technische universität
dortmund

Functionalized Organotin Compounds as Synthons for Tin-containing Heterocycles and Periphery-functionalized Organotinoxo Clusters

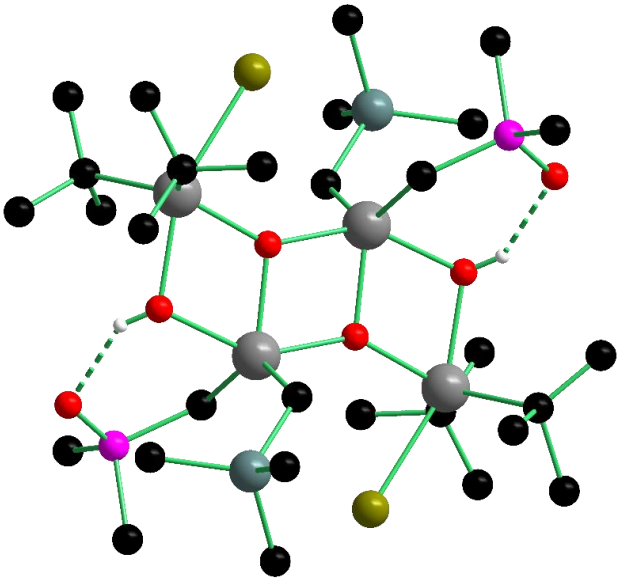

Thesis presented for obtaining the degree of

DOKTOR DER NATURWISSENSCHAFTEN

(Doctor rer. nat.)

by

Dipl. Chem. Samer Baba Haj

First Reviewer: Prof. Dr. Klaus Jurkschat

Second Reviewer: Prof. Dr. Stefanie Dehnen

Thesis defended the 24th July 2015

ACKNOWLEDGMENT

The present work was carried out from August 2009 until December 2013
at the Institute of Inorganic Chemistry of the Technische Universität Dortmund

under the supervision of

Prof. Dr. KLAUS JURKSCHAT

whom I pay my greatest gratitude and thanks for the interesting and fascinating topic, for his skillful guidance and encouragement throughout the course of this research. Your advices and supports are always for me a source of motivation.

My sincere thanks and regards go also to

Prof. Dr. STEFANIE DEHNEN

for writing the second review report

This work was also realized with funding from Damascus University that provided me a scholarship. I am grateful to Damascus University for this support.

Heartiest thanks are also extended to all the scientific co-workers of the research group of Prof. Dr. K. JURKSCHAT for the willingness to support this work.

In particular I would like to thank:
Dr. CHRISTINA DIETZ, Dr. THOMAS ZÖLLER, and M. Sc. MICHAEL LUTTER
for performing the X-ray diffraction analyses.

I also appreciate the technical staff for their day to day service

No words can express my gratitude and profound thanks to my parents and sisters whose prayers, affection, love, care and perpetual encouragement helped me not only during my studies but throughout my life.

My beloved daughter LEEN deserves greatest thanks for being such a good girl always cheering me up, and wished me 'All the Best', innocently and wholeheartedly.

I would also like to express my thanks to my sweetheart, my baby daughter DANA, who was one of my sources of optimism

Finally, and most importantly, I would like to thank my wife NOUR who always trust and support me. Thank you for your encouragement throughout my PhD studies!

Contents

List of Abbreviations

General abbreviations			
R	Organic group	c	Consentration
Ar	Aryl	M	Molarity
Ph	Phenyl	mL	Milliliter
Me	Methyl	t	Time
Et	Ethyl	min	Minutes
n-Bu	*n*-Butyl	h	Hours
t-Bu	*tert*-Butyl	T	Temperature
Cy	Cyclohexyl	*i*	Ipso-position in aromatic ring
X	Halide	*o*	Ortho-position in aromatic ring
THF	Tetrahydrofuran	*m*	Meta-position in aromatic ring
DMSO	Dimethyl sulfoxide	*p*	Para-position in aromatic ring
eq	Equation	Calcd	Calculated
Spectroscopy			
MS	Mass spectrometry	MHz	Megaherz
ESI	Electrospray Ionization	s	Singulett
m/z	Mass per charge	d	Dublett
NMR	Nuclear magnetic resonance	t	Triplett
ppm	Parts per million	m	Multiplett
δ	Chemical shift in ppm	dd	doublet of doublet
J	Coupling constant	IR	Infrarot
Hz	Hertz		
Molecular Structure Determination			
a, b, c	Unit cell dimensions	Z	Number of molecules in the unit cell
Å	Angström	σ	Standard deviation
α, β, γ	Unit cell angles	μ	Absorption coefficient
°	Degree	F(000)	number of electrons in the unit cell
V	Volume of the unit cell	Dc	Density

General Introduction

Among organometallics, organotin compounds probably show the most diverse range of applications. They generally show high biological activity and have been reported to be efficient homogeneous catalysts for a variety of organic reactions such as transesterification under virtually neutral conditions,[1] highly selective acylation of alcohols,[2] polyurethane synthesis,[3] and polymerization of butyrolactones.[4] They also find application in PVC stabilization,[5] glass coating,[6] silicone vulcanization,[7] and as ionophores in sensors.[8] The diversity of applications of organotin compounds are attributed to the fact that, they are easy to handle and provide the desired product in excellent yields under virtually mild conditions.

Selected Applications of Organotin Compounds

1. Transesterification[1]

Transesterification is a classical reaction that still find great demand in modern synthetic chemistry, and is widely applied in industry.

Transesterification has been carried out traditionally and most frequently by the use of acid catalysts such as sulfuric, sulfonic, phosphoric, and hydrochloric acids. On the industrial scale, this presents problems of corrosion and of decomposition and colouration of the excess alcohol.

Tin-based Lewis acids are very efficient catalysts for transesterification reactions under mild conditions. They offer yields up to 100% in reactants ratio of 1:1.

Many different types of organotin compounds have been patented as catalysts, e.g. Bu_2SnO, $BuSnO_2H$, $Bu_2Sn(OAc)_2$, but the most effective appear to be the tetraorganodistannoxanes, $XR_2SnOSnR_2Y$ (X, Y = electronegative substituents),[9] which feature ladder-type structures induced by molecular association (Chart 1). Distannoxanes may act as bidentate Lewis acids as a result of the proximate location of two different tin atoms.

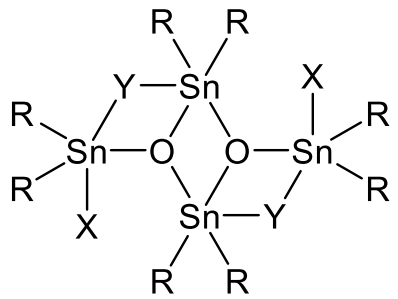

X, Y = electronegative substituent.

Chart 1. Dimeric tetraorganodistannoxanes.

An example is provided by the transesterification of methyl butyrate and benzyl alcohol.

$$C_3H_7COOMe + PhCH_2OH \xrightarrow{\text{Distannoxane}} C_3H_7COOCH_2Ph + MeOH$$

The reaction affords high yields up to 100% using distannoxane catalysts in low concentrations (0.05 mol %) at almost neutral conditions.

One mechanism suggested for the distannoxane-catalyzed transesterification is demonstrated in Scheme 3. The initial step is the formation of alkoxydistannoxane which undergoes coordination of the ester. Subsequent alcoholysis of the last adduct affords the transesterified product and consequently regenerate the alkoxydistannoxane.

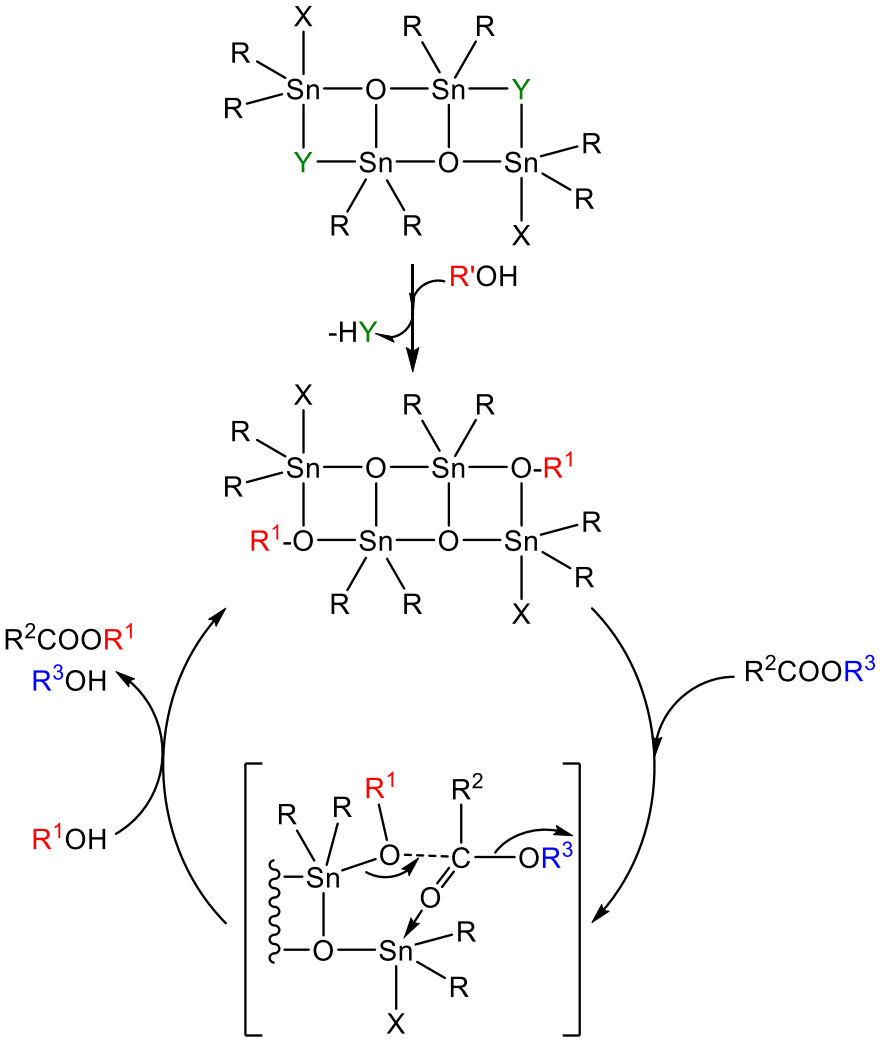

Scheme 3. Probable mechanism for distannoxane-catalyzed transesterification.

2. PVC Stabilization.[5]

The most important application of organotin compounds is as stabilizer for PVC. In the course of fabrication of poly(vinyl chloride), it exposed to high temperatures (about 200 °C) which may cause elimination of some HCl at allylic defects in the polymer. The release of HCl catalyzes progressive elimination with the formation of a conjugated polyene (Scheme 1). As a consequence, the color changes to yellow, then red, and then black, after which the polymer becomes hard and brittle.

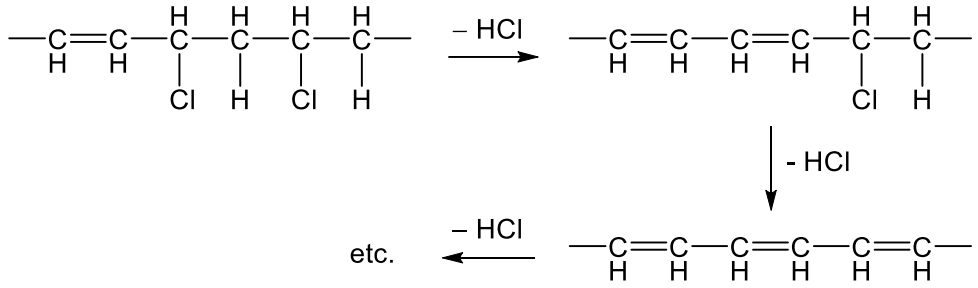

Scheme 1. Progressive elimination of HCl from PVC.

Di- and triorganotin thiolates have been the most widely used organotin compounds as stabilizers for PVC. They perform at least in a dual function.
First they exchange the chlorine atom at the allylic sites giving the allyl mercaptane that is thermally more stable and does not act as a site for initiating the elimination of HCl.

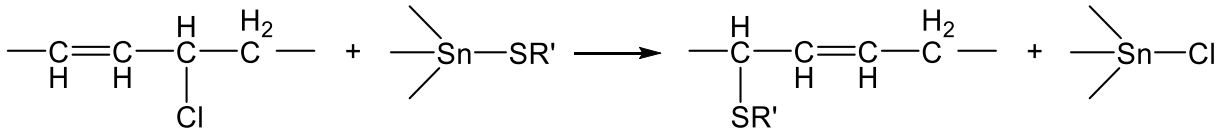

Second they scavenge the HCl which is eliminated, to give the organotin chlorides and thiol. The latter do not catalyze further elimination.

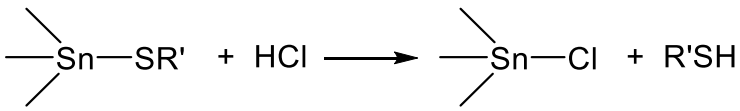

The use of organotin thiolates as stabilizers makes it possible to manufacture clear PVC products that have gained approval for food packaging because of the low leach rate and low toxicity of the stabilizers.

3. Glass Coating.[6]

Tin (IV) oxide, SnO_2, holds the advantage as being a cheap material that shows high thermodynamic stability in air. Organotin(IV) oxides have been employed in the

preparation of nanoscale particles of SnO_2.[9] The identity of the organic group attached to the Sn center plays an important role in the decomposition process.[10]

At the end of 1960s thin films of tin oxide on glass were deposited using $SnCl_2$ or $SnCl_4$ in the presence of O_2. Now it is produced by pyrolysis of organotin(IV) compounds, usually butyltin trichloride.[11] Films of up to 10 nm thickness are used to strengthen glassware so that lighter and cheaper glass containers can be used. Films of greater than 1 μm can be doped to provide semiconductors or conductors, and find applications such as in deicing windscreens, security glass, or display systems. The glass finds increasing application in window glazing because of its low heat emissivity.

4. Silicone Vulcanization.[7]

Organotin compounds have been extensively used as catalysts within the silicone industry in a diversity of applications where the formation of Si–O bonds is required. They are used for room temperature vulcanization (RTV) of polysiloxanes. The aim of this transformation is to form heavy resins, coatings and elastomers.

A liquid linear polysiloxane, with terminal OH groups, is mixed with alkyl silicate as a cross-linking agent, together with a condensation catalyst, generally an organotin compound. The organotin dicarboxylate is one example of the condensation catalyst. It is hydrolysed to the hydroxycarboxylate, which transforms the terminal OH groups into the more reactive SiO–Sn groups. These react with the tetraethoxysilane to initiate the cross-linking.[7b]

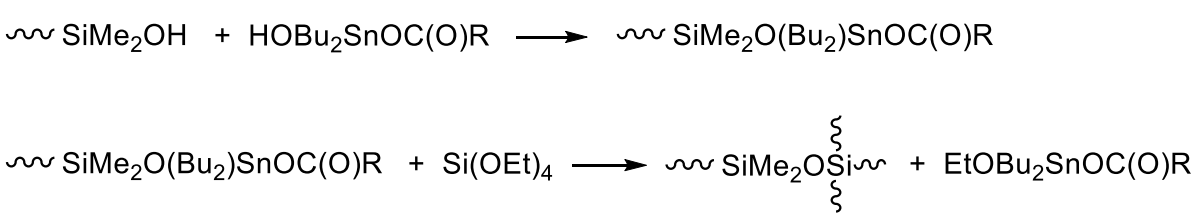

Scheme 2. RTV of Polysiloxanes catalyzed by organotin dicarboxylate.

This work deals with different topics in organotin chemistry. The goal of the work is to synthesize organotin compounds that are promising as catalysts for a diversity of organic reactions, and hold potential in material science.

The **first chapter** deals with the syntheses of functionally-substituted organotin compounds and their hydrolysis-behavior giving different types of periphery-functionalized organotinoxo clusters. It will be demonstrated the reactions of the diorganotin dihalides $\{Ph_2P(O)CH_2\}RSnX_2$ with different molar equivalents di-*tert*-butyltin oxides affording the corresponding O-capped clusters $[\{Ph_2P(O)CH_2\}R(\mu\text{-}OH)Sn]_3(\mu_3\text{-}O)(\mu_3\text{-}X)$ and the ladder-type unsymmetrically-substituted dimeric tetraorganodistannoxanes $[t\text{-}Bu_2(X)SnOSn(OH)R\{CH_2P(O)Ph_2\}]_2$, containing the P=O functional group (Figure 1). Organotinoxo clusters feature mild Lewis acidity as well as thermal and hydrolytic stability. Therefore, they find applications as catalysts for a variety of organic reactions.[1-3, 12] The involving of the functional group could affect the catalytic activity of this type of compounds.

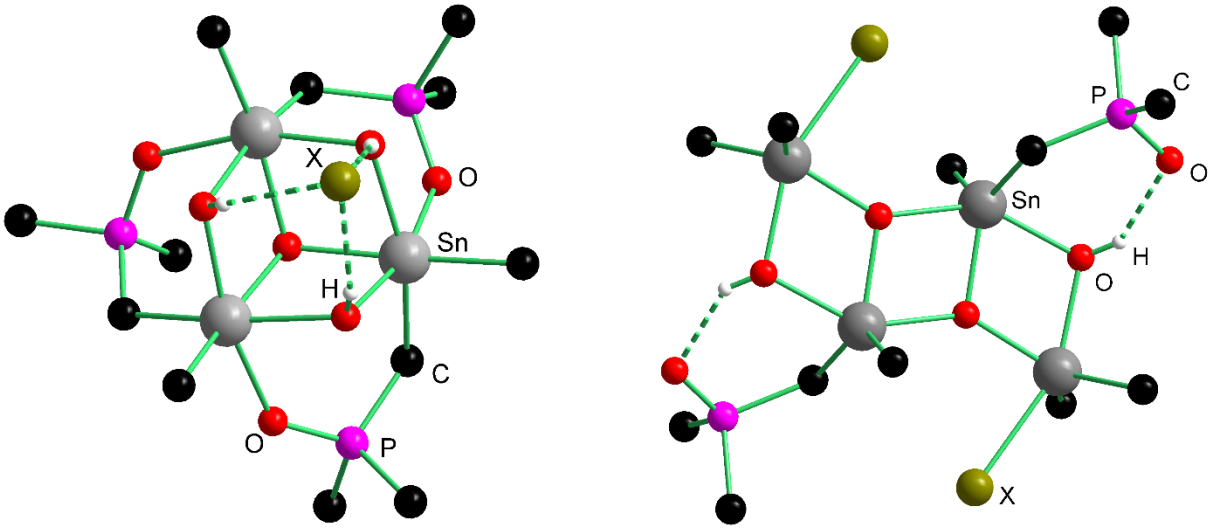

Figure 1. O-capped clusters (on left) and dimeric tetraorganodistannoxanes (on right).

The **second chapter** concerns the syntheses of *cyclo*-siloxanes and silsesquioxanes containing tin atoms that are bound to the silicon atoms by carbon linkage ($SnCH_2Si$) (Chart 2). These compounds could be interpreted as single source precursors for structurally modified polysiloxanes and silicates.

The hydrolyses behavior of the organotin halides $O(Me_2SiCH_2)_2SnX_2$ affording the symmetrically- and/or the unsymmetrically-substituted dimeric tetraorganodistannoxanes depending on the identity of the halogen (X) will also be investigated.

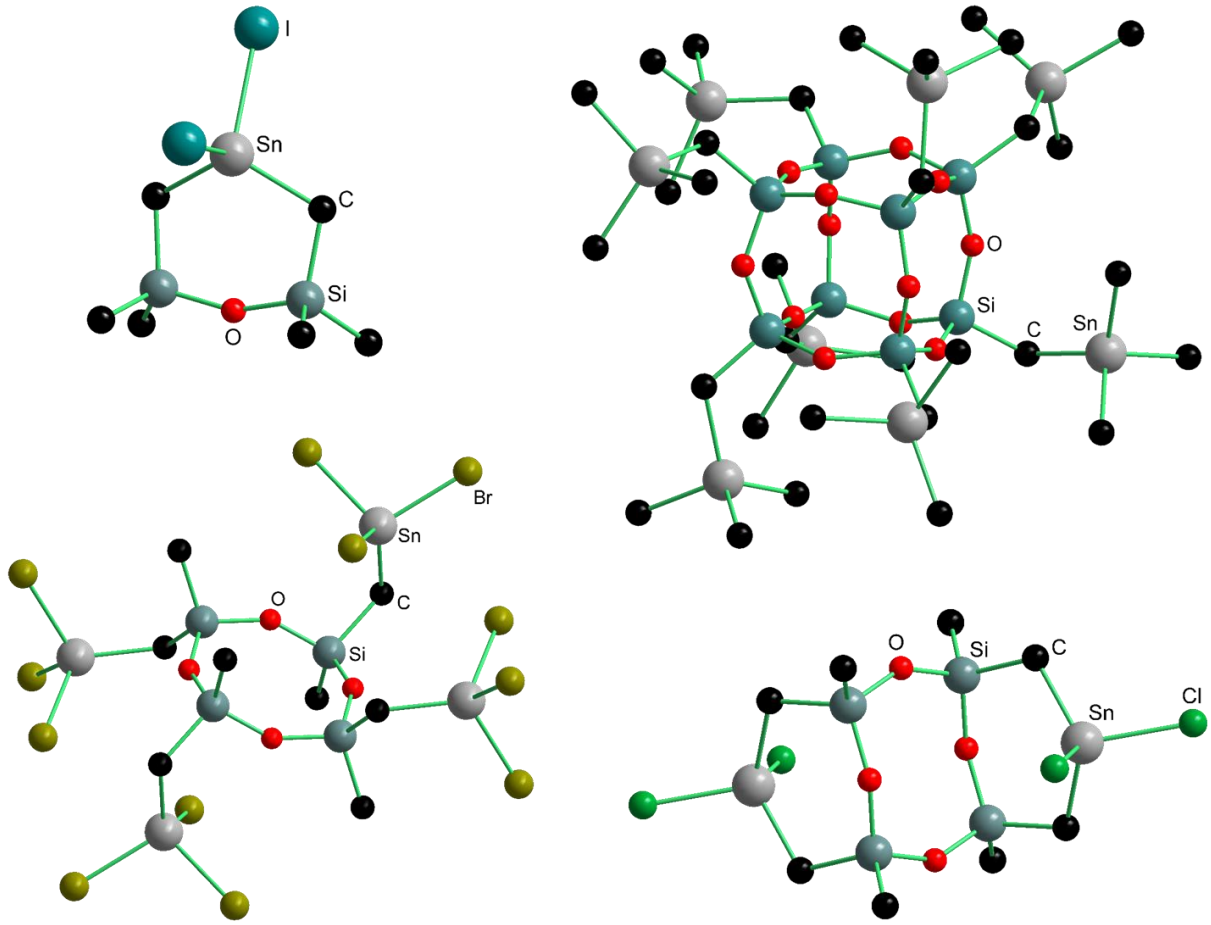

Chart 2. Tin-substituted siloxanes and silsesquioxanes.

The **third chapter** deals with the syntheses of the eight-membered *cyclo*-stannasiloxanes, *cyclo*-$[RR'SnOMe_2SiCH_2]_2$ which have tin and silicon atoms binded together via a methylene bridge. The reactivity of these compounds towards different organoelement oxides affording the corresponding six-membered *cyclo*-metallasiloxanes *cyclo*-$[Me_2SiCH_2(RR')SnOMO]$ (M = organoelement fragment) will be presented (Scheme 4).

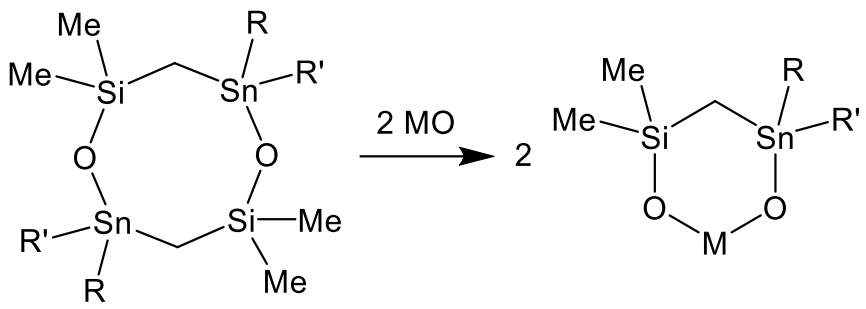

Scheme 4.

Metal-supported siloxanes hold potential as precursors for the preparation of ceramic materials and model compounds that effectively mimic heterogeneous silica-supported catalysts.[13] Metallasiloxanes have been commonly used as heterogeneous catalysts in a variety of organic transformations.[13h, 14]

The evidence for intramolecular Si–O bond activation supported by the molecular structure of $[Me_2(i\text{-PrO})SiCH_2]_2SnBr_2$ (Chart 3), and NMR studies at variable temperatures will be highlighted in the **fourth chapter**.

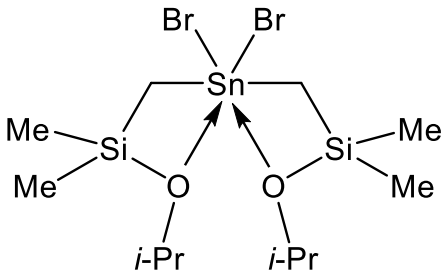

Chart 3. Drawing of $[Me_2(i\text{-PrO})SiCH_2]_2SnBr_2$.

References

1. (a) Otera, J., *Chem. Rev.* **1993**, *93*, 1449; (b) Otera, J.; Ioka, S.; Nozaki, H., *J. Org. Chem.* **1989**, *54*, 4013; (c) Otera, J.; Yano, T.; Kawabata, A.; Nozaki, H., *Tetrahedron Lett.* **1986**, *27*, 2383; (d) Otera, J.; Dan-Oh, N.; Nozaki, H., *J. Chem. Soc., Chem. Commun.* **1991**, 1742; (e) Otera, J.; Danoh, N.; Nozaki, H., *J. Org. Chem.* **1991**, 56, 5307.
2. (a) Otera, J.; Dan-oh, N.; Nozaki, H., *Tetrahedron* **1992**, *48*, 1449; (b) Orita, A.; Mitsutome, A.; Otera, J., *J. Org. Chem.* **1998**, *63*, 2420; (c) Durand, S.; Sakamoto, K.; Fukuyama, T.; Orita, A.; Otera, J.; Duthie, A.; Dakternieks, D.; Schulte, M.; Jurkschat, K., *Organometallics* **2000**, *19*, 3220.
3. Houghton, R. P.; Mulvaney, A. W., *J. Organomet. Chem.* **1996**, *517*, 107.
4. Kemnitzer, J. E.; McCarthy, S. P.; Gross, R. A., *Macromolecules* **1993**, *26*, 6143.
5. Arkis, E., Organotin Compounds as PVC Stabilizers. In Tin Chemistry: Fundamentals, Frontiers, and Applications, Davies, A. G.; Gielen, M.; Pannell, K. H.; Tiekink, E. R. T., Eds. Wiley: **2008**.
6. de Lima, G. M., Materials Chemistry and Structural Chemistry of Tin Compounds. In Tin Chemistry: Fundamentals, Frontiers, and Applications, Davies, A. G.; Gielen, M.; Pannell, K. H.; Tiekink, E. R. T., Eds. Wiley: **2008**.
7. (a) Cervantes, J.; Zárraga, R.; Salazar-Hernández, C., *Appl. Organomet. Chem.* **2012**, *26*, 157; (b) van Der Weij, F. W., *Makromol. Chem.* **1980**, *181*, 2541.
8. (a) Chaniotakis, N. A.; Jurkschat, K.; Rühlemann, A., *Anal. Chim. Acta* **1993**, *282*, 345; (b) Chaniotakis, N.; Jurkschat, K.; Müller, D.; Perdikaki, K.; Reeske, G., *Eur. J. Inorg. Chem.* **2004**, 2283; (c) Perdikaki, K.; Tsagkatakis, I.; Chaniotakis, N. A.; Altmann, R.; Jurkschat, K.; Reeske, G., *Anal. Chim. Acta* **2002**, *467*, 197.
9. Pereira, A. G.; Porto, A. O.; Silva, G. G.; de Lima, G. M.; Siebald, H. G. L.; Neto, J. L., *Phys. Chem. Chem. Phys.* **2002**, *4*, 4528.
10. Pereira, A. G.; Batalha, L. A. R.; Porto, A. O.; de Lima, G. M.; Silva, G. G.; Ardisson, J. D.; Siebald, H. G. L., *Mater. Res. Bull.* **2003**, *38*, 1805.
11. Korotkov, R. Y.; Ricou, P.; Farran, A. J. E., *Thin Solid Films* **2006**, *502*, 79.

12. (a) Tin Chemistry: Fundamentals, Frontiers, and Applications. Wiley: **2008**; (b) Orita, A.; Tanabe, S.; Ono, T.; Otera, *J., Adv. Synth. Catal.* **2010**, *352*, 1419; (c) Otera, J.; Yano, T.; Okawara, R., *Organometallics* **1986**, *5*, 1167; (d) Otera, J.; Yano, T.; Himeno, Y.; Nozaki, H., *Tetrahedron Lett.* **1986**, *27*, 4501; (e) Otera, J.; Nozaki, H., *Tetrahedron Lett.* **1986**, *27*, 5743; (f) Otera, J.; Kawada, K.; Yano, T., *Chem. Lett.* **1996**, *25*, 225; (g) Houghton, R. P.; Mulvaney, A. W., *J. Organomet. Chem.* **1996**, *518*, 21; (h) Suciu, E. N.; Kuhlmann, B.; A. Knudsen, G.; Michaelson, R. C., *J. Organomet. Chem.* **1998**, *556*, 41; (i) Padelkova´, Z.; Vanka´tova´, H.; Cisarova´, I.; Nechaev, M. S.; Zevaco, T. A.; Walter, O.; Ruzicka, A., *Organometallics* **2009**, *28*, 2629; (j) Okawara, R., *Proc. Chem. Soc.* **1961**, 383; (k) Schulte, M.; Mehring, M.; Paulus, I.; Schurmann, M.; Jurkschat, K.; Dakternieks, D.; Duthie, A.; Orita, A.; Otera, J., *Phosphorus, Sulfur Silicon Relat. Elem.* **1999**, *150*, 201; (l) Otera, J., *Acc. Chem. Res.* **2004**, *37*, 288; (m) An, D. L.; Peng, Z.; Orita, A.; Kurita, A.; Man-e, S.; Ohkubo, K.; Li, X.; Fukuzumi, S.; Otera, J., *Chem. Eur. J.* **2006**, *12*, 1642.

13. (a) Beckmann, J.; Jurkschat, K., *Coord. Chem. Rev.* **2001**, *215*, 267; (b) King, L.; Sullivan, A. C., *Coord. Chem. Rev.* **1999**, *189*, 19; (c) Murugavel, R.; Voigt, A.; Walawalkar, M. G.; Roesky, H. W., *Chem. Rev.* **1996**, *96*, 2205; (d) Kung, M. C.; Riofski, M. V.; Missaghi, M. N.; Kung, H. H., *Chem. Commun.* **2014**, *50*, 3262; (e) MMLevitsky; Zavin, B. G.; Bilyachenko, A. N., *Russ. Chem. Rev.* **2007**, *76*, 847 ; (f) Murugavel, R.; Bhattacharjee, M.; Roesky, H. W., *Appl. Organomet. Chem.* **1999**, *13*, 227; (g) Cordes, D. B.; Lickiss, P. D.; Rataboul, F., *Chem. Rev.* **2010**, *110*, 2081; (h) Fandos, R.; Gallego, B.; Otero, A.; Rodriguez, A.; Ruiz, M. J.; Terreros, P., *Dalton Trans.* **2007**, 871.

14. (a) Murugavel, R.; Roesky, H. W., *Angew. Chem. Int. Ed.* **1997**, *36*, 477; (b) Conley, M. P.; Delley, M. F.; Siddiqi, G.; Lapadula, G.; Norsic, S.; Monteil, V.; Safonova, O. V.; Copéret, C., *Angew. Chem. Int. Ed.* **2014**, *53*, 1872.

1 Periphery-Functionalized Organotinoxo Clusters. Syntheses and Structures

1.1 Organotin Derivatives Containing the $Ph_2P(O)CH_2$ moiety: Tetraorganodistannoxanes and Trinuclear Organotinoxo Clusters

1.1.1 Introduction

Among the versatile applications of organotin compounds, their use in catalysis continues to attract considerable attention.[1] In this context organotinoxo clusters represent an important class owing to their mild Lewis acidity and their thermal and hydrolytic stability.

Organotinoxo clusters have received considerable interest over the last few decades in view of the wide structural diversity shown by this type of compounds, their potential in material science, and their catalytic activity for a variety of organic reactions.[1b, 2]

Their potential in organic synthesis has been demonstrated especially for transesterifications under virtually neutral conditions,[2c-g] highly selective acylation of alcohols,[2h-j] urethane formation,[2n] and alkyl carbonate synthesis.[2p, 2q]

Several types of organotinoxo clusters having a tin-oxo core resembling ladder, double ladder, drum, cube, butterfly, and football structures have been synthesized (Figure 1).[1b]

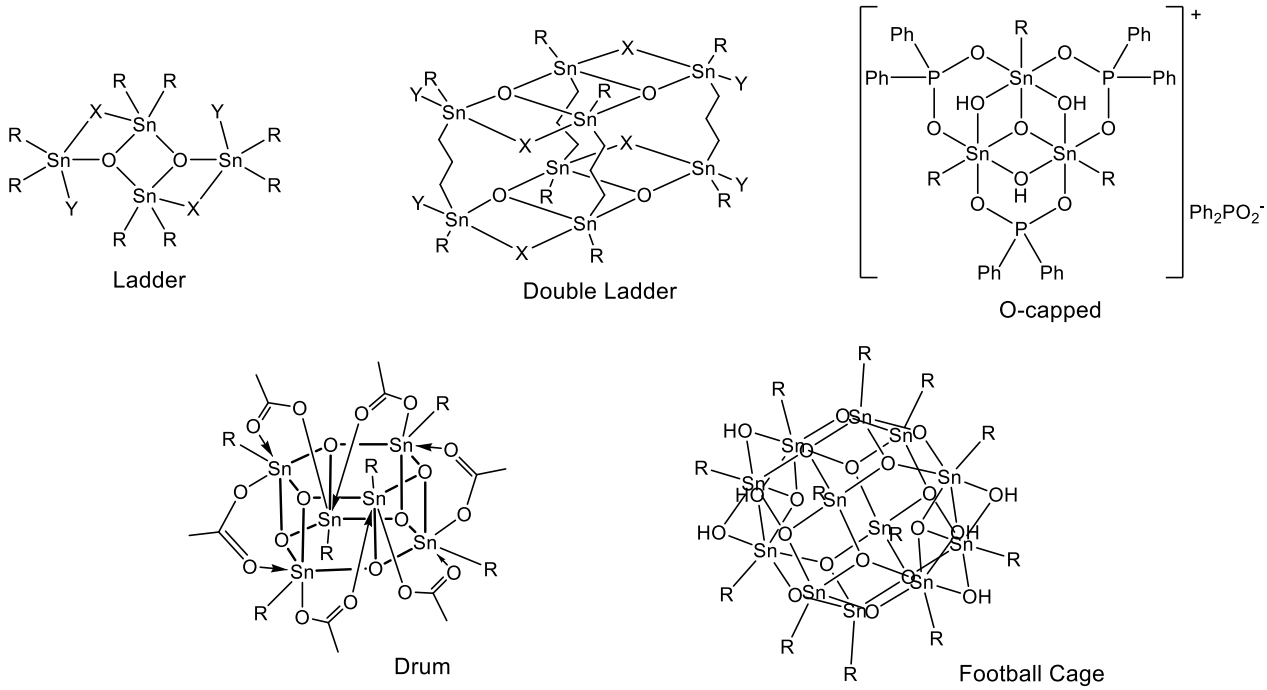

Figure 1. Examples for some types of organotinoxo clusters.

The nuclearity of these clusters often varies from trimeric to octadecameric. While clusters made up of an even number of tin atoms are very common, clusters with an odd number of tin atoms feature by their absence or rarity (excepting Sn_3 clusters). Most organotinoxo clusters reported are symmetric and exhibit mirror planes and inversion centers.

Organotinoxo clusters are synthesized by the hydrolysis of organotin compounds of the type R_nSnX_{4-n} (X = electronegative substituent). The molecular structure of the resulting tinoxo-hydroxo clusters depends on the identity and number of the organic substituent R, the functional group X and the reaction conditions. These compounds can formally be interpreted as intermediates along the hydrolysis pathway of the organotin compounds as the complete base hydrolysis of the organotin compounds leads to the corresponding organotin oxides (Scheme 1).

Hydrolyses of the monoorganotin compounds lead to Sn_{12} oxide-hydroxides, the most documented monoorganotinoxo cluster,[3] or Sn_9 oxide-pentachloride-hexahydroxides.[4] For bulky groups and depending on the identity of the base, Sn_6 oxide hydroxide,[5] Sn_4 pure oxide[6] or Sn_3 oxide-trichlorides/trihydroxides[7] were

reported. The first intermediate along the hydrolysis pathway was also reported as Sn_2 aqua-hydroxide-chloride $\{RSn(\mu_2\text{-}OH)Cl_2(H_2O)\}_2$.[8]

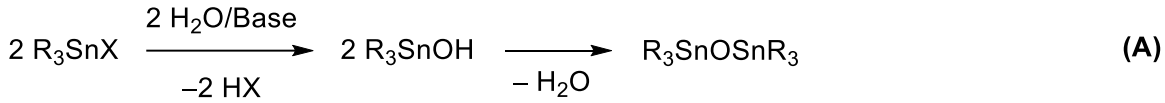

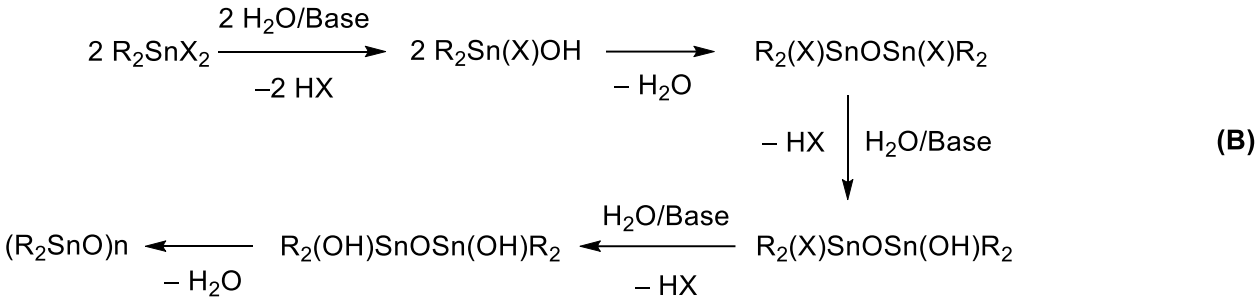

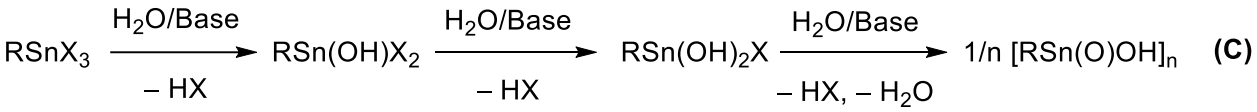

Scheme 1. Hydrolyses under basic conditions of organotin compounds of the type R_nSnX_{4-n}, (n = 1–3; R = alkyl, aryl; X = electronegative substituent).

Complete hydrolyses of the diorganotin compounds R_2SnX_2 (X = electronegative substituent) proceed via formation of insoluble polymeric diorganotin oxides $(R_2SnO)_n$ (n = ∞) for sterically nondemanding substituents as a result of intramolecular cross-linking.[9] Bulky substituents inhibit cross linking, and thus well-defined molecular organotin oxides such as $(t\text{-}Bu_2SnO)_3$,[10] $[O(Me_2SiCH_2)_2SnO]_3$,[11] $[(t\text{-}C_5H_{11})_2SnO]_3$,[10] $[(2,6\text{-}Et_2C_6H_3)_2SnO]_3$,[12] $[(2,4,6\text{-}Me_3C_6H_2)_2SnO]_3$,[13], $[\{2,4,6\text{-}(CF_3)_3C_6H_2\}_2SnO]_3$,[14] $[(Me_3Si)_2CH(Me)SnO]_3$,[15] and $[\{(Me_3Si)_2CH\}_2SnO]_2$[16] are formed. However the controlled hydrolyses of R_2SnX_2 commonly afford dimeric tetraorganodistannoxanes $[R_2(X)SnOSn(X)R_2]_2$ and $[R_2(X)SnOSn(OH)R_2]_2$ (path a). These compounds can also be synthesized by the acidic hydrolysis of diorganotin oxides (paths b), or by the oxidation of functional distannanes (path c) (Scheme 2).

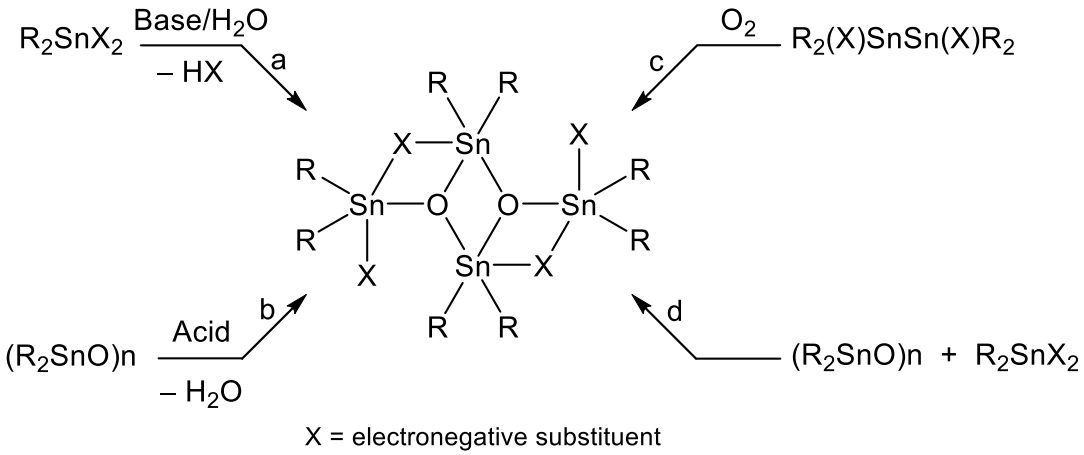

Scheme 2. Synthesis of dimeric tetraorganodistannoxanes.

The most elegant route to synthesize the dimeric tetraorganodistannoxanes is by the reaction between equimolar amounts of diorganotin oxides and diorganotin compounds R_2SnX_2 (path d, Scheme 2). Reaction of R_2SnX_2 with diorganotin oxides having different organic substituents on the tin atom R'_2SnO could result in unsymmetrically-substituted dimeric distannoxanes $[R_2(X)SnOSn(X)R'_2]_2$, in which the tin atom with more bulky organic substituents is placed in the exo-cyclic position (Chart 1).

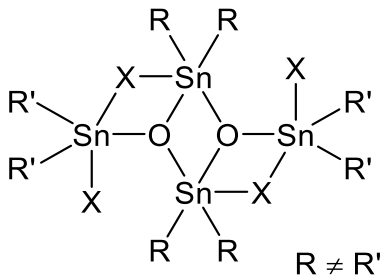

Chart 1. Unsymmetrically-substituted dimeric tetraorganodistannoxanes.

Dimeric tetraorganodistannoxanes feature a planar central Sn_2O_2 ring and adopt the so called ladder-like structure both in solution and in the solid state.[17]

The applications of dimeric tetraorganodistannoxanes in organic syntheses were especially developed by *Otera* and coworkers and the catalytic activity of these compounds was reported to be the result of the kinetic lability in solution of the ladder-like structure motif found in the solid state.[3e]

To the best of our knowledge, there are only few reports on unsymmetrically substituted tetraorganodistannoxanes containing different diorganotin moieties, and much less on those which have different organic substituents on the same tin atom.
In this work the synthesis of a set of $Ph_2P(O)CH_2$-functionalized organotinoxo clusters is reported. The involving of this group results in formation of the first diorganotinoxo clusters that have a trinuclear O-capped structure. Hence, this allows to synthesize organotinoxo clusters of small nuclearity in the same way the bulky substituents do.
Also reported are the syntheses of a few unsymmetrically substituted ladder-like dimeric tetraorganodistannoxanes. These are the first examples of organotinoxo clusters that have a functional group in the periphery which could affect the catalytic activity of this type of compounds.

1.1.2 Results and Discussion

1.1.2.1 Syntheses and structures of the $Ph_2P(O)CH_2$-substituted tetraorganotin compounds $Ph_2P(O)CH_2SnR_2R'$ (1, R = R' = Ph; 2, R = Ph, R' = Me_3SiCH_2; 3, R = R' = Cy; 4, R = Ph, R' = $Ph_2P(O)CH_2$)

Reactions of one molar equivalent $Ph_2P(O)CH_2Li$ with triphenyltin chloride, (trimethylsilylmethyl)diphenyltin iodide and tricyclohexyltin chloride, and of two molar equivalents $Ph_2P(O)CH_2Li$ with diphenyltin dichloride afforded the corresponding $Ph_2P(O)CH_2$-substituted tetraorganotins $Ph_2P(O)CH_2SnPh_3$, **1**, $[Ph_2P(O)CH_2](Me_3SiCH_2)SnPh_2$, **2**, $Ph_2P(O)CH_2SnCy_3$, **3**, and $[Ph_2P(O)CH_2]_2SnPh_2$, **4**, respectively, in moderate yields for **1**–**3** and low yield for **4** (Scheme 3).
Compounds **1**–**4** show good solubility in common organic solvents as THF, chloroform and dichloromethane.

The ^{119}Sn NMR spectra of compounds **1**–**3** show, as expected, doublet resonances at δ –116 [$^2J(^{119}Sn–^{31}P)$ = 62 Hz] for **1**; at –68 [$^2J(^{119}Sn–^{31}P)$ = 58 Hz] for **2** and at –63 [$^2J(^{119}Sn–^{31}P)$ = 62 Hz] for **3**. Compound **4** shows a triplet resonance at δ –93 [$^2J(^{119}Sn–^{31}P)$ = 64 Hz]. The ^{1}H NMR spectra show for the methylene protons (SnCH_2P) doublet resonances at δ 2.45 (for **1**), 2.16 (for **2**), 1.63 (for **3**) and 2.34 (for

4) with $^{2}J(^{1}H–^{31}P)$ coupling constants of about 11.4 ± 0.4 Hz. $^{117/119}Sn$ coupling satellites were detected for compounds **1**, **2** and **4** of $^{2}J(^{1}H–^{117/119}Sn)$ = 58 ± 5 Hz. This could not be observed for compound **3** because of the overlapping from the *cyclo*-hexyl protons which display resonances in the same range.

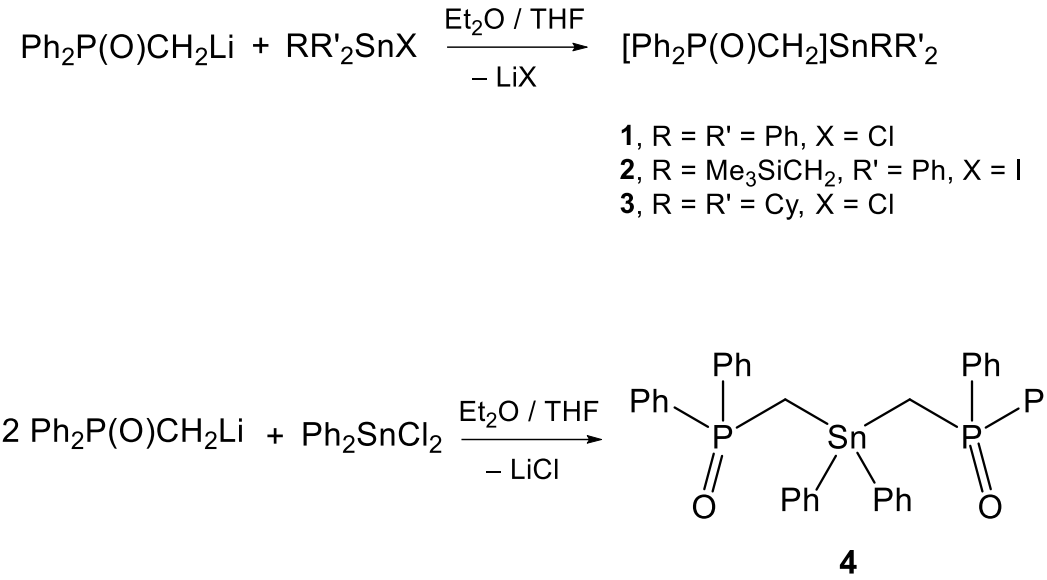

Scheme 3. Syntheses of the $Ph_2P(O)CH_2$-substituted tetraorganotin compounds **1**–**4**.

In the ^{13}C NMR spectra of compounds **1**–**4** doublets for $SnCH_2P$ carbon atom were observed at δ 14.3 (for **1**), 14.0 (for **2**), 7.2 (for **3**) and 14.0 (for **4**) with $^{1}J(^{13}C–^{31}P)$ of 67 ±1 Hz. The NMR data of compounds **1**–**4** are listed in Table 1.

Table 1. Selected NMR data of compounds **1**–**4**.

				$SnCH_2P$				
	$\delta^{119}Sn$	$\delta^{31}P$	$^{2}J(^{31}P–^{117/119}Sn)$	^{1}H			^{13}C	
				δ	$^{2}J(^{1}H–^{31}P)$	$^{2}J(^{1}H–^{117/119}Sn)$	δ	$^{1}J(^{13}C–^{31}P)$
1	d, –116	33.0	58/62	2.45	11.3	57.4/60.0	14.3	66
2	d, –68	33.2	57	2.16	11.7	54.2/56.7	14.0	67
3	d, –63	33.9	49	1.63	11.7	–	7.2	68
4	t, –93	33.7	62/65	2.34	11.0	60.6/63.0	14.0	67

Chemical shifts are given in ppm, and coupling constants in Hz.

Recrystallization of **1** and **3** from their solutions in CH_2Cl_2/ethyl acetate and of **2** from hot hexane provided colorless single crystals suitable for X-ray diffraction analysis.

The molecular structures of **1**, **2** and **3** are shown in Figures 2, 3 and 4, respectively, and selected bond lengths and bond angles are summarized in Table 2.

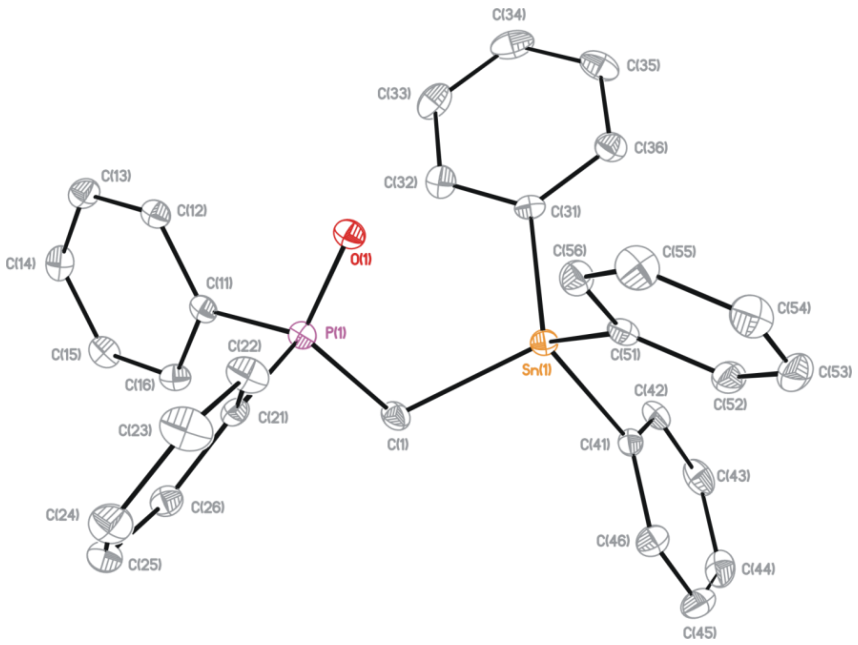

Figure 2. General view (SHELXTL) of a molecule of **1** showing 30% probability displacement ellipsoids and the crystallographic numbering scheme. Hydrogen atoms are omitted for clarity.

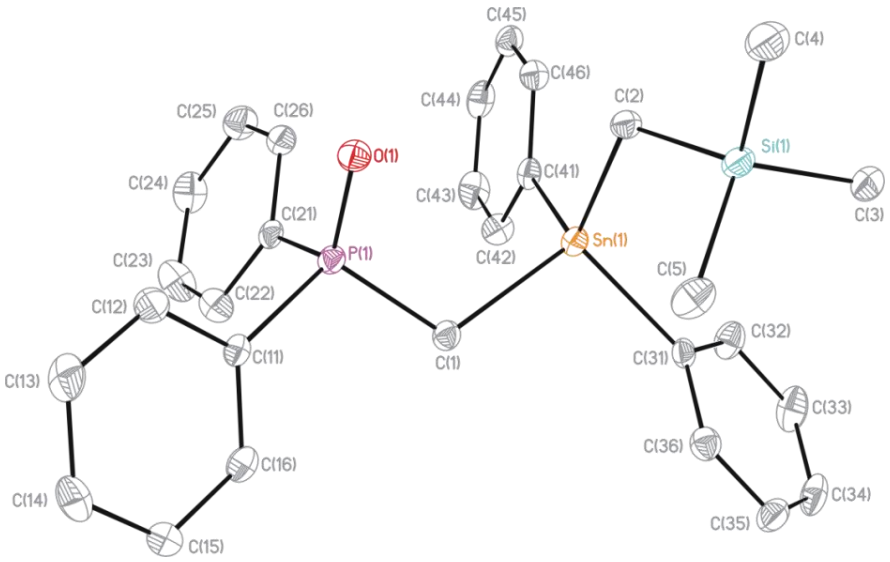

Figure 3. General view (SHELXTL) of a molecule of **2** showing 30% probability displacement ellipsoids and the crystallographic numbering scheme. Hydrogen atoms are omitted for clarity.

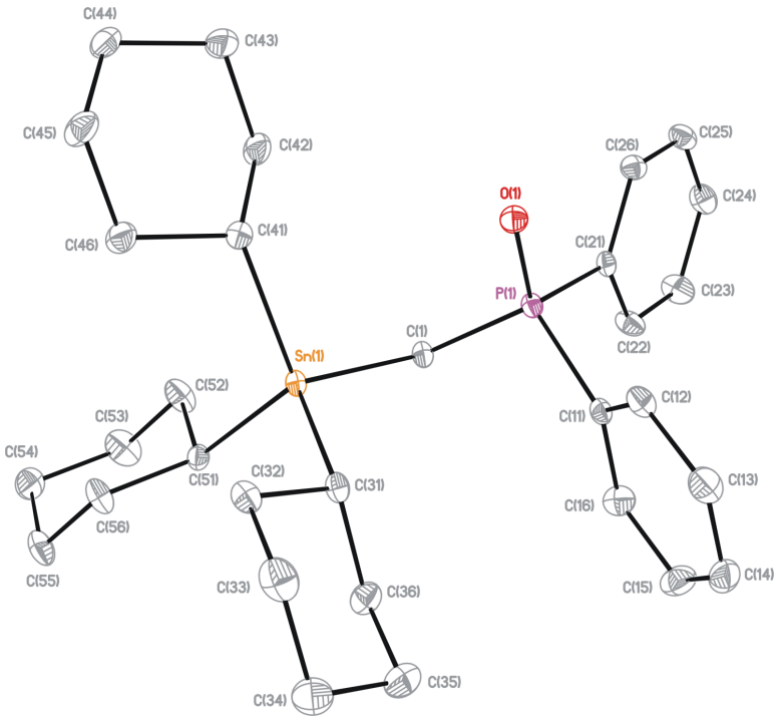

Figure 4. General view (SHELXTL) of a molecule of **3** showing 30% probability displacement ellipsoids and the crystallographic numbering scheme. Hydrogen atoms are omitted for clarity.

Table 2. Selected bond lengths (Å) and bond angles (deg) in compounds **1**–**3**.

	1	**2**	**3**
Sn(1)–C(1)	2.160(3)	2.161(2)	2.1631(19)
Sn(1)–C(31)	2.138(3)	2.143(3)	2.159(2)
Sn(1)–C (41)	2.138(3)	2.133(2)	2.155(2)
Sn(1)–Y	2.142(3)	2.125(2)	2.1585(19)
P(1)–O(1)	1.4915(18)	1.4831(17)	1.4858(13)
Sn(1)···O(1)	3.1607(19)	3.4810(17)	3.5498(14)
Sn(1)–C(1)–P(1)	109.73(13)	113.42(12)	114.79(10)
C(1)–Sn(1)–C(31)	109.32(11)	102.87(9)	111.09(8)
C(1)–Sn(1)–C(41)	103.99(10)	109.49(10)	108.18(8)
C(1)–Sn(1)–Y	111.75(11)	110.30(10)	102.13(7)
C(31)–Sn(1)–C(41)	107.85(11)	105.88(10)	109.16(8)
C(31)–Sn(1)–Y	116.45(10)	116.59(9)	110.84(8)
C(41)–Sn(1)–Y	106.64(10)	111.22(10)	115.24(8)

1, Y= C(51); **2**, Y= C(2); **3**, Y= C(51).

The tin atoms in **1**, **2** and **3** can be seen as being [4+1]-coordinated, with four carbon atoms [C(1), C(31), C(41) and C(51)/C(2)] forming a distorted tetrahedron that is face-attacked by O(1) at Sn(1)–O(1) distances of 3.1607(19)Å for **1**, 3.4810(17) Å for **2**, and 3.5498(14) Å for **3**. The C–Sn–C angles range between 103.99(10)° and 116.45(10) for **1**, between 102.87(9) and 116.59(9) for **2** and between 102.13(7) and 115.24(8) for **3**, whilst all Sn–C lengths lie between 2.125(2) and 2.1631(19) Å. The difference is greatest in P(1)–C(1)–Sn(1) angle of 109.73(13) for **1**, 113.42(12) for **2** and 114.79(10) for **3**. The difference could be related to the bigger steric hindrance of the trimethylsilylmethyl substituent in **2** and the *cyclo*-hexyl groups in **3** with respect to that for the phenyl groups in **1**. All other bond lengths and angles do not show any particularities.

1.1.2.2 Syntheses and structures of the $Ph_2P(O)CH_2$-substituted organotin halides $Ph_2P(O)CH_2SnRR'X$ (5, R = R' = Ph, X = I; 6, R = R' = Ph, X = Br; 8, R = Ph, R' = Me_3SiCH_2, X = I; 9, R = Ph, R' = Me_3SiCH_2, X = Br), $Ph_2P(O)CH_2Sn(R)X_2$ (7, R = Ph, X = Br; 11, R = Ph, X = Cl; 10, R = Me_3SiCH_2, X = Br; 12, R = Me_3SiCH_2, X = Cl), and $Ph_2P(O)CH_2SnCl_3$, 13

Halogenation and proto-destannylation of **1** and **2** afforded the corresponding organotin (IV) halides **5**–**12**, and reaction of **3** with tin tetrachloride gave the organotin trichloride $[Ph_2P(O)CH_2]SnCl_3$, **13**, in almost quantitative yields (Scheme 4).

Substitution of the tin atom with Me_3SiCH_2 group instead of the phenyl group increases the solubility in organic solvents, as the phenyl-substituted compounds **5–7** and **11** are poorly soluble in common organic solvents like hexane, dichloromethane and chloroform, while the Me_3SiCH_2-substituted compounds **8**–**10** are well soluble in THF, chloroform and dichloromethane. Compound **12** is moderate soluble in dichloromethane and chloroform.

The organotin trichloride $Ph_2P(O)CH_2SnCl_3$, **13**, is poorly soluble in the organic solvents, however, it is slightly soluble in a mixture of acetone/CH_2Cl_2. The poor solubility of this type of compounds could be related to the polymeric structure as a result of P=O→Sn interaction. This interaction increases by increasing the Lewis acidity of the tin atom.

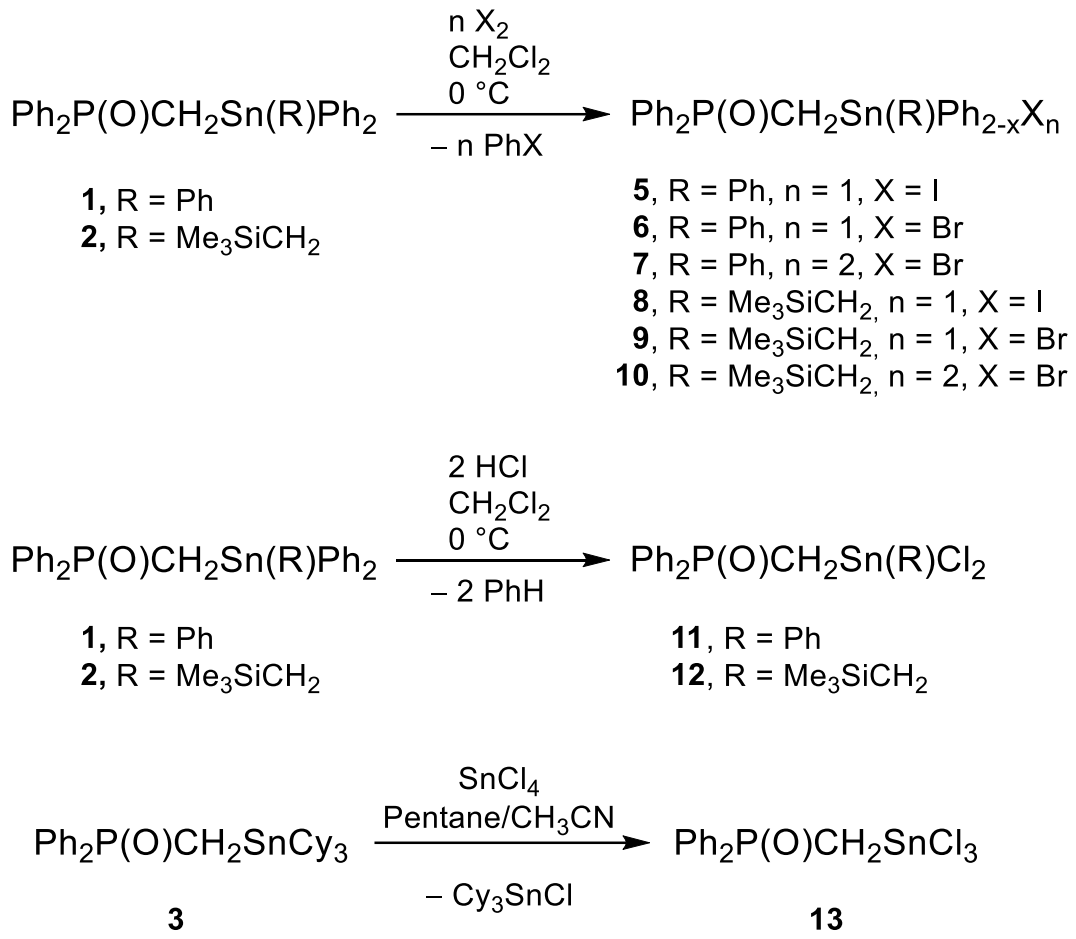

Scheme 4. Syntheses of the organotin halides **5**–**13** containing the $Ph_2P(O)CH_2$ substituent.

The very low solubility of compounds **7**, **11** and **13** prohibits recording NMR spectra. Compounds **5**, **8**–**10** and **12** show broad signals in ^{119}Sn NMR spectra according to the labile P=O→Sn interaction. Recording the ^{119}Sn NMR spectra at low temperatures to reduce the lability of the interaction was excluded because of the low or moderate solubilities of the compounds which should decrease at low temperatures.

The ^{31}P NMR spectra of compounds **5**, **7**–**10** and **12** show single resonances with $^{117/119}$Sn satellites at δ 37.8 [$^2J(^{31}P–^{117/119}Sn)$ = 75 Hz] for **5**; 40.8 [$^2J(^{31}P–^{117/119}Sn)$ = 76 Hz] for **6**; 36.0 [$^2J(^{31}P–^{117/119}Sn)$ = 60 Hz] for **8**; 37.5 [$^2J(^{31}P–^{117/119}Sn)$ = 64 Hz] for **9**; 39.6 [$^2J(^{31}P–^{117/119}Sn)$ = 88 Hz] for **10** and 39.6 [$^2J(^{31}P–^{117/119}Sn)$ = 96 Hz] for **12**. The pattern of the resonances in ^{31}P NMR spectra of compounds **5**, **8**–**10**, and **12**

show that each phosphorus atom couples with one tin atom, and corresponding, the compounds present as monomers in solution. The resonance for compound **6** is too broad so no prediction for the structure of the compound in solution could be done. For the methylene groups $SnCH_2P$ in compounds **5**, **6**, **8**–**10** and **12** doublet resonances between δ 2.76 and δ 3.02 with $^{117/119}Sn$ coupling satellites were observed in ^{1}H NMR spectra (for more details please see table 3). The ^{13}C NMR spectra of compounds **5**, **6** and **8**–**10** show also doublet resonances for the methylene groups. The NMR data of compounds **5**, **6**, **8**–**10** and **12** are listed in Table 3.

Table 3. Selected NMR data of compounds **5**, **6**, **8**–**10** and **12**.

	$\delta^{119}Sn$	$\delta^{31}P$	$^{2}J(^{31}P–^{117/119}Sn)$	$SnCH_2P$				
				^{1}H			^{13}C	
				δ	$^{2}J(^{1}H–^{31}P)$	$^{2}J(^{1}H–^{117/119}Sn)$	δ	$^{1}J(^{13}C–^{31}P)$
5	–148	37.8	75	3.02	9.2	73.2/76.1	27.1	63
6	–	40.8	76	2.88	10.6	79.8	25.6	64
8	–74	36.0	60	2.80	8.8	69.2	25.4	63
9	–41	37.5	64	2.76	9.3	72.6	25.7	64
10	–206	39.6	88	3.00	11.0	87.1	32.1	64
12	–151	39.6	96	2.79	11.7	91.2	–	–

Chemical shifts are given in ppm, and coupling constants in Hz.

Reactions of $[Ph_2P(O)CH_2]_2SnPh_2$, **4**, with one or two molar equivalents of elemental iodine in order to get the corresponding organotin iodides $[Ph_2P(O)CH_2]_2SnPhI$ and $[Ph_2P(O)CH_2]_2SnI_2$ were not successful. Black insoluble precipitates were observed and their elemental analyses do not fit with those calculated for the expected compounds.

Compound **4** was reacted with one molar equivalent elemental bromine. The ^{119}Sn NMR spectrum of a solution of the crude product in $CDCl_3$ showed, in addition to a signal at δ –93 for the starting material, one very broad signal at –180 (integral 96, $v_{1/2} \approx 1400$ Hz). The ^{31}P NMR spectrum of the same solution showed broad signal at δ 38.0 ($v_{1/2}$ = 98 Hz) that is comparable with that found for the triorganotin bromide **9** (δ 37.5). In addition, a resonance of the starting material at δ 33.6 (integral 4), as well as a signal for $Ph_2P(O)Me$ at δ 30.1 (integral 22) were observed. The ^{1}H NMR

spectrum showed a broad signal at δ 2.40 and six small resonances between δ 1.80 and δ 2.02, in addition to resonances between 7.06 and 7.83 ppm for the aromatic protons. The latter statement hints at formation of the proposed compound $[Ph_2P(O)CH_2]_2SnPhBr$ (Signals at δ –180 in ^{119}Sn NMR spectrum, δ 37.8 in ^{31}P NMR spectrum, and δ –2.40 in ^{1}H NMR spectrum). However, it hints also to the lability and instability of the Sn–CH_2 bond as the compound decomposes giving $Ph_2P(O)Me$.

The course of the reaction between compound **4** and two molar equivalents of elemental bromine was monitored by NMR spectroscopy. The ^{31}P NMR spectrum of a solution of the crude product in $CDCl_3$ showed six signals at δ 28.3 (integral 12), 30.3 (integral 33, $Ph_2P(O)Me$), 31.6 (integral 8), 43.8 (integral 30, $J(^{31}P–^{117/119}Sn)$ = 123 Hz, $J(^{31}P–^{117/119}Sn)$ = 280 Hz), 47.5 (integral 3), 47.6 (integral 14, $J(^{31}P–^{117/119}Sn)$ = 187 Hz, $J(^{31}P–^{117/119}Sn)$ = 223 Hz). The ^{1}H and ^{119}Sn NMR spectra of a same solution were rather complex. Due to the low yield of compound **4**, no further investigations of the bromination and iodination reactions were carried out.

Recrystallization of the triorganotin halides **5** and **6** from hot solutions in dichloromethane/hexane provided colorless single crystals suitable for X-ray diffraction analyses. Compound **6** shows pseudo-polymorphism with different bond lengths and angles, one molecular structure is asymmetric (**6**) and is similar to that of **5** and the other is symmetric (**6'**). The molecular structures of **5** and **6** are shown in Figure 5, and that of **6'** is shown in Figure 6. Selected bond lengths and bond angles of **5**, **6** and **6'** are summarized in Table 4.

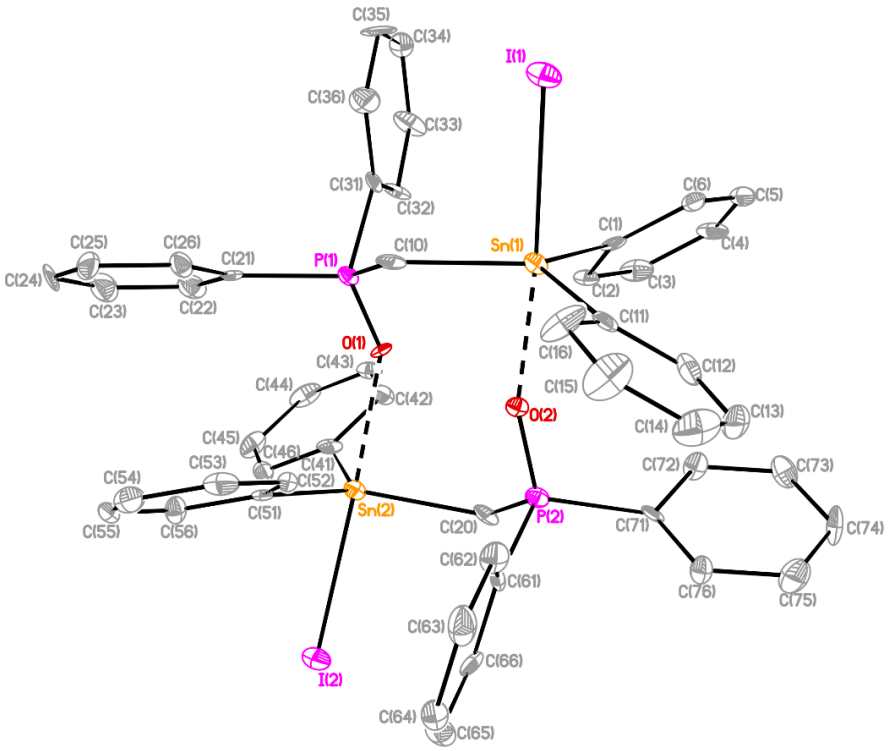

Figure 5. General view (SHELXTL) of a molecule of **5** [compound **6** (X = Br) is isostructural] showing 30% probability displacement ellipsoids and the crystallographic numbering scheme. Hydrogen atoms are omitted for clarity.

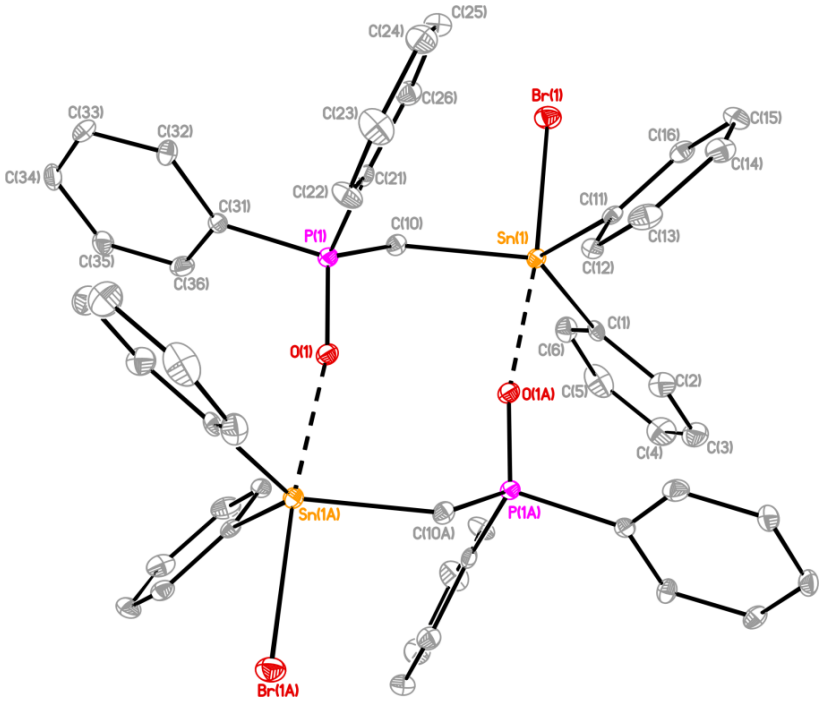

Figure 6. General view (SHELXTL) of a molecule of **6'** showing 30% probability displacement ellipsoids and the crystallographic numbering scheme. Hydrogen atoms are omitted for clarity.

Table 4. Selected bond lengths (Å) and bond angles (deg) in **5**, **6** and **6'**.

	5 (X = I)	**6** (X = Br)	**6'** (X = Br)
Sn–X	2.8850(7) / 2.9084(7)	2.6757(4) / 2.6564(4)	2.6481(5)
Sn–O	2.257(4) / 2.297(4)	2.297(2) / 2.269(2)	2.259(2)
Sn–C_{Ph}	2.136(3) / 2.131(3) / 2.133(3) / 2.133(3)	2.131(3) / 2.134(4) / 2.132(3) / 2.137(3)	2.130(3) / 2.131(3)
Sn(1)–C_{CH2}	2.153(6) / 2.138(6)	2.154(3) / 2.150(3)	2.153(3)
P–O	1.470(4) / 1.483(4)	1.487(2) / 1.503(2)	1.499(2)
X–Sn–O	173.70(11) / 176.04(10)	175.98(5) / 173.89(5)	170.12(6)
X–Sn–C_{CH2}	92.37(17) / 94.20(16)	93.28(8) / 93.98(8)	89.44(9)
X–Sn–C_{Ph}	96.39(11) / 91.48(11) / 94.52(11) / 91.71(10)	92.16(8) / 93.08(9) / 93.62(8) / 96.13(9)	92.22(9) / 98.69(9)
O–Sn–C_{CH2}	83.0(2) / 88.29(19)	88.04(10) / 84.64(10)	84.38(11)
O–Sn–C_{Ph}	89.70(15) / 84.71(15) / 84.15(14) /89.58(15)	83.84(10) / 82.14(11) / 88.88(10) / 89.66(10)	84.26(11) / 91.06(11)
C_{CH2}–Sn–C_{Ph}	121.7(2) /112.91(19) / 119.98(19) /121.9(2)	113.96(12) / 114.83(14) / 122.13(13) / 120.98(13)	120.05(13) / 119.05(12)
C_{Ph}–Sn–C_{Ph}	116.55(18) / 124.69(17)	123.08(13) / 122.40(15)	119.82(13)
O–P–C_{CH2}	114.7(3) / 110.3(3)	111.09(14) / 114.07(14)	112.00(15)
Sn–C–P	117.6(3) / 119.2(3)	116.71(15) / 118.37(15)	121.00(17)
P–O–Sn	141.3(2) / 161.1(3)	156.22(14) / 142.87(12)	167.17(15)

X-ray diffraction analyses show that the triorganotin halides **5** and **6**, respectively **6'**, are dimers in the solid state as a result of two intermolecular P=O→Sn interactions resulting in formation of eight-membered rings like that described for the analogous compound $[Ph_2P(O)CH_2SnPh_2Cl]_2$ (**A**).[18] The tin atoms in these compounds are penta-coordinated with three carbon atoms [C(1), C(10) and C(11) for Sn(1); C(20), C(41) and C(51) for Sn(2)] in the equatorial position and one oxygen [O(1a)/O(2) for Sn(1); O(1) for Sn(2)] and the halogen atom in the axial positions. Each tin atom exhibits a distorted trigonal bipyramidal environment. The molecular structures of **5** and **6** are similar and both are asymmetric, whereas **6'** is symmetric.

The O–Sn–X angle of 173.70(11)°, 176.04(10)° for **5**, 175.98(5)°, 173.89(5)° for **6** and 170.12(6)° for **6'** are close to that found in (**A**) of 170.7(1)° being close to the

ideal value of 180°. The angle between the carbon atoms in the equatorial position in **6'** are also close to the ideal value (120°) ranging between 119.05(12)° and 120.05(13)° while those for **5** and **6** are much distorted ranging between 112.91(19)° and 124.69(17)°. The equatorial substituents are displaced toward the axial oxygen. The angles (Hal–Sn–L_{eq}) and (O–Sn–L_{eq}) are almost slightly bigger respectively slightly smaller than 90°. The Sn–O–P angles are remarkably large in **6'** of 167.17(15)° being close to that for (**A**) of 167.5(2)°, but the asymmetric polymorph (**6**) and its iodo-analogous (**5**) show two largely different values of 142.87(12)° and 156.22(14) for **6** and 141.3(2)° and 161.1(3)° for **5**. The O–Sn distances range between 2.257(4) and 2.297(4) Å being a little longer than that found in (**A**) of 2.170(5). The Sn–I distances are 2.8850(7) and 2.9084(7) Å in **5** and the Sn–Br distances are 2.6757(4) and 2.6564(4) Å in compound **6** and 2.6481(5) Å in **6'**.

An electrospray mass spectrum (ESI MS, positive mode) of $[Ph_2P(O)CH_2]Ph_2SnI$, **5**, showed a major mass cluster centered at *m/z* 1479.6 that fits with the hydrolysis product $[(\{Ph_2P(O)CH_2\}Ph_2Sn)_3\mu_3\text{-}O]^+$ (**B**) (Chart 2). The formation of the latter organotinoxo cluster **B** under the experimental conditions employed indicated the lability of Sn–I bond.

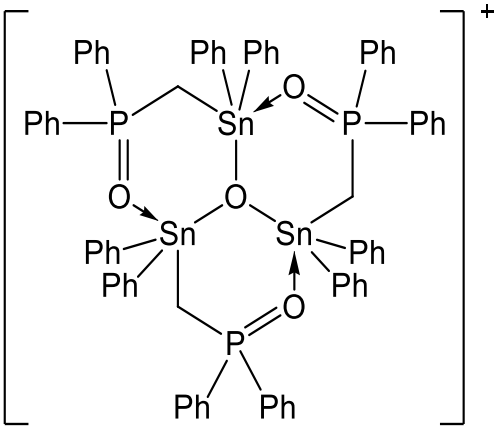

B m/z 1479.6

Chart 2. Drawing of the hydrolysis product of compound **5**.

An ESI MS spectrum of the triorganotin bromide $[Ph_2P(O)CH_2]Ph_2SnBr$, **6**, in acetonitrile shows a major mass cluster centered at *m/z* 258.1 that is assigned to $[Ph_2P(O)Me + H + MeCN]^+$ indicating the lability of $Ph_2P(O)CH_2$–Sn bond. This fits with the lability of the analog one $Ph_2P(S)CH_2$–Sn which was studied by *Fackler* et al.[18] Other mass clusters were observed at *m/z* 489.1 $[Ph_2P(O)CH_2SnPh_2]^+$, 530.1

$[Ph_2P(O)CH_2SnPh_2 + MeCN]^+$ and 705.2 $[Ph_2P(O)CH_2SnPh_2 + Ph_2P(O)Me]^+$ indicating the presence of the monomeric structure in solution. A mass cluster with low relative abundance at *m/z* 1055.2 for $[2M – Br]^+$ was also observed indicating the presence of the dimeric structure in solution.

The ESI MS spectra of the triorganotin halides $Ph_2P(O)CH_2SnPh(CH_2SiMe_3)X$ (**8**, X = I; **9**, X = Br) show mass clusters based on the monomeric structure ($[M – X]^+$ and $[M + H/Na])^+$, as well mass cluster that relate to the dimeric structure ($[2M – X]^+$ and $[2M + H/Na]^+$). Those which relate to the dimeric structure are also of low relative abundance (2–5 %).

ESI MS spectra of the diorganotin dihalides $[Ph_2P(O)CH_2]RSnX_2$, **7**, **10**, **11** and **12** in acetonitrile showed major mass cluster centered at *m/z* 1281.2 for **7** and **11**, and at *m/z* 1311.3 for **10** and **12** that fits perfectly with the protonated hydrolysis product $[\{Ph_2P(O)CH_2\}RSnO]_3$ (R = Ph, Me_3SiCH_2) **C** and **D** respectively (Chart 3). Another mass cluster centered at *m/z* 1065.1 for **7** and at 1095.2 for **10** and **12** that corresponds to [**C** – $Ph_2P(O)CH_2]^+$ and [**D** – $Ph_2P(O)CH_2]^+$, respectively, were also observed.

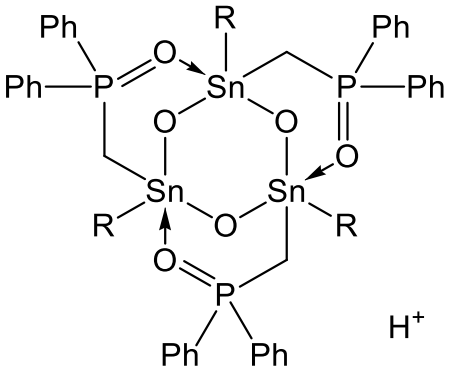

C, R = Ph, m/z 1281.2
D, R = CH_2SiMe_3, m/z 1311.3

Chart 3. Drawing of the hydrolysis products of compounds **5, 10**–**12**.

Recrystallization of $[Ph_2P(O)CH_2](Me_3SiCH_2)SnCl_2$, **12**, from CH_2Cl_2 afforded colorless single crystals. The molecular structure of **12** is shown in Figure 7 and selected bond lengths and bond angles are summarized in Table 5.

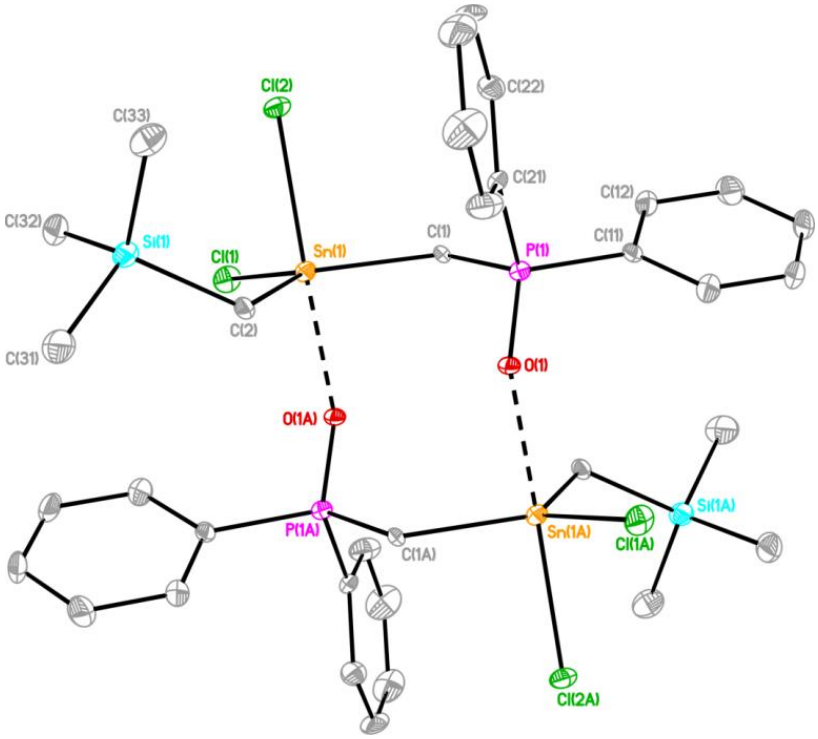

Figure 7. General view (SHELXTL) of a molecule of **12** showing 30% probability displacement ellipsoids and the crystallographic numbering scheme. Hydrogen atoms are omitted for clarity.

Table 5. Selected bond lengths (Å) and bond angles (deg) in the diorganotin dichloride $[Ph_2P(O)CH_2](Me_3SiCH_2)SnCl_2$,**12**.

Sn(1)–O(1a)	2.272(2)	Sn(1)–C(1)	2.124(3)
Sn(1)–Cl(1)	2.3418(10)	Sn(1)–C(2)	2.114(3)
Sn(1)–Cl(2)	2.4634(9)	P(1)–O(1)	1.498(2)
O(1a)–Sn(1)–Cl(2)	173.26(6)	Cl(1)–Sn(1)–C(2)	121.60(10)
O(1a)–Sn(1)–Cl(1)	84.17(6)	C(1)–Sn(1)–C(2)	127.22(13)
O(1a)–Sn(1)–C(1)	84.01(11)	Sn(1)–C(1)–P(1)	113.26(16)
O(1a)–Sn(1)–C(2)	90.17(11)	Sn(1)–C(2)–Si(1)	120.83(17)
Cl(2)–Sn(1)–Cl(1)	91.20(3)	Sn(1)–O(1a)–P(1a)	140.64(13)
Cl(2)–Sn(1)–C(1)	93.01(9)	O(1)–P(1)–C(1)	111.69(15)
Cl(2)–Sn(1)–C(2)	96.43(9)	O(1)–P(1)–C(11)	111.69(16)
Cl(1)–Sn(1)–C(1)	109.92(9)	O(1)–P(1)–C(21)	109.32(16)

X-ray diffraction analysis shows that compound **12** is a symmetric dimer in the solid state as a result of two intramolecular P=O→Sn interaction resulting in formation of an eight-membered ring like those described for the analogous compounds

$[Ph_2P(O)CH_2SnPh_2Cl]_2$ (**A**)[18] and $[Ph_2P(O)CH_2SnPh_2Br]_2$ **6'**. Each tin atom in **12** is penta-coordinated with the C(1), C(2) and Cl(1) atoms in the equatorial positions and the O(1a) and Cl(2) atoms in the axial positions, and exhibits a distorted trigonal bipyramidal environment.

The axial O–Sn–Cl angle of 173.26(6)° is a little bigger than those found in **A** and **6'** of 170.7(1)° and 170.12(6)°, respectively, and closer to the ideal value (180°). The Cl(1)–Sn(1)–C(2) angle [121.60(10)°] is remarkably bigger than Cl(1)–Sn(1)–C(1) [109.92(9)], and the angle between the equatorial carbon atoms C(1)–Sn(1)–C(2) [127.22(13)°] is bigger than those in **A** and **6'**. The equatorial ligands are displaced toward the axial oxygen, making the O–Sn–L_{eq} smaller than the corresponding Cl(2)–Sn–L_{eq} angles. The Sn–O–P angle [140.64(13)°] is remarkably small with respect to those in **A** [167.5(2)°] and **6'** [167.17(15)°]. The O–Sn distance of 2.272(2) Å agree with those found in **5**, **6** and **6'** [2.257(4) to 2.297(4) Å] and a little longer than that found in **A** (2.170(5) Å). Finally, the Sn(1)–Cl(2) distance of 2.3418(10) Å is shorter than the corresponding distance in **A** of 2.512(1) Å, and shorter than the distance to the equatorial chlorine atom [Sn(1)–Cl(1) 2.4634(9) Å].

1.1.2.3 Hydrolysis of $[Ph_2P(O)CH_2](Me_3SiCH_2)SnBr_2$, 10, in aerobic conditions affording the monoorganotinoxo cluster $(Me_3SiCH_2Sn)_{12}O_{14}(OH)_6Br_2$, 10a

Attempts to recrystallize **10** from CH_2Cl_2/ethyl acetate at aerobic conditions afforded after a few weeks the hydrolysis product, the Sn_{12} monoorganotinoxo cluster $(Me_3SiCH_2Sn)_{12}O_{14}(OH)_6Br_2$, **10a**, as colorless crystals. This is a result of Sn–C cleavage and complete hydrolysis of compound **10** (Scheme 5). The ^{31}P NMR spectrum of the residue showed a singlet at δ 30.9 for $Ph_2P(O)Me$ confirming the cleavage of Sn–CH_2P bond.

$$12\ [Ph_2P(O)CH_2](Me_3SiCH_2)SnBr_2 \xrightarrow[-\ Ph_2P(O)Me\ -\ HBr]{H_2O} (Me_3SiCH_2Sn)_{12}O_{14}(OH)_6Br_2$$

10 **10a**

Scheme 5. Hydrolysis of compound **10** in moist air.

The hydrolysis of Sn–Br bonds in **10** result in the formation of Sn–OH bonds and HBr. It is supposed that the latter is responsible for the Sn–C bond cleavage. Subsequent condensation of the resulting monoorganotin compound results in the formation of the monoorganotinoxo cluster **10a**. The Sn–C_{Ph} bond cleavage was reported before by *Chandrasekhar* et al. as the reaction of the diorganotin dichloride Ph_2SnCl_2 with cycPO_2H (1,1,2,3,3-pentamethyltrimethylenephosphinic acid) gave the monoorganotinoxo cluster $[(PhSn)_3(\mu_3\text{-}O)(\mu\text{-}cyc PO_2)_3(\mu\text{-}OH)_3][cycPO_2]$.

Compound **10a** has a melting point above 350° and its ESI MS spectrum in the positive mode shows a major mass cluster centered at *m/z* 1398.9 that fits exactly with the $[(Me_3SiCH_2Sn)_{12}O_{14}(OH)_6]^{2+}$ macrocation. A mass cluster at *m/z* 1371.1 that correspond to $[(Me_3SiCH_2Sn)_{12}O_{17}]^{2+}$ with about 34% relative abundance was also detected.

The molecular structure of **10a** is shown in Figure 8 and selected bond lengths and bond angles of Sn(1) and Sn(2) are summarized in Table 6; those of Sn(3)–Sn(6) could be found in the cif-file and the corresponding table in the supporting CD.

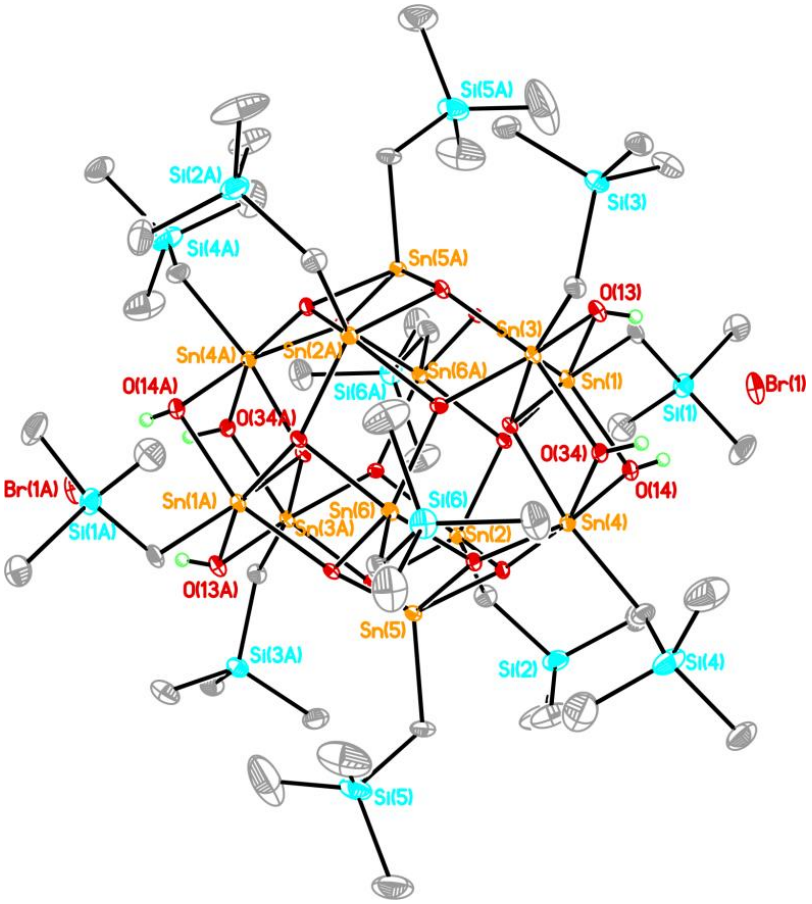

Figure 8. General view (SHELXTL) of a molecule of **10a** showing 30% probability displacement ellipsoids and the crystallographic numbering scheme. Hydrogen atoms that are bound to carbon atoms are omitted for clarity.

Table 6. Selected bond lengths (Å) and bond angles (deg) which relate to Sn(1) and Sn(2) in **10a**.

Sn(1)–O(134)	2.097(3)	Sn(2)–O(245)	2.016(3)
Sn(1)–O(126)	2.102(3)	Sn(2)–O(126)	2.026(2)
Sn(1)–O(156a)	2.116(3)	Sn(2)–O(236a)	2.083(3)
Sn(1)–O(14)	2.120(3)	Sn(2)–O(235)	2.098(2)
Sn(1)–O(13)	2.126(3)	Sn(2)–C(21)	2.101(4)
Sn(1)–C(11)	2.125(4)	O(134)–Sn(1)–O(126)	87.45(10)
O(134)–Sn(1)–O(156a)	86.70(10)	O(156a)–Sn(1)–C(11)	99.46(14)
O(126)–Sn(1)–O(156a)	76.43(10)	O(14)–Sn(1)–C(11)	98.74(15)
O(134)–Sn(1)–O(14)	76.46(11)	O(134)–Sn(1)–O(13)	76.50(11)
O(126)–Sn(1)–O(14)	91.09(12)	O(126)–Sn(1)–O(13)	159.38(11)
O(156a)–Sn(1)–O(14)	159.54(11)	O(156a)–Sn(1)–O(13)	89.64(12)
O(134)–Sn(1)–C(11)	170.75(15)	O(14)–Sn(1)–O(13)	97.50(13)
O(126)–Sn(1)–C(11)	100.64(14)	C(11)–Sn(1)–O(13)	96.54(14)
O(245)–Sn(2)–O(126)	96.48(11)	O(236a)–Sn(2)–O(235)	77.50(10)
O(245)–Sn(2)–O(236a)	135.28(10)	O(245)–Sn(2)–C(21)	113.11(15)
O(126)–Sn(2)–O(236a)	77.67(10)	O(126)–Sn(2)–C(21)	112.26(15)
O(245)–Sn(2)–O(235)	77.43(10)	O(236a)–Sn(2)–C(21)	109.96(15)
O(126)–Sn(2)–O(235)	136.52(10)	O(235)–Sn(2)–C(21)	109.56(14)
Sn(3)–O(13)–Sn(1)	102.20(13)	Sn(6a)–O(126)–Sn(1)	103.12(11)
Sn(1)–O(14)–Sn(4)	102.33(13)	Sn(3)–O(134)–Sn(1)	104.12(10)
Sn(2)–O(126)–Sn(6a)	102.30(11)	Sn(4)–O(134)–Sn(1)	104.43(11)
Sn(2)–O(126)–Sn(1)	134.97(15)	Sn(2)–O(245)–Sn(4)	135.94(13)

The structure of compound **10a** is isostructural with that of $(Me_3SiCH_2Sn)_{12}O_{14}(OH)_6Cl_2$[3e] and resembles those of $(BuSn)_{12}O_{14}(OH)_6X_2$ (X = Cl,[3a] OH,[3b] 4-$CH_3C_6H_4$–SO_3[3c]) and (*i*-PrSn)$_{12}O_{14}(OH)_6Cl_2$[3d] basing on the centrosymmetric $[(Me_3SiCH_2Sn)_{12}O_{14}(OH)_6]^{2+}$ macrocation. This cation is composed of six five-coordinate tin atoms with distorted square pyramidal environment (Sn(2/2a), Sn(5/5a), Sn(6/6a)) and six six-coordinated octahedrally configurated tin atoms (Sn(1/1a), Sn(3/3a), Sn(4/4a)), which are connected via μ_3-O (O126, O134, O156, O235, O236, O245, O456, and their symmetric counterparts) and μ_2-OH bridges

(O13, O14, O34, and their symmetric counterparts). The μ_2-OH groups bridge the six-coordinate tin atoms pairwise and define the cage poles (Figure 9). The Sn–O distances are between 2.013(2) and 2.128(3) Å. The charge of the cationic core is balanced by two bromide anions which are held to the cation by O–H···Br hydrogen bridges of 3.229(3)–3.288(3) Å.

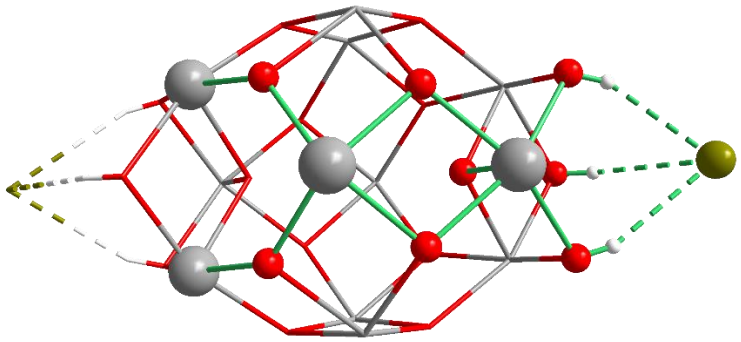

Figure 9. Reduced molecular structure of **10a**. The organic groups are omitted for clarity.

The structure can be seen as being composed of two O-capped clusters each consists of three six-coordinated tin atoms. The O-capped clusters are bound through six five-coordinate tin atoms that are connected to the O-capped clusters via μ_3-O bridges.

An electrospray mass spectrum (ESI MS, positive mode) of the organotin trichloride $[Ph_2P(O)CH_2]SnCl_3$, **13**, shows a mass cluster at *m/z* 1118.9 that fits with the protonated hydrate of the trimeric organostannonic acid $[\{(Ph_2P(O)CH_2Sn(O)OH\}_3 + H_3O]^+$, **E** (Chart 4, on left), the hydrolysis product of **13**. The latter has a similar structural core like those observed in the bulky stannonic acids $[(Me_3Si)_3CSn(O)OH]_3$[7a] and $[2,6–Mes_2C_6H_3Sn(O)OH]_3$[7b] (Chart 4) indicating that the intramolecularly coordinating substituents play a similar role like the bulky groups in defining the structural type of the organotinoxo cluster.

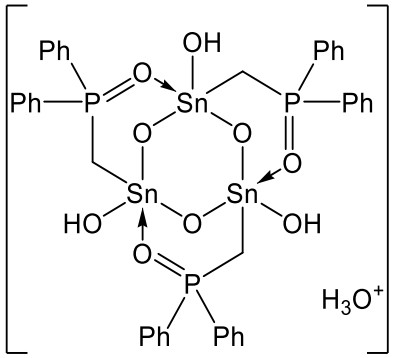

E m/z 1118.9

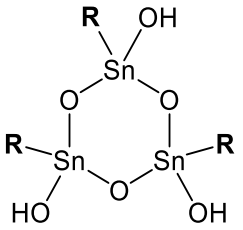

R = $(Me_3Si)_3C$[7a], 2,6-$Mes_2C_6H_3$[7b]

Chart 4. Drawing of the hydrolysis product of compound **13** (on left), and the bulky stannonic acids reported in the literature (on right).

1.1.2.4 Hydrolysis of the organotin trichloride $Ph_2P(O)CH_2SnCl_3$, 13, in aerobic conditions affording the monoorganotinhydroxo cluster $[Ph_2P(O)CH_2SnCl_2(\mu\text{-}OH)]_2$, 13a

Compound **13** is sensitive toward air moisture, and under recrystallization from acetone at aerobic conditions it reacts with water to give some colorless single crystals of the acetone solvate of the hydrolysis product $[\{Ph_2P(O)CH_2SnCl_2(\mu\text{-}OH)\}_2\cdot 2C_3H_6O]$, **13a** (eq. 1).

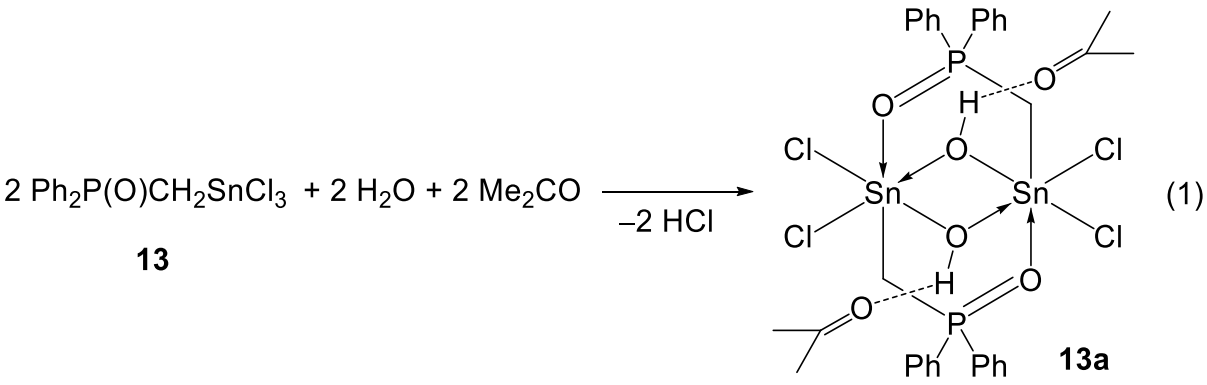

(1)

Compound **13a** can be interpreted as being the first intermediate along the hydrolysis pathway of compound **13**. It has a structure that resemble those reported on the Sn_2 aqua-hydroxide-chloride clusters $\{RSn(\mu_2\text{-}OH)Cl_2(H_2O)\}_2$[8a-e] by replacing the $H_2O\rightarrow Sn$ interaction by $P{=}O\rightarrow Sn$, and those having a functional group in the organic

substituents that afford N→Sn or O→Sn intramolecular interactions having the formula $\{RSn(\mu_2–OH)Cl_2\}_2$.[19]

The molecular structure of **13a** is shown in Figure 10 and selected bond lengths and bond angles are summarized in Table 7.

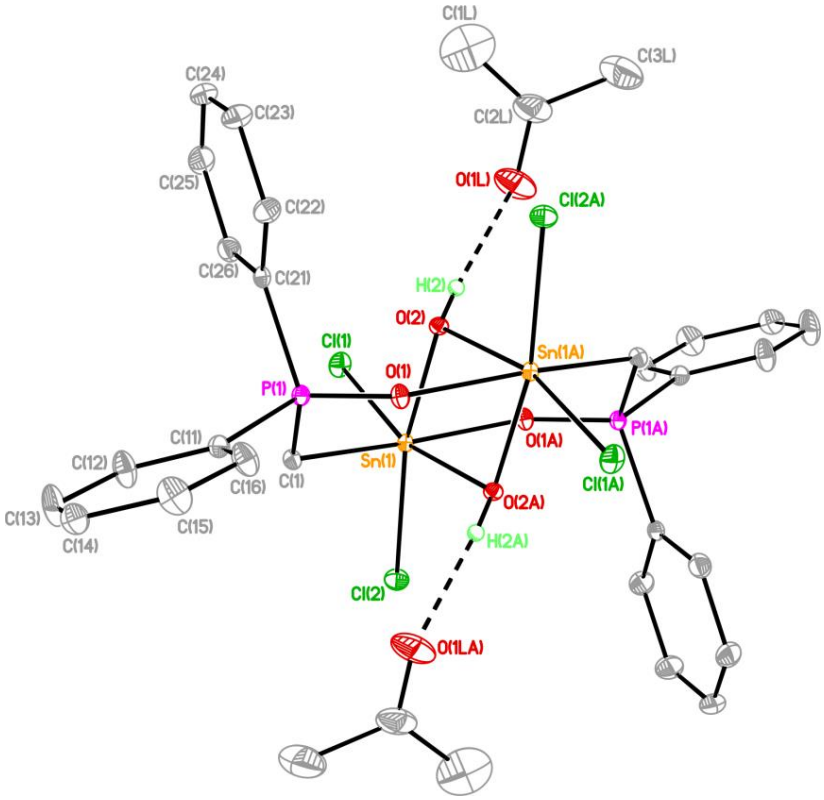

Figure 10. General view (SHELXTL) of a molecule of **13a** showing 30% probability displacement ellipsoids and the crystallographic numbering scheme. Hydrogen atoms that are bound to carbon atoms are omitted for clarity.

Table 7. Selected bond lengths (Å) and bond angles (deg) in **13a**.

Sn(1)–O(1a)	2.1060(14)	Sn(1)–C(1)	2.178(2)
Sn(1)–O(2)	2.0992(14)	P(1)–O(1)	1.5307(14)
Sn(1)–O(2a)	2.1047(14)	Sn(1)–Sn(1a)	3.2962(3)
Sn(1)–Cl(1)	2.3878(5)	H(2)–O(1L)	1.99(3)
Sn(1)–Cl(2)	2.3855(5)	O(2)–O(1L)	2.727(2)
Cl(2)–Sn(1)–O(2)	168.58(4)	Cl(1)–Sn(1)–C(1)	101.08(6)
Cl(1)–Sn(1)–O(2a)	165.44(4)	Cl(1)–Sn(1)–O(1a)	88.31(4)
C(1)–Sn(1)–O(1a)	166.24(6)	O(2a)–Sn(1)–C(1)	88.54(7)
Cl(2)–Sn(1)–C(1)	98.07(5)	O(2a)–Sn(1)–O(1a)	80.45(5)
Cl(2)–Sn(1)–Cl(1)	96.287(19)	O(1)–P(1)–C(1)	115.02(9)

Cl(2)–Sn(1)–O(2a)	93.11(4)	O(1)–P(1)–C(11)	105.61(9)
Cl(2)–Sn(1)–O(1a)	90.79(4)	O(1)–P(1)–C(21)	110.66(9)
O(2)–Sn(1)–C(1)	87.00(6)	Sn(1)–(O1a)–P(1a)	129.32(8)
O(2)–Sn(1)–Cl(1)	92.74(4)	Sn(1)–(C1a)–P(1a)	113.83(10)
O(2)–Sn(1)–O(2a)	76.73(6)	O(2)–H(2)–O(1L)	169(3)
O(2)–Sn(1)–O(1a)	82.49(6)	Sn(1)–O(2)–Sn(1a)	103.27(6)

X-ray diffraction analysis shows that compound **13a** is a centro-symmetric dimer in the solid state as a result of an intramolecular P=O→Sn interaction. The tin atoms in **13a** are six-coordinated with the O(1a), O(2), O(2a), Cl(1), Cl(2), and C(1) atoms forming a distorted octahedron (Figure 11).

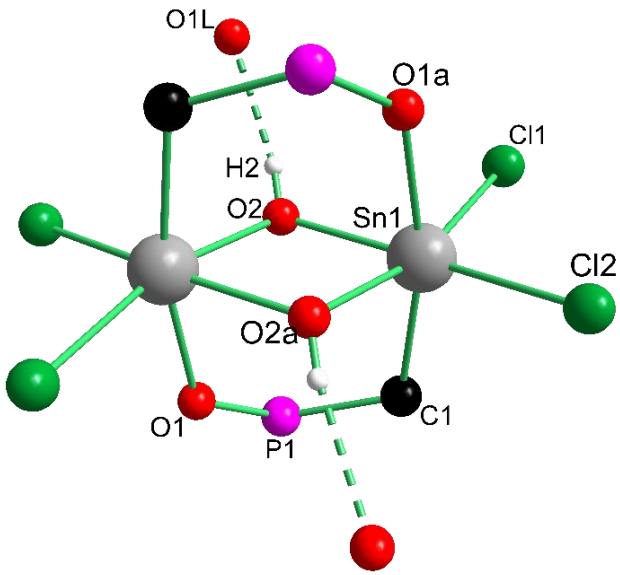

Figure 11. Reduced ball-and-sticks molecular structure of **13a**. The phenyl groups at the phosphorus atom, and the carbon atoms in the acetone molecules are omitted for clarity.

The chlorine atoms are in the opposite position to the hydroxide anion. The angles between the opposite atoms with respect to the tin atoms are close to 180° ranging between 165.44(4) and 168.58(4)°. If Cl(2) and O(2) are considered axial, then the equatorial substituents are displaced toward the axial oxygen, making the Cl(2)–Sn–L_{eq} and O(2)–Sn–L_{eq} angles respectively slightly wider and slightly narrower than 90°. The only exception is O(2)–Sn(1)–Cl(1) of 92.74(4)° but this is still smaller than Cl(2)–Sn(1)–Cl(1) of 96.287(19)°. No significant difference is observed between the Sn–O

bond lengths ranging from 2.0992(14) to 2.1060(14) Å. The P–O bond distance of 1.5307(14) Å resembles those in **14**·$CHCl_3$, **15**·$CHCl_3$ and **16**·$CHCl_3$ of 1.531(3), 1.520(5) and 1.519(2) Å, respectively. The acetone molecules are fixed through hydrogen bonds of O(2)···O(1L) 2.727(2) Å with the bridging hydroxyl groups, and the chlorine atoms make intermolecular hydrogen bonds with the phenyl groups and the acetone molecules [Cl(1)···C(3L) 3.691(4) Å; Cl(1)···C(12) 3.781(3) Å]. These afford the compound **13a** to be assembled into three-dimensional polymer in the solid state (Figure 12).

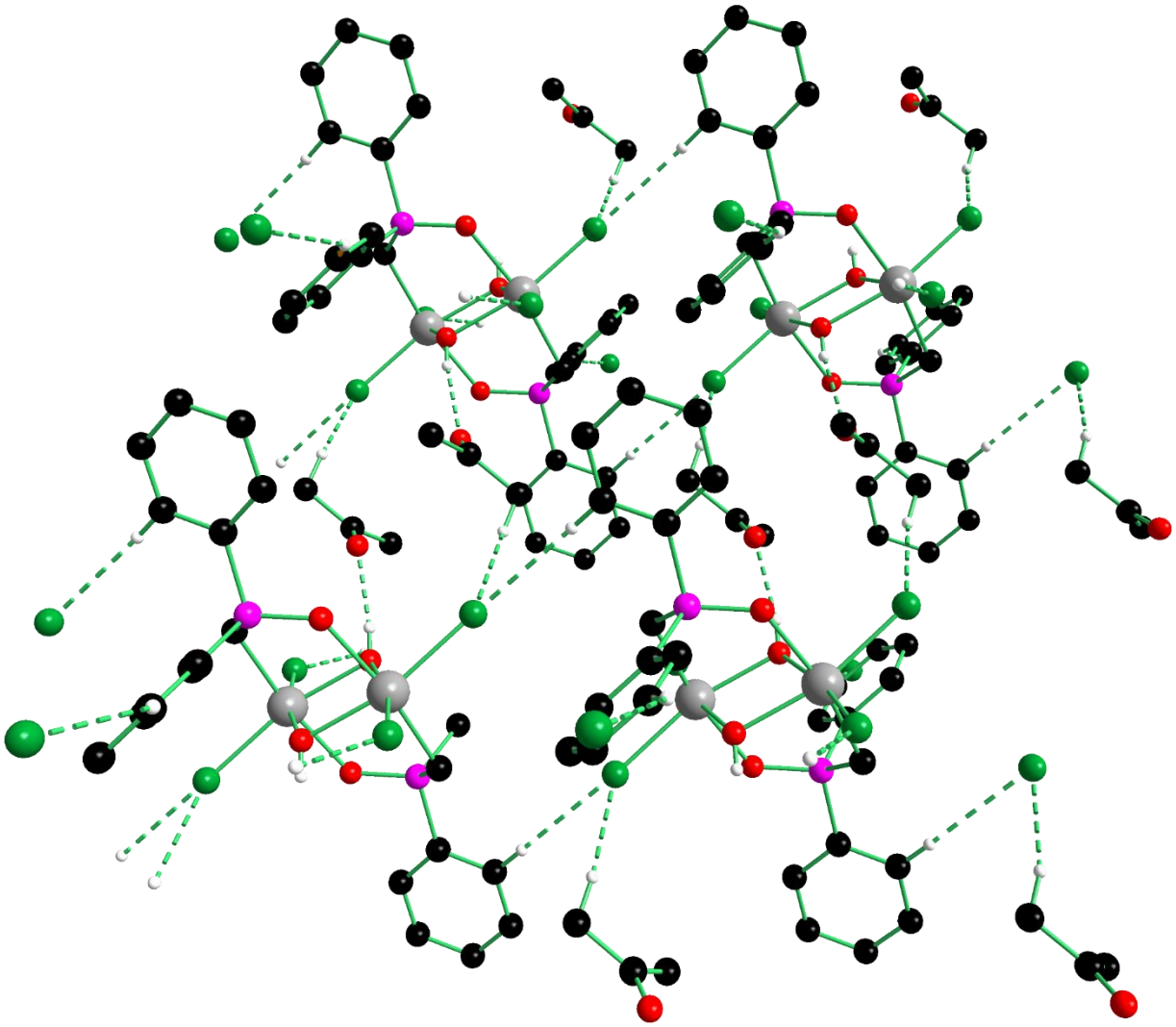

Figure 12. Three-dimensional structure of compound **13a**. Tin is presented as gray circles, chlorine as green circles, phosphorus as purple circles, oxygen as red circles, carbon as black circles and hydrogen as white circles. Hydrogen atoms that are not a part of hydrogen bridges are omitted for clarity.

1.1.2.5 Syntheses and structures of the O-capped clusters [{$Ph_2P(O)CH_2$}R(μ-OH)Sn]$_3$(μ_3-O)(μ_3-X) (14, R = Ph, X = Br; 15, R = Ph, X = I; 16, R = Ph, X = Cl; 17, R = CH_2SiMe_3, X = Br) and the ladder-like unsymmetrically substituted tetraorganodistannoxanes [*t*-Bu_2(X)SnOSn(OH)R{$CH_2P(O)Ph_2$}]$_2$ (18, R = Ph, X = Cl; 19, R = Me_3SiCH_2, X = Br; 20, R = Me_3SiCH_2, X = Cl)

Reaction of the diorganotin dibromide $[Ph_2P(O)CH_2](Ph)SnBr_2$, **7**, with one molar equivalent di-*tert*-butyltin oxide afforded in quantitative yield the trinuclear O-capped cluster, $[(Ph_2P(O)CH_2)Ph(\mu\text{-}OH)Sn]_3(\mu_3\text{-}O)(\mu_3\text{-}Br)$, **14**, containing a cationic stannoxane core and a counter bromide anion (Scheme 6). This type of structure has been reported in the literature for monoorganotinoxo clusters.[20]

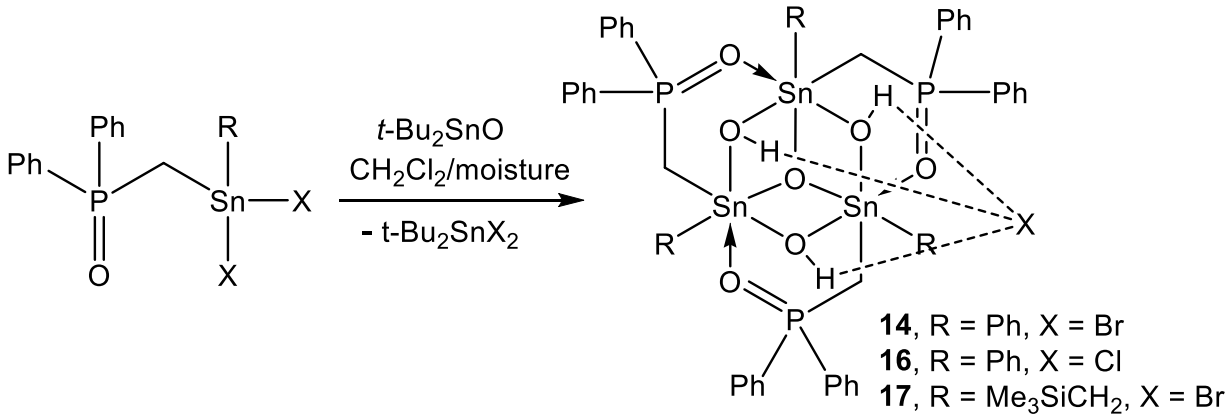

Scheme 6. Syntheses of the trinuclear O-capped clusters **14**, **16** and **17**.

The ^{31}P NMR spectrum of compound **14** in $CDCl_3$ (Figure 13) shows a single resonance at δ 52.2 with $^2J(^{31}P–^{117/119}Sn)$ coupling constants of 96/100 Hz and 109/115 Hz with the two environmentally different tin atoms. The ^{119}Sn NMR spectrum (Figure 13) displays a doublet of doublet at δ –442 with $^2J(^{119}Sn–^{117}Sn)$ coupling constant of 147 Hz. Finally the ^1H NMR spectrum reveals a doublet resonance at δ 1.92 [$^2J(^1H–^{31}P)$ = 11.0 Hz] for *CH*$_2$–Sn protons and a singlet at δ 5.98 for the O*H* protons. The identity of **14** was also confirmed using single crystal X-ray diffraction analysis (see below).

In the same manner, the diorganotin dichloride $[Ph_2P(O)CH_2](Ph)SnCl_2$, **11**, was stirred with one molar equivalent di-*tert*-butyltin oxide (Scheme 6). The crude ^{119}Sn

NMR spectrum showed a doublet of doublet resonance at δ –442 (integral 76) with $^{2}J(^{119}Sn–^{31}P)$ of 99 Hz and 113 Hz and $^{2}J(^{119}Sn–^{117}Sn)$ coupling constant of 144 Hz. The corresponding ^{31}P NMR spectrum shows a resonance at δ 52.2 [$^{2}J(^{31}P–^{117/119}Sn)$ = 95/99 Hz, $^{2}J(^{31}P–^{117/119}Sn)$ = 108/112 Hz]. The latter signals were attributed to the trinuclear O-capped cluster, $[(Ph_2P(O)CH_2)Ph(\mu\text{-}OH)Sn]_3(\mu_3\text{-}O)(\mu_3\text{-}Cl)$, **16**, having an analogous structure to that of compound **14** by replacing the bromide anion in **14** with chloride.

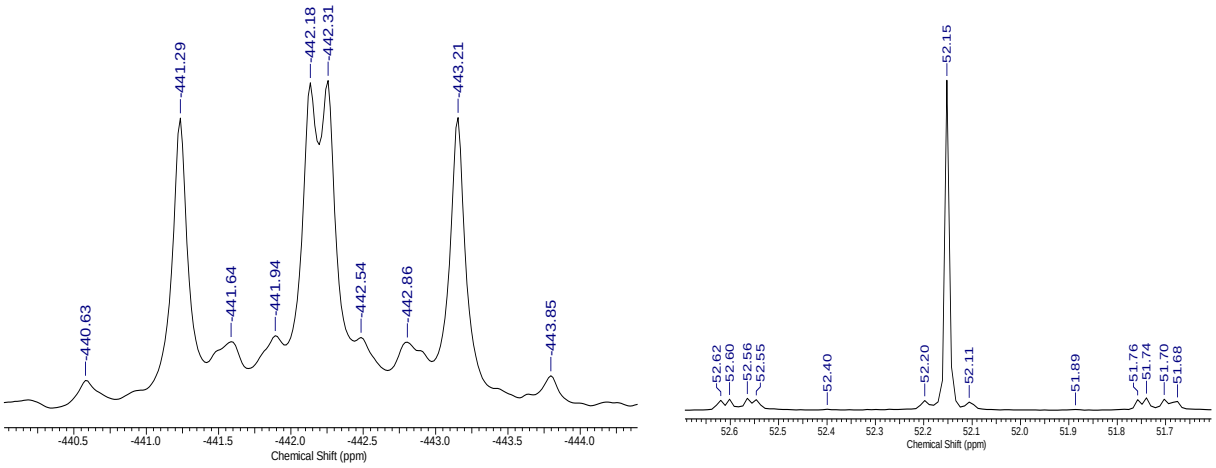

Figure 13. Expansion of the signals related to compound **14** in $^{119}Sn\{^{1}H\}$ NMR spectrum (111.85 MHz, 296 K) (on left), and in $^{31}P\{^{1}H\}$ NMR spectrum (121.50 MHz, 296 K) (on right) measured in $CDCl_3$.

In addition to these signals in ^{119}Sn NMR a singlet at δ –215 (integral 2), a singlet at δ –217 (integral 10), a doublet at δ –273 with $^{2}J(^{119}Sn–^{31}P)$ of 41 Hz (integral 10), and a doublet at δ –276 with $^{2}J(^{119}Sn–^{31}P)$ of 43 Hz (integral 2) were observed. The corresponding ^{31}P NMR spectrum shows a resonance at δ 35.4 with $^{2}J(^{31}P–^{117/119}Sn)$ coupling constant of 39 Hz. As the diorganotin dichloride **11** was stirred with two molar equivalents di-*tert*-butyltin oxide (Scheme 7), only the last four signals in ^{119}Sn NMR spectrum and the singlet at δ 35.4 in ^{31}P NMR spectrum were observed, and no signals for compound **16** were seen. The chemical shift of the signals in ^{119}Sn NMR spectrum are indicative of penta-coordinated tin atoms and those at δ –215 and δ –217 are in agreement with that found in Sn' in the ladder-like diorganotinoxo cluster $[t\text{-}Bu_2(Cl)(Sn')O(Sn)(CH_2SiMe_3)_2(OH)]_2$[17f] at δ –218 (Chart 5).

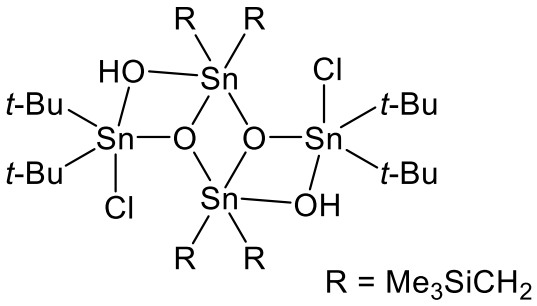

Chart 5. Drawing of [*t*-Bu_2(Cl)(Sn')O(Sn)$(CH_2SiMe_3)_2$(OH)]$_2$.[17f]

These signals were attributed to the ladder-like unsymmetrically substituted tetraorganodistannoxane [*t*-Bu_2(Cl)SnOSnPh{$CH_2P(O)Ph_2$}(OH)]$_2$, **18** (Scheme 7). Two isomeric forms of **18** (cis and trans, see Chart 6), each with two chemically and magnetically different tin atoms, result in four resonances observed in the ^{119}Sn NMR spectrum (δ –215, –217, –273, –276).

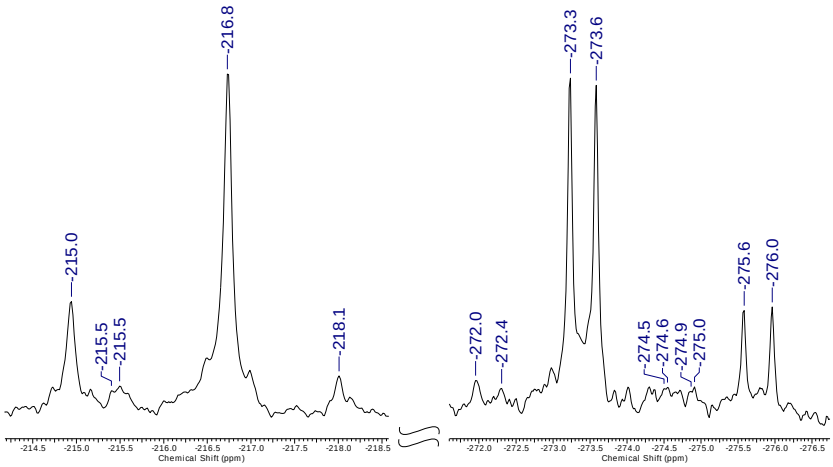

Figure 14. Expansion of the signals assigned to compound **18** in ^{119}Sn{^{1}H} NMR spectrum (111.88 MHz, 296 K) measured in $CDCl_3$.

The singlet at δ –217 and the doublet at δ –273 belong to one isomer with the $Ph_2P(O)CH_2$-substituents either cis or trans to each other, and the singlet at δ –215 and the doublet at δ –276 belong to the other isomer (Figure 14). The structure of **18** was confirmed by single crystal X-ray diffraction analysis (see below).

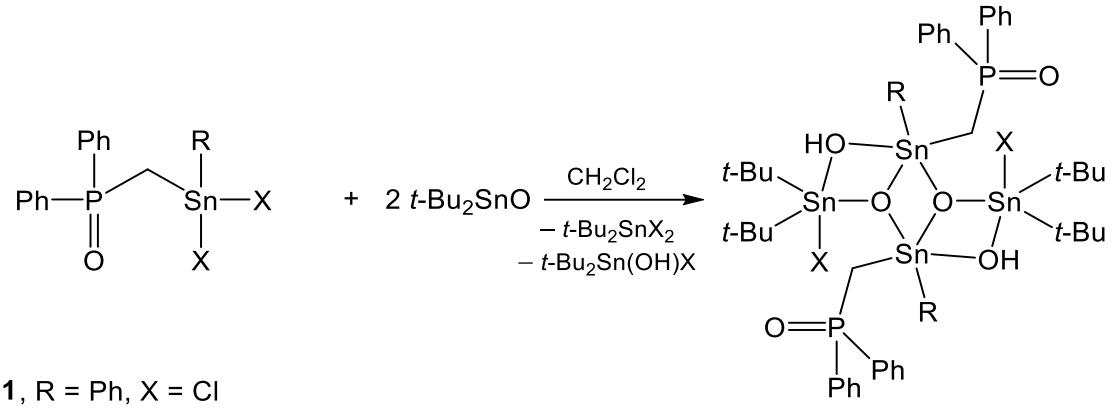

11, R = Ph, X = Cl
10, R = Me_3SiCH_2, X = Br
12, X = Me_3SiCH_2, X = Cl

18, R = Ph, X = Cl
19, R = Me_3SiCH_2, X = Br
20, X = Me_3SiCH_2, X = Cl

Scheme 7. Syntheses of the unsymmetrically substituted tetraorganodistannoxanes **18**–**20**.

The same behavior was observed in course of the reaction of $[Ph_2P(O)CH_2](Me_3SiCH_2)SnBr_2$, **10**, with $(t\text{-}Bu_2SnO)_3$. The reaction of **10** with one molar equivalent di-*tert*-butyltin oxide afforded two compounds. The trinuclear O-capped cluster, $[\{Ph_2P(O)CH_2\}(Me_3SiCH_2)(\mu\text{-}OH)Sn]_3(\mu_3\text{-}O)(\mu_3\text{-}Br)$, **17**, and the unsymmetrically substituted dimeric tetraorganodistannoxane $[t\text{-}Bu_2(Br)SnOSn(CH_2SiMe_3)\{CH_2P(O)Ph_2\}(OH)]_2$, **19**, with a ratio of about 6:1 according to the ^{31}P NMR spectrum. On the other hand, the reaction of compound **10** with two molar equivalents di-*tert*-butyltin oxide gave the tetraorganodistannoxane **19** only (Schemes 6 and 7).

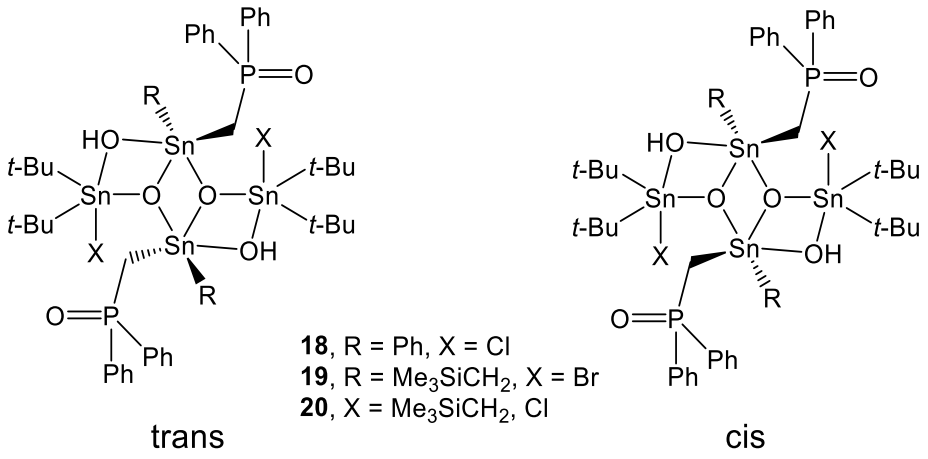

18, R = Ph, X = Cl
19, R = Me_3SiCH_2, X = Br
20, X = Me_3SiCH_2, Cl

trans cis

Chart 6. Presentation of the two isomers of compounds **18**–**20**.

Reaction of $[Ph_2P(O)CH_2](Me_3SiCH_2)SnBr_2$, **12**, with two molar equivalents di-*tert*-butyltin oxide provided the unsymmetrically substituted tetraorganodistannoxane $[Bu_2(Cl)SnOSn(CH_2SiMe_3)\{CH_2P(O)Ph_2\}(OH)]_2$, **20** (Scheme 7; Chart 6). For compounds **18**–**20**, only the trans isomers were detected in the solid state.

Interestingly, halide exchange in the O-capped cluster **14** with iodide is very facile as the reaction of **14** with sodium iodide provided the analogous compound $[\{Ph_2P(O)CH_2\}Ph(\mu\text{-}OH)Sn]_3(\mu_3\text{-}O)(\mu_3\text{-}I)$, **15**, with iodide as counter anion instead of bromide. On the other hand, no reaction of **14** with sodium fluoride under the same conditions was observed (Scheme 8). Compound **15** is isostructural with **14** indicating that the exchange of bromide with iodide anion does not affect the structure of the compound.

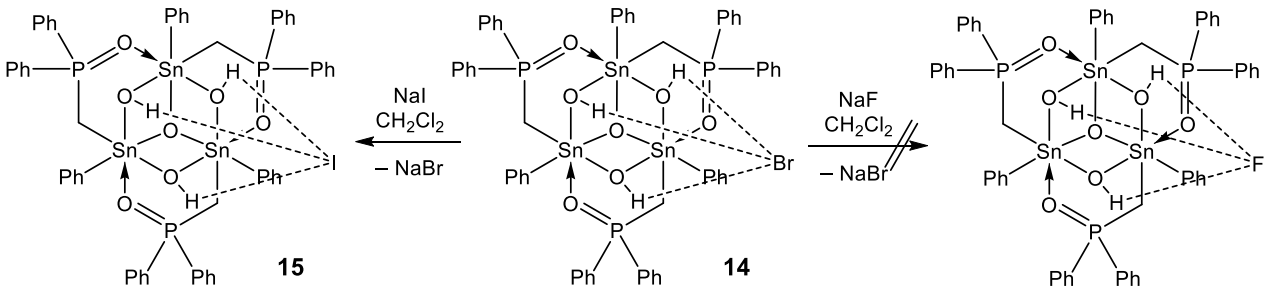

Scheme 8. Halide anion exchange experiments on the O-capped cluster **14**.

The NMR spectra of **15** are similar to those of **14**. They differ only slightly with the resonance of the O*H* protons. In **15** a singlet at δ 5.54 was observed (**14**, δ 5.98).

The ESI MS spectra of the O-capped clusters **14**, **15** and **16** (positive ion mode, CH_3CN) show the two most intense peaks observed in the original diorganotin dibromide $[Ph_2P(O)CH_2]PhSnBr_2$, **7**, as mass clusters centered at *m/z* 1281.2 (for the protonated complete condensed organotinoxo cluster $[\mathbf{C} + H]^+$; **C** = $[\{Ph_2P(O)CH_2\}PhSnO]_3$) and at *m/z* 1065.2 (for $[\mathbf{C} - Ph_2P(O)CH_2]^+$) were observed. The peak at *m/z* 1065.2 has less relative abundance in the spectra of **14**, **15** and **16** with respect to the same peak observed in the diorganotin dibromide **7**.
An ESI MS spectrum of **18** in the positive mode show mass clusters at *m/z* 1281.2 for $[\mathbf{C} + H]^+$, at *m/z* 1299.3 for $[\mathbf{C} + H_3O]^+$, at *m/z* 1065.1 for $[\mathbf{C} - Ph_2P(O)CH_2]^+$ and at *m/z* 747.2 for $[(t\text{-}Bu_2SnO)_3 + H]^+$.

Recrystallization of **14** from a solution in chloroform respectively of **15** and **16** from a mixture of chloroform/toluene provided colorless single crystals. The molecular structures of **14**·$CHCl_3$, **15**·$CHCl_3$ and **16**·$CHCl_3$ are shown in Figure 15 and selected bond lengths and bond angles of Sn(1) are summarized in Table 8; those of Sn(2) and Sn(3) could be found in the cif-file and the corresponding table in the supporting CD.

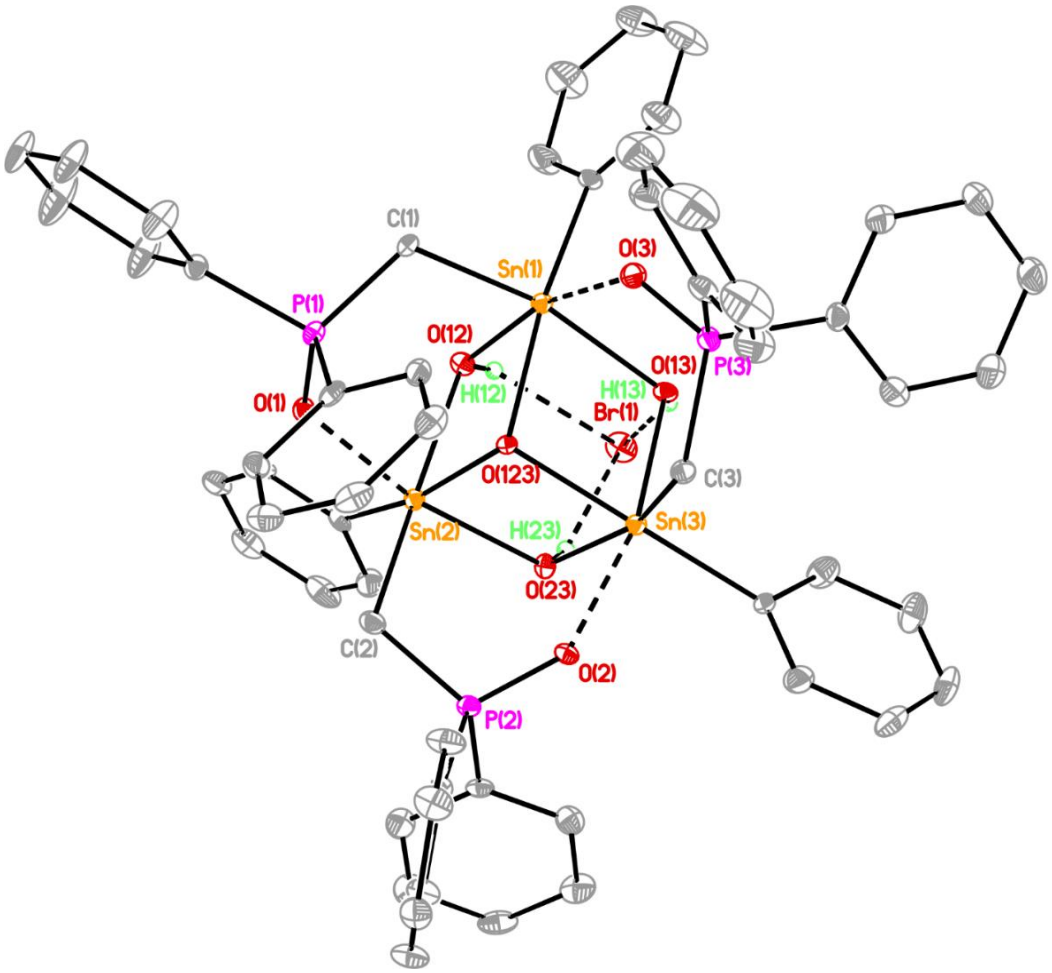

Figure 15. General view (SHELXTL) of a molecule of **14**·$CHCl_3$ [**15**·$CHCl_3$ (X = I) and **16**·$CHCl_3$ (X = Cl) are isostructural] showing 30% probability displacement ellipsoids and the crystallographic numbering scheme. The chloroform solvate molecule is omitted for clarity. Hydrogen atoms that are bound to carbon atoms are omitted for clarity.

Table 8. Selected bond lengths (Å) and bond angles (deg) which relate to Sn(1) in the O-capped clusters **14**·$CHCl_3$ (X = Br), **15**·$CHCl_3$ (X = I) and **16**·$CHCl_3$ (X = Cl).

	14·$CHCl_3$	**15**·$CHCl_3$	**16**·$CHCl_3$
Sn(1)–O(123)	2.110(2)	2.099(4)	2.0815(18)
Sn(1)–O(12)	2.111(3)	2.118(5)	2.108(2)
Sn(1)–O(13)	2.180(3)	2.164(5)	2.186(2)
Sn(1)–O(3)	2.145(2)	2.174(5)	2.1394(19)
Sn(1)–C(1)	2.192(4)	2.211(7)	2.202(3)
Sn(1)–C(11)	2.148(4)	2.144(6)	2.132(3)
P(1)–O(1)	1.531(3)	1.520(5)	1.519(2)
H(12)–X(1)	2.71(4)	2.76(2)	2.49(3)
H(13)–X(1)	2.57(4)	2.62(3)	2.38(3)
H(23)–X(1)	2.51(4)	2.83(4)	2.40(3)
Sn(1)–O(12)–Sn(2)	100.55(12)	100.78(19)	100.64(10)
Sn(1)–O(13)–Sn(3)	100.66(11)	100.48(18)	100.24(9)
Sn(1)–O(123)–Sn(2)	104.69(10)	104.7(2)	104.49(8)
Sn(1)–O(123)–Sn(3)	104.14(10)	103.67(18)	104.46(8)
O(123)–Sn(1)–C(11)	168.79(12)	170.5(2)	169.63(10)
O(123)–Sn(1)–C(1)	88.19(12)	85.8(2)	87.30(9)
O(123)–Sn(1)–O(12)	77.57(10)	77.26(18)	77.74(8)
O(123)–Sn(1)–O(13)	75.94(9)	76.59(17)	76.09(8)
O(123)–Sn(1)–O(3)	89.05(9)	87.66(17)	88.89(7)
C(11)–Sn(1)–C(1)	101.76(14)	103.4(3)	102.76(11)
C(11)–Sn(1)–O(12)	96.72(13)	99.2(2)	98.74(11)
C(11)–Sn(1)–O(13)	94.65(12)	94.6(2)	94.23(10)
C(11)–Sn(1)–O(3)	95.63(13)	94.6(2)	93.49(10)
C(1)–Sn(1)–O(12)	92.09(13)	95.3(2)	94.31(10)
C(1)–Sn(1)–O(13)	162.97(12)	160.3(2)	161.79(9)
C(1)–Sn(1)–O(3)	92.31(12)	90.4(2)	90.41(9)
O(3)–Sn(1)–O(12)	165.76(10)	163.43(18)	165.57(8)
O(3)–Sn(1)–O(13)	81.45(10)	80.29(18)	81.97(8)
O(12)–Sn(1)–O(13)	90.50(11)	89.45(18)	89.47(9)
Sn(1)–C(1)–P(1)	116.82(19)	113.3(3)	114.28(15)
Sn(1)–O(3)–P(3)	135.49(15)	128.9(3)	131.76(12)

The molecular geometry around Sn(1), Sn(2) and Sn(3) differ only slightly. Consequently, only that of Sn(1) is discussed in detail. The X-ray diffraction analyses of **14**·$CHCl_3$, **15**·$CHCl_3$ and **16**·$CHCl_3$ show that they are isostuctural and belong to the well-known family of O-capped clusters described by Holmes[20b] (Chart 7) by replacing one oxygen of the bridging phosphinate ligand with carbon at each tin atom.

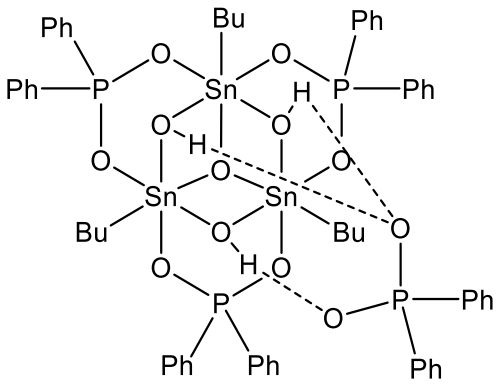

Chart 7. Drawing of the O-capped cluster reported by Holmes.[20b]

The basic framework based on a cationic core resemble those of $[(PhSn)_3(\mu_3\text{-}O)(\mu\text{-}cycPO_2)_3(\mu\text{-}OH)_3]^+$,[20e] $[\{2,4,6\text{–}i\text{-}Pr_3C_6H_2Sn(\mu_2\text{-}OH)(\eta^2\mu^2)\text{–}p\text{-}MeC_6H_4SO_3\}_3(\mu_3\text{-}O)]^+$,[20c] $[\{MeSn(HTDP)(\mu\text{-}OH)\}_3(\mu_3\text{-}O)]^+$ (TDP = thiamine diphosphate),[20f] $[\{n\text{-}BuSn(\mu\text{-}OH)O_2Pcyc_2\}_3(\mu_3\text{-}O)]^+$,[20d] $[((PhCH_2)Sn(\mu\text{-}OH)\{O_2P(C_6H_{11})_2\})_3(\mu_3\text{-}O)]^+$ [20h] and $[\{n\text{-}BuSn(\mu\text{-}OH)O_2PPh_2\}_3(\mu_3\text{-}O)]^+$,[20g] being consisting of a cationic $Sn_3(\mu\text{-}OH)_3$ ring in a *cyclo*-hexane chair conformation that is capped from one side with a triply bridging oxygen atom (Figure 16).

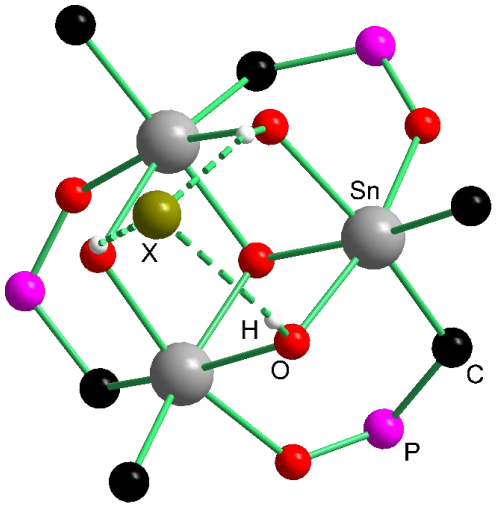

Figure 16. Reduced ball-and-sticks molecular structure of compounds **14–16** (X = Br, I, Cl). The phenyl groups at the phosphorus atom are omitted for clarity.

The hydrogen atoms in the hydroxyl groups are arranged in the reverse orientation trapping the counter anion by three hydrogen bonds. The $Sn_3(\mu\text{-}OH)_3$ ring is centered by an μ_3-oxygen, resulting in a cubane-type arrangement with alternating corners occupied by Sn and O atoms, and with one tin atom missing.

The oxygen atom in the $Ph_2P(O)CH_2$ substituents intramolecularly coordinate the next tin atom resulting in three six-membered phosphorus and tin containing rings.

The tin atoms are hexa-coordinated with the O(123), O(12), O(13), O(3), C(1) and C(11) atoms forming a distorted octahedron. The angles between the opposite atoms with respect to the tin atoms are close to 180° ranging between 162.97(12)° and 168.79(12)° for **14**·$CHCl_3$, between 160.3(2)° and 170.5(2)° for **15**·$CHCl_3$ and between 161.79(9)° and 169.63(10)° for **16**·$CHCl_3$. If the phenyl group and O(123) are considered axial, then the equatorial ligands are displaced towards the axial oxygen, making the Ph–Sn–L_{eq} and O(123)–Sn–L_{eq} angles respectively slightly wider and slightly narrower than 90°.
The Sn–O–Sn angle at the capping oxygen O(123) ranging between 104.14(10)° and 104.69(10)° for **14**·$CHCl_3$, between 104.7(2)° and 103.67(18)° for **15**·$CHCl_3$ and between 104.46(8)° and 104.49(8)° for **16**·$CHCl_3$ are close to that observed in $[(PhSn)_3(\mu_3\text{-}O)(\mu\text{-}cycPO_2)_3(\mu\text{-}OH)_3][cycPO_2]\cdot CH_3CN$ (103.6°).[20e] The Sn–O bond lengths in the basic framework range from 2.111(3) to 2.196(3) for **14**·$CHCl_3$, from 2.106(5) to 2.202(5) for **15**·$CHCl_3$ and from 2.101(2) to 2.186(2) for **16**·$CHCl_3$.

It should also be mentioned that an analogous structure type is known for titanium carboxylate,[21] cobalt[22] and molypdenum[23] complexes, and zirconium carboxylates[24] and phosphates[25] (Chart 8).

Recrystallization of **18** from a solution in CH_2Cl_2/toluene, of **19** from chloroform and of **20** from CH_2Cl_2 provide colorless single crystals of **18**·H_2O·3toluene, **19**·$CHCl_3$ and **20** respectively, that are suitable for X-ray diffraction analyses.

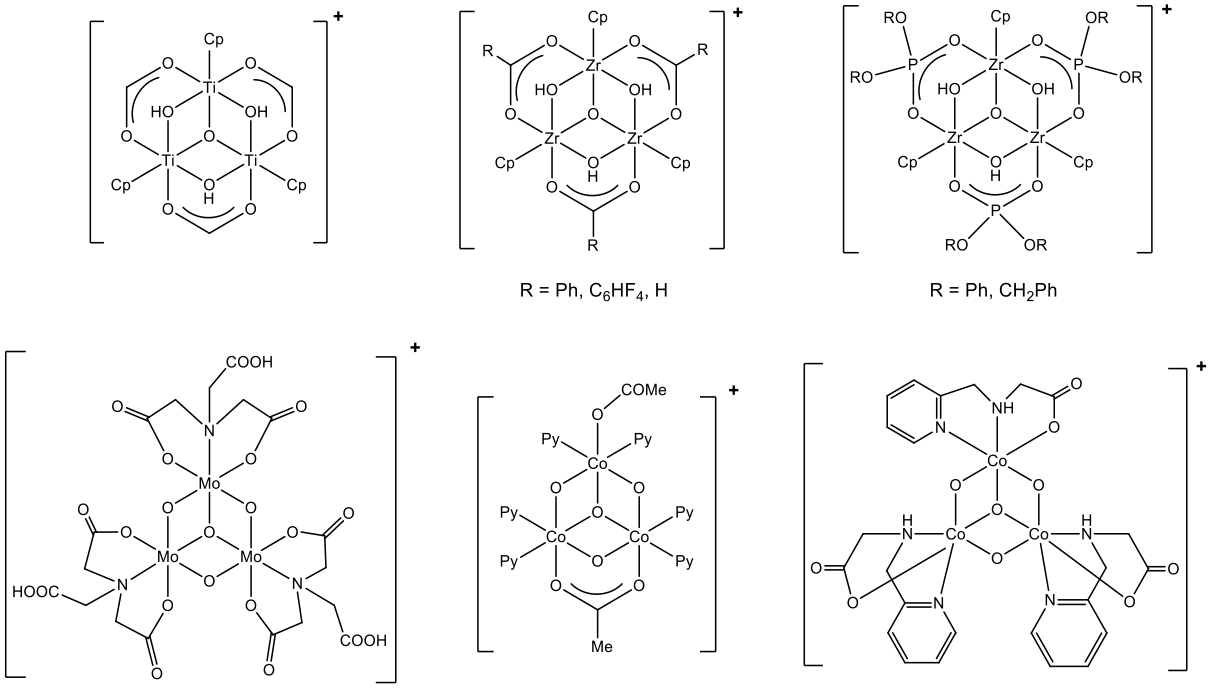

Chart 8. Examples for O-capped clusters reported in the literature.

The molecular structures of **18**·H_2O·3toluene, **19**·$CHCl_3$ and **20** are shown in Figures 17 and 18, and selected bond lengths and bond angles are summarized in Tables 9 and 10.

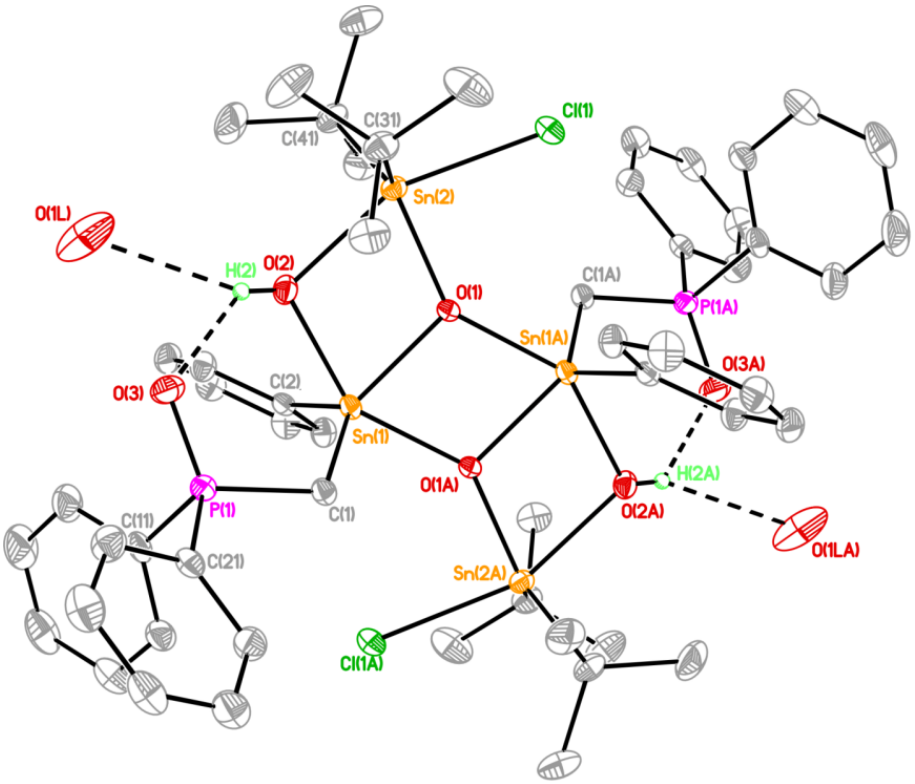

Figure 17. General view (SHELXTL) of a molecule of **18**·H_2O.3toluene showing 30% probability displacement ellipsoids and the crystallographic numbering scheme. The

toluene solvate molecules are omitted for clarity. The molecule contains one water molecule, however, its protons could not be found. Hydrogen atoms that are bound to carbon atoms are omitted for clarity.

Table 9. Selected bond lengths (Å) and bond angles (deg) in **18**·H_2O·$3C_7H_8$.

Sn(1)–O(1)	2.046(2)	Sn(2)–O(1)	2.0433(19)
Sn(1)–O(2)	2.103(2)	Sn(2)–O(2)	2.171(2)
Sn(1)–O(1a)	2.1125(19)	Sn(2)–Cl(1)	2.4971(9)
Sn(1)–C(1)	2.140(3)	Sn(2)–C(31)	2.173(3)
Sn(1)–C(2)	2.111(3)	Sn(2)–C(41)	2.177(3)
P(1)–O(3)	1.482(2)	P(1)–C(1)	1.787(3)
H(2)–O(3)	2.15(3)	H(2)–O(1L)	2.36(3)
O(2)–O(3)	2.805(3)	O(2)–O(1L)	3.045(8)
O(2)–Sn(1)–O(1a)	147.58(8)	Cl(1)–Sn(2)–O(2)	156.02(6)
O(2)–Sn(1)–C(1)	95.08(11)	Cl(1)–Sn(2)–O(1)	83.91(6)
O(2)–Sn(1)–C(2)	94.45(10)	Cl(1)–Sn(2)–C(31)	94.99(10)
O(2)–Sn(1)–O(1)	73.61(8)	Cl(1)–Sn(2)–C(41)	99.50(10)
O(1a)–Sn(1)–C(1)	98.41(10)	O(2)–Sn(2)–O(1)	72.23(8)
O(1a)–Sn(1)–C(2)	99.66(10)	O(2)–Sn(2)–C(31)	92.74(12)
O(1a)–Sn(1)–O(1)	73.99(8)	O(2)–Sn(2)–C(41)	94.67(12)
O(1)–Sn(1)–C(1)	116.66(10)	O(1)–Sn(2)–C(31)	114.46(11)
O(1)–Sn(1)–C(2)	114.26(10)	O(1)–Sn(2)–C(41)	120.14(10)
C(1)–Sn(1)–C(2)	128.85(11)	C(31)–Sn(2)–C(41)	124.53(13)
Sn(1)–O(1)–Sn(2)	110.43(9)	Sn(1)–O(2)–Sn(2)	103.56(10)
Sn(1)–O(1)–Sn(1a)	106.01(8)	Sn(2)–O(1)–Sn(1a)	143.48(10)
Sn(1)–C(1)–P(1)	114.27(15)		

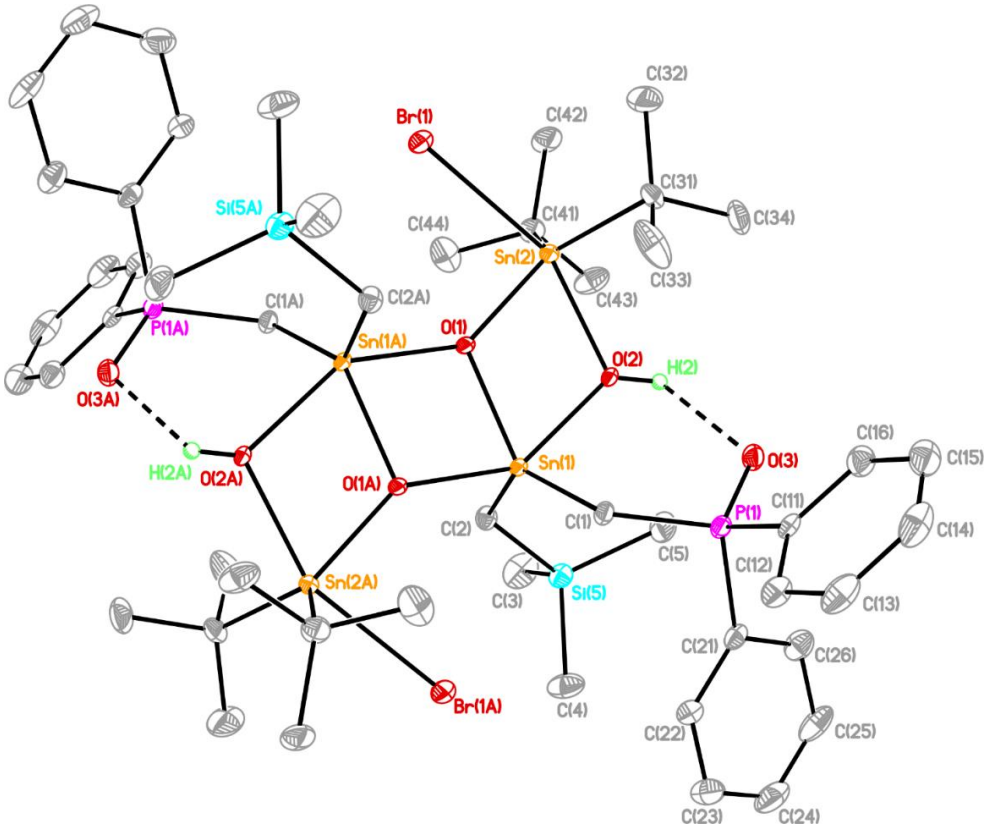

Figure 18. General view (SHELXTL) of a molecule of **19**·$CHCl_3$ [compound **20** (X = Cl) is isostructural] showing 30% probability displacement ellipsoids and the crystallographic numbering scheme. The chloroform solvate molecule is omitted for clarity. Hydrogen atoms that are bound to carbon atoms are omitted for clarity. [The carbon atoms C(32) and C(34) in compound **20** are disordered over two positions with a ratio of 50:50)].

Table 10. Selected bond lengths (Å) and bond angles (deg) in **19**·$CHCl_3$ and **20**.

	19·$CHCl_3$ (X = Br)	**20** (X = Cl)
Sn(1)–O(1)	2.051(2)	2.0534(19)
Sn(1)–O(2)	2.129(2)	2.128(2)
Sn(1)–O(1a)	2.117(2)	2.124(2)
Sn(1)–C(1)	2.142(3)	2.147(3)
Sn(1)–C(2)	2.103(3)	2.107(3)
Sn(2)–O(1)	2.037(2)	2.0313(19)
Sn(2)–(O2)	2.155(2)	2.203(2)
Sn(2)–X(1)	2.7023(4)	2.5389(8)
Sn(2)–C(31)	2.185(3)	2.189(3)
Sn(2)–C(41)	2.180(3)	2.186(3)
P(1)–O(3)	1.488(2)	1.491(2)

O(2)–O(3)	2.703(3)	2.793(3)
H(2)–O(3)	2.03(3)	2.02(2)
O(2)–Sn(1)–O(1a)	146.32(8)	146.94(8)
O(2)–Sn(1)–O(1)	73.32(8)	74.04(8)
O(2)–Sn(1)–C(1)	94.07(11)	95.42(10)
O(2)–Sn(1)–C(2)	96.60(11)	98.54(11)
O(1a)–Sn(1)–O(1)	73.39(9)	73.42(8)
O(1a)–Sn(1)–C(1)	95.01(10)	92.93(10)
O(1a)–Sn(1)–C(2)	100.53(11)	98.88(11)
O(1)–Sn(1)–C(1)	114.48(10)	114.88(10)
O(1)–Sn(1)–C(2)	112.30(10)	112.10(11)
C(1)–Sn(1)–C(2)	133.14(12)	132.99(13)
X(1)–Sn(2)–O(2)	155.71(6)	156.71(6)
X(1)–Sn(2)–O(1)	82.66(6)	83.88(6)
X(1)–Sn(2)–C(31)	95.66(9)	95.90(9)
X(1)–Sn(2)–C(41)	94.14(9)	95.22(9)
O(2)–Sn(2)–O(1)	73.05(8)	72.87(8)
O(2)–Sn(2)–C(31)	96.22(11)	93.84(11)
O(2)–Sn(2)–C(41)	95.69(11)	95.22(11)
O(1)–Sn(2)–C(31)	119.64(11)	111.71(10)
O(1)–Sn(2)–C(41)	113.75(11)	119.59(10)
C(31)–Sn(2)–C(41)	126.50(14)	128.33(12)
Sn(1)–O(1)–Sn(2)	110.43(9)	111.04(9)
Sn(1)–O(1)–Sn(1a)	106.61(9)	106.58(8)
Sn(1)–O(2)–Sn(2)	103.19(9)	102.03(9)
Sn(2)–O(1)–Sn(1a)	142.50(11)	142.10(10)
Sn(1)–C(1)–P(1)	118.14(16)	118.60(15)
Sn(1)–C(2)–Si(5)	122.87(16)	122.60(17)

Compounds **18**–**20** exist as ladder-type compounds that contain pentacoordinated tin atoms. They can be viewed, as most reported tetraorganodistannoxans,[17c-g, 26] as centrosymmetric dimers, where one half of the molecule comprises the crystallographic asymmetric unit and the other half is generated by an inversion center. All tin atoms are five-coordinate. The endo-cyclic tin atom have square-

pyramidal environment by two carbon and two oxygen atoms [C(1), C(2), O(1a), O(2)] in the equatorial positions and one triply bridging oxygen atom (O(1)) as the axial ligand (geometrical parameter[27] τ = 0.31 for **18**·H_2O·$3C_7H_8$, 0.22 for **19**·$CHCl_3$, 0.23 for **20**). The exo-cyclic tin atoms exhibit distorted trigonal bipyramidal geometry with the equatorial positions being occupied by the C(31), C(41) and O(1) atoms, and the axial positions by O(2) and the halogen atoms, chlorine in **18**·H_2O·$3C_7H_8$ and **20**, and bromine in **19**·$CHCl_3$ (geometrical goodness[28] ΔΣ(θ) 80.7 for **18**·H_2O·$3C_7H_8$, 87.4 for **19**·$CHCl_3$, 84.6 for **20**).

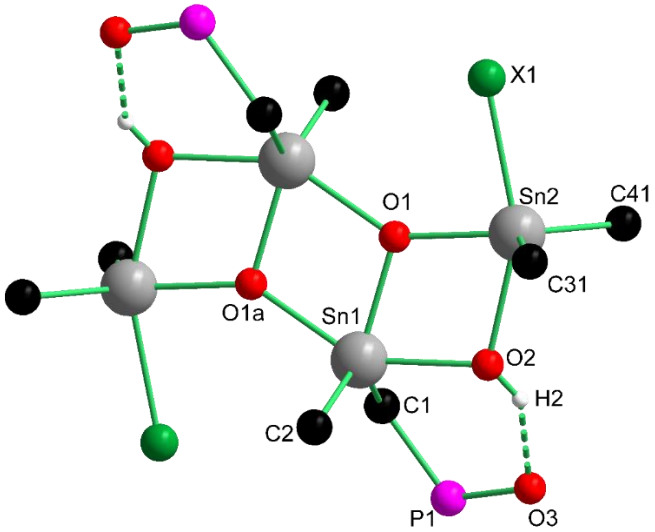

Figure 19. Reduced ball-and-sticks molecular structure of compound **18** and **19** (X = Cl, Br). The phenyl and *tert*-butyl groups, and the solvate molecules are omitted for clarity.

The Sn–O distances range between 2.0433(19) and 2.171(2) Å for **18**·H_2O·$3C_7H_8$, between 2.037(2) and 2.155(2) Å for **19**·$CHCl_3$, and between 2.0313(19) and 2.203(2) Å for **20**. The Sn_{endo}–μ_2-OH–Sn_{exo} bridges are asymmetric [**18**·H_2O·$3C_7H_8$, Sn(1)–O(2) 2.103(2) Å, Sn(2)–O(2) 2.171(2) Å; **19**·$CHCl_3$, Sn(1)–O(2) 2.129(2) Å, Sn(2)–O(2) 2.155(2) Å; **20**, Sn(1)–O(2) 2.128(2) Å, Sn(2)–O(2) 2.203(2) Å]. The Sn_{endo}–μ_3-O–Sn_{exo} angles (Sn(2)–O(1)–Sn(1a) 143.44(10)° in **18**·H_2O·$3C_7H_8$, 142.50(11)° in **19**·$CHCl_3$ and 142.10(10)° in **20**) are bigger than that in $[(Me_3SiCH_2)_2(HO)SnOSn(OH)t\text{-}Bu_2]_2$[17f] of 139.3(1)°. The axial angles at the tin atoms (O(2)–Sn_{endo}–O(1a), 147.58(8)° in **18**·H_2O·$3C_7H_8$, 146.32(8)° in **19**·$CHCl_3$ and 146.94(8)° in **20**; O(2)–Sn_{exo}–Hal, 156.02(6)° in **18**·H_2O·$3C_7H_8$, 155.71(6)° in **19**·$CHCl_3$ and 156.71(6)° in **20**) are in agreement with those found in $[(Me_3SiCH_2)_2(HO)SnOSn(OH)t\text{-}Bu_2]_2$[17f] (146.26(9) and 156.71(7)° respectively).

The hydrogen atom in the bridging hydroxide anion in compound **18**·H_2O·$3C_7H_8$ is fixed by two hydrogen bonds. One to the oxygen atom in the P=O group [O(2)···O(3) 2.805(3) Å], and one to the water molecule [O(2)···O(1L) 3.045(8) Å]. In compounds **19**·$CHCl_3$ and **20** the hydrogen atoms are fixed by one hydrogen bond to the oxygen atoms in the P=O groups [**19**·$CHCl_3$, O(2)···O(3) 2.703(3) Å; **20**, O(2)···O(3) 2.793(3) Å].

1.1.3 Conclusion.

A series of novel organotin compounds containing the $Ph_2P(O)CH_2$ moiety was synthesized and characterized. The organotin halides $[Ph_2P(O)CH_2]PhRSnX$ (**6**, R = Ph, X = Br; **8**, R = Me_3SiCH_2, X = I; **9**, R = Me_3SiCH_2, X = Br) and $[Ph_2P(O)CH_2](Me_3SiCH_2)SnX_2$ (**10**, X = Br; **12**, X = Cl) are monomeric in solution, whereas X-ray diffraction analyses proved that the triorganotin halides $[Ph_2P(O)CH_2]Ph_2SnX$ (**5**, X = I; **6**, X = Br) and the diorganotin dichloride $[Ph_2P(O)CH_2](Me_3SiCH_2)SnCl_2$, **12**, are dimers in the solid state. This is a result of two intermolecular P=O→Sn interactions resulting in the formation of eight-membered rings. Reactions of the diorganotin dihalides $[Ph_2P(O)CH_2]RSnX_2$ with different stoichiometric amounts of di-*tert*-butyltin oxide afforded different types of diorganotinoxo clusters. The reactions of $[Ph_2P(O)CH_2]RSnX_2$ (**7**, R = Ph, X = Br; **11**, R = Ph, X = Cl; **10**, R = Me_3SiCH_2, X = Br) with one molar equivalent *t*-Bu_2SnO afforded the O-capped clusters $[(Ph_2P(O)CH_2)R(\mu\text{-}OH)Sn]_3(\mu_3\text{-}O)(\mu_3\text{-}X)$ (**14**, R = Ph, X = Br; **16**, R = Ph, X = Cl; **17**, R = Me_3SiCH_2, X = Br), being composed of cationic stannoxane core and a counter halide anion that is stabilized by three hydrogen bonds. Interestingly, under the reaction with sodium iodide, the O-capped cluster **14** suffers halide anion exchange providing the iodide containing analogous compound $[(Ph_2P(O)CH_2)Ph(\mu\text{-}OH)Sn]_3(\mu_3\text{-}O)(\mu_3\text{-}I)$, **15**, whereas no reaction with sodium fluoride was observed. The diorganotinoxo clusters **14–16** are isostructural as proved by X-ray diffraction analyses and by their NMR data in solution. The reactions of the diorganotin dihalides $[Ph_2P(O)CH_2]RSnX_2$ (**11**, R = Ph, X = Cl; **10**, R = Me_3SiCH_2, X = Br; **12**, R = Me_3SiCH_2, X = Cl) with two molar equivalents *t*-Bu_2SnO afforded the ladder-like unsymmetrically-substituted dimeric tetraorganodistannoxanes $[t\text{-}Bu_2(X)SnOSnR\{CH_2P(O)Ph_2\}(OH)]_2$ (**18**, R = Ph, X = Cl; **19**, R = Me_3SiCH_2, X = Br; **20**, R =

Me_3SiCH_2, X = Cl). The complete hydrolysis of the diorganotin dibromide $[Ph_2P(O)CH_2](Me_3SiCH_2)SnBr_2$, **10**, in moist air afforded, after a long reaction time, under Sn–C cleavage, the Sn_{12} monoorganotinoxo cluster $(Me_3SiCH_2Sn)_{12}O_{14}(OH)_6Br_2$, **10a**, consisting of the centrosymmetric macrocation $[(Me_3SiCH_2Sn)_{12}O_{14}(OH)_6]^{2+}$ and two bromide counter anions that are stabilized by hydrogen bonds. Compound **10a** is isostructural with the monoorganotinoxo cluster $(Me_3SiCH_2Sn)_{12}O_{14}(OH)_6Cl_2$ reported by Jurkschat et al.[3e] Recrystallization of the organotin trichloride $[Ph_2P(O)CH_2]SnCl_3$, **13**, from acetone in aerobic conditions gave some crystals of $[\{Ph_2P(O)CH_2SnCl_2(\mu\text{-}OH)\}_2{\cdot}2C_3H_6O]$, **13a**, that is the first intermediate along the hydrolysis pathway of compound **13**. Compound **13a** is a polymer in the solid state as a result of hydrogen bridges.

1.2 Syntheses, Structures and Hydrolyses Behavior of Organotin Halides Containing the [*p*-$Ph_2P(O)C_6H_4$]Me_2SiCH_2 moiety

1.2.1 Introduction

In Chapter (1.1) it is reported that the organotin compounds containing the $Ph_2P(O)CH_2$ substituent prefer to make P=O→Sn intramolecular coordination as a result of the PCH_2Sn linkage being flexible. Therefore, the hydrolysis of organotin halides results in tinoxo clusters with small nuclearity, because of strong P=O→Sn interactions which fills the electronic sphere around the tin atoms.

This statement prompted us to synthesize other P=O functionalized organotin halides, containing the less labile [$Ph_2P(O)C_6H_4$]Me_2SiCH_2 moiety. These should in turn, under hydrolysis conditions, allow the synthesis of organotinoxo clusters with higher nuclearity, or should allow the formation of organotinoxo cluster by means of intermolecular donor-acceptor interactions or hydrogen bridges.

In this section the syntheses of the diorganotin halides [{*p*-$Ph_2P(O)C_6H_4$}Me_2SiCH_2](Ph)SnX_2 (**25**, X = Br; **26**, X = Cl) and their reaction with 1/3 molar equivalent (*t*-$Bu_2SnO)_3$ is reported. Also reported is the synthesis of [*p*-$Ph_2PC_6H_6$]Sn(*t*-Bu_2)Cl, **29**, the first tin-containing frustrated Lewis pair.

1.2.2 Results and Discusion

1.2.2.1 Syntheses of the tetraorganotin compound [$Ph_2P(O)C_6H_4$]$Me_2SiCH_2SnPh_3$, 24, containing the [*p*-$Ph_2P(O)C_6H_4$]Me_2SiCH_2 substituent

Reaction of (4-Bromophenyl)diphenylphosphane[29], **21**, with one molar equivalent *n*-BuLi followed by the reaction with one molar equivalent chloro(chloromethyl)-

dimethylsilane afforded (chloromethyl)dimethyl(4-diphenyl-phosphinophenyl)silane, **22**, in almost quantitative yield (Scheme 9).

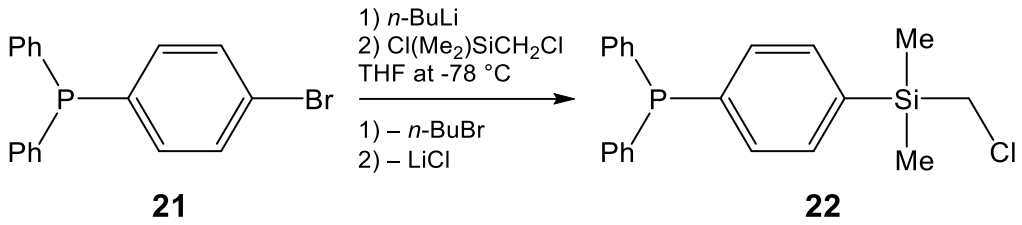

21 **22**

Scheme 9. Synthesis of compound **22**.

Compound **22** is a white solid that is soluble in THF, CH_2Cl_2, $CHCl_3$ and hexane.

Reaction of compound **22** with one molar equivalent sodium triphenylstannide in THF at –78 °C gave in quantitative yield dimethyl(4-diphenylphpsphinophenyl)silylmethy-triphenyltin, **24**, as light yellowish waxy oil that is soluble in hexane, CH_2Cl_2, $CHCl_3$ and toluene (Scheme 10).

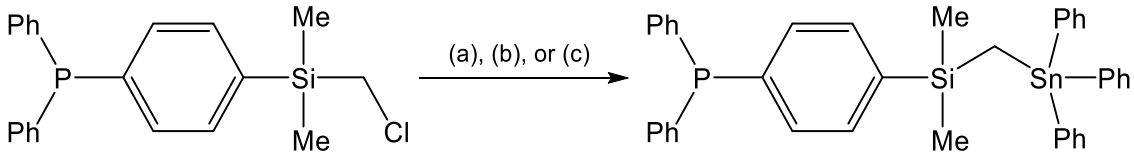

22 **23**

Scheme 10. Synthesis of compound **23**; (a) Reaction with Ph_3SnNa at –78 °C in THF. (b) Lithiation of **22** using *n*-BuLi, followed by reaction with Ph_3SnCl at –78 °C in THF. (c) Reaction of the Grignard reagent of **22** with Ph_3SnF in THF/toluene at room temperature.

Compound **23** could also be obtained by lithiation of compound **22** using *n*-BuLi, followed by the reaction with triphenyltin chloride in THF at –78°C (Scheme 9). Reaction of the Grignard reagent of compound **22**, $[Ph_2PC_6H_4]Me_2SiCH_2MgCl$, with triphenyltin fluoride afforded compound **23** in low yield (integral 15 in ^{119}Sn NMR spectrum) (Scheme 9).

For a solution of compound **23** in $CDCl_3$ single resonances in each ^{119}Sn (δ –90), ^{29}Si (δ –1.4 [$^2J(^{29}Si–^{117/119}Sn)$ = 20 Hz]), and ^{31}P NMR spectra (δ –4.5) were observed.

The ^{1}H NMR spectrum of the same solution showed a single resonance for the SnC*H*$_2$Si protons at *δ* 0.64 [^{2}J(^{1}H–$^{117/119}$Sn) = 75.4 Hz]. For the carbon atom of the methylene group a single resonance at *δ* –5.5 was observed in ^{13}C NMR spectrum. No satellites ^{1}J(^{13}C–$^{117/119}$Sn) were detected, because the signal is too small with respect to those for the phenyl groups. The ESI MS spectrum for compound **23** showed a major mass cluster centered at *m/z* 699.2 that fits with the protonated oxidized adduct [Ph$_2$P(O)C$_6$H$_4$]Me$_2$SiCH$_2$SnPh$_3$ + H]$^+$.

Compound **23** was oxidized with potassium permanganate in acetone at room temperature giving [Ph$_2$P(O)C$_6$H$_4$]Me$_2$SiCH$_2$SnPh$_3$, **24**, as high viscous oil in almost quantitative yield. Compound **24** is soluble in acetone, toluene, THF, CH_2Cl_2 and $CHCl_3$ (Scheme 11).

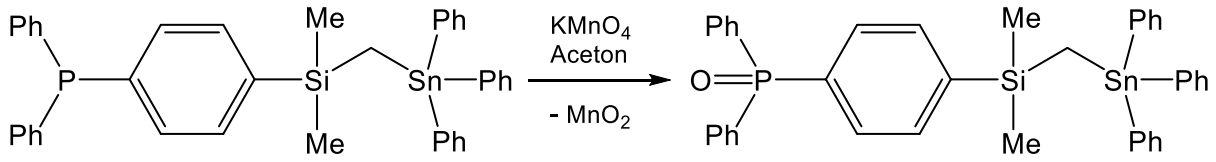

23 **24**

Scheme 11. Synthesis of compound **24**.

The ^{119}Sn and ^{29}Si NMR spectra of compound **24** show no particularity. They differ only slightly from those in compound **23**. However, the resonance in ^{31}P NMR spectrum showed, as expected, low-field shift of 30.8 ppm in comparison to that in compound **23**, as a single resonance at *δ* 26.3 was observed. The ESI MS spectrum in positive mode showed two major mass clusters. One centered at *m/z* 707.2 that is assigned to [M + Na]$^+$ and another one at *m/z* 1405.5 that fits with [2M + K]$^+$.

1.2.2.2 Syntheses and structure of the [*p*-Ph$_2$P(O)C$_6$H$_4$]Me$_2$SiCH$_2$-substituted diorganotin halides [*p*-Ph$_2$P(O)C$_6$H$_4$]Me$_2$SiCH$_2$(Ph)SnX$_2$ (25, X = Br; 26, X = Cl)

Bromination and proto-destannylation of the tetraorganotin compound **24** afforded the corresponding diorganotin(IV) halides [{Ph$_2$P(O)C$_6$H$_4$}Me$_2$SiCH$_2$](Ph)SnX$_2$ (**25**, X = Br; **26**, X = Cl) as high melting solids in almost quantitative yields (Scheme 12).

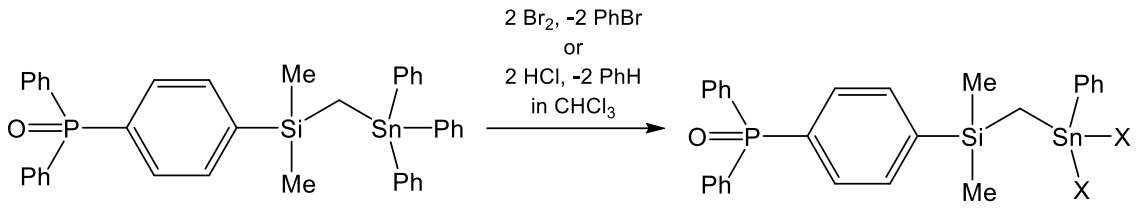

24

25, X = Br
26, X = Cl

Scheme 12. Syntheses of the diorganotin dihalides **25** and **26**.

Compound **25** is moderate soluble in $CHCl_3$ and CH_2Cl_2, whereas compound **26** has a very poor solubility in most common organic solvents like hexane, $CHCl_3$, CH_2Cl_2 and THF. The ^{119}Sn NMR spectrum of a solution of compound **25** in $CDCl_3$ showed a broad signal at δ –84 ($\nu_{1/2}$ = 490 Hz) that is approximately 53 ppm low-frequency shifted with respect to the diorganotin dibromide $[Me_2(i\text{-PrO})SiCH_2]PhSnBr_2$ (δ –31, $CDCl_3$). This is a result of the stronger P=O→Sn intermolecular interaction. The ^{31}P NMR spectrum of the same solution showed also a broad signal at δ –32.7 ($\nu_{1/2}$ = 56 Hz). The broadness of the signals in ^{119}Sn and ^{31}P NMR spectra hints to intermolecular P=O→Sn interaction that is fast on the NMR time scale at room temperature. The ^{1}H NMR spectrum showed a single resonance for SnCH_2Si protons at δ 1.42 [$^2J(^1H–^{117/119}Sn)$ = 103.2/106.8 Hz]. On the other hand, the ^{31}P NMR spectrum of compound **26** in $CDCl_3$ showed a single resonance at δ 33.7 ($\nu_{1/2}$ = 17 Hz). The low solubility of **26** in organic solvents prohibited recording a ^{119}Sn NMR spectrum.

An electrospray mass spectra of compound **25** showed in the positive mode two major mass clusters, at *m/*z 707.0 for $[M + H]^+$, and 1410.8 for $[2M + H]^+$. In the negative mode a mass cluster at *m/*z 784.8 for $[M + Br]^-$ was observed. Compound **26**, on the other side, shows four major mass cluster in the positive mode centered at *m/*z 617.0 $[M + H]^+$, 577.1 $[M – 2Cl + 2OH + H]^+$, 1141.2 $[2M – 4Cl + 3OH]^+$ and 1197.0 $[2M – Cl]^+$, and two in the negative mode at *m/*z 650.9 $[M – 2Cl + 3OH + 3H_2O]^-$ and 669.0 $[M – 2Cl + 3OH + 4H_2O]^-$.

A ^{119}Sn NMR spectrum of compound **25** in $CDCl_3$-solution to which had been added one molar equivalent tetraphenylphosphonium bromide, Ph_4PBr, showed resonance at δ –206 for the tetraphenylphosphonium diorganotribromidostannate [*p*-

$Ph_2P(O)C_6H_4]PhSnBr_3^-$ Ph_4P^+, **27**. Compound **27** is yellowish waxy oil that is soluble in CH_2Cl_2, $CHCl_3$ and acetonitrile.

Recrystallization of compound **25** from its solution in $CHCl_3$/toluene provided colorless single crystals suitable for X-ray diffraction analysis. The molecular structure of **25** is shown in Figure 20 and selected bond lengths and bond angles are summarized in Table 11.

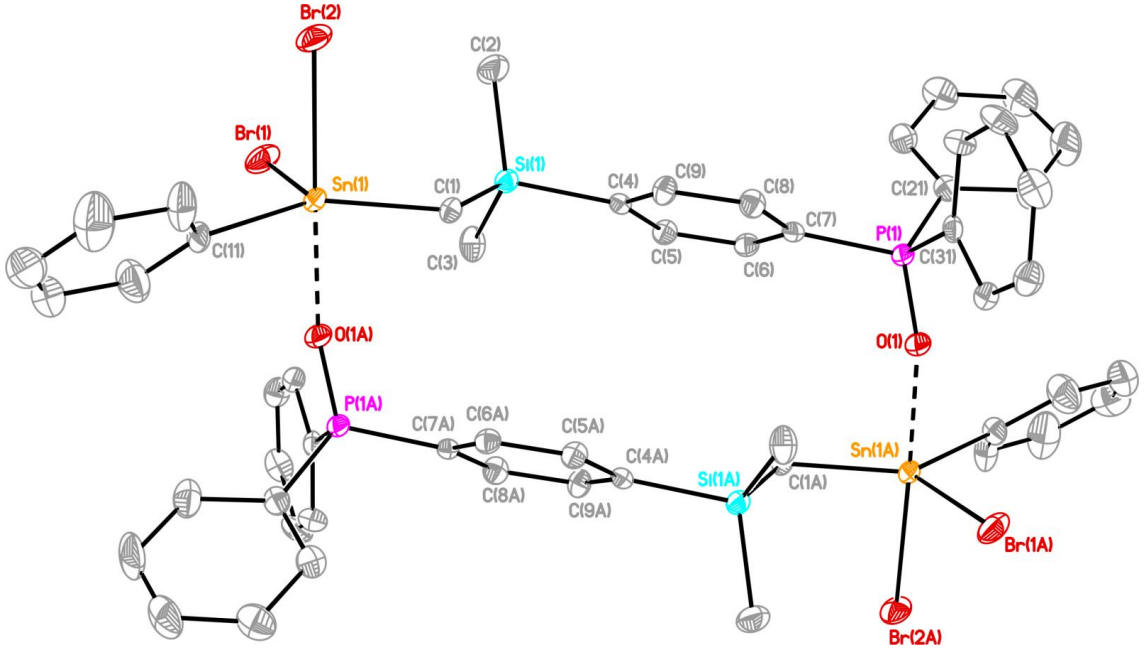

Figure 20. General view (SHELXTL) of a molecule of **25** showing 30% probability displacement ellipsoids and the crystallographic numbering scheme. Hydrogen atoms are omitted for clarity.

Table 11. Selected bond lengths (Å) and bond angles (deg) in compound **25**.

Sn(1)–O(1a)	2.290(3)	Sn(1)–C(1)	2.121(4)
Sn(1)–Br(1)	2.5187(6)	Sn(1)–C(11)	2.193(5)
Sn(1)–Br(2)	2.6384(6)	P(1)–O(1)	1.504(3)
Br(2)–Sn(1)–O(1a)	177.30(8)	Br(1)–Sn(1)–C(11)	107.1(2)
Br(2)–Sn(1)–Br(1)	95.33(2)	C(1)–Sn(1)–C(11)	138.5(2)
Br(2)–Sn(1)–C(1)	93.10(12)	Sn(1)–C(1)–Si(1)	117.7(2)
Br(2)–Sn(1)–C(11)	91.84(19)	Sn(1)–O(1a)–P(1a)	165.2(2)
O(1a)–Sn(1)–Br(1)	87.37(8)	O(1a)–Sn(1)–C(1)	85.75(14)
Br(1)–Sn(1)–C(1)	113.37(11)	O(1a)–Sn(1)–C(11)	87.4(2)

Compound **25** is a dimer in the solid state as a result of two P=O→Sn intermolecular interactions. The tin atom is penta-coordinated with the C(1), C(11) and Br(1) atoms in the equatorial positions, and the Br(2) and O(1a) atoms occupying the axial positions. The tin atom exhibits distorted trigonal bipyramidal environment.

The bond lengths and angles around the tin atom are comparable with those found in $[Ph_2P(O)CH_2(Ph_2)SnBr]_2$, **6'**. The O–Sn–Br angle of 177.30(8)° in compound **25** is very close to the ideal value (180°) and is slightly larger than that of 170.12(6)° in compound **6'**. The angles (Br–Sn–L_{eq}) and (O–Sn–L_{eq}) are slightly bigger respectively slightly narrower than the ideal value 90°. The Br–Sn–L_{eq} angles lie between 91.84(19) and 95.33(2)°, and the O–Sn–L_{eq} angles range between 85.75(14) and 87.4(2)°. The angles between the equatorial ligands lie relatively in bigger range. The Br(1)–Sn–C_{eq} angles are 107.1(2) and 113.37(11)°, whereas the C(1)–Sn–C(11) is 138.5(2)°. The P–O–Sn angle of 165.2(2)° in compound **25** is slightly smaller than that of 167.17(15)° found in compound **6'**. The silicon and phosphorus atoms in compound **25** are tetra-coordinated and show tetrahedral environment. The angle around the silicon and phosphorus atoms are in the ranges [106.6(2) – 112.6(3)°] and [107.1(2) – 111.93(19)°], respectively, and they do not show any particularity.
The O–Sn distance is 2.290(3) Å in compound **25** being a little longer than that of 2.259(2) Å seen in compound **6'**. The Br–Sn bond lengths are 2.5187(6) and 2.6384(6) Å with the smaller value for the bromine atom in the axial position. All other bond lengths show no particularity.

1.2.2.3 Experiments to synthesize the diorganotinoxo cluster containing the [*p*-$Ph_2P(O)C_6H_4$]Me_2SiCH_2 moiety

The course of reaction between **25** and 1/3 molar equivalents $(t\text{-}Bu_2SnO)_3$, as water free oxygen source, was monitored using NMR spectroscopy. The ^{119}Sn NMR spectrum ($CDCl_3$) showed, in addition to the signal of $t\text{-}Bu_2SnBr_2$ (at δ 77), more than 16 signals with different integrals, in the range between –197 and –258 ppm (Figure 21). It was difficult to assign the signals, but it is expected that, among these signals, there are ten that correspond to the exo-cyclic and endo-cyclic tin sites, respectively, of five dimeric tetraorganodistannoxane isomers **28a**–**28e** (Chart 9), each having four

magnetically equivalent bromine atoms. These are the theoretically expected isomers of the dimeric tetraorganodistannoxane resulted by hydrolysis of **25**, as the hydrolysis of diorganotin halides mostly results in the ladder-like tetraorganostannoxanes. Other possible products are the partially hydrolyses products of the latter isomers by replacing the bridging bromine atom by hydroxyl group, and the unsymmetrically substituted dimeric tetraorganodistannoxanes by involving the *t*-Bu_2Sn moieties in the reaction products. This could explain the presence of over 16 signals. Experiments to purify the reaction products by recrystallization from different organic solvents failed. The dimeric tetraorganodistannoxane, $[(Me_3SiCH_2)Ph(Cl)SnOSn(Cl)Ph(CH_2\text{-}SiMe_3)]_2$,[30] containing two different substituents bound at the same tin atom, was reported and showed in the ^{119}Sn NMR spectrum of a pure sample 10 signals corresponding to the five expected isomers.

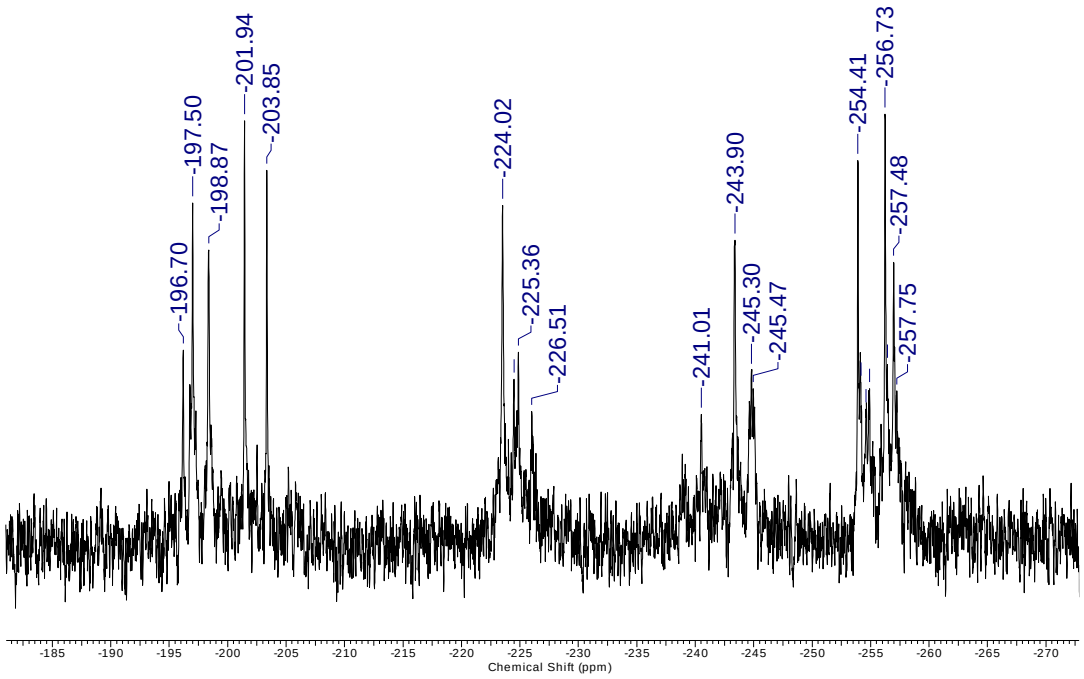

Figure 21. Expansion of the $^{119}Sn\{^1H\}$ NMR spectrum (111.92 MHz, 294 K) of the crude reaction product of **25** and 1/3 (*t*-$Bu_2SnO)_3$ measured in $CDCl_3$.

The ^{31}P NMR spectrum showed many signals (over 11 signal) between 28.9 and 31.0 ppm. Some of these signals are broad, this could be a result of overlapping signals.

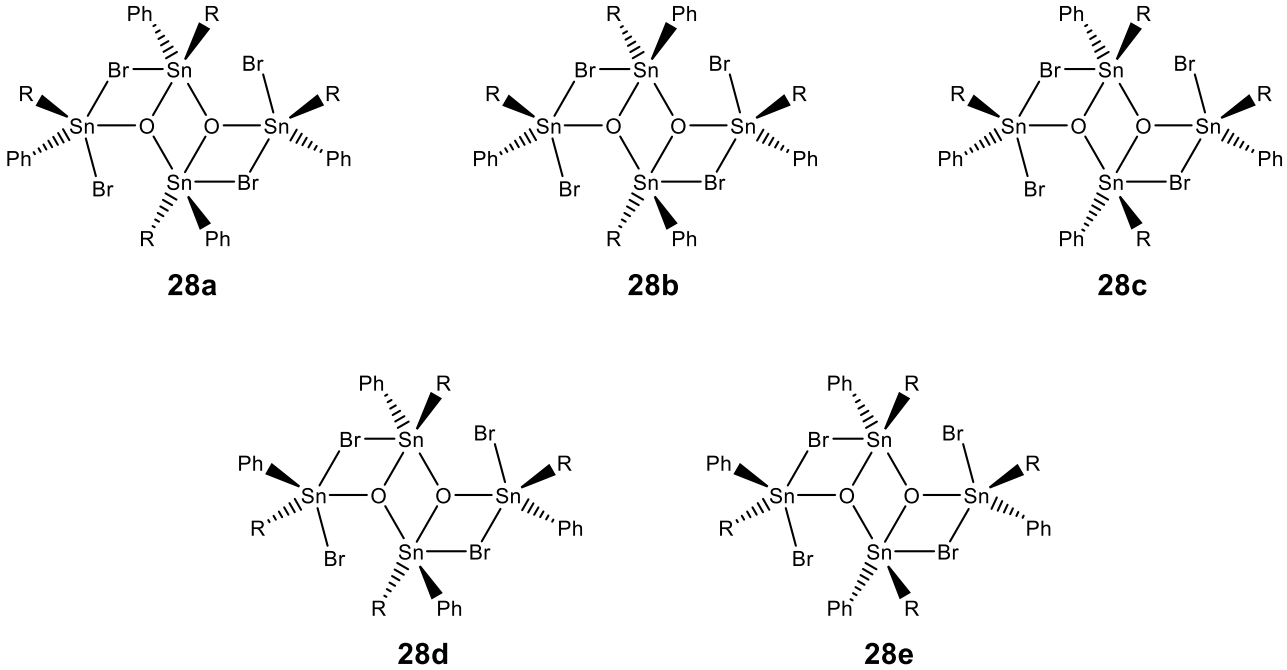

Chart 9. Expected isomers for the symmetric dimeric tetraorganodistannoxane **28**.

The ESI MS spectrum of the crude reaction product showed two main mass clusters centered at 1119.3 that is assigned to $[2RPhSnO - Ph + OH + H_2O + K]^+$, and at 1431.4 for $[2RPhSnO + t\text{-}Bu_2SnO + 2H_2O + Na]^+$ (R = $[Ph_2P(O)C_6H_4]Me_2SiCH_2$).

The reaction of compound **26** with $1/3(t\text{-}Bu_2SnO)_3$ was also monitored using NMR spectroscopy. The ^{119}Sn NMR spectrum of the crude reaction product showed, in addition to a signal at δ 54 for $t\text{-}Bu_2SnCl_2$, many broad signals in the range between –209 and –253 ppm, which are in the range of penta-coordinated tin atoms that are characteristic for tin atoms in the ladder-like dimeric tetraorganodistannoxanes. The ^{31}P NMR spectrum showed broad signals between 28.9 and 31.0 ppm. Attempt to separate the products by recrystallization from different organic solvents failed.

1.2.2.4 Synthesis of the first tin-containing Frustrated Lewis Pair (FLP)

A rather hot topic of contemporary research is the field of so-called Frustrated Lewis Pairs (FLPs). These are a combination of Lewis acids and Lewis bases that are sterically precluded from forming Lewis acid–base adducts. Frustrated Lewis pairs have been the subject of recent interest because of the high latent reactivity of such species in the activation of small molecules.[31] So far, the chemistry of frustrated Lewis pairs is dominated by systems containing phosphorus or nitrogen as the Lewis base center, and boron or aluminum as the Lewis acid center. However, this concept was extended to include transition metals as the Lewis acid. Recently the zirconocene phosphinoaryloxide complexes has shown high reactivity to activate a large variety of reactions like hydrogen cleavage, CO_2 activation, alkene and alkyne addition, and tetrahydrofuran ring opening.[31e, 32] Despite that the novelty of metal-free catalysis cannot be hold for tin-containing FLPs, the FLP model is valuable in understanding the reactivity of this system via ditopic activation. To the best of our knowledge, the combination of tin/phosphorus has not yet been investigated in this respect.

Reaction of *t*-Bu_2SnCl_2 with one molar equivalent $Ph_2PC_6H_4Li$ in THF at –40 °C affords $Ph_2PC_6H_4$(*t*-Bu_2)SnCl, **29**, in moderate yield (Integral 66 in the ^{119}Sn NMR spectrum). As a byproduct the tetraorganotin compound [$Ph_2PC_6H_4$]$_2$(*t*-Bu_2)Sn, **30**, was also observed (Integral 19) (Scheme 12).

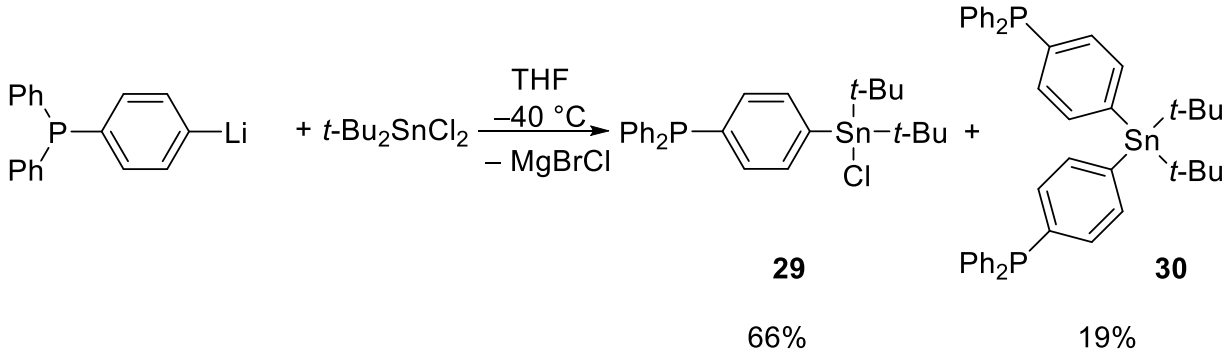

Scheme 12. Reaction of *t*-Bu_2SnCl_2 with $Ph_2PC_6H_4Li$.

The ^{119}Sn NMR spectrum (Figure 18) showed a doublet resonance that was assigned to compound **29** at δ 40 ppm with $^{4}J(^{119}\text{Sn}–^{31}\text{P})$ of 6 Hz, and no $^{1}J(^{119}\text{Sn}–^{31}\text{P})$ coupling was observed. This confirms the absence of P→Sn intermolecular interaction, which is the prerequisite for FLPs. In ^{31}P NMR spectrum of the same solution a signal at δ 4.3 [$^{4}J(^{31}\text{P}–^{117/119}\text{Sn})$ = 6.7 Hz] was observed that was assigned to compound **29**. For compound **30** a triplet resonance in ^{119}Sn NMR spectrum at δ –92 [$^{4}J(^{119}\text{Sn}–^{31}\text{P})$ = 5 Hz] was observed. The corresponding ^{31}P NMR spectrum showed a resonance at δ –4.4 [$^{4}J(^{31}\text{P}–^{117/119}\text{Sn})$ = 5.5 Hz] that was assigned to compound **30**.

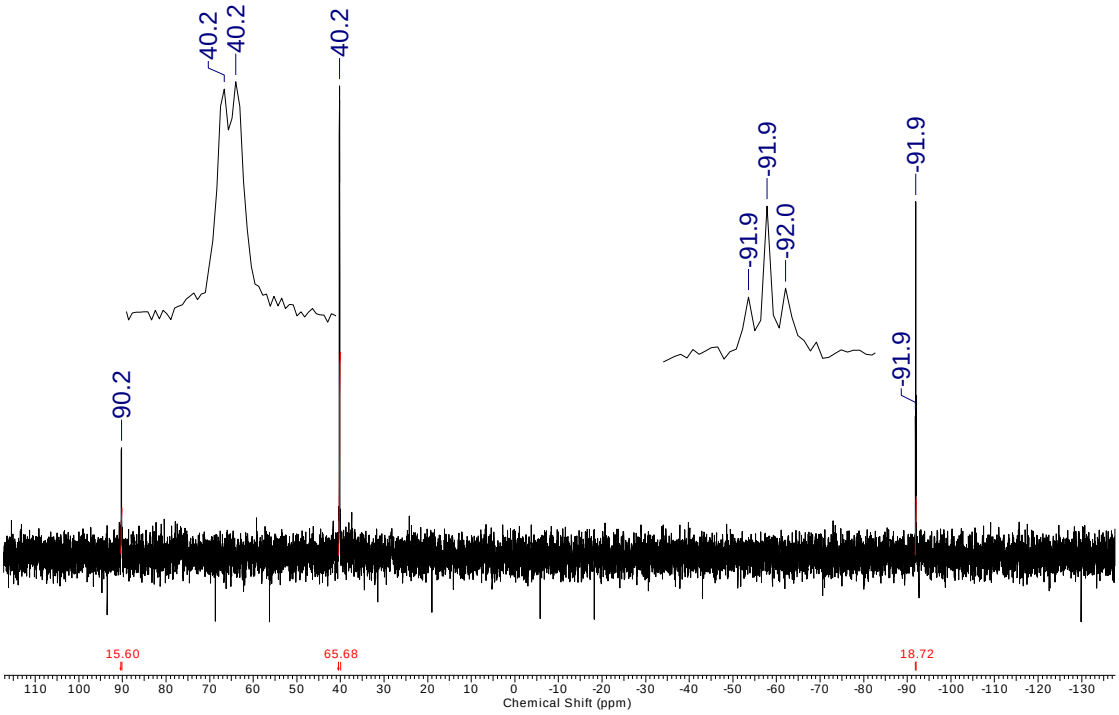

Figure 18. Expansion of the ^{119}Sn{^{1}H} NMR spectrum (111.92 MHz, 294 K) of the crude reaction product of $Ph_2PC_6H_4MgBr$ and 1/3 $(t\text{-}Bu_2SnO)_3$, measured in $CDCl_3$.

In ^{119}Sn NMR spectrum a signal at δ 90 (Integral 15) was also observed, this should contain no phosphine ligand. Recrystallization of the crude reaction product in moist air resulted in few crystals of $[t\text{-}Bu_2Sn(OH)Br]_2$.

1.2.3 Conclusion

The diorganotin halides [{*p*-$Ph_2P(O)C_6H_4$}Me_2SiCH_2]$PhSnX_2$ (**25**, X = Br; **26**, X = Cl) were synthesized and characterized. Reactions with (*t*-$Bu_2SnO)_3$ as water-free oxygen source resulted in complex mixtures. The ^{119}Sn NMR spectra hint to five-coordinated tin atoms present in ladder-like diorganotinoxo clusters as signals in the range between δ –197 and –258 were observed. However, the reaction products could not be purified. Also reported is the synthesis of the first tin-containing frustrated Lewis pair ($Ph_2PC_6H_4$)*t*-Bu_2SnCl, **29**. The compound shows no P→Sn interaction as proved by the absence couplings between these nuclei in the corresponding NMR spectra. This is a prerequisite for FLPs.

1.3 Experimental Section

General Considerations

All solvents were purified by distillation under argon from appropriate drying agents, if not otherwise stated. $Me_3SiCH_2SnPh_3$,[33] *t*-Bu_2SnCl_2,[34] and di-*tert*-butyltin oxide,[35] were synthesized according to literature method. $Me_3SiCH_2SnPh_2I$ was synthesized from $Me_3SiCH_2SnPh_3$[33] according to the representative procedure (A). Triphenyltin chloride, tricyclohexyltin chloride, diphenyltin dichloride, triphenylphosphane oxide, methyl lithium (1.6 M in diethyl ether), hydrogen chloride (1.0 M in diethyl ether), *n*-BuLi (1.6 M in hexane), tin tetrachloride, chloro(chloromethyl)dimethylsilane, and hexaphenylditin were commercially available, and they were used without further purification. Bruker DPX–300 and DRX–400 spectrometers were used to obtain ^{1}H, ^{13}C, ^{29}Si, ^{31}P, and ^{119}Sn NMR spectra at ambient temperature. The ^{1}H, ^{13}C, ^{29}Si, ^{31}P and ^{119}Sn NMR chemical shifts are given in ppm and were referenced to Me_4Si (^{1}H, ^{13}C, ^{29}Si), H_3PO_4 (^{31}P), and Me_4Sn (^{119}Sn). Elemental analyses were performed on a LECO–CHNS–932 analyzer. The electrospray mass spectra were recorded with a Thermoquest–Finnigan instrument, using CH_3CN, methanol or CH_2Cl_2 as the mobile phase.

Representative procedure for the preparation of organotin iodides (Procedure A)

Iodine was added in portions at 0 °C to a solution of the compound in dichloromethane or chloroform. After the complete addition the mixture was allowed to reach room temperature and stirred overnight. The solvent and iodobenzene were removed in vacuo. The stoichiometric ratio (iodine : compound) equal the number of phenyl groups in the compound that have to be replaced with iodine.

Representative procedure for the preparation of organotin bromides (Procedure B)

A solution of bromine in dichloromethane or chloroform was added drop-wise at 0 °C to a solution of the compound in dichloromethane or chloroform. After 2 hours of stirring the mixture was allowed to reach room temperature and stirred overnight at ambient temperature. The solvent and bromobenzene were removed in vacuo. The

stoichiometric ratio (bromine : compound) equal the number of phenyl groups in the compound that have to be replaced with bromine.

Representative procedure for the preparation of organotin chlorides (Procedure C)

To a solution of the compound in dichloromethane was added in one portion a solution of hydrogen chloride (1.0 M in diethyl ether) at 0 °C and the mixture was stirred for 30 minutes at the same temperature. Then the mixture was allowed to reach ambient temperature and stirred overnight. The solvent and benzene were removed in vacuo. The stoichiometric ratio (HCl : compound) equal the number of phenyl groups in the compound that have to be replaced with chlorine.

Representative procedure for the preparation of compounds 1–4 (Procedure D)

(1.05 eq.) Methyllithium (1.6 M in diethyl ether) was added drop-wise at 0 °C to a suspension of triphenylphosphine oxide (TPPO) (1.00 eq.) in diethyl ether (3 mL/1 mmol TPPO). After complete addition the mixture was allowed to reach room temperature and stirred for 2 h at the same temperature. Then a solution of the organotin halide (0.90 eq.) in diethylether (3 mL/1 mmol TPPO) and THF (1 mL/1 mmol TPPO) was added drop-wise at room temperature. After stirring overnight the filtrate was hydrolyzed with ammonium chloride. The organic phase was separated and the aqueous phase was extracted with diethyl ether. The organic phases were combined and dried with magnesium sulfate. Removal of the solvents in vacuo afforded yellowish viscous oil. Purification of the oil by column chromatography using silica gel/CH_2Cl_2 and elution with CH_2Cl_2 followed with ethyl acetate gave the corresponding compounds as white solids.

Synthesis of $Ph_2P(O)CH_2SnPh_3$, 1

Compound **1** was synthesized by modified procedure of that described in the literature.[36] The compound was synthesized according to the procedure (D) using Ph_3SnCl as the organotin halide. Mp 136.0–138.0 °C; yield 56%; single crystals of **1** suitable for X-ray diffraction analysis were obtained by slow evaporation of a solution of the compound in CH_2Cl_2/ethyl acetate.

Anal. Calcd for $C_{31}H_{27}OPSn$ (565.22 g/mol): C, 65.88; H, 4.81. Found: C, 66.0; H, 4.9. **^{1}H NMR** (300.13, $CDCl_3$): δ 2.45 (d, 2H, $^2J(^1H–^{31}P)$ = 11.3 Hz, $^2J(^1H–^{117/119}Sn)$ =

57.4/60.0 Hz, PC*H*$_2$Sn), 7.27–7.75 (m, 25H, Ar H). **^{13}C{^{1}H} NMR** (75.48, $CDCl_3$): *δ* 14.3 (d, ^1J(^{13}C–^{31}P) = 66 Hz, P*C*H$_2$Sn), 128.2 (d, ^3J(^{13}C–^{31}P) = 12 Hz, C$_m$; Ph–P), 128.4 (s, ^3J(^{13}C–$^{117/119}$Sn) = 54 Hz, C$_m$; Ph–Sn), 128.9 (s, ^4J(^{13}C–$^{117/119}$Sn) = 12 Hz, C$_p$; Ph–Sn), 130.4 (d, ^2J(^{13}C–^{31}P) = 9 Hz, C$_o$; Ph–P), 130.9 (d, ^4J(^{13}C–^{31}P) = 2 Hz, C$_p$; Ph–P), 135.7 (d, ^1J(^{13}C–^{31}P) = 100 Hz, C$_i$; Ph–P), 137.0 (s, ^2J(^{13}C–$^{117/119}$Sn) = 40 Hz, C$_o$; Ph–Sn), 137.4 (s, ^1J(^{13}C–$^{117/119}$Sn) = 527/554 Hz, ^3J(^{13}C–^{31}P) = 1 Hz, C$_i$; Ph–Sn). **^{31}P{^{1}H} NMR** (121.50, $CDCl_3$): *δ* 33.0 (s, ^2J(^{31}P–$^{117/119}$Sn) = 60 Hz). **^{119}Sn{^{1}H} NMR** (111.92, $CDCl_3$): *δ* –116 (d, ^2J(^{119}Sn–^{31}P) = 63 Hz, ^1J(^{119}Sn–^{13}C$_{CH2}$) = 211 Hz, ^1J(^{119}Sn–^{13}C$_{Ph}$) = 554 Hz).

Synthesis of {Ph$_2$P(O)CH$_2$}(Me$_3$SiCH$_2$)SnPh$_2$, 2

The compound was synthesized according to the procedure (D) using (Me$_3$SiCH$_2$)Ph$_2$SnI as the organotin halide. Mp 96.5–98.5 °C; yield 54%; single crystals of **2** suitable for X-ray diffraction analysis were obtained by slow evaporation of a solution of the compound in hexane.

Anal. Calcd for $C_{29}H_{33}OPSiSn$ (575.33 g/mol): C, 60.54; H, 5.78. Found: C, 60.6; H, 5.8. **^{1}H NMR** (300.13, $CDCl_3$): *δ* 0.10 (s, 9H, *Me$_3$*Si), 0.42 (s, 2H, ^2J(^{1}H–$^{117/119}$Sn) = 80.9/84.5 Hz, SiC*H*$_2$Sn), 2.16 (d, 2H, ^2J(^{1}H–^{31}P) = 11.7 Hz, ^2J(^{1}H–$^{117/119}$Sn) = 54.2/56.7 Hz, PC*H*$_2$Sn), 7.29–7.72 (m, 20H, Ar H). **^{13}C{^{1}H} NMR** (75.84, $CDCl_3$): *δ* –3.5 (s, ^1J(^{13}C–$^{117/119}$Sn) = 283/296 Hz, Si*C*H$_2$Sn), 1.3 (s, ^1J(^{13}C–^{29}Si) = 51 Hz, ^3J(^{13}C–$^{117/119}$Sn) = 18 Hz, *Me$_3$*Si), 14.0 (d, ^1J(^{13}C–^{31}P) = 67 Hz, ^1J(^{13}C–$^{117/119}$Sn) = 209/218 Hz, P*C*H$_2$Sn), 128.2 (s, ^3J(^{13}C–$^{117/119}$Sn) = 52 Hz, C$_m$; Ph–Sn), 128.3 (*Ph*–P) , 128.6 (s, C$_p$; Ph–Sn), 130.3 (d, *J*(^{13}C–^{31}P) = 9 Hz, *Ph*–P), 130.9 (d, *J*(^{13}C–^{31}P) = 2 Hz, *Ph*–P), 136.2 (d, ^1J(^{13}C–^{31}P) = 99 Hz, C$_i$; Ph–P), 136.6 (s, ^2J(^{13}C–$^{117/119}$Sn) = 41 Hz, C$_o$; Ph–Sn), 139.4 (s, ^1J(^{13}C–$^{117/119}$Sn) = 493/514 Hz, C$_i$; Ph–Sn). **^{31}P{^{1}H} NMR** (121.50, $CDCl_3$): *δ* 33.2 (s, ^2J(^{31}P–$^{117/119}$Sn) = 58 Hz, ^1J(^{31}P–^{13}C$_{Ph}$) = 99 Hz). **^{29}Si{^{1}H} NMR** (59.63, $CDCl_3$): *δ* 3.0 (^2J(^{29}Si–$^{117/119}$Sn) = 23 Hz). **^{119}Sn{^{1}H} NMR** (111.92, $CDCl_3$): *δ* –68 (d, ^2J(^{119}Sn–^{31}P) = 58 Hz).

Synthesis of Ph$_2$P(O)CH$_2$SnCy$_3$, 3

The compound was synthesized according to the procedure (D) using Cy$_3$SnCl as the organotin halide. Mp 178.0–180.0 °C; yield 60%; single crystals of **3** suitable for X-ray diffraction analysis were obtained by slow evaporation of a solution of the compound in CH_2Cl_2/ethyl acetate.

Anal. Calcd for $C_{31}H_{45}OPSn$ (583.36 g/mol): C, 63.83; H, 7.77. Found: C, 63.3; H, 7.7. **^{1}H NMR** (300.13, $CDCl_3$): *δ* 1.63 (d, 2H, $^{2}J(^{1}H–^{31}P)$ = 11.7 Hz, PC*H*$_2$Sn), 1.12–1.81 (m, 33H, Cy H), 7.38–7.42 (m, 6H, Ar H (*meta, para*), 7.76–7.83 (m, 4H, Ar H (*orto*)). **^{13}C{^{1}H} NMR** (75.48, $CDCl_3$): *δ* 7.2 (d, $^{1}J(^{13}C–^{31}P)$ = 68 Hz, P*C*H$_2$Sn), 27.0 (C*4*; Cy–Sn), 27.8 ($^{1}J(^{13}C–^{117/119}Sn)$ = 327/343 Hz, C1; Cy–Sn), 29.1 ($J(^{13}C–^{117/119}Sn)$ = 61 Hz, Cy–Sn), 31.9 ($J(^{13}C–^{117/119}Sn)$ = 17 Hz, Cy–Sn), 128.2 ($J(^{13}C–^{31}P)$ = 11 Hz, Ph–P), 130.3 ($J(^{13}C–^{31}P)$ = 9 Hz, Ph–P), 130.7 ($J(^{13}C–^{31}P)$ = 3 Hz, Ph–P), 137.4 ($^{1}J(^{13}C–^{31}P)$ = 98 Hz, C$_i$; Ph–P). **^{31}P{^{1}H} NMR** (121.50, $CDCl_3$): *δ* 33.9 (s, $^{2}J(^{31}P–^{117/119}Sn)$ = 49 Hz). **^{119}Sn{^{1}H} NMR** (111.92, $CDCl_3$): *δ* –63 (d, $^{2}J(^{119}Sn–^{31}P)$ = 49 Hz).

Synthesis of {Ph$_2$P(O)CH$_2$}$_2$SnPh$_2$, 4

The compound was synthesized according to the procedure (D) using Ph_2SnCl_2 as the organotin halide with (0.45 eq) Ph_2SnCl_2 instead of (0.90 eq) since the organotion compound is bifunctional. The extraction of the aqueous phase was performed with CH_2Cl_2 instead of diethyl ether. M.p. 153.5–156.5 °C; yield 9%.

^{1}H NMR (400.13, $CDCl_3$): *δ* 2.34 (d, 2H, $^{2}J(^{1}H–^{31}P)$ = 11.0 Hz, $^{2}J(^{1}H–^{117/119}Sn)$ = 60.6/63.0 Hz, PC*H*$_2$Sn), 7.13–7.67 (m, 30H, Ar H). **^{13}C{^{1}H} NMR** (100.63, $CDCl_3$): *δ* 14.0 (d, $^{1}J(^{13}C–^{31}P)$ = 67 Hz, P*C*H$_2$Sn), 128.0 (s, $^{3}J(^{13}C–^{117/119}Sn)$ = 57 Hz, C$_m$; Ph–Sn), 128.2 (d, $J(^{13}C–^{31}P)$ = 13 Hz, *Ph*–P), 128.7 (s, C$_p$; Ph–Sn), 130.2 (d, $J(^{13}C–^{31}P)$ = 10 Hz, *Ph*–P), 130.9 (d, $^{4}J(^{13}C–^{31}P)$ = 3 Hz, C$_m$; Ph–P), 135.6 (d, $^{1}J(^{13}C–^{31}P)$ = 100 Hz, C$_i$; Ph–P), 136.5 (s, $^{2}J(^{13}C–^{117/119}Sn)$ = 43 Hz, C$_o$; Ph–Sn), 137.1 (s, C$_i$; Ph–Sn). **^{31}P{^{1}H} NMR** (81.02, $CDCl_3$): *δ* 33.7 (s, $^{2}J(^{31}P–^{117/119}Sn)$ = 64 Hz, $^{1}J(^{31}P–^{13}C_{Ph})$ = 100 Hz). **^{119}Sn{^{1}H} NMR** (111.92, $CDCl_3$): *δ* –93 (t, $^{2}J(^{119}Sn–^{31}P)$ = 64 Hz). **Electrospray MS**: m/z (%), positive mode, 705.2 (100, $[M + H]^+$), 1427.5 (10).

Synthesis of Ph$_2$P(O)CH$_2$SnPh$_2$I, 5

The compound was synthesized according to the iodination procedure (A). The residue was washed with hexane and a small amount of cold chloroform. Drying in vacuo gave compound **5** (yield 96%) as yellowish solid of mp 194.5–195.5 °C. Single crystals of **5** suitable for X-ray diffraction analysis were obtained by slow evaporation of a solution of the compound in hot CH_2Cl_2/hexane.

Anal. Calcd for $C_{25}H_{22}IOPSn$ (1230.03 g/mol): C, 48.82; H, 3.61. Found: C, 48.7; H, 3.6. **^{1}H NMR** (300.13, $CDCl_3$): *δ* 3.02 (d, 2H, $^{2}J(^{1}H–^{31}P)$ = 9.2 Hz, $^{2}J(^{1}H–^{117/119}Sn)$ = 73.2/76.1 Hz, PC*H*$_2$Sn), 7.30–7.92 (m, 20H, Ar H). **^{13}C{^{1}H} NMR** (75.48, $CDCl_3$): *δ*

27.1 (d, $^{1}J(^{13}C–^{31}P)$ = 63 Hz, P*C*H$_2$Sn), 128.5 (s, $^{3}J(^{13}C–^{117/119}Sn)$ = 73 Hz, C$_m$; Ph–Sn), 128.6 (*Ph*–P), 129.6 (s, C$_p$; Ph–Sn), 130.5 (d, $J(^{13}C–^{31}P)$ = 11 Hz, *Ph*–P), 131.8 (d, $J(^{13}C–^{31}P)$ = 2, *Ph*–P), 133.2 (d, $^{1}J(^{13}C–^{31}P)$ = 101 Hz, C$_i$; Ph–P), 136.1 (s, $^{2}J(^{13}C–^{117/119}Sn)$ = 54 Hz, C$_o$; Ph–Sn), 138.1 (s, C$_i$; Ph–Sn). **$^{31}P\{^{1}H\}$ NMR** (121.50, CDCl$_3$): *δ* 37.8 (s, $^{2}J(^{31}P–^{117/119}Sn)$ = 75 Hz). **$^{119}Sn\{^{1}H\}$ NMR** (111.92, CDCl$_3$)**:** *δ* –148 (broad signal). **Electrospray MS**: m/z (%), positive mode, 1479.6 (100, [({Ph$_2$P(O)CH$_2$}Ph$_2$Sn)$_3$μ$_3$-O]$^+$), 489.1 (5, [M – I]$^+$), 993.2 (5, [2M – 2I + OH]$^+$), negative mode, 127.0 (100, [I]$^–$), 582.8 (15, [M – I + 2OH]$^–$), 380.8 (9, [I$_3$]$^–$).

Synthesis of Ph$_2$P(O)CH$_2$SnPh$_2$Br, 6

The compound was synthesized according to the bromination procedure (B). The residue was washed with hexane and a small amount of cold chloroform. Drying in vacuo gave compound **6** (yield 97%) as white solid of mp 195.5–197.5 °C. Single crystals of **6** suitable for X-ray diffraction analysis were obtained by slow evaporation of a solution of the compound in hot CH$_2$Cl$_2$/hexane.

Anal. Calcd for C$_{25}$H$_{22}$BrOPSn (1136.03 g/mol): C, 52.86; H, 3.90. Found: C, 52.6; H, 3.9. **^{1}H NMR** (300.13, CDCl$_3$): *δ* 2.88 (d, 2H, $^{2}J(^{1}H–^{31}P)$ = 10.6 Hz, $^{2}J(^{1}H–^{117/119}Sn)$ = 79.8 Hz, PC*H*$_2$Sn), 7.22–7.79 (m, 20H, Ar H). **$^{13}C\{^{1}H\}$ NMR** (75.48, CDCl$_3$): *δ* 25.6 (d, $^{1}J(^{13}C–^{31}P)$ = 64 Hz, P*C*H$_2$Sn), 128.3 (s, $^{3}J(^{13}C–^{117/119}Sn)$ = 76 Hz, C$_m$; Ph–Sn), 128.6 (d, $J(^{13}C–^{31}P)$ = 12 Hz, *Ph*–P), 129.2 (s, C$_p$; Ph–Sn), 130.6 (d, $J(^{13}C–^{31}P)$ = 11 Hz, *Ph*–P), 132.0 (d, $J(^{13}C–^{31}P)$ = 2 Hz, *Ph*–P), 132.7 (d, $^{1}J(^{13}C–^{31}P)$ = 102 Hz, C$_i$; Ph–P), 135.8 (s, $^{2}J(^{13}C–^{117/119}Sn)$ = 55 Hz, C$_o$; Ph–Sn), 141.2 (s, C$_i$; Ph–Sn). **$^{31}P\{^{1}H\}$ NMR** (121.50, CDCl$_3$): *δ* 40.8 (s, $^{2}J(^{31}P–^{117/119}Sn)$ = 76 Hz). **$^{119}Sn\{^{1}H\}$ NMR** (111.92, CDCl$_3$): No resounance (because of the very poor solubility). **Electrospray MS**: m/z (%), positive mode, 258.1 (100, [Ph$_2$P(O)Me + H + MeCN]$^+$), 217.1 (30, [Ph$_2$P(O)Me + H]$^+$), 489.1 (27, [M – Br]$^+$), 530.1 (15, [M – Br + MeCN]$^+$), 567.1 (10), 569.1 (5, [M + H]$^+$), 705.2 (12, [M – Br + Ph$_2$P(O)Me]$^+$), 993 (2, [2M – 2Br + OH]$^+$), 1021.2 (7), 1055.2 (4, [2M – Br]$^+$).

Synthesis of Ph$_2$P(O)CH$_2$SnPhBr$_2$, 7

The compound was synthesized according to the bromination procedure (B). The residue was washed with hexane and cold dichloromethane. Drying in vacuo gave compound **7** (yield 99%) as white solid which decompose over 248 °C. The very poor

solubility of the compound in common organic solvents prohibits recording the NMR spectra.

Anal. Calcd for $C_{19}H_{17}Br_2OPSn$ (570.81 g/mol): C, 39.98; H, 3.00. Found: C, 40.0; H, 3.1. **Electrospray MS**: m/z (%), positive mode, 1281.2 (100, $[(\{Ph_2P(O)CH_2\}PhSnO)_3 + H]^+$), 1065.1 (96, $[(\{Ph_2P(O)CH_2\}PhSnO)_3 – Ph_2P(O)Me + H]^+$), 1203 (43), 855.1 (12, $[(\{Ph_2P(O)CH_2\}PhSnO)_2 + H]^+$).

Synthesis of $\{Ph_2P(O)CH_2\}(Me_3SiCH_2)PhSnI$, 8

The compound was synthesized according to the iodination procedure (A). The residue was washed with hexane followed by drying in vacuo to give compound **8** (yield 98%) as yellowish solid of mp 115–116 °C.

Anal. Calcd for $C_{23}H_{28}IOPSiSn$ (625.13 g/mol): C 44.19; H 4.51. Found: C 44.6; H 4.4. **^{1}H NMR** (300.13, $CDCl_3$): δ 0.02 (s, 9H, *Me*$_3$Si), 0.95 (s, 2H, $^2J(^1H–^{117/119}Sn)$ = 90.4 Hz, Si*C*H$_2$Sn), 2.80 (d, 2H, $^2J(^1H–^{31}P)$ = 8.8 Hz, $^2J(^1H–^{117/119}Sn)$ = 69.2 Hz, P*C*H$_2$Sn), 7.28–7.94 (m, 15H, Ar H). **^{13}C{^{1}H} NMR** (100.63, $CDCl_3$): δ 1.2 ($^1J(^{13}C–^{29}Si)$ = 52 Hz, *Me*$_3$Si), 6.3 (Si*C*H$_2$Sn), 25.4 (d, $^1J(^{13}C–^{31}P)$ = 63 Hz, P*C*H$_2$Sn), 128.3 (s, $^3J(^{13}C–^{117/119}Sn)$ = 68 Hz, C$_m$; Ph–Sn), 128.6 (d, $J(^{13}C–^{31}P)$ = 12 Hz, *Ph*–P), 129.4 (s, C$_p$; Ph–Sn), 130.4 (d, $J(^{13}C–^{31}P)$ = 10 Hz, *Ph*–P), 131.7 (*Ph*–P), 134.1 (d, $^1J(^{13}C–^{31}P)$ = 100 Hz, C$_i$; Ph–P), 136.0 (s, $^2J(^{13}C–^{117/119}Sn)$ = 54 Hz, C$_o$; Ph–Sn), 138.0 (s, C$_i$; Ph–Sn). **^{31}P{^{1}H} NMR** (121.50, $CDCl_3$): δ 36.0 (s, $^2J(^{31}P–^{117/119}Sn)$ = 60 Hz). **^{29}Si{^{1}H} NMR** (59.63, $CDCl_3$): δ 3.5 (s, $^2J(^{29}Si–^{117/119}Sn)$ = 34 Hz). **^{119}Sn{^{1}H} NMR** (111.90, $CDCl_3$): δ –74 (broad signal). **Electrospray MS**: m/z (%), positive mode, 217.0 (100, $[Ph_2P(O)Me + H]^+$), 548.9 (83, $[M – I + H_2O + MeOH]^+$), 499.1 (54, $[M – I]^+$, 627.0 (10, $[M + H]^+$), 649.0 (7, $[M + Na]^+$), 1123.0 (2, $[2M – I]^+$), 1251.0 (3, $[2M + H]^+$), 1272.9 (3, $[2M + Na]^+$).

Synthesis of $\{Ph_2P(O)CH_2\}(Me_3SiCH_2)PhSnBr$, 9

The compound was synthesized according to the bromination procedure (B). The residue was washed with hexane and a small amount of cold dichloromethane. Drying in vacuo afforded compound **9** (yield 98%) as white solid of mp 147.5–149.5 °C.

Anal. Calcd for $C_{23}H_{28}BrOPSiSn$ (578.13 g/mol): C, 47.78; H, 4.88. Found: C, 47.8; H, 4.9. **^{1}H NMR** (400.13, $CDCl_3$): δ 0.00 (s, 9H, *Me*$_3$Si), 0.72 (s, 2H, $^2J(^1H–^{117/119}Sn)$ = 94.6 Hz, Si*C*H$_2$Sn), 2.76 (d, 2H, $^2J(^1H–^{31}P)$ = 9.3 Hz, $^2J(^1H–^{117/119}Sn)$ = 72.6 Hz,

PC*H*$_2$Sn), 7.31–7.90 (m, 15H, Ar H). **^{13}C{^{1}H} NMR** (100.63, $CDCl_3$): *δ* 1.2 (^1J(^{13}C–^{29}Si) = 52 Hz, ^3J(^{13}C–$^{117/119}$Sn) = 25 Hz, *Me*$_3$Si), 7.5 (^1J(^{13}C–$^{117/119}$Sn) = 346/356 Hz, Si*C*H$_2$Sn), 25.7 (d, ^1J(^{13}C–^{31}P) = 64 Hz, P*C*H$_2$Sn), 128.3 (s, C$_m$; Ph–Sn), 128.6 (d, J(^{13}C–^{31}P) = 13 Hz, *Ph*–P), 129.4 (s, C$_p$; Ph–Sn), 130.5 (d, J(^{13}C–^{31}P) = 10 Hz, *Ph*–P), 131.8 (*Ph*–P), 133.8 (d, ^1J(^{13}C–^{31}P) = 100 Hz, C$_i$; Ph–P), 135.8 (s, ^2J(^{13}C–$^{117/119}$Sn) = 55 Hz, C$_o$; Ph–Sn), 140.4 (s, C$_i$; Ph–Sn). **^{31}P{^{1}H} NMR** (121.49, $CDCl_3$): *δ* 37.5 (s, ^2J(^{31}P–$^{117/119}$Sn) = 64 Hz). **^{29}Si{^{1}H} NMR** (59.63, $CDCl_3$): *δ* 3.2 (s, ^2J(^{29}Si–$^{117/119}$Sn) = 35 Hz). **^{119}Sn{^{1}H} NMR** (111.90, $CDCl_3$): *δ* –41 (broad, $v_{1/2}$ = 795 Hz). **Electrospray MS**: m/z (%), positive mode, 499.1 (100, $[M - Br]^+$), 601.1 (2, $[M + Na]^+$), 637.2 (3, $[M + 2\ H_2O + Na]^+$), 1095.2 (5, $[2M - Br + H_2O]^+$), 1312.3 (5, $[2M - Br + H_2O + Ph_2P(O)Me]^+$).

Synthesis of {Ph$_2$P(O)CH$_2$}(Me$_3$SiCH$_2$)SnBr$_2$, 10

The compound was synthesized according to the bromination procedure (B). The residue was washed with hexane and a small amount of cold dichloromethane. Drying in vacuo afforded compound **10** (yield 98%) as white solid of mp186.0–188.0 °C.

Anal. Calcd for $C_{17}H_{23}Br_2OPSiSn$ (580.93 g/mol): C, 35.15; H, 3.99. Found: C, 35.9; H, 4.0. **^{1}H NMR** (400.13, $CDCl_3$): *δ* 0.03 (s, 9H, *Me*$_3$Si), 0.75 (s, 2H, ^2J(^{1}H–$^{117/119}$Sn) = 118.9/121.1 Hz, SiC*H*$_2$Sn), 3.00 (d, 2H, ^2J(^{1}H–^{31}P) = 11.0 Hz, ^2J(^{1}H–$^{117/119}$Sn) = 87.1 Hz, PC*H*$_2$Sn), 7.47–7.78 (m, 10H, Ar H). **^{13}C{^{1}H} NMR** (75.48, $CDCl_3$): *δ* 1.1 (s, ^1J(^{13}C–^{29}Si) = 52 Hz, ^3J(^{13}C–$^{117/119}$Sn) = 36 Hz, *Me*$_3$Si), 19.8 (s, Si*CH*$_2$Sn), 32.1 (d, ^1J(^{13}C–^{31}P) = 64 Hz, P*C*H$_2$Sn), 128.9 (d, J(^{13}C–^{31}P) = 13 Hz, *Ph*–P), 131.2 (d, J(^{13}C–^{31}P) = 11 Hz, *Ph*–P), 131.7 (d, ^{1}J(^{13}C–^{31}P) = 105 Hz, C$_i$; Ph–P), 132.8 (d, J(^{13}C–^{31}P) = 2 Hz, *Ph*–P). **^{31}P{^{1}H} NMR** (121.49, $CDCl_3$): *δ* 39.6 (s, ^2J(^{31}P–$^{117/119}$Sn) = 88 Hz). **^{29}Si{^{1}H} NMR** (59.63, $CDCl_3$): *δ* = 2.8 (s, ^2J(^{29}Si–$^{117/119}$Sn) = 52 Hz). **^{119}Sn{^{1}H} NMR** (111.90, $CDCl_3$): *δ* –206 (broad, $v_{1/2}$ = 538 Hz). **Electrospray MS**: m/z (%), positive mode, 1311.3 (100, $[(\{Ph_2P(O)CH_2\}\{Me_3SiCH_2\}SnO)_3 + H]^+$), 1375.1 (16, $[(\{Ph_2P(O)CH_2\}\{Me_3SiCH_2\}SnO)_3 + 2\ MeOH + H]^+$), 1095.2 (56, $[(\{Ph_2P(O)CH_2\}\{Me_3SiCH_2\}SnO)_3 - Ph_2P(O)CH_2]^+$), 939.0 (24, $[(\{Ph_2P(O)CH_2\}\{Me_3SiCH_2\}SnO)_2 + 2\ MeOH + H]^+$), 875.1 (10, $[(\{Ph_2P(O)CH_2\}\{Me_3SiCH_2\}SnO)_2 + H]^+$).

Recrystallization of compound **10** from a solution in CH_2Cl_2/ethyl acetate at aerobic conditions afforded after a few weeks the hydrolysis product $(Me_3SiCH_2Sn)_{12}O_{14}(OH)_6Br_2$, **10a**, as colorless crystals of mp >300.

Anal. Calcd for $C_{48}H_{138}Br_2O_{20}Si_{12}Sn_{12}$ (2956.72 g/mol): C, 19.50; H, 4.70. Found: C, 19.8; H, 4.6. **Electrospray MS**: m/z (%), positive mode, 1398.9 (100, $[(Me_3SiCH_2Sn)_{12}O_{14}(OH)_6]^{2+}$), 1371.1 (32, $[(Me_3SiCH_2Sn)_{12}O_{17}]^{2+}$), negative mode, 81.2 (100, $[Br]^-$).

Synthesis of $Ph_2P(O)CH_2SnPhCl_2$, 11

The compound was synthesized according to the chlorination procedure (C). The residue was washed with hexane and cold dichloromethane affording, after drying in vacuo, compound **11** (yield 98%) as white solid that decomposes over 265 °C. The compound is very poor soluble in common organic solvents, so no NMR spectra could be recorded.

Anal. Calcd for $C_{19}H_{17}Cl_2OPSn$ (481.91 g/mol): C, 47.35; H, 3.56. Found: C, 47.5; H, 3.5. **Electrospray MS**: m/z (%), positive mode, 1281.2 (100, $[(\{Ph_2P(O)CH_2\}PhSnO)_3 + H]^+$), 1299.1 (28, $[(\{Ph_2P(O)CH_2\}PhSnO)_3 + H_2O + H]^+$), 217 (34, $[Ph_2P(O)Me + H]^+$).

Synthesis of $\{Ph_2P(O)CH_2\}(Me_3SiCH_2)SnCl_2$, 12

The compound was synthesized according to the chlorination procedure (C). The residue was washing with cold hexane and dried in vacuo giving compound **12** (yield 94%) as white solid of mp 221–223°C.

^{1}H NMR (200.13, $CDCl_3$): δ 0.00 (s, 9H, *Me*$_3$Si), 0.50 (s, 2H, $^2J(^1H–^{117/119}Sn)$ = 123.6 /129.0 Hz, SiC*H*$_2$Sn), 2.79 (d, 2H, $^2J(^1H–^{31}P)$ = 11.7 Hz, $^2J(^1H–^{117/119}Sn)$ = 91.2 Hz, PC*H*$_2$Sn), 7.42–7.78 (m, 10H, Ar H). **$^{31}P\{^1H\}$ NMR** (81.02, $CDCl_3$): δ 41.0 (s (broad), $^2J(^{31}P–^{117/119}Sn)$ = 96 Hz). **$^{29}Si\{^1H\}$ NMR** (59.63, $CDCl_3$): δ 2.5 (s, $^2J(^{29}Si–^{117/119}Sn)$ = 53 Hz). **$^{119}Sn\{^1H\}$ NMR** (111.90, $CDCl_3$): δ = –151 (broad, $v_{1/2}$ = 433 Hz). **Electrospray MS**: m/z (%), positive mode, 1311.3 (100, $[(\{Ph_2P(O)CH_2\}\{Me_3SiCH_2\}SnO)_3 + H]^+$), 1095.2 (15, $[(\{Ph_2P(O)CH_2\}\{Me_3SiCH_2\}SnO)_3 – Ph_2P(O)CH_2]^+$), 875.2 (4, $[(\{Ph_2P(O)CH_2\}\{Me_3SiCH_2\}SnO)_2 + H]^+$).

Synthesis of $Ph_2P(O)CH_2SnCl_3$, 13

(0.36 g, 1.37 mmol) of tin tetrachloride was added to a solution of **3** (0.80 g, 1.37 mmol) in acetonitrile (75 ml) and pentane (50 mL) and the mixture was stirred for two days at room temperature. The white precipitate was separated and washed with

CH_2Cl_2 before it was extensively evaporated in vacuo to give compound **13** (0.57 g, 94%) as white solid of mp 262.5–264.5 °C.

Anal. Calcd for $C_{13}H_{12}Cl_3OPSn$ (440.26 g/mol): C, 35.47; H, 2.75. Found: C, 35.3; H, 2.7. **Electrospray MS**: m/z (%), positive mode, 152 (100), 1118.9 (35, $[\{Ph_2P(O)CH_2Sn(O)OH\}_3 + H_2O + H]^+$), 1157.0 (8, $[\{Ph_2P(O)CH_2Sn(O)OH\}_3 + H_2O + K]^+$).

Compound **13** was dissolved in hot acetone and exposed to air to give after few days single crystals of the acetone solvate of the hydolysis product $Ph_2P(O)CH_2(Cl_2)Sn(\mu_2\text{-}OH)_2Sn(Cl_2)CH_2P(O)Ph_2{\cdot}2C_3H_6O$, **13a**, which decompose over 231–234 °C. The crystals were suitable for X-ray diffraction analysis.

Anal. Calcd for $C_{26}H_{26}Cl_4O_4P_2Sn_2$ (843.63 g/mol): C 37.02; H 3.11. Found: C 35.7; H 3.2.

Synthesis of $[\{Ph_2P(O)CH_2\}Ph(\mu\text{-}OH)Sn]_3(\mu_3\text{-}O)(\mu_3\text{-}Br)$, 14

A mixture of **7** (1.40 g, 2.45 mmol) and di-*tert*-butyltin oxide (0.61 g, 2.45 mmol) in dichloromethane (50 mL) was stirred at room temperature for two hours. After evaporating the solvent in vacuo the residue was washed more times with cold hexane. Drying in vacuo gave **14** (1.09 g, 96 %) as white solid of mp 131.0–133.0 °C. Single crystals of **14** suitable for X-ray diffraction analysis were obtained by slow evaporation of a solution of the compound in CH_2Cl_2/hexane.

Anal. Calcd for $C_{57}H_{54}BrO_7P_3Sn_3$ (1380.95 g/mol): C, 49.61; H, 3.94. Found: C, 49.8; H, 4.0. **^{1}H NMR** (300.13, $CDCl_3$): δ 1.92 (d, 2H, $^2J(^1H–^{31}P)$ = 11.0 Hz, PC*H*$_2$Sn), 5.98 (s, 1H, O*H*), 7.21–7.83 (m, 15H, Ar H). **^{13}C{^{1}H} NMR** (100.63, $CDCl_3$): δ 21.5 (d, $^1J(^{13}C–^{31}P)$ = 62 Hz, P*C*H$_2$Sn), 127.9 ($^3J(^{13}C–^{117/119}Sn)$ = 103/108 Hz, C$_m$; Ph–Sn), 128.1 (C$_p$; Ph–Sn), 128.2 (d, $J(^{13}C–^{31}P)$ = 13 Hz, *Ph*–P), 130.9 (d, $J(^{13}C–^{31}P)$ = 11 Hz, *Ph*–P), 131.0 (d, $J(^{13}C–^{31}P)$ = 11 Hz, *Ph*–P), 131.7 (d, $J(^{13}C–^{31}P)$ = 3 Hz, *Ph*–P), 131.7 (d, $J(^{13}C–^{31}P)$ = 3 Hz, *Ph*–P), 132.4 (d, $^1J(^{13}C–^{31}P)$ = 107 Hz, C$_i$; Ph–P), 134.4 ($^2J(^{13}C–^{117/119}Sn)$ = 68 Hz, C$_o$; Ph–Sn), 134.6 (d, $^1J(^{13}C–^{31}P)$ = 104 Hz, C$_i$; Ph–P), 150.6 (C$_i$; Ph–Sn). **^{31}P{^{1}H} NMR** (121.50, $CDCl_3$): δ 52.2 (s, $^2J(^{31}P–^{117/119}Sn)$ = 96/100 Hz, $^2J(^{31}P–^{117/119}Sn)$ = 109/115 Hz). **^{119}Sn{^{1}H} NMR** (111.92, $CDCl_3$): δ –442 (dd, $^2J(^{119}Sn–^{31}P)$ = 101 Hz, $^2J(^{119}Sn–^{31}P)$ = 114 Hz, $^2J(^{119}Sn–^{117/119}Sn)$ = 147 Hz). **Electrospray MS**: m/z (%), positive mode, 1281.2 (100, $[(\{Ph_2P(O)CH_2\}PhSnO)_3 + H]^+$), 1065.2 (16, $[(\{Ph_2P(O)CH_2\}PhSnO)_3 – Ph_2P(O)CH_2]^+$), 217.1 (19, $[Ph_2P(O)Me + H]^+$), negative mode, 81.1 (100, $[Br]^-$).

Synthesis of [{$Ph_2P(O)CH_2$}Ph(μ-OH)Sn]$_3$(μ_3-O)(μ_3-I), 15

A mixture of **14** (57 mg, 0.041 mmol) and Sodium iodide (6.2 mg, 0.041 mmol) in dichloromethane (40 mL) was stirred overnight at room temperature. The mixture was filtrated and the filtrate was evaporated in vacuo to give compound **15** (56 mg, 95%) as light yellowish solid of mp 146–148 °C. Single crystals of (**15**·$CHCl_3$) suitable for X-ray diffraction analysis were obtained by slow evaporation of a solution of the compound in $CHCl_3$/toluene.

Anal. Calcd for $C_{58}H_{55}Cl_3IO_7P_3Sn_3$ (1547.33 g/mol): C, 45.05; H, 3.59. Found: C, 45.8; H, 3.7. **^{1}H NMR** (300.13, $CDCl_3$): δ 1.93 (d, 2H, $^2J(^1H–^{31}P)$ = 11.3 Hz, PCH_2Sn), 5.54 (s, 1H, O*H*), 7.20–7.87 (m, 15H, Ar H). **^{13}C{^{1}H} NMR** (100.63, $CDCl_3$): δ 21.7 (d, $^1J(^{13}C–^{31}P)$ = 62 Hz, P*C*H_2Sn), 127.9 ($^3J(^{13}C–^{117/119}Sn)$ = 103/109 Hz, C$_m$; Ph–Sn), 128.2 (d, $J(^{13}C–^{31}P)$ = 5 Hz, *Ph*–P), 128.3 (C$_p$; Ph–Sn), 128.4 (d, $J(^{13}C–^{31}P)$ = 6 Hz, Ph–P), 130.9 (d, $J(^{13}C–^{31}P)$ = 10 Hz, *Ph*–P), 131.0 (d, $J(^{13}C–^{31}P)$ = 11 Hz, *Ph*–P), 131.7 (d, $J(^{13}C–^{31}P)$ = 3 Hz, *Ph*–P), 132.3 (d, $^1J(^{13}C–^{31}P)$ = 106 Hz, C$_i$; Ph–P) 131.8 (d, $J(^{13}C–^{31}P)$ = 3 Hz, *Ph*–P), 134.4 ($^2J(^{13}C–^{117/119}Sn)$ = 70 Hz, C$_o$; Ph–Sn), 134.6 (d, $^1J(^{13}C–^{31}P)$ = 104 Hz, C$_i$; Ph–P), 150.4 (C$_i$; Ph–Sn). **^{31}P{^{1}H} NMR** (121.50, $CDCl_3$): δ 52.1 (s, $^2J(^{31}P–^{117/119}Sn)$ = 96/ 100 Hz, $^2J(^{31}P–^{117/119}Sn)$ = 110/115 Hz). **^{119}Sn{^{1}H} NMR** (111.92, $CDCl_3$): δ –442 (dd, $^2J(^{119}Sn–^{31}P)$ = 101 Hz, $^2J(^{119}Sn–^{31}P)$ = 114 Hz, $^2J(^{119}Sn–^{117/119}Sn)$ = 148 Hz). **Electrospray MS**: m/z (%), positive mode, 1281.2 (100, [({$Ph_2P(O)CH_2$}PhSnO)$_3$ + H]$^+$), 1065.2 (5, [({$Ph_2P(O)CH_2$}PhSnO)$_3$ – $Ph_2P(O)CH_2$]$^+$), 151.1 (10), 217.1 (5, [$Ph_2P(O)Me$ + H]$^+$), negative mode, 127.0 (100, [I]$^–$), 380.7 (11, [I_3]$^–$).

Reaction of compound 11 with one molar equivalent di-*tert*-butyltin oxide affording the O-capped cluster, [{$Ph_2P(O)CH_2$}Ph(μ-OH)Sn]$_3$(μ_3-O)(μ_3-Cl), 16, and the tetraorganodistannoxane, [{$Ph_2P(O)CH_2$}Ph(OH)SnOSn(Cl)*t*-Bu_2]$_2$, 18

A mixture of **11** (96 mg, 0.20 mmol) and di-*tert*-butyltin oxide (50 mg, 0.20 mmol) in $CDCl_3$ (1.2 mL) was stirred overnight at room temperature then ^{31}P and ^{119}Sn NMR spectra were recorded.

^{31}P{^{1}H} NMR (121.50, $CDCl_3$): δ 52.2 (78%, s, $^2J(^{31}P–^{117/119}Sn)$ = 95/99 Hz, $^2J(^{31}P–^{117/119}Sn)$ = 108/112 Hz, **16**), 35.4 (19%, s, $^2J(^{31}P–^{117/119}Sn)$ = 39 Hz, **18**), 30.9 (3%, s, $Ph_2P(O)Me$). **^{119}Sn{^{1}H} NMR** (111.88, $CDCl_3$): δ 54 (s, *t*-Bu_2SnCl_2), –442 (77%, dd, $^2J(^{119}Sn–^{31}P)$ = 99 Hz, $^2J(^{119}Sn–^{31}P)$ = 112 Hz, $^2J(^{119}Sn–^{117/119}Sn)$ = 143 Hz, **16**), –

215 (2%, s, **18**), –217 (10%, s, **18**), –273 (10%, d, $^{2}J(^{119}Sn–^{31}P)$ = 41 Hz, **18**), –276 (2%, d, $^{2}J(^{119}Sn–^{31}P)$ = 43 Hz, **18**).

The last solution was dryed in vacuo and the residue was washed with cold hexane. Recrystallization from $CHCl_3$/toluene afforded single crystals of (**16**·$CHCl_3$) of mp 140–141 °C suitable for X-ray diffraction analysis.
Anal. Calcd for $C_{58}H_{55}Cl_4O_7P_3Sn_3$ (1455.88 g/mol): C 47.88; H 3.81. Found: C 46.3; H 4.0. **Electrospray MS**: m/z (%), positive mode, 1281.2 (100, $[(\{Ph_2P(O)CH_2\}PhSnO)_3 + H]^+$), 1299.2 (10, $[(\{Ph_2P(O)CH_2\}PhSnO)_3 + H_2O + H]^+$), 1065.1 (6, $[(\{Ph_2P(O)CH_2\}PhSnO)_3 – Ph_2P(O)CH_2]^+$).

Reaction of compound 10 with one molar equivalent di-*tert*-butyltin oxide affording the O-capped cluster, [{$Ph_2P(O)CH_2$}(Me_3SiCH_2)(μ-OH)Sn]$_3$(μ_3-O)(μ_3-Br), 17, and the tetraorganodistannoxane, [{$Ph_2P(O)CH_2$}(Me_3SiCH_2)(OH)SnOSn(Br)*t*-Bu_2]$_2$, 19

A mixture of **10** (150 mg, 0.26 mmol) and di-*tert*-butyltin oxide (65 mg, 0.26 mmol) in dichloromethane (25 mL) was stirred at room temperature for 2 hours. The solvent was evaporation in vacuo before ^{31}P, ^{119}Sn NMR spectra were recorded.
$^{31}P\{^{1}H\}$ NMR (121.50, $CDCl_3$): δ 49.7 (50%, s, $^{2}J(^{31}P–^{117/119}Sn)$ = 102/107 Hz, $^{2}J(^{31}P–^{117/119}Sn)$ = 120/126 Hz, **17**), 33.2 (5%, **19**), 33.1 (4%, **19**), 30.9 (8%, $Ph_2P(O)Me$), 5.4 (22%, s), –2.5 (6%, s). **$^{119}Sn\{^{1}H\}$ NMR** (111.86, $CDCl_3$)**:** δ –389 (dd, $^{2}J(^{119}Sn–^{31}P)$ = 108 Hz, $^{2}J(^{119}Sn–^{31}P)$ = 125 Hz, $^{2}J(^{119}Sn–^{117/119}Sn)$ = 136 Hz, **17**), 76 (*t*-Bu_2SnBr_2), –201 (s, **19**) , –202 (s, **19**), –210 (d, **19**), –211 (d, **19**).
Electrospray MS: m/z (%), positive mode, 217.1 (100, $[Ph_2P(O)Me + H]^+$), 1095.1 (5, $[(\{Ph_2P(O)CH_2\}\{Me_3SiCH_2\}SnO)_3 – Ph_2P(O)CH_2]^+$).

Synthesis of [{$Ph_2P(O)CH_2$}Ph(OH)SnOSn(Cl)*t*-Bu_2], 18

A mixture of **11** (96 mg, 0.20 mmol) and di-*tert*-butyltin oxide (100 mg, 0.40 mmol) in $CDCl_3$ (1.4 mL) was stirred overnight at room temperature before ^{31}P and ^{119}Sn NMR spectra were recorded.
$^{31}P\{^{1}H\}$ NMR (121.50, $CDCl_3$): δ 35.4 (s, $^{2}J(^{31}P–^{117/119}Sn)$ = 38 Hz). **$^{119}Sn\{^{1}H\}$ NMR** (111.92, $CDCl_3$): δ –30 (s, *t*-$Bu_2Sn(OH)Cl$), –215 (10%, s, $^{4}J(^{119}Sn_{exo}–^{117/119}Sn_{exo})$ = 48 Hz, $^{2}J(^{119}Sn_{exo}–^{117/119}Sn_{endo})$ = 276 Hz, *t*-Bu_2Sn), –217 (40%, s, $^{2}J(^{119}Sn_{exo}–^{117/119}Sn_{endo})$ = 280/299 Hz, $^{2}J(^{119}Sn_{exo}–^{117/119}Sn_{exo})$ = 56 Hz), –273 (40%, d, $^{2}J(^{119}Sn–$

^{31}P) = 39 Hz, ^{2}J(^{119}Sn$_{endo}$–$^{117/119}$Sn$_{exo}$) = 280/297 Hz, ^{2}J(^{119}Sn$_{endo}$–$^{117/119}$Sn$_{endo}$) = 58 Hz), –276 (10%, d, ^{2}J(^{119}Sn–^{31}P) = 43 Hz, ^{2}J(^{119}Sn$_{endo}$–$^{117/119}$Sn$_{endo}$) = 55 Hz).

The solvent was evaporated and the mixture was washed three times with cold hexane. After drying in vacuo 124 mg (93%) of **18** as white solid were obtained. Recrystallization from $CHCl_3$/toluene afforded colorless crystalls of mp 163–165 °C.

Anal. Calcd for $C_{54}H_{72}Cl_2O_6P_2Sn_4$ (1424.77 g/mol): C, 45.52; H, 5.09. Found: C, 45.2; H, 5.6. **Electrospray MS**: m/z (%), positive mode, 1281.2 (100, [({$Ph_2P(O)CH_2$}PhSnO)$_3$ + H]$^+$), 1299.3 (13, [({$Ph_2P(O)CH_2$}PhSnO)$_3$ + H_2O + H]$^+$), 1065.2 (8, [({$Ph_2P(O)CH_2$}PhSnO)$_3$ – $Ph_2P(O)CH_2$]$^+$), 747.1 (4, [(*t*-Bu_2SnO)$_3$ + H]$^+$), negative mode, 161.0 (100, [2Cl + H + 5H_2O]$^-$), 357.0 (53, [*t*-$Bu_2Sn(OH)_3$ + 4H_2O]$^-$), 569.2 (24, [{*t*-$Bu_2Sn(OH)_2$}$_2$ + OH + H_2O]$^-$).

Synthesis of [{$Ph_2P(O)CH_2$}(Me_3SiCH_2)(OH)SnOSn(Br)*t*-Bu_2]$_2$, 19

A mixture of **10** (163 mg, 0.28 mmol) and di-*tert*-butyltin oxide (140 mg, 0.56 mmol) in CH_2Cl_2 (1.4 mL) was stirred for 2 hours at room temperature. Then the solvent was evaporated and the residue was washed more times with cold hexane followed with extensive drying in vacuo to give 200 mg (93%) of **19** as white solid of mp 181.5–183.5 °C. Colorless single crystals of **19**·$CHCl_3$ suitable for the X-ray diffraction analysis were obtained by slow evaporation of $CDCl_3$ in the NMR tube.

Anal. Calcd for $C_{50}H_{84}Br_2O_6P_2Si_2Sn_4$ (1533.90 g/mol): C, 39.10; H, 5.52. Found: C, 39.1; H, 5.4. **^{1}H NMR** (300.13, $CDCl_3$): (***a*** *and* ***b*** *refer to the isomers of compound* ***19***) *δ* –0.16 (s, 9H, *Me*$_3$Si (**a**)), –0.14 (s, 9H, *Me*$_3$Si (**b**)), 0.60 (d, 1H, *J* = 12.1), 0.66 (d, 1H, *J* = 12.4), 0.82 (d, 1H, *J* = 12.4), 0.83 (d, 1H, *J* = 12.4), 1.37 (s, 18H, ^{3}J(^{1}H–$^{117/119}$Sn) = 115.2 Hz, *t*-Bu_2Sn, (**a**)), 1.38 (s, 2H, SiC*H*$_2$Sn (**a**)), 1.41 (s, 2H, SiC*H*$_2$Sn (**b**)), 1.43 (s, 18H, ^{3}J(^{1}H–$^{117/119}$Sn) = 114.5 Hz, *t*-Bu_2Sn (**b**)), 5.99 (s, 1H, O*H* (**b**)), 6.01 (s, 1H, O*H* (**a**)), 7.41–8.08 (m, 10H (**a**) + 10H (**b**), Ar H). **^{31}P{^{1}H} NMR** (121.49, $CDCl_3$): *δ* 33.2 (62%, s, ^{2}J(^{31}P–$^{117/119}$Sn) = 40 Hz), 33.1 (38%, s, ^{2}J(^{31}P–$^{117/119}$Sn) = 42 Hz). **^{29}Si{^{1}H} NMR** (59.63, $CDCl_3$): *δ* 1.5 (s, ^{2}J(^{29}Si–$^{117/119}$Sn) = 20 Hz), 1.4 (s, ^{2}J(^{29}Si–$^{117/119}$Sn) = 23 Hz). **^{119}Sn{^{1}H} NMR** (111.92, $CDCl_3$): *δ* –201.7 (19%, s, ^{4}J(^{119}Sn$_{exo}$–$^{117/119}$Sn$_{exo}$) = 41 Hz, *t*-Bu_2Sn), –202.1 (31%, s, ^{2}J(^{119}Sn$_{exo}$–$^{117/119}$Sn$_{exo}$) = 41 Hz), –210.1 (19%, d, ^{2}J(^{119}Sn–^{31}P) = 43 Hz), –211.1 (31%, d, ^{2}J(^{119}Sn–^{31}P) = 41 Hz, ^{2}J(^{119}Sn$_{endo}$–$^{117/119}$Sn$_{endo}$) = 41 Hz). **Electrospray MS**: m/z (%), positive mode, 1311.2 (100, [({$Ph_2P(O)CH_2$}{Me_3SiCH_2}SnO)$_3$ + H]$^+$), 1329.3 (16, [({$Ph_2P(O)CH_2$}{Me_3SiCH_2} SnO)$_3$ + H_2O + H]$^+$), 1095.1 (6,

[({$Ph_2P(O)CH_2$}{Me_3SiCH_2}SnO)$_3$ – $Ph_2P(O)CH_2$]$^+$), 935.2(16), 687.1 (14, [{$Ph_2P(O)CH_2$} (Me_3SiCH_2)SnO·*t*-Bu_2SnO + H]$^+$), 729.1 (15, [{$Ph_2P(O)CH_2$}(Me_3SiCH_2)SnO·*t*-Bu_2SnO + MeCN + H]$^+$), 747.1 (6, [(*t*-Bu_2SnO)$_3$ + H]$^+$).

Synthesis of [{$Ph_2P(O)CH_2$}(Me_3SiCH_2)(OH)SnOSn(Cl)*t*-Bu_2]$_2$, 20

A mixture of **11** (50 mg, 0.10 mmol) and di-*tert*-butyltin oxide (50 mg, 0.20 mmol) in $CDCl_3$ (0.8 mL) was stirred for 10 minutes at room temperature then ^{31}P and ^{119}Sn NMR spectra were recorded.

^{31}P{^{1}H} NMR (121.49, $CDCl_3$): *δ* 33.1 (44%, s, ^2J(^{31}P–$^{117/119}$Sn) = 41 Hz), 33.0 (57%, s, ^2J(^{31}P–$^{117/119}$Sn) = 42 Hz). **^{119}Sn{^{1}H} NMR** (111.92, $CDCl_3$): *δ* –30 (s, *t*-Bu_2Sn(OH)Cl), –83 (s, *t*-Bu_2SnO), –108 (s, Sn_{exo} [*t*-Bu_2(Cl)SnOSn(Cl)*t*-Bu_2]$_2$), –143 (s, Sn_{endo} [*t*-Bu_2(Cl)SnOSn(Cl)*t*-Bu_2]$_2$), –205.6 (28%, d, ^2J(^{119}Sn–^{31}P) = 43 Hz, ^2J($^{119}Sn_{endo}$–$^{117/119}Sn_{endo}$) = 20 Hz), –206.6 (22%, d, ^2J(^{119}Sn–^{31}P) = 43 Hz, ^2J($^{119}Sn_{endo}$–$^{117/119}Sn_{endo}$) = 20 Hz), –216.6 (28%, s, ^2J($^{119}Sn_{exo}$–$^{117/119}Sn_{endo}$) = 290 Hz, *t*-Bu_2Sn), –216.8 (22%, s, ^2J($^{119}Sn_{exo}$–$^{117/119}Sn_{endo}$) = 290 Hz).

The solvent was evaporated in vacuo and the residue was washed with hexane. Recrystallization from a solution in toluene/$CHCl_3$ afforded white amorphous solide of mp 181-183 °C.

Electrospray MS: m/z (%), positive mode, 1311.4 (100, [({$Ph_2P(O)CH_2$}{Me_3SiCH_2}SnO)$_3$ + H]$^+$), 1065.1 (50, [{$Ph_2P(O)CH_2$}{Me_3SiCH_2}SnO · 2 *t*-Bu_2SnO + 4 MeOH + H]$^+$), 1095.1 (25, [({$Ph_2P(O)CH_2$}{Me_3SiCH_2}SnO)$_3$ – $Ph_2P(O)CH_2$]$^+$), 875.3 (15, [({$Ph_2P(O)CH_2$}{Me_3SiCH_2}SnO)$_2$ + H]$^+$), 687.1 (3), 541.2 (3).

Synthesis of {4-$Ph_2PC_6H_4$}Br, 21

Compound **21** was synthesized by modified procedure of that described in the literature.[29] A solution of *n*-butyllithium (75 mL, 1.6 M in hexane, 120 mmole) was added drop-wise over 1.5 h at –78 °C to a solution of 1,4-dibromobenzene (28.31 g, 120 mmol) in THF (500 mL) with vigorous stirring. Then a solution of diphenylphosphine chloride (26.46 g, 120 mmol) in THF (150 mL) was added over 1.5 h at the same temperature. The reaction mixture was stirred overnight and allowed to reach room temperature. The THF was evaporated and (500 mL) hexane was added. The mixture was filtrated off under argon and the filtrate was concentrated in vacuo. Methanol (400 mL) was added and the mixture was stirring

overnight giving white precipitate which was filtered off. Washing the residue with methanol and drying in vacuo gave compound **21** (34.60 g, 84.5%) as white solid of mp 77–79 °C.

Anal. Calcd for $C_{18}H_{14}BrP$ (341.19 g/mol): C, 63.37; H, 4.14. Found: C, 63.0; H, 4.1. **^{1}H NMR** (300.13, $CDCl_3$): *δ* 7.16–7.50 (m, 14H, Ar H). **^{13}C{^{1}H} NMR** (100.63, C_6D_6): *δ* 124.0 (s, *C*–Br), 129.2 (d, $^{3}J(^{13}C–^{31}P)$ = 7 Hz, C_m), 129.4 (s, C_p), 132.3 (d, $^{3}J(^{13}C–^{31}P)$ = 7 Hz, C_m), 134.4 (d, $^{2}J(^{13}C–^{31}P)$ = 19 Hz, C_o), 136.0 (d, $^{2}J(^{13}C–^{31}P)$ = 20 Hz, C_o), 137.5 (d, $^{1}J(^{13}C–^{31}P)$ = 14 Hz, C_i), 137,7 (d, $^{1}J(^{13}C–^{31}P)$ = 12 Hz, C_i). **^{31}P{^{1}H} NMR** (121.50, $CDCl_3$): *δ* –5.6. **Electrospray MS**: m/z (%), positive mode, 341.0 (100, [**21** + H]$^{+}$)

Synthesis of {4-$Ph_2PC_6H_4$}Me_2SiCH_2Cl, 22

A solution of *n*-butyllithium (32.5 mL, 1.6 M in hexane, 52 mmole) was added dropwise over 15 minutes at –78 °C to a solution of **21** (17.05 g, 50 mmol) in THF (200 mL). The resulting mixture was dropped at –78 °C over a solution of chloro(chloromethyl) dimethylsilane (6.94 g, 48.5 mmol) in THF (50 mL). The reaction mixture was stirred for 1 h at the same temperature, before it was allowed to reach room temperature and stirred overnight. Then THF was evaporated, hexane (200 mL) was added, and the mixture was filtered off under inert conditions. The filtrate was concentrated and the residue was dried in vacuo to give compound **22** (16.7 g, 91%) as white solid of mp 51–53 °C.

Anal. Calcd for $C_{21}H_{22}ClPSi$ (368.91 g/mol): C 68.37; H 6.01. Found: C 69.2; H 5.8.

^{1}H NMR (400.13, $CDCl_3$): *δ* 0.44 (s, 6H, Me_2Si), 2.98 (s, 2H, SiCH_2Cl), 7.31–7.54 (m, 14H, Ar H). **^{13}C{^{1}H} NMR** (100.63, $CDCl_3$): *δ* –4.6 (s, Me_2Si), 30.2 (s, SiCH_2Cl), 128.5 (d, $J(^{13}C–^{31}P)$ = 25 Hz, *Ph*), 128.7 (d, $J(^{13}C–^{31}P)$ = 27 Hz, *Ph*), 132.9 (d, $J(^{13}C–^{31}P)$ = 18 Hz, *Ph*), 133.7 (d, $J(^{13}C–^{31}P)$ = 19 Hz, *Ph*), 133.8 (d, $J(^{13}C–^{31}P)$ = 19 Hz, *Ph*), 136.5 (s, *Ph*), 136.8 (d, $J(^{13}C–^{31}P)$ = 11 Hz, *Ph*), 139.1 (d, $J(^{13}C–^{31}P)$ = 13 Hz, *Ph*). **^{31}P{^{1}H} NMR** (121.50, $CDCl_3$): *δ* –4.55. **^{29}Si{^{1}H} NMR** (59.63, $CDCl_3$): *δ* –2.8. **Electrospray MS**: m/z (%), positive mode, 277.1 (100, $[Ph_3MeP]^{+}$), 369.1 (85, [**22** + H]$^{+}$), 383.1 (100, [**22** + Me]$^{+}$).

Synthesis of {4-$Ph_2PC_6H_4$}$Me_2SiCH_2SnPh_3$, 23

To a solution of hexaphenyldistannane (2.09 g, 3.0 mmol) in THF (75mL) were added sodium (0.14 g, 6.0 mmol) and a catalytic amount of naphthalene, and the mixture

was stirred for two days at room temperature (until all the sodium has been reacted). The resulting black solution was added drop-wise at –70°C to a solution of **22** (2.20 g, 6.0 mmol) in THF (50mL). The mixture was stirred overnight at room temperature before THF was distilled off under reduced pressure. Cold water (100 mL) was added over the residue and the mixture was extracted three times each with 75 mL CH_2Cl_2. The combined organic phases were dried with $MgSO_4$ and the solvent was evaporated in vacuo giving compound **23** (3.87 g, 95 %) as light yellowish waxy oil.

^{1}H NMR (300.13, C_6D_6): *δ* 0.26 (s, 6H, *Me*$_2$Si), 0.64 (s, 2H, $^{2}J(^{1}H–^{117/119}Sn)$ = 75.4 Hz, SiC*H*$_2$Sn), 7.41–7.68 (m, 29H, Ar H). **^{13}C{^{1}H} NMR** (75.47, C_6D_6): *δ* –5.5 (s, Si*C*H$_2$Sn), 0.5 (s, $^{3}J(^{13}C–^{117/119}Sn)$ = 13 Hz, *Me*$_2$Si), 129.2 (s, *Ph*), 129.3 (d, $J(^{13}C–^{31}P)$ = 3 Hz, *Ph*), 129.5 (s, *Ph*), 133.8 (d, $J(^{13}C–^{31}P)$ = 19 Hz, *Ph*), 134.3 (d, $J(^{13}C–^{31}P)$ = 7 Hz, *Ph*), 134.6 (d, $J(^{13}C–^{31}P)$ = 20 Hz, *Ph*), 137.6 (s, *Ph*), 138.0 (d, $J(^{13}C–^{31}P)$ = 9 Hz, *Ph*), 138.4 (d, $J(^{13}C–^{31}P)$ = 12 Hz, *Ph*), 139.0 (d, $J(^{13}C–^{31}P)$ = 12 Hz, *Ph*), 140.1 (s, *Ph*), 141.9 (s, *Ph*). **^{31}P{^{1}H} NMR** (121.50, C_6D_6): *δ* –4.6. **^{29}Si{^{1}H} NMR** (59.63, C_6D_6): *δ* –1.4 ($^{2}J(^{29}Si–^{119}Sn)$ = 21 Hz). **^{119}Sn{^{1}H} NMR** (111.92, C_6D_6): *δ* –90, –127 (5%, Ph_4Sn). **Electrospray MS**: m/z (%), positive mode, 699.2 (100, $[\{Ph_2P(O)C_6H_4\}Me_2SiCH_2SnPh_3 + H]^+$), 733.2 (10, $[\{Ph_2P(O)C_6H_4\}Me_2SiCH_2SnPh_3 + MeOH + H]^+$).

Synthesis of {4-Ph$_2$P(O)C$_6$H$_4$}Me$_2$SiCH$_2$SnPh$_3$, 24

A saturated solution of potassium permanganate in acetone was added to a stirred solution of compound **23** (3.70 g, 5.4 mmol) in acetone until stability of the pink color of permanganate. The mixture was filtered off and acetone was evaporated in vacuo. The residue was dissolved in toluene and the solution was filtered off again. After evaporating the toluene in vacuo compound **24** was obtained (3.6 g, 95%) as light yellowish waxy oil.

^{1}H NMR (300.13, C_6D_6): *δ* 0.20 (s, 6H, *Me*$_2$Si), 0.57 (s, 2H, $^{2}J(^{1}H–^{117/119}Sn)$ = 75.0 Hz, SiC*H*$_2$Sn), 7.06–7.90 (m, 29H, Ar H). **^{13}C{^{1}H} NMR** (100.63, C_6D_6): *δ* –5.7 (s, Si*C*H$_2$Sn), 0.3 (s, $^{3}J(^{13}C–^{117/119}Sn)$ = 13 Hz, *Me*$_2$Si), 128.9 (d, $J(^{13}C–^{31}P)$ = 12 Hz, *Ph*), 129.2 (s, *Ph*), 129.4 (d, $J(^{13}C–^{31}P)$ = 6 Hz, *Ph*), 129.6 (s, *Ph*), 131.9 (d, $J(^{13}C–^{31}P)$ = 3 Hz, *Ph*), 132.8 (d, $J(^{13}C–^{31}P)$ = 10 Hz, *Ph*), 134.0 (d, $J(^{13}C–^{31}P)$ = 12 Hz, *Ph*), 134.3 (d, $J(^{13}C–^{31}P)$ = 11 Hz, *Ph*), 135.3 (d, $J(^{13}C–^{31}P)$ = 11 Hz, *Ph*), 137.6 (s, *Ph*), 139.8 (s, *Ph*), 145.7 (s, *Ph*). **^{31}P{^{1}H} NMR** (121.49, C_6D_6): *δ* 26.3. **^{29}Si{^{1}H} NMR** (59.63, C_6D_6): *δ* –1.0 ($^{2}J(^{29}Si–^{119}Sn)$ = 21 Hz). **^{119}Sn{^{1}H} NMR** (111.92, C_6D_6): *δ* –91

(94%), –127 (6%, Ph_4Sn). **Electrospray MS**: m/z (%), positive mode, 339.1 (100), 1405.5 (55, $[2M + K]^+$), 707.2 (42, $[M + Na]^+$).

Synthesis of {4-$Ph_2P(O)C_6H_4$}$Me_2SiCH_2(Ph)SnBr_2$, 25

The compound was synthesized according to the bromination procedure (B). The residue was washed with hexane and a small amount of cold dichloromethane. Drying in vacuo afforded compound **25** (yield 98.0%) as light brownish solid of mp 212–214 °C.

^{1}H NMR (300.13, $CDCl_3$): *δ* 0.49 (s, 6H, Me_2Si), 1.44 (s, 2H, $^2J(^1H–^{117/119}Sn)$ = 105.0 Hz, $SiCH_2Sn$), 7.22–7.63 (m, 19H, Ar H). **^{31}P{^{1}H} NMR** (121.49, $CDCl_3$): *δ* 32.7. **^{119}Sn{^{1}H} NMR** (111.92, $CDCl_3$): *δ* –84. **Electrospray MS**: m/z (%), positive mode, 279.1 (100), 707.0 (90, $[M + H]^+$), 1410.8 (26, $[2M + H]^+$), negative mode, 304.6 (100), 784.8 (37, $[M + Br]^–$).

Synthesis of {$Ph_2P(O)C_6H_4$}$Me_2SiCH_2(Ph)SnCl_2$, 26

The compound was synthesized according to the chlorination procedure (C). The residue was washed with hexane and a small amount of cold dichloromethane. Drying in vacuo afforded compound **26** (yield 96.0%) as white solid of mp 238–240 °C.

^{31}P{^{1}H} NMR (121.49, $CDCl_3$): δ 33.68. **Electrospray MS**: m/z (%), positive mode, 279.1 (100), 577.1 (51, $[M – 2Cl + OH + H_2O]^+$), 617.0 (44, $[M + H]^+$), 1141.2 (25, $[2M – 4Cl + 3OH]^–$), 1197.0 (12 ,$[2M – Cl]^+$), negative mode, 650.9 (100, $[M – 2Cl + 3OH + 3H_2O]^–$), 669.0 (92, $[M – 2Cl + 3OH + 4H_2O]^–$).

Synthesis of ($Ph_2PC_6H_4$)*t*-Bu_2SnCl, 29

A solution of *n*-butyllithium (3.3 mL, 1.8 M in hexane, 5.9 mmol) was added drop-wise over 15 min at –78 °C to a solution of **21** (1.00 g, 2.93 mmol) in THF (25 mL) and the mixture was stirred for 40 minutes at the same temperature. The resulting mixture was dropped at –50 °C over a solution of di-*tert*-buthyltin dichloride (0.89 g, 2.93 mmol) in THF (25 mL). The reaction mixture was stirred for 1 h at the same temperature, before it was allowed to reach room temperature with stirring overnight. The solvents were evaporated, toluene (50 mL) was added, and the mixture was filtered off under argon. The filtrate was concentrated and the residue was dried in vacuo giving yellowish oil (1.50 g).

$^{31}P\{^{1}H\}$ NMR (121.49, C_6D_6): *δ* –4.29 (49%, $^{5}J(^{31}P–^{117/119}Sn)$ = 6.7 Hz), 4.36 (36%, $^{5}J(^{31}P–^{117/119}Sn)$ = 5.6 Hz), 4.41 (13%), 26.23 (1%), 26.51 (1%). **$^{119}Sn\{^{1}H\}$ NMR** (111.92, C_6D_6): *δ* 40 (66%, d, $^{5}J(^{119}Sn–^{31}P)$ = 5 Hz, $(Ph_2PC_6H_4)$*t*-Bu_2SnCl (**29**)), –92 (19%, t, $^{5}J(^{119}Sn–^{31}P)$ = 5 Hz, $(Ph_2PC_6H_4)_2$*t*-Bu_2Sn (**30**)), 90 (15%).

1.4 References

1. (a) Davies, A. G., *Organotin Chemistry*. Wiley **2004**; (b) Davies, A. G.; Gielen, M.; Pannell, K. H.; Tiekink, E. R. T., *Tin Chemistry: Fundamentals, Frontiers, and Applications*. Wiley **2008**.
2. (a) Orita, A.; Tanabe, S.; Ono, T.; Otera, J., *Adv. Synth. Catal.* **2010**, *352*, 1419; (b) Otera, J.; Yano, T.; Okawara, R., *Organometallics* **1986**, *5*, 1167; (c) Otera, J., *Chem. Rev.* **1993**, *93*, 1449; (d) Otera, J.; Ioka, S.; Nozaki, H., *J. Org. Chem.* **1989**, *54*, 4013; (e) Otera, J.; Yano, T.; Kawabata, A.; Nozaki, H., *Tetrahedron Lett.* **1986**, *27*, 2383; (f) Otera, J.; Dan-Oh, N.; Nozaki, H., *J. Chem. Soc., Chem. Commun.* **1991**, 1742; (g) Otera, J.; Danoh, N.; Nozaki, H., *J. Org. Chem.* **1991**, *56*, 5307; (h) Durand, S.; Sakamoto, K.; Fukuyama, T.; Orita, A.; Otera, J.; Duthie, A.; Dakternieks, D.; Schulte, M.; Jurkschat, K., *Organometallics* **2000**, *19*, 3220; (i) Otera, J.; Dan-oh, N.; Nozaki, H., *Tetrahedron* **1992**, *48*, 1449; (j) Orita, A.; Mitsutome, A.; Otera, J., *J. Org. Chem.* **1998**, *63*, 2420; (k) Otera, J.; Yano, T.; Himeno, Y.; Nozaki, H., *Tetrahedron Lett.* **1986**, *27*, 4501; (l) Otera, J.; Nozaki, H., *Tetrahedron Lett.* **1986**, *27*, 5743; (m) Otera, J.; Kawada, K.; Yano, T., *Chem. Lett.* **1996**, *25*, 225; (n) Houghton, R. P.; Mulvaney, A. W., *J. Organomet. Chem.* **1996**, *517*, 107; (o) Houghton, R. P.; Mulvaney, A. W., *J. Organomet. Chem.* **1996**, *518*, 21; (p) Suciu, E. N.; Kuhlmann, B.; A. Knudsen, G.; Michaelson, R. C., *J. Organomet. Chem.* **1998**, *556*, 41; (q) Padelkova´, Z.; Vanka´tova´, H.; Cisarova´, I.; Nechaev, M. S.; Zevaco, T. A.; Walter, O.; Ruzicka, A., *Organometallics* **2009**, *28*, 2629; (r) Okawara, R., *Proceedings of the Chemical Society* **1961**, 383; (s) Schulte, M.; Mehring, M.; Paulus, I.; Schurmann, M.; Jurkschat, K.; Dakternieks, D.; Duthie, A.; Orita, A.; Otera, J., *Phosphorus, Sulfur Silicon Relat. Elem.* **1999**, *150*, 201; (t) Otera, J., *Acc. Chem. Res.* **2004**, *37*, 288; (u) An, D. L.; Peng, Z.; Orita, A.; Kurita, A.; Man-e, S.; Ohkubo, K.; Li, X.; Fukuzumi, S.; Otera, J., *Chem. Eur. J.* **2006**, *12*, 1642.
3. (a) Dakternieks, D.; Zhu, H.; Tiekink, E. R. T.; Colton, R., *J. Organomet. Chem.* **1994**, *476*, 33; (b) Banse, F.; Ribot, F.; Toledano, P.; Maquet, J.; Sanchez, C., *Inorg. Chem.* **1995**, *34*, 6371; (c) Eychenne-Baron, C.; Ribot, F.; Steunou, N.; Sanchez, C. m.; Fayon, F.; Biesemans, M.; Martins, J. C.; Willem, R., *Organometallics* **2000**, *19*, 1940; (d) Puff, H.; Reuter, H., *J. Organomet.*

Chem. **1989**, *373*, 173; (e) Beckmann, J.; Jurkschat, K.; Kaltenbrunner, U.; Rabe, S.; Schürmann, M.; Dakternieks, D.; Duthie, A.; Müller, D., *Organometallics* **2000**, *19*, 4887; (f) Ribot, F.; Veautier, D.; Guillaudeu, S. J.; Lalot, T., *J. Mater. Chem.* **2005**, *15*, 3973.

4. Puff, H.; Reuter, H., *J. Organomet. Chem.* **1989**, *368*, 173.
5. Prabusankar, G.; Jousseaume, B.; Toupance, T.; Allouchi, H., *Angew. Chem. Int. Ed. Engl.* **2006**, *45*, 1255.
6. Wraage, K.; Pape, T.; Herbst-Irmer, R.; Noltemeyer, M.; Schmidt, H.-G.; Roesky, H. W., *Eur. J. Inorg. Chem.* **1999**, 869.
7. (a) Janssen, J.; Magull, J.; Roesky, H. W., *Angew. Chem. Int. Ed. Engl.* **2002**, *41*, 1365; (b) Ahmad, S. U.; Beckmann, J.; Duthie, A., *Chem. Asian J.* **2010**, *5*, 160.
8. (a) Zobel, B.; Duthie, A.; Dakternieks, D.; Tiekink, E. R. T., *Organometallics* **2001**, *20*, 2820; (b) Holmes, R. R.; Shafieezad, S.; Chandrasekhar, V.; Holmes, J. M.; Day, R. O., *J. Am. Chem. Soc.* **1988**, *110*, 1174; (c) Lecomte, C.; Protas, J.; Devaud, M., *Acta Crystallogr., Sect. B* **1976**, *32*, 923; (d) Johnson, S. E.; Knobler, C. B., *Organometallics* **1994**, *13*, 4928; (e) Puff, H.; Reuter, H., *J. Organomet. Chem.* **1989**, *364*, 57; (f) Beckmann, J.; Duthie, A.; Grassmann, M., *J. Organomet. Chem.* **2009**, *694*, 161.
9. (a) Harris, R. K.; Sebald, A., *J. Organomet. Chem.* **1987**, *331*, C9; (b) Lohmann, D. H., *J. Organomet. Chem.* **1965**, *4*, 382; (c) Harrison, P. G.; Phillips, R. C.; Thornton, E. W., *J. Chem. Soc., Chem. Commun.* **1977**, 603.
10. Puff, H.; Schuh, W.; Sievers, R.; Wald, W.; Zimmer, R., *J. Organomet. Chem.* **1984**, *260*, 271.
11. Baba Haj, S.; Schürmann, M.; Iovkova-Berends, L.; Herres-Pawlis, S.; Jurkschat, K., *Organometallics* **2012**, *31*, 4716.
12. Masamune, S.; Sita, L. R.; Williams, D. J., *J. Am. Chem. Soc.* **1983**, *105*, 630.
13. Weber, U.; Pauls, N.; Winter, W.; Stegmann, H. B., *Z. Naturforsch., B* **1982**, *37*, 1316.
14. Grützmacher, H.; Pritzkow, H., *Chem. Ber.* **1993**, *126*, 2409.
15. Belsky, V. K.; Zemlyansky, N. N.; Borisova, I. V.; Kolosova, N. D.; Beletskaya, I. P., *J. Organomet. Chem.* **1983**, *254*, 189.
16. Edelman, M. A.; Hitchcock, P. B.; Lappert, M. F., *J. Chem. Soc., Chem. Commun.* **1990**, 1116.

17. (a) Gross, D. C., *Inorg. Chem.* **1989**, *28*, 2355; (b) Harrison, P. G.; Begley, M. J.; Molloy, K. C., *J. Organomet. Chem.* **1980**, *186*, 213; (c) Puff, H.; Bung, I.; Friedrichs, E.; Jansen, A., *J. Organomet. Chem.* **1983**, *254*, 23; (d) Vollano, J. F.; Day, R. O.; Holmes, R. R., *Organometallics* **1984**, *3*, 745; (e) Beckmann, J.; Henn, M.; Jurkschat, K.; Schürmann, M.; Dakternieks, D.; Duthie, A., *Organometallics* **2001**, *21*, 192; (f) Beckmann, J.; Jurkschat, K.; Rabe, S.; Schürmann, M.; Dakternieks, D., *Z. Anorg. Allg. Chem.* **2001**, *627*, 458; (g) Yap, Q. L.; Lo, K. M.; Ng, S. W., *Acta Crystallogr., Sect. E* **2010**, *66*, m8; (h) Yano, T.; Nakashima, K.; Otera, J.; Okawara, R., *Organometallics* **1985**, *4*, 1501; (i) Teoh, S.-G.; Looi, E.-S.; Teo, S.-B.; Ng, S.-W., *J. Organomet. Chem.* **1996**, *509*, 57; (j) Narula, S. P.; Kaur, S.; Shankar, R.; Bharadwaj, S. K.; Chadha, R. K., *J. Organomet. Chem.* **1996**, *506*, 181; (k) Vatsa, C.; Jain, V. K.; Kesavadas, T.; Tiekink, E. R. T., *J. Organomet. Chem.* **1991**, *408*, 157; (l) Baumeister, U.; Dakternieks, D.; Jurkschat, K.; Schürmann, M., *Main Group Met. Chem.* **2002**, *25*, 521.

18. Fackler Jr, J. P.; Garzon, G.; Kresinski, R. A.; Murray III, H. H.; Raptis, R. G., *Polyhedron* **1994**, *13*, 1705.

19. (a) Howie, R. A.; Harrison William, T. A.; de Lima Geraldo, M.; Wardell James, L.; Wardell Solange, M. S. V., *Z. Krist.* **2011**, *226*, 739; (b) Ok-Sang, J.; Jong, H. J.; Youn, S. S., *J. Organomet. Chem.* **1992**, *439*, 23; (c) Vicente, J.; Chicote, M.-T.; Ramirez-de-Arellano, M.-d.-C.; Jones, P. G., *J. Chem. Soc., Dalton Trans.* **1992**, 1839.

20. (a) Holmes, R. R., *Acc. Chem. Res.* **1989**, *22*, 190; (b) Holmes, R. R., *Phosphorus, Sulfur Silicon Relat. Elem.* **1999**, *150*, 1; (c) Prabusankar, G.; Jousseaume, B.; Toupance, T.; Allouchi, H., *Dalton Trans.* **2007**, 3121; (d) Swamy, K. C. K.; Day, R. O.; Holmes, R. R., *Inorg. Chem.* **1992**, *31*, 4184; (e) Chandrasekhar, V.; Thirumoorthi, R., *Inorg. Chem.* **2009**, *48*, 10330; (f) Casas, J. S.; Castellano, E. E.; Couce, M. D.; García-Tasende, M. S.; Sánchez, A.; Sordo, J.; Taboada, C.; Vázquez-López, E. M., *Inorg. Chem.* **2001**, *40*, 946; (g) Day, R. O.; Holmes, J. M.; Chandrasekhar, V.; Holmes, R. R., *J. Am. Chem. Soc.* **1987**, *109*, 940; (h) C. Kumara Swamy, K.; A. Said, M.; Nagabrahmanandachari, S.; M. Poojary, D.; Clearfield, A., *J. Chem. Soc., Dalton Trans.* **1998**, 1645.

21. Döppert, K.; Thewalt, U., *J. Organomet. Chem.* **1986**, *301*, 41.

22. (a) Beattie, J. K.; Hambley, T. W.; Klepetko, J. A.; Masters, A. F.; Turner, P., *Polyhedron* **1998**, *17*, 1343; (b) Ama, T.; Yonemura, T.; Yamaguchi, M., *Bull. Chem. Soc. Jpn* **2006**, *79*, 1063.
23. Zhou, Z.-H.; Xu, Q.; Lin, J.; Ng, S.-W., *Inorg. Chem. Commun.* **2007**, *10*, 1461.
24. (a) Thewalt, U.; Döppert, K.; Lasser, W., *J. Organomet. Chem.* **1986**, *308*, 303; (b) Zhang, R.-F.; Li, C.-P.; Wang, Q.-F.; Ma, C.-L., *J. Coord. Chem.* **2010**, *63*, 2105; (c) Boutonnet, F.; Zablocka, M.; Igau, A.; Jaud, J.; Majoral, J.-P.; Schamberger, J.; Erker, G.; Werner, S.; Kruger, C., *J. Chem. Soc., Chem. Commun.* **1995**, 823.
25. Zhang, R.; Li, C.; Wang, Q.; Chunlin, M., *Struct. Chem.* **2010**, *21*, 745.
26. Jurkschat, K., Tetraorganodistannoxanes: Simple Chemistry From a Personal Perspective. In *Tin Chemistry: Fundamentals, Frontiers, and Applications*, Eds. Davies, A. G.; Gielen, M.; Pannell, K. H.; Tiekink, E. R. T., Wiley **2008**, and references cited therein.
27. Addison, A. W.; Rao, T. N.; Reedijk, J.; van Rijn, J.; Verschoor, G. C., *J. Chem. Soc., Dalton Trans.* **1984**, 1349.
28. (a) Dräger, M., *J. Organomet. Chem.* **1983**, *251*, 209; (b) Kolb, U.; Beuter, M.; Dräger, M., *Inorg. Chem.* **1994**, *33*, 4522; (c) Dräger, M., *Z. Anorg. Allg. Chem.* **1976**, *423*, 53; (d) Beuter, M.; Kolb, U.; Zickgraf, A.; Bräu, E.; Bletz, M.; Dräger, M., *Polyhedron* **1997**, *16*, 4005.
29 Ravindar, V.; Hemling, H.; Schumann, H.; Blum, J., *Synth. Commun.* **1992**, *22*, 841.
30. Beckmann, J.; Dakternieks, D.; Duthie, A.; Tiekink, E. R. T., *Dalton Trans.* **2003**, 755.
31. (a) Erker, G.; Stephan, D. W., *Frustrated Lewis Pairs I, Uncovering and Understanding*. Springer **2013**; (b) Erker, G.; Stephan, D. W., *Frustrated Lewis Pairs II, Expanding the Scope*. Springer **2013**; (c) Stephan, D. W.; Erker, G., *Angew. Chem. Int. Ed. Engl.* **2010**, *49*, 46; (d) Stephan, D. W., *Org. Biomol. Chem.* **2012**, *10*, 5740; (e) Chapman, A. M.; Haddow, M. F.; Wass, D. F., *J. Am. Chem. Soc.* **2011**, *133*, 18463; (f) Appelt, C.; Slootweg, J. C.; Lammertsma, K.; Uhl, W., *Angew. Chem. Int. Ed. Engl.* **2012**, *51*, 5911; (g) Li, Y.; Kang, Y.; Lu, J.-S.; Wyman, I.; Ko, S.-B.; Wang, S., *Organometallics* **2014**, *33*, 964; (h) Chase, P. A.; Welch, G. C.; Jurca, T.; Stephan, D. W., *Angew. Chem. Int. Ed. Engl.* **2007**, *46*, 8050; (i) Zhao, X.; Stephan, D. W., *Chem.*

Commun. **2011**, *47*, 1833; (j) Welch, G. C.; Cabrera, L.; Chase, P. A.; Hollink, E.; Masuda, J. D.; Wei, P.; Stephan, D. W., *Dalton Trans.* **2007**, 3407; (k) Ménard, G.; Stephan, D. W., *Angew. Chem. Int. Ed. Engl.* **2011**, *50*, 8396; (l) McCahill, J. S. J.; Welch, G. C.; Stephan, D. W., *Angew. Chem. Int. Ed. Engl.* **2007**, *46*, 4968.

32. Wass, D.; Chapman, A., Frustrated Lewis Pairs Beyond the Main Group: Transition Metal-Containing Systems. In *Frustrated Lewis Pairs II*, Eds. Erker, G.; Stephan, D. W., Springer **2013**, and references cited therein.
33. Papetti, S.; Post, H. W., *J. Org. Chem.* **1957**, *22*, 526.
34. Kandil, S. A.; Allred, A. L., *J. Chem. Soc. A* **1970**, 2987.
35. Puff, H.; Schuh, W.; Sievers, R.; Wald, W.; Zimmer, R., *J. Organomet. Chem.* **1984**, *260*, 271.
36. Seyferth, D.; Welch, D. E.; Heeren, J. K., *J. Am. Chem. Soc.* **1964**, *86*, 1100.

1.5 Appendix

Crystallographic Data and Structure Refinements

Intensity data for all crystals were collected on a XcaliburS CCD diffractometer (Oxford Diffraction) fitted with graphite-monochromated Mo Kα (λ = 0.71073 Å) radiation at 173 K.

The structure was solved with direct methods using SHELXS-97.[1] Refinements were carried out against F^2 by using SHELXL-97.[1] All non-hydrogen atoms were refined using anisotropic displacement parameters. The C−H hydrogen atoms were positioned with idealized geometry and refined using a riding model. For decimal rounding of numerical parameters and su values the rules of IUCr have been employed.[2] The Figures were created using SHELXTL[3] and Diamond 3.2i.[4] The crystallographic data are given in tables A1–A6.

References

1. Sheldrick, G., *Acta Crystallographica Section A* **2008,** *64* (1), 112.
2. Clegg, W., *Acta Crystallographica Section E* **2003,** *59* (1), e2.
3. *Sheldrick, G. M. SHELXTL, release 5.1 Software Reference Manual; Brucker AXS, Inc.: Madison, Wisconsin, 1997.*
4. *Diamond - Crystal and Molecular Structure Visualization, Crystal Impact - Dr. H. Putz & Dr. K. Brandenburg GbR, Kreuzherrenstr. 102, 53227 Bonn, Germany http://www.crystalimpact.com/diamond*.

Table A1. Crystal data and structure refinements of the tetraorganotins **1**, **2** and **3**.

	1	**2**	**3**
Empirical formula	C_{31} H_{27} O P Sn	C_{29} H_{33} O P Si Sn	C_{31} H_{45} O P Sn
Formula weight	565.19	575.30	583.33
Temperature / K	173(2) K	173(2)	173(2)
Wavelength /°A	0.71073 A	0.71073	0.71073
Crystal system	Triclinic	Monoclinic	Monoclinic
space group	P-1	P 21/c	P21/c
a /°A	6.1238(2)	9.2050(4)	10.9356(5)
b /°A	10.5300(4)	27.0105(11)	10.8620(5)
c /°A	21.5777(8)	11.0422(4)	25.3611(12)
α /°	77.507(3)	90	90
β /°	82.791(3)	94.113(4)	108.701(4
γ /°	74.178(3)	90	90
Volume /°A^3	1303.72(8)	2738.37(19)	2853.4(2)
Z	2	4	4
Dc /$g.cm^{-3}$	1.440	1.395	1.358
Absorption coefficient /mm^{-1}	1.062	1.054	0.972
F(000)	572	1176	1216
Crystal size /mm	0.46 x 0.15 x 0.07	0.34 x 0.23 x 0.07	0.50 x 0.35 x 0.18
Range for data collection /°	2.05 to 25.50	2.00 to 25.49	2.53 to 25.50
Reflections collected	15180	16232	16931
Independent reflections	4865	5093	5317
Refinement method	Full-matrix least-squares on F^2	Full-matrix least-squares on F^2	Full-matrix least-squares on F^2
Data / restraints / Parameters	4865 / 0 / 307	5093 / 0 / 301	5317 / 0 / 307
Goodness-of-fit on F^2	0.953	0.855	0.977
Final R indices [$I>2\sigma(I)$]	R1 = 0.0277, wR2 = 0.0594	R1 = 0.0266, wR2 = 0.0461	R1 = 0.0221, wR2 = 0.0523
R indices (all data)	R1 = 0.0372, wR2 = 0.0604	R1 = 0.0460, wR2 = 0.0478	R1 = 0.0300, wR2 = 0.0533
Largest diff. peak and hole / e.A^{-3}	0.788 and -0.570	0.470 and -0.347	0.328 and -0.336

Table A2. Crystal data and structure refinements of the triorganotin halides **5**, **6**, and **6'**.

	5	**6**	**6'**
Empirical formula	$C_{50}H_{44}I_2O_2P_2Sn_2$	$C_{50}H_{44}Br_2O_2P_2Sn_2$	$C_{50}H_{44}Br_2O_2P_2Sn_2$
Formula weight	1229.97	1135.99	1135.99
Temperature / K	173(2)	173(2)	173(2)
Wavelength /°A	0.71073	0.71073	0.71073
Crystal system	Triclinic	Triclinic	Triclinic
space group	P-1	P-1	P-1
a /°A	11.8603(7)	11.8698(5)	10.1293(7)
b /°A	12.3981(7)	12.2448(4)	10.5555(8)
c /°A	18.9901(11)	18.4967(6)	11.4731(9)
α /°	73.947(5)	88.875(3)	102.989(7)
β /°	74.109(5)	72.016(3)	109.045(7)
γ /°	62.036(6)	63.502(4)	95.404(6)
Volume /°A^3	2335.8(2)	2266.27(16)	1111.04(16)
Z	2	2	1
Dc /g.cm^{-3}	1.749	1.665	1.698
Absorption coefficient /mm^{-1}	2.497	2.975	3.034
F(000)	1192	1120	560
Crystal size /mm	0.24 x 0.19 x 0.08	0.35 x 0.22 x 0.14	0.14 x 0.12 x 0.11
Range for data collection /°	2.26 to 26.50	2.34 to 25.50	2.16 to 25.50
Reflections collected	18512	30703	8319
Independent reflections	9675	8444	4136
Refinement method	Full-matrix least-squares on F^2	Full-matrix least-squares on F^2	Full-matrix least-squares on F^2
Data / restraints / parameters	9675 / 0 / 427	8444 / 0 / 523	4136 / 0 / 262
Goodness-of-fit on F^2	0.666	0.858	0.815
Final R indices [$I>2\sigma(I)$]	R1 = 0.0416, wR2 = 0.0475	R1 = 0.0274, wR2 = 0.0519	R1 = 0.0296, wR2 = 0.0446
R indices (all data)	R1 = 0.1147, wR2 = 0.0522	R1 = 0.0466, wR2 = 0.0536	R1 = 0.0511, wR2 = 0.0463
Largest diff. peak and hole / e.A^{-3}	1.023 and -1.094	0.771 and -0.565	0.514 and -0.607

Table A3. Crystal data and structure refinements of the Compounds **12**, **10a**, and **13a**.

	12	**10a**	**13a**
Empirical formula	C_{34} H_{46} Cl_4 O_2 P_2 Si_2 Sn_2	C_{48} H_{138} Br_2 O_{20} Si_{12} Sn_{12}	C_{32} H_{38} Cl_4 O_6 P_2 Sn_2
Formula weight	984.01	2956.76	959.74
Temperature / K	173(2) K	173(2)	173(2)
Wavelength /°A	0.71073	0.71073	0.71073
Crystal system	Monoclinic	Monoclinic	Triclinic
space group	P2(1)/c	C2/c	P-1
a /°A	9.8312(5)	25.6338(6)	9.0465(4)
b /°A	9.4168(5)	17.0668(4)	10.4970(5)
c /°A	24.4503(15)	23.4312(5)	11.5929(6)
α /°	90	90	65.682(5)
β /°	112.889(5)	90.774(2)	83.802(4)
γ /°	90	90	76.499(4)
Volume /°A^3	2085.3(2)	10249.9(4)	975.39(8)
Z	2	4	1
Dc /$g.cm^{-3}$	1.567	1.916	1.634
Absorption coefficient /mm^{-1}	1.617	3.837	1.675
F(000)	984	5696	476
Crystal size /mm	0.30 x 0.07 x 0.06	0.34 x 0.25 x 0.12	0.50 x 0.49 x 0.47
Range for data collection /°	2.25 to 25.50	2.25 to 25.50	2.83 to 25.49
Reflections collected	12590	35801	8172
Independent reflections	3888	9544	3617
Refinement method	Full-matrix least-squares on F^2	Full-matrix least-squares on F^2	Full-matrix least-squares on F^2
Data / restraints / parameters	3888 / 0 / 211	9544 / 0 / 436	3617 / 0 / 214
Goodness-of-fit on F^2	0.763	0.856	1.473
Final R indices [$I>2\sigma(I)$]	R1 = 0.0300, wR2 = 0.0355	R1 = 0.0261, wR2 = 0.0473	R1 = 0.0190, wR2 = 0.0549
R indices (all data)	R1 = 0.0679, wR2 = 0.0370	R1 = 0.0431, wR2 = 0.0487	R1 = 0.0201, wR2 = 0.0552
Largest diff. peak and hole / $e.A^{-3}$	0.609 and -0.519	1.693 and -1.035	0.525 and -0.647

Table A4. Crystal data and structure refinements of the trinuclear O-capped clusters **14**·$CHCl_3$, **15**·$CHCl_3$ and **16**·$CHCl_3$.

	14·$CHCl_3$	**15**·$CHCl_3$	**16**·$CHCl_3$
Empirical formula	C_{57} H_{54} Br O_7 P_3 Sn_3	C_{58} H_{55} Cl_3 I O_7 P_3 Sn_3	C_{58} H_{55} Cl_4 O_7 P_3 Sn_3
Formula weight	1379.89	1546.25	1454.80
Temperature / K	173(2)	173(2)	173(2)
Wavelength /°A	0.71073	0.71073	0.71073
Crystal system	Monoclinic	Monoclinic	Monoclinic
space group	P2(1)/n	Cc	P2(1)/n
a /°A	13.0485(4)	24.3698(13)	13.2841(5)
b /°A	19.7096(6)	11.2735(4)	22.6752(8)
c /°A	25.1356(7)	23.6381(16)	20.0715(7)
α /°	90	90	90
β /°	100.101(3)	115.589(3)	104.597(4)
γ /°	90	90	90
Volume /°A^3	6364.2(3)	5857.2(5)	5850.8(4)
Z	4	4	4
Dc /g.cm^{-3}	1.440	1.753	1.652
Absorption coefficient /mm^{-1}	1.916	2.066	1.586
F(000)	2728	3032	2888
Crystal size /mm	0.44 x 0.29 x 0.13	0.34 x 0.29 x 0.14	0.33 x 0.07 x 0.06
Range for data collection /°	2.22 to 25.50	2.01 to 25.50	2.28 to 25.50
Reflections collected	43664	16225	46785
Independent reflections	11770	9376	10894
Refinement method	Full-matrix least-squares on F^2	Full-matrix least-squares on F^2	Full-matrix least-squares on F^2
Data / restraints / parameters	11770 / 0 / 652	9376 / 11 / 685	10894 / 0 / 688
Goodness-of-fit on F^2	0.907	0.803	0.609
Final R indices [I>2σ(I)]	R1 = 0.0291, wR2 = 0.0670	R1 = 0.0340, wR2 = 0.0745	R1 = 0.0249, wR2 = 0.0418
R indices (all data)	R1 = 0.0461, wR2 = 0.0692	R1 = 0.0439, wR2 = 0.0772	R1 = 0.0589, wR2 = 0.0450
Largest diff. peak and hole / e.A^{-3}	0.500 and -0.441	0.969 and -1.193	0.402 and -0.414

Table A5. Crystal data and structure refinements of the dimeric tetraorganodistannoxanes **18**·C_7H_8·H_2O and **19**·$CHCl_3$.

	18·C_7H_8·H_2O	**19**·$CHCl_3$	**20**
Empirical formula	C_{75} H_{98} Cl_2 O_7 P_2 Sn_4	C_{51} H_{85} Br_2 Cl_3 O_6 P_2 Si_2 Sn_4	C_{50} H_{84} Cl_2 O_6 P_2 Si_2 Sn_4
Formula weight	1719.13	1653.24	1444.95
Temperature / K	173(2)	173(2)	173(2)
Wavelength /°A	0.71073	0.71073	0.71073
Crystal system	Triclinic	Triclinic	Monoclinic
space group	P-1	P -1	I2/a
a /°A	12.8880(5)	10.3620(3)	20.7092(8)
b /°A	13.2569(5)	12.0901(4)	13.7834(5)
c /°A	13.3108(5)	14.8613(5)	22.8912(10)
α /°	68.537(3)	75.580(3)	90
β /°	61.882(4)	88.186(3)	106.230(4)
γ /°	82.198(3)	82.951(3)	90
Volume /°A^3	1864.85(14)	1789.51(10)	6273.7(4)
Z	1	1	4
Dc /g.cm^{-3}	1.531	1.534	1.530
Absorption coefficient /mm^{-1}	1.489	2.724	1.789
F(000)	868	818	2896
Crystal size /mm	0.50 x 0.15 x 0.13	0.22 x 0.16 x 0.16	0.41 x 0.04 x 0.03
Range for data collection /°	2.38 to 25.50	2.43 to 25.50	2.347 to 25.500
Reflections collected	18187	6671	24589
Independent reflections	6946	6671	5836
Refinement method	Full-matrix least-squares on F^2	Full-matrix least-squares on F^2	Full-matrix least-squares on F2
Data / restraints / parameters	6946 / 2 / 371	6671 / 19 / 330	5836 / 16 / 329
Goodness-of-fit on F^2	0.871	0.963	0.816
Final R indices [I>2σ(I)]	R1 = 0.0274, wR2 = 0.0678	R1 = 0.0226, wR2 = 0.0610	R1 = 0.0256, wR2 = 0.0680
R indices (all data)	R1 = 0.0387, wR2 = 0.0699	R1 = 0.0302, wR2 = 0.0618	R1 = 0.0366, wR2 = 0.0740
Largest diff. peak and hole / e.A^{-3}	0.969 and -0.528	0.514 and -0.415	0.540 and -0.466

Table A6. Crystal data and structure refinements of the $\{Ph_2P(O)C_6H_4\}Me_2SiCH_2(Ph)SnBr_2$, **25**.

Empirical formula	C_{27} H_{27} Br_2 O P Si Sn
Formula weight	705.05
Temperature / K	173(2)
Wavelength /°A	0.71073
Crystal system	Monoclinic
space group	P2(1)/c
a /°A	11.0187(6)
b /°A	13.2020(7)
c /°A	19.2105(9)
α /°	90
β /°	102.523(5)
γ /°	90
Volume /°A^3	2728.0(2)
Z	4
Dc /$g.cm^{-3}$	1.717
Absorption coefficient /mm^{-1}	3.987
F(000)	1384
Crystal size /mm	0.24 x 0.09 x 0.08
Range for data collection /°	2.172 to 25.500
Reflections collected	26849
Independent reflections	5071
Refinement method	Full-matrix least-squares on F^2
Data / restraints / parameters	5071 / 72 / 294
Goodness-of-fit on F^2	1.047
Final R indices [$I>2\sigma(I)$]	R1 = 0.0376, wR2 = 0.0944
R indices (all data)	R1 = 0.0545, wR2 = 0.1005
Largest diff. peak and hole / $e.A^{-3}$	0.974 and -1.127

2. Tin-containing Siloxanes and Related Dimeric Tetraorganodistannoxanes: Syntheses and Structures

2.1 Introduction

Organosiloxanes and silicates are an important and diverse body of materials. They are based on Si–O bonds and consequently they can be classified in common groups of compounds according to the structural units present in the compound. They can be described using the letters M, D, T, and Q (Table 1). Linear silicone fluids are composed mainly of D units. The base polymers for silicone elastomers or silicone rubbers consist of D units that bear cross-linkable functional groups. The main structural feature of the highly branched silicone resins are T units, often combined with D units to make the resins more flexible. Silicone resins can also contain Q and M units.

Organosiloxanes are generally produced by the hydrolysis of organosilanes having electronegative subtituents like chloro or alkoxy groups.
Hydrolysis of diorganodichlorosilanes affords either the corresponding cyclic organosiloxanes or polymerize directly to the linear polyorganosiloxanes (also called

siloxanes). The latter can be prepared from *cyclo*-organosiloxanes by the so-called ring-opening polymerization (ROP) that is promoted by cationic or anionic catalysts. The ring-opening polymerization procedure of the methyl-substituted six-membered trisiloxane ring, *cyclo*-$(Me_2SiO)_3$, (D3) is employed for the preparation of high-molecular weight polymers.[1]

Table 1. Structural units in organosiloxanes and silicates.

Siloxane structural unit		Example
Symbol	Functionality	
M	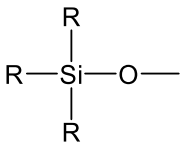	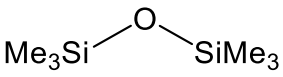
D	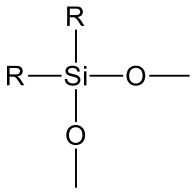	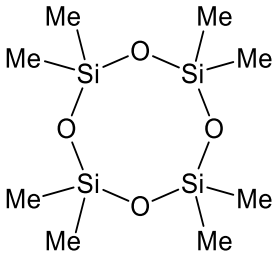
T	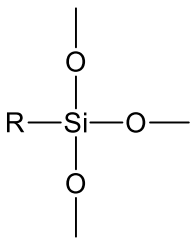	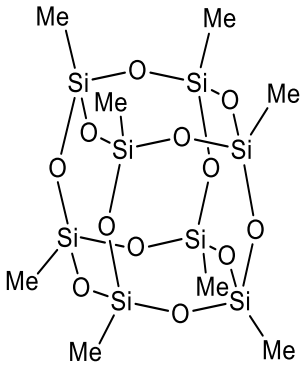
Q	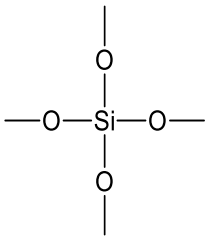	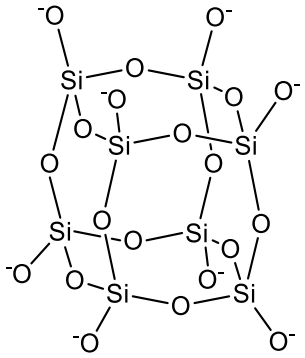

Polyorganosiloxanes are the most important inorganic polymers. The worldwide industrial production of siloxanes was enormously increased since the early 1940s, by the development of methylchlorosilane synthesis (Rochow-Müller direct synthesis) at the industrial scale.

In 2002, the total production of siloxanes was estimated to be 2 million tons per year presenting a business volume of about 8 Billion Euros.[2] The miscellaneous molecular structures and the close relationship between structure and properties, not achievable by any other class of polymers, raise the motivation to develop siloxane-based materials. A large diversity of industrial silicone products have been developed ranging from linear chains (fluids) to slightly and highly cross-linked networks (rubbers and resins respectively). These unique physical properties allowed their use in a diverse range of applications in areas like proceeding aids, personal care, paints and protective coating, adhesives, lubricants, automotive, and medical areas.[3]

Hydrolysis of monoorganosilanes from the type $RSiX_3$ (X = halide, alkoxide) affords the corresponding silsesquioxanes $(RSiO_{1.5})_n$. These compounds have often been described as having hybrid properties, that is, some from the chemically inert and thermally stable inorganic Si–O–Si fragment and some from the potentially reactive and readily modified R-Si fragment. This is a result of their formula unit being between that for the inorganic ceramic materials and that for the organic polymers. In particular, much interest has been paid to the cubic T8 silsesquioxane $(RSiO_{1.5})_8$, consisting of a rigid, crystalline silica-like core that is perfectly defined spatially (0.5–0.7 nm) and linked covalently to eight R groups.[1b, 4]
Silsesquioxanes have been used in a diversity of contexts such as in molecular science,[4f, 5] as catalysts,[4a, 6] as building blocks,[5c, 7] as cores for branched dendritic macromolecules,[6a, 8] as binders for ceramics,[9] as atomic scavengers,[10] in liquid crystals,[11] as redox-active materials,[12] for the preparation of optical device,[13] or to support effects like electrochromism,[14] sensing with modified electrodes,[15] and hole transport in light emitting diod materials.[16]

In the last three decades metal-supported siloxanes have attracted considerable attention, due to their potential as precursors for the preparation of ceramic materials and model compounds that effectively mimic heterogeneous silica-supported

catalysts.[4a, 17] Such compounds have been widely used as heterogeneous catalysts in a variety of organic transformations.[17g, 18]

The most tin-containing siloxanes are based on Sn–O–Si bonds and are called stannasiloxanes (or silastannoxanes). A large diversity of stannasiloxanes are reported in the literature ranging from the linear stannasiloxanes ($R_3SiOSnR'_3$),[19] during the cyclic stannasiloxanes of different ring sizes (*cyclo*-$R'_2Sn(OR_2Si)_2O$,[20] *cyclo*-$O(R_2SiOR'_2Sn)_2O$,[21] and *cyclo*-$R_2Si(OR'_2SnO)_2R_2Si$,[21b]), to more complicated oxo clusters like the cubic clusters (T_7-$OSnMe_3$,[22] and $T_8(OSnR_3)_8$[7d, 23]) (Chart 1).

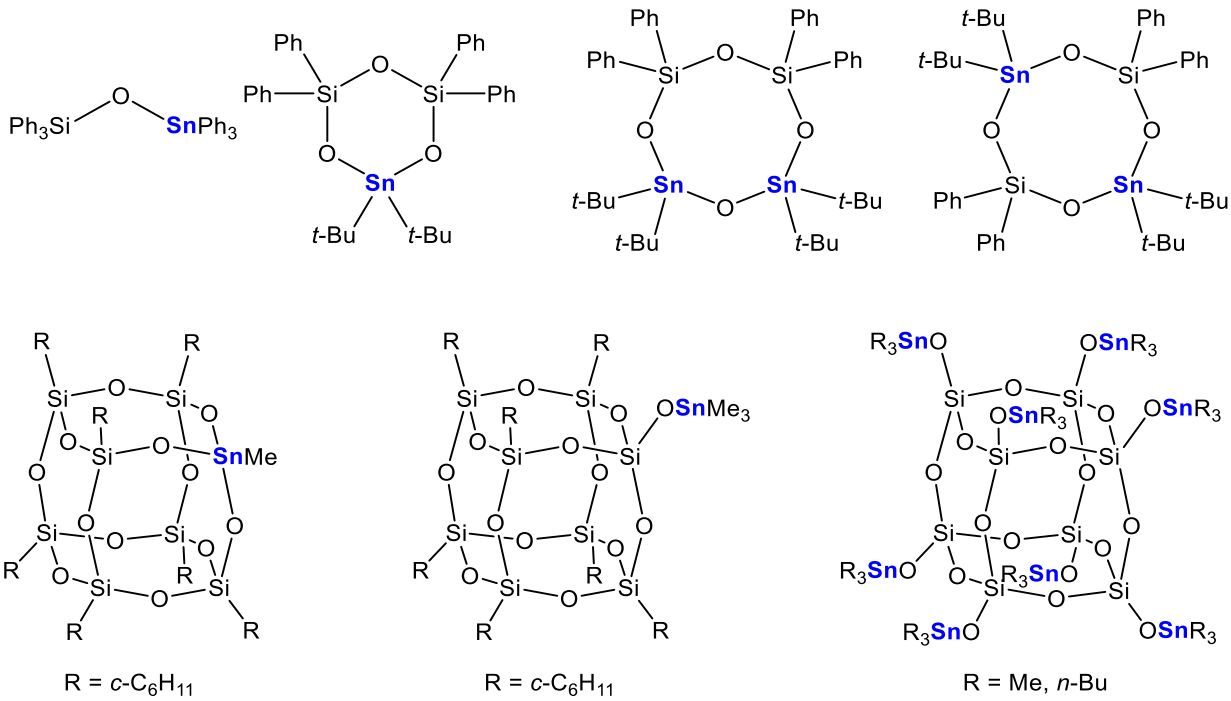

Chart 1. Different types of stannasiloxanes.

However, the high kinetic lability of the Sn–OSi bond makes the stannasiloxanes not particularly stable and unsuitable for industrial use. The eight-membered stannasiloxane $RR'Sn(OPh_2SiO)_2SnRR'$ reacts with different organoelements oxides affording, upon insertion of the organoelement moiety in the labile Sn–OSi bond, the corresponding six-membered ring (Scheme 1),[17a, 24] and the tin-substituted spherosilicates react with many high valent transition metal and main group chlorides (e.g. $AlCl_3$, $SiCl_4$, $TiCl_4$, $VOCl_3$) to cleanly metathesize the trialkyltin group for the metal chloride (Scheme 2)[7c, 25].

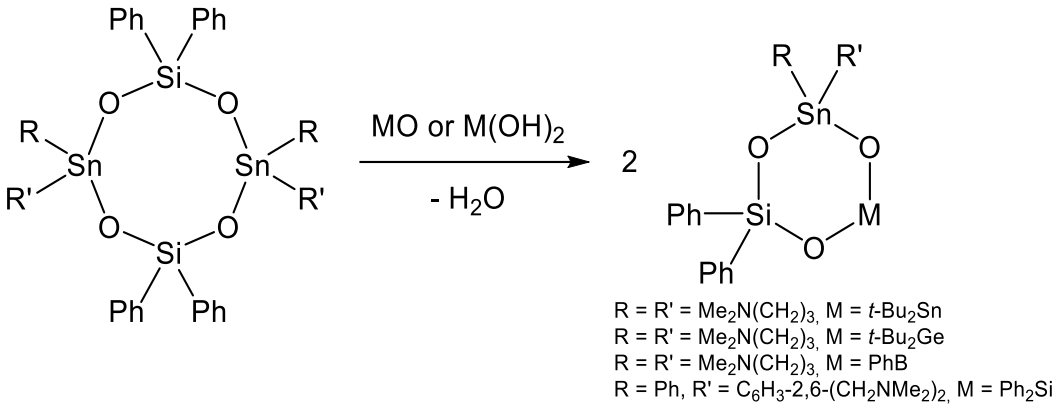

Scheme 1. Insertion of the organoelement oxide moiety in the labile Sn–OSi bond.

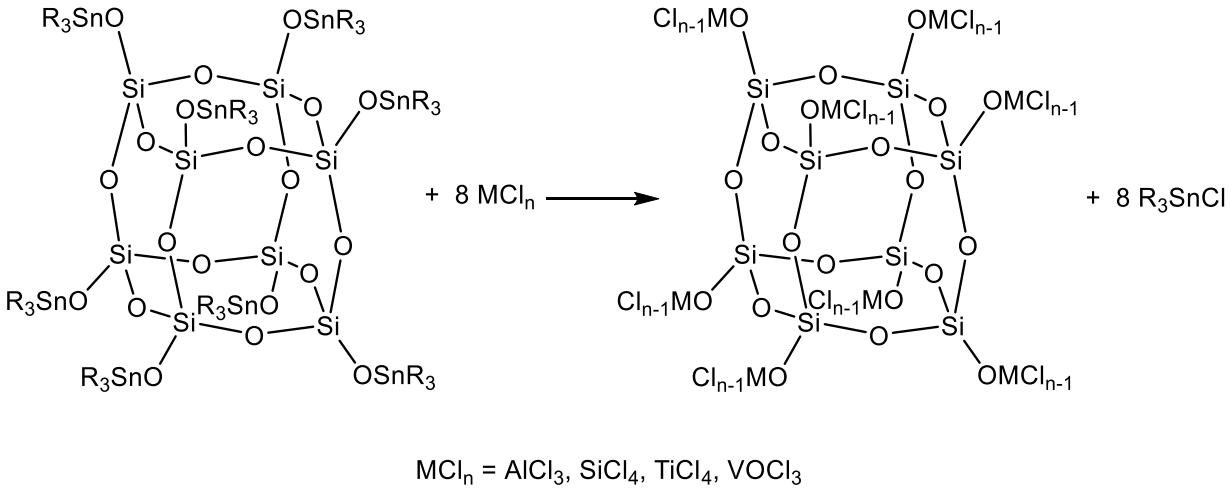

Scheme 2. Metathesize of the tin-substituted spherosilicate.

On the other hand, tin-containing siloxanes, in which the tin atom is covalently bound to the siloxane framework, not by oxygen linkage, are more stable. However these are less researched. To the best of our knowledge the *cyclo*-siloxanes (**A**)[26] and (**B**)[27], and the silsesquioxane tethered fluorene ligands (*c*-$C_5H_9)_7Si_8O_{12}CH_2$-9-Flu(9-$SnMe_3$) (**C**)[28], are the only such examples (Chart 2).

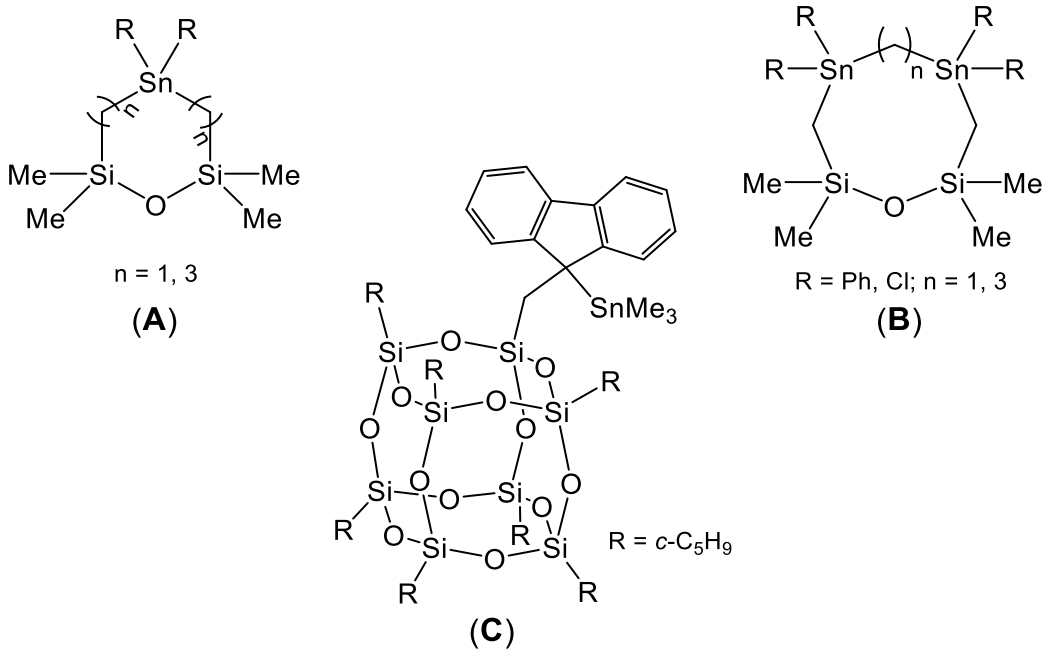

Chart 2. Tin-supported siloxanes in which the tin atom is bound to the silicon atom by carbon linkage.

In this chapter we report on the syntheses of *cyclo*-siloxanes and silsesquioxanes that contain tin atoms bound to the silicon atoms via carbon linkage ($SnCH_2Si$) (Chart 3).

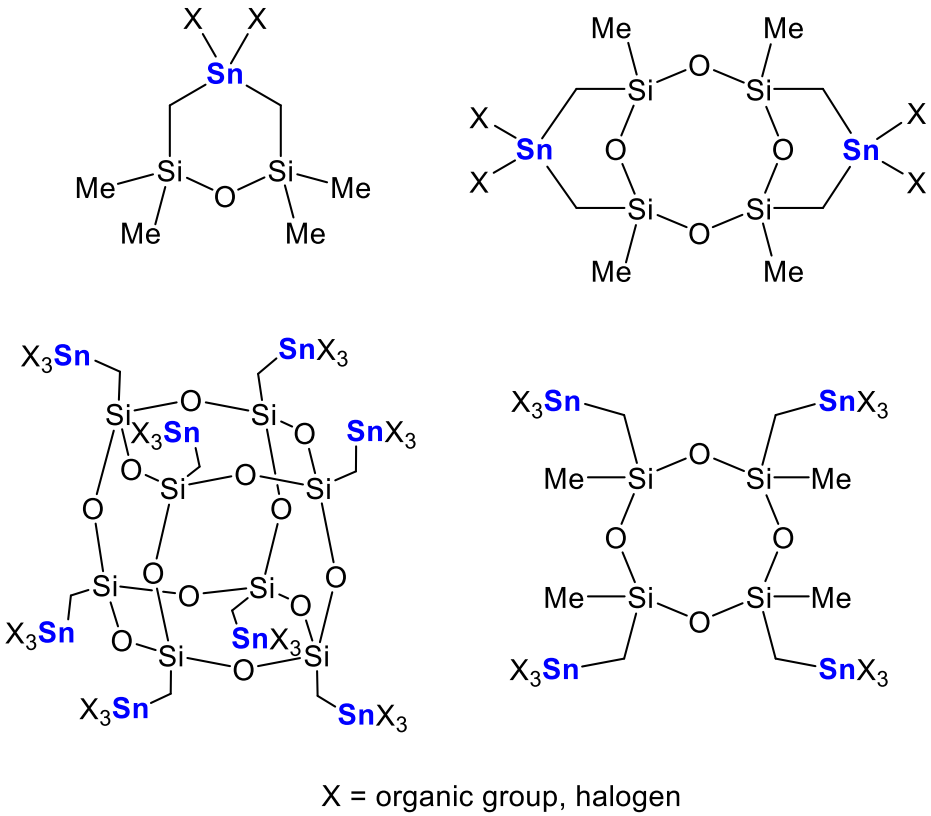

Chart 3. Tin-substituted siloxanes and silsesquioxanes.

These compounds could be interpreted as single source precursors for structurally modified polysiloxanes and silicates.

Also reported is the assembling of the tin-containing six-membered *cyclo*-siloxanes, $X_2Sn(CH_2Me_2Si)_2O$, by means of hydrolysis condensation of the Sn–X bonds, in presence of water-free oxygen source, resulting in the corresponding ladder-like diorganotinoxo clusters in which the tin atoms are part of the *cyclo*-siloxane ring.

2.2 Results and Discussion

2.2.1 Syntheses, structures and reactivity of the tin-containing six-membered *cyclo*-siloxanes 1–7

The reaction of diphenyltin dichloride, Ph_2SnCl_2, with two molar equivalents of the Grignard reagent $Me_2(i\text{-PrO})SiCH_2MgCl$[29] followed with acidic hydrolysis provided the tin-containing six-membered *cyclo*-siloxane *cyclo*-$Ph_2Sn(CH_2Me_2Si)_2O$, **1**, in very good yield (Scheme 3). Compound **1** has been reported before by Mironov et al. by the reaction of $Cl_2Sn(CH_2Me_2Si)_2O$ with PhMgX, however, no spectroscopic details or molecular structure were given in this report.[26a]

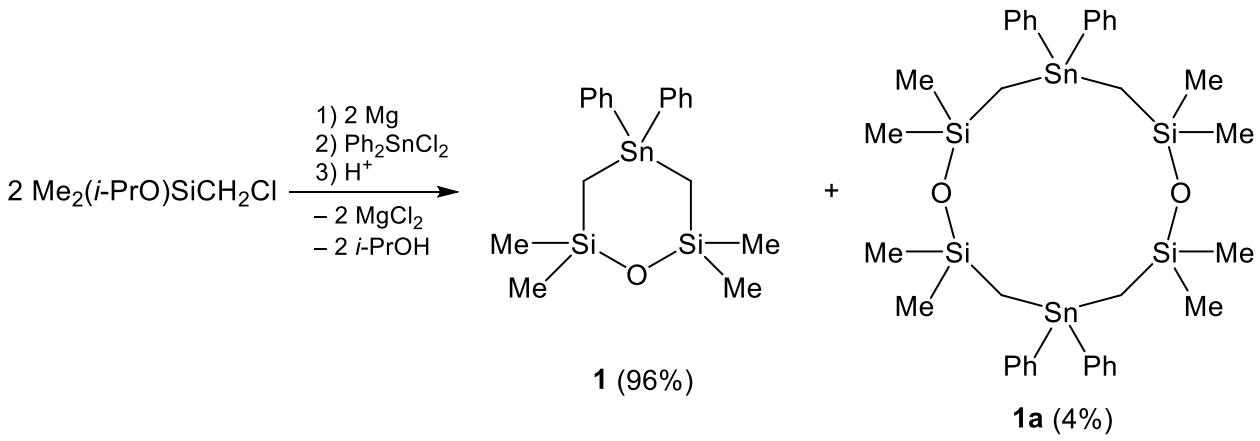

Scheme 3. Synthesis of *cyclo*-$Ph_2Sn(CH_2Me_2Si)_2O$, **1**.

The ^{119}Sn NMR spectrum of the reaction product (in $CDCl_3$) reveals a singlet resonance at δ –57 (integral 96) that is assigned to compound **1**. In addition, there is

a singlet at δ –53 (integral 4) that is tentatively attributed to the twelve-membered ring $Ph_2Sn(CH_2Me_2SiOSiMe_2CH_2)_2SnPh_2$, **1a**. The ^{13}C NMR spectrum of the same solution displayed a single resonance for the methylene group Si*C*H_2Sn at δ –5.1 with $^1J(^{13}C–^{117/119}Sn)$ coupling constants of 225/236 Hz, and the ^1H NMR spectrum showed a signal for Si*C*H_2Sn protons at δ 0.39 with $^2J(^1H–^{117/119}Sn)$ coupling constant of 70.8 Hz.

Halogenation and proto-destannylation of *cyclo*-$Ph_2Sn(CH_2Me_2Si)_2O$, **1**, afforded the corresponding cyclic organotin (IV) halides *cyclo*-$PhISn(CH_2Me_2Si)_2O$, **2**, and *cyclo*-$X_2Sn(CH_2Me_2Si)_2O$ (**3**, X = I; **4**, X = Br; **5**, X = Cl), respectively, in very good yields (Scheme 4).

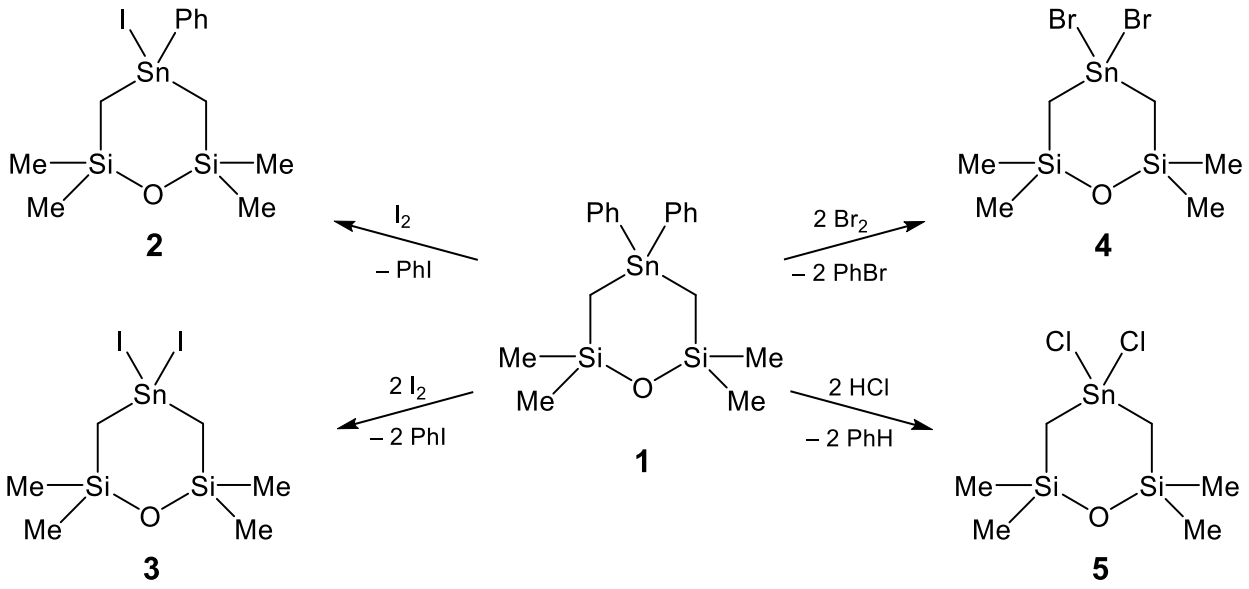

Scheme 4. Syntheses of the organotin halides **2**–**5**.

Compounds **2**–**5** are tin-containing *cyclo*-siloxanes containing halogen substituents at the tin atoms which in turn allow further modification by simple reactions. This was proved by the reaction of *cyclo*-$PhISn(CH_2Me_2Si)_2O$, **2**, with the Grignard reagent $Me_2N(CH_2)_3MgCl$ affording in high yield the *cyclo*-siloxane *cyclo*-$\{Me_2N(CH_2)_3\}PhSn(CH_2Me_2Si)_2O$, **6** (Scheme 5).

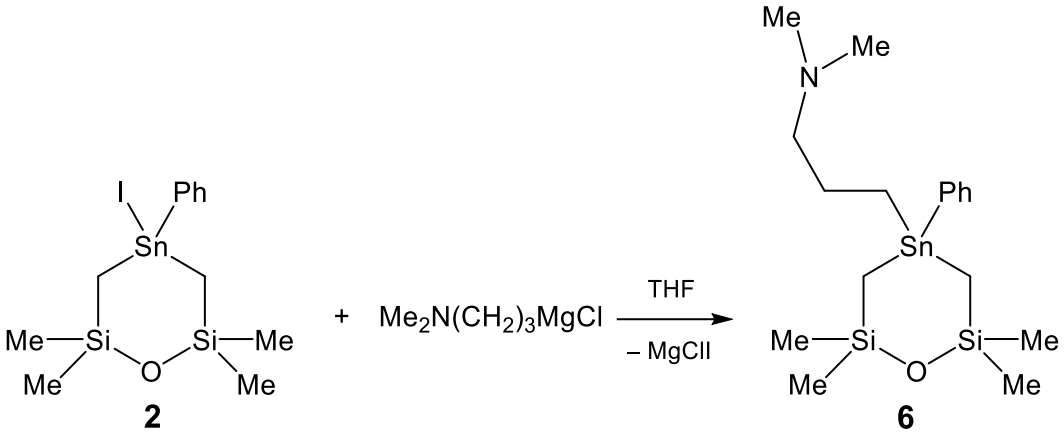

Scheme 5. Synthesis of *cyclo*-{$Me_2N(CH_2)_3$}PhSn($CH_2Me_2Si)_2O$, **6**.

Reaction of compound **6** with one molar equivalent elemental iodine provided, under Sn–C_{Ph} bond cleavage, the triorganotin iodide *cyclo*-{$Me_2N(CH_2)_3$}ISn($CH_2Me_2Si)_2O$, **7**, in very good yield (Scheme 6). The high base amine group in compound **7** seems to suffer partial protonation in time, in presence of air moisture, as evidenced by a broad singlet at *δ* 9.28 for N*H* proton observed in the ^{1}H NMR spectrum.

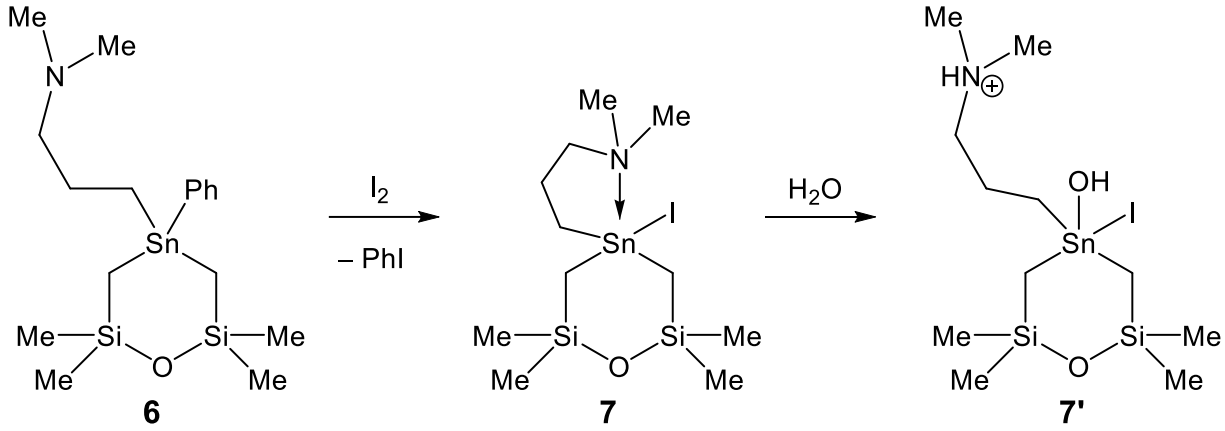

Scheme 6. Synthesis of compound **7** and its protonation in moist air.

The solubility of compounds **1–7** in common organic solvents such as CH_2Cl_2, $CHCl_3$, toluene and THF is excellent. The NMR data of compounds **1–7** and the parent compounds $(Me_3SiCH_2)_2SnX_2$ (X = Ph[30], Cl[31], Br[31]) are listed in Table 2.

Table 2. Selected NMR data of compounds **1**–**7**, and of $(Me_3SiCH_2)_2SnX_2$ (X = Ph, Cl, Br).

			$SnCH_2Si$	
	δ ^{119}Sn	δ ^{29}Si	δ ^{1}H	δ ^{13}C
		[^2J(^{29}Si–$^{117/119}$Sn)]	[^2J(^{1}H–$^{117/119}$Sn)]	[^1J(^{13}C–$^{117/119}$Sn)]
1	–57	10.2 [35]	0.39 [70.8]	–5.1 [26]
$(Me_3SiCH_2)_2SnPh_2$[30]	–49	–	0.26	–3.6
2	–29	9.9 [39]	0.87 [79.8]	3.06 [211/221]
3	–207	9.7 [41]	1.49 [98.4/102.8]	13.6 [200/210]
4	54	9.6 [40]	1.18 [105.4/110.5]	13.7 [233/245]
$(Me_3SiCH_2)_2SnBr_2$[31]	68	3.4 [37]	1.01 [89]	14.0 [296]
5	145	9.6 [39]	1.00 [109.4/114.4]	12.6 [260/272]
$(Me_3SiCH_2)_2SnCl_2$[31]	147	3.1 [38]	0.79 [91]	13.0 [328]
6	–24	9.9 [36]	0.10, 0.22 [68.3]	–5.7 [215/224]
7	60	9.4 [43]	0.73 [72.8/76.1]	3.8 [206/215]

The chemical shifts are given in ppm, and the coupling constants are given in Hz.

The ^{119}Sn NMR spectra of compounds **1**–**7** showed resonances at δ –57, –29, –207, 54, 145, –24 and 60, respectively. In addition, resonances with an integral of approx 4% at δ –52, –21, –180, 121 and –18 in the ^{119}Sn NMR spectra of compounds **1**, **2**, **3**, **5** and **6**, respectively, were observed. With caution, these relate to the dimers of the corresponding compounds 1a, 2a, 3a, 5a, and 6a, repectively, being based on the twelve-membered *cyclo*-siloxane ring $Sn(CH_2Me_2SiOSiMe_2CH_2)_2Sn$.

The resonances for the compounds *cyclo*-$Ph_2Sn(CH_2Me_2Si)_2O$, **1**, (δ –57), *cyclo*-$Br_2Sn(CH_2Me_2Si)_2O$, **4**, (δ 54) and *cyclo*-$Cl_2Sn(CH_2Me_2Si)_2O$, **5**, (δ 145) are slightly high-field shifted in comparison with those for the parent compound $Me_3SiCH_2)_2SnX_2$ (X = Ph[30] , Br[31], Cl[31]) at δ –49, 68 and 147, respectively. This is a result of the weak O···Sn interactions present in compounds **1**, **4**, and **5**.

The ^2J(^{1}H–$^{117/119}$Sn) coupling constant for the methylene protons $SnCH_2Si$ increases as the Lewis acidity of the tin atom increases being in the range between 68.3 Hz for the tetraorganotin compound *cyclo*-$\{Me_2N(CH_2)_3\}PhSn(CH_2Me_2Si)_2O$, **6**, and 109.8/114.5 Hz for the diorganotin dichloride *cyclo*-$Cl_2Sn(CH_2Me_2Si)_2O$, **5**. The

$^{1}J(^{13}C–^{117/119}Sn)$ coupling constant for the Sn*C*H_2Si methylene carbon atom in the diorganotin dihalides *cyclo*-$X_2Sn(CH_2Me_2Si)_2O$ (**3**, X = I; **4**, X = Br; **5**, X = Cl) increases in the order I < Br < Cl being between 200/210 Hz and 260/272 Hz.

The electrospray mass spectra (ESI MS, positive mode) of the tetraorganotin compounds *cyclo*-$Ph_2Sn(CH_2Me_2Si)_2O$, **1**, and *cyclo*-$\{Me_2N(CH_2)_3\}PhSn(CH_2Me_2Si)_2O$, **6**, showed the corresponding $[M + nMeCN + H/Na]^+$ and $[M – Ph]^+$ mass clusters. That for the triorganotin iodide *cyclo*-$PhISn(CH_2Me_2Si)_2O$, **2**, showed a mass cluster centered at *m/z* 429.1 for $[M – I + 4H_2O]^+$ and another with nearly the same relative abundance centered at *m/z* 729.1 for the hydrolysis product $[2M – 2I + OH]^+$.

The ESI MS spectrum of the amine substituted triorganotin iodide *cyclo*-$\{Me_2N(CH_2)_3\}ISn(CH_2Me_2Si)_2O$, **7**, showed in positive mode mass clusters at *m/z* 493.9, 366.0, and 402.0 for $[M + H]^+$, $[M – I]^+$, and $[M – I + 2H_2O]^+$, respectively.

The ESI MS spectra of the diorganotin halides **3**–**5** showed a major mass cluster centered at *m/z* 885.1. This fits exactly with the protonated hydrolysis product $[\{O(Me_2SiCH_2)_2SnO\}_3 + H]^+$ (Chart 4, **A**) that was also observed in the ESI MS spectrum of [*i-P*r$O(Me_2)SiCH_2]_2SnBr_2$.[32] A mass cluster centered at *m/z* 959.1 for [**A** + $4H_2O]^+$ with about 33% relative abundance was also observed.

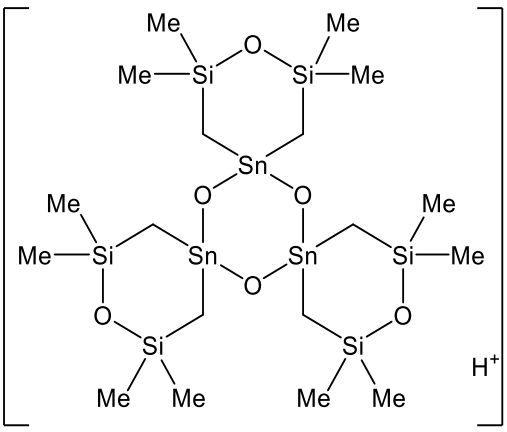

A *m/z* 885.1

Chart 4.

The hydrolysis under basic conditions of the diorganotin diiodide *cyclo*-$I_2Sn(CH_2SiMe_2)_2O$, **3**, by reaction with trimethylamine and water in toluene afforded white solid that is poorly soluble in $CHCl_3$ and CH_2Cl_2 and slightly soluble in toluene. The elemental analysis of the reaction product agrees with the diorganotin oxide $[O(Me_2SiCH_2)_2SnO]_n$, **8** (Scheme 7), and the mass spectrum in positive mode in the range between 0 and 2000 *m/z* showed many mass clusters that relate to the different oligomers of the oxide, $[nM + aH_2O + bMeCN + H/Na]^+$, (M = $[O(Me_2SiCH_2)_2SnO]$, n = 1 – 6).

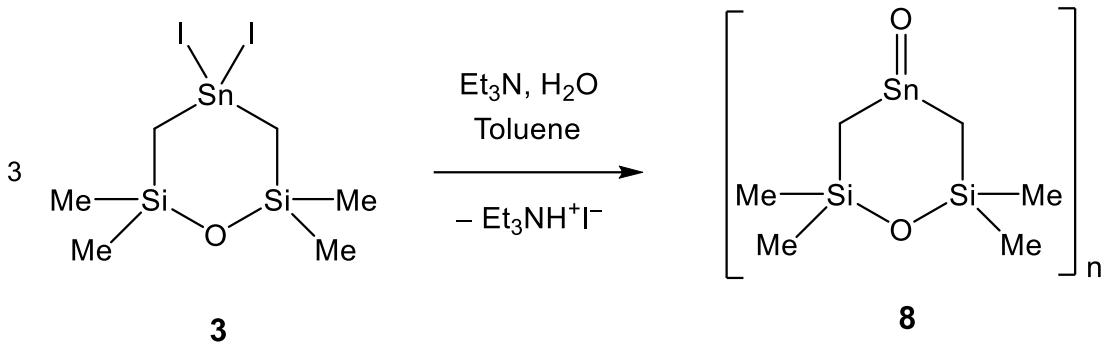

3 **8**

Scheme 7. Synthesis of the diorganotin oxide $[O(Me_2SiCH_2)_2SnO]_n$, **8**.

2.2.1.1 Molecular structures of the tin-containing six-membered siloxanes (1, 2, 3, and 6), and the twelve-membered siloxane, 5a

Recrystallization of *cyclo*-$Ph_2Sn(CH_2Me_2Si)_2O$, **1**, from a solution in ethanol, of *cyclo*-$PhISn(CH_2Me_2Si)_2O$, **2**, from acetonitrile, of *cyclo*-$I_2Sn(CH_2Me_2Si)_2O$, **3**, from hexane, and of *cyclo*-$\{Me_2N(CH_2)_3\}PhSn(CH_2Me_2Si)_2O$, **6** from CH_2Cl_2/hexane, afforded colorless single crystals suitable for the X-ray diffraction analyses. Compound **6** crystallized as **6**·HI. Recrystallization of **5** from CH_2Cl_2/EtOH afforded few crystals of the twelve membered ring, **5a**. The molecular structures of compounds **1**–**3**, **5a** and **6**·HI are shown in Figures 1–5, respectively, and selected bond lengths and bond angles are summarized in Tables 3–5.

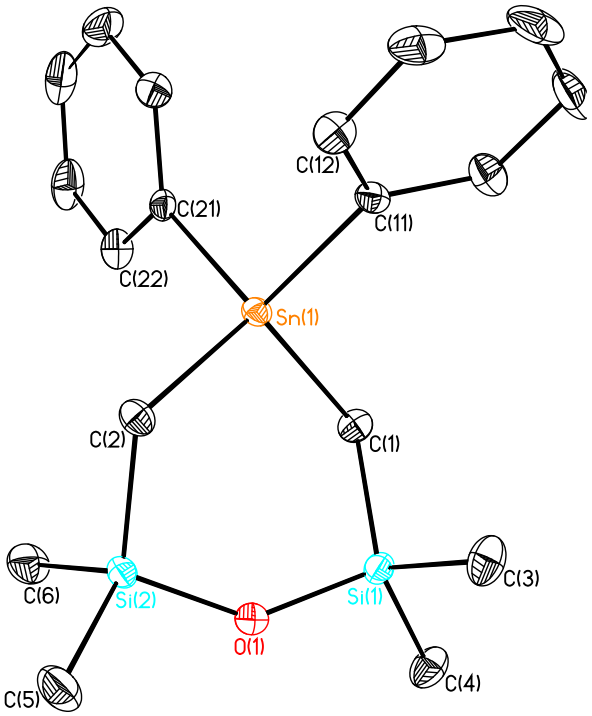

Figure 1. General view (SHELXTL) of a molecule of *cyclo*-$Ph_2Sn[CH_2Si(Me_2)]_2O$, **1**, showing 30% probability displacement ellipsoids and the crystallographic numbering scheme. Hydrogen atoms are omitted for clarity.

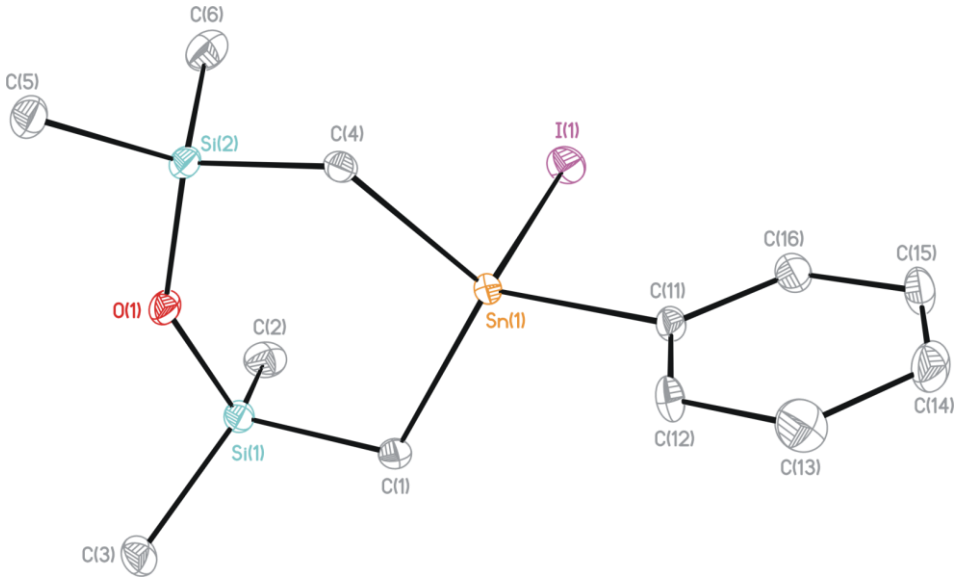

Figure 2. General view (SHELXTL) of a molecule of *cyclo*-$PhISn[CH_2Si(Me_2)]_2O$, **2**, showing 30% probability displacement ellipsoids and the crystallographic numbering scheme. Hydrogen atoms are omitted for clarity.

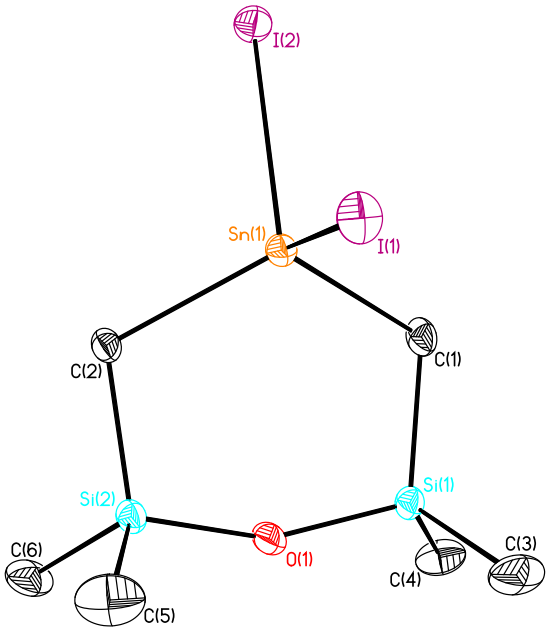

Figure 3. General view (SHELXTL) of a molecule of *cyclo*-$I_2Sn[CH_2Si(Me_2)]_2O$, **3**, showing 30% probability displacement ellipsoids and the crystallographic numbering scheme. Hydrogen atoms are omitted for clarity.

Table 3. Selected bond lengths /Å and bond angles /° in **1**–**3**.

	1	**2**	**3**
$Sn–C_{Ph}$	2.141(4), 2.137(4)	2.140(3)	–
Sn–I	–	2.7151(3)	2.7005(7), 2.7020(7)
$Sn–C_{CH2}$	2.143(4), 2.159(3)	2.131(3), 2.135(3)	2.132(7), 2.139(7)
Si–O	1.646(3), 1.629(3)	1.643(2), 1.639(2)	1.632(6), 1.621(6)
Sn–O	3.5072(29)	3.4082(18)	3.2382(61)
A–Sn–B	107.22(14)	103.80(8)	104.96(2)
$C_{CH2}–Sn–C_{Ph}$	109,49(14)–111.32(15)	113.32(11), 116.22(11)	–
C_{CH2}–Sn–I	–	105.93(8), 108.49(8)	108.2(2)–109.8(2)
$C_{CH2}–Sn–C_{CH2}$	108.03(15)	108.48(11)	114.8(3)
O–Si–C	106.61(19)–109.68(18)	107.53(12)–109.56(13)	107.4(4)–109.0(4)
Si–C–Sn	111.94(18), 112.88(18)	112.94(14), 113.25(14)	110.4(3), 110.7(4)
Si–O–Si	140.5(2)	142.84(14)	153.9(4)

1, A=C(21), B=C(11); **2**, A=I(1), B=C(11); **3**, A=I(1), B=I(2).

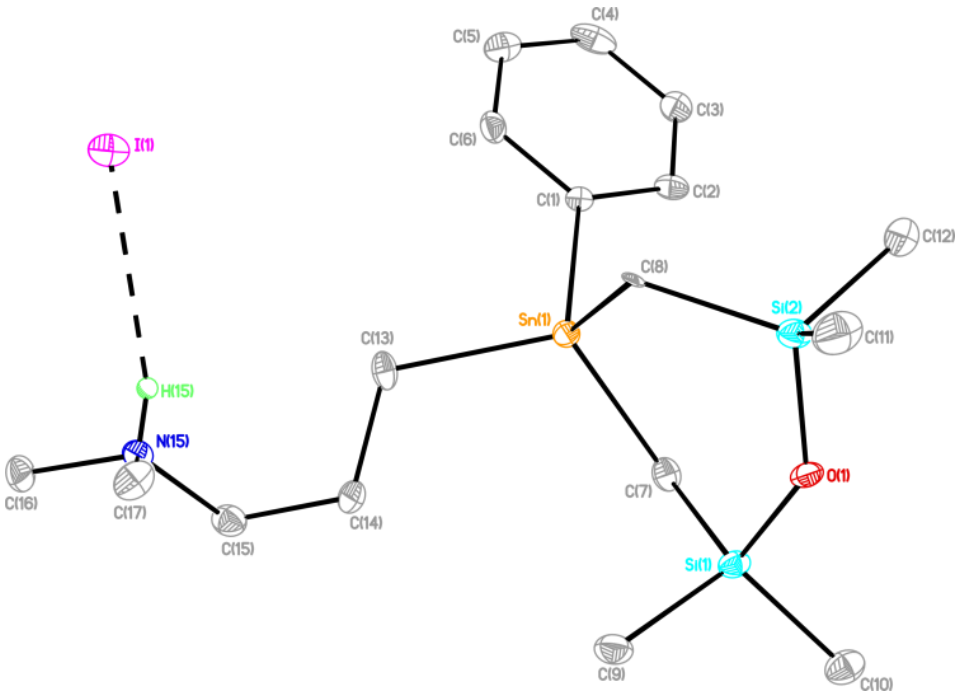

Figure 4. General view (SHELXTL) of a molecule of **6**·HI showing 30% probability displacement ellipsoids and the crystallographic numbering scheme. Hydrogen atoms are omitted for clarity.

Table 4. Selected bond lengths /Å and bond angles /° in **6**·HI.

Sn(1)–C(1)	2.168(2)	Si(1)–O(1)	1.637(3)
Sn(1)–C(7)	2.145(5)	Si(2)–O(1)	1.648(4)
Sn(1)–C(8)	2.124(5)	H(15)...I(1)	2.76(5)
Sn(1)–C(13)	2.165(5)	N(15)...I(1)	3.476(5)
Sn(1)–O(1)	3.5393(31)	Si(1)–O(1)–Si(2)	140.1(3)
C(1)–Sn(1)–C(7)	111.55(16)	C(13)–Sn(1)–C(7)	113.8(2)
C(1)–Sn(1)–C(8)	109.96(15)	C(13)–Sn(1)–C(8)	109.99(18)
C(1)–Sn(1)–C(13)	105.06(16)	C(7)–Sn(1)–C(8)	106.49(19)
Sn(1)–C(7)–Si(1)	112.9(2)	Sn(1)–C(13)–C(14)	115.8(4)
Sn(1)–C(8)–Si(2)	116.3(2)	I(1)–H(15)–N(15)	151(5)

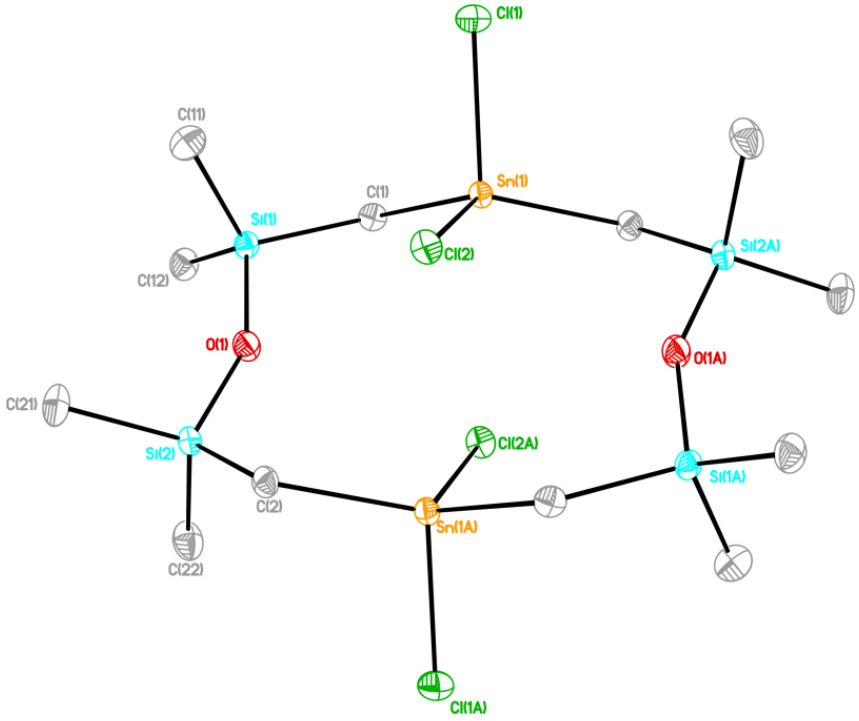

Figure 5. General view (SHELXTL) of a molecule of $Cl_2Sn(CH_2Me_2SiOSiMe_2CH_2)_2SnCl_2$, **5a**, showing 30% probability displacement ellipsoids and the crystallographic numbering scheme. Hydrogen atoms are omitted for clarity.

Table 5. Selected bond lengths /Å and bond angles /° in **5a**.

Sn(1)–C(1)	2.111(3)	Sn(1)–O(1a)	3.7150(19)
Sn(1)–C(2a)	2.106(3)	Sn(1)–Cl(2a)	3.3861(8)
Sn(1)–Cl(1)	2.3619(8)	Si(1)–O(1)	1.619(2)
Sn(1)–Cl(2)	2.3581(7)	Si(2)–O(1)	1.625(2)
Sn(1)–O(1)	3.7680(19)		
Cl(1)–Sn(1)–Cl(2)	96.91(3)	Cl(2a)–Sn(1)–Cl(1)	173.590(25)
Cl(1)–Sn(1)–C(1)	102.92(8)	Cl(2a)–Sn(1)–C(1)	79.314(85)
Cl(1)–Sn(1)–C(2a)	105.47(9)	Sn(1)–Cl(2)–Sn(1a)	103.297(25)
Cl(2)–Sn(1)–C(1)	111.59(8)	Cl(2a)–Sn(1)–Cl(2)	76.703(23)
Cl(2)–Sn(1)–C(2a)	112.77(7)	Cl(2a)–Sn(1)–C(2a)	77.821(21)
C(1)–Sn(1)–C(2a)	122.92(11)	Sn(1)–C(1)–Si(1)	118.75(13)
Si(1)–O(1)–Si(2)	152.52(14)	Sn(1a)–C(2)–Si(2)	119.01(14)

The tetraorganotin compounds *cyclo*-$Ph_2Sn(CH_2Me_2Si)_2O$, **1**, and [*cyclo*-{$[Me_2NH(CH_2)_3]PhSn(CH_2Me_2Si)_2O]^+$ I^-, **6**·HI, exhibit distorted twist-boat conformations, whereas the organotin halides *cyclo*-$PhISn(CH_2Me_2Si)_2O$, **2**, and *cyclo*-$I_2Sn(CH_2Me_2Si)_2O$, **3**, show distorted chair conformations (Figure 6).[33] The torsion angles within the six-membered ring in compounds **1**–**3**, and **6**·HI are given in Table 6. All tin and silicon atoms in compounds **1**–**3** and **6**·HI exhibit distorted tetrahedral environment.

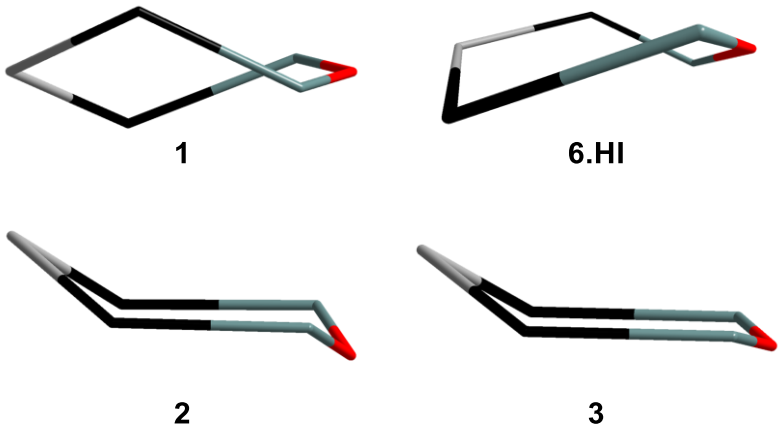

Figure 6. The molecular structure of compounds **1**, **2**, **3** and **6**·HI. Tin is presented in gray, silicon is presented in green, carbon is presented in black, and oxygen is presented in red. All atoms bound to the six-membered ring are omitted for clarity.

Table 6. Torsion angles within the six-membered rings in compounds **1**–**3** and **6**·HI.

	1	**2**	**3**	**6**·HI
Sn(1)–C_{CH2}–Si(1)–O(1)	49.3(2)	–34.07(19)	25.2(5)	–50.0(3)
C_{CH2}–Si(1)–O(1)–Si(2)	–28.6(4)	47.3(3)	–28.7(12)	34.6(4)
Si(1)–O(1)–Si(2)–C_{CH2}	–22.3(4)	–49.1(3)	28.1(12)	13.7(4)
O(1)–Si(2)–C_{CH2}–Sn(1)	41.9(2)	37.67(18)	–24.0(5)	–39.0(3)
Si(2)–C_{CH2}–Sn(1)–C_{CH2}	–18.2(2)	–40.94(18)	35.2(5)	18.9(3)
C_{CH2}–Sn(1)–C_{CH2}–Si(1)	–27.7(2)	38.67(18)	–35.9(5)	26.2(3)

The Si–O–Si bond angles in compounds **1** and **6**·HI, which contain tin atoms with relatively low Lewis acidity, are in the range of 140°. They are in the same order of magnitude as those found in the six-membered rings containing the Si–O–Si

fragment like $HN\{(CH_2)_2O\}_2Sn(CH_2Me_2Si)_2O$[34] [143.1(7)°, 143.1(6)°], and $I_2Te(CH_2Me_2Si)_2O$ [144.3(4)°][35]. The low Lewis acidity of the tin atoms in **1** and **6**·HI results in lower Si–O···Sn interactions with Sn–O distance above 3.50 Å in both compounds.

In compounds *cyclo*-$PhISn(CH_2Me_2Si)_2O$, **2**, and *cyclo*-$I_2Sn(CH_2Me_2Si)_2O$, **3**, containing tin atoms with enhanced Lewis acidity, the Sn···O distances are 3.4082(18) (**2**) and 3.2382(61) Å (**3**).

The C–Sn–C angle in the six-membered ring in **3** of 114.8(3)° is larger than that in **1** [108.03(15)°], **6**·HI [106.49(19)°] and **2** [108.48(11)°]. This could also be attributed to the stronger O···Sn interaction in **3** in comparison to that in **1**, **6**·HI and **2**. The O···Sn interaction compresses the C–Sn–C angle resulting in bigger value. The Si–O bond lengths in **1**, **6**·HI, **2** and **3** ranging between 1.621(6) and 1.648(4) Å are rather similar to those in $HN\{(CH_2)_2O\}_2Sn(CH_2Me_2Si)_2O$[34] [1.61(1)–1.64(1) Å] and $I_2Te(CH_2Me_2Si)_2O$[35] [1.608(6), 1.625(6) Å]. All other bond lengths and angles do not show any particularity.

The compound $Cl_2Sn(CH_2Me_2SiOSiMe_2CH_2)_2SnCl_2$, **5a**, is a twelve-membered ring in which the four silicon atoms are nearly in the same plane and the carbon atoms bound to one tin atom are placed in the opposite direction to those bound to the other tin atom with respect to the plane. The oxygen atoms are also placed oppositely, one being above the plane and one below it (Figure 7).

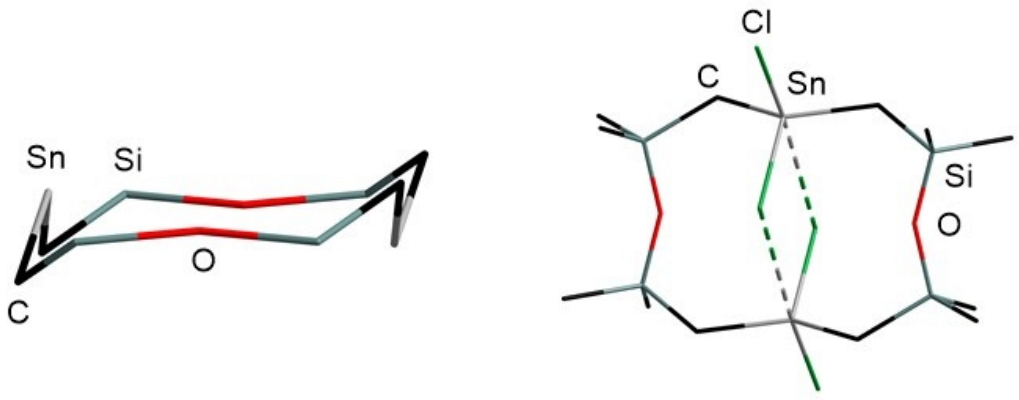

Figure 7. Two views for $Cl_2Sn(CH_2Me_2SiOSiMe_2CH_2)_2SnCl_2$, **5a**. All hydrogen atoms are omitted for clarity. In the view on left, all atoms bound to the twelve-membered ring are omitted for clarity.

The Sn–C [2.106(3) and 2.111(3) Å], Si–O [1.619(2) and 1.625(2) Å], and Si–C bonds [1.845(3) to 1.865(3) Å] in compound **5a** are comparable with those in the diorganotin diiodide *cyclo*-$I_2Sn(CH_2Me_2Si)_2O$, **3**, whereas the Sn···O distance in **5a** of 3.7150(19) Å is longer than that in **3** of 3.2382(61) Å. This is a result of the intramolecular Cl→Sn interaction of 3.3861(8) Å in compound **5a** (which is shorter than the sum of the van der Waals radii of tin and chlorine (3.91 Å)[36]) that compete with the O→Sn interaction. The tin atoms in compound **5a** show distorted trigonal bipyramidal environment with the Cl(1) and Cl(2a) atoms in the axial positions [Cl(1)–Sn(1)–Cl(2a) 173.590(25)°] and the Cl(2), C(1) and C(2a) atoms in the equatorial positions. The equatorial ligands are displaced toward the coordinating chlorine atom Cl(2a), making the Cl(1)–Sn–L_{eq} angles between 96.91(3)° and 105.47(9)°, and the Cl(2a)–Sn–L_{eq} angles between 76.703(23)° and 79.314(85)°. The C–Sn–C bond angle of 122.92(11)° is relatively big with respect to that in **3** of 114.8(3)°, and the Cl(2)–Sn–C angles are around 112°. The Si–O–Si angle is close to that in **3** being around 153°. The two tin atoms and four chlorine atoms in the twelve-membered ring are nearly in the same plane.

2.2.1.2 Experiments to polymerize compound 1 by the so-called ring-opening polymerization (ROP)

Compound **1** hold potential in developing materials with interesting properties on the molecular level. One of the most important motivations in inorganic heterocyclic compounds is the fact that (i) they are single source precursors for inorganic polymers which have more than one element in the skeleton, and (ii) polymers obtained by ring-opening polymerization (ROP) have mostly molecular weights of narrow ranges in contrast to the polymers obtained by polymerization of non-cyclic monomers using other polymerization techniques.

Different anionic initiators were applied for the polymerization of *cyclo*-siloxanes.and other cyclic compounds.[1c, 37]

Attempts to obtain the silicon- and tin-containing polymer starting from compound **1**, by the so-called anionic ring-opening polymerization (ROP), were not successful. The reactions of compound **1** were performed separately with potassium hydroxide, KOH, tetra-*n*-buthylammonium fluoride, *n*-$Bu_4N^+F^-$, lithium siloxanolate, *n*-$BuMe_2SiO^-Li^+$, or

sodium methoxide, MeO^-Na^+, as anionic initiators at high temperatures (170–190°C except the experiment with sodium methoxide which was done in THF at reflux), in diphenyl ether or THF as a solvent or under solvent-free conditions (in case of KOH as initiator). In all experiments only the starting material was observed in the NMR spectra of the reaction mixtures. Increasing the reactivity of the siloxanolate or fluoride anions by complexing the counter ion using 12–crown–4 to complex lithium cations (*n*-$BuMe_2SiO^-Li^+$/12–crown–4), or tetraglyme to complex potassium cations (KF/tetraglyme) did not change the result.

Waymouth et al. reported that N-heterocyclic carbenes are effective catalysts for the ring-opening polymerization of the five-membered *cyclo*-siloxane $(CH_2Me_2Si)_2O$ giving a high molecular weight polymer.[38] Compound **1** was stirred with the high nucleophile N-heterocyclic carbene (NHC), 1,3-bis(2,6-diisopropylphenyl)-1,3-dihydro-2H-imidazol-2-ylidene, as initiator in solvent-free condition at 80°C, however no polymerization was observed.

Furthermore, the microwave-assisted experiments (at 100W for 20 min) to polymerize compound **1** using KOH or MeONa as initiator were unsuccessful (Scheme 8, Table 7).

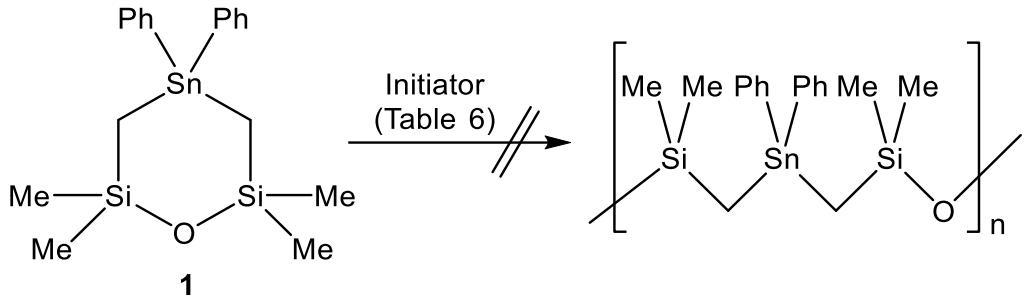

Scheme 8.

Table 7. Experiments to polymerize compound **1**.

	Initiator	Ratio (**1** : initiator)	Solvent	Temperature	Time
1	*n*–$Bu(Me_2)SiOLi$	250:1	Ph_2O	170 °C	3 h
2	*n*–$Bu(Me_2)SiOLi$	50:1	Ph_2O	190 °C	3 h
3	*n*–$Bu(Me_2)SiOLi$ / 12-Crown-4	20:1	Ph_2O	170 °C	3 h
4	*n*–Bu_4NF	20:1	Ph_2O	170 °C	24 h

5	KF / Tetraglyme	20:1	Ph_2O	170 °C	24 h
6	KOH	100:1	–	170 °C	3 h
7	KOH	20:1	–	170 °C	3 h
8	MeONa	25:1	THF	66 °C	3 h
9	NHC[a]	1000:1	–	80 °C	1 h
10	KOH	3:1	Diglyme	150 °C	20 min[b]
11	MeONa	25:1	Diglyme	160 °C	20 min[b]

In runs (1–6) DMSO was used as promoter. (a) The N-heterocyclic carbene (NHC) that was using in run (9) is 1,3-Bis(2,6-diisopropylphenyl)-1,3-dihydro-2H-imidazol-2-ylidene. (b) In runs (10 and 11) the reaction was performed in a Microwave oven at 100W.

The fact, that *cyclo*-$Ph_2Sn(CH_2SiMe_2)_2O$, **1**, does not undergo anionic ring opening polymerization, could probably be attributed to the low Lewis acidity of the silicon atom within the ring, which is not high enough to be attacked by the nucleophilic initiator in order to start the polymerization. The same statement was made for *cyclo*-carbosiloxanes by Islamov and co-worker.[39] They reported that the *cyclo*-carbosiloxane which has a structure of *cyclo*-hexamethyltrisiloxane by replacing two oxygen atoms with methylene groups (Chart 5, D_3C_2) polymerizes with difficulty using nucleophilic initiator giving low yield of a liquid polymer, whereas that containing two oxygen atoms and one methylene group (Chart 5, D_3C_1) is much readily to polymerize giving high-molecular polymer with a yield of about 80%.

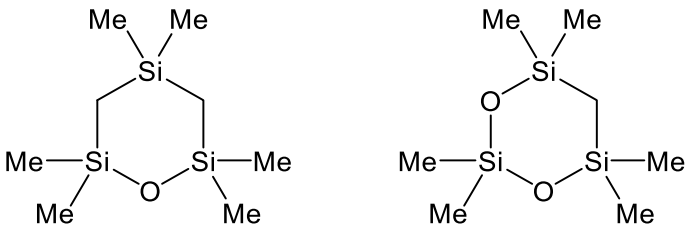

D_3C_2 **D_3C_1**

Chart 5.

Depending on the previous discussion, it was planned to synthesize cyclic siloxane, in which the silicon atoms are bound to two oxygen atoms. These silicon atoms could have enough Lewis acidity to be attacked by the anionic polymerization initiator, in order to polymerize the compound by the so-called ring-opening polymerization.

2.2.2 Syntheses and Structures of the tri-cyclic siloxanes [{X_2Sn-$(CH_2MeSi)_2O$}$O]_2$, (12, X = Ph; 13, X = I; 14, X = Br; 15, X = Cl)

2.2.2.1 Synthesis of the oligomers mixture *cyclo*-[{$Ph_2Sn(CH_2MeSi)_2O$}$O]_n$, 13

The reaction of diphenyltin dichloride, Ph_2SnCl_2, with two molar equivalents of the Grignard reagent Me(*i*-PrO)$_2$SiCH$_2$MgCl afforded the tetraorganotin compound [Me(*i*-PrO)$_2$SiCH$_2$]$_2$SnPh$_2$, **10**, in very good yield (Scheme 9).

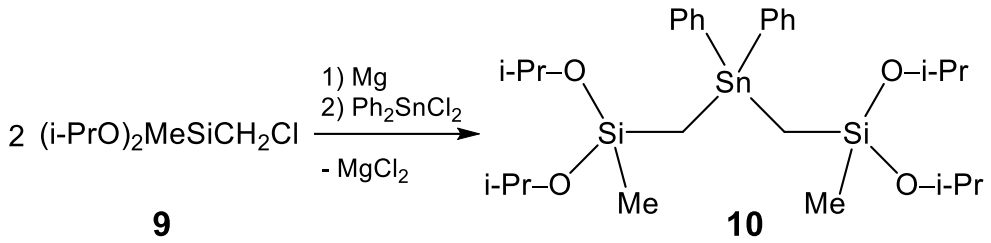

Scheme 9. Synthesis of [Me(*i*-PrO)$_2$SiCH$_2$]$_2$SnPh$_2$ **10**.

A ^{119}Sn NMR spectrum of a solution of compound **10** in $CDCl_3$ showed a singlet resonance at *δ* –55. The corresponding ^{29}Si NMR spectrum showed a resonance at *δ* –8.0. The methylene groups SnCH$_2$Si reveal a signal in ^{13}C NMR spectrum at *δ* –4.8 [^1J(^{13}C–$^{117/119}$Sn) 249/260 Hz], and a signal in ^{1}H NMR spectrum at *δ* 0.47 [^2J(^{1}H–$^{117/119}$Sn) 74.3/77.7 Hz].

A solution of compound **10** in CH_2Cl_2 was stirred for three days with a solution of NaOH in EtOH/water in attempt to obtain the cyclic compound that has two oxygen-bound silicon atoms by the hydrolysis of Si–O–*i*-Pr bonds. The crude reaction product was completely soluble in $CHCl_3$, CH_2Cl_2 and THF. The ^{119}Sn NMR spectrum (in $CDCl_3$) showed three broad resonances at *δ* –50.2, –53.0 and –53.2. In ^{29}Si NMR spectrum also three broad signals at *δ* –18.6, –19.0 and –19.3 were observed. The resonances in ^{29}Si NMR spectrum are about 11 ppm up-field shifted in comparison to the resonance in compound **10** at δ –8.0. The ^{1}H NMR spectrum showed very broad signal between 0.03 and 0.47 ppm and no signals for *i*-propoxy groups were observed. These indicate that the Si–O–*i*-Pr bonds were hydrolyzed in presence of

water affording different oligomers of the expected ring {[$Ph_2Sn(CH_2MeSi)_2O$]O}$_n$, **11** (Scheme 10).

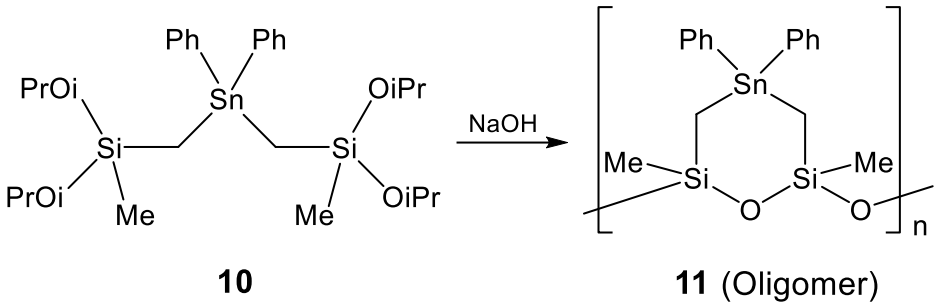

10 **11** (Oligomer)

Scheme 10. Hydrolysis of [Me(*i*-PrO)$_2$SiCH$_2$]$_2$SnPh$_2$, **10**.

No reaction was observed as compound **10** was stirred separately with aqueous solution of NH_4Cl at *p*H = 5 for two days, and with aqueous solution of KF for three days.

2.2.2.2 Syntheses of the tri-cyclic siloxanes [{$X_2Sn(CH_2MeSi)_2O$}O]$_2$, (12, X = Ph; 13, X = I; 14, X = Br; 15, X = Cl)

Attempt to polymerize the mixture of oligomers, **11**, using sodium methoxide as initiator did not afford the corresponding polymer. It afforded a dimeric compound, the tricyclic siloxane {[$Ph_2Sn(CH_2MeSi)_2O$]O}$_2$, **12**, containing the eight-membered tetrasiloxane ring (Scheme 11).

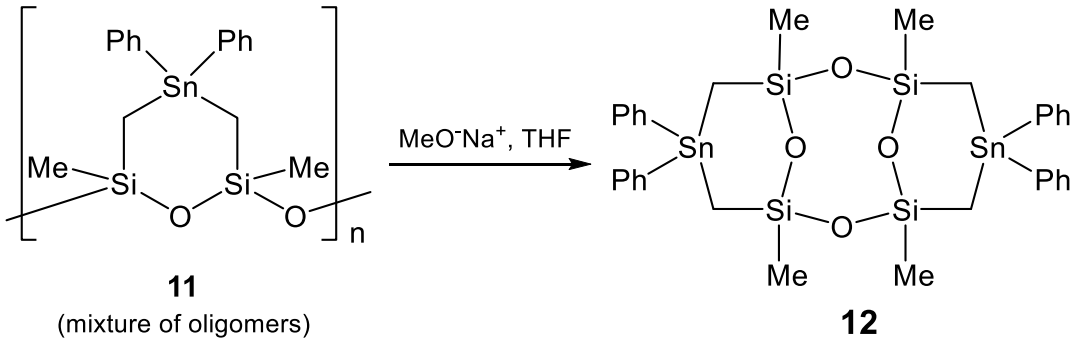

11
(mixture of oligomers)

12

Scheme 11. Synthesis of {[$Ph_2Sn(CH_2MeSi)_2O$]O}$_2$, **12**.

A ^{29}Si NMR spectrum of compound **12** in $CDCl_3$ showed a single resonance at δ –16.6 [$^2J(^{29}Si–^{117/119}Sn)$ = 36 Hz]. That of $\{[CH_2(CH_2MeSi)_2O]O\}_2$[40] in C_6D_6 showed a singlet at δ –13.0. For the methylene group $SnCH_2Si$ in compound **12** a resonance in ^{13}C NMR spectrum at δ –5.8 [$^1J(^{13}C–^{117/119}Sn)$ = 228/239 Hz, $^1J(^{13}C–^{29}Si)$ = 68 Hz], and an AB-type resonance in ^{1}H NMR spectrum at δ 0.40 [J_{AB} = 13.5 Hz, $^2J(^1H–^{117/119}Sn)$ = 67.3/70.3 Hz] were observed.

The mixture of oligomers **11** was stirred overnight in methanol. The ^{29}Si NMR spectrum of the residue (in $CDCl_3$) showed three sharp resonances at δ –15.2 [$^2J(^{29}Si–^{117/119}Sn)$ = 35 Hz], –15.9, –16.6 [$^2J(^{29}Si–^{117/119}Sn)$ = 36 Hz, assigned to compound **12**], in addition to a broad signal at 18.5. This clarifies that the reformation of the oligomeric mixture **11** into the dimer **12** does not happen in absence of the nucleophilic initiator.

Halogenation and proto-destannylation of **12** afforded the corresponding organotin (IV) halides $\{[X_2Sn(CH_2MeSi)_2O]O\}_2$, (**13**, X = I; **14**, X = Br; **15**, X = Cl) in good yields (Schemes 12).

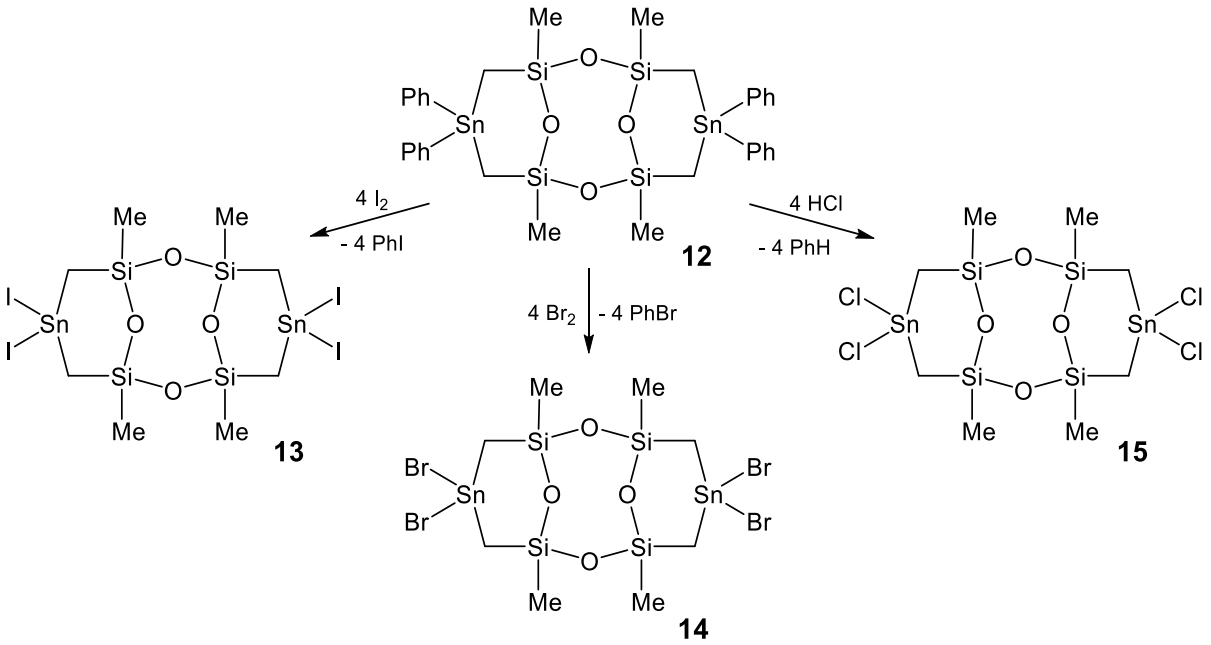

Scheme 12. Syntheses of the organotin halides $[\{X_2Sn(CH_2MeSi)_2O\}O]_2$ (**13**, X = I; **14**, X = Br; **15**, X = Cl).

The low solubility of the compounds $[\{X_2Sn(CH_2MeSi)_2O\}O]_2$ (**13**, X = I; **14**, X = Br; **15**, X = Cl) in $CDCl_3$ afforded not particularly clean NMR spectra. The ^{119}Sn NMR

spectra in $CDCl_3$ showed main signal at δ –228, 44, and 139 assigned to compounds **13**, **14** and **15**, respectively. These chemical shifts are comparable with those for the mono-cyclic analogous compounds *cyclo*-$I_2Sn(CH_2Me_2Si)_2O$, **3**, (at δ –207), *cyclo*-$Br_2Sn(CH_2Me_2Si)_2O$, **4**, (at δ 54) and *cyclo*-$Cl_2Sn(CH_2Me_2Si)_2O$, **5**, (at δ 145), respectively. The ^{1}H NMR spectra of compounds **14** and **15** showed, like compound **12**, an AB-type resonance for Sn*CH*$_2$Si protons (**14**, δ 1.17 [J_{AB} 14.0 Hz, $^2J(^1H–^{117/119}Sn)$ = 105.0/109.8Hz]; **15**, δ 1.00 [J_{AB} = 14.0 Hz, $^2J(^1H–^{117/119}Sn)$ = 107.4/112.4 Hz]). In the ^{13}C NMR spectra of compounds **13**–**15** singlet resonances for Sn*C*H$_2$Si carbon atoms were observed (**13**, δ 12.0; **14**, δ 12.1 ($^1J(^{13}C–^{117/119}Sn)$ = 247/259 Hz, **15**, δ 11.1 ($^1J(^{13}C–^{117/119}Sn)$ = 274/288 Hz), (Table 8). No further reactions were done on compounds **13**–**15** because of lack of these compounds.

Table 8. Selected NMR data of $[\{X_2Sn(CH_2MeSi)_2O\}O]_2$, (**12**, X = Ph; **13**, X = I; **14**, X = Br; **15**, X = Cl).

	δ ^{119}Sn	δ ^{29}Si	SnCH$_2$Si	
		$[^2J(^{29}Si–^{117/119}Sn]$	δ ^{1}H $[^2J(^1H–^{117/119}Sn)]$	δ ^{13}C $[^1J(^{13}C–^{117/119}Sn)]$
12	–54	–16.6 [36]	0.40 [67.3/70.3]	–5.8 [228/239]
13	–228	–20.4 [40]	–	12.0
14	44	–20.9 [40]	1.17 [105.0/109.8]	12.1 [247/259]
15	139	–20.0 [39]	1.00 [107.4/112.4]	11.1 [274/288]

The chemical shifts are given in ppm, and the coupling constants are given in Hz.

An ESI MS spectrum (positive mode) of compound **13** showed a mass cluster centered at *m/z* 800.8 that is assigned to [**13** – 2I + OH]$^+$. In the negative mode a major mass cluster at *m/z* 1164.4 for [**13** + I]$^-$ was observed. The ESI MS spectrum of compound **14** (positive mode) showed two mass clusters at *m/z* 664.9 ([**14** – 4 Br + 3 OH]$^+$) and *m/z* 558.3 ([**14** – 4 Br + 3 OH + 2 MeCN]$^+$). And that of compound **15** in the negative mode showed a major mass cluster centered at *m/z* 706.7 ([**17** + Cl]$^-$).

2.2.2.3 Molecular structures of the tricyclic siloxanes [{Ph$_2$Sn-(CH$_2$MeSi)$_2$O}O]$_2$, 12, and [{Cl$_2$Sn(CH$_2$MeSi)$_2$O}O]$_2$, 15

Recrystallization of **12** from methanol and of **15** from CH_2Cl_2 afforded colorless single crystals suitable for X-ray diffraction analyses. The molecular structures of

compounds **12** and **15** are shown in Figures 8 and 9, and selected bond lengths and bond angles are summarized in Table 9.

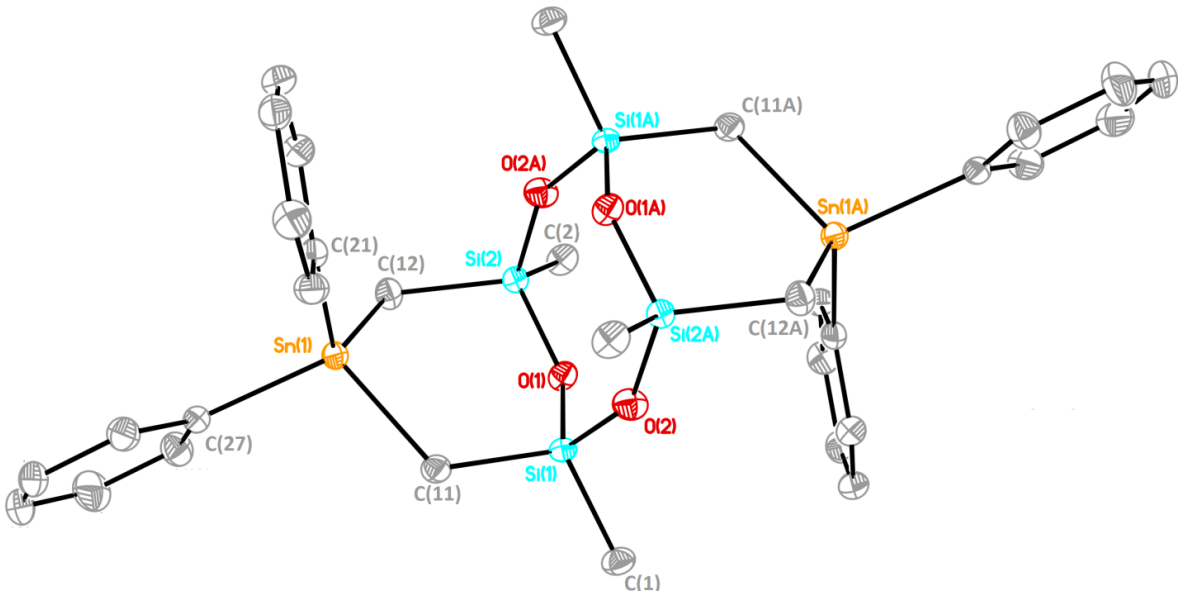

Figure 8. General view (SHELXTL) of a molecule of **12** showing 30% probability displacement ellipsoids and the crystallographic numbering scheme. Hydrogen atoms are omitted for clarity.

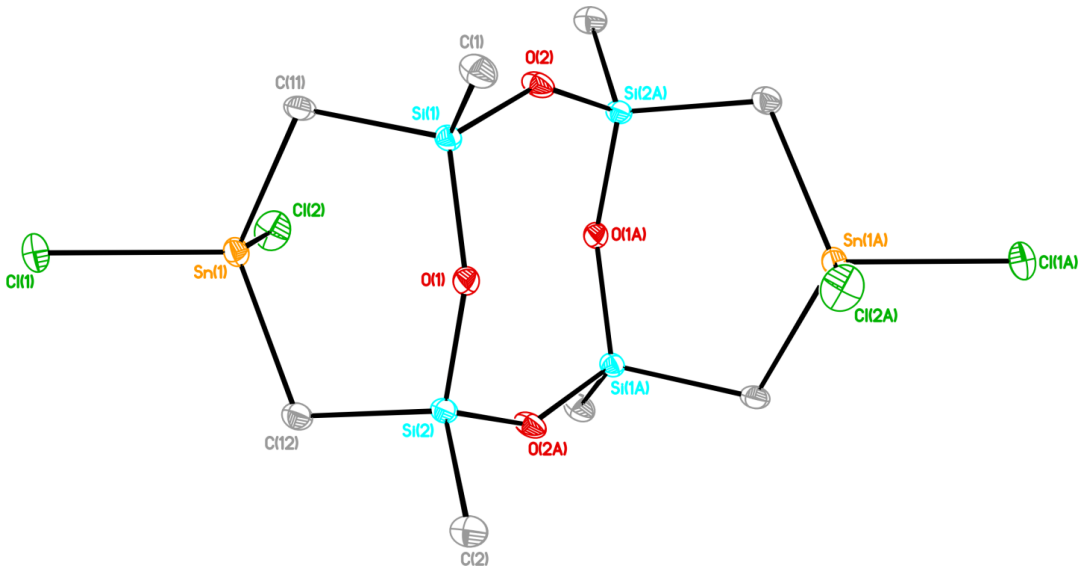

Figure 9. General view (SHELXTL) of a molecule of **15** showing 30% probability displacement ellipsoids and the crystallographic numbering scheme. Hydrogen atoms are omitted for clarity.

Table 9. Selected bond lengths /Å and bond angles /° in **12** and **15**.

	12	**15**
Sn(1)–C(11)	2.1665(13)	2.109(3)
Sn(1)–C(12)	2.1558(13)	2.115(4)
Sn(1)–A	2.1424(13)	2.3391(11)
Sn(1)–B	2.1515(13)	2.3468(11)
Si(1)–O(1)	1.6386(9)	1.625(3)
Si(1)–O(2)	1.6298(10)	1.630(3)
Si(2)–O(1)	1.6399(10)	1.625(2)
Si(2)–O(2a)	1.6275(10)	1.617(3)
Sn(1)–O(1)	3.4663(12)	3.2164(27)
C(11)–Sn(1)–C(12)	107.93(5)	118.79(14)
C(11)–Sn(1)–A	108.50(5)	109.86(11)
C(11)–Sn(1)–B	108.91(5)	108.30(11)
C(12)–Sn(1)–A	114.70(5)	105.35(11)
C(12)–Sn(1)–B	110.32(5)	108.42(10)
A–Sn(1)–B	106.37(5)	105.31(4)
O(1)–Si(1)–O(2)	108.86(5)	109.69(14)
O(1)–Si(2)–O(2a)	109.71(5)	108.05(13)
Si(1)–O(1)–Si(2)	140.74(6)	153.20(17)
Si(1)–O(2)–Si(2a)	152.16(7)	146.32(16)
Sn(1)–C(11)–Si(1)	116.34(6)	111.41(18)
Sn(1)–C(12)–Si(2)	111.24(6)	110.59(17)

12, A=C(21), B=C(27); **15**, A=Cl(2), B=Cl(1).

Compounds **12** and **15** are tricyclic compounds. They consist of two six-membered silalkyltin *cyclo*-siloxanes that are connected via Si–O bonds forming one distorted eight-membered *cyclo*-siloxane ring. The six-membered rings are trans with respect to the eight membered tetrasiloxane ring.

The six-membered rings have chair conformations which are more distorted in **12** in comparison to those found in **15**.[33] The eight-membered tetrasiloxane ring in compound **12** exhibits boat-chair conformation.[41] That in compound **15** have a crown-conformation.[41] The torsion angles within the six- and the eight-membered rings in compounds **12** and **15** are given in Table 10. The four silicon [Si(1), Si(2), Si(1a),

Si(2a)] and two oxygen atoms [O(2), O(2a)] in the tetrasiloxane rings are, especially in **15**, nearly in the same plane, and the other two oxygen atoms (O1, O1a) displace in the opposite directions with respect to the plane. The molecules have ladder-like structures and resemble those of $[\{M(CH_2MeSi)_2O\}O]_2$, M = CH_2[40], Me_2Ge[42] (Figure 10).

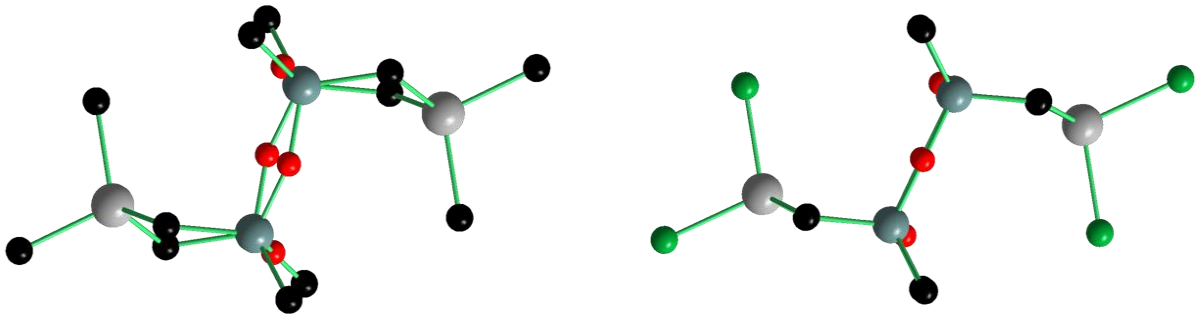

12 **15**

Figure 10. Reduced ball-and-sticks molecular structure of **12** and **15**. The phenyl groups are omitted for clarity.

Table 10. Torsion angles within the six- and the eight-membered rings in compounds **12** and **15**.

	12	**15**
Sn(1)–C(11)–Si(1)–O(1)	–22.05(9)	–18.2(2)
C(11)–Si(1)–O(1)–Si(2)	42.05(12)	32.9(4)
Si(1)–O(1)–Si(2)–C(12)	–56.42(12)	–34.3(4)
O(1)–Si(2)–C(12)–Sn(1)	46.09(8)	20.3(2)
Si(2)–C(12)–Sn(1)–C(11)	–40.05(9)	–24.0(3)
C(12)–Sn(1)–C(11)–Si(1)	28.14(9)	23.0(3)
O(2)–Si(1)–O(1)–Si(2)	–77.47(11)	–83.9(4)
Si(1)–O(1)–Si(2)–O(2a)	60.21(12)	83.0(4)
O(1)–Si(2)–O(2a)–Si(1a)	17.88(18)	–12.91(37)
Si(2)–O(2a)–Si(1a)–O(1a)	55.41(17)	14.9(4)

Replacing the phenyl groups in **12** with chlorine substituent in **15** increases the Lewis acidity at the tin atoms, affording shorter Sn–CH_2 bonds, [Sn–CH_2; **12**, 2.1665(13) Å and 2.1558(13) Å; **15**, 2.109(3) Å and 2.115(4) Å], and stronger O···Sn interactions,

[Sn–O; **12**, 3.4663(12) Å; **15**, 3.2164(27) Å]. The stronger O···Sn interactions result in turn in bigger Si(1)–O(1)–Si(2) and CH_2–Sn–CH_2 angles, [Si(1)–O(1)–Si(2); **12**, 140.74(6)°; **15**, 153.20(17)°], [CH_2–Sn–CH_2; **12**, 107.93(5)°; **15**, 118.79(14)°]. The bigger Si(1)–O(1)–Si(2) angle in **15** with respect to that in **12** affords smaller Si(1)–O(2)–Si(2a) angle in order to reduce the ring strain in the eight-membered tetrasiloxane ring, [Si(1)–O(2)–Si(2a); **12**, 152.16(7)°; **15**, 146.32(16)°]. The Si–O bond lengths range between 1.617(3) and 1.6399(10) Å and show no particularity. The Sn–C_{Ph} bond lengths in **12** are 2.1424(13) and 2.1515(13) Å, whereas the Sn–Cl bond lengths in **15** are 2.3391(11) and 2.3468(11) Å.

2.2.3 Synthesis of the tin-substituted siloxane *cyclo*-{Br_3SnCH_2MeSiO}$_4$, 18

The reaction of triphenyltin chloride, Ph_3SnCl, with one molar equivalent of the Grignard reagent Me(*i*-PrO)$_2$$SiCH_2MgCl$ afforded the tetraorganotin compound Me(*i*-PrO)$_2$$SiCH_2SnPh_3$, **16**, in very good yield (Scheme 13).

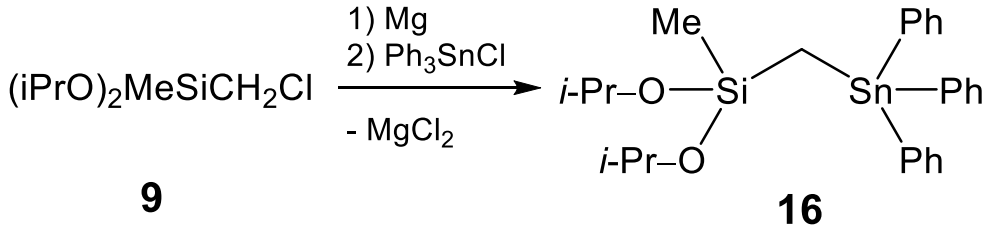

9 **16**

Scheme 13. Synthesis of Me(*i*-PrO)$_2$$SiCH_2SnPh_3$, **16**.

A ^{119}Sn NMR spectrum of compound **16** in $CDCl_3$ showed a singlet resonance at δ –92. The ^{29}Si NMR spectrum of the same solution showed a signal at δ –8.1 [^2J(^{29}Si–$^{117/119}$Sn) = 20 Hz].

Reaction of compound **16** with three molar equivalents elemental bromine provided the monoorganotin tribromide Me(*i*-PrO)$_2$$SiCH_2SnBr_3$, **17**, in very good yield (Scheme 14).

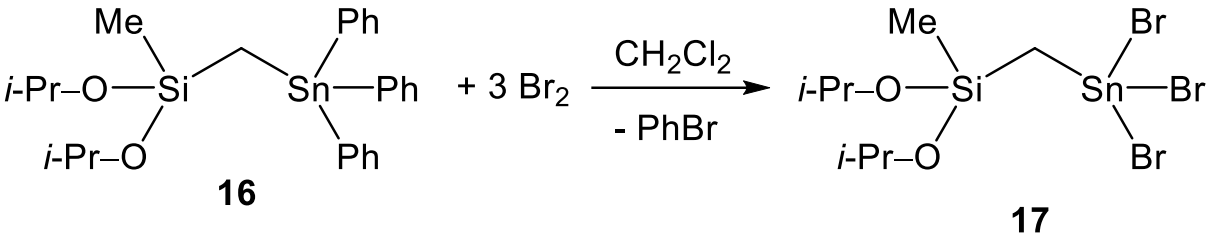

Scheme 14. Synthesis of Me(*i*-PrO)$_2$SiCH$_2$SnBr$_3$, **17**.

A ^{119}Sn NMR spectrum of compound **17** in $CDCl_3$ showed relatively broad resonance at δ –216. The broadness of the signal is a result of intra- or intermolecular Si–O···Sn interaction. In the ^{29}Si NMR spectrum of the same solution a resonance at δ –15.1 [^2J(^{29}Si–$^{117/119}$Sn) = 70 Hz] was observed. For the methylene group a resonance in ^{1}H NMR spectrum at δ 1.67 [^2J(^{1}H–$^{117/119}$Sn) = 128.8/135.0 Hz] as well as a resonance in ^{13}C NMR spectrum at δ 19.3 [^1J(^{13}C–$^{117/119}$Sn) = 390/408 Hz] were observed.

A solution of compound **17** in $CDCl_3$ in a not completely closed NMR-tube was kept in air to evaporate slowly giving single crystals of the periphery functionalized tetrasiloxane ring {Br$_3$SnCH$_2$MeSiO}$_4$, **18**, of mp 210–212 °C. The hydrolysis/condensation is catalyzed by the high Lewis acidity at the tin atom (Scheme 15).[32]

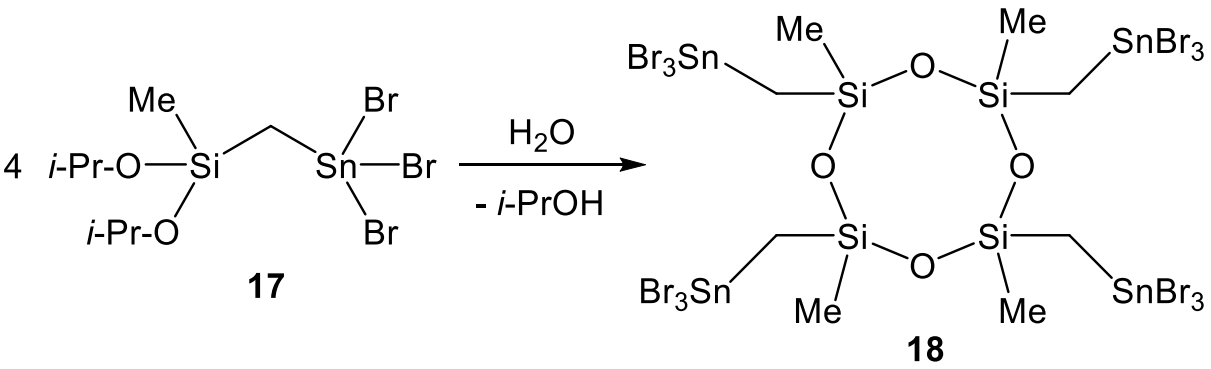

Scheme 15. Hydrolysis of Me(*i*-PrO)$_2$SiCH$_2$SnBr$_3$, **17**, in presence of moist air.

The ^{29}Si NMR spectrum of the crude hydrolysis product in $CDCl_3$ showed one main resonance at δ –22.4 and four smaller resonances at δ –22.0, –22.5, –22.6 and –22.7. The chemical shifts are comparable with that found in the tricyclic tin-containing

siloxane [{$Br_2Sn(CH_2MeSi)_2O$}$O]_2$, **14**, at *δ* –20.9 having the same tetrasiloxane ring. The ^{119}Sn NMR spectrum showed also one main broad resonance at *δ* –195.6 and four broad resonances at *δ* –195.3, –195.4, –195.9 and –196.9. These are about 20 ppm low-field shifted in comparison with that for the origin compound **17** at *δ* –216 that adopt Si–O···Sn interaction. The interaction becomes much weaker after the hydrolysis.

The ESI MS spectrum of compound **18** in negative mode showed a mass cluster centered at *m/z* 1803.2 that fits exactly with [**18** + Br]$^-$.

2.2.3.1 Molecular structure of the tin-substituted *cyclo*-tetrasiloxane {Br_3SnCH_2MeSiO}$_4$, 18

The molecular structures of compound **18** is shown in Figures 11 and selected bond lengths and bond angles are summarized in Table 11.

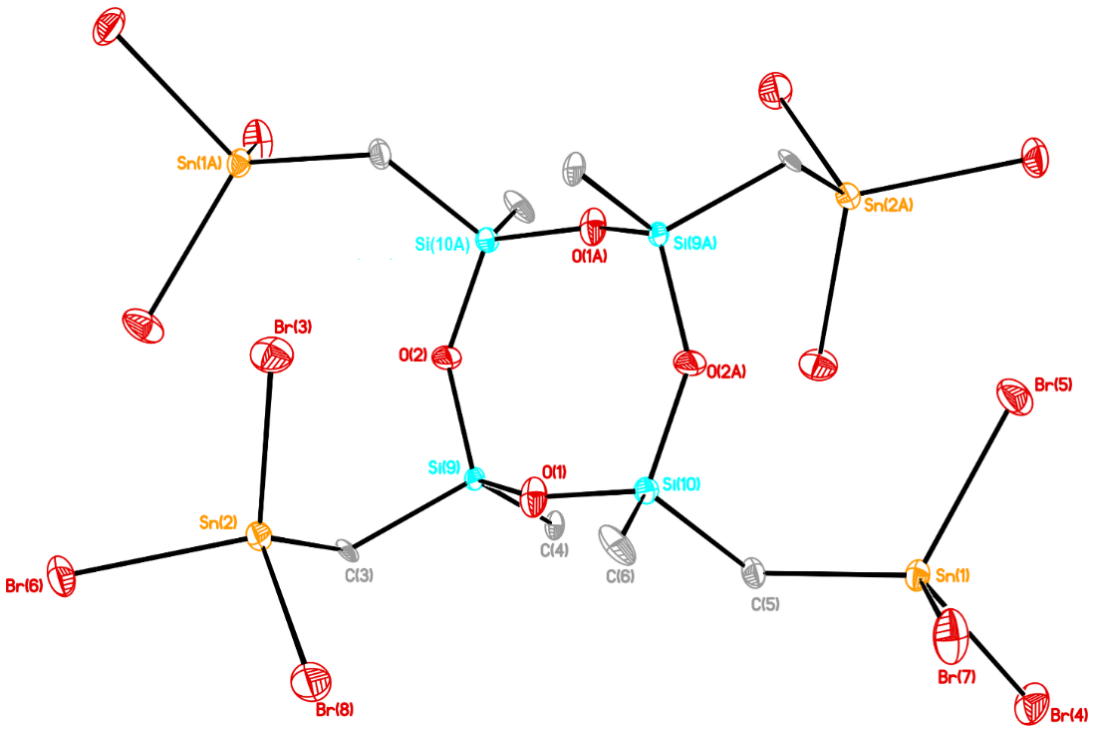

Figure 11. General view (SHELXTL) of a molecule of **18** showing 30% probability displacement ellipsoids and the crystallographic numbering scheme. Hydrogen atoms are omitted for clarity.

Table 11. Selected bond lengths /Å and bond angles /° in $[(Br_3SnCH_2)MeSiO]_4$, **18**.

Si(9)–O(1)	1.63(2)	Si(10)–O(1)	1.63(2)
Si(9)–O(2)	1.621(19)	Si(10)–O(2a)	1.621(18)
Sn(1)-Br(4)	2.448(3)	Sn(2)-Br(3)	2.458(3)
Sn(1)-Br(5)	2.463(3)	Sn(2)-Br(6)	2.457(3)
Sn(1)-Br(7)	2.447(3)	Sn(2)-Br(8)	2.459(4)
Sn(1)-C(5)	2.10(3)	Sn(2)-C(3)	2.11(2)
Si(9)–O(1)–Si(10)	149.5(13)	Si(10)–O(2a)–Si(9a)	147.4(14)
Si(9)–C(3)–Sn(2)	114.1(11)	Si(10)–C(5)–Sn(1)	117.0(14)
O(1)–Si(9)–O(2)	109.4(11)	O(1)–Si(10)–O(2a)	108.6(11)
C(3)–Sn(2)–Br(3)	118.6(6)	C(5)–Sn(1)–Br(4)	113.1(7)
C(3)–Sn(2)–Br(6)	111.4(7)	C(5)–Sn(1)–Br(5)	114.7(7)
C(3)–Sn(2)–Br(8)	113.4(7)	C(5)–Sn(1)–Br(7)	115.3(7)
Br(3)–Sn(2)–Br(6)	107.60(13)	Br(4)–Sn(1)–Br(5)	103.73(14)
Br(3)–Sn(2)–Br(8)	101.92(14)	Br(4)–Sn(1)–Br(7)	103.32(14)
Br(6)–Sn(2)–Br(8)	102.40(13)	Br(5)–Sn(1)–Br(7)	105.34(14)

Compound **18** consists of one eight-membered *cyclo*-siloxane ring in distorted chair conformation. Two silicon and four oxygen atoms in compound **18** are nearly in the same plane. The remaining two silicon atoms displace in opposite directions with respect to the plane. The Si–O bond lengths range between 1.621(19) and 1.63(2) Å and show no particularity. The Si–O–Si bond angles are 147.4(14) and 149.5(13)°. The Si–C_{CH2} bonds {1.88(2) and 1.88(3)} are slightly longer than the Si–C_{Me} bonds {1.82(3) and 1.85(3)}. Each two Br_3SnCH_2 substituents that are bound to the siloxane ring are in the same direction and locate oppositely to the other two substituents. The Sn–C bond lengths are 2.10(3) and 2.11(2) Å and the Sn–Br bonds lie between 2.447(3) and 2.463(3) Å. Four bromine atoms in compound **18** make Br···H–C hydrogen bonds with the methyl hydrogens resulting in the compound to be assembled in two dimensional polymer (Br···C 3.67(3) Å) (Figure 12).

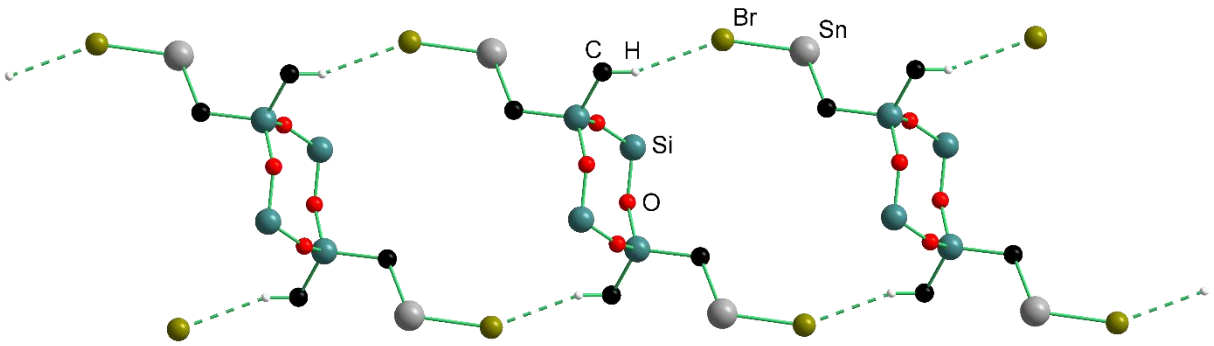

Figure 12. Two-dimensional structure of compound **18**. Atoms that are not part of hydrogen bonds are omitted for clarity.

2.2.4 Syntheses and structures of the tin-substituted cube-octameric silsesquioxane T_8R_8 (20, R = Ph_3SnCH_2; 21, R = $PhBr_2SnCH_2$)

The reaction of triphenyltin chloride, Ph_3SnCl, with one molar equivalent of the Grignard reagent $(i\text{-PrO})_3SiCH_2MgCl$ provided the tetraorganotin compound $(i\text{-PrO})_3SiCH_2SnPh_3$, **19**, in very good yield (Scheme 16).

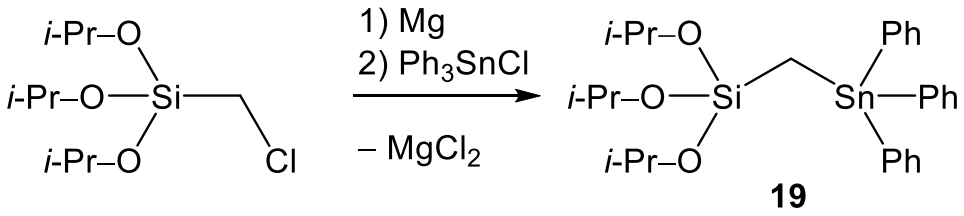

Scheme 16. Synthesis of $(i\text{–PrO})_3SiCH_2SnPh_3$, **19**.

The ^{119}Sn NMR spectrum of compound **19** in $CDCl_3$ showed a resonance at δ –93. The ^{29}Si NMR spectrum of the same solution showed a signal at δ –47.2. The ^{1}H NMR spectrum reveals singlet resonance for the methylene protons at δ 0.45 [$^{2}J(^{1}H–^{117/119}Sn)$ = 74.6/77.9 Hz].

2.2.4.1 Synthesis of the cube-octameric silsesquioxane $(Ph_3SnCH_2SiO_{1.5})_8$, 20, by the sol-gel reaction of $(i\text{-PrO})_3SiCH_2SnPh_3$, 19, under microwave irradiation

A solution of compound **19** in bis(2-methoxyethyl)ether (diglyme), to which the sol-gel reaction catalyst (1 M KOH_{eq}) was added, was stirred overnight at room temperature. After irradiating the mixture in a microwave oven (100W, 6 min), the tin-containing cube-octameric silsesquioxane $(Ph_3SnCH_2SiO_{1.5})_8$, **20**, was obtained in moderated yield (Scheme 17).

Compound **20** shows good solubility in CH_2Cl_2 and $CHCl_3$ and moderate solubility in hexane. A ^{119}Sn NMR spectrum of the solution of compound **20** in $CDCl_3$ showed a single resonance at δ –91 [$^4J(^{119}Sn–^{29}Si)$ = 72 Hz], and a ^{29}Si NMR spectrum displayed three signals at δ 66.05, 66.15, and 66.21 in an integral ratio of about (2:1:1).

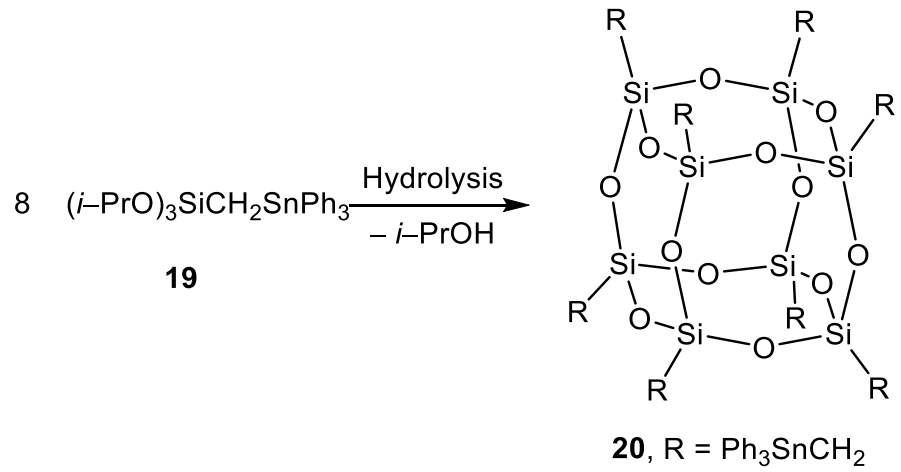

Scheme 17. Synthesis of the tin-substituted POSS $(Ph_3SnCH_2SiO_{1.5})_8$, **20**.

The chemical shifts of the resonances in ^{29}Si NMR spectrum are close to the measurement reported for T_8Me_8 at δ 66.2.[43] The presence of more than one signal in the spectrum was reported before for octamethylsilsesquioxane, and is attributed to the distortion of the silicon-oxygen framework along the body diagonal of about 0.06 Å. This corresponds to a splitting of 0.7 ppm of the signal in the ^{29}Si NMR spectrum for octamethylsilsesquioxane.[43] In compound **20** the distortion was measured from the molecular structure to be 0.05 Å.

2.2.4.1.1 Molecular structure of the tin-substituted cube-octameric silsesquioxane $(Ph_3SnCH_2SiO_{1.5})_8$, 20

Recrystallization of **20** by slow evaporation of a solution in diglyme afforded colorless single crystals suitable for X-ray diffraction analysis. The molecular structure of compound **20** is shown in Figure 13 and selected bond lengths and bond angles are summarized in Table 12. Most bond lengths and bond angles which relate to Si(2)–Si(8) are not given in Table 12 as they are very similar to those around Si(1). They could be found in the cif-file and the Table in the supporting CD.

Compound **20** consists of an inorganic Si_8O_{12} cubic core that is periphery functionalized by eight Ph_3SnCH_2 groups. All tin and silicon atoms are four-coordinated and exhibit distorted tetrahedral environment.

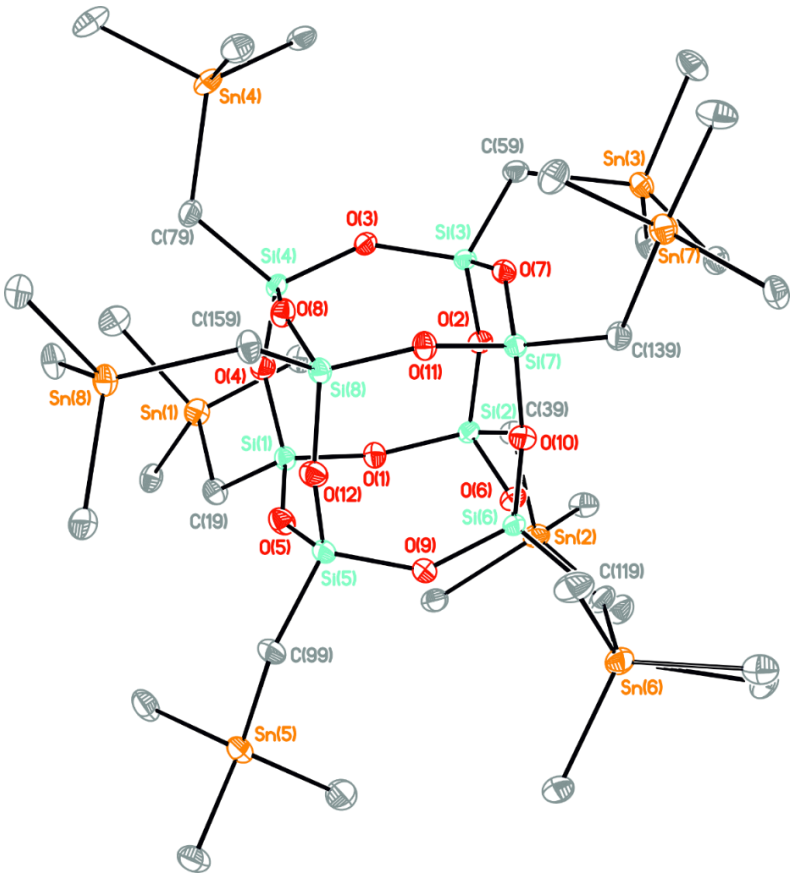

Figure 13. General view (SHELXTL) of a molecule of **20** showing 30% probability displacement ellipsoids and the crystallographic numbering scheme. Phenyl groups are omitted for clarity.

Table 12. Selected bond lengths /Å and bond angles /° in $(Ph_3SnCH_2SiO_{1.5})_8$, **20**.

Si(1)–O(1)	1.615(3)	Si(1)–O(5)	1.625(3)
Si(1)–O(4)	1.611(2)	Sn(1)–C(19)	2.136(3)
Si(1)–C(19)–Sn(1)	116.01(18)	Si(5)–C(99)–Sn(5)	120.8(2)
Si(2)–C(39)–Sn(2)	121.99(18)	Si(6)–C(119)–Sn(6)	118.3(2)
Si(3)–C(59)–Sn(3)	116.62(17)	Si(7)–C(139)–Sn(7)	129.31(18)
Si(4)–C(79)–Sn(4)	118.80(18)	Si(8)–C(159)–Sn(8)	115.83(17)
O(1)–Si(1)–O(4)	107.57(13)	O(7)–Si(7)–O(10)	107.99(13)
O(1)–Si(1)–O(5)	110.85(13)	O(7)–Si(7)–O(11)	107.40(12)
O(4)–Si(1)–O(5)	108.21(14)	O(10)–Si(7)–O(11)	108.55(13)
Si(1)–O(1)–Si(2)	149.25(17)	Si(3)–O(7)–Si(7)	141.05(15)
Si(2)–O(2)–Si(3)	160.47(17)	Si(4)–O(8)–Si(8)	154.99(17)
Si(3)–O(3)–Si(4)	142.92(15)	Si(5)–O(9)–Si(6)	143.23(16)
Si(1)–O(4)–Si(4)	151.61(16)	Si(6)–O(10)–Si(7)	171.17(18)
Si(1)–O(5)–Si(5)	147.37(17)	Si(7)–O(11)–Si(8)	138.07(16)
Si(2)–O(6)–Si(6)	137.43(16)	Si(5)–O(12)–Si(8)	153.31(17)

The bond lengths in compound **20** lie in the rather narrow ranges 1.604(2) – 1.629(2) Å for Si–O bonds, 1.819(3) – 1.830(3) Å for Si–C bonds, and 2.118(4) – 2.148(3) Å for Sn–C_{CH2} bonds.

The O–Si–O and C–Si–O bond angles are also almost similar being in the ranges 106.84(13) – 110.92(13)° and 105.22(14) – 114.23(15)°, respectively. Most Si–CH_2–Sn bond angles are close to 119° (in a range of 119 ±3°). The only exception is Si(7)–C(139)–Sn(7) of 129.31(18)°. The Si–O–Si bond angles range from 137.43(16) to 171.17(18)°.

2.2.4.2 Synthesis of the $PhBr_2SnCH_2$-substituted cube-octameric silsesquioxane $(PhBr_2SnCH_2SiO_{1.5})_8$, 21

Reaction of the Ph_3SnCH_2-substituted silsesquioxane **20** with 16 molar equivalents of elemental bromine in $CHCl_3$ afforded $(PhBr_2SnCH_2SiO_{1.5})_8$, **21**, as light yellowish oil (Scheme 18).

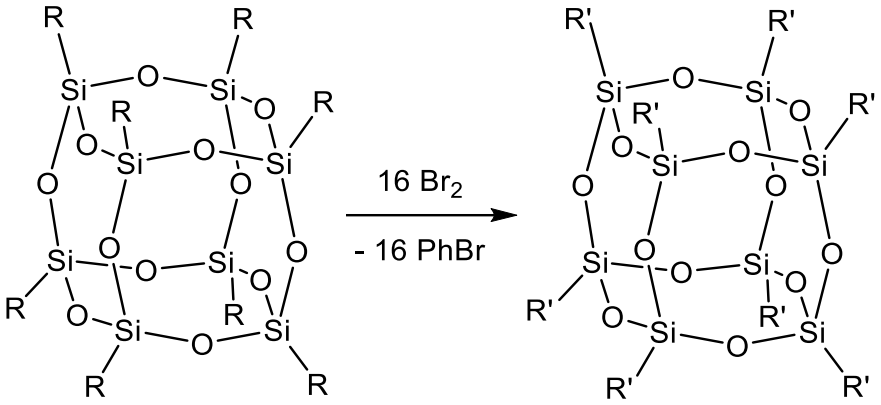

20, R = Ph_3SnCH_2 **21**, R' = $PhBr_2SnCH_2$

Scheme 18. Synthesis of $(PhBr_2SnCH_2SiO_{1.5})_8$, **21**.

The ^{29}Si NMR spectrum of a solution of the reaction product in $CDCl_3$ showed main signal at δ –69.6 [$^2J(^{29}Si–^{117/119}Sn)$ = 20 Hz]. In addition, two small signals at δ 72.3 and 69.3 were observed. A ^{119}Sn NMR spectrum reveals three resonances at δ –22.2, –22.6 and –23.2, in an integral ratio of (6 : 1 : 1). With caution it is supposed that all the resonances belong to compound **21**, and the tin atoms are not chemically equivalent because of the distortion of the silicon-oxygen framework along the body diagonal.

A ^{119}Sn NMR spectrum of $[Me(i\text{-}PrO)_2SiCH_2]PhSnBr_2$ in $CDCl_3$ showed a single resonance at δ –33 that is relatively low-field shifted in comparison with that for compound **21**. This is attributed to the higher O···Sn interaction in $[Me(i\text{-}PrO)_2SiCH_2]PhSnBr_2$ with respect to that found in compound **21**.

Compound **21** is the first cube-octameric silsesquioxane that is periphery-substituted by organotinhalide-moieties. The halide groups on the tin atoms are functional groups that are readily modifiable by reactions with Grignard reagents.

2.2.5 Hydrolyses studies of the organotin halides based on the six-membered siloxanes 2–5

Few crystals of the novel ladder-like diorganotinoxo cluster [{O(Me$_2$SiCH$_2$)$_2$Sn(I)OEt}$_2$ Sn$_2$O$_2$\{(CH$_2$Me$_2$Si)$_2$O}$_2$], **22**, were isolated as a solution of *cyclo*-PhISn(CH$_2$SiMe$_2$)$_2$O, **2**, which contained 4% of *cyclo*-I$_2$Sn(CH$_2$SiMe$_2$)$_2$O, **3** and its dimer **3a** as impurities, in CH$_2$Cl$_2$/hexane/ethanol, was kept in moist air for about four months. This is a result of partial hydrolysis of the "impurities" **3** and **3a** resulting in the dimeric tetraorganodistannoxane [{O(Me$_2$SiCH$_2$)$_2$Sn(I)X}$_2$Sn$_2$O$_2$\{(CH$_2$Me$_2$Si)$_2$O}$_2$] (X = I, OH), followed by replacing iodide or hydroxide anions by ethoxide anions in presence of ethanol (Scheme 19). The facile replacement of hydroxide and halide anions by alkoxide in dimeric tetraorganodistannoxanes was reported by *Otera* and co-workers some thirty years ago.[44]

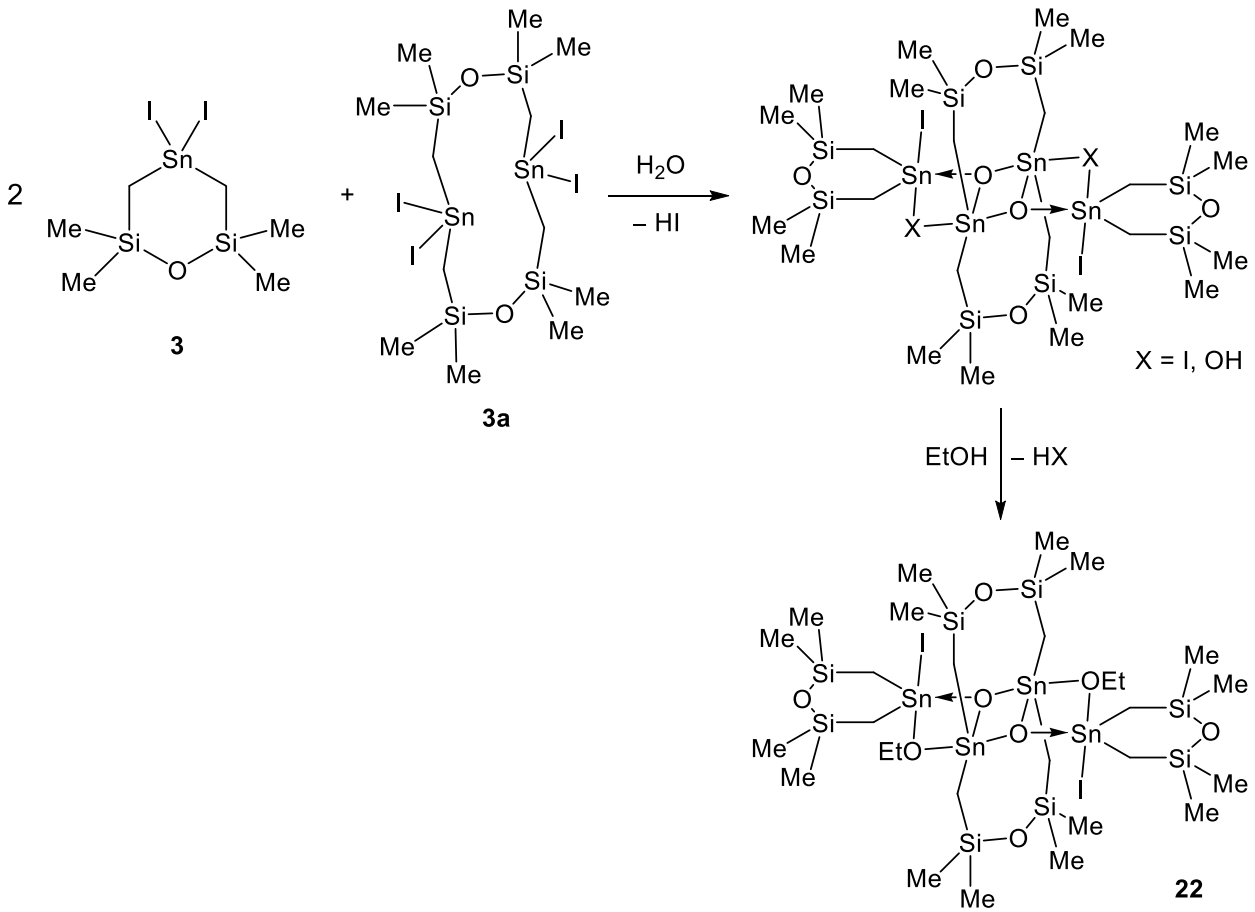

Scheme 19. Proposed mechanism for the formation of compound **22**.

Compound **22** is high melting solid (m.p. 202–204 °C) that is very poor soluble in common organic solvents such as CH_2Cl_2, chloroform, THF, acetonitrile, toluene, and methanol.

The Molecular structure of **22** is shown in Figure 14, and selected bond lengths and bond angles are summarized in Table 13. These will be discussed with those of compounds **23**–**27** in section 2.2.5.3.

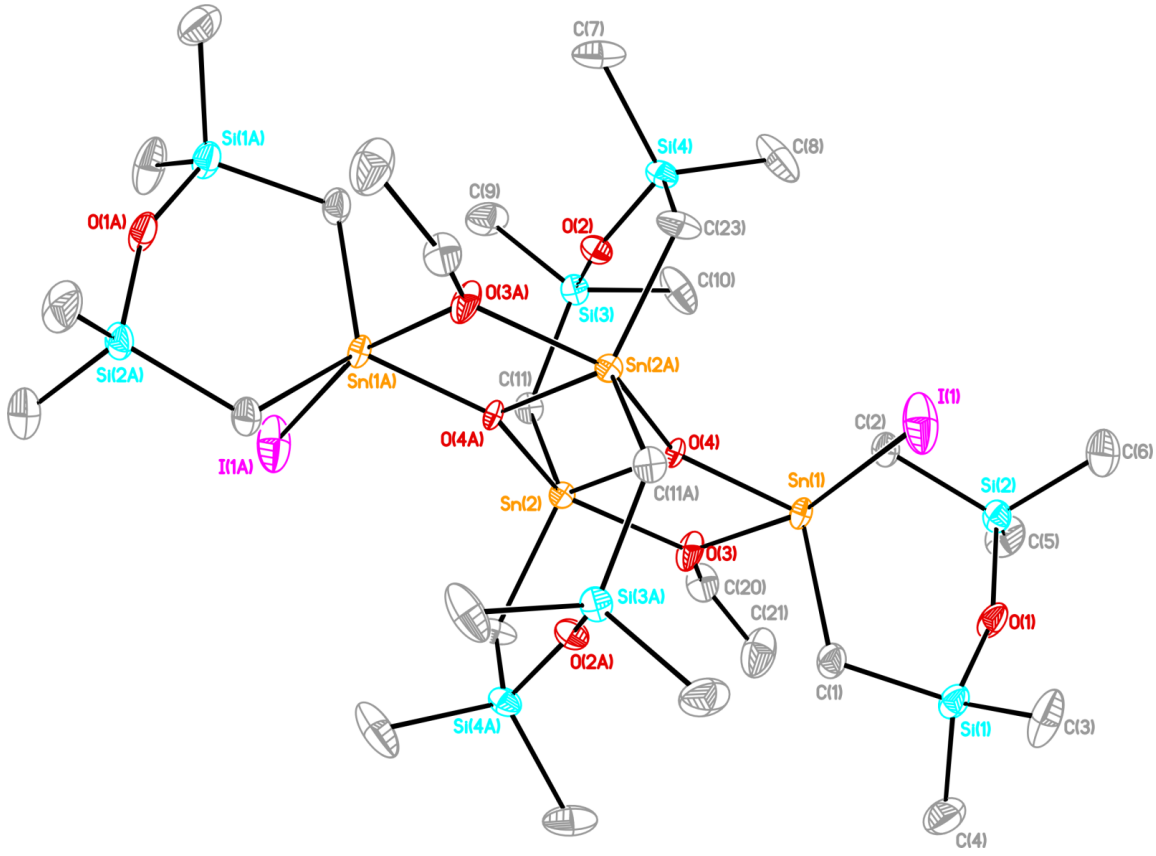

Figure 14. General view (SHELXTL) of a molecule of **22** showing 30% probability displacement ellipsoids and the crystallographic numbering scheme.

Table 13. Selected bond lengths /Å and bond angles /° in **22**.

Sn(1)–O(3)	2.155(6)	Sn(2)–O(3)	2.155(6)
Sn(1)–I(1)	2.8580(9)	Sn(2)–O(4a)	2.126(5)
Sn(1)–O(4)	2.014(5)	Sn(2)–O(4)	2.038(5)
Sn(1)–C(1)	2.106(8)	Sn(2)–C(11)	2.103(7)
Sn(1)–C(2)	2.124(8)	Sn(2)–C(23a)	2.117(8)
O(1)–Si(1)	1.619(6)	O(2)–Si(3)	1.616(5)
O(1)–Si(2)	1.632(6)	O(2)–Si(4)	1.639(6)
O(3)–Sn(1)–I(1)	164.55(14)	O(3)–Sn(2)–O(4a)	147.1(2)
O(3)–Sn(1)–O(4)	73.0(2)	O(3)–Sn(2)–O(4)	72.5(2)
O(3)–Sn(1)–C(1)	94.4(3)	O(3)–Sn(2)–C(11)	97.1(3)
O(3)–Sn(1)–C(2)	94.3(3)	O(3)–Sn(2)–C(23a)	95.0(3)
I(1)–Sn(1)–O(4)	91.71(14)	O(4a)–Sn(2)–O(4)	74.6(2)
I(1)–Sn(1)–C(1)	94.6(3)	O(4a)–Sn(2)–C(11)	99.7(3)
I(1)–Sn(1)–C(2)	92.2(2)	O(4a)–Sn(2)–C(23a)	99.5(3)
O(4)–Sn(1)–C(1)	116.7(3)	O(4)–Sn(2)–C(11)	117.5(2)
O(4)–Sn(1)–C(2)	123.6(3)	O(4)–Sn(2)–C(23a)	120.0(3)
C(1)–Sn(1)–C(2)	119.0(3)	C(11)–Sn(2)–C(23a)	122.3(3)
Sn(1)–O(4)–Sn(2)	111.8(2)	Sn(2)–O(4)–Sn(2a)	105.4(2)
Sn(1)–O(3)–Sn(2)	102.2(2)	Sn(1)–O(4)–Sn(2a)	142.1(2)
Sn(1)–C(1)–Si(1)	113.3(4)	Sn(2)–C(11)–Si(3)	118.5(4)
Sn(1)–C(2)–Si(2)	110.8(4)	Sn(2)–C(23a)–Si(4a)	119.1(4)
Si(1)–O(1)–Si(2)	155.2(4)	Si(3)–O(2)–Si(4)	147.0(4)

2.2.5.1 Reaction of the diorganotin diiodide *cyclo*-$I_2Sn(CH_2Me_2Si)_2O$, 3, with silver acetate

The reaction of **3**/**3a** with two molar equivalents of silver acetate gave a poorly soluble solid material from which, by extraction/crystallization from CH_2Cl_2, single crystals of $[\{O(Me_2SiCH_2)_2Sn(OAc)OAc\}Sn_2O_2\{(CH_2Me_2Si)_2O\}_2]$, **23** were obtained (Scheme 20). The endo-cyclic tin atoms in compound **23** are involved in the twelve-membered ring, $Sn(CH_2SiOSiCH_2)_2Sn$.

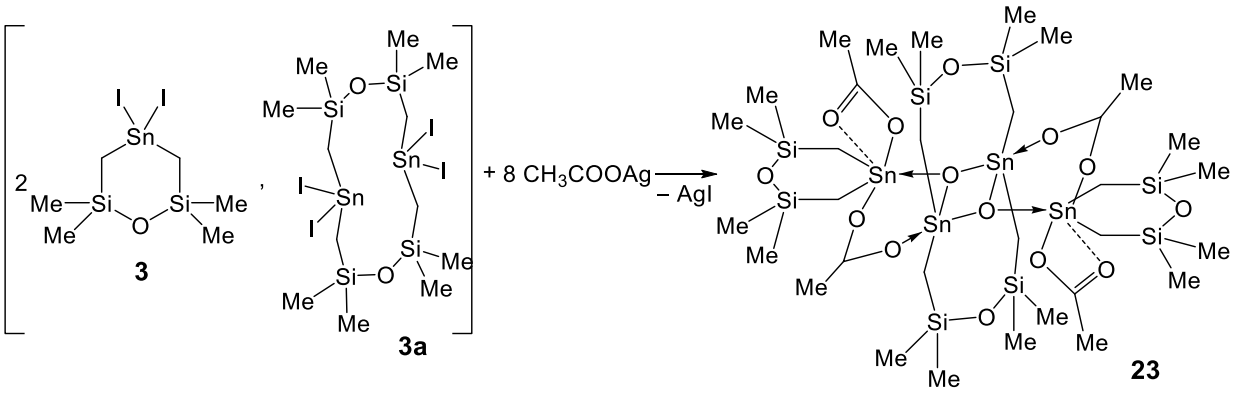

Scheme 20. Synthesis of compound **23**.

The Molecular structure of **23** is shown in Figure 15, and selected bond lengths and bond angles are summarized in Table 14. These will be discussed with those of compounds **22**, **24**–**27** in section 2.2.5.3.

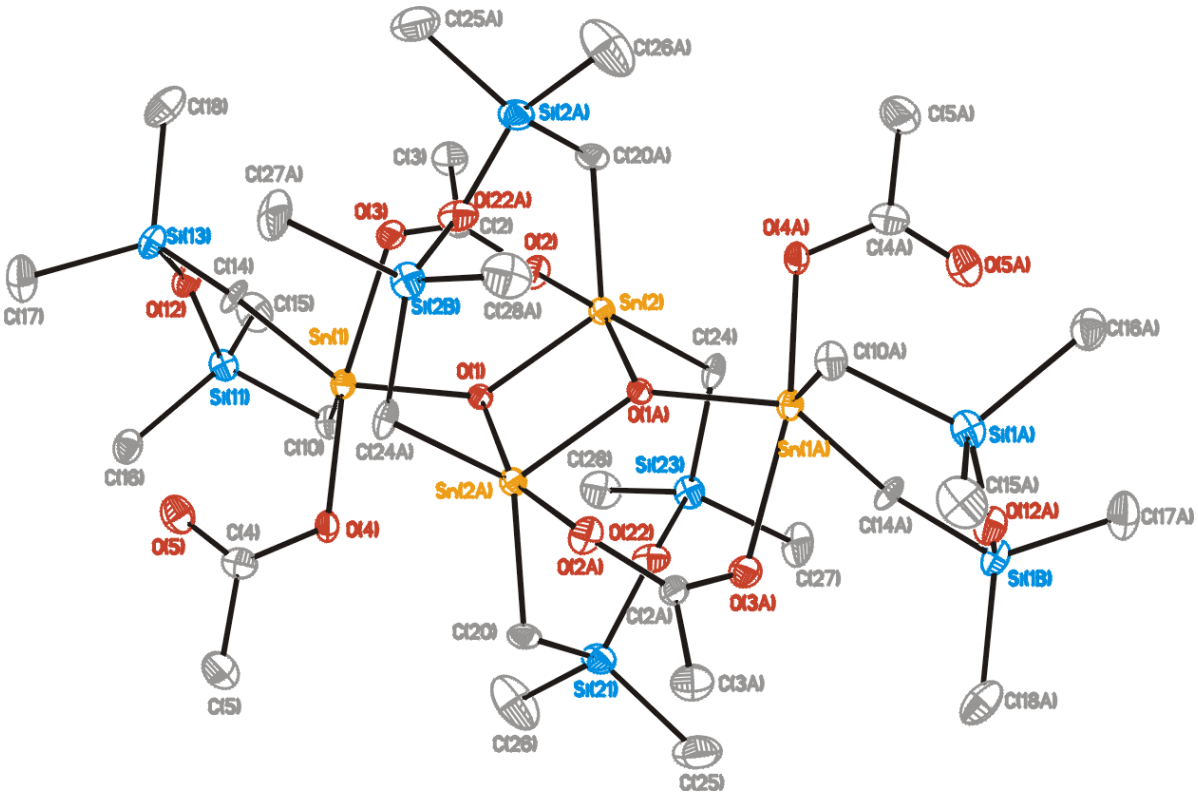

Figure 15. General view (SHELXTL) of a molecule of **23** showing 30% probability displacement ellipsoids and the crystallographic numbering scheme.

Table 14. Selected bond lengths /Å and bond angles /° in **23**.

Sn(1)–O(1)	2.019(3)	Sn(2)–O(1a)	2.163(3)
Sn(1)–O(3)	2.285(4)	Sn(2)–O(2)	2.250(3)
Sn(1)–O(4)	2.103(4)	Sn(2)–O(1)	2.022(3)
Sn(1)–O(5)	2.850(4)	Sn(2)–O(4a)	3.049(4)
Sn(1)–C(10)	2.125(5)	Sn(2)–C(20a)	2.123(5)
Sn(1)–C(14)	2.107(5)	Sn(2)–C(24)	2.120(5)
O(12)–Si(11)	1.631(4)	O(22)–Si(21)	1.608(4)
O(12)–Si(13)	1.638(4)	O(22)–Si(23)	1.642(4)
O(4)–Sn(1)–O(3)	167.51(15)	O(2)–Sn(2)–O(1a)	162.39(13)
O(4)–Sn(1)–O(1)	80.83(14)	O(2)–Sn(2)–O(1)	87.87(13)
O(4)–Sn(1)–C(10)	99.67(18)	O(2)–Sn(2)–C(20a)	88.83(17)
O(4)–Sn(1)–C(14)	102.81(17)	O(2)–Sn(2)–C(24)	84.98(17)
O(3)–Sn(1)–O(1)	86.79(13)	O(1a)–Sn(2)–O(1)	75.76(14)
O(3)–Sn(1)–C(10)	87.50(18)	O(1a)–Sn(2)–C(20a)	104.14(16)
O(3)–Sn(1)–C(14)	81.49(17)	O(1a)–Sn(2)–C(24)	96.78(17)
O(1)–Sn(1)–C(10)	117.69(17)	O(1)–Sn(2)–C(20a)	116.46(17)
O(1)–Sn(1)–C(14)	117.81(18)	O(1)–Sn(2)–C(24)	117.71(17)
C(10)–Sn(1)–C(14)	122.4(2)	C(20a)–Sn(2)–C(24)	125.1(2)
O(5)–Sn(1)–O(3)	142.36(13)	O(4a)–Sn(2)–O(2)	138.039(110)
O(5)–Sn(1)–O(4)	49.95(12)	O(4a)–Sn(2)–O(1a)	58.825(106)
O(5)–Sn(1)–O(1)	130.77(12)	O(4a)–Sn(2)–O(1)	134.066(127)
O(5)–Sn(1)–C(10)	77.31(17)	O(4a)–Sn(2)–C(20a)	72.246(178)
O(5)–Sn(1)–C(14)	78.27(17)	O(4a)–Sn(2)–C(24)	76.853(144)
Sn(1)–O(1)–Sn(2)	130.28(15)	Sn(1)–O(4)–Sn(2a)	88.829(121)
Sn(1)–O(1)–Sn(2a)	122.56(16)	Sn(2)–O(1)–Sn(2a)	104.24(14)
Sn(1)–C(10)–Si(11)	108.9(2)	Sn(2a)–C(20)–Si(21)	119.5(3)
Sn(1)–C(14)–Si(13)	110.0(3)	Sn(2)–C(24)–Si(23)	115.3(3)
Si(11)–O(12)–Si(13)	148.8(2)	Si(21)–O(22)–Si(23)	149.4(3)

2.2.5.2 Reaction of the diorganotin dihalides *cyclo*-$X_2Sn(CH_2Me_2Si)_2O$ (3, X = I; 4, X = Br; 5, X = Cl) with (t-$Bu_2SnO)_3$

The reactions of the diorganotin halides *cyclo*-$X_2Sn(CH_2Me_2Si)_2O$ (**3**, X = I; **4**, X = Br; **5**, X = Cl) with one molar equivalent di-*tert*-butyltin oxide, t-Bu_2SnO, provided, according to the halide bound to the tin atom, the symmetrically substituted dimeric tetraorganodistannoxane, and/or the unsymmetrically substituted dimeric tetraorganodistannoxane (mixed dimeric tetraorganodistannoxane). The latter is a result of involving the t-Bu_2Sn moieties in the reaction product (Chart 6).

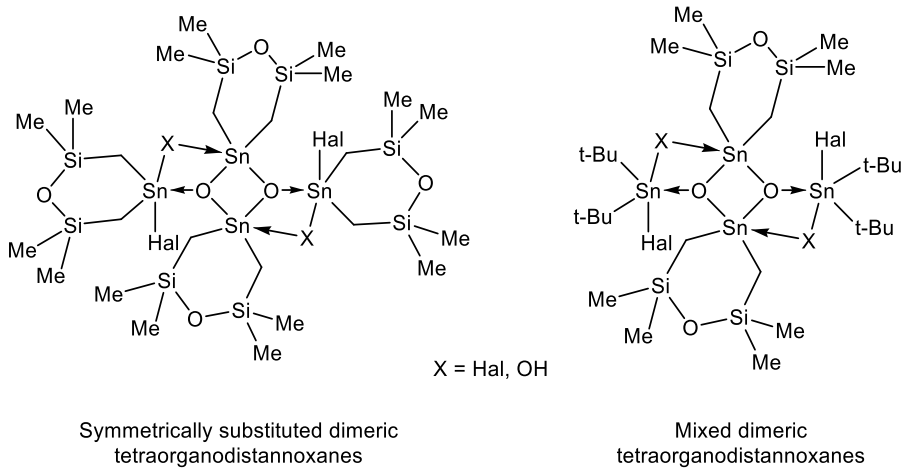

Chart 6. Symmetrically substituted- and mixed dimeric tetraorganodistannoxanes.

The Reaction of the diorganotin diiodide **3** with di-*tert*-butyltin oxide afforded only the symmetrically substituted dimeric tetraorganodistannoxanes $[O(Me_2SiCH_2)_2(I)SnOSn(\mathbf{X})(CH_2Me_2Si)_2O]_2$ (X = I, OH), **24** (Scheme 21).

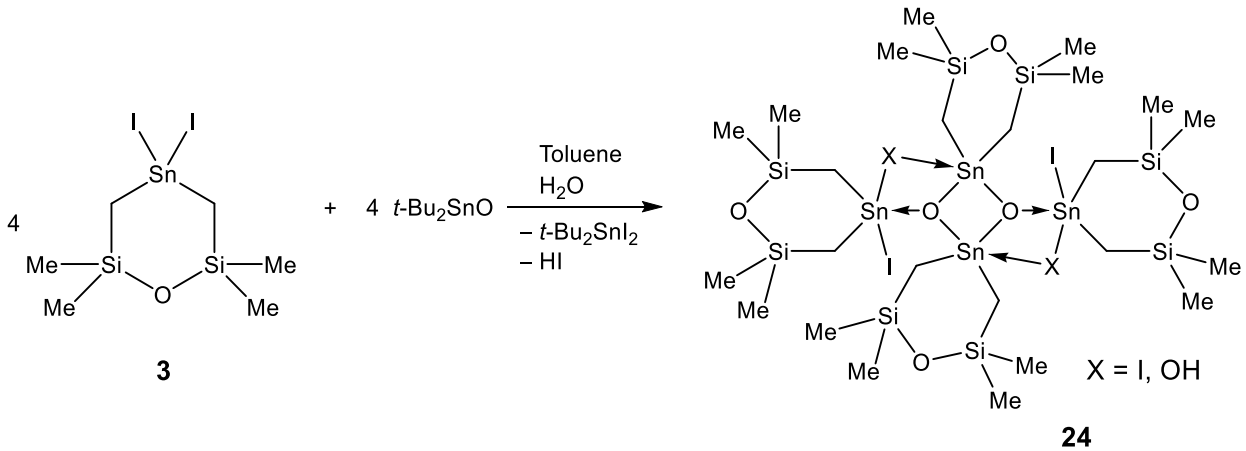

Scheme 21. Reaction of *cyclo*-$I_2Sn(CH_2Me_2Si)_2O$, **3** with (t-$Bu_2SnO)_3$.

A ^{119}Sn NMR spectrum of the crude product in $CDCl_3$-solution showed in addition to the resonance of *t*-Bu_2SnI_2, eight resonances between –139 and –241 ppm, two equally intense resonances at *δ* –139 [^2J(^{119}Sn–$^{117/119}$Sn) = 272 Hz] and *δ* –236 [^2J(^{119}Sn–$^{117/119}$Sn) = 272 Hz] with sum integral of about 52%. These are assigned to the compound in which the bridging groups are hydroxide anions, $[O(Me_2SiCH_2)_2(I)SnOSn(\mathbf{OH})(CH_2Me_2Si)_2O]_2$, **24a**. Two equally intense resonances at *δ* –145 ($W_{1/2}$ = 26 Hz) and *δ* –183 ($W_{1/2}$ = 18 Hz) with sum integral of about 23% were also observed. Those correspond to the compound in which the bridging groups are iodide anions, $[O(Me_2SiCH_2)_2(I)SnOSn(\mathbf{I})(CH_2Me_2Si)_2O]_2$, **24b**. Four nearly equal resonances at *δ* –147 ($v_{1/2}$ = 41 Hz), –152, –207 ($v_{1/2}$ = 25 ppm) and *δ* –241 ($W_{1/2}$ = 18 ppm) with a sum integral of about 25% were also observed. These are assigned with caution to $[O(Me_2SiCH_2)_2(I)SnOSn(\mathbf{I})(CH_2Me_2Si)_2O][O(Me_2SiCH_2)_2(I)SnOSn(\mathbf{OH})(CH_2Me_2Si)_2O]$, **24c**, the intermediate hydrolysis product between **24b** and **24a**.

Recrystallization of the crude product from a solution in CH_2Cl_2/hexane afforded single crystals of **24a** suitable for X-ray diffraction analysis. The ^{119}Sn NMR spectrum of a solution of the crystals in $CDCl_3$ showed two resonances at *δ* –139 and –236 with ^2J(^{119}Sn–$^{117/119}$Sn) coupling constant of 272 Hz for each resonance. The ^{1}H NMR spectrum showed four resonances for the silicon-bound methyl groups at *δ* 0.15, 0.16, 0.31 and 0.37. For the methylene protons a complex pattern between 0.60 and 1.15 was observed. In ^{13}C NMR spectrum four singlet resonances at *δ* 3.6, 3.7, 3.8 and 3.9 for the silicon-bound methyl groups, and a singlet at *δ* 13.0 [^1J(^{13}C–$^{117/119}$Sn) = 379 Hz] and a singlet at *δ* 20.3 [^1J(^{13}C–$^{117/119}$Sn) = 405/419 Hz] for Sn*C*H_2Si carbon atoms were observed. We expect that the resonance at *δ* 20.3 in ^{13}C NMR spectrum correspond to the methylene group bound to the endo-cyclic tin atom as the endo-cyclic tin atom has more Lewis acidity with respect to that in the exo-cyclic one. This results in low-field shift for the carbon atom in the ^{13}C NMR spectrum. A ^{29}Si NMR spectrum showed two singlets [*δ* 8.3 (^2J(^{29}Si–$^{117/119}$Sn) = 51 Hz); 9.0 (^2J(^{29}Si–$^{117/119}$Sn) = 45 Hz)], one for the silicon atom in the six-membered ring bound to the endo-cyclic tin atom and the other for that bound to the exo-cyclic one.

The Molecular structure of **24a** is shown in Figure 16, and selected bond lengths and bond angles are summarized in Table 15. These will be discussed with those of compounds **22**, **23**, **25**–**27** in section 2.2.5.3.

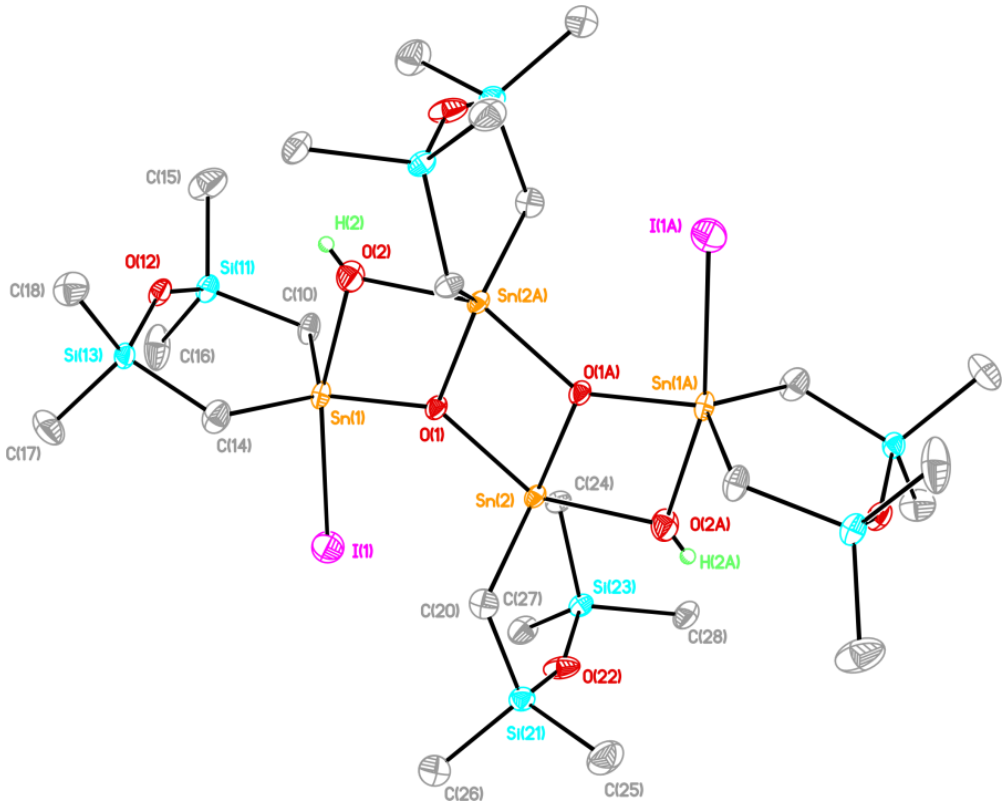

Figure 16. General view (SHELXTL) of a molecule of **24a** showing 30% probability displacement ellipsoids and the crystallographic numbering scheme.

Table 15. Selected bond lengths /Å and bond angles /° in **24a**.

Sn(1)–O(1)	2.019(3)	Sn(1)–C(14)	2.130(5)
Sn(1)–O(2)	2.221(4)	Sn(2)–C(20)	2.113(5)
Sn(1)–I(1)	2.8206(6)	Sn(2)–C(24)	2.089(4)
Sn(2)–O(1)	2.128(3)	O(12)–Si(11)	1.640(3)
Sn(2)–O(2a)	2.169(4)	O(12)–Si(13)	1.639(4)
Sn(2)–O(1a)	2.039(3)	O(22)–Si(21)	1.627(4)
Sn(1)–C(10)	2.110(5)	O(22)–Si(23)	1.627(4)
O(2)–Sn(1)–I(1)	164.86(10)	O(1)–Sn(2)–O(2a)	147.27(14)
O(2)–Sn(1)–O(1)	72.81(14)	O(1)–Sn(2)–O(1a)	73.74(13)
O(2)–Sn(1)–C(10)	88.7(2)	O(1)–Sn(2)–C(20)	103.80(17)

O(2)–Sn(1)–C(14)	90.1(2)	O(1)–Sn(2)–C(24)	100.49(16)
I(1)–Sn(1)–O(1)	92.17(9)	O(2a)–Sn(2)–O(1a)	73.56(14)
I(1)–Sn(1)–C(10)	97.08(16)	O(2a)–Sn(2)–C(20)	94.16(18)
I(1)–Sn(1)–C(14)	98.55(18)	O(2a)–Sn(2)–C(24)	93.51(17)
O(1)–Sn(1)–C(10)	118.02(16)	O(1a)–Sn(1)–C(20)	121.26(17)
O(1)–Sn(1)–C(14)	116.76(17)	O(1a)–Sn(1)–C(24)	117.81(17)
C(10)–Sn(1)–C(14)	121.98(19)	C(20)–Sn(1)–C(24)	120.2(2)
Sn(1)–O(1)–Sn(2a)	112.89(15)	Sn(2a)–O(1)–Sn(2)	106.26(13
Sn(1)–O(1)–Sn(2)	140.85(17)	Sn(2a)–O(2)–Sn(1)	100.74(16)
Sn(1)–C(10)–Si(11)	109.8(2)	Sn(2)–C(20)–Si(21)	108.4(2)
Sn(1)–C(14)–Si(13)	109.7(2)	Sn(2)–C(24)–Si(23)	110.1(2)
Si(11)–O(12)–Si(13)	144.3(3)	Si(21)–O(22)–Si(23)	156.0(3)

In contrast to the diorganotin diiodide **3**, the reaction of the diorganotin dichloride **5** with *t*-Bu_2SnO gave only the mixed dimeric tetraorganodistannoxane $[O(Me_2SiCH_2)_2(Cl)SnOSn(Cl)t\text{-}Bu_2]_2$, **25** (Scheme 22). This compound has very poor solubility in common organic solvents. The elemental analysis confirms the empirical formula, and the reaction product is compatible with that reported for the reaction between $(Me_3SiCH_2)_2SnCl_2$ and *t*-Bu_2SnO which afforded also the mixed dimeric tetraorganodistannoxane $[(Me_3SiCH_2)_2(Cl)SnOSn(Cl)t\text{-}Bu_2]_2$.[45]

Recrystallization of **25** from a solution in CH_2Cl_2/toluene in moist air afforded single crystals suitable for the X-ray diffraction analysis.

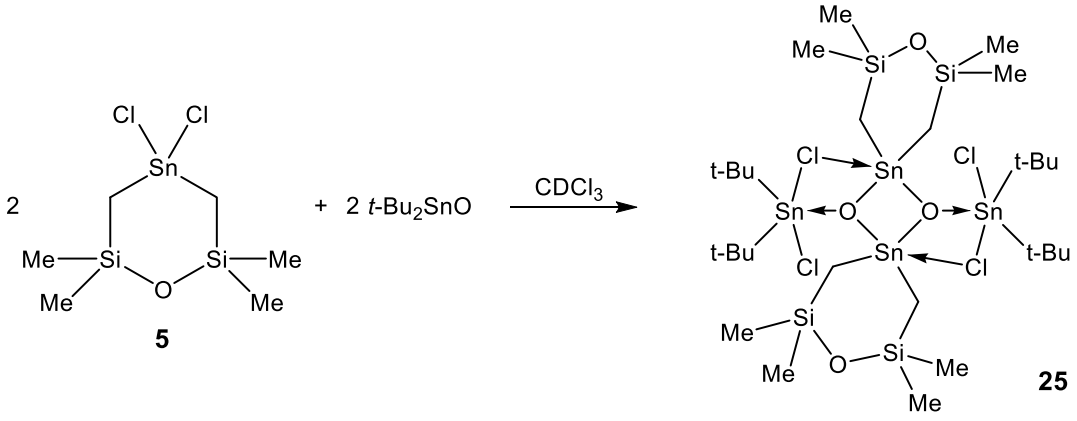

Scheme 22. Synthesis of compound **25**.

The Molecular structure of **25** is shown in Figure 17, and selected bond lengths and bond angles are summarized in Table 16. These will be discussed with those of compounds **22**–**24**, **26**, **27** in section 2.2.5.3.

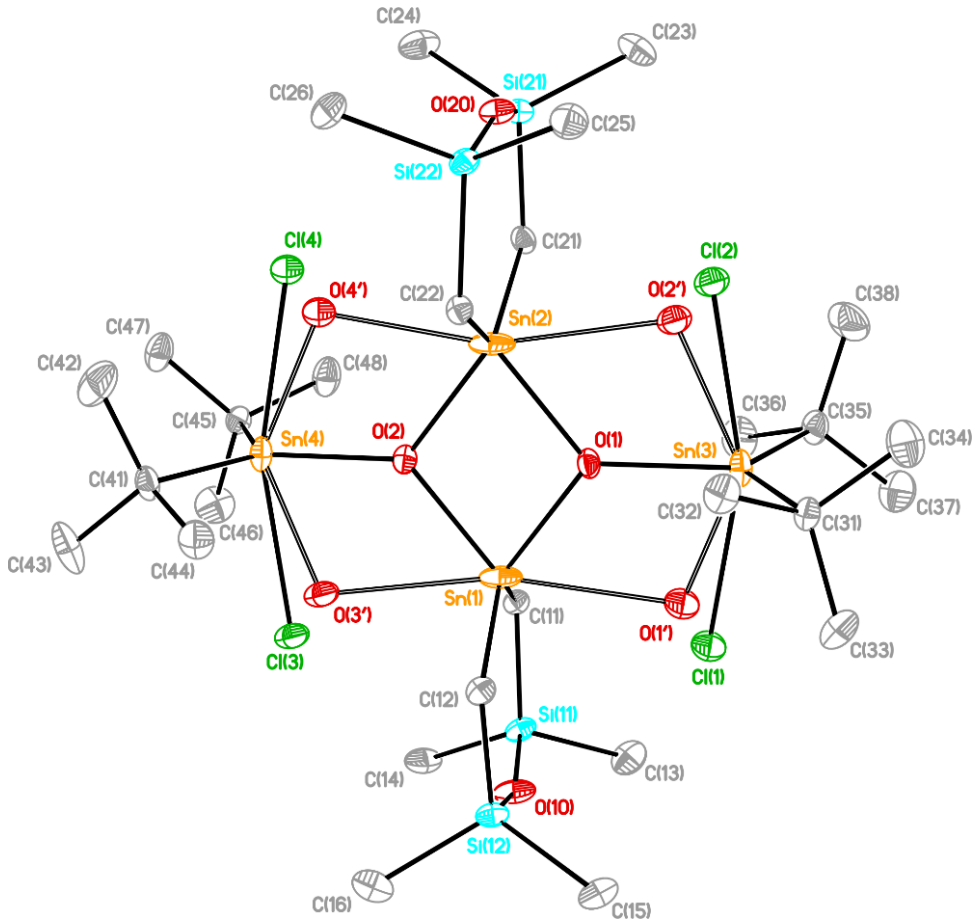

Figure 17. General view (SHELXTL) of a molecule of **25** showing 30% probability displacement ellipsoids and the crystallographic numbering scheme. The bridging chloride are partially replaced by hydroxide anions. The chlorides are disordered with OH groups, Cl1:O1‘ and Cl4:O4‘ with a ratio of 85:15; Cl2:O2‘ and Cl3:O3‘ with a ratio of 90:10, so that a total of half OH group is distributed onto the molecule. The protons of these OH groups could not be found. The *t*-Butyl group is disordered over two positions with a ratio of 60:40.

Table 16. Selected bond lengths /Å and bond angles /° which relate to Sn(1) and Sn(3) in **25**.

Sn(1)–O(1)	2.055(2)	Sn(3)–O(1)	2.033(2)
Sn(1)–O(2)	2.072(3)	Sn(3)–O(1')	2.08(2)
Sn(1)–O(1')	2.49(2)	Sn(3)–O(2')	2.20(3)
Sn(1)–O(3')	2.52(3)	Sn(3)–Cl(1)	2.5894(14)
Sn(1)–C(11)	2.094(3)	Sn(3)–Cl(2)	2.5804(13)
Sn(1)–C(12)	2.097(3)	Sn(3)–C(31)	2.175(4)
Sn(1)–Cl(1)	2.9738(14)	Sn(3)–C(35)	2.178(4)
Sn(1)–Cl(3)	3.0678(13)	Si(12)–O(10)	1.627(3)
Si(11)–O(10)	1.632(2)	O(1')–Sn(1)–C(12)	86.2(5)
O(1')–Sn(1)–O(3')	166.0(8)	O(3')–Sn(1)–O(1)	134.0(7)
O(1')–Sn(1)–O(1)	59.9(5)	O(3')–Sn(1)–O(2)	58.7(7)
O(1')–Sn(1)–O(2)	135.3(5)	O(3')–Sn(1)–C(11)	84.8(8)
O(1')–Sn(1)–C(11)	89.5(5)	O(3')–Sn(1)–C(12)	86.6(7)
O(1)–Sn(1)–O(2)	75.44(10)	O(2)–Sn(1)–C(11)	108.40(12)
O(1)–Sn(1)–C(11)	113.97(12)	O(2)–Sn(1)–C(12)	112.78(12)
O(1)–Sn(1)–C(12)	110.78(12)	C(11)–Sn(1)–C(12)	124.80(14)
Cl(1)–Sn(3)–Cl(2)	161.89(4)	Cl(1)–Sn(3)–O(1')	12.8(6)
Cl(1)–Sn(3)–O(1)	80.64(8)	Cl(1)–Sn(3)–C(31)	95.52(11)
Cl(1)–Sn(3)–O(2')	147.0(8)	Cl(1)–Sn(3)–C(35)	93.15(12)
Cl(2)–Sn(3)–O(1)	81.28(8)	Cl(2)–Sn(3)–C(31)	91.71(11)
Cl(2)–Sn(3)–O(2')	14.9(8)	Cl(2)–Sn(3)–C(35)	95.04(12)
Cl(2)–Sn(3)–O(1')	149.1(6)	O(1)–Sn(3)–C(31)	116.85(12)
O(1)–Sn(3)–O(2')	66.4(8)	O(1)–Sn(3)–C(35)	113.74(13)
O(1)–Sn(3)–O(1')	68.0(6)	O(2')–Sn(3)–O(1')	134.3(10)
O(1')–Sn(3)–C(31)	99.2(6)	O(2')–Sn(3)–C(31)	98.8(9)
O(1')–Sn(3)–C(35)	99.9(6)	O(2')–Sn(3)–C(35)	100.3(9)
C(31)–Sn(3)–C(35)	129.40(14)	Sn(1)–O(1)–Sn(2)	104.76(11)
Sn(1)–O(1)–Sn(3)	126.46(13)	Sn(2)–O(1)–Sn(3)	128.77(13)
Sn(1)–O(1')–Sn(3)	105.6(9)	Sn(2)–O(2')–Sn(3)	104.1(11)
Sn(1)–C(11)–Si(11)	109.18(16)	Sn(1)–C(12)–Si(12)	109.83(17)
Si(11)–O(10)–Si(12)	157.14(18)		

The reaction between the diorganotin dibromide **4** and (*t*-$Bu_2SnO)_3$ was also monitored using ^{119}Sn NMR spectroscopy. The ^{119}Sn NMR spectrum ($CDCl_3$) of the crude product revealed, in addition to the signal of *t*-Bu_2SnBr_2 at *δ* 76, sixteen resonances between –94 and –211 ppm. It was difficult to assign all the resonances, but comparing the chemical shift of these signals with those of [*n*-Bu_2(X1)SnOSn(Br)*n*-Bu_2][*n*-Bu_2(X2)SnOSn(Br)*n*-Bu_2], X1, X2 = Br, OH,[46] confirmed the presence of [O($Me_2SiCH_2)_2$(**Br**)SnOSn(Br)($CH_2Me_2Si)_2$O]$_2$ (**26a**, *δ* –96, –129; total integral 18%). The resonances between –94 and –178 suggest the presence of the partial hydrolysis product of **26a**, [O($Me_2SiCH_2)_2$(**OH**)SnOSn(Br)($CH_2Me_2Si)_2$O] [O($Me_2SiCH_2)_2$(**X**)SnOSn(Br)($CH_2SiMe_2)_2$O], X = Br, OH, **26b**. The presence of a signal at *δ* –205, which is up-field shifted in comparison to those of **26a** and its hydrolysis products **26b**, hints to the *t*-Bu_2Sn moiety being present in the mixed dimeric tetraorganodistannoxane. This signal and the equally intense signal at *δ* –149 propose the presence of the diorganotinoxo cluster [O($Me_2SiCH_2)_2$(**X**)SnOSn(Br)*t*-$Bu_2]_2$, X = Br or OH, **27**.

Recrystallization of the crude reaction mixture from a solution in CH_2Cl_2/hexane afforded some crystals of the symmetrically substituted dimeric tetraorganodistannoxane, **26**.

Slow evaporation of the reaction mixture in air to dryness gave a white precipitate that was washed with hexane and dried in vacuo. The elemental analysis and X-ray diffraction analysis of the latter solid fit with the mixed dimeric tetraorganodistannoxane, **27**, containing bridging groups are hydroxide anions (Scheme 23).

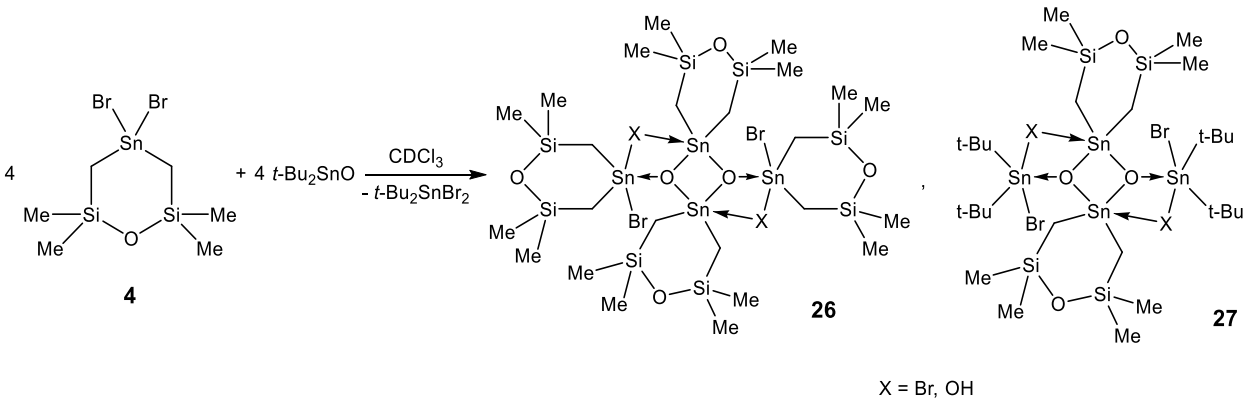

Scheme 23. Reaction of *cyclo*-$Br_2Sn(CH_2Me_2Si)_2O$, **4** with (*t*-$Bu_2SnO)_3$.

The Molecular structure of **26**, **27** are shown in Figures 18 and 19, respectively, and selected bond lengths and bond angles are summarized in Tables 17 and 18, respectively. These will be discussed with those of compounds **22**–**25** in section 2.2.5.3.

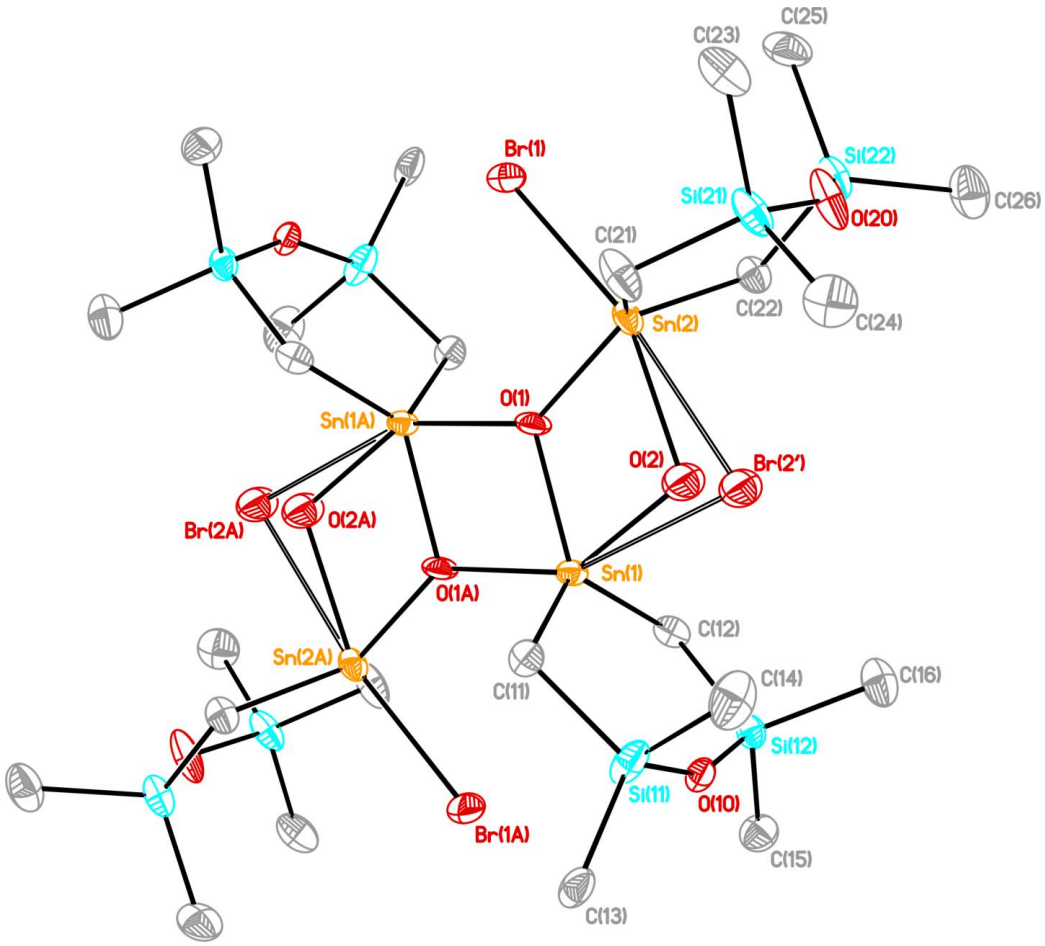

Figure 18. General view (SHELXTL) of a molecule of **26**, showing 30% probability displacement ellipsoids and the crystallographic numbering scheme. The bridging bromide are partially replaced by hydroxide anions. The bromide Br2' is disordered by a ratio of 50:50 with OH group (O2), in which the proton could not be found. The methyl groups C13 and C14 are disordered over two positions by a ratio of 60:40.

Table 17. Selected bond lengths /Å and bond angles /° in **26**.

Sn(1)–O(1)	2.047(4)	Sn(2)–O(1)	2.015(3)
Sn(1)–O(2)	2.063(10)	Sn(2)–O(2)	2.258(10)
Sn(1)–O(1a)	2.116(4)	Sn(2)–Br(1)	2.6097(9)
Sn(1)–Br(2')	2.8344(16)	Sn(2)–Br(2')	2.7583(16)
Sn(1)–C(11)	2.108(5)	Sn(2)–C(21)	2.102(6)
Sn(1)–C(12)	2.096(6)	Sn(2)–C(22)	2.107(5)
Si(11)–O(10)	1.629(4)	Si(21)–O(20)	1.639(4)
Si(12)–O(10)	1.620(4)	Si(22)–O(20)	1.624(5)
O(1a)–Sn(1)–O(2)	143.6(3)	Br(1)–Sn(2)–O(2)	155.7(3)
O(1a)–Sn(1)–Br(2')	155.87(10)	Br(1)–Sn(2)–Br(2')	173.01(4)
O(1a)–Sn(1)–O(1)	74.19(15)	Br(1)–Sn(2)–O(1)	89.43(11)
O(1a)–Sn(1)–C(11)	102.6(2)	Br(1)–Sn(2)–C(21)	97.0(2)
O(1a)–Sn(1)–C(12)	101.9(2)	Br(1)–Sn(2)–C(22)	96.50(18)
O(2)–Sn(1)–O(1)	69.6(3)	O(2)–Sn(2)–O(1)	66.3(3)
O(2)–Sn(1)–C(11)	97.3(4)	O(2)–Sn(2)–C(21)	96.2(4)
O(2)–Sn(1)–C(12)	93.2(3)	O(2)–Sn(2)–C(22)	94.5(3)
Br(2')–Sn(1)–O(1)	81.69(11)	Br(2')–Sn(2)–O(1)	84.22(12)
Br(2')–Sn(1)–C(11)	87.95(18)	Br(2')–Sn(2)–C(21)	83.7(2)
Br(2')–Sn(1)–C(12)	90.61(17)	Br(2')–Sn(2)–C(22)	89.14(18)
O(1)–Sn(1)–C(11)	118.5(2)	O(1)–Sn(2)–C(21)	119.80(19)
O(1)–Sn(1)–C(12)	119.48(18)	O(1)–Sn(2)–C(22)	118.94(19)
C(11)–Sn(1)–C(12)	121.1(2)	C(21)–Sn(2)–C(22)	119.6(2)
O(2)–Sn(1)–Br(2')	12.8(3)	O(2)–Sn(2)–Br(2')	18.4(3)
Sn(1)–C(11)–Si(11)	109.2(3)	Sn(2)–C(21)–Si(21)	111.8(3)
Sn(1)–C(12)–Si(12)	110.4(3)	Sn(2)–C(22)–Si(22)	110.3(3)
Si(11)–O(10)–Si(12)	153.2(3)	Si(21)–O(20)–Si(22)	148.3(3)
Sn(1)–O(1)–Sn(1a)	105.81(15)	Sn(1)–O(2)–Sn(2)	106.7(4)
Sn(1)–O(1)–Sn(2)	117.3(2)	Sn(2)–O(1)–Sn(1a)	136.82(19)
Sn(2)–Br(2')–Sn(1)	76.68(4)		

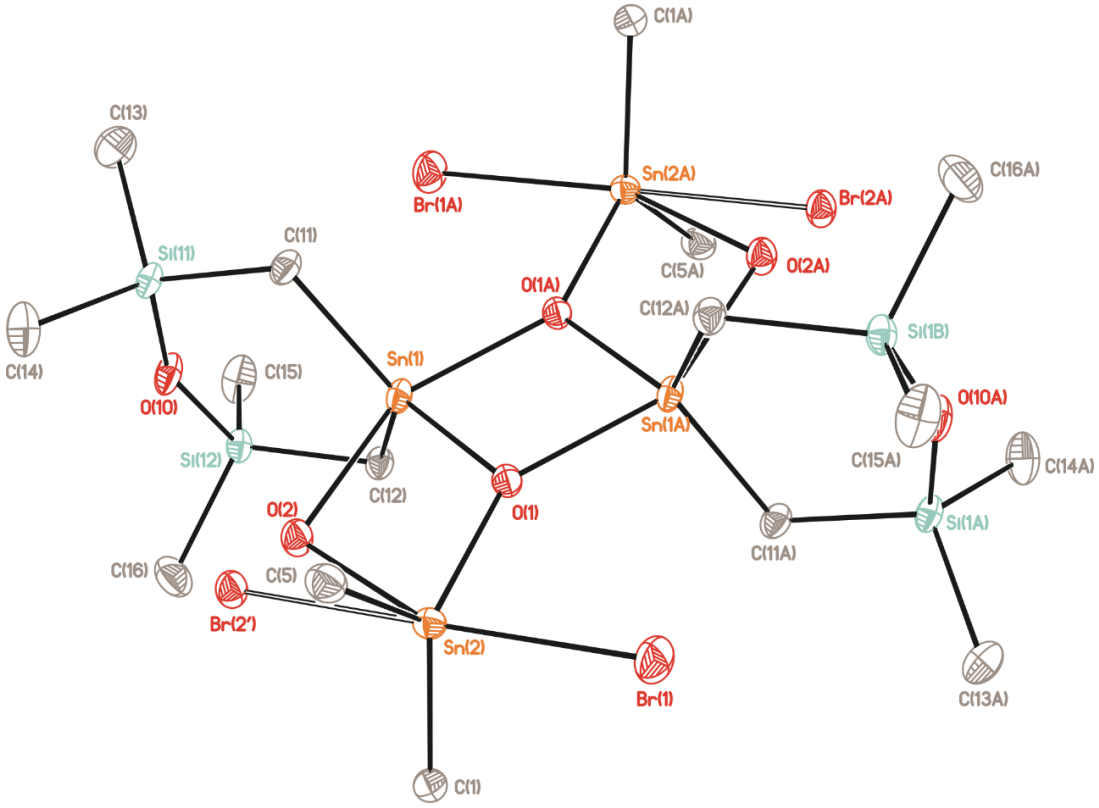

Figure 19. General view (SHELXTL) of a molecule of **27**, showing 30% probability displacement ellipsoids and the crystallographic numbering scheme. The bridging hydroxide are partially replaced by bromide anions. The OH anion (O2) is disordered by a ratio of 95:5 with bromide anion (Br2). The proton in the bridging hydroxide anion could not be found. The methyl groups in the *t*-Bu group are omitted for clarity. The *t*-Bu groups at C1 are disordered over two positions by a ratio of 50:50.

Table 18. Selected bond lengths /Å and bond angles /° in **27**.

Sn(1)–O(1)	2.052(3)	Sn(2)–O(1)	2.033(3)
Sn(1)–O(1a)	2.115(3)	Sn(2)–O(2)	2.222(3)
Sn(1)–O(2)	2.213(4)	Sn(2)–Br(1)	2.6795(7)
Sn(1)–C(11)	2.108(4)	Sn(2)–Br(2‘)	2.542(10)
Sn(1)–C(12)	2.119(4)	Sn(2)–C(1)	2.21(2)
Sn(2)–C(1‘)	2.15(3)	Sn(2)–C(5)	2.197(5)
Si(11)–O(10)	1.631(3)	Si(12)–O(10)	1.636(3)
O(1a)–Sn(1)–O(2)	146.50(13)	Br(1)–Sn(2)–O(2)	157.47(10)
O(1a)–Sn(1)–O(1)	74.60(14)	Br(1)–Sn(2)–O(1)	85.41(9)
O(1a)–Sn(1)–C(11)	104.01(16)	Br(1)–Sn(2)–C(1)	96.7(4)
O(1a)–Sn(1)–C(12)	103.26(16)	Br(1)–Sn(2)–C(5)	95.15(14)

O(2)–Sn(1)–O(1)	71.91(12)	O(2)–Sn(2)–O(1)	72.06(13)
O(2)–Sn(1)–C(11)	92.22(17)	O(2)–Sn(2)–C(1)	92.6(4)
O(2)–Sn(1)–C(12)	92.41(16)	O(2)–Sn(2)–C(5)	94.76(17)
O(1)–Sn(1)–C(11)	118.09(16)	O(1)–Sn(2)–C(1)	114.6(4)
O(1)–Sn(1)–C(12)	118.83(16)	O(1)–Sn(2)–C(5)	115.31(16)
C(11)–Sn(1)–C(12)	121.34(19)	C(1)–Sn(1)–C(5)	129.3(4)
Br(2‘)–Sn(2)–Br(1)	179.3(2)	Br(2‘)–Sn(2)–C(1)	83.4(6)
Br(2‘)–Sn(2)–O(1)	93.9(3)	Br(2‘)–Sn(2)–C(5)	85.4(3)
Sn(1)–O(1)–Sn(2)	114.48(15)	Sn(1)–C(11)–Si(11)	109.3(2)
Sn(1)–O(1)–Sn(1a)	105.40(14)	Sn(1)–C(12)–Si(12)	109.8(2)
Sn(2)–O(1)–Sn(1a)	140.11(17)	Si(11)–O(10)–Si(12)	155.2(2)
Sn(1)–O(2)–Sn(2)	101.55(14)		

To the best of our knowledge, all known mixed dimeric tetraorganodistannoxanes $[R_2(X)SnOSn(X)R'_2]_2$ in the literature are accomplished from the reactions of diorganotin dichlorides[45, 47] or difluorides[48] with an appropriate diorganotin oxides, and no one was reported from the reaction of diorganotin dibromide or diiodide with the oxide. The more bulky organic substituents (R, R') are bound to the exo-cyclic tin atom.

Reactions of R_2SnX_2 (X = Cl, F) with R'_2SnO result mostly in the mixed dimeric tetraorganodistannoxanes. The only exception is expressed in the reaction of $[Me_3SiCH_2(Cl_2)SnCH_2(Me_2)Si]_2C_2$ with $(t\text{-}Bu_2SnO)_3$ providing the symmetrically substituted dimeric tetraorganodistannoxane $\{[Me_3SiCH_2(Cl)SnCH_2Me_2SiC{\equiv}CSiMe_2\text{-}CH_2Sn(Cl)CH_2SiMe_3]O\}_2$.[49] The diorganotin oxide, $(t\text{-}Bu_2SnO)_3$, acts in this reaction as water-free oxygen source, and it is not involved in the reaction product.

From the last discussion, the identity of the halogen substituent in the diorganotin dihalides R_2SnX_2 in reactions with R'_2SnO seems to play an important role in determining the structure of the dimeric tetraorganodistannoxane obtained, whether symmetric or mixed. However, this is not the only determining factor. Diorganotin dihalides, R_2SnX_2, with high Lewis acid tin centers favor to build mixed dimeric tetraorganodistannoxanes on reactions with diorganotin oxides, R'_2SnO.

When the diorganotin halides, $O(Me_2SiCH_2)_2SnX_2$; **3**, X = I; **4**, X = Br; **5**, X = Cl, react with *t*-Bu_2SnO, the corresponding di-*tert*-butyltin halides, *t*-Bu_2SnX_2, produce as by-products (Scheme 24). If the Lewis acidity at the tin atom in the latter is high enough to interact with the intermediate hydrolyses products $R_2(X)Sn(Y)O[SnR_2]_2O$ (X = Hal; Y = Hal, OH) resulted by the hydrolyses of the organotin halides **3**–**5**, the mixed tetraoranodistannoxanes will be favored. Because of the bulky ter*t*-butyl substituents at the tin atom, the latter places in the exo-cyclic center (Scheme 25).

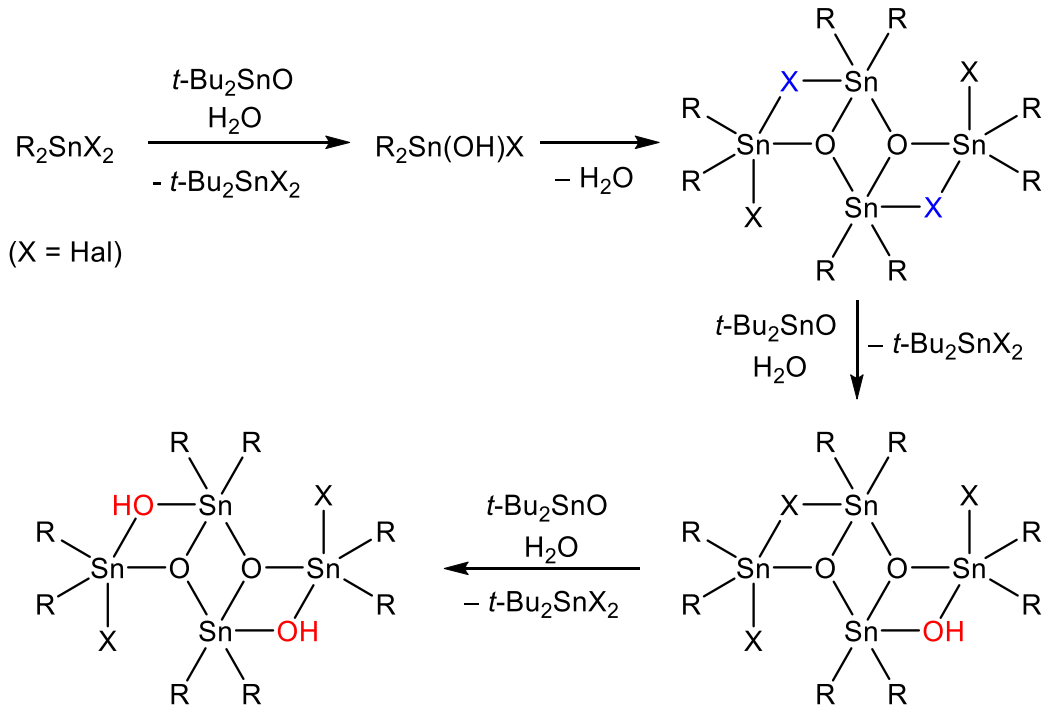

Scheme 24.

One possibility is that the Lewis acidity of *t*-Bu_2SnCl_2 is high enough to form a complex with the intermediate hydrolyses products of the organotin chloride **5** and build the mixed dimeric tetraorganodistannoxane (Scheme 25), and that of *t*-Bu_2SnI_2 is too small so only the symmetric dimeric tetraorganodistannoxane was formed. The Lewis acidity at the tin atom in *t*-Bu_2SnBr_2 is in the middle, and in consequence the symmetrically- and the unsymmetrically-substituted dimeric tetraorganodistann-oxanes were isolated.

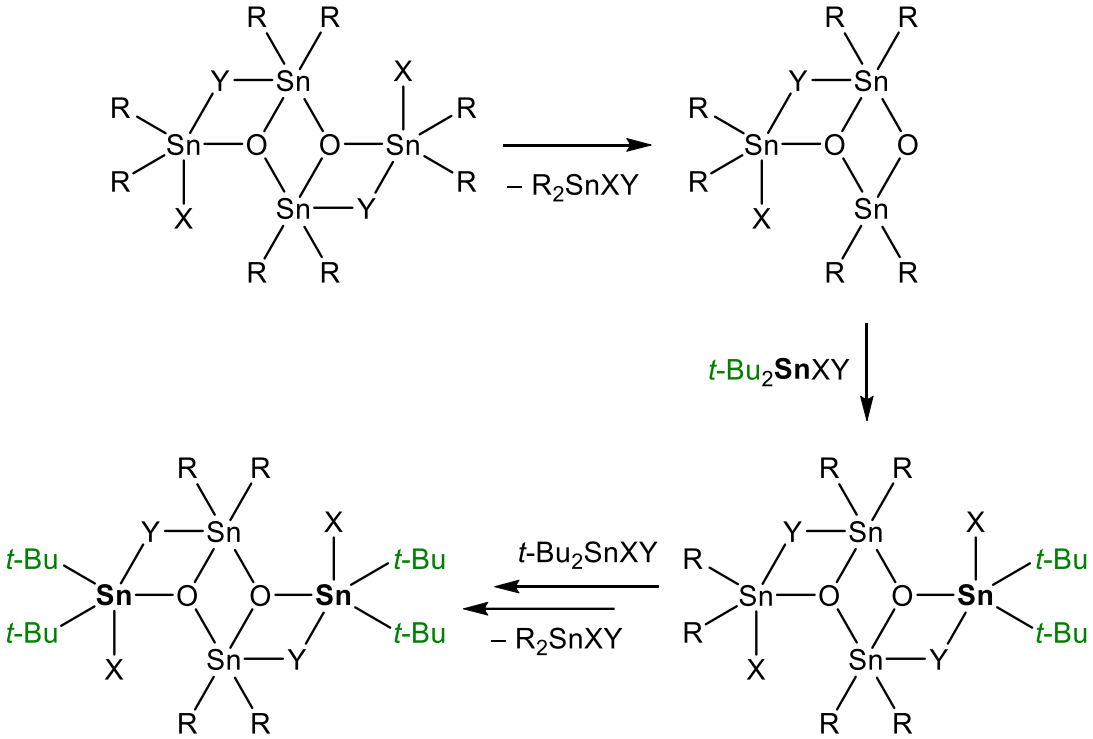

Scheme 25.

The diorganotinoxo clusters **22**, **23** and **25** are poorly soluble in common organic solvents whereas compounds **24**, **26** and **27** are well soluble in CH_2Cl_2, $CHCl_3$ and toluene.

2.2.5.3 The molecular structures of the diorganotinoxo clusters 22–27

Compounds **22**, **23**, **24a**, **25**, **26** and **27** exist as ladder-like compounds that contain pentacoordinated tin atoms. Compounds **22**, **23**, **24a**, **26** and **27** can be viewed as centrosymmetric dimers, as one half of the molecule comprises the crystallographic asymmetric unit and the other half is generated by an inversion center (Figure 20). Compound **25** does not show symmetry but the bond lengths and angles in one half are very close to those in the other half.
The molecular geometries around Sn(1) and Sn(3) in compound **25** differ only slightly from those in Sn(2) and Sn(4), respectively. Consequently, only those of Sn(1) and Sn(3) are discussed in detail. The bond lengths and bond angles which relate to Sn(2) and Sn(4) in **25** could be found in the cif-file and the table in the supporting CD.

Each tin atom in compounds **22**, **23** and **24a** exhibits distorted trigonal bipyramidal geometry with the equatorial positions being occupied by two carbon atoms and one triply bridging oxygen atom, and the axial positions by two oxygen atoms for the endo-cyclic tin atoms. The axial position around the exo-cyclic tin atoms in **22** and **24a** is occupied by one iodine and one bidentate oxygen atom (deprotonated ethanol in **22** and hydroxyl group in **24a**). In compound **23** the axial position is occupied by two carboxylate-oxygen atoms (Figure 20).

The bridging halide anions bound to the exo- and endo-cyclic tin atoms in compounds **25**, **26** and **27** are replaced partially by hydroxy groups. The protons of these were not detected by the X-ray diffraction measurement.

All tin atoms in compounds **26** and **27** show distorted trigonal bipyramidal geometry with the equatorial positions being occupied by two carbon atoms and one oxygen atom. On the other hand, the endo-cyclic tin atoms in compound **25** exhibit distorted octahedral geometries with two carbon and two oxygen atoms in the equatorial positions. The exo-cyclic tin atoms show distorted trigonal bipyramidal geometries with two carbon atoms and one oxygen atom in the equatorial positions (Figure 20). The axial positions in **25**, **26** and **27** are occupied by two oxygen atoms, by one oxygen atom and one halogen, or by two halogen atoms, and that is because of the partial replacement of the bridging halide groups.

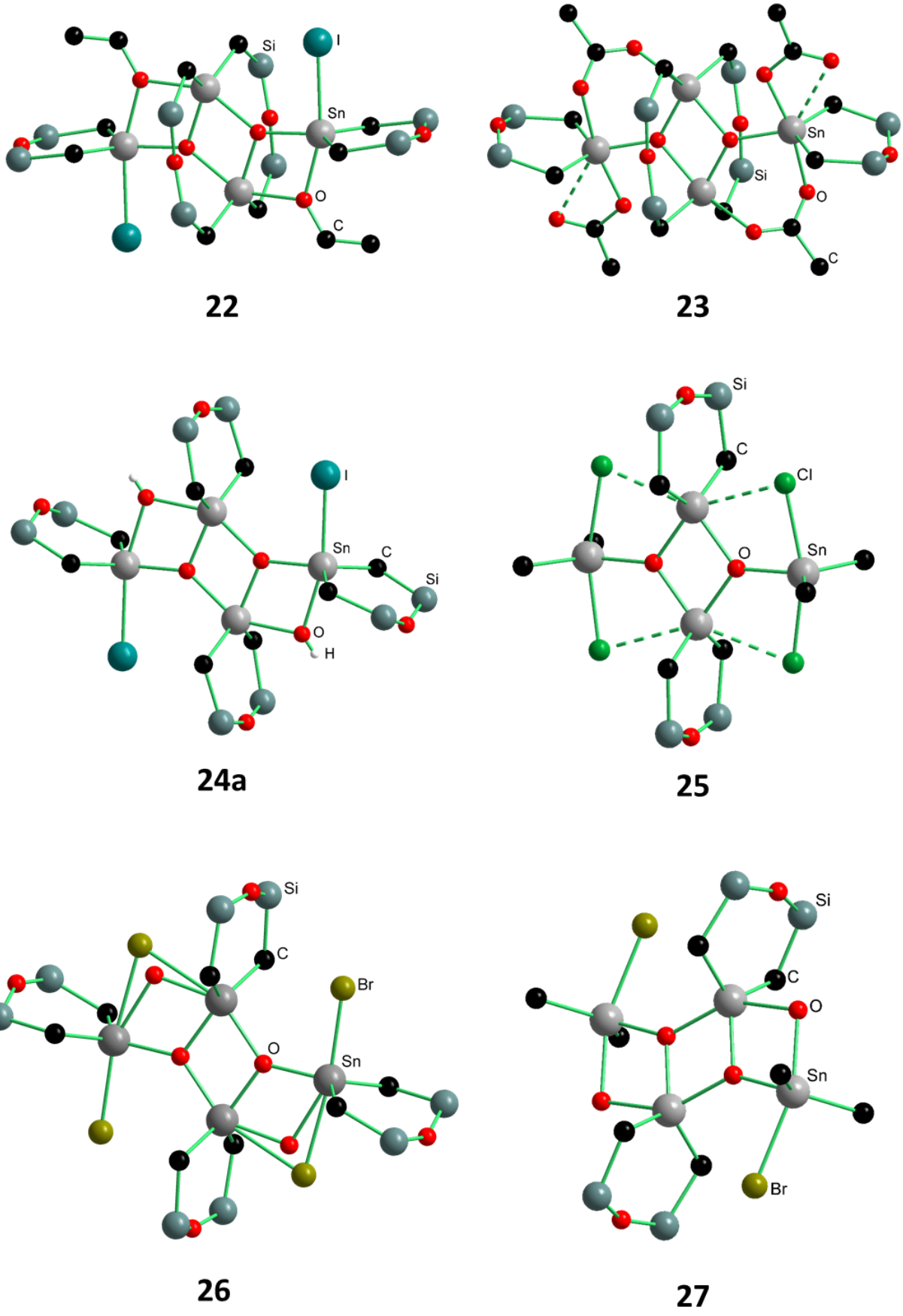

Figure 20. Simplified molecular Structures of compounds **22**–**27**. The bridging OH in **25** and Br in **27** are omitted as these show relatively low occupation-ratios.

The Sn_{endo}–μ_2-O–Sn_{exo} bridge is symmetric in compound **22** (Sn–O 2.155(6) Å). This is, however, asymmetric in **24a** [Sn(1)–O(2) 2.221(4) Å; Sn(2a)–O(2) 2.169(4) Å], **26** [Sn(1)–O(2) 2.063(10) Å; Sn(2)–O(2) 2.258(10) Å], and **27** [Sn(1)–O(2) 2.213(4) Å; Sn(2)–O(2) 2.222(3) Å]. The carboxylate anion in **23** coordinates the endo- and the exo-cyclic tin atoms in a bidentate mode with almost equal Sn–O bond lengths of 2.250(3) Å to the endo-cyclic tin atom and 2.285(4) Å to the exo-cyclic one. The Sn–O distances are between 2.014(5) and 2.155(6) Å in **22**, between 2.019(3) and 2.285(4) Å in **23**, between 2.019(3) and 2.221(4) Å in **24a**, between 2.015(3) and 2.258(10) in **26**, and between 2.033(3) and 2.222(3) in **27**.

In compound **25** the μ_3-O–Sn_{endo} bond lengths range between 2.055(2) and 2.072(3) Å, and the μ_3-O–Sn_{exo} are between 2.022(2) and 2.033(2) Å. The bridging hydroxyl groups locate closer to the exo-cyclic tin atoms [μ_2-O–Sn_{endo}, 2.44(2)–2.52(2) Å; μ_2-O–Sn_{exo}, 2.08(2)–2.20(2) Å]. The Sn_{exo}–Cl bond lengths are between 2.5757(12) and 2.5957(13) Å being of the same order of magnitude as those in [*t*-Bu_2(Cl)SnOSn(Cl)(CH_2SiMe_3)$_2$]$_2$[45] of 2.584(2) and 2.545(2) Å. The Sn_{endo}–Cl bond lengths in **25** range between 2.9738(14) and 3.0847(13). Those in [*t*-Bu_2(Cl)SnOSn(Cl)(CH_2SiMe_3)$_2$]$_2$[45] are 2.857(2) and 3.115(2) Å. The Sn_{endo}–μ_3-O–Sn_{exo} angles in **22** [Sn(1)–O(4)–Sn(2a) 142.1(2)°], **24a** [Sn(1)–O(1)–Sn(2) 140.85(17)°], **26** [Sn(1a)–O(1)–Sn(2) 136.82(19)°], and **27** [Sn(1a)–O(1)–Sn(2) 140.11(17)°] are remarkably bigger than those in **23** [Sn(1)–O(1)–Sn(2) 130.28(15)°] and **25** [Sn_{endo}–μ_3-O–Sn_{exo}, 126.46(13)° to 128.77(13)°]. This is a result of the intramolecular Sn(2a)–O(4) interaction of 3.0484(46) Å in compound **23**, and of Sn···OH/Cl interaction in **25**.

Interestingly the endo-cyclic tin atoms in **22** and **23** are involved in twelve-membered rings, Sn($CH_2SiOSiCH_2$)$_2$Sn, present in compounds **3a**–**5a**, the dimer of compounds **3**–**5**. However, the exo-cyclic tin atoms in all compounds are part of six-membered rings. The six-membered rings in **22**, **24a** and **27** exhibit boat conformation. Those in **23** exhibit half chair conformation, and those in **26** show twist-boat conformation. The six-membered rings in **25** are almost planar. The silicon atoms in all compounds show distorted tetrahedral environment.

2.3 Conclusion

A series of tin-substituted *cyclo*-siloxanes and polyhedral oligomeric silsesquioxanes (POSS) was synthesized and characterized. The silicon atoms in these siloxanes are bound to one, two or three oxygen atoms. Halogenation and proto-destannylation of the mono-cyclic siloxane *cyclo*-$Ph_2Sn(CH_2Me_2Si)_2O$, **1**, the tri-cyclic siloxane $[\{Ph_2Sn(CH_2MeSi)_2O\}O]_2$, **12**, and of the tin-substituted POSS $(Ph_3SnCH_2SiO_{1.5})_8$, **20**, afforded the corresponding organotin halides *cyclo*-$PhISn(CH_2Me_2Si)_2O$, **2**, *cyclo*-$X_2Sn(CH_2Me_2Si)_2O$ (**3**, X = I; **4**, X = Br; **5**, X = Cl), $[\{X_2Sn(CH_2MeSi)_2O\}O]_2$ (**13**, X = I; **14**, X = Br; **15**, X = Cl), and $(Br_2PhSnCH_2SiO_{1.5})_8$, **21**, containing halogen substituents that are readily modifiable by reactions with Grignard reagents. This was proved by the reaction of *cyclo*-$PhISn(CH_2Me_2Si)_2O$, **2**, with the Grignard reagent $Me_2N(CH_2)_3MgCl$ affording the siloxane *cyclo*-$\{Me_2N(CH_2)_3\}PhSn(CH_2Me_2Si)_2O$, **6**, which contains a periphery amine group.

The reaction of the diorganotin halides *cyclo*-$X_2Sn[CH_2Si(Me_2)]_2O$ (**3**, X = I; **4**, X = Br; **5**, X = Cl), with *t*-Bu_2SnO afforded the corresponding symmetrically and/or the unsymmetrically substituted dimeric tetraorganodistannoxanes, and that is according to the halogen substituent bound to the tin atom. The diorganotin diiodide **3** reacts with *t*-Bu_2SnO to give only the symmetrically substituted dimeric tetraorganodistannoxanes $[O(Me_2SiCH_2)_2(I)SnOSn(\mathbf{X})(CH_2SiMe_2)_2O]_2$ (X = OH, I), **24**. In contrast, the diorganotin dichloride **5** reacts with *t*-Bu_2SnO giving only the unsymmetrically substituted dimeric tetraorganodistannoxane $[O(Me_2SiCH_2)_2(Cl)Sn\text{-}OSn(Cl)t\text{-}Bu_2]_2$, **25**. The reaction of the diorganotin dibromide **4** with *t*-Bu_2SnO afforded the symmetrically- as well as the unsymmetrically substituted dimeric tetraorganodistannoxanes $[O(Me_2SiCH_2)_2(Br)SnOSn(\mathbf{X})(CH_2SiMe_2)_2O]_2$ (X = OH, Br), **26**, and $[O(Me_2SiCH_2)_2(X)SnOSn(Br)t\text{-}Bu_2]_2$ (X = OH, Br), **27**, respectively. Experiments to polymerize the six-membered *cyclo*-siloxane *cyclo*-$Ph_2Sn(CH_2\text{-}Me_2Si)_2O$, **1**, using different anionic initiators were not successful.

2.4 Experimental Section

General Considerations

All solvents were dried and purified according to standard procedures and freshly distilled prior to use. Me_2(*i*-PrO)$SiCH_2Cl$,[50] $Me_2N(CH_2)_3Cl$,[51] and (*t*-$Bu_2SnO)_3$,[52] were synthesised according to literature methods. Cl(Me_2)$SiCH_2Cl$, $Cl_2MeSiCH_2Cl$, [$Me_2N(CH_2)_3Cl$]·HCl, diphenyltin dichloride, diphenylphosphonic acid, silver perchlorate and silver carboxylate were commercially available, and they were used without further purification. Bruker DPX–300 and DRX–400 spectrometers were used to obtain ^{1}H, ^{13}C, ^{29}Si, and ^{119}Sn NMR spectra at ambient temperature. Solution ^{1}H, ^{13}C, ^{29}Si, and ^{119}Sn NMR chemical shifts are given in ppm and were referenced to Me_4Si (^{1}H, ^{13}C, ^{29}Si), and Me_4Sn (^{119}Sn). Elemental analyses were performed on a LECO–CHNS–932 analyzer. The electrospray mass spectra were recorded with a Thermoquest–Finnigan instrument, using CH_3CN, CH_3OH or CH_2Cl_2 as the mobile phase. The *m/z* values reported correspond to those of the most intense peak in the corresponding isotope pattern.

Synthesis of *cyclo*-$Ph_2Sn(CH_2Me_2Si)_2O$, 1

A solution of diphenyltin dichloride (40.45 g, 120 mmol) in THF (250 mL) was added drop-wise to the Grignard reagent prepared from Me_2(*i*-PrO)$SiCH_2Cl$ (46.13 g, 260 mmol) and magnesium turnings (6.86 g, 280 mmol) in THF (200 mL). Then the mixture was heated at reflux for 2 hours and stirred 18 hours at room temperature, before 150 mL of cold saturated ammonium chloride was added. The latter mixture was stirred for two hours at room temperature before it was acidified with diluted hydrochloric acid and extracted three times each with (200 ml) of diethyl ether. The organic phases were combined and dried with magnesium sulphate, and the solvents were evaporated in vacuo. Distillation of the residue at reduced pressure (105°C, 3.6 X 10^{-6}) gave (42.09 g, 82%) of compound **1** as colorless liquid which solidified after one day. Recrystallization from ethanol gave white crystals of mp 43–45 °C suitable for X-ray diffraction analysis.

Anal. Calcd for $C_{18}H_{26}OSi_2Sn$ (433.28 g/mol): C, 49.90; H, 6.05. Found: C, 49.8; H, 6.1.

^{1}H NMR (400.13, $CDCl_3$): *δ* 0.23 (s, 12 H, *Me*$_2$Si), 0.39 (s, 4 H, $^{2}J(^{1}H–^{117/119}Sn)$ = 68.8/71.7 Hz, SiC*H*$_2$Sn), 7.41–7.67 (m, 10H, Ar H). **^{13}C{^{1}H} NMR** (100.63, $CDCl_3$): *δ* –5.1 ($^{1}J(^{13}C–^{117/119}Sn)$ = 226/236 Hz, $^{1}J(^{13}C–^{29}Si)$ = 53 Hz, Si*C*H$_2$Sn), 3.2 ($^{1}J(^{13}C–^{29}Si)$ = 60 Hz, $^{3}J(^{13}C–^{117/119}Sn)$ = 12 Hz, *(Me*$_2$Si), 128.3 ($^{3}J(^{13}C–^{117/119}Sn)$ = 50 Hz, C$_m$), 128.7 ($^{4}J(^{13}C–^{117/119}Sn)$ = 12 Hz, C$_p$), 136.1 ($^{2}J(^{13}C–^{117/119}Sn)$ = 39 Hz, C$_o$), 140.8 ($^{1}J(^{13}C–^{117/119}Sn)$ = 469/491 Hz, C$_i$). **^{29}Si{^{1}H} NMR** (59.63, $CDCl_3$): *δ* 10.2 ($^{2}J(^{29}Si–^{119}Sn)$ = 35 Hz, $^{1}J(^{29}Si–^{13}C)$ = 61 Hz). **^{119}Sn{^{1}H} NMR** (111.92, $CDCl_3$): *δ* –57 [96%, ($^{1}J(^{119}Sn–^{13}C_{CH2})$ = 237 Hz, $^{1}J(^{119}Sn–^{13}C_{Ph})$ = 491 Hz), **1**], –52 (4%, **1a**). **Electrospray MS**: *m/z* (%), positive mode, 475.2 (100, $[M + MeCN + H]^+$), 497.1 (25, $[M + MeCN + Na]^+$), 538.2 (20, $[M + 2MeCN + Na]^+$), 357 (17, $[M – Ph]^+$).

Synthesis of *cyclo*-PhISn(CH$_2$Me$_2$Si)$_2$O, 2

Iodine (3.05 g, 12 mmol) was added in small portions at 0 °C to a solution of **1** (5.20 g, 12 mmol) in CH_2Cl_2 (100 mL). Then the mixture was allowed to reach room temperature and stirred overnight. Removing the solvent and iodobenzene in vacuo gave compound **2** as colorless oil (94% yield, judged by ^{119}Sn NMR spectrum). Recrystallization from a solution in MeCN gave single crystals of **2** of mp 31.5–33.5 °C suitable for X-ray diffraction analysis.

^{1}H NMR (400.13, $CDCl_3$): *δ* 0.26 (s (broad, $W_{1/2}$ = 28 Hz), 12H, *Me*$_2$Si), 0.87 (s, 4H, $^{2}J(^{1}H–^{117/119}Sn)$ = 79.8 Hz, SiC*H*$_2$Sn), 7.37–7.71 (m, 5H, Ar H). **^{13}C{^{1}H} NMR** (100.63, $CDCl_3$): *δ* 3.06 ($^{1}J(^{13}C–^{117/119}Sn)$ = 211/221 Hz, Si*C*H$_2$Sn), 3.16 ($^{1}J(^{13}C–^{29}Si)$ = 62 Hz, *Me*$_2$Si), 128.7 ($^{3}J(^{13}C–^{117/119}Sn)$ = 60 Hz, C$_m$), 129.8 ($^{4}J(^{13}C–^{117/119}Sn)$ = 14 Hz, C$_p$), 135.0 ($^{2}J(^{13}C–^{117/119}Sn)$ = 52, C$_o$), 139.1 ($^{1}J(^{13}C–^{117/119}Sn)$ = 494/518 Hz, C$_i$). **^{29}Si{^{1}H} NMR** (59.63, $CDCl_3$): *δ* 9.9 ($^{2}J(^{29}Si–^{119}Sn)$ = 39 Hz, **2**), 9.8 ($^{2}J(^{29}Si–^{119}Sn)$ = 39 Hz, **3**). **^{119}Sn{^{1}H} NMR** (111.92, $CDCl_3$): *δ* –29 (93%, **2**), –21 (3%, **2a**), –207 (4%, **3**). **Electrospray MS**: *m/z* (%), positive mode, 429.1 (100, $[M – I + 4H_2O]^+$), 729.1 (92, $[2M – 2I + OH]^+$), 651 (25), 801.2 (25).

Synthesis of *cyclo*-I$_2$Sn(CH$_2$Me$_2$Si)$_2$O, 3

Iodine (6.40 g, 25 mmol) was added in portions at 0 °C to a solution of **1** (5.20 g, 12 mmol) in CH_2Cl_2 (100 mL). Then the mixture was allowed to reach room temperature and stirred overnight. Removing the solvent and iodobenzene in vacuo and washing with a small amount of cold hexane gave compound **3** (5.97 g, 93%) as yellowish

solid. Recrystallization from hexane gave colorless crystals of mp 73–75 °C suitable for the X-ray diffraction analysis.

Anal. Calcd for $C_6H_{16}I_2OSi_2Sn$ (532.88 g/mol): C, 13.52; H, 3.03. Found: C, 13.2; H, 3.1.

^{1}H NMR (300.13, $CDCl_3$): *δ* 0.26 (s, 12 H, $^4J(^1H–^{117/119}Sn)$ = 6.6 Hz, *Me*$_2$Si), 1.49 (s, 4 H, $^2J(^1H–^{117/119}Sn)$ = 98.4/102.8 Hz, SiC*H*$_2$Sn). **^{13}C{^{1}H} NMR** (75.48, $CDCl_3$): *δ* 3.0 ($^1J(^{13}C–^{29}Si)$ = 62 Hz, $^3J(^{13}C–^{117/119}Sn)$ = 19 Hz, *Me*$_2$Si), 13.6 ($^1J(^{13}C–^{117/119}Sn)$ = 200/210 Hz, $^1J(^{13}C–^{29}Si)$ = 49 Hz, Si*C*H$_2$Sn). **^{29}Si{^{1}H} NMR** (59.63, $CDCl_3$): *δ* 9.7 ($^2J(^{29}Si–^{117/119}Sn)$ = 41 Hz). **^{119}Sn{^{1}H} NMR** (111.92, $CDCl_3$): *δ* –207 (96.5%, **3**), –180 (3.5%, **3a**). **Electrospray MS**: *m/z* (%), positive mode, 885.1 (100, $[\{O(Me_2SiCH_2)_2SnO\}_3 + H]^+$), 959.1 (35, $[\{O(Me_2SiCH_2)_2SnO\}_3 + 4H_2O + H$.

Synthesis of *cyclo*-$Br_2Sn(CH_2Me_2Si)_2O$, 4

A solution of bromine (147 mg, 0.92 mmol) in dichloromethane (15 mL) was added drop-wise at 0 °C to a solution of compound **1** (200 mg, 0.46 mmol) in dichloromethane (25 mL). After 2 hours of stirring the mixture was allowed to reach room temperature and stirred overnight at ambient temperature. Then the solvent and bromobenzene were removed in vacuo. The residue was washed with small amount of cold hexane and dried in vacuo to give compound **4** (196 mg, 97%) as white solid of mp 69–70 °C.

Anal. Calcd for $C_6H_{16}Br_2OSi_2Sn$ (438.88 g/mol): C, 16.42; H, 3.67. Found: C, 16.2; H, 3.6.

^{1}H NMR (400.13, $CDCl_3$): *δ* 0.27 (s, 12 H, $^4J(^1H–^{117/119}Sn)$ = 7.3 Hz, *Me*$_2$Si), 1.18 (s, 4 H, $^2J(^1H–^{117/119}Sn)$ = 105.9/110.4 Hz, SiC*H*$_2$Sn). **^{13}C{^{1}H} NMR** (100.63, $CDCl_3$): *δ* 2.8 ($^1J(^{13}C–^{29}Si)$ = 62 Hz, $^3J(^{13}C–^{117/119}Sn)$ = 19 Hz, *Me*$_2$Si), 13.8 ($^1J(^{13}C–^{117/119}Sn)$ = 233/245 Hz, $^1J(^{13}C–^{29}Si)$ = 49 Hz, Si*C*H$_2$Sn). **^{29}Si{^{1}H} NMR** (59.63, $CDCl_3$): *δ* 9.6 ($^2J(^{29}Si–^{119}Sn)$ = 40 Hz). **^{119}Sn{^{1}H} NMR** (111.92, $CDCl_3$): *δ* 54. **Electrospray MS**: *m/z* (%), positive mode, 885.1 (100, $[\{O(Me_2SiCH_2)_2SnO\}_3 + H]^+$), 947.0 (100, $[\{O(Me_2SiCH_2)_2SnO\}_3 + MeCN + Na^+]$), 1243.0 (30, $[\{O(Me_2SiCH_2)_2SnO\}_4 + MeCN + Na^+]$).

Synthesis of *cyclo*-$Cl_2Sn(CH_2Me_2Si)_2O$, 5

To a solution of compound **1** (217 mg, 0.50 mmol) in dry dichloromethane (20 mL) was added in one portion a solution of hydrogen chloride (1.00 mL, 1.0 M in diethyl

ether) at 0 °C and the mixture was stirred for 30 min at the same temperature. Then the mixture was allowed to reach the ambient temperature and stirred overnight. The solvents and benzene were removed in vacuo and the residue was washed with small amount of cold hexane followed by drying in vacuo to give compound **5** (168 mg, 96.0%) as white solid of mp 76–77 °C.

Anal. Calcd for $C_6H_{16}Cl_2OSi_2Sn$ (349.91 g/mol): C, 20.59; H, 4.61. Found: C, 20.6; H, 4.7.

^{1}H NMR (400.13, $CDCl_3$): *δ* 0.27 (s, 12 H, $^4J(^1H–^{117/119}Sn)$ = 7.3 Hz, Me_2Si), 1.00 (s, 4 H, $^2J(^1H–^{117/119}Sn)$ = 109.4/114.4 Hz, $SiCH_2Sn$). **^{13}C{^{1}H} NMR** (100.63, $CDCl_3$): *δ* 2.8 ($^1J(^{13}C–^{29}Si)$ = 62 Hz, $^3J(^{13}C–^{117/119}Sn)$ = 19 Hz, Me_2Si), 12.6 ($^1J(^{13}C–^{117/119}Sn)$ = 260/272 Hz, $^1J(^{13}C–^{29}Si)$ = 49 Hz, $SiCH_2Sn$). **^{29}Si{^{1}H} NMR** (59.63, $CDCl_3$): *δ* 9.6 ($^2J(^{29}Si–^{119}Sn)$ = 39 Hz). **^{119}Sn{^{1}H} NMR** (111.92, $CDCl_3$): *δ* 145 (96%, **5**), 121 (4%, **5a**). **Electrospray MS**: *m/z* (%), positive mode, 903.0 (100, $[\{O(Me_2SiCH_2)_2SnO\}_3 + H_2O + H]^+$), 885.1 (80, $[\{O(Me_2SiCH_2)_2SnO\}_3 + H]^+$), 355.9 (80), 591.0 (40), 1197.0 (40), 1473.3 (40), 1733.4 (40).

Synthesis of *cyclo*-{$Me_2N(CH_2)_3$}$PhSn(CH_2Me_2Si)_2O$, 6

The Grignard reagent prepared from $Me_2N(CH_2)_3Cl$ (0.82 g, 6.74 mmol) and magnesium turnings (0.17 g, 7.10 mmol) in THF (25 mL) was added to a solution of **2** (2.60 g, 5.39 mmol) in THF (30 ml) and the mixture was stirred overnight at room temperature. THF was evaporated in vacuo and the residue was hydrolysed with cold water. The mixture was extracted three times with (50 mL) diethyl ether each. The organic phase was dried with magnesium sulphate and the solvent was evaporated in vacuo. The residue was purified by column chromatography using silica gel/CH_2Cl_2 and elution with CH_2Cl_2 followed with ethanol to give, after drying in vacuo, compound **6** (1.83 g, 59.6%) as white solid of mp 108.5–110.5 °C. Recrystallization from CH_2Cl_2/n-hexane gave colourless crystals of (**6**·HI) suitable for X-ray diffraction analysis.

^{1}H NMR (400.13, $CDCl_3$): *δ* 0.07 (s, 6H, Me_2Si), 0.16 (s, 6H, Me_2Si), 0.22 (s (broad), 4 H, $SiCH_2Sn$), 1.04 (t, 2 H, $^3J(^1H–^1H)$ = 8.28 Hz, $^2J(^1H–^{117/119}Sn)$ = 52.4 Hz, CH_2CH_2Sn), 2.04 (m, 2H, $CH_2CH_2CH_2$), 2.69 (s, 6H, Me_2N), 2.97 (t, 2H, CH_2N), 7.33–7.59 (m, 5H, Ar H). **^{13}C{^{1}H} NMR** (100.63, $CDCl_3$): *δ* –5.7 ($^1J(^{13}C–^{117/119}Sn)$ = 215/224 Hz, $SiCH_2Sn$), 3.0 (Me_2Si), 3.3 (Me_2Si), 8.8 ($^1J(^{13}C–^{117/119}Sn)$ = 361/370 Hz, CH_2CH_2Sn), 21.4 ($CH_2CH_2CH_2$), 42.8 (Me_2N), 60.7 (CH_2N), 128.4 (C_m), 128.7 (C_p),

135.8 (^2J(^{13}C–$^{117/119}$Sn) = 37 Hz, C_o), 140.2 (C_i). **^{29}Si{^{1}H} NMR** (59.63, $CDCl_3$): *δ* 9.9 (^2J(^{29}Si–^{119}Sn) = 36 Hz. **^{119}Sn{^{1}H} NMR** (111.92, $CDCl_3$): *δ* –24 (96%, **6**), –18 (4%, **6a**). **Electrospray MS**: *m/z* (%): Positive Mode: 444.2 (100, $[M + H]^+$), 366.1 (81, $[M – Ph]^+$), 412 (37).

Synthesis of *cyclo*-{$Me_2N(CH_2)_3$}ISn($CH_2Me_2Si)_2O$, 7

Iodine (0.26 g, 1.03 mmol) was added in portions at 0 °C to a solution of **6** (0.45 g, 1.02 mmol) in dichloromethane (50 mL). Then the mixture was allowed to reach room temperature and stirred overnight. Removing of the solvent and iodobenzene in vacuo gave (0.50 g, 100 %) of **7** as yellowish solid.

^{1}H NMR (300.13, $CDCl_3$): *δ* 0.21 (s, 12H, Me_2Si), 0.73 (s, 4H, ^2J(^{1}H–$^{117/119}$Sn) = 72.8/76.1 Hz, SiCH_2Sn), 1.53 (t, 2H, ^2J(^{1}H–^{1}H) = 8.0 Hz, ^2J(^{1}H–$^{117/119}$Sn) = 49.0, CH_2–CH_2–Sn), 2.23 (m, 2H, $CH_2CH_2CH_2$), 2.96 (s, 6H, Me_2N), 3.28 (t, 2H, ^3J(^{1}H–^{1}H) = 7.7 Hz, CH_2–N), 9.28 (s, 1H, NH, **7a**). **^{13}C{^{1}H} NMR** (75.48, $CDCl_3$): *δ* 3.2 (^1J(^{13}C–^{29}Si) = 62 Hz, ^3J(^{13}C–$^{117/119}$Sn) = 62 Hz, Me_2Si), 3.8 (^1J(^{13}C–$^{117/119}$Sn) = 207/215 Hz, SiCH_2Sn) , 15.2 (^1J(^{13}C–$^{117/119}$Sn) = 238/250 Hz, CH_2CH_2Sn), 22.0 ($CH_2CH_2CH_2$), 43.9 (Me_2N), 60.3 (CH_2–N). **^{29}Si{^{1}H} NMR** (59.63, $CDCl_3$): *δ* 9.4 (^1J(^{29}Si–^{119}Sn) = 43 Hz. **^{119}Sn{^{1}H} NMR** (111.92, $CDCl_3$): *δ* 61. **Electrospray MS**: *m/z* (%): Positive mode: 146 .0 (100), 493.9 (85, $[M + H]^+$), 445.9 (20), 366.0 (23, $[M – I]^+$), 406.8 (16, $[M – I + OH + Na]^+$), 402.0 (14, $[M – I + 2H_2O]^+$), negative mode, 127.0 (100, $[I]^–$), 619.8 (10, $[M + I]^–$).

Reaction of *cyclo*-$I_2Sn(CH_2Me_2Si)_2O$ with trimethylamine

To a solution of compound **3** (0.26 g, 0.49 mmol) in toluene (40 mL) triethylamine (0.34 mL, 2.44 mmol) was added in one portion and the solution was stirred for two days at room temperature. The white precipitate was filtered off and the filtrate was washed three times with 15 mL water each. The organic phase was evaporated in vacuo and the residue was washed with dichloromethane. Drying in vacuo afforded compound **8** (0.13 g, 90%) as white solid of mp 160–162 °C that is very poor soluble in $CDCl_3$ and slightly soluble in toluene and benzene.

Anal. Calcd for $(C_6H_{16}O_2Si_2Sn)_n$ (295.07)$_n$ g/mol: C, 24.42; H, 5.47. Found: C, 24.3; H, 5.3.

Electrospray MS: *m/z* (%): Positive mode (in the range 0 – 2000 *m/z*): 338.0 (26, $[M + MeCN + H]^+$), 380.0 (100), 633.0 (72, $[2M + MeCN + H]^+$), 885.0 (27, $[3M + H]^+$),

947.0 (50, [3M + MeCN + Na]$^+$), 1181.2 (7, [4M + H]$^+$), 1221.1 (8, [4M + MeCN + H]$^+$), 1555.2 (12, [5M + H_2O + MeCN + Na]$^+$), 1868.5 (16, [6M + 2 H_2O + MeCN + Na]$^+$); (M = $O(Me_2SiCH_2)_2SnO$).

Synthesis of Me(*i*-PrO)$_2$SiCH$_2$Cl, 9

The ompound was synthesized was synthesized by modified procedure of that described in the literature.[53]

i-Propanol (30.0 mL, 0,39 mol) was added drop-wise at –30 °C to a solution of dichloro(chloromethyl)methylsilane, $Cl_2MeSiCH_2Cl$, (25.7 g, 0.157 mol) in hexane (150 mL). The mixture was stirred for about 30 min at the same temperature, before it was heated at reflux for about 3 hours. Then *i*-propanol (20 ml, 0.26 mol) was added and the mixture was heated at reflux for one additional hour. The mixture was stirred overnight at room temperature and the excess of *i*-propanol was removed in vacuo giving compound **9** (32.46 g, 98 %) as colorless liquid.

^{1}H NMR (300.13, $CDCl_3$): *δ* 0.25 (s, 3H; CH_3Si), 1.19 (d, 12H, Me_2CH), 2.73 (s, 2H; CH_2Cl), 4.18 (s, 2H, CHO). **^{13}C{^{1}H} NMR** (75.48, $CDCl_3$): *δ* –5.4 ($^1J(^{13}C–^{29}Si)$ = 77.8 Hz, MeSi), 25.5 (Me_2CH), 27.7 ($^1J(^{13}C–^{29}Si)$ = 79.9, $SiCH_2Cl$), 65.6 (CHO). **^{29}Si{^{1}H} NMR** (59.63, $CDCl_3$): *δ* –18.4 ($^1J(^{29}Si–^{13}C)$ = 79 Hz).

Synthesis of {Me(*i*-PrO)$_2$SiCH$_2$}$_2$SnPh$_2$, 10

A solution of diphenyltin dichloride (5.00 g, 14.5 mmole) in THF (50 mL) was added drop-wise to the Grignard reagent prepared from Me(*i*-PrO)$_2$SiCH$_2$Cl (7.20 g, 34.1 mmol) and magnesium turnings (0.85 g, 35 mmole) in THF (25 mL). Then the mixture was stirred overnight at room temperature and the solvent was evaporated in vacuo. The residue was extracted three times with hexane under inert conditions, before hexane was removed in vacuo to give compound **10** (8.22 g, 91%) as colourless liquid.

^{1}H NMR (400.13, C_6D_6): *δ* 0.12 (s, 6H, MeSi), 0.47 (s, 4H, $^2J(^1H–^{117/119}Sn)$ = 74.3/77.6 Hz, $SiCH_2Sn$), 1.09, 1.14 (d, 24H, $^3J(^1H–^1H)$ = 6.3 Hz, Me_2CH), 4.06 (m, 4H, CHO, $^3J(^1H–^1H)$ = 6.0 Hz), 7.19–7.83 (m, 10H, Ar H). **^{13}C{^{1}H} NMR** (100.63, C_6D_6): *δ* –4.8 ($^1J(^{13}C–^{117/119}Sn)$ = 249/260 Hz, $^1J(^{13}C–^{29}Si)$ = 74 Hz, $SiCH_2Sn$), 0.5 ($^1J(^{13}C–^{29}Si)$ = 73 Hz, Me_2Si), 26.4 (d, Me_2CH), 65.2 (CHO), 128.6 (C_m), 129.0 (C_p), 137.7 ($^2J(^{13}C–^{117/119}Sn)$ = 37.9, C_o), 142.4 ($^1J(^{13}C–^{117/119}Sn)$ = 480/503 Hz, Ar–C_i).

^{29}Si{^{1}H} NMR (59.63, C_6D_6): δ –8.0 ($^{1}J(^{29}Si–^{13}C)$ = 73, $^{2}J(^{29}Si–^{117/119}Sn)$ = 21 Hz. **^{119}Sn{^{1}H} NMR** (111.92, $CDCl_3$): δ –55.

Synthesis of [{$Ph_2Sn(CH_2MeSi)_2O$}O]$_2$, 12

A solution of **12** (1.00 g, 1.6 mmol) in dichloromethane (20 mL) was stirred with a solution of sodium hydroxide (0.50 g, 12.5 mmol) in water (5 mL) and ethanol (40 mL) for two days at room temperature in aerobic conditions. The organic solvents were evaporated and the residue was extracted with CH_2Cl_2. The organic phase was dried with magnesium sulfate. Then dichloromethane was evaporated in vacuo to give (0.67 g) of the oligomeric compound **11** as highly viscous oil which solidified at the next day. The latter was dissolved in THF (25 mL) and treated with a solution of sodium methanolate (3.5 mg) in methanol (1 mL). The mixture was heated at reflux for 3 hours and kept overnight at room temperature without stirring. At the next day white precipitate was observed. This was washed with water and dried in vacuo to give compound **12** (0.58 g, 86%) as white solid. Recrystallization from methanol afforded colorless crystals of mp 161–164 °C suitable for X-ray diffraction analysis.

Anal. Calcd for $C_{32}H_{40}O_4Si_4Sn_2$ (838.42 g/mol): C, 45.84; H, 4.81. Found: C, 45.8; H, 4.6.

^{1}H NMR (300.13, $CDCl_3$): δ 0.14 (s, 12H, *Me*Si), 0.40 (AB system, 8H, $^{2}J(^{1}H–^{117/119}Sn)$ = 67.3/70.3 Hz, Si*C*H_2Sn), 7.39–7.66 (m, 20H, Ar H). **^{13}C{^{1}H} NMR** (75.48, $CDCl_3$): δ –5.8 ($^{1}J(^{13}C–^{117/119}Sn)$ = 228/239 Hz, $^{1}J(^{13}C–^{29}Si)$ = 68 Hz, Si*C*H_2Sn), 1.4 ($^{1}J(^{13}C–^{29}Si)$ = 58 Hz, $^{3}J(^{13}C–^{117/119}Sn)$ = 14 Hz, *Me*Si), 128.2, 128.4 (C_m), 128.7 (C_p), 136.0, 136.4 ($^{2}J(^{13}C–^{117/119}Sn)$ = 39 Hz, C_o), 140.1, 140.7 ($^{1}J(^{13}C–^{117/119}Sn)$ = 503 Hz, C_i). **^{29}Si{^{1}H} NMR** (59.63, $CDCl_3$): δ –16.6 ($^{1}J(^{29}Si–^{13}C)$ = 36 Hz). **^{119}Sn{^{1}H} NMR** (111.92, $CDCl_3$): δ 54. **Electrospray MS**: *m/z* (%): Positive mode: 152 (100), 761.0 (8, $[M - Ph]^-$).

Synthesis of [{$I_2Sn(CH_2SiMe)_2O$}O]$_2$, 13

Iodine (92 mg, 0.36 mmol) was added in portions at 0 °C to a solution of compound **12** (76 mg, 0.09 mmol) in chloroform (25 mL). After the complete addition the mixture was allowed to reach room temperature and stirred overnight. Then the solvent and iodobenzene were removed in vacuo. The residue was washed with hexane and a small amount of cold chloroform followed by drying in vacuo to give compound **13** (66 mg, 70%) as light yellowish solid.

The NMR sample was not completely soluble in $CDCl_3$. **$^{13}C\{^1H\}$ NMR** (75.48, $CDCl_3$): *δ* 1.5 (*Me*$_2$Si), 1.6 (*Me*$_2$Si), 12.0 (Si*C*H$_2$Sn). **$^{29}Si\{^1H\}$ NMR** (59.63, $CDCl_3$): *δ* –20.47 ($^2J(^{29}Si–^{117/119}Sn)$ = 40 Hz), –18 (6%), –17 (10%). **$^{119}Sn\{^1H\}$ NMR** (111.91, $CDCl_3$): *δ* –228 (50%, **13**), –226 (16%), –221 (5%), –220 (10%), –42 (7%), –30 (12%). **Electrospray MS**: *m/z* (%), positive mode, 880.8 (100, $[M – 2I + OH]^+$), 750.8 (35), negative mode, 380.8 (100, $[I_3]^–$), 127.1 (44, $[I]^–$), 1164.4 (22, $[M + I]^–$), 1114.6 (15).

Synthesis of [{Br$_2$Sn(CH$_2$SiMe)$_2$O}O]$_2$, 14

A solution of bromine (51 mg, 0.32 mmol) in dichloromethane (5 mL) was added drop-wise at 0 °C to a solution of compound **12** (67 mg, 0.08 mmol) in dichloromethane (20 mL). After 2 hours of stirring the mixture was allowed to reach room temperature and stirred overnight at ambient temperature. The solvent and bromobenzene were removed in vacuo. The residue was washed with hexane and a small amount of cold dichloromethane. Drying in vacuo afforded compound **14** (60 mg, 88%) as white solid of mp 256–258 °C.

Anal. Cacd for $C_8H_{20}Br_4O_4Si_4Sn_2$ (849.58 g/mol): C, 11.31; H, 2.37. Found: C, 11.5; H, 2.5.

The NMR sample was not completely soluble in $CDCl_3$. **^1H NMR** (300.13, $CDCl_3$): *δ* 0.34 (s, 12 H, $^4J(^1H–^{117/119}Sn)$ = 9.5 Hz, *Me*$_2$Si), 1.17 (AB pattern, 8H, J_{AB} 14.0 Hz, $^2J(^1H–^{117/119}Sn)$ 105.0/109.8 Hz, SiC*H*$_2$Sn). **$^{13}C\{^1H\}$ NMR** (100.63, $CDCl_3$): *δ* 1.2 (*Me*$_2$Si), 12.1 ($^1J(^{13}C–^{117/119}Sn)$ = 247/259 Hz, Si*CH*$_2$Sn). **$^{29}Si\{^1H\}$ NMR** (59.63, $CDCl_3$): *δ* –20.9 ($^2J(^{29}Si–^{117/119}Sn)$ = 40 Hz, **14**), –19.7, –17.2. **$^{119}Sn\{^1H\}$ NMR** (111.92, $CDCl_3$): *δ* 44 (87%, **14**), 40 (7%), 26 (6%). **Electrospray MS**: *m/z* (%), positive mode, 270.7 (100), 558.3 (22, $[M – 4 Br + 3 OH]^–$), 664.9 (22, $[M – 4 Br + 3 OH + 2 MeCN]^+$), 1300.9 (4, $2 M – 8 Br + 7 OH + 3 MeCN]^+$).

Synthesis of [{Cl$_2$Sn(CH$_2$SiMe)$_2$O}O]$_2$, 15

To a solution of compound **12** (85 mg, 0.10 mmol) in dry dichloromethane (20 mL) was added in one portion a solution of hydrogen chloride (0.50 mL, 1.0 M in diethyl ether) at 0 °C and the mixture was stirred for 30 min at the same temperature. The mixture was stirred overnight at ambient temperature. Then the solvents were removed in vacuo and the residue was washed with hexane and small amount of cold dichloromethane. Drying in vacuo gave compound **15** (55 mg, 81%) as white solid.

Recrystallization from CH_2Cl_2 afforded single crystals of **15** of mp 247–250 °C suitable for X-ray diffraction analysis.

Anal. Calcd for $C_8H_{20}Cl_4O_4Si_4Sn_2$ (671.78 g/mol): C, 14.30; H, 3.00. Found: C, 14.3; H, 2.9.

The NMR sample was not completely soluble in $CDCl_3$. **^{1}H NMR** (300.13, $CDCl_3$): δ 0.35 (s, 12H, *Me*Si), 1.00 (AB pattern, 8H, J_{AB} 14.0 Hz, $^2J(^1H–^{117/119}Sn)$ 107.4/112.4 Hz, SiC*H*$_2$Sn). **^{13}C{^{1}H} NMR** (100.63, $CDCl_3$): δ 1.1 (*Me*$_2$Si), 11.1 ($^1J(^{13}C–^{117/119}Sn)$ = 274/288 Hz, Si*C*H$_2$Sn). **^{29}Si{^{1}H} NMR** (59.63, $CDCl_3$): δ –21.0 ($^1J(^{29}Si–^{13}C)$ = 39 Hz), –20 (13%), –17 (13%). **^{119}Sn{^{1}H} NMR** (111.92, $CDCl_3$): δ 139(57%), 142 (11%), 133 (8%), 110 (8%), 46 (15%). **Electrospray MS**: *m/z* (%), negative mode, 170.9 (100), 384.8 (68, $[Cl_3Sn\{CH_2Me(OH)Si\}_2O + MeOH]^-$), 706.7 (55, [**15** + Cl]$^-$).

Synthesis of Me(*i*-PrO)$_2$SiCH$_2$SnPh$_3$, 16

A solution of triphenyltin chloride (7.10 g, 17.5 mmole) in THF (50 mL) was added drop-wise to the Grignard reagent prepared from Me(*i*-PrO)$_2$SiCH$_2$Cl (4.10 g, 19.4 mmol) and magnesium turnings (0.52 g, 21.4 mmole) in THF (20 mL). Then the mixture was stirred overnight at room temperature and the solvent was evaporated in vacuo. Hexane was added and the mixture was stirred for 30 min before it was filtered off under inert conditions. The hexane was evaporated in reduced pressure to give compound **16** (8.65 g, 94%) as colourless liquid.

^{1}H NMR (300.13, $CDCl_3$): δ 0.00 (s, 3H; *Me*$_2$Si), 0.49 (s, 2H, $^2J(^1H–^{117/119}Sn)$ = 74.6/78.3 Hz, SiC*H*$_2$Sn), 1.04 (d, 6H, $^3J(^1H–^1H)$ = 5.9 Hz, *Me*$_2$CH), 1.10 (d, 6H, $^3J(^1H–^1H)$ = 5.9 Hz, *Me*$_2$CH), 4.07 (m, 2H, *CH*O, $^3J(^1H–^1H)$ = 6.0 Hz), 7.33–7.63 (m, 15H, Ar H). **^{13}C{^{1}H} NMR** (75.48, $CDCl_3$): δ –6.6 ($^1J(^{13}C–^{117/119}Sn)$ = 256/270 Hz, Si*C*H$_2$Sn), –1.3 (*Me*$_2$Si), 25.5 (*Me*$_2$CH), 25.6 (*Me*$_2$CH), 64.8 (*C*HO), 128.2 ($^3J(^{13}C–^{117/119}Sn)$ = 50 Hz, C$_m$), 128.6 (C$_p$), 137.0 ($^2J(^{13}C–^{117/119}Sn)$ = 38 Hz, C$_o$), 139.7 ($^1J(^{13}C–^{117/119}Sn)$ = 494/517 Hz, C$_i$). **^{29}Si{^{1}H} NMR** (59.63, $CDCl_3$): δ –8.1 $^2J(^{29}Si–^{117/119}Sn)$ = 20 Hz. **^{119}Sn{^{1}H} NMR** (111.92, $CDCl_3$): δ –92.

Synthesis of Me(*i*-PrO)$_2$SiCH$_2$SnBr$_3$, 17

A solution of bromine (1.37 g, 8.57 mmol) in dichloromethane (30 mL) was added drop-wise at 0 °C to a solution of compound **17** (1.50 g, 2.86 mmol) in dichloromethane (15 mL). After 2 hours of stirring the mixture was allowed to reach room temperature and stirred overnight at ambient temperature. The solvent and

bromobenzene were removed in vacuo to give compound **19** (1.43 g, 94%) as light yellowish oil.

^{1}H NMR (300.13, $CDCl_3$): δ 0.34 (s, 3H, *Me*$_2$Si), 1.24 (d, 6H, $^{3}J(^{1}H–^{1}H)$ = 6.2 Hz, *Me*$_2$CH), 1.25 (d, 6H, $^{3}J(^{1}H–^{1}H)$ = 6.2 Hz, *Me*$_2$CH), 1.67 (s, 2H, $^{2}J(^{1}H–^{117/119}Sn)$ = 128.8/135.0 Hz, SiC*H*$_2$Sn), 4.24 (m, 3H, *CH*O, $^{3}J(^{1}H–^{1}H)$ = 6.0 Hz). **^{13}C{^{1}H} NMR** (75.48, $CDCl_3$): δ –1.5 ($^{3}J(^{13}C–^{117/119}Sn)$ = 24 Hz, $^{1}J(^{13}C–^{29}Si)$ = 77 Hz, *Me*$_2$Si), 19.3 ($^{1}J(^{13}C–^{117/119}Sn)$ = 390/408 Hz, $^{1}J(^{13}C–^{29}Si)$ = 69 Hz, Si*C*H$_2$Sn), 25.4 (*Me*$_2$CH), 25.5 (*Me*$_2$CH), 66.6 (*C*HO). **^{29}Si{^{1}H} NMR** (59.63, $CDCl_3$): δ –15.2 ($^{2}J(^{29}Si–^{117/119}Sn)$ = 70 Hz, **17**), 20.7. **^{119}Sn{^{1}H} NMR** (111.91, $CDCl_3$): δ –216 (94%, **17**), –209 (6%).

Slow evaporation of a solution of compound **17** in $CDCl_3$ in the NMR-tube afforded single crystals of the cyclic tetrasiloxane ring $\{Br_3SnCH_2MeSiO\}_4$, **18**, of mp 210–212 °C suitable for the X-ray diffraction analysis.

^{29}Si{^{1}H} NMR (59.63, $CDCl_3$): δ –22.0, –22.4, –22.5, –22.6, –22.7. **^{119}Sn{^{1}H} NMR** (111.92, $CDCl_3$): δ —–195.3, –195.4, –195.6, –195.9, –196.9. **Electrospray MS**: *m/z* (%), negative mode, 304.6 (100, [**D** – 2 Br + OH + O]$^-$), 375.0 (75), 1517.7 (15, [**D**$_4$ – 3Br + 2O]$^-$), 1660 (15, [**D**$_4$ – Br + O]$^-$), 528.7 (15, [**D**$_2$ – 6Br + 2OH + 2O]$^-$), 1375.9 (7, [**D**$_3$ + Br]$^-$), 1803.2 (2, [**D**$_4$ + Br]$^-$); [**D** = $(Br_3SnCH_2)MeSiO$].

Synthesis of (*i*-PrO)$_3$SiCH$_2$SnPh$_3$, 19

A solution of triphenyltin chloride (12.00 g, 31.0 mmole) in THF (75 mL) was added drop-wise to the Grignard reagent prepared from (*i-P*rO)$_3$SiCH$_2$Cl (8.80 g, 34.5 mmol) and magnesium turnings (0.93 g, 38.0 mmole) in THF (25 mL). Then the mixture was stirred overnight at room temperature and the solvent was evaporated in vacuo. Hexane was added and the mixture was stirred for 30 min before it was filtered off under inert conditions. The solvent was evaporated under reduced pressure to give compound **19** (15.10 g, 96%) as colourless liquid.

^{1}H NMR (300.13, $CDCl_3$): δ 0.45 (s, 2H, $^{2}J(^{1}H–^{117/119}Sn)$ = 74.6/77.9 Hz, Si*CH*$_2$Sn), 1.09 (d, 18H, $^{3}J(^{1}H–^{1}H)$ = 6.2 Hz, *Me*$_2$CH), 4.16 (m, 3H, *CH*–O, $^{3}J(^{1}H–^{1}H)$ = 6.0 Hz), 7.36–7.67 (m, 15H, Ar H). **^{13}C{^{1}H} NMR** (75.47, $CDCl_3$): δ –10.30 (*Me*$_2$Si), 25.4 (*Me*$_2$CH), 65.0 (*CH*O), 128.1 ($^{3}J(^{13}C–^{117/119}Sn)$ = 49; C$_m$), 128.6 ($^{4}J(^{13}C–^{117/119}Sn)$ = 12; C$_p$), 137.1 ($^{2}J(^{13}C–^{117/119}Sn)$ = 39; C$_o$), 139.9 ($^{1}J(^{13}C–^{117/119}Sn)$ = 498/521 Hz, C$_i$). **^{29}Si{^{1}H} NMR** (59.63, $CDCl_3$): δ –47.2 $^{2}J(^{29}Si–^{117/119}Sn)$ = 25 Hz. **^{119}Sn{^{1}H} NMR** (111.92, $CDCl_3$): δ –93.

Synthesis of the polyhedral oligosilsesquioxane (POSS) $(Ph_3SnCH_2SiO_{1.5})_8$, 20

A mixture of compound **19** (1.30 g, 2.28 mmol) and $KOH_{aq.}$ (1mL, 1M) in diglyme (30 mL) was stirred at room temperature at least for two hours. Then the mixture was placed at the center of the microwave oven and irradiated at 100W for 6 min (the temperature rose to 135°C). Hexane (50 mL) was added and the mixture was filtered off. The filtrate was kept to evaporate slowly in aerobic conditions affording after a few days white precipitate. This was separated and dried in vacuo to give compound **20** (0.32 g, 34%) as white solid of mp 385 °C (dec.).

Anal. Cacd for $C_{152}H_{136}O_{12}Si_8Sn_8$ (3329.11 g/mol): C, 54.84; H, 4.12. Found: C, 53.5; H, 4.9.

^{29}Si{^{1}H} NMR (59.63, $CDCl_3$): δ –66.05 (50%), 66.15 (25%), 66.21 (25%). **^{119}Sn{^{1}H} NMR** (111.92, $CDCl_3$): δ –91 [J(^{119}Sn–^{29}Si) = 72 Hz].

Synthesis of the polyhedral oligosilsesquioxane $(Br_2PhSnCH_2SiO_{1.5})_8$, 21

A solution of bromine (153 mg, 960 µmol) in dichloromethane (10 mL) was added drop-wise at 0 °C to a solution of compound **20** (200 mg, 60 µmol) in dichloromethane (15 mL). After 2 hours of stirring the mixture was allowed to reach room temperature and stirred overnight at ambient temperature. Then the solvent and bromobenzene were removed in vacuo to give quantitatively compound **23** as yellowish viscous oil.

^{29}Si{^{1}H} NMR (59.63, $CDCl_3$): δ –69.6 (^2J(^{29}Si–$^{117/119}$Sn) = 20 Hz), 69.3, 72.3. **^{119}Sn{^{1}H} NMR** (111.92, $CDCl_3$): δ –22.2 (76%), 22.6 (13%), 23.2 (11 %).

Synthesis of $[O(Me_2SiCH_2)_2(OAc)SnO(OAc)(CH_2Me_2Si)_2O]_2$, 23

A suspension of **3** (200 mg, 0.375 mmol) and silver acetate (125 mg, 0.750 mmol) in CH_2Cl_2 (25 mL) and acetonitrile (25mL) was stirred overnight at room temperature. The mixture was filtered off and the filtrate was evaporated in vacuo giving compound **23** (28 mg, 22%) as poorly soluble colorless crystalline solid of mp 164–167 °C.

Anal. Calcd for $C_{32}H_{76}O_{14}Si_8Sn_4$ (1384.41 g/mol): C, 27.76; H, 5.53. Found: C, 28.1; H, 5.7.

Synthesis of $[O(Me_2SiCH_2)_2](I)SnOSn(OH)[(CH_2Me_2Si)_2O]_2$, 24a

A mixture of **3** (250 mg, 0.47 mmol) and *t*-Bu_2SnO (117 mg, 0.47 mmol) was heated at reflux in toluene (25 mL) until the solution became clear. Then the solvent was

evaporated in vacuo to give yellowish oily residue. Recrystallization of the residue from CH_2Cl_2/hexane in air gave (127 mg, 75%) of **24a** as colorless crystals of mp 211–213 °C suitable for X-ray diffraction analysis.

Anal. Cacd for $C_{24}H_{66}I_2O_8Si_8Sn_4$ (1436.11 g/mol): C, 20.07; H, 4.63. Found: C, 20.3; H, 5.2.

$^{13}C\{^1H\}$ NMR (75.48, $CDCl_3$): δ 3.6, 3.7, 3.8, 4.0 Me_2Si), 13.0 ($SiCH_2Sn$), 20.3 ($^1J(^{13}C–^{117/119}Sn)$ = 405/419 Hz, $SiCH_2Sn$). **$^{29}Si\{^1H\}$ NMR** (59.63, $CDCl_3$): δ 8.3 ($^2J(^{29}Si–^{119}Sn)$ = 51 Hz), 9.0 ($^2J(^{29}Si–^{119}Sn)$ = 45 Hz). **$^{119}Sn\{^1H\}$ NMR** (111.92, $CDCl_3$): δ –139 ($^2J(^{119}Sn–^{117/119}Sn)$ = 273 Hz), –236 ($^2J(^{119}Sn–^{117/119}Sn)$ = 271 Hz). **Electrospray MS**: *m/z* (%), positive mode, 887.0 (100, $[\{O(Me_2SiCH_2)_2SnO\}_3 + H]^+$), 619.0 (20), 1205.0 (6), 1179.1 (3, $[\{O(Me_2SiCH_2)_2SnO\}_4 + H]^+$).

Reaction of *cyclo*-$Cl_2Sn(CH_2Me_2Si)_2O$, 5, with di-*tert*-Butyltin oxide

A mixture of **5** (60 mg, 0.17 mmol) and *t*-Bu_2SnO (43 mg, 0.17 mmol) was stirred in CH_2Cl_2 (25 mL) overnight. The precipitate was separated and washed with hexane and CH_2Cl_2. Drying in vacuo afforded compound **25** (0.99 mg, 96%) as white solid of mp 246.5–247.5 °C. Recrystallization of **25** from a solution in CH_2Cl_2/toluene in moist air afforded single crystals suitable for X-ray diffraction analysis.

Anal. Cacd for $C_{28}H_{68}Cl_4O_4Si_4Sn_4$ (1197.83 g/mol): C, 28.08.07; H, 5.72. Found: C, 27.8; H, 5.3.

Electrospray MS: *m/z* (%), positive mode, 887.0 (100, $[\{O(Me_2SiCH_2)_2SnO\}_3 + H]^+$), 839.1 (84, $[(t\text{-}Bu_2SnO)_3 + 3H_2O + K]^+$), negative mode, 384.8 (100, $[O(Me_2SiCH_2)_2Sn(OH)_2Cl + 2H_2O]^-$), 339.0 (15, $[t\text{-}Bu_2Sn(OH)_2Cl + 2H_2O]^-$).

2.5 References

1. (a) Pouget, E.; Tonnar, J.; Lucas, P.; Lacroix-Desmazes, P.; Ganachaud, F.; Boutevin, B., *Chem. Rev.* **2009**, *110*, 1233; (b) Abe, Y.; Gunji, T., *Prog. Polym. Sci.* **2004**, *29*, 149; (c) Chojnowski, J., *J. Inorg. Organomet. Polym.* **1991**, *1*, 299; (d) Manners, I., *Angew. Chem. Int. Ed. Engl.* **1996**, *35*, 1602; (e) Rehahn, M., *Acta Polym.* **1998**, *49*, 201; (f) Moretto, H.-H.; Schulze, M.; Wagner, G., Silicones. In *Ullmann's Encyclopedia of Industrial Chemistry*, Wiley 2000.
2. *European Silicones Centre ; http://www.silicones.eu/*.
3. (a) Compañ, V.; Andrio, A.; López-Alemany, A.; Riande, E.; Refojo, M. F., *Biomaterials* **2002**, *23*, 2767; (b) Čermák, J.; Sasíh, M.; Kolář, D.; Dobeš, P., *J. Synth. Lub.* **1984**, *1*, 127; (c) Interrante, L. V.; Rathore, J. S., *Dalton Trans.* **2010**, *39*, 9193; (d) Astapov, B. A., *Polym. Sci. Ser. D* **2013**, *6*, 69.
4. (a) Cordes, D. B.; Lickiss, P. D.; Rataboul, F., *Chem. Rev.* **2010**, *110*, 2081; (b) Mehdi, A.; Reye, C.; Corriu, R., *Chem. Soc. Rev.* **2011**, *40*, 563; (c) Tateyama, S.; Kakihana, Y.; Kawakami, Y., *J. Organomet. Chem.* **2010**, *695*, 898; (d) Harrison, P. G., *J. Organomet. Chem.* **1997**, *542*, 141; (e) Lorenz, V.; Edelmann, F. T., *Z. Anorg. Allg. Chem.* **2004**, *630*, 1147; (f) Ayandele, E.; Sarkar, B.; Alexandridis, P., *Nanomaterials* **2012**, *2*, 445.
5. (a) Riollet, V.; Quadrelli, E. A.; Copéret, C.; Basset, J.-M.; Andersen, R. A.; Köhler, K.; Böttcher, R.-M.; Herdtweck, E., *Chem. Eur. J.* **2005**, *11*, 7358; (b) Zhang, Y.; Ye, Z., *Chem. Commun.* **2008**, 1178; (c) Zamora, M.; Bruña, S.; Alonso, B.; Cuadrado, I., *Macromol.* **2011**, *44*, 7994; (d) Marciniec, B.; Kownacki, I.; Franczyk, A.; Kubicki, M., *Dalton Trans.* **2011**, *40*, 5073; (e) J. Feher, F.; D. Wyndham, K., *Chem. Commun.* **1998**, 323; (f) Loy, D. A.; Jamison, G. M.; Baugher, B. M.; Myers, S. A.; Assink, R. A.; Shea, K. J., *Chem. Mater.* **1996**, *8*, 656.
6. (a) Ropartz, L.; Morris, R. E.; Foster, D. F.; Cole-Hamilton, D. J., *Chem. Commun.* **2001**, 361; (b) Ropartz, L. c.; Morris, R. E.; Schwarz, G. P.; Foster, D. F.; Cole-Hamilton, D. J., *Inorg. Chem. Commun.* **2000**, *3*, 714.
7. (a) Miao, J.; Zhu, L., *J. Phys. Chem. B* **2010**, *114*, 1879; (b) Díaz, U.; García, T.; Velty, A.; Corma, A., *Chem. Eur. J.* **2012**, *18*, 8659; (c) Ghosh, N. N.; Clark, J. C.; Eldridge, G. T.; Barnes, C. E., *Chem. Commun.* **2004**, 856; (d) Clark, J.

C.; Saengkerdsub, S.; Eldridge, G. T.; Campana, C.; Barnes, C. E., *J. Organomet. Chem.* **2006**, *691*, 3213.

8. (a) Hong, B.; Thoms, T. P. S.; Murfee, H. J.; Lebrun, M. J., *Inorg. Chem.* **1997**, *36*, 6146; (b) Chen, D.; Yi, S.; Wu, W.; Zhong, Y.; Liao, J.; Huang, C.; Shi, W., *Polymer* **2010**, *51*, 3867.
9. Mine, T.; Komazaki, S. Compositions for ceramic moldings. 1985.
10. (a) Päch, M.; Stösser, R., *J. Phys. Chem. A* **1997**, *101*, 8360; (b) Hayashino, Y.; Isobe, T.; Matsuda, Y., *ChemPhysChem* **2001**, *2*, 748.
11. (a) Saez, I. M.; Goodby, J. W., *Liq. Cryst.* **1999**, *26*, 1101; (b) Elsa; Mehl, G. H.; Goodby, J. W.; Photinos, D. J., *Chem. Commun.* **2000**, 851.
12. Abad, D. R.; Henig, J.; Mayer, H. A.; Reißig, T.; Speiser, B., *Organometallics* **2014**, *33*, 4777.
13. Prasad, P. N. In *Sol-gel processed inorganic and organically modified composites for nonlinear optics and photonics*, **1990**; pp 168.
14. Ak, M.; Gacal, B.; Kiskan, B.; Yagci, Y.; Toppare, L., *Polymer* **2008**, *49*, 2202.
15. de Jesus, C. G.; dos Santos, V.; Canestraro, C. D.; Zucolotto, V.; Fujiwara, S. T.; Gushikem, Y.; Wohnrath, K.; Pessoa, C. A., *J. Nanosci. Nanotechnol.* **2011**, *11*, 3499.
16. Chan, K. L.; Sonar, P.; Sellinger, A., *J. Mater. Chem.* **2009**, *19*, 9103.
17. (a) Beckmann, J.; Jurkschat, K., *Coord. Chem. Rev.* **2001**, *215*, 267; (b) King, L.; Sullivan, A. C., *Coord. Chem. Rev.* **1999**, *189*, 19; (c) Murugavel, R.; Voigt, A.; Walawalkar, M. G.; Roesky, H. W., *Chem. Rev.* **1996**, *96*, 2205; (d) Kung, M. C.; Riofski, M. V.; Missaghi, M. N.; Kung, H. H., *Chem. Commun.* **2014**, *50*, 3262; (e) MMLevitsky; Zavin, B. G.; Bilyachenko, A. N., *Russ. Chem. Rev.* **2007**, *76*, 847 ; (f) Murugavel, R.; Bhattacharjee, M.; Roesky, H. W., *Appl. Organomet. Chem.* **1999**, *13*, 227; (g) Fandos, R.; Gallego, B.; Otero, A.; Rodriguez, A.; Ruiz, M. J.; Terreros, P., *Dalton Trans.* **2007**, 871.
18. (a) Murugavel, R.; Roesky, H. W., *Angew. Chem. Int. Ed. Engl.* **1997**, *36*, 477; (b) Conley, M. P.; Delley, M. F.; Siddiqi, G.; Lapadula, G.; Norsic, S.; Monteil, V.; Safonova, O. V.; Copéret, C., *Angew. Chem. Int. Ed. Engl.* **2014**, *53*, 1872.
19. Morosin, B.; Harrah, L. A., *Acta Crystallogr., Sect. B* **1981**, *37*, 579.
20. Beckmann, J.; Jurkschat, K.; Kaltenbrunner, U.; Pieper, N.; Schürmann, M., *Organometallics* **1999**, *18*, 1586.

21. (a) Beckmann, J.; Jurkschat, K.; Schollmeyer, D.; Schürmann, M., *J. Organomet. Chem.* **1997**, *543*, 229; (b) Beckmann, J.; Mahieu, B.; Nigge, W.; Schollmeyer, D.; Schürmann, M.; Jurkschat, K., *Organometallics* **1998**, *17*, 5697.
22. Feher, F. J.; Newman, D. A.; Walzer, J. F., *J. Am. Chem. Soc.* **1989**, *111*, 1741.
23. Feher, F. J.; Weller, K. J., *Organometallics* **1990**, *9*, 2638.
24. (a) Beckmann, J.; Jurkschat, K.; Pieper, N.; Schurmann, M., *Chem. Commun.* **1999**, 1095; (b) Fridrichova, A.; Mairychova, B.; Padelkova, Z.; Lycka, A.; Jurkschat, K.; Jambor, R.; Dostal, L., *Dalton Trans.* **2013**.
25. Feher, F. J.; Weller, K. J., *Chem. Mater.* **1994**, *6*, 7.
26. (a) Mironov, V.; Shiryaev, V.; Stepina, E'.; Makhalkina, L.; Lapina, A.; Bochkarev, V.; Nehaeva, A., *Russ. J. Gen. Chem. Engl. trans.* **1976**, *42*, 1043; (b) Merker, R. L.; Scott, M. J., *J. Am. Chem. Soc.* **1959**, *81*, 975.
27. (a) Schulte, M.; Schürmann, M.; Jurkschat, K., *Chem. Eur. J.* **2001**, *7*, 347; (b) Schulte, M.; Gabriele, G.; Schürmann, M.; Jurkschat, K.; Duthie, A.; Dakternieks, D., *Organometallics* **2003**, *22*, 328.
28. Severn, J. R.; Duchateau, R.; van Santen, R. A.; Ellis, D. D.; Spek, A. L.; Yap, G. P. A., *Dalton Trans.* **2003**, 2293.
29. Andrianov, K. A.; Golubenko, A., *J. Gen. Chem. USSR Engl. Transl.* **1975**, *45*.
30. Kong, X.; Grindley, T. B.; Bakshi, P. K.; Cameron, T. S., *Organometallics* **1993**, *12*, 4881.
31. Beckmann, J.; Henn, M.; Jurkschat, K.; Schürmann, M.; Dakternieks, D.; Duthie, A., *Organometallics* **2001**, *21*, 192.
32. Baba Haj, S.; Schürmann, M.; Iovkova-Berends, L.; Herres-Pawlis, S.; Jurkschat, K., *Organometallics* **2012**, *31*, 4716.
33. Nelson, D. J.; Brammer, C. N., *J. Chem. Educ.* **2011**, *88*, 292.
34. Gurkova, S. N.; Tandura, S. N.; Gusev, A. I.; Alekseev, N. V.; Chernyshev, A. E.; Stepina, E. M.; Koveleva, E. A.; Grachevand, A. A.; Shiryaev, V. I., *Organomet. Chem. USSR* **1988**, *1*, 464.
35. Al-Rubaie, A. Z.; Uemura, S.; Masuda, H., *J. Organomet. Chem.* **1991**, *410*, 309.
36. Bondi, A., *J. Phys. Chem.* **1964**, *68*, 441.

37. (a) Lee, M. K.; Meier, D. J., *Polymer* **1993**, *34*, 4882; (b) Sieburth, S. M.; Mu, W., *J. Org. Chem.* **1993**, *58*, 7584; (c) Ibemesi, J.; Gvozdic, N.; Keumin, M.; Lynch, M. J.; Meier, D. J., *Polym. Prepr.* **1985**, *26*, 18; (d) Fielden, M.; Britcher, L. G.; Clarke, S. R.; Embery, C. J.; Matisons, J. G., *Polym. Prepr.* **2001**, *42*, 165; (e) Bostick, E. E., *Polym. Prepr.* **1969**, *10*, 877; (f) Harkness, B. R.; Tachikawa, M.; Mita, I., *Macromolecules* **1995**, *28*, 1323; (g) Kostjuk, S. V.; Ortega, E.; Ganachaud, F.; Améduri, B.; Boutevin, B., *Macromolecules* **2009**, *42*, 612; (h) Chen, Y.-Y.; Wu, G.; Qiu, Z.-C.; Wang, X.-L.; Zhang, Y.; Lu, F.; Wang, Y.-Z., *J. Polym. Sci., Part A: Polym. Chem.* **2008**, *46*, 3207.

38. Brown, H. A.; Chang, Y. A.; Waymouth, R. M., *J. Am. Chem. Soc.* **2013**, *135*, 18738.

39. Islamov, T. K.; Nametkin, N. S.; Gusel'nikov, L. E., *Bull. Acad. Sci. USSR, Div. Chem. Sci.* **1969**, *18*, 2573.

40. Loy, D. A.; Carpenter, J. P.; Alam, T. M.; Shaltout, R.; Dorhout, P. K.; Greaves, J.; Small, J. H.; Shea, K. J., *J. Am. Chem. Soc.* **1999**, *121*, 5413.

41. Pakes, P. W.; Rounds, T. C.; Strauss, H. L., *J. Phys. Chem.* **1981**, *85*, 2469.

42. Gar, T.; Buyakov, A.; Gusev, A.; Los‘, M.; Kisin, A.; Mironov, V., *Russ. J. Gen. Chem. Engl. trans.* **1976**, *46*, 837.

43. Iwamura, T.; Adachi, K.; Chujo, Y., *Chem. Lett.* **2010**, *39*, 354.

44. (a) Yano, T.; Nakashima, K.; Otera, J.; Okawara, R., *Organometallics* **1985**, *4*, 1501; (b) Otera, J.; Yano, T.; Okawara, R., *Organometallics* **1986**, *5*, 1167.

45. Beckmann, J.; Jurkschat, K.; Rabe, S.; Schürmann, M.; Dakternieks, D., *Z. Anorg. Allg. Chem.* **2001**, *627*, 458.

46. Beckmann, J.; Dakternieks, D.; Kuan, F. S.; Tiekink, E. R. T., *J. Organomet. Chem.* **2002**, *659*, 73.

47. (a) Patel, Y.; George, J.; Pillai, S. M.; Munshi, P., *Green Chem.* **2009**, *11*, 1056; (b) Lu, Y. W., Lin Hong; Lan, Zhi Li; Li, Jing; Xie, Qing Lan, *Chin. Chem. Lett.* **2002**, *13*, 185; (c) Lu, Y. L., Zhi-Li; Li, Jing; Xie, Qing-Lan, *Gaodeng Xuexiao Huaxue Xuebao* **2001**, *22*, 66; (d) He, X.-L. L., Sen; Guo, Xuan; Lu, Lu-De; Wang, Xin; Yang, Xu-Jie, *Yingyong Huaxue* **2007**, *24*, 1268.

48. Beckmann, J.; Dakternieks, D.; Duthie, A.; Jurkschat, K.; Schürmann, M., *Z. Anorg. Allg. Chem.* **2003**, *629*, 99.

49. Schulte, M.; Schurmann, M.; Jurkschat, K.; Dakternieks, D., *Chem. Commun.* **1999**, *0*, 1291.

50. Andrianov, K. A.; Golubenko, A., *J. Gen. Chem. USSR Engl. trans.* **1975**, *45*.
51. Zickgraf, A.; Beuter, M.; Kolb, U.; Dräger, M.; Tozer, R.; Dakternieks, D.; Jurkschat, K., *Inorg. Chim. Acta* **1998**, *275–276*, 203.
52. Puff, H.; Schuh, W.; Sievers, R.; Wald, W.; Zimmer, R., *J. Organomet. Chem.* **1984**, *260*, 271.
53. Erhardt, S. A.; Hoffmann, F.; Daiß, J. O.; Stohrer, J.; Herdtweck, E.; Rieger, B., *Chem. Eur. J.* **2013**, *19*, 4818.

2.6 Appendix

Crystallographic Data and Structure Refinements

Intensity data for the crystals of compounds **3**, **5a**, **6**.HI, **15**, **20**, **23a**, **25'**, **26'**, and **27'** were collected on a XcaliburS CCD diffractometer (Oxford Diffraction) fitted with graphite-monochromated Mo Kα (λ = 0.71073 Å) radiation at 173 K. Those of the crystals of **1**, **2**, **22**, and **24a** were collected on Nonius Kappa CCD diffractometer, and of **12**, and **18** were collected on SMART CCD Bruker AXS diffractometer.

The structure was solved with direct methods using SHELXS-97.[1] Refinements were carried out against F^2 by using SHELXL-97.[1] All non-hydrogen atoms were refined using anisotropic displacement parameters. The C−H hydrogen atoms were positioned with idealized geometry and refined using a riding model. For decimal rounding of numerical parameters and su values the rules of IUCr have been employed.[2] The Figures were created using SHELXTL[3] and Diamond 3.2i.[4] The crystallographic data are given in tables B1–B6.

References

1. Sheldrick, G., *Acta Crystallographica Section A* **2008,** *64* (1), 112.
2. Clegg, W., *Acta Crystallographica Section E* **2003,** *59* (1), e2.
3. *Sheldrick, G. M. SHELXTL, release 5.1 Software Reference Manual; Brucker AXS, Inc.: Madison, Wisconsin, 1997.*
4. *Diamond - Crystal and Molecular Structure Visualization, Crystal Impact - Dr. H. Putz & Dr. K. Brandenburg GbR, Kreuzherrenstr. 102, 53227 Bonn, Germany http://www.crystalimpact.com/diamond*.

Table B1. Crystal data and structure refinements of the tetraorganotin compounds **1** and **6**·HI.

	1	**6.HI**
Empirical formula	C_{18} H_{26} O Si_2 Sn	C_{17} H_{34} I N O Si_2 Sn
Formula weight	433.26	570.22
Temperature / K	173(1)	173(2)
Wavelength /°A	0.71073	0.71073
Crystal system	Monoclinic	Monoclinic
space group	Pc	P2(1)/c
a /°A	6.4782(2)	17.3430(12)
b /°A	8.4161(3)	12.5787(8)
c /°A	18.9026(7)	11.2749(8)
α /°	90	90
β /°	94.159(3)	106.466(7)
γ /°	90	90
Volume /°A^3	1027.88(6)	2358.8(3)
Z	2	4
Dc /g.cm^{-3}	1.4	1.606
Absorption coefficient /mm^{-1}	1.359	2.498
F(000)	440	1128
Crystal size /mm	0.36 x 0.20 x 0.18	0.14 x 0.10 x 0.03
Range for data collection /°	2.16 to 25.49	2.03 to 25.50
Reflections collected	4912	16080
Independent reflections	2667	4365
Refinement method	Full-matrix least-squares on F^2	Full-matrix least-squares on F^2
Data / restraints / parameters	2667 / 2 / 203	4365 / 0 / 200
Goodness-of-fit on F^2	1.02	0.615
Final R indices [$I>2\sigma(I)$]	R1 = 0.0188, wR2 = 0.0440	R1 = 0.0296, wR2 = 0.0543
R indices (all data)	R1 = 0.0201, wR2 = 0.0442	R1 = 0.0813, wR2 = 0.0597
Largest diff. peak and hole / e.A^{-3}	0.380 and -0.275	0.870 and -0.457

Table B2. Crystal data and structure refinements of the organotin halides **2**, **3** and **5a**.

	2	**3**	**5a**
Empirical formula	C_{12} H_{21} I O Si_2 Sn	C_6 H_{16} I_2 O Si_2 Sn	C_{12} H_{32} Cl_4 O_2 Si_4 Sn_2
Formula weight	483.06	532.86	699.92
Temperature / K	173(2)	173(1)	173(2)
Wavelength /°A	0.71073	0.71073	0.71073
Crystal system	Monoclinic	Triclinic	Monoclinic
space group	P 21/n	P-1	P 21/c
a /°A	7.0770(3)	8.2905(4)	6.7987(4)
b /°A	11.5716(5)	8.3156(5)	11.2135(6)
c /°A	21.3924(10)	12.4289(6)	17.9728(10)
α /°	90	90.682(4)	90
β /°	90.549(4)	101.060(4)	97.079(5)
γ /°	90	113.174(5)	90 deg
Volume /°A^3	1751.79(13)	769.45(7)	1359.75(13)
Z	4	2	2
Dc /g.cm^{-3}	1.832	2.3	1.709
Absorption coefficient /mm^{-1}	3.344	2.3	2.411
F(000)	928	488	688
Crystal size /mm	0.30 x 0.22 x 0.06	0.24 x 0.20 x 0.12	0.25 x 0.16 x 0.10
Range for data collection /°	2.59 to 25.49	2.68 to 25.49	2.28 to 25.50
Reflections collected	13983	6577	8212
Independent reflections	3261	2840	2534
Refinement method	Full-matrix least-squares on F^2	Full-matrix least-squares on F^2	Full-matrix least-squares on F^2
Data / restraints / parameters	3261 / 0 / 154	2840 / 0 / 113	2534 / 0 / 113
Goodness-of-fit on F^2	0.850	1.009	1.015
Final R indices [I>2σ(I)]	R1 = 0.0219, wR2 = 0.0391	R1 = 0.0493, wR2 = 0.1188	R1 = 0.0224, wR2 = 0.0501
R indices (all data)	R1 = 0.0368, wR2 = 0.0406	R1 = 0.0557, wR2 = 0.1215	R1 = 0.0295, wR2 = 0.0523
Largest diff. peak and hole / e.A^{-3}	0.423 and -0.470	6.869 and -1.302	0.372 and -0.368

Table B3. Crystal data and structure refinements of the tricyclic silalkyltin siloxane $[\{X_2Sn(CH_2MeSi)_2O\}O]_2$ (**12**, X = Ph; **15**, X = Cl).

	12	**15**
Empirical formula	$C_{32}H_{40}O_4Si_4Sn_2$	$C_8H_{20}Cl_4O_4Si_4Sn_2$
Formula weight	838.38	671.78
Temperature / K	173(2)	173(2)
Wavelength /°A	0.71073	0.71073
Crystal system	Triclinic	Triclinic
space group	P -1	P-1
a /°A	9.1063(4)	8.0144(9)
b /°A	10.5156(5)	8.5699(9)
c /°A	11.0339(5)	9.2476(10)
α /°	117.7415(10)	109.379(9)
β /°	103.5152(11)	107.809(9)
γ /°	93.2995(11)	98.965(9)
Volume /°A^3	892.09(7)	546.54(12)
Z	1	1
Dc /g.cm^{-3}	1.561	2.041
Absorption coefficient /mm^{-1}	1.567	3.002
F(000)	420	324
Crystal size /mm	0.50 x 0.30 x 0.13	0.39 x 0.08 x 0.05
Range for data collection /°	2.18 to 27.98	2.53 to 25.50
Reflections collected	29500	6010
Independent reflections	4277	2047
Refinement method	Full-matrix least-squares on F^2	Full-matrix least-squares on F^2
Data / restraints / parameters	4277 / 0 / 192	2047 / 0 / 102
Goodness-of-fit on F^2	1.055	0.870
Final R indices [I>2σ(I)]	R1 = 0.0141, wR2 = 0.0372	R1 = 0.0265, wR2 = 0.0480
R indices (all data)	R1 = 0.0148, wR2 = 0.0377	R1 = 0.0360, wR2 = 0.0493
Largest diff. peak and hole / e.A^{-3}	0.379 and -0.299	0.526 and -0.505

Table B4. Crystal data and structure refinements of the tin-containing tetrasiloxane $[(Ph_3SnCH_2)MeSiO]_4$, **18**, and the octameric silsesquioxane $(Ph_3SnCH_2SiO_{1.5})_8$, **20**.

	18	**20**
Empirical formula	$C_8 H_{20} Br_{12} O_4 Si_4 Sn_4$	$C_{152}H_{136}O_{12}Si_8Sn_8$
Formula weight	1726.28	3328.85
Temperature / K	173(2)	173(2)
Wavelength /°A	0.71073	0.71073
Crystal system	Monoclinic	Triclinic
space group	P 21/c	P–1
a /°A	10.0466(11)	17.3801(3)
b /°A	9.4689(11)	17.8078(3)
c /°A	20.435(2)	27.1261(5)
α /°	90	74.913(2)
β /°	101.995(3)	84.665(2)
γ /°	90	61.676(2)
Volume /°A^3	1901.5(4)	7131.1(2)
Z	2	2
Dc /$g.cm^{-3}$	3.015	1.550
Absorption coefficient /mm^{-1}	15.347	1.503
F(000)	1552	3312
Crystal size /mm	0.35 x 0.35 x 0.15	0.47 x 0.40 x 0.26
Range for data collection /°	2.04 to 27.92	2.28 to 25.50
Reflections collected	5146	136052
Independent reflections	5146	26527
Refinement method	Full-matrix least-squares on F^2	Full–matrix least–squares on F^2
Data / restraints / parameters	5146 / 12 / 148	26527 / 18 / 1579
Goodness-of-fit on F^2	1.068	1.238
Final R indices [$I>2\sigma(I)$]	R1 = 0.1153, wR2 = 0.3080	R1 = 0.0361, wR2 = 0.0946
R indices (all data)	R1 = 0.1606, wR2 = 0.3467	R1 = 0.0455, wR2 = 0.0984
Largest diff. peak and hole / e.A^{-3}	4.749 and -3.569	1.669 and –0.872

Table B5. Crystal data and structure refinements of the dimeric tetraorganodistannoxanes **22**, **23a** and **24a**.

	22	**23a**	**24a**
Empirical formula	C_{28} H_{74} I_2 O_8 Si_8 Sn_4	C_{32} H_{76} O_{14} Si_8 Sn_4	C_{24} H_{66} I_2 O_8 Si_8 Sn_4
Formula weight	1492.15	1384.41	1436.05
Temperature / K	173(2)	173(2)	173(2)
Wavelength /°A	0.71073	0.71073	0.71073
Crystal system	Triclinic	Orthorhombic	Triclinic
space group	P-1	P b c a	P -1
a /°A	9.7151(6)	15.9051(13)	8.7752(4)
b /°A	11.9295(9)	15.7582(13)	12.4184(5)
c /°A	12.9327(7)	22.6357(17)	12.7512(5)
α /°	84.870(5)	90	89.695(3)
β /°	78.835(5)	90	74.667(4)
γ /°	70.004(7)	90	74.703(4)
Volume /°A^3	1381.40(15)	5673.3(8)	1289.51(9)
Z	1	4	1
Dc /$g.cm^{-3}$	1.794	1.621	1.849
Absorption coefficient /mm^{-1}	3.113	1.959	3.331
F(000)	724	2768	692
Crystal size /mm	0.28 x 0.20 x 0.18	0.16 x 0.15 x 0.03	0.27 x 0.21 x 0.10
Range for data collection /°	2.27 to 25.50	2.21 to 25.50	2.30 to 25.50
Reflections collected	10157	26817	14917
Independent reflections	5121	5281	4806
Refinement method	Full-matrix least-squares on F^2	Full-matrix least-squares on F^2	Full-matrix least-squares on F^2
Data / restraints / parameters	5121 / 6 / 235	5281 / 0 / 272	4806 / 0 / 219
Goodness-of-fit on F^2	1.049	0.666	1.094
Final R indices [$I>2\sigma(I)$]	R1 = 0.0468, wR2 = 0.1136	R1 = 0.0340, wR2 = 0.0487	R1 = 0.0304, wR2 = 0.0787
R indices (all data)	R1 = 0.0736, wR2 = 0.1181	R1 = 0.0962, wR2 = 0.0524	R1 = 0.0425, wR2 = 0.0805
Largest diff. peak and hole / e.A^{-3}	2.669 and -2.714	1.109 and -0.639	0.759 and -1.562

Table B6. Crystal data and structure refinements of the dimeric tetraorganodistannoxanes **25'**, **26'**, and **27'**.

	25'	**26'**	**27'**
Empirical formula	C_{28} $H_{68.50}$ $Cl_{3.50}$ $O_{4.50}$ Si_4 Sn_4	C_{24} H_{65} Br_3 O_7 Si_8 Sn_4	C_{28} H_{70} $Br_{2.10}$ $O_{5.90}$ Si_4 Sn_4
Formula weight	1188.52	1404.97	1256.17
Temperature / K	173(2)	173(2)	173(2)
Wavelength /°A	0.71073	0.71073	0.71073
Crystal system	Triclinic	Monoclinic	Triclinic
space group	P-1	P2(1)/c	P-1
a /°A	12.3700(4)	14.2488(6)	12.2144(4)
b /°A	12.3898(4)	10.2226(5)	13.0338(5)
c /°A	17.6248(7)	17.6654(7)	17.7816(7)
α /°	72.612(3)	90	106.857(3)
β /°	89.805(3)	91.914(4)	95.059(3)
γ /°	67.932(3)	90	113.158(3)
Volume /°A^3	2370.75(16)	2571.70(19)	2424.22(17)
Z	2	2	2
Dc /$g.cm^{-3}$	1.665	1.814	1.721
Absorption coefficient /mm^{-1}	2.410	4.469	3.897
F(000)	1176	1364	1229
Crystal size /mm	0.32 x 0.25 x 0.10	0.26 x 0.24 x 0.10	0.280 x 0.180 x 0.140
Range for data collection /°	2.15 to 29.27	2.30 to 25.50	2.457 to 25.497
Reflections collected	22397	16816	32538
Independent reflections	10990	4785	9012
Refinement method	Full-matrix least-squares on F^2	Full-matrix least-squares on F^2	Full-matrix least-squares on F2
Data / restraints / parameters	10990 / 36 / 463	4785 / 0 / 223	9012 / 54 / 463
Goodness-of-fit on F^2	0.816	0.804	1.293
Final R indices [$I>2\sigma(I)$]	R1 = 0.0337, wR2 = 0.0498	R1 = 0.0383, wR2 = 0.0867	R1 = 0.0382, wR2 = 0.0998
R indices (all data)	R1 = 0.0780, wR2 = 0.0540	R1 = 0.0633, wR2 = 0.0909	R1 = 0.0467, wR2 = 0.1028
Largest diff. peak and hole / e.A^{-3}	1.238 and -1.858	2.026 and -1.625	3.517 and -0.869

3. Novel *cyclo*-Stannasiloxanes and Related Organotinoxo Clusters. Syntheses and Structures

3.1 Introduction

Carbon is not the most abundant element. It comprises only 0.08 % of the earth crust. Despite this, organic polymers fill the world around us. They are used in miscellaneous areas as packaging materials, car tires, clothing, compact discs and a lot more.[1] The enormous development of organic polymers is attributed to their ease of preparation and the cheap of petroleum derivative monomers. In contrary, inorganic polymers are much less developed. Only three classes of inorganic polymers are well-characterized, namely polysiloxanes[2] $(R_2SiO)_n$, polysilanes[3] $(R_2Si)_n$, and polyphosphazenes[4] $(R_2PN)_n$ (Chart 1).

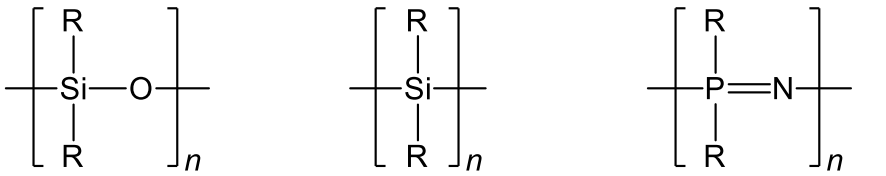

Polysiloxanes Polysiloxanes Polyphosphazenes

Chart 1.

Polysiloxanes are the most important inorganic polymers. They show a variety of molecular structures and demonstrate intimate relationship between structure and properties not easily achievable by other classes of polymers. Consequently a wide diversity of applications is known. The ring-opening polymerization (ROP) procedure of the *cyclo*-siloxanes is applied for the production of high-molecular weight

polysiloxanes.[2a] This initiated activities concerning the synthesis, characterization and reactivity of *cyclo*-metallasiloxanes.[5] Such compounds can be seen as model compounds for structurally modified silica surfaces and minerals, and they hold potential as single source precursors for new inorganic materials and polymers.[5a, 6] A rich structural diversity of *cyclo*-metallasiloxanes incorporating various heteroatoms, such as B, Al, Ge, Sn, P, Ti, Zr, Hf, Mo, W, Pb, Sb, and Bi exists among the *cyclo*-metallasiloxanes.[5b, 6a, 7] The first tin-containing *cyclo*-metallasiloxanes, *cyclo*-*t*-$Bu_2Si(OMe_2SnO)_2Si$*t*-Bu_2, was prepared in 1986 by Klingebiel et al.[7c] In 1997, Jurkschat et al. reported on the syntheses and molecular structures of the *cyclo*-stannasiloxanes *cyclo*-*t*-$Bu_2Sn[O(t\text{-}Bu_2)Si]_2O$ (Figure 1, type **A**) and *cyclo*-*t*-$Bu_2Si[O(t\text{-}Bu_2)SnO]_2Si$*t*-$Bu_2$ (Figure 1, type **B**) by the reaction of $(t\text{-}Bu_2SnO)_3$ with *t*-Bu_2SiCl_2.[8] These followed by the syntheses and reactivity studies of a series of *cyclo*-stannasiloxanes of different ring sizes and variable substituents at both the silicon and tin atoms.[5a]

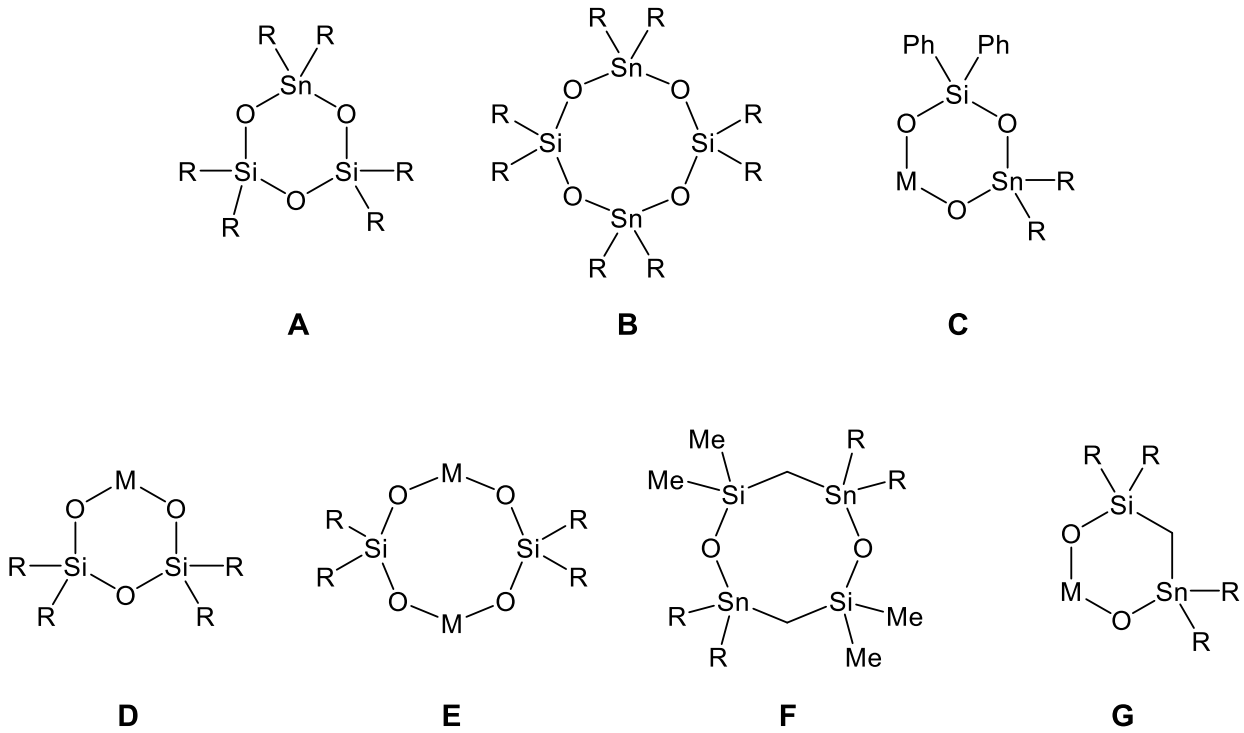

Figure 1. Selected types of cyclo-stannasiloxanes and *cyclo*-metallasiloxanes.

The studies showed that the reactivity of the *cyclo*-stannasiloxanes differ drastically from that of the parent *cyclo*-siloxanes as a result of the higher kinetic lability of the

Sn–O bond in comparison to the Si–O bond. Consequently, reactions involving Sn–O bonds usually proceed rapidly at room temperature on the laboratory time scale.[5a] Whilst ROP of *cyclo*-$(Ph_2SiO)_3$ occurs at temperatures between 150-190 °C in presence of initiators, the *cyclo*-stannasiloxane *cyclo*-$R_2Sn(OPh_2Si)_2O$ (R = *t*-Bu, *i*-Pr) undergoes ROP upon crystallization, in absence of any initiator, giving the first well-defined polymetallasiloxanes $(R_2SnOPh_2SiOPh_2SiO)_n$.[5a, 9] However, the polymer is not stable and depolymerization occurs upon dissolving in solvent (eq. 1).[9] The release of the ring strain is foreseen to be the thermodynamic driving force for the ROP process.

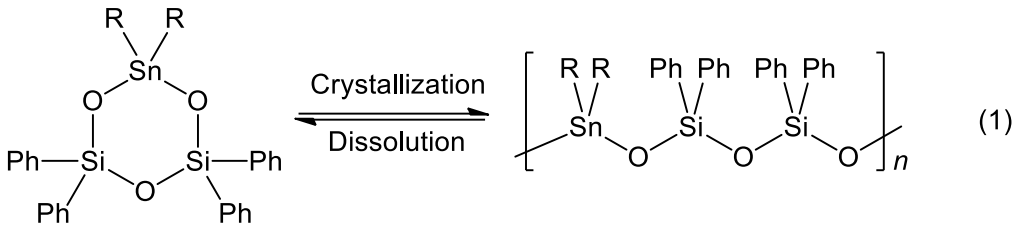

(1)

R = *t*-Bu, *i*-Pr

The borasiloxane *cyclo*-$PhB(OPh_2Si)_2O$ presents, in contrary to the *cyclo*-stannasiloxane *cyclo*-$R_2Sn(OPh_2Si)_2O$, as a six-membered ring both in solution and in the solid state.[7g]

The ability of *cyclo*-stannasiloxanes to undergo ring-opening polymerization strongly depends on the identity of the exocyclic substituents at the tin and silicon atoms, as the crystallization of the ferrocenyl-substituted six-membered *cyclo*-stannasiloxane *cyclo*-$Fc_2Sn(OPh_2Si)_2O$ (Fc = $CpFeC_5H_4$) does not give the corresponding polymer, but it dimerizes affording the corresponding twelve-membered cyclic stannasiloxane *cyclo*-$[(Fc_2Sn(OPh_2SiOPh_2SiO)_2SnFc_2]$ (eq. 2).[5a] However, the connectivity of the atoms within the ring plays also a major role. Thus, the five-membered stannasiloxane *cyclo*-*t*-$Bu_2Sn(OSiPh_2)_2$ containing a Si–Si bond does not polymerize upon crystallization. It reversibly dimerizes providing the ten-membered *cyclo*-stannasiloxane *cyclo*-*t*-Bu_2Sn $(OPh_2SiPh_2SiO)_2Snt$-Bu_2 (eq. 3).[5a]

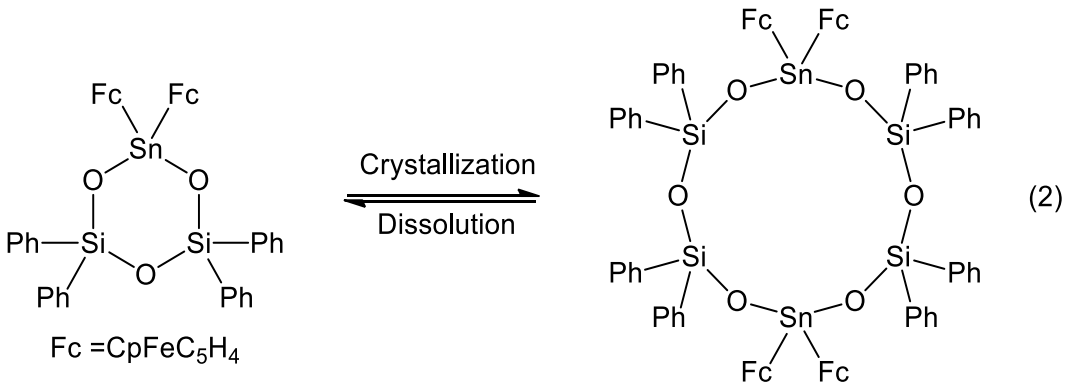

(2)

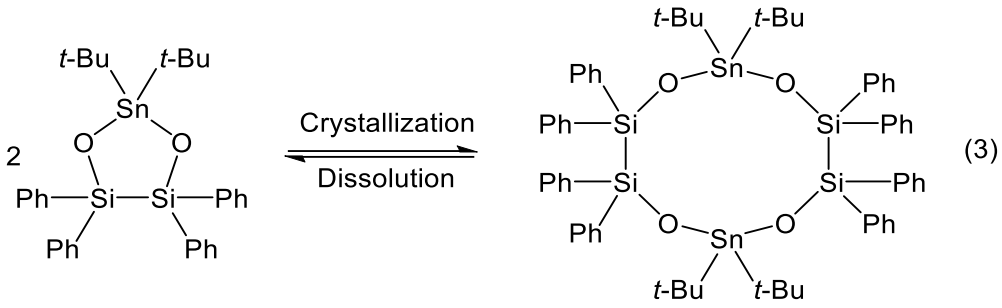

(3)

The ring strain in the *cyclo*-stannasiloxanes is of great importance. Thus, the reaction of the eight-membered stannasiloxane ring *cyclo*-(Ph_2SiO*t*-$Bu_2SnO)_2$ with 2/3 molar equivalents *cyclo*-(*t*-$Bu_2SnO)_3$ quantitatively provided in situ the six-membered stannasiloxane ring $Ph_2Si(OSn$*t*-$Bu_2)_2O$. However, this reaction is an equilibrium and removal of the solvent quantitatively yields the starting compounds (eq. 4).[7r]

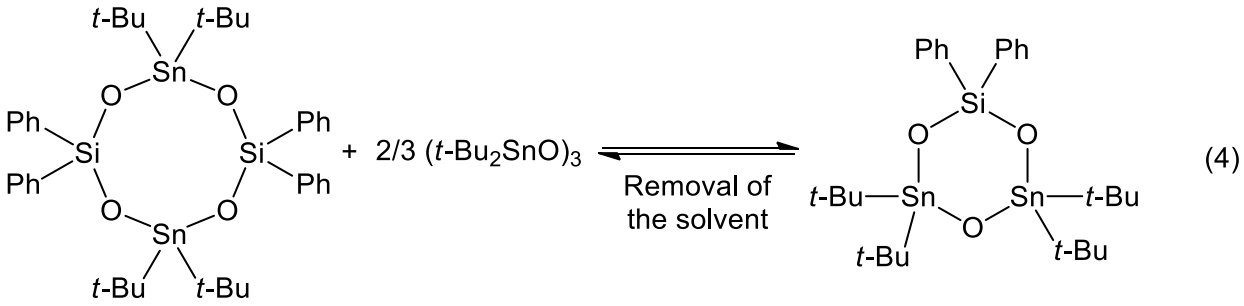

(4)

Furthermore, all attempts to isolate the six-membered stannasiloxane ring *cyclo*-$Ph_2Si(OSnPh_2)_2CH_2$ failed, as it irreversibly rearranges into the eight-membered stannasiloxane ring *cyclo*-$O(SiPh_2OSnPh_2)_2CH_2$ and $(Ph_2SnOH)_2CH_2$ (eq. 5).[5a] These observations are attributed to the higher ring strain in the six-membered *cyclo*-stannasiloxanes in comparison to that in the eight-membered rings.

On the other hand, the six-membered metallasiloxanes containing a *built-in* liganed *cyclo*-[$Me_2N(CH_2)_3]_2Sn(OPh_2Si)_2O$,[10] *cyclo*-$LPhSn(OR_2Si)_2O$, *cyclo*-$LSb(OR_2Si)_2O$, and *cyclo*-$LBi(OR_2Si)_2O$, (R = Ph, Me; L = C_6H_3–2,6-$(CH_2NMe_2)_2$)[5b] (Figure 1, Type **D**) do not polymerize or dimerize upon crystallization.

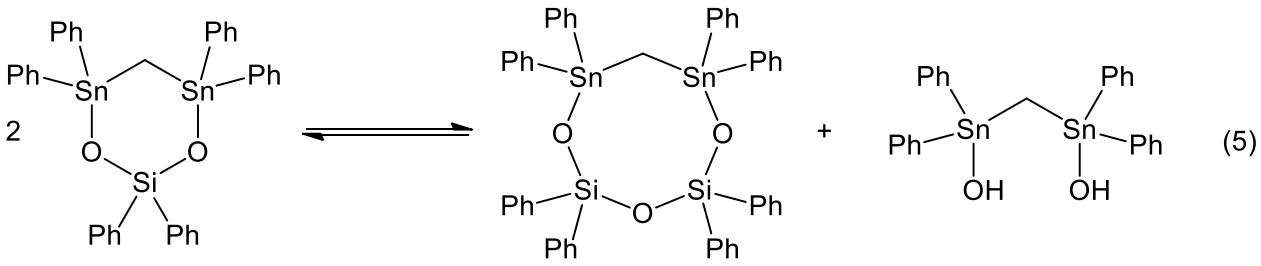

(5)

The reaction of *cyclo*-stannasiloxanes with organoelement oxides allowed the isolation of new interesting *cyclo*-metallasiloxanes of different ring size thank to the kinetically labile Sn–OSi bond. Thus, the reaction of the eight-membered *cyclo*-stannasiloxanes $RR'Sn(OPh_2SiO)_2SnR_2$ [R = $Me_2N(CH_2)_3$] with (*t*-$Bu_2SnO)_3$, *t*-$Bu_2Ge(OH)_2$ or $PhB(OH)_2$ gave the six-membered metallasiloxanes *cyclo*-(R_2SnOPh_2SiOMO), (M = *t*-Bu_2Sn, *t*-Bu_2Ge, or PhB) (Figure 1, type **C**) (eq. 6),[11] and the reaction of $LPhSn(OPh_2SiO)_2SnLPh$ [L = C_6H_3–2,6-$(CH_2NMe_2)_2$] with $Ph_2Si(OH)_2$ gives the six membered stannasiloxane *cyclo*-$LPhSn(OPh_2Si)_2O$ (eq. 6).[5b]

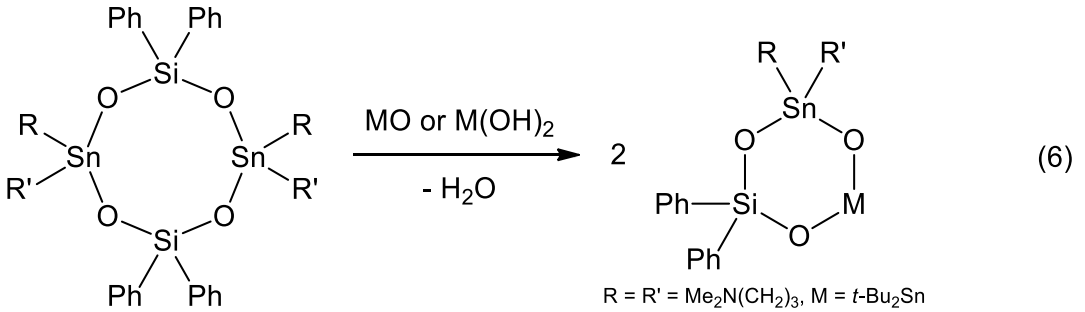

(6)

Furthermore, the reactions of the five-membered cyclic stannasiloxane *cyclo*-*t*-$Bu_2Sn(OPh_2Si)_2$, respectively, the six-membered cyclic stannasiloxane *cyclo*-*t*-$Bu_2Sn(OPh_2Si)_2O$ with (*t*-$Bu_2SnO)_3$ result in ring enlargement giving the corresponding seven- respectively eight-membered stannasiloxanes *cyclo*-O(*t*-$Bu_2SnOPh_2Si)_2$[5a] and *cyclo*-O(*t*-$Bu_2SnOPh_2Si)_2O$ (eq. 7 and 8).[7r, 9]

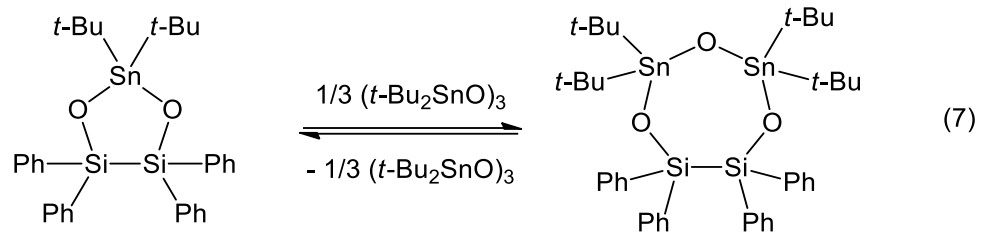

(7)

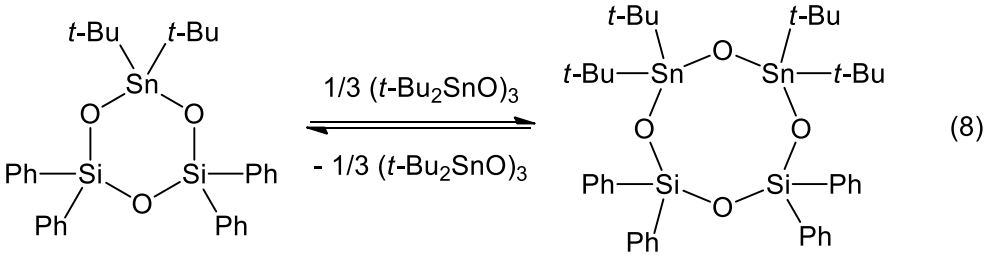

(8)

To the best of our knowledge, *cyclo*-stannasiloxanes which have tin and silicon atoms linked via a strong carbon linkage (Figure 1, **F** and **G**) are almost unexplored. As systematic studies showed that even very similar compounds can have drastically different chemical reactivity, this raises the interest to synthesis the *cyclo*-stannasilloxanes of type **F** (Figure 1) and study their behavior against organoelement oxides.

Herein, it is reported on the syntheses of the eight-membered stannasiloxanes, *cyclo*-[RR'$SnOMe_2SiCH_2]_2$, compounds **6**–**8**, of type **F** (Figure 1) with different organic substituents at the tin atom. These react differently with organoelement oxides giving a variety of novel metallasiloxanes, *cyclo*-[Me_2SiCH_2(RR')SnOMO] (Figure 1, **G**). Among these, compound **17**, *cyclo*-[Me_2SiCH_2(*t*-Bu_2)$SnOPh_2GeO$], containing $SnGeSiCO_2$ central cores, is the first example for such species being composed of four different group 14 elements in the six-membered ring skeleton. The molecular structures of these compounds are discussed based on multinuclear NMR spectroscopy, ESI MS spectroscopy, and in the case of compounds **6**–**8** also by single crystal X-ray diffraction studies. The organotinoxo cluster [*t*-Bu_2SnO{$O(Me_2)SiCH_2$}$Sn(OH)Ph]_2$, **10**, formed by the aerobic hydrolysis of the six-membered stannasiloxane *cyclo*-[$Me_2SiCH_2Ph_2SnO$(*t*-Bu_2)SnO], **9**, is also reported.

3.2 Results and discussion

3.2.1 Syntheses and structures of the eight-membered stannasiloxanes *cyclo*-(RR'SnOMe$_2$SiCH$_2$)$_2$ (6, R = R' = Ph; 7, R = Me$_2$N(CH$_2$)$_3$, R' = Ph; 8, R = R' = *t*-Bu)

The hydrolyses under basic conditions of the triorganotin halides [Me$_2$(*i*-PrO)SiCH$_2$]RR'SnX (**2**, R = R' = Ph, X = I; **4**, R = Me$_2$N(CH$_2$)$_3$, R' = Ph, X = I; **5**, R = R' = *t*-Bu, X = Cl, OH) provided the corresponding eight-membered stannasiloxanes *cyclo*-(RR'SnOMe$_2$SiCH$_2$)$_2$ (**6**, R = R' = Ph; **7**, R = Me$_2$N(CH$_2$)$_3$, R' = Ph; **8**, R = R' = *t*-Bu), respectively, in very good yields (Scheme 1).

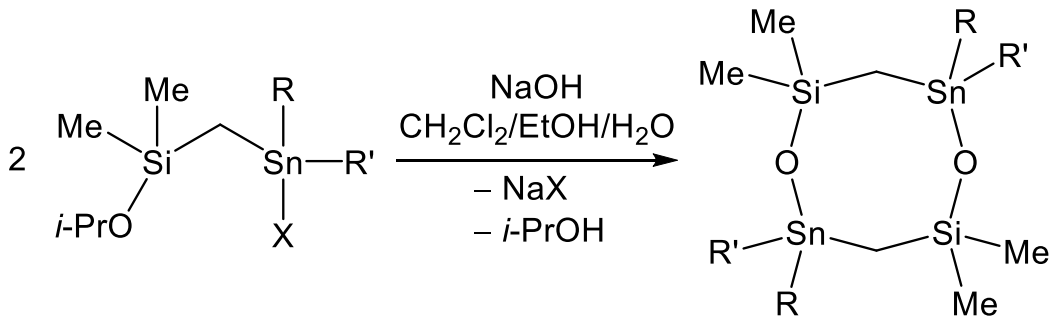

2, R = R' = Ph, X = I
4, R = Me$_2$N(CH$_2$)$_3$, R' = Ph, X = I
5, R = R' = *t*-Bu, X = Cl, OH

6, R = R' = Ph
7, R = Me$_2$N(CH$_2$)$_3$, R' = Ph
8, R = R' = *t*-Bu

Scheme 1. Syntheses of compounds **6**–**8**.

The ^{119}Sn NMR spectra of solutions of compounds **6** and **8** in CDCl$_3$ show single resonances at *δ* –31 and 34, respectively. The corresponding ^{29}Si NMR spectra show singlet resonances with $^{117/119}$Sn coupling satellites with two magnetically different tin atoms at *δ* 8.6 [^2J(^{29}Si–$^{117/119}$Sn) = 33 Hz, ^2J(^{29}Si–$^{117/119}$Sn) = 54 Hz] for compound **6** and at *δ* 1.8 [^2J(^{29}Si–$^{117/119}$Sn) = 46 Hz, ^2J(^{29}Si–$^{117/119}$Sn) = 56 Hz] for **8**. On the other hand, compound **7** adopts chirality at the tin atom with the phenyl groups are either cis or trans to each other. Consequently, two resonances were observed in ^{119}Sn NMR spectrum at *δ* –53 (integral 45) and –55 (integral 55), as well two resonances in ^{29}Si NMR spectrum at *δ* 1.4 [^2J(^{29}Si–$^{117/119}$Sn) = 38 Hz, ^2J(^{29}Si–$^{117/119}$Sn) = 47 Hz] and at *δ* 1.0 [^2J(^{29}Si–$^{117/119}$Sn) = 42 Hz, ^2J(^{29}Si–$^{117/119}$Sn) = 49 Hz] (Table 1), indicating the presence of two diastereomers.

Table 1. Selected data from the NMR spectra of the cyclic stannasiloxanes *cyclo*-(RR'SnOMe$_2$SiCH$_2$)$_2$ (**6**, R = R' = Ph; **7**, R = Me$_2$N(CH$_2$)$_3$, R' = Ph; **8**, R = R' = *t*-Bu).

	δ ^{29}Si	δ ^{119}Sn	$^{2}J(^{29}Si–^{117/119}Sn)$ (Hz)
6	8.6	–31	33, 54
7	1.0;	–53;	42, 49;
	1.4	–55	38, 47
8	1.8	34	46, 56

The ESI MS spectra of compounds **6**–**8** in the positive mode showed respectively major mass clusters that are assigned to the protonated compounds centered at *m/z* (723.1, [**6** + H]$^+$; 741.2, [**7** + H]$^+$; and 643.2, [**8** + H]$^+$). In addition, mass clusters for the species [Me$_2$(OH)SiCH$_2$RR'Sn + nH$_2$O + mMeCN]$^+$, (n, m = natural number between 0 and 4) were also observed.

The compounds **6**–**8** show good solubility in common organic solvents such as dichloromethane, chloroform, toluene and THF. They each crystallized in the triclinic space group P–1 with one molecule in the unit cell. The molecular structures of compounds **6**–**8** are shown in Figures 2–4, respectively, and selected bond lengths and bond angles are summarized in Table 2.

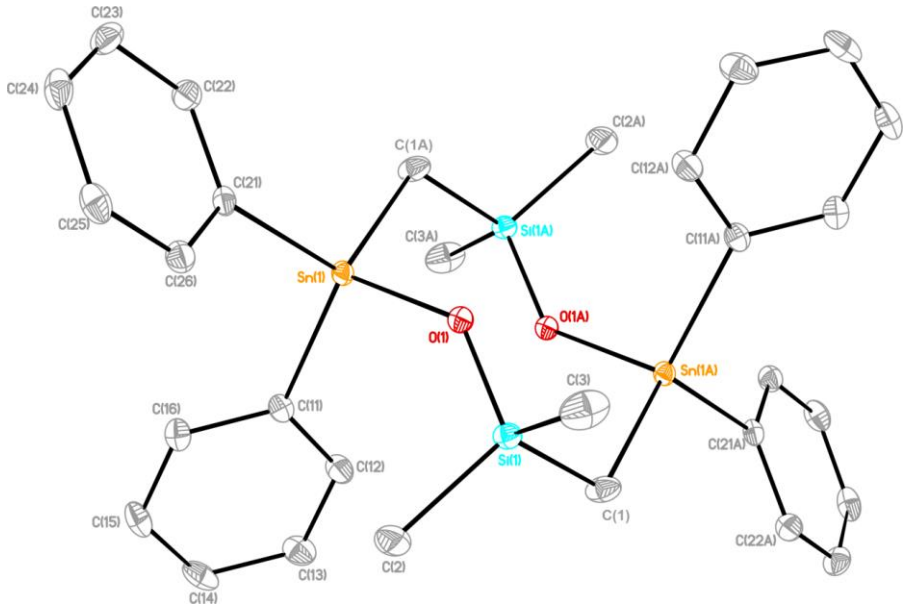

Figure 2. General view (SHELXTL) of a molecule of **6** showing 30% probability displacement ellipsoids and the crystallographic numbering scheme. Hydrogen atoms are omitted for clarity.

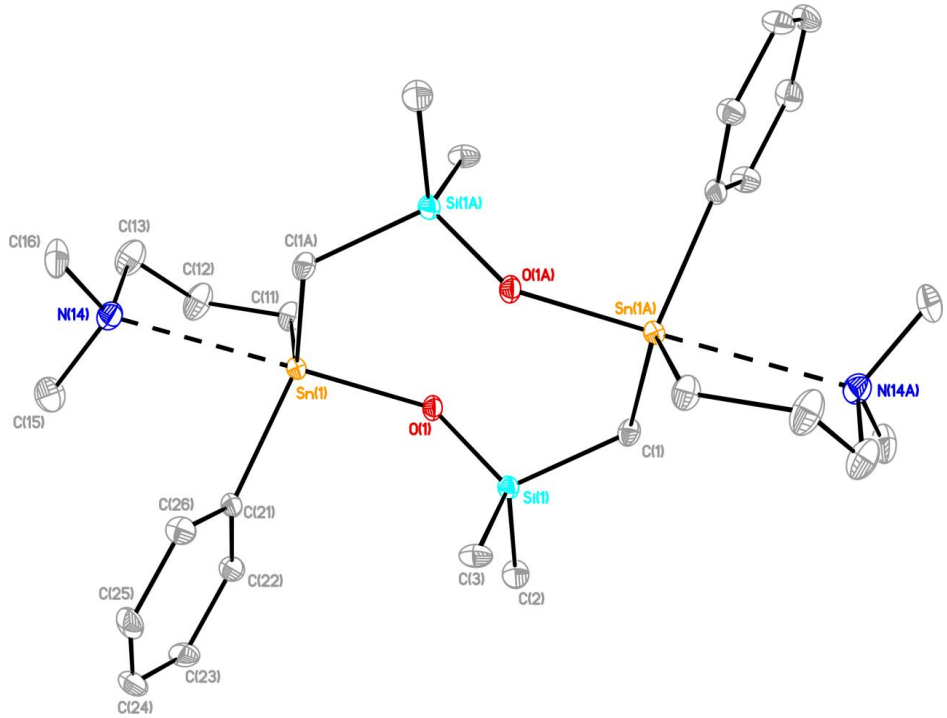

Figure 3. General view (SHELXTL) of a molecule of **7** showing 30% probability displacement ellipsoids and the crystallographic numbering scheme. Hydrogen atoms are omitted for clarity.

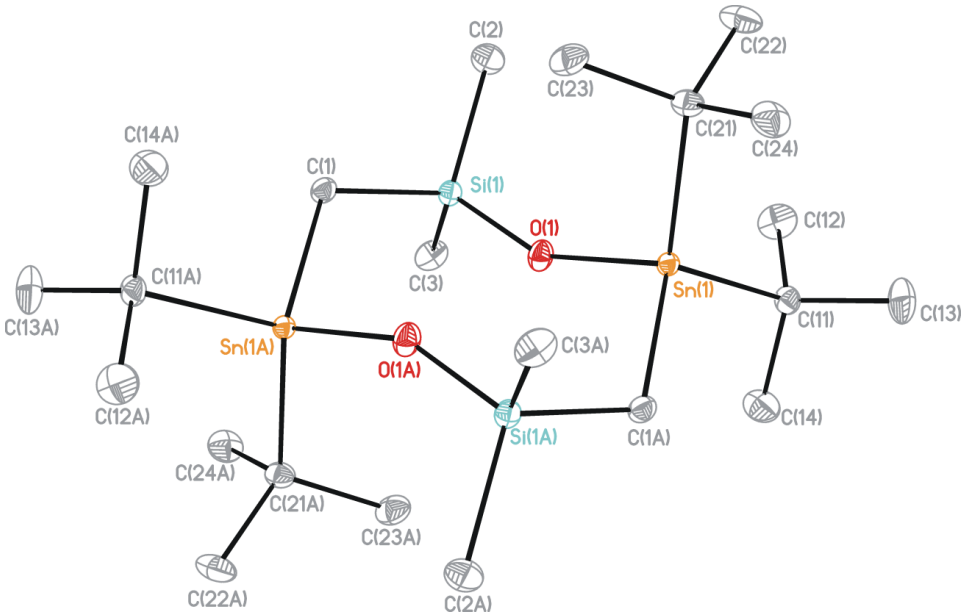

Figure 4. General view (SHELXTL) of a molecule of **8** showing 30% probability displacement ellipsoids and the crystallographic numbering scheme. Hydrogen atoms are omitted for clarity.

Table 2. Selected bond lengths (Å) and bond angles (deg) in the stannasiloxanes *cyclo*-(RR'SnOMe$_2$SiCH$_2$)$_2$ (**6**, R = R' = Ph; **7**, R = Me$_2$N(CH$_2$)$_3$, R' = Ph; **8**, R = R' = *t*-Bu).

	6	**7**	**8**
Sn(1)–O(1)	1.9815(14)	2.020(4)	1.9687(13)
Sn(1)–C(1a)	2.125(2)	2.135(6)	2.1361(17)
Si(1)–O(1)	1.6264(15)	1.610(4)	1.6072(13)
Sn(1)–C(11)	2.137(2)	2.141(6)	2.1739(18)
Sn(1)–C(21)	2.137(2)	2.136(6)	2.1746(19)
Sn(1)–N(14)	–	2.766(6)	–
O(1)–Sn(1)–C(1a)	103.71(8)	101.8(2)	105.84(7)
O(1)–Sn(1)–C(11)	106.62(7)	93.2(2)	100.41(6)
O(1)–Sn(1)–C(21)	102.84(7)	99.8(2)	108.76(7)
C(1a)–Sn(1)–C(11)	118.33(9)	119.0(3)	110.10(7)
C(1a)–Sn(1)–C(21)	113.91(8)	116.8(2)	113.53(7)
C(11)–Sn(1)–C(21)	109.76(8)	118.1(3)	116.81(7)
Sn(1)–O(1)–Si(1)	137.52(8)	140.7(2)	152.29(9)
Sn(1)–C(1a)–Si(1A)	113.86(11)	116.1(3)	117.89(9)
N(14)–Sn(1)–O(1)	–	166.94(17)	–
N(14)–Sn(1)–C(1a)	–	88.7(2)	–
N(14)–Sn(1)–C(11)	–	74.7(2)	–
N(14)–Sn(1)–C(21)	–	82.1(2)	–

The *cyclo*-stannasiloxanes **6**–**8** can be viewed as centrosymmetric compounds, where one half of the molecule comprises the crystallographic asymmetric unit and the other half is generated by an inversion center. The torsion angles within the eight-membered rings in compounds **6**–**8** are listed in Table 3 showing the consequence (+, +, –, +, –, –, +, –) which is characteristic for chair conformation of *cyclo*-octane.[12]

The C(1), O(1), Si(1), C(1a), O(1a) and Si(1a) atoms in compounds **6** and **8** are nearly in the same plane and the Sn(1) and Sn(1a) atoms displaced in the opposite directions from this plane (Figure 5). Compound **7**, however, shows a ladder-like structure with two oxygen and two silicon atoms in one plane and each one tin atom and one carbon atom above and below the plane (Figure 5). All tin and silicon atoms in compounds **6** and **8** and the silicon atoms in **7** are four-coordinated and show

distorted tetrahedral geometry. The tin atoms in compound **7** can be seen as being [4+1]-coordinated, with three carbon atoms and one oxygen atom forming a distorted tetrahedron that is face-attacked by the N(14) atom at a N–Sn distance of 2.766(6) Å.

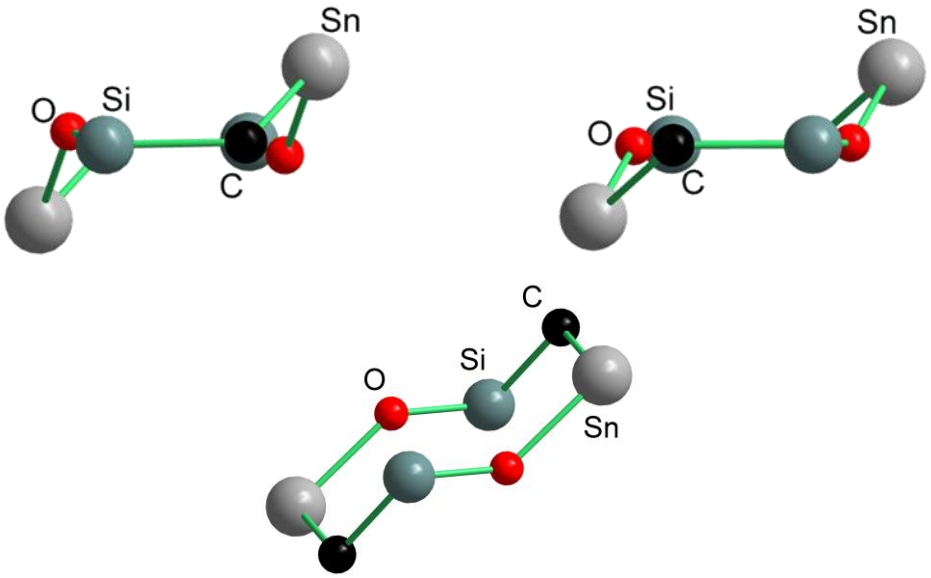

Figure 5. Reduced ball-and-sticks molecular structure of compounds **6** (above left), **8** (above right) and **7** (below). All atoms bound to the eight-membered rings were omitted for clarity.

Table 3. Torsion angles within the eight-membered rings in compounds **6**–**8**.

	6	**7**	**8**
Sn(1)–O(1)–Si(1)–C(1)	90.71(15)	–139.9(4)	–89.86(18)
O(1)–Si(1)–C(1)–Sn(1a)	23.27(15)	69.3(4)	–30.86(13)
Si(1)–C(1)–Sn(1a)–O(1a)	–66.99(13)	–22.9(4)	58.99(12)
C(1)–Sn(1a)–O(1a)–Si(1a)	137.64(13)	–89.0(4)	–132.80(17)

All bond lengths and bond angles in *cyclo*-$(Ph_2SnOMe_2SiCH_2)_2$, **6**, are comparable with the corresponding bond lengths and angles in *cyclo*-$(t\text{-}Bu_2SnOMe_2SiCH_2)_2$, **8**. These are in the same order of magnitude as those in the dicyclic stannasiloxane **H** (Chart 2).[13] The only exceptions are expressed in the Sn–O–Si angles of 137.52(8) in **6** and 152.29(9) in **8** being both bigger than the corresponding angles in compound **H** of 126.0(4) and 127.6(4). This angle in $Ph_3SiOSnPh_3$ of 144.2(6)[14] is bigger than the angle in **6** but smaller than that in **8**. Interestingly, the bond lengths in *cyclo*-$[\{Me_2N(CH_2)_3\}PhSnOMe_2SiCH_2]_2$, **7**, seem to not be affected by the N→Sn

interaction. They are rather similar to the corresponding distances found in compounds **6** and **8**. However, the bond angles differ slightly in order to approach the ideal angles in the trigonal bipyramidal configuration.

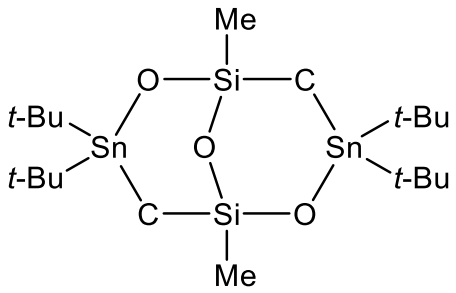

Chart 2. Schematic drawing of the dicyclic stannasiloxane **H**.[13]

The axial O–Sn–N angle in compound **7** of 166.94(17)° is smaller than the ideal value in the trigonal bipyramid of 180°. The carbon atoms are displaced toward the axial oxygen atom making the N–Sn–C angles smaller than 90° being between 74.7(2)° and 88.7(2)°. The O–Sn–C angles are between 93.2(2)° and 101.8(2)° in compound **7** being smaller than the corresponding angles in compounds **6** (102.84(7)°–106.62(7)°) and **8** (100.41(6)°–108.76(7)°). The Sn–O bond lengths in compounds **6**–**8** range between 1.9687(13) and 2.020(4) Å, and the Si–O bond lengths are between 1.6072(13) and 1.6264(15) Å.

3.2.2 Syntheses of the six-membered stannasiloxane *cyclo*-[$Me_2SiCH_2(Ph_2)SnO(t\text{-}Bu_2)SnO$], 9, and the related organotinoxo clusters

Reaction of the stannasiloxane *cyclo*-$(Ph_2SnMe_2OSiCH_2)_2$, **6**, with one, two and four molar equivalents di-*tert*-butyltin oxide, respectively, at room temperature afforded, upon insertion of the oxide in the kinetically labile Sn–OSi bond, and regardless of the stoichiometric ratio applied, the six-membered stannasiloxane *cyclo*-[$Me_2SiCH_2(Ph_2)SnO(t\text{-}Bu_2)SnO$], **9** (Scheme 2). Compound **9** contains two differently substituted tin atoms. The first *cyclo*-stannasiloxane with two differently substituted tin atoms *cyclo*-[$Ph_2SiO(R_2)SnO(t\text{-}Bu_2)SnO$], R = $Me_2N(CH_2)_3$, was reported in 1999 by Jurkschat et al. by the reaction of *cyclo*-$(Ph_2SiOR_2SnO)_2$ with di-*tert*-butyltin oxide.[11] The ^{119}Sn NMR spectrum of compound **9** in $CDCl_3$ showed two equally intense

singlet resonances at δ –13 (OPh$_2$*Sn*CH$_2$) and at δ –93 (O*t*-Bu$_2$*Sn*O) with ^2J(^{119}Sn–$^{117/119}$Sn) coupling constant of 317/335 Hz for each resonance (Figure 6). The ^{29}Si NMR spectrum displayed a single resonance at δ 5.9 with ^2J(^{29}Si–$^{117/119}$Sn) couplings of 43 and 49 Hz (Table 6).

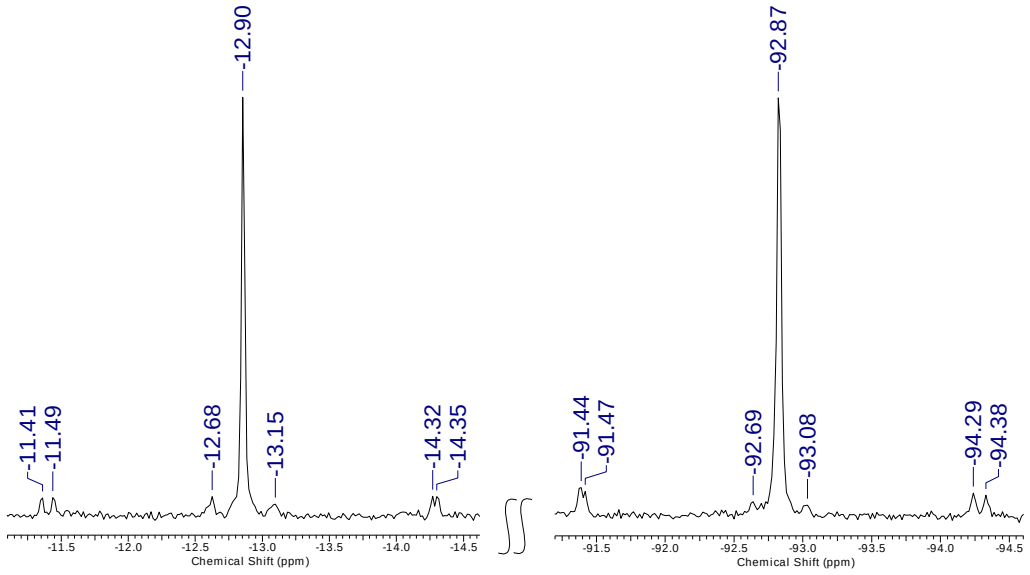

Figure 6. Expansion of the signals related to compound **9** in the ^{119}Sn{^{1}H} NMR spectrum (111.91 MHz, 298 K) measured in CDCl$_3$.

The ESI MS spectrum of compound **9** shows a major mass cluster centered at *m/z* 611.1 which fits with the protonated compound [**9**+H]$^+$. Compound **9** show good solubility in dichloromethane and chloroform.

Recrystallization of **9** by slow evaporation of a solution of the compound in CH$_2$Cl$_2$/hexane in aerobic conditions gave, as the mixture was dried, a few single crystals suitable for X-ray diffraction analysis of the ladder-type dimeric tetraorganodistannoxane [PhSn(CH$_2$Me$_2$SiO)Sn(μ_3-O)(μ-OH)*t*-Bu$_2$]$_2$, **10**. This is a result of Sn–C$_{Ph}$ bond cleavage in presence of moist air. *Chandrasekhar* et al. reported before on Sn–C$_{Ph}$ bond cleavage as the reaction of the diorganotin dichloride Ph$_2$SnCl$_2$ with cycPO$_2$H (1,1,2,3,3-pentamethyltrimethylenephosphinic acid) gave the monoorganotinoxo cluster [(PhSn)$_3$(μ_3-O)(μ-*cyc*PO$_2$)$_3$(μ-OH)$_3$][cycPO$_2$].

Compound **10** is a high melting solid (mp 266–270°C) that is soluble in CH$_2$Cl$_2$ and chloroform.

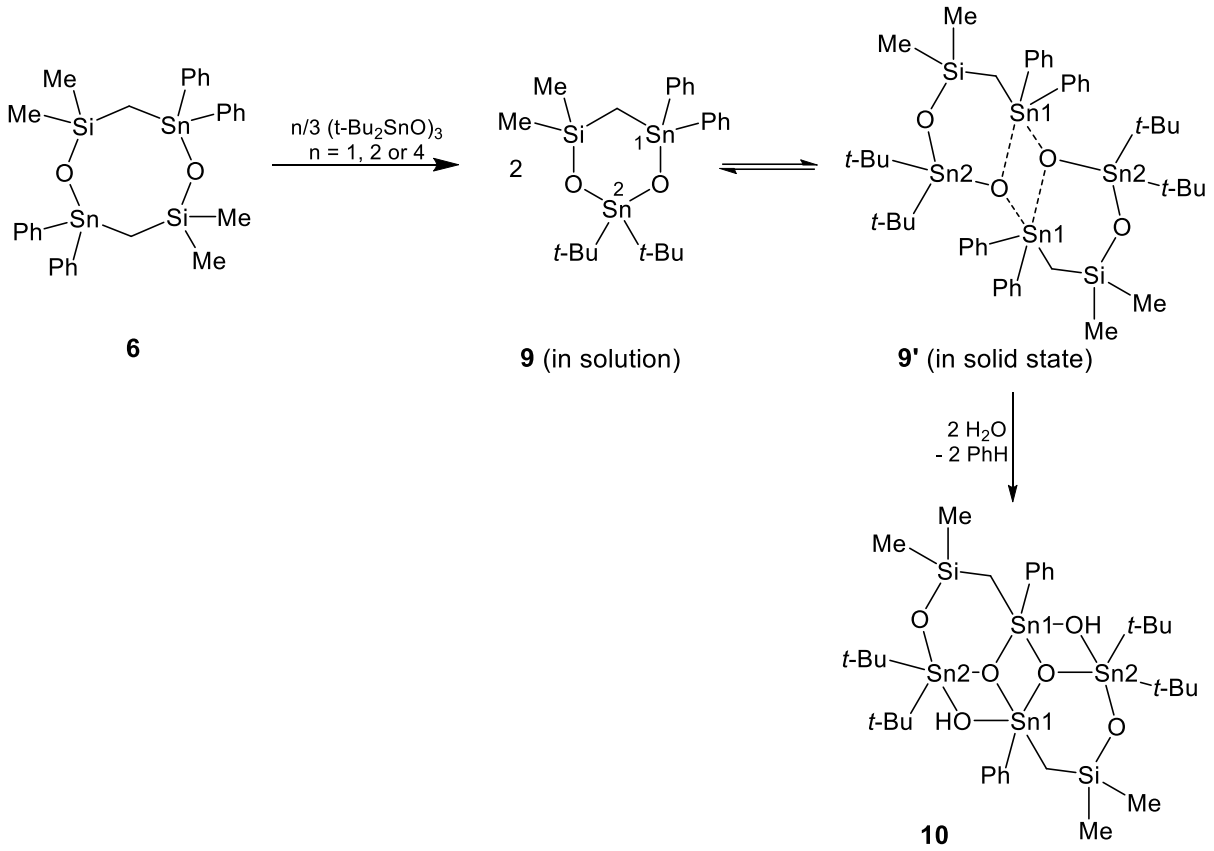

Scheme 2. Synthesis of compound **9** and its hydrolysis in moist air to give the ladder-type diorganotinoxo cluster **10**.

In attempt to synthesize compound **10**, a solution of **9** in CH_2Cl_2 was stirred for a few days at room temperature in the presence of catalytic amount water, but surprisingly no reaction was observed. Then compound **9** was dried and kept for a few weeks in moist air before ^{29}Si and ^{119}Sn NMR spectra were recorded. The ^{29}Si NMR spectrum showed two signals, at δ 8.6 for the eight-membered *cyclo*-stannasiloxane **6**, and at δ –2.4 with $^{2}J(^{29}Si–^{117/119}Sn)$ of 40 and 69 Hz. The corresponding ^{119}Sn NMR spectrum shows resonances at δ –219 and –260 that are characteristic for penta-coordinated tin atoms found in ladder-type diorganotinoxo clusters.[15] The signal at δ –219 [$^{2}J(^{119}Sn_{endo}–^{29}Si)$ = 41 Hz, $^{2}J(^{119}Sn_{endo}–^{117/119}Sn_{exo})$ = 228/242 Hz, $^{2}J(^{119}Sn_{endo}–^{117}Sn_{endo})$ = 82 Hz] could be related to the endo-cyclic tin atom (Sn1) in compound **10**, however that at δ –260 [$^{2}J(^{119}Sn_{exo}–^{29}Si)$ = 71 Hz, $^{2}J(^{119}Sn_{exo}–^{117/119}Sn_{endo})$ = 228/242 Hz, $^{4}J(^{119}Sn_{exo}–^{117}Sn_{exo})$ = 84 Hz] was assigned to the exo-cyclic one (Sn2) (Figure 7). In addition, a resonance at δ –31 (compound **6**, 23%) and five uncertain signals at –38 (11%), –54 (6%), –25 (1%), –44 (1%) and –60 (1%) were observed in

the ^{119}Sn NMR spectrum. The last five signals are supposed to be related to the hydrolyses products that contain the *t*-Bu$_2$Sn moiety as they do not have corresponding signals in ^{29}Si NMR spectrum and keeping in mind that compound **6** was observed in ^{29}Si and ^{119}Sn NMR spectra.

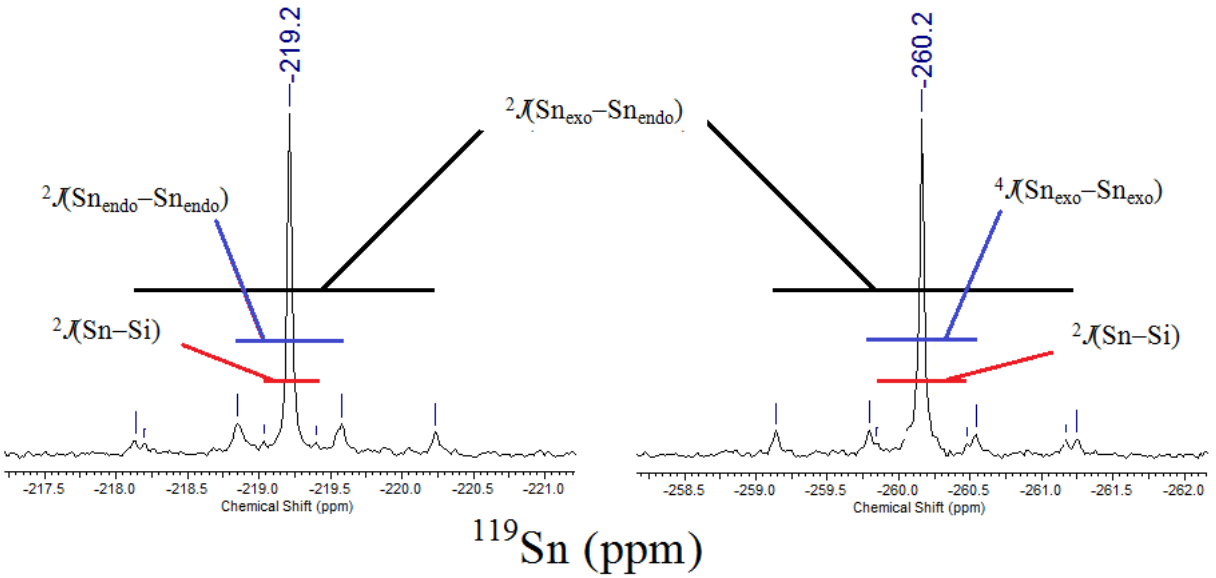

Figure 7. Expansion of the signals related to compound **10** in the ^{119}Sn{^{1}H} NMR spectrum (111.92 MHz, 294 K) measured in $CDCl_3$.

We suppose that the cleavage of Sn–C$_{Ph}$ bond is forced by activation of Sn1 in **9** in term of O→Sn molecular interaction. For this reason we assume that compound **9** presents as dimer in the solid state as the distance O→Sn will be smaller, and consequently the activation of Sn1 will be stronger, in the flexible twelve-membered ring in the dimeric structure of **9** in comparison to that in the rigid six-membered ring in the monomeric structure. The rearrangement of the six-membered cyclic stannasiloxanes upon recrystallization giving the corresponding twelve-membered rings was also described for *cyclo*-[R$_2$Sn(OPh$_2$Si)$_2$O]$_n$ (R=CpFeC$_5$H$_4$).[5a] Activation of the tin atom (Sn1) in the six-membered stannasiloxane **9** in term of intermolecular O→Sn interaction is another possibility for the cleavage of Sn–C$_{Ph}$ bond in presence of moist air giving compound **10**. The intermolecular O→Sn interaction vanish upon dilution (in solution), explaining why stirring a solution of compound **9** in presence of water does not afford compound **10**.

Interestingly, when $CDCl_3$ was allowed to evaporate slowly from a solution of **9** (93%), **6** (4%) and *t*-Bu_2SnO (3%) in closed NMR-tube a few single crystals of the ladder-like hydrolysis product [*t*-Bu_2(μ-OH)Sn(μ_3-O)SnPh(CH_2Me_2SiO)Sn*t*-Bu_2(μ_3-O)]$_2$, **11**, suitable for X-ray diffraction analysis were isolated (for molecular structure see below). Compound **11** is built by insertion of two *t*-Bu_2SnO moieties in the labile Sn–OH bonds in **10** (Scheme 3).

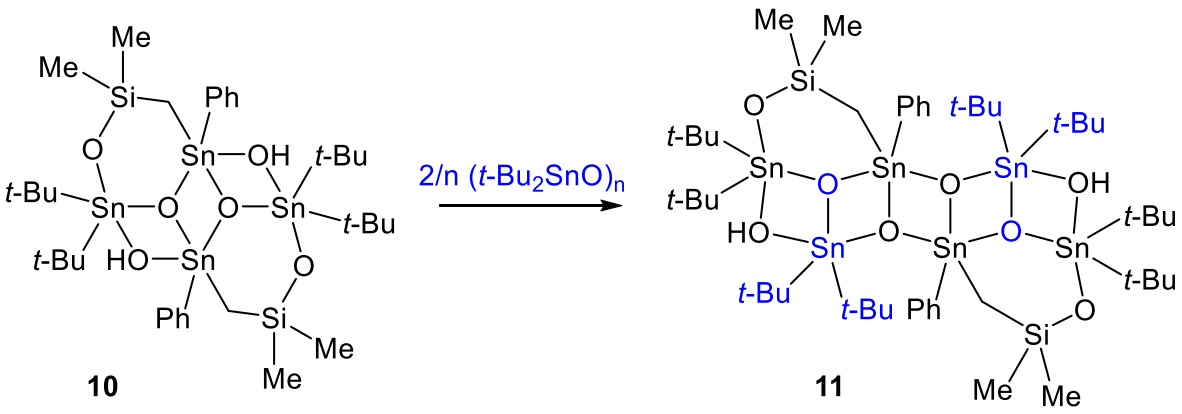

Scheme 3. Reaction of compound **10** with di-*tert*-butyltin oxide providing the Sn_6-diorganotinoxo cluster **11**.

3.2.2.1 Molecular structures of the ladder-like diorganotinoxo clusters 10 and 11

The compounds **10** and **11** crystallized in the monoclinic space groups P 2/n 1 and P 2_1/n respectively, with two molecules in the unit cell. The molecular structures of compounds **10** and **11** are shown in Figures 8 and 9, respectively, and selected bond lengths and bond angles are summarized in Tables 4 and 5 respectively.

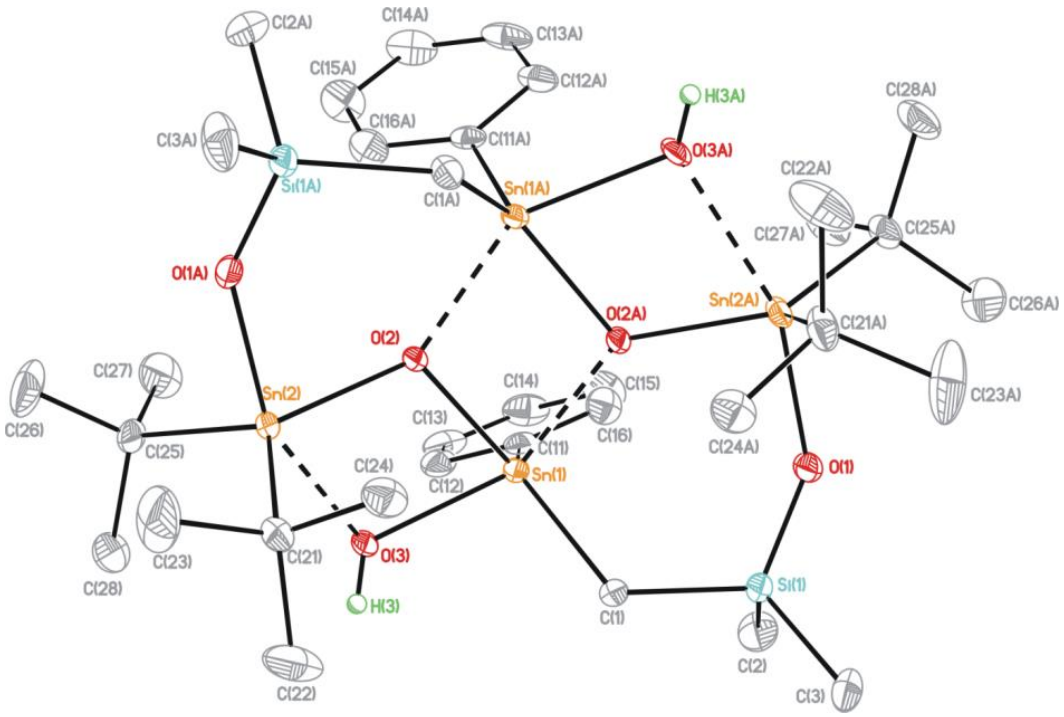

Figure 8. General view (SHELXTL) of a molecule of **10** showing 30% probability displacement ellipsoids and the crystallographic numbering scheme. Carbon-bound hydrogen atoms are omitted for clarity.

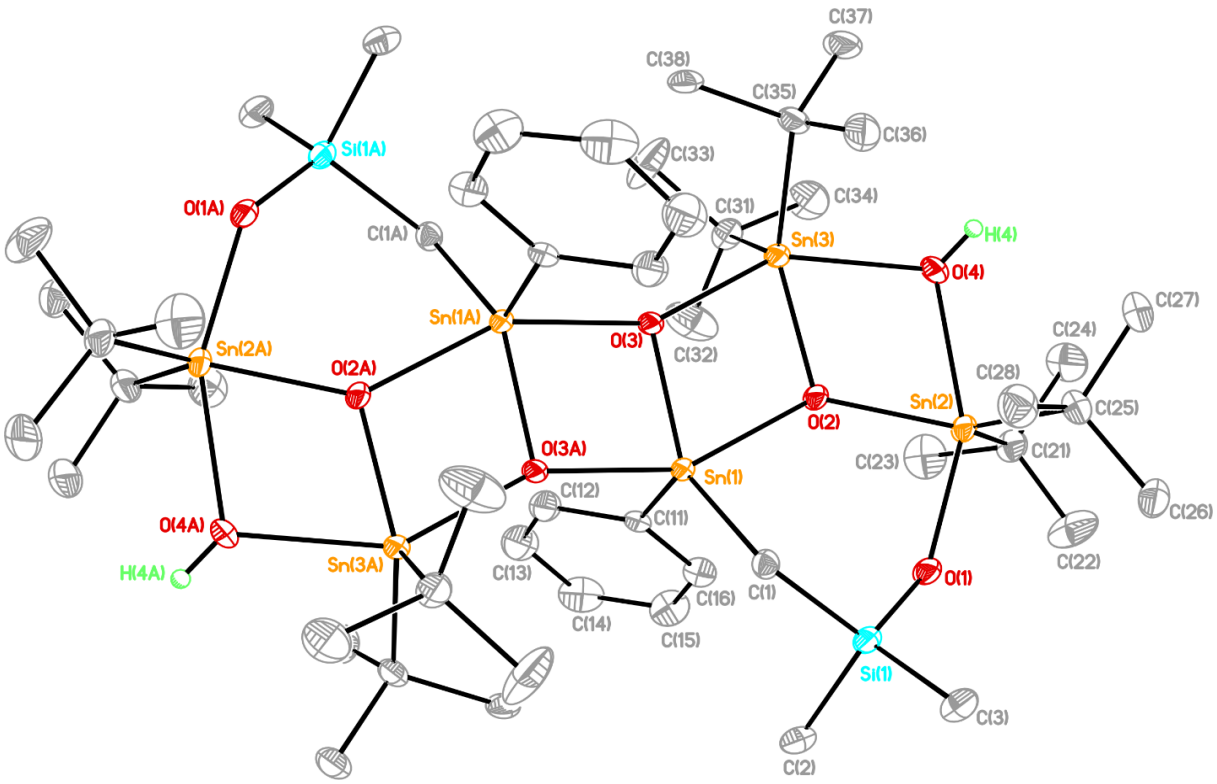

Figure 9. General view (SHELXTL) of a molecule of **11** showing 30% probability displacement ellipsoids and the crystallographic numbering scheme. Carbon-bound hydrogen atoms are omitted for clarity.

Table 4. Selected bond lengths (Å) and bond angles (deg) in **10**.

Sn(1)–O(2)	2.0344(17)	Sn(2)–O(2)	2.0329(16)
Sn(1)–O(2A)	2.1266(16)	Sn(2)–O(3)	2.301(2)
Sn(1)–O(3)	2.0936(18)	Sn(2)–O(1A)	2.0253(18)
Sn(1)–C(1)	2.119(3)	Sn(2)–C(21)	2.167(3)
Sn(1)–C(11)	2.123(3)	Sn(2)–C(25)	2.165(3)
Si(1)–O(1)	1.5993(19)		
O(3)–Sn(1)–O(2A)	146.87(7)	O(3)–Sn(2)–O(2)	69.22(7)
O(3)–Sn(1)–O(2)	73.54(7)	O(3)–Sn(2)–C(21)	94.60(10)
O(3)–Sn(1)–C(1)	99.68(9)	O(3)–Sn(2)–C(25)	90.60(10)
O(3)–Sn(1)–C(11)	99.25(10)	O(1A)–Sn(2)–O(2)	87.32(7)
O(2A)–Sn(1)–O(2)	74.30(7)	O(1A)–Sn(2)–C(21)	99.80(10)
O(2A)–Sn(1)–C(1)	93.59(8)	O(1A)–Sn(2)–C(25)	98.04(9)
O(2A)–Sn(1)–C(11)	98.78(9)	O(2)–Sn(2)–C(21)	113.29(9)
O(2)–Sn(1)–C(1)	127.54(9)	O(2)–Sn(2)–C(25)	122.73(10)
O(2)–Sn(1)–C(11)	109.68(9)	C(21)–Sn(2)–C(25)	121.58(11)
C(1)–Sn(1)–C(11)	122.67(11)	Sn(1)–C(1)–Si(1)	114.29(13)
O(3)–Sn(2)–O(1A)	155.92(7)	Sn(2A)–O(1)–Si(1)	143.13(11)

Table 5. Selected bond lengths (Å) and bond angles (deg) in **11**.

Sn(1)–O(2)	2.128(2)	Sn(2)–C(21)	2.191(4)
Sn(1)–O(3a)	2.141(2)	Sn(2)–C(25)	2.200(5)
Sn(1)–O(3)	2.040(3)	Sn(3)–O(4)	2.149(3)
Sn(1)–C(1)	2.119(4)	Sn(3)–O(3)	2.161(2)
Sn(1)–C(11)	2.121(5)	Sn(3)–O(2)	2.049(3)
Sn(2)–O(1)	2.060(3)	Sn(3)–C(31)	2.195(5)
Sn(2)–O(4)	2.273(3)	Sn(3)–C(35)	2.186(5)
Sn(2)–O(2)	2.035(2)	Si(1)–O(1)	1.612(3)
O(2)–Sn(1)–O(3a)	151.44(10)	O(3a)–Sn(1)–C(1)	97.64(12)
O(2)–Sn(1)–O(3)	74.62(10)	O(3a)–Sn(1)–C(11)	98.63(13)
O(2)–Sn(1)–C(1)	93.09(13)	O(3)–Sn(1)–C(1)	129.00(15)
O(2)–Sn(1)–C(11)	98.53(13)	O(3)–Sn(1)–C(11)	110.36(13)
O(3a)–Sn(1)–O(3)	78.07(11)	C(1)–Sn(1)–C(11)	120.45(16)

O(1)–Sn(2)–O(4)	156.15(10)	O(4)–Sn(2)–C(21)	93.28(15)
O(1)–Sn(2)–O(2)	86.92(10)	O(4)–Sn(2)–C(25)	94.14(16)
O(1)–Sn(2)–C(21)	97.42(15)	O(2)–Sn(2)–C(21)	118.06(14)
O(1)–Sn(2)–C(25)	98.14(15)	O(2)–Sn(2)–C(25)	118.41(14)
O(4)–Sn(2)–O(2)	69.24(11)	C(21)–Sn(2)–C(25)	121.88(17)
O(4)–Sn(3)–O(3)	141.87(11)	O(3)–Sn(3)–C(31)	105.52(14)
O(4)–Sn(3)–O(2)	71.54(11)	O(3)–Sn(3)–C(35)	99.52(13)
O(4)–Sn(3)–C(31)	100.78(14)	O(2)–Sn(3)–C(31)	110.09(15)
O(4)–Sn(3)–C(35)	93.83(14)	O(2)–Sn(3)–C(35)	134.66(15)
O(3)–Sn(3)–O(2)	73.74(9)	C(31)–Sn(3)–C(35)	114.81(19)
Sn(1)–O(2)–Sn(2)	137.16(13)	Sn(1)–O(2)–Sn(3)	105.66(10)
Sn(1)–O(3)–Sn(3)	104.75(10)	Sn(1)–O(3)–Sn(1a)	101.93(11)
Sn(2)–O(4)–Sn(3)	103.10(13)	Sn(2)–O(2)–Sn(3)	116.05(13)
Sn(3)–O(3)–Sn(1a)	153.32(14)	Si(1)–O(1)–Sn(2)	138.74(17)
Si(1)–C(1)–Sn(1)	113.8(2)		

Compounds **10** and **11** exist as ladder-type compounds that contain penta-coordinated tin atoms. They can be viewed as symmetric dimers as one half of the molecules comprise the crystallographic asymmetric unit and other half is generated by a C_2 proper axis (in compound **10**) or inversion center (in compound **11**). All tin atoms are five-coordinated. The endo-cyclic tin atoms have square pyramidal environment by two carbons and two oxygen atoms in the equatorial positions and one triply-bridging oxygen atom as the axial ligand (geometrical parameter[16] $\tau = 0.32$ for **10**, 0.37 and 0.12 for Sn(1) respectively Sn(3) in **11**). The exo-cyclic tin atoms exhibit distorted trigonal bipyramidal geometry with the equatorial positions being occupied by two carbons and one triply-bridging oxygen atom, and the axial positions by one silicon-bound oxygen atom and one μ_2 oxygen atom (geometrical goodness[17] $\Delta\Sigma(\theta)$ 72.4 for **10**, 75.9 for **11**). The Sn–O distances range between 2.0253(18) and 2.301(2) Å for **10** and between 2.035(2) and 2.273(3) for **11**. The Sn_{endo}–μ_2-O–Sn_{exo} bridges are asymmetric (**10**, Sn(1)–O(3) 2.0936(18) Å, Sn(2)–O(3) 2.301(2) Å; **11**, Sn(3)–O(4) 2.149(3) Å, Sn(2)–O(4) 2.273(3) Å). The silicon-containing substituents bound to the endo-cyclic tin atoms are trans in compound **10** but cis in **11** with respect to the central Sn_2O_2 ring.

Compound **10** can be viewed as one twelve-membered ring or two six-membered rings like those found in the dimer or the monomer structure of compound **9**, respectively, by replacing one phenyl group at the tin atoms with one hydroxyl group. The substitution enhances the Lewis acidity at the tin atom affording stronger O→Sn interactions, and consequently, a ladder-like structure results. The latter consists of three four-membered rings and two six-membered rings (Figure 10).

Compound **11**, on the other hand, comprises of two eight-membered rings [$Me_2SiCH_2(Ph)Sn(\mu_3\text{-}O)O(t\text{-}Bu_2)Sn(\mu\text{-}OH)Sn(t\text{-}Bu_2)$] like those described by Jurkschat[18] and Pannell[19] by replacing one oxygen atom with a carbon atom. These two rings are bridged via two O→Sn interactions giving also the ladder-like structure (Figure 9). The three tin atoms in the eight-membered rings are linked through one (μ_3-O) atom giving three smaller rings. Two four-membered rings that are nearly planar, and one six-membered ring which exhibits twist-boat conformation.

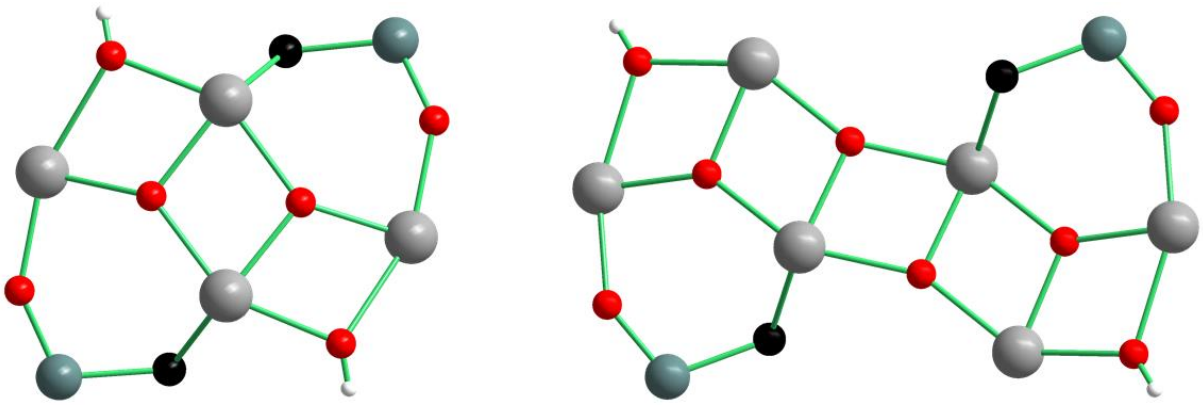

Figure 10. Reduced ball-and-sticks molecular structure of compounds **10** (left) and **11** (right). Tin is presented as gray circles, silicon as green circles, oxygen as red circles, carbon as black circles and hydrogen as white circles. The organic substituents are omitted for clarity.

No reactions were observed as compound **6** was stirred with the diorgano group 14 element oxides *cyclo*-$(Me_2SiO)_3$, $(Ph_2GeO)_n$ and Ph_2PbO in CH_2Cl_2 or hot chloroform, with the diorganotellurium oxide $(p\text{-}MeOC_6H_4)_2TeO$ in CH_2Cl_2, and with the poorly soluble diorganotin oxides $[Me_3SiCH_2Sn(O)]_2(CH_2)_8$, Me_2SnO and $n\text{-}Bu_2SnO$ in CH_2Cl_2 at ambient temperature or in toluene at reflux.

3.2.3 Syntheses of the six-membered metallasiloxanes *cyclo*-[Me_2SiCH_2(*t*-Bu_2)SnO(*t*-Bu_2)SnO], 12, and *cyclo*-[Me_2SiCH_2(*t*-Bu_2)SnO(*p*-$MeOC_6H_4)_2$TeO],13

Stirring a solution of the stannasiloxane *cyclo*-[*t*-$Bu_2SnOMe_2SiCH_2]_2$, **8**, with 2/3 (*t*-$Bu_2SnO)_3$ at ambient temperature showed, on the contrary of **6**, no reaction. However, refluxing the mixture in $CHCl_3$ for 5 hours provided the six-membered stannasiloxane *cyclo*-[Me_2SiCH_2(*t*-Bu_2)SnO(*t*-Bu_2)SnO], **12** (Scheme 4).

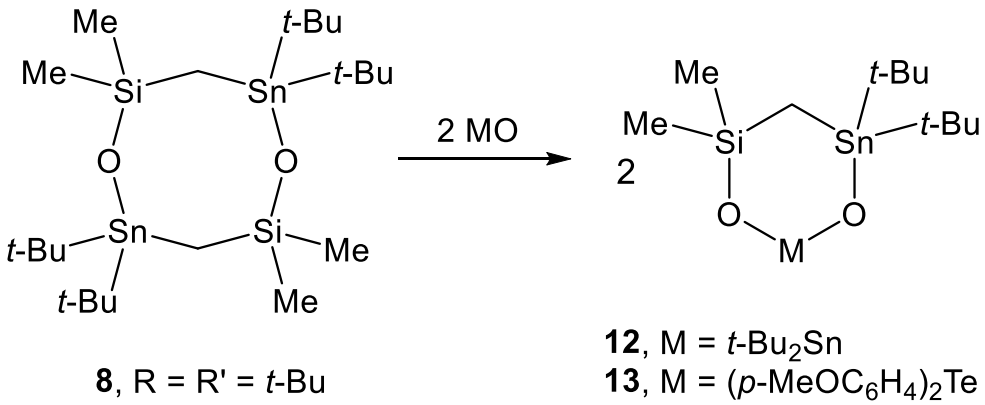

8, R = R' = *t*-Bu

12, M = *t*-Bu_2Sn
13, M = (*p*-$MeOC_6H_4)_2Te$

Scheme 4. Syntheses of compounds **12** and **13**.

A ^{119}Sn NMR spectrum of compound **12** in $CDCl_3$ showed two resonances, at δ 49 that is assigned to O(*t*-Bu_2)*Sn*CH_2, and δ –98 that corresponds to O(*t*-Bu_2)*Sn*O with $^2J(^{119}Sn–^{117/119}Sn)$ of 351/367 Hz for each tin atom (Figure 11).

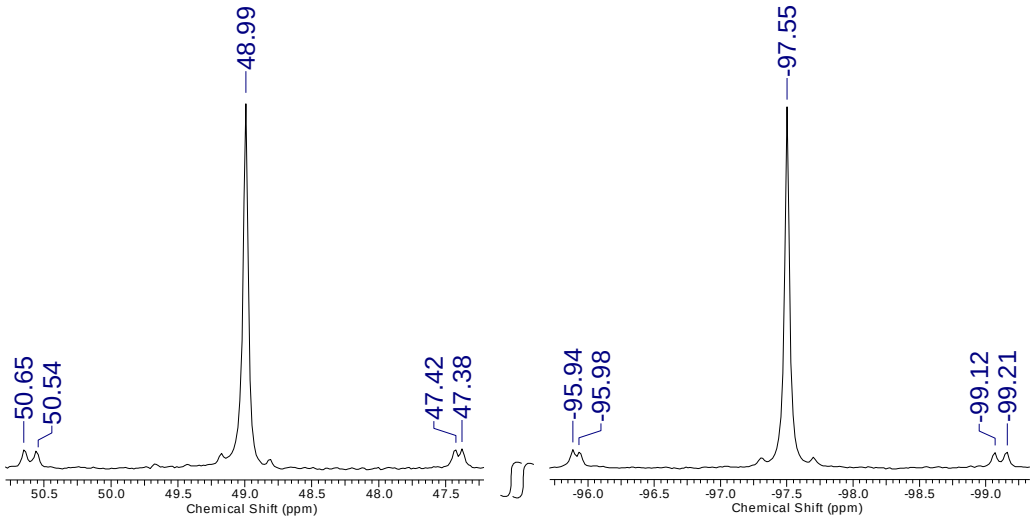

Figure 11. Expansion of the signals related to compound **12** in the $^{119}Sn\{^1H\}$ NMR spectrum (111.92 MHz, 297 K) measured in $CDCl_3$.

A ^{29}Si NMR spectrum displayed a resonance at δ 5.2 with $^{2}J(^{29}Si–^{117/119}Sn)$ couplings of 40 and 44 Hz (Table 5). The ESI MS spectrum in negative mode showed a major mass cluster centered at 587.1 that fits with [**12** + OH]$^{-}$. Compound **12** shows good solubility in CH_2Cl_2 and chloroform.

Stirring the stannasiloxane *cyclo*-[*t*-$Bu_2SnO(Me_2)SiCH_2]_2$, **8**, with two molar equivalents of Ph_2GeO in chloroform gave no reaction.

Table 6. Selected NMR data of compounds **9**, **12**, **16** and **17**.

	δ ^{29}Si (ppm)	$^{2}J(^{29}Si–^{117/119}Sn)$ (Hz)	δ ^{119}Sn (ppm)	$^{2}J(^{119}Sn–^{117/119}Sn)$ / $^{2}J(^{119}Sn–^{73}Ge)$* (Hz)
9	5.9	43, 49	–13, –93	317/335
12	5.2	40, 44	49, –98	351/367
16	6.5	40	–23, –89	292
17	10.7	42	–59	60*

No reaction was observed as a solution of compound **8** in $CHCl_3$ was stirred with two molar equivalents (*p*-$MeOC_6H_4)_2TeO$ at ambient temperature. The very poor solubility of the organotellurium oxide in chloroform at room temperature could be the reason for this. The reaction was repeated in refluxing toluene affording light yellowish filtrate and a white precipitate. The precipitate is not soluble in $CDCl_3$, benzene, and methanol and its elemental analysis does not consist with that for R_2TeO (R = *p*-$MeOC_6H_4$). After concentrating the filtrate a yellow viscous oil was obtained. The ^{29}Si-INEPT NMR spectrum of the latter showed three signals, one at δ 1.8 that is assigned to compound **8**, and two additional signals at δ 6.9 [$^{2}J(^{29}Si–^{117/119}Sn)$ = 41 Hz] and δ –10.3 [$^{2}J(^{29}Si–^{117/119}Sn)$ = 31 Hz]. The integral of the last two signals were almost equal also after repeating the reaction with longer refluxing time (we should not take the integral in ^{29}Si-INEPT NMR spectra as evidence, but it could maybe give an overview). The ^{119}Sn NMR spectrum showed one relatively broad resonance at δ 35 ($v_{1/2}$= 2.2 Hz, *J* = 32 and 41 Hz) that is only 1 ppm high-frequency shifted with respect to that in compound **8** (δ 34). The signal pattern in ^{119}Sn NMR spectrum suggests the presence of two overlapped signals at 34.84 (*J* = 41) and 34.82 (*J* = 31). An ESI MS spectrum of the filtrate in positive mode showed three major mass clusters at *m/z* 451.0 for [R_2TeO + 5 H_2O + H]$^{+}$, 697.1 for the protonated and

hydrated six-membered ring *cyclo*-[Me_2SiCH_2(*t*-Bu_2)SnO(*p*-$MeOC_6H_4$)$_2$TeO], **13** (Chart 3), and 1019.2 for the protonated and hydrated ten-membered ring [Me_2SiCH_2(*t*-Bu_2)SnO($MeOC_6H_4$)$_2$TeO(Me_2)$SiCH_2$(*t*-Bu_2)SnO], **14**, (Chart 3). Compound **14** results from insertion of one molecule of the organotellurium oxide in the labile Sn–OSi bond in the eight-membered ring **8**. In negative mode, a mass cluster centered at m/z 733.1 that is assigned to [**13** + 2 H_2O + OH]$^-$ was observed.

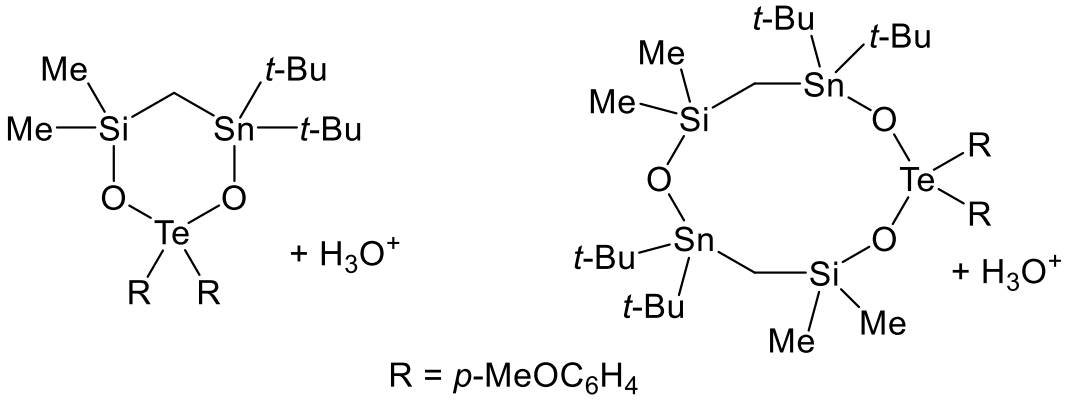

R = *p*-$MeOC_6H_4$

m/z 697.1 *m/z* 1019.2

Chart 3.

The ESI MS spectra confirm the presence of the six-membered *cyclo*-tellurosiloxane **13**, which could not be separated clean. We have no straightforward explanation for the presence of two resonances in the ^{29}Si NMR spectrum. One suggestion is that compound **8** reacts with R_2TeO giving the six-membered ring **13** and its dimeric structure the twelve-membered ring **13a**, as it is known that tellurium is able to build larger rings, and the chemical shift in the ^{29}Si NMR spectrum depends on the ring size. However, this possibility does not explain why the integrals of both resonances are equal.

Recording the ^{119}Sn NMR spectrum of the latter reaction mixture in $CDCl_3$ after 1–2 months showed a new resonance at δ –259 (integral approx 25). Slow evaporation of the solvent in the NMR tube afforded few single crystals of [{(*p*-$MeOC_6H_4$)$_2$TeOSn(*t*-Bu_2)CO_3}$_2$]·2$CHCl_3$, **15**. This is a result of hydrolysis cleavage of Sn–CH_2Si bonds followed by fixation of CO_2 molecule between the Lewis acidic tin and tellurium atoms. Compound **15** was reported before by Beckmann et al. by the reaction of *t*-Bu_2SnO with R_2TeO (R = *p*-$MeOC_6H_4$) in presence of gaseous CO_2, or when a (*t*-$Bu_2SnO)_3$/(*p*-$MeOC_6H_4$)$_2$TeO solution was exposed for several days to air.[20]

Compound **15** crystallized in the monoclinic space group P 2_1/c with two molecules in the unit cell. The molecular structure of compound **15** is shown in Figure 12 and the selected bond lengths and bond angles are given in the Appendix (Table C4).

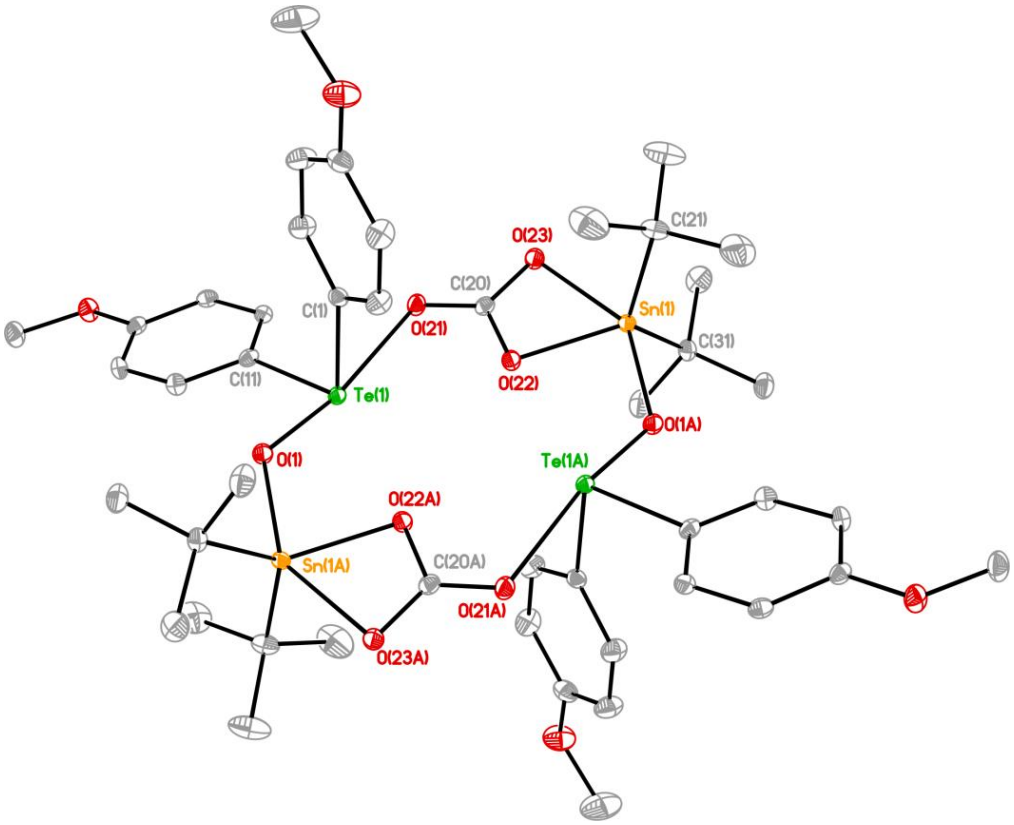

Figure 12. General view (SHELXTL) of a molecule of **15** showing 30% probability displacement ellipsoids and the crystallographic numbering scheme. Hydrogen atoms and chloroform solvate molecules were omitted for clarity.

3.2.4 Syntheses of the six-membered metallasiloxanes *cyclo*-[Me_2SiCH_2{$Me_2N(CH_2)_3$}PhSnO(*t*-Bu_2)SnO], 16, and *cyclo*-[Me_2SiCH_2{$Me_2N(CH_2)_3$}PhSnO(Ph_2)GeO], 17

The reaction of the eight-membered intramolecularly coordinated stannasiloxane *cyclo*-[{$Me_2N(CH_2)_3$}PhSnOMe_2SiCH_2]$_2$, **7** with 2/3 molar equivalents *cyclo*-(*t*-$Bu_2SnO)_3$ at ambient temperature provided the six-membered *cyclo*-stannasiloxane *cyclo*-[Me_2SiCH_2(*t*-Bu_2)SnO(*t*-Bu_2)SnO], **16** (Scheme 5). Compound **16** contains two *t*-Bu_2Sn moieties that are connected to one silicon atom by oxygen or carbon bridges.

Furthermore, the reaction of compound **7** with diphenylgermanium oxide, Ph_2GeO, in chloroform at reflux afforded the first six-membered *cyclo*-metallasiloxane *cyclo*-[Me_2SiCH_2(*t*-Bu_2)SnO(Ph_2)GeO], **17**, being composed of four different group 14 elements (Scheme 5).

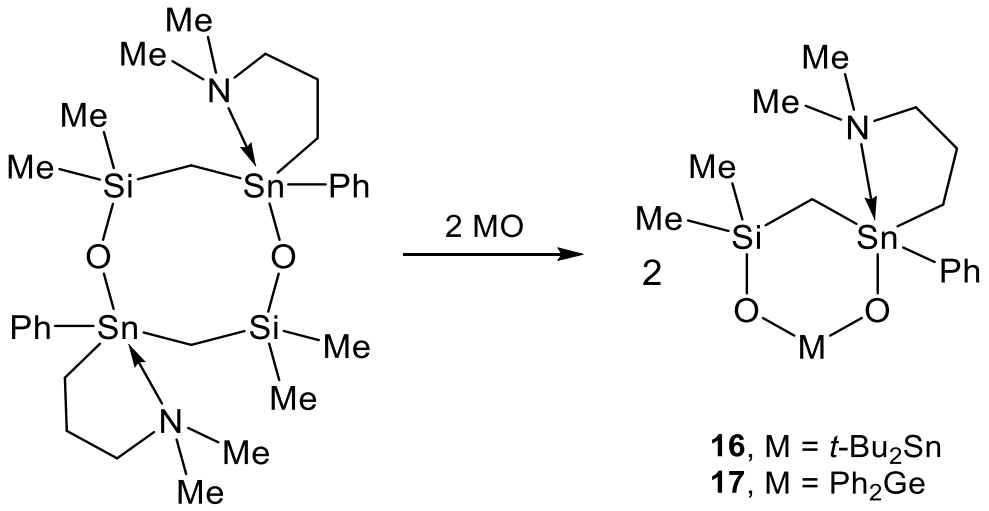

Scheme 5. Syntheses of compounds **16** and **17**.

A ^{119}Sn NMR spectrum of a solution of compound **16** in $CDCl_3$ showed two resonances, at δ –23 (^2J(^{119}Sn–$^{117/119}$Sn) = 292 Hz) assigned to O(RPh)*Sn*CH_2Si (R = $Me_2N(CH_2)_3$), and δ –89 (^2J(^{119}Sn–$^{117/119}$Sn) = 293 Hz) that corresponds to O(*t*-Bu_2)*Sn*O. The ^{29}Si NMR spectrum of the same solution showed a resonance at δ 6.5 [^2J(^{29}Si–$^{117/119}$Sn) = 40 Hz].

On the other hand, the ^{29}Si NMR spectrum of compound **17** shows a singlet at δ 10.7 [^2J(^{29}Si–$^{117/119}$Sn) = 42 Hz], and the ^{119}Sn NMR spectrum displays a single resonance at δ –59 [^2J(^{119}Sn–^{29}Si) = 43 Hz, ^2J(^{119}Sn–^{73}Ge) = 60 Hz] (Figure 13).

Heating compound **7** and R_2TeO (R=*p*-$MeOC_6H_4$) in chloroform at reflux showed no reaction.

The reason for these observations is foreseen be the ring strain in the cyclic compounds, as the release of the ring strain is normally the thermodynamic driving force of this type of reactions.

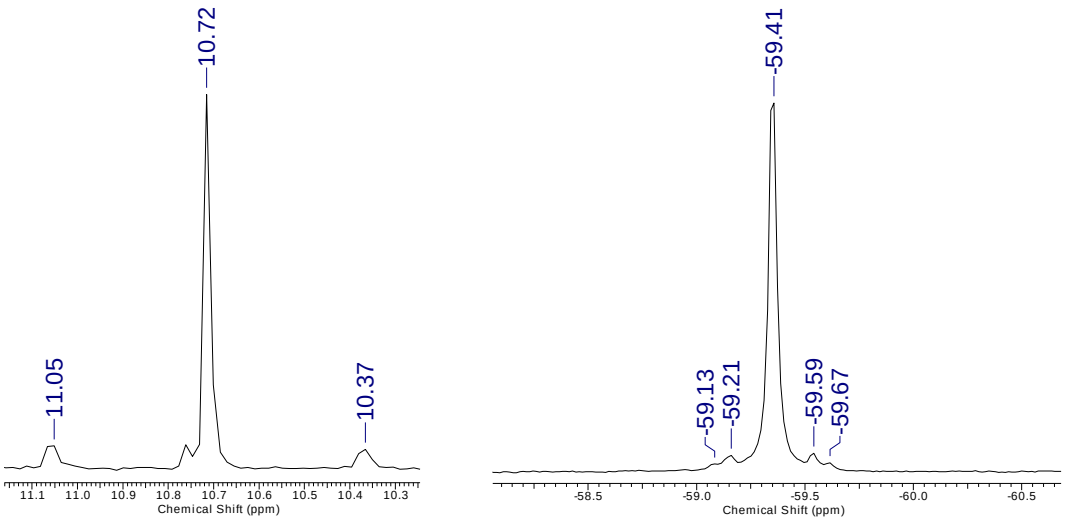

^{29}Si NMR spectrum

^{119}Sn NMR spectrum

Figure 13. Expansion of the signals related to compound **17** in the $^{29}Si\{^{1}H\}$ and $^{119}Sn\{^{1}H\}$ NMR spectra measured in $CDCl_3$.

3.3 Conclusion

A series of novel eight membered stannasiloxanes *cyclo*-$(RR'SnOMe_2SiCH_2)_2$ (**6**, R = R' = Ph; **7**, R = $Me_2N(CH_2)_3$, R' = Ph; **8**, R = R' = *t*-Bu) were synthesized and completely characterized. Changing the organic substituents bound at the tin atom affects the chemical reactivity of the resulting eight-membered rings. Compound **6**, which has two phenyl groups bound at the tin atom, reacts rapidly at room temperature with *t*-Bu_2SnO providing the six-membered stannasiloxane *cyclo*-$[Me_2SiCH_2(Ph_2)SnO(t\text{-}Bu_2)SnO]$, **9**. No reaction was observed as a solution of compound **6** was stirred with a variety of different diorganoelement oxides at different reaction conditions. On contact with air moisture, compound **9** surprisingly undergoes $Sn–C_{Ph}$ bond cleavage to give the ladder-like diorganotinoxo cluster $[PhSn(CH_2Me_2SiO)(\mu_3\text{-}O)Sn(\mu\text{-}OH)t\text{-}Bu_2]_2$, **10**. The latter reacts with two molar equivalents *t*-Bu_2SnO affording the Sn_6 diorganotinoxo cluster $[(t\text{-}Bu_2)(\mu\text{-}OH)Sn(\mu_3\text{-}O)Sn(Ph)(CH_2Me_2SiO)Sn(t\text{-}Bu_2)(\mu_3\text{-}O)]_2$, **11**. The eight-membered stannasiloxane **8**, containing two *t*-butyl groups bound at the tin atom, does not react with *t*-Bu_2SnO at ambient temperature. However, it reacts in $CHCl_3$ at reflux providing the six-membered stannasiloxane *cyclo*-$[Me_2SiCH_2(t\text{-}Bu_2)SnO(t\text{-}Bu_2)SnO]$, **12**. The course of

the reaction between compound **8** and two molar equivalents (p-$MeOC_6H_4)_2TeO$ was also studied. The ESI MS spectrum of the product verifies the presence of the six-membered tellurasiloxane *cyclo*-[Me_2SiCH_2(t-Bu_2)SnO(p-$MeOC_6H_4)_2TeO$], **13**. However, the ^{29}Si NMR spectrum showed two equally intense signals. This fact could not be explained. Compound **13** could not be isolated from the reaction mixture. Reaction of the stannasiloxane *cyclo*-[{$Me_2N(CH_2)_3$}$PhSnOMe_2SiCH_2]_2$, **7**, with t-Bu_2SnO and Ph_2GeO provided the six-membered metallasiloxanes *cyclo*-[Me_2SiCH_2{$Me_2N(CH_2)_3$}PhSnOMO] (**16**, M = t-Bu_2Sn; **17**, M = Ph_2Ge). Compound **17** is the first six-membered ring being composed of four different group 14 elements in the ring skeleton. The *cyclo*-metallasiloxanes *cyclo*-[CH_2(RR')SnO(Me_2)$Si]_2$ (**6**–**8**) and *cyclo*-[Me_2SiCH_2(RR')SnOMO] (**9**, **12**, **13**, **16**, and **17**) can be interpreted as model compounds for structurally modified silica surfaces. They also hold potential as single source precursors for new inorganic polymers and structurally modified polysiloxanes by the so-called Ring-Opening Polymerization.[5a]

3.4 Experimental Section

General Considerations

All solvents were purified by distillation under argon from appropriate drying agents, if not otherwise stated. $Me_2(i\text{-}PrO)SiCH_2Cl$,[21] $Me_2N(CH_2)_3Cl$,[22] $t\text{-}Bu_2SnCl_2$,[23] $(t\text{-}Bu_2SnO)_3$,[24] $(p\text{-}MeOC_6H_4)_2TeO$,[25] were synthesized according to literature methods. Ph_2GeO was synthesized by modified procedure of that described in the literature.[26] Triphenyltin chloride and diphenylgermanium dichloride were commercially available, and they were used without further purification. Bruker DPX-300 and DRX-400 spectrometers were used to obtain ^{1}H, ^{13}C, ^{29}Si, and ^{119}Sn NMR spectra at ambient temperature. Solution ^{1}H, ^{13}C, ^{29}Si-INEPT, and ^{119}Sn NMR chemical shifts are given in ppm and were referenced to Me_4Si (^{1}H, ^{13}C, ^{29}Si), and Me_4Sn (^{119}Sn). Elemental analyses were performed on a LECO–CHNS–932 analyzer. No elemental analysis were performed for compounds that are oils. The electrospray mass spectra were recorded with a Thermoquest–Finnigan instrument, using CH_3CN or CH_2Cl_2 as the mobile phase.

Synthesis of diphenylgermanium oxide, Ph_2GeO

A solution of sodium hydroxide (300 mg, 7.5 mmol) in water (15 mL) and ethanol (10 mL) was added to a solution of Ph_2GeCl_2 (280 mg, 0.94 mmol) in CH_2Cl_2 (15 mL) and the mixture was stirred for 3 days at room temperature before CH_2Cl_2 and ethanol were evaporated. The residue was extracted with CH_2Cl_2. The organic phase was separated and CH_2Cl_2 was evaporated to give Ph_2GeO (0.21 g, 92%) as white solid of mp 148 °C.

Anal. Calcd for $C_{12}H_{10}OGe$ (242.85 g/mol): C, 59.35; H, 4.15. Found: C, 59.5, H, 4.2.

^{1}H NMR (400.13 MHz, C_6D_6): δ 7.30–7.63 (m, 10H, Ar H). **$^{13}C\{^{1}H\}$ NMR** (75.48 MHz, C_6D_6): δ 128.2 (C_m), 130.3 (C_p), 133.6 (C_o), 135.9 (C_i). **Electrospray MS**: *m/z* (%), positive mode, 729.0 (100, $[(Ph_2GeO)_3 + H]^+$), 285.9 (67, $[Ph_2GeO + MeCN + H]^+$), 487.0 (32, $[(Ph_2GeO)_2 + H]^+$), 527.0 (20, $[(Ph_2GeO)_2 + H_2O + Na]^+$), 769.1 (20, $[(Ph_2GeO)_3 + 2H_2O + 2MeCN - Ph]^+$), 568.0 (18, $[(Ph_2GeO)_2 + H_2O + MeCN + Na]^+$), 895.0 (11, $[(Ph_2GeO)_4 - Ph]^+$), 973.0 (3, (32, $[(Ph_2GeO)_4 + H]^+$).

Synthesis of $Me_2(i\text{-}PrO)SiCH_2SnPh_3$, 1

A solution of triphenyltin chloride (104.08 g, 270 mmol) in THF (350 mL) was added drop-wise to the Grignard reagent prepared from $Me_2(i\text{-}PrO)SiCH_2Cl$ (50.02 g, 300 mmol) and magnesium turnings (8.02 g, 330 mmol) in THF (230 mL) and the mixture was stirred overnight at room temperature. The mixture was then heated at reflux for one hour before it was cooled to room temperature and the solvent was evaporated in vacuo. The viscous oil obtained was extracted in a soxhlet extractor using hexane as a solvent. After evaporating the solvent compound **1** (121.30 g, 93%) was obtained as colorless liquid.

^{1}H NMR (300.13 MHz, C_6D_6): δ 0.16 (s, 6H, *Me*$_2$Si), 0.55 (s, 2H, $^2J(^1H–^{117/119}Sn)$ = 75.1/77.2 Hz, SiC*H*$_2$Sn), 1.08 (d, 6H, $^3J(^1H–^1H)$ = 5.8 Hz, *Me*$_2$CH), 3.87 (m, 1H, C*H*O), 7.27–7.77 (m, 15H, Ar H). **^{13}C{^{1}H} NMR** (75.48 MHz, C_6D_6): δ –3.7 ($^1J(^{13}C–^{29}Si)$ = 60 Hz, $^1J(^{13}C–^{117/119}Sn)$ = 258/270 Hz, Si*C*H$_2$Sn), 1.9 ($^1J(^{13}C–^{29}Si)$ = 58 Hz, $^3J(^{13}C–^{117/119}Sn)$ = 12 Hz, *Me*$_2$Si), 26.3 (*Me*$_2$CH), 65.51 (*C*HO), 129.0 (C_m), 129.4 (C_p), 137.8 ($^2J(^{13}C–^{117/119}Sn)$ = 38 Hz, C_o), 140.5 ($^1J(^{13}C–^{117/119}Sn)$ = 488/512 Hz, C_i). **^{29}Si{^{1}H} NMR** (59.63 MHz, C_6D_6): δ 14.2 ($^2J(^{29}Si–^{117/119}Sn)$ = 25 Hz, $^2J(^{29}Si–^{13}C)$ = 57 Hz). **^{119}Sn{^{1}H} NMR** (111.92 MHz, C_6D_6): δ –89 ($^1J(^{119}Sn–^{13}C_{CH2})$ = 271 Hz, $^1J(^{119}Sn–^{13}C_{Ph})$ = 513 Hz). **Electrospray MS**: *m/z* (%), positive mode, 405.1 (100, $[M – Ph]^+$), 446.1 (38, $[M – Ph + MeCN]^+$), 477.1 (10, $[M – Ph + 4H_2O]$), 83.2 (69).

Synthesis of $\{Me_2(i\text{-}PrO)SiCH_2\}SnPh_2I$, 2

Iodine (2.64 g, 10.4 mmol) was added in portions at 0 °C to a solution of **1** (5.00 g, 10.4 mmol) in CH_2Cl_2 (50 mL) and the mixture was allowed to reach room temperature and stirred overnight. Removing of the solvent and iodobenzene in vacuo gave (5.07 g, 92%) of compound **2** as colorless oil.

^{1}H NMR (400.13, $CDCl_3$): δ 0.25 (s, 6H, *Me*$_2$Si), 1.06 (d, 6H, $^3J(^1H–^1H)$ = 6.0 Hz, *Me*$_2$CH), 1.15 (s, 2H, $^2J(^1H–^{117/119}Sn)$ = 87.4/91.4 Hz, SiC*H*$_2$Sn), 4.01 (m, 1H, $^3J(^1H–^1H)$ = 6.1 Hz, C*H*O), 7.43–7.88 (m, 10H, Ar H). **^{13}C{^{1}H} NMR** (100.63, $CDCl_3$): δ 1.2 ($^1J(^{13}C–^{29}Si)$ = 58 Hz, $^3J(^{13}C–^{117/119}Sn)$ = 15 Hz, *Me*$_2$Si), 4.6 ($^1J(^{13}C–^{117/119}Sn)$ = 251/262 Hz, $^1J(^{13}C–^{29}Si)$ = 57 Hz, Si*C*H$_2$Sn), 25.5 (*Me*$_2$CH), 65.5 (*C*HO), 128.5 ($^3J(^{13}C–^{117/119}Sn)$ = 61 Hz, C_m), 129.6 ($^4J(^{13}C–^{117/119}Sn)$ = 14 Hz, C_p), 136.0 ($^2J(^{13}C–^{117/119}Sn)$ = 50 Hz, *Co*), 138.4 ($^1J(^{13}C–^{117/119}Sn)$ = 536/562 Hz, C_i). **^{29}Si{^{1}H} NMR** (59.63, $CDCl_3$): δ 15.1 ($^2J(^{29}Si–^{117/119}Sn)$ = 30 Hz). **^{119}Sn{^{1}H} NMR** (111.91, $CDCl_3$): δ –67 (92%, $^1J(^{119}Sn–^{13}C_{CH2})$ = 263 Hz, $^1J(^{119}Sn–^{13}C_{Ph})$ = 561 Hz), –7 (1%), –60 (3%),

–114 (2%, Ph_3SnI), –217 (2%, $Me_2(i\text{-}PrO)SiCH_2PhSnI_2$). **Electrospray MS**: *m/z* (%), positive mode, 723.1 (100, $[O(Me_2SiCH_2SnPh_2)_2 + OH]^+$), 795.2 (13, $[O(Me_2SiCH_2SnPh_2)_2 + 4H_2O + OH]^+$), 833.1 (2, $[O(Me_2SiCH_2SnPh_2)_2 + I]^+$]), negative mode, 127.0 (100, $[I]^-$), 380.8 (10, $[I_3]^-$), 488.9 (3, $[Ph_2(I)SnCH_2Me_2SiO]^-$).

Synthesis of $\{Me_2(i\text{-}PrO)SiCH_2\}\{Me_2N(CH_2)_3\}SnPh_2$, 3

The Grignard reagent prepared from $Me_2N(CH_2)_3Cl$ (610 mg, 5.00 mmol) and magnesium turnings (134 mg, 5.50 mmol) in THF (10 mL) was added at room temperature to a solution of **2** (2.12 g, 4.00 mmol) in THF (15 mL) and the mixture was stirred overnight. The solvent was evaporated and hexane (50 mL) was added and the mixture obtained was filtered under inert conditions. The residue was extensively evaporated in vacuo to give compound **3** (1.63 g, 83%) as colorless oil.

^{1}H NMR (300.13 MHz, $CDCl_3$): δ 0.06 (s, 6H, *Me*$_2$Si), 0.32 (s, 2H, $^2J(^1H–^{117/119}Sn)$ = 73.6 Hz, Si*CH*$_2$Sn), 1.11 (d, 6H, $^3J(^1H–^1H)$ = 5.8 Hz, *Me*$_2$CH), 1.31 (t, 2H, CH_2CH_2Sn), 1.81 (m, 2H, $CH_2CH_2CH_2$), 2.17 (s, 6H, *Me*$_2$N), 2.28 (t, 2H, C*H*$_2$N), 3.98 (m, 1H, C*H*O), 7.34–7.63 (m, 10H, Ar H). **^{29}Si{^{1}H}NMR** (59.63 MHz, $CDCl_3$): δ 15.1 ($^2J(^{29}Si–^{117/119}Sn)$ = 18 Hz). **^{119}Sn{^{1}H} NMR** (111.92 MHz, $CDCl_3$): δ –62.

Synthesis of $\{Me_2(i\text{-}PrO)SiCH_2\}\{Me_2N(CH_2)_3]PhSnI$, 4

Iodine (0.76 g, 3.00 mmol) was added in portions at 0 °C to a solution of compound **3** (1.47 g, 3.00 mmol) in CH_2Cl_2 (50 mL). After the complete addition the mixture was allowed to reach room temperature and stirred overnight, before the solvent and iodobenzene were removed in vacuo to give compound **4** (1.40 g, 86%) as yellowish viscous oil.

^{29}Si{^{1}H} NMR (59.63, $CDCl_3$): δ 9.4 ($^2J(^{29}Si–^{117/119}Sn)$ = 20 Hz. **^{119}Sn{^{1}H} NMR** (111.92, $CDCl_3$): δ 3 (87%, **4**), 4 (13%, **4**·H_2O). **Electrospray MS**: *m/z* (%), positive mode, 741.2 (100, $[\mathbf{7} + H]^+$, 603.1 (32), 372 (7).

Synthesis of $\{Me_2(i\text{-}PrO)SiCH_2\}t\text{-}Bu_2SnCl$, 5

The Grignard reagent prepared from $Me_2(i\text{-}PrO)SiCH_2Cl$ (2.19 g, 13.16 mmol) and magnesium turnings (0.35 g, 14.48 mmol) in THF (30 mL) was added drop-wise at –50 °C over one hour to a solution of $t\text{-}Bu_2SnCl_2$ (4.00 g, 13.16 mmol) in THF (15 mL) and the mixture was allowed to reach room temperature and stirred overnight. The solvent was evaporated, hexane (100 mL) was added, and the mixture was stirred for

15 min before it was filtered under inert conditions. Hexane was evaporated and the residue was distilled at 133–138 °C giving (3.95 g) of a mixture of two compounds with the ratio (4 : 1) according to the ^{119}Sn NMR spectrum that could be related to compounds **5** and **5'** (**5'**, R*t*-Bu$_2$SnOH or (R*t*-Bu$_2$Sn)$_2$O [R = Me$_2$(*i*-PrO)SiCH$_2$] resulted by hydrolysis/condensation of compound **5**).

Compound (5): **^{1}H NMR** (400.13, $CDCl_3$): δ 0.21 (s, 6H, *Me*$_2$Si), 0.29 (s, 2H, ^2J(^{1}H–$^{117/119}$Sn) = 64.2/66.8 Hz, SiC*H*$_2$Sn), 1.15 (d, 6H, ^3J(^{1}H–^{1}H) = 6.3 Hz, *Me*$_2$CH), 1.32 (s, 18H, ^3J(^{1}H–$^{117/119}$Sn) = 80.8/84.8 Hz, *t*-Bu$_2$Sn), 4.01 (m, 1H, ^3J(^{1}H–^{1}H) = 6.0 Hz, C*H*O). **^{13}C{^{1}H} NMR** (100.63, $CDCl_3$): δ –0.1 (^1J(^{13}C–$^{117/119}$Sn) = 111/115 Hz, ^1J(^{13}C–^{29}Si) = 58 Hz, Si*C*H$_2$Sn), 1.1 (^1J(^{13}C–^{29}Si) = 58 Hz, ^3J(^{13}C–$^{117/119}$Sn) = 9 Hz, *Me*$_2$Si), 25.8 (*Me*$_2$CH), 29.9 (*Me*$_3$C), 34.9 (^1J(^{13}C–$^{117/119}$Sn) = 371/389 Hz, Me$_3$*C*Sn), 65.1 (*C*HO). **^{29}Si{^{1}H} NMR** (59.63, $CDCl_3$): δ 14.66 (^2J(^{29}Si–$^{117/119}$Sn) = 16 Hz, ^1J(^{29}Si–^{13}C) = 58 Hz). **^{119}Sn{^{1}H} NMR** (111.92, $CDCl_3$): δ –122 (80%).

Compound (5'): **^{1}H NMR** (400.13, $CDCl_3$): δ 0.21 (s, 6H, *Me*$_2$Si), 0.35 (s, 2H, ^2J(^{1}H–$^{117/119}$Sn) = 62.8/65.0 Hz, SiC*H*$_2$Sn), 1.15 (d, 6H, ^3J(^{1}H–^{1}H) = 6.3 Hz, *Me*$_2$CH), 1.33 (s, 18H, ^3J(^{1}H–$^{117/119}$Sn) = 81.8/85.3 Hz, *t*-Bu$_2$Sn), 4.01 (m, 1H, ^3J(^{1}H–^{1}H) = 6.0 Hz, C*H*O). **^{13}C{^{1}H} NMR** (100.63, $CDCl_3$): δ 0.0 (^1J(^{13}C–$^{117/119}$Sn) = 103/107 Hz, ^1J(^{13}C–^{29}Si) = 58 Hz, Si*C*H$_2$Sn), 1.2 (^1J(^{13}C–^{29}Si) = 58 Hz, ^3J(^{13}C–$^{117/119}$Sn) = 9 Hz, *Me*$_2$Si), 25.8 (*Me*$_2$CH), 30.0 (*Me*$_3$C), 34.6 (^1J(^{13}C–$^{117/119}$Sn) = 361/378 Hz, Me$_3$*C*Sn), 65.1 (*C*HO). **^{29}Si{^{1}H} NMR** (59.63, $CDCl_3$): δ 14.71 (^1J(^{29}Si–^{13}C) = 58 Hz). **^{119}Sn{^{1}H} NMR** (111.92, $CDCl_3$): δ –128 (20%).

Electrospray MS: *m/z* (%), positive mode, 365.1 (100, [Me$_2$(*i*-PrO)SiCH$_2$(*t*-Bu$_2$)Sn]$^+$), 323.1 (19, [Me$_2$(HO)SiCH$_2$(*t*-Bu$_2$)Sn]$^+$), negative mode, 393.0 (100, Me$_2$(HO)SiCH$_2$(*t*-Bu$_2$)Sn(OH)$_2$ + 2H$_2$O]$^-$), 437.0 (23).

Synthesis of the eight-membered stannasiloxane *cyclo*-[Ph$_2$SnOMe$_2$SiCH$_2$]$_2$, 6

A solution of sodium hydroxide (0.90 g, 22.6 mmol) in water (50 mL) and ethanol (10 mL) was added to a solution of **2** (1.50 g, 2.82 mmol) in CH_2Cl_2 (25 mL) and the mixture was stirred for 3 days at room temperature before CH_2Cl_2 and ethanol were evaporated in vacuo. The residue was extracted with CH_2Cl_2/water. The organic phase was separated and the solvent was evaporated, before the residue was recrystallized from a solution in CH_2Cl_2/hexane to give (0.98 g, 96%) of **6** as colorless crystals of mp 167–169 °C suitable for X-ray diffraction analysis.

Anal. Calcd for $C_{30}H_{36}O_2Si_2Sn_2$ (722.20 g/mol): C, 49.89; H, 5.02. Found: C, 49.8, H, 5.1.

^{1}H NMR (300.13, $CDCl_3$): δ 0.15 (s, 12H, *Me*$_2$Si), 0.58 (s, 4H, $^2J(^1H–^{117/119}Sn)$ = 73.6/76.5 Hz, SiC*H*$_2$Sn), 7.37–7.78 (m, 20H, Ar H). **^{13}C{^{1}H} NMR** (75.48, $CDCl_3$): δ 3.3 ($^1J(^{13}C–^{29}Si)$ = 84 Hz, $^1J(^{13}C–^{117/119}Sn)$ = 326/341 Hz, Si*C*H$_2$Sn), 4.5 ($^1J(^{13}C–^{29}Si)$ = 59 Hz, $^3J(^{13}C–^{117/119}Sn)$ = 18 Hz, *Me*$_2$Si), 128.4 ($^3J(^{13}C–^{117/119}Sn)$ = 58 Hz, C_m), 129.4 ($^4J(^{13}C–^{117/119}Sn)$ = 12 Hz, C_p), 135.9 ($^2J(^{13}C–^{117/119}Sn)$ = 46 Hz, C_o), 142.1 ($^1J(^{13}C–^{117/119}Sn)$ = 572/599 Hz, C_i). **^{29}Si{^{1}H} NMR** (59.63, $CDCl_3$): δ 8.6 ($^2J(^{29}Si–^{117/119}Sn)$ = 33 Hz, $^2J(^{29}Si–^{117/119}Sn)$ = 54 Hz, $^1J(^{29}Si–^{13}C)$ = 87 Hz). **^{119}Sn{^{1}H} NMR** (111.92, $CDCl_3$): δ –31 ($^1J(^{119}Sn–^{13}CH_2)$ = 341 Hz, $^1J(^{119}Sn–^{13}C_i)$ = 598 Hz). **Electrospray MS**: *m/z* (%), positive mode, 723.1 (100, [**6** + H]$^+$), 363.0 (78, [$Me_2(HO)SiCH_2(Ph_2)Sn$]$^+$), 404.0 (35, [$Me_2(HO)SiCH_2Ph_2Sn$ + MeCN]$^+$).

Synthesis of the eight-membered stannasiloxane *cyclo*-[{Me$_2$N(CH$_2$)$_3$}PhSnO Me$_2$SiCH$_2$]$_2$, 7

A solution of sodium hydroxide (0.55 g, 13.75 mmol) in water (40 mL) and ethanol (10 mL) was added to a solution of **4** (1.50 g, 2.78 mmol) in CH_2Cl_2 (25 mL) and the mixture was stirred for 3 days at room temperature before CH_2Cl_2 and ethanol were evaporated in vacuo. The residue was extracted with CH_2Cl_2. The organic phase was separated and the solvent was evaporated to give compound **7** (0.95 g, 92%) as white light yellowish solid. Recrystallization from chloroform afforded colorless single crystals of mp 142.5–144.5 °C suitable for X-ray diffraction analysis.

Anal. Calcd for $C_{28}H_{50}N_2O_2Si_2Sn_2$ (740.266 g/mol): C, 45.43; H, 6.81; N, 3.78. Found: C, 45.1, H, 7.2, N, 4.1.

^{13}C{^{1}H} NMR (75.47, $CDCl_3$): δ 3.2 (*Me*$_2$Si), 3.4 (*Me*$_2$Si), 4.7 (Si*C*H$_2$Sn), 5.0 (Si*C*H$_2$Sn), 5.1 (Si*C*H$_2$Sn), 5.3 (Si*C*H$_2$Sn), 14.6 (CH$_2$*C*H$_2$Sn), 14.6 (CH$_2$*C*H$_2$Sn), 22.4 (CH$_2$*C*H$_2$CH$_2$), 46.1 (*Me*$_2$N), 46.1 (*Me*$_2$N), 61.6 (*C*H$_2$N), 127.7 ($^3J(^{13}C–^{117/119}Sn)$ = 54/57 Hz, C_m), 128.9 (C_p), 128.9 (C_p), 135.4 ($^2J(^{13}C–^{117/119}Sn)$ = 45 Hz, C_o), 135.5 ($^2J(^{13}C–^{117/119}Sn)$ = 47 Hz, C_o), 146.6 (C_i), 146.7 (C_i). **^{29}Si{^{1}H} NMR** (59.63, $CDCl_3$): δ 1.4 ($^2J(^{29}Si–^{117/119}Sn)$ = 39/47 Hz), 1.0 ($^2J(^{29}Si–^{117/119}Sn)$ = 40/48 Hz), 4.7. **^{119}Sn{^{1}H} NMR** (111.92, $CDCl_3$): δ = –55 (50%, $^2J(^{119}Sn–^{29}Si)$ = 48 Hz), –53 (43%, $^2J(^{119}Sn–^{29}Si)$ = 48 Hz), –66 (4%), 4 (3%). **Electrospray MS**: *m/z* (%), positive mode, 444.1 (100, [{$Me_2(OH)SiCH_2$}{$Me_2N(CH_2)_3$}PhSn + 4H_2O]+), 741.2 (80, [**7** + H]$^+$), 366.1 (27).

Synthesis of the eight-membered stannasiloxane *cyclo*-[*t*-Bu$_2$SnOMe$_2$SiCH$_2$]$_2$, 8

A solution of sodium hydroxide (0.32 g, 8.0 mmol) in water (15 mL) and ethanol (10 mL) was added to a solution of the mixture **5**/**5'** (0.396 g, 1.0 mmol based on [Me$_2$(*i*-PrO)SiCH$_2$Sn(*t*-Bu)$_2$]$^+$) in CH_2Cl_2 (15 mL) and the mixture was stirred for 3 days at room temperature before CH_2Cl_2 and ethanol were evaporated. The residue was extracted with CH_2Cl_2. The organic phase was separated and the solvent was evaporated before the residue was recrystallized from a solution in CH_2Cl_2/hexane to give (0.29 g, 90%) of **8** as colorless crystals of mp 100.5–102.5 °C suitable for X-ray diffraction analysis.

Anal. Calcd for $C_{22}H_{52}O_2Si_2Sn_2$ (642.20 g/mol): C, 41.14; H, 8.16. Found: C, 41.1, H, 8.2.

^{1}H NMR (400.13, $CDCl_3$): δ –0.10 (s, 4H, $^2J(^1H–^{117/119}Sn)$ = 55.0 Hz, Si*C*H$_2$Sn), 0.12 (s, 12H, *Me*$_2$Si), 1.2 (s, 36H, $^3J(^1H–^{117/119}Sn)$ = 71.8/75.3 Hz, *Me*$_3$CSn). **^{13}C{^{1}H} NMR** (100.63, $CDCl_3$): δ –0.8 ($^1J(^{13}C–^{117/119}Sn)$ = 190/198 Hz, $^1J(^{13}C–^{29}Si)$ = 54 Hz, Si*C*H$_2$Sn), 5.4 ($^1J(^{13}C–^{29}Si)$ = 59 Hz, $^3J(^{13}C–^{117/119}Sn)$ = 15 Hz, *Me*$_2$Si), 30.0 (*Me*$_3$C), 31.5 ($^1J(^{13}C–^{117/119}Sn)$ = 409/428 Hz, Me$_3$*C*Sn). **^{29}Si{^{1}H} NMR** (59.63, $CDCl_3$): δ 1.8 ($^2J(^{29}Si–^{117/119}Sn)$ = 46 Hz, $^2J(^{29}Si–^{117/119}Sn)$ = 56/60 Hz). **^{119}Sn{^{1}H} NMR** (111.92, $CDCl_3$): δ 34 ($^1J(^{119}Sn–^{13}C_{CH2})$ = 198 Hz, $^1J(^{119}Sn–^{13}C_{t\text{-Bu}})$ = 428 Hz, $^2J(^{119}Sn–^{29}Si)$ = 48 Hz, $^2J(^{119}Sn–^{29}Si)$ = 60 Hz). **Electrospray MS**: *m/z* (%), positive mode, 323.0 (100, [Me$_2$(HO)SiCH$_2$(*t*-Bu$_2$)Sn]$^+$), 364.1 (16, [Me$_2$(HO)SiCH$_2$(*t*-Bu$_2$)Sn + MeCN]$^+$), 643.2 (16, [**8** + H]$^+$).

Synthesis of *cyclo*-[Me$_2$SiCH$_2$(Ph$_2$)SnO*t*-Bu$_2$SnO], 9

A mixture of di-*tert*-butyltin oxide (100 mg, 0.40 mmol) and **6** (145 mg, 0.20 mmol) in CH_2Cl_2 (3 mL) was stirred for 10 minutes at room temperature. Then the solvent was evaporated giving (225 g, 92%) of **9** as a white solid of mp 145–149°C.

^{1}H NMR (400.13, $CDCl_3$): δ 0.18 (s, 12H, *Me*$_2$Si), 0.56 (s, 4H, $^2J(^1H–^{117/119}Sn)$ = 71.3/73.8 Hz, SiC*H*$_2$Sn), 1.36 (s, 36H, $^3J(^1H–^{117/119}Sn)$ = 91.4/95.9 Hz, *Me*$_3$CSn), 7.37–7.73 (m, 20H, Ar H). **^{13}C{^{1}H} NMR** (100.63, $CDCl_3$): δ 3.0 ($^1J(^{13}C–^{117/119}Sn)$ = 282/295 Hz, Si*C*H$_2$Sn), 4.4 ($^1J(^{13}C–^{29}Si)$ = 59 Hz, $^3J(^{13}C–^{117/119}Sn)$ = 17 Hz, *Me*$_2$Si), 29.8 (*Me*$_3$C), 38.4 (Me$_3$*C*Sn), 128.4 ($^3J(^{13}C–^{117/119}Sn)$ = 57 Hz, C_m), 129.3 ($^4J(^{13}C–^{117/119}Sn)$ = 13 Hz, C_p), 135.7 ($^2J(^{13}C–^{117/119}Sn)$ = 47 Hz, C_o), 142.5 ($^1J(^{13}C–^{117}Sn)$ = 568 Hz, $^1J(^{13}C–^{119}Sn)$ = 595 Hz, C_i). **^{29}Si{^{1}H} NMR** (59.63, $CDCl_3$): δ 5.9 ($^2J(^{29}Si–^{117/119}Sn_{t\text{-Bu}})$ = 43 Hz, $^2J(^{29}Si–^{117/119}Sn_{Ph})$ = 49 Hz), 8.5 (**6**). **^{119}Sn{^{1}H} NMR** (111.91,

$CDCl_3$): δ –13 ($^2J(^{119}Sn–^{117}Sn)$ = 317 Hz, $^2J(^{119}Sn–^{119}Sn)$ = 334 Hz, $^2J(^{119}Sn–^{29}Si)$ = 51 Hz, $CH_2Sn(Ph_2)O$), –93 ($^2J(^{119}Sn–^{117}Sn)$ = 317 Hz, $^2J(^{119}Sn–^{119}Sn)$ = 337 Hz, $^2J(^{119}Sn–^{29}Si)$ = 44 Hz, $OSn(t\text{-}Bu_2)O$), –31 (3%, **6**), –84 (5%, $(t\text{-}Bu_2SnO)_3$). **Electrospray MS**: *m/z* (%), positive mode, 541.1 (100, $[(t\text{-}Bu_2SnO)_2 + MeCN + H]^+$), 807.3 (35 , $[(t\text{-}Bu_2SnO)_3 + MeCN + H_2O + H]^+$), negative mode, 397 (100, $[Me_2(OH)SiCH_2(Ph_2)Sn(OH)_2]^-$).

Attempt at recrystallizing compound **9** by slow evaporation of $CDCl_3$ from the NMR sample afforded single crystals of **10** of mp 266-270 °C suitable for the X-ray diffraction analysis.

Electrospray MS of compound 10: *m/z* (%), positive mode, 352.0 (100, $[t\text{-}Bu_2Sn(OH)_2 + 2\ MeCN + H]^+$), 1083.1 (16, [**10** – OH]$^+$), 833 (4, $[(t\text{-}Bu_2SnO)_3 + 2MeCN + H]^+$), negative mode, 248.9 (100), 397 (43, $[Me_2(OH)SiCH_2(Ph_2)Sn(OH)_2]^-$).

Synthesis of *cyclo*-[Me_2SiCH_2(*t*-Bu_2)SnO*t*-Bu_2SnO], 12

A mixture of di-*tert*-butyltin oxide (60 mg, 0.24 mmol) and **8** (77 mg, 0.12 mmol) in $CHCl_3$ (25 mL) was heated at reflux for 5 hours. The mixture was allowed to cool to room temperature and the solvent was evaporated in vacuo to give white solid.

^{1}H NMR (300.13, $CDCl_3$): δ –0.10 (s, 4H, $^2J(^1H–^{117/119}Sn)$ = 57.0 Hz, Si*C*H_2Sn), 0.17 (s, 12H, *Me*$_2$Si), 1.27 (s, 36H, $^3J(^1H–^{117/119}Sn)$ = 72.7/74.6 Hz, *Me*$_3$CSn), 1.33 (s, 36H, $^3J(^1H–^{117/119}Sn)$ = 89.3/93.7 Hz, *Me*$_3$CSn). **^{13}C{^{1}H} NMR** (75.47, $CDCl_3$): δ –1.4 (Sn*C*H_2Si), 5.0 ($^3J(^{13}C–^{117/119}Sn)$ = 9 Hz, *Me*$_2$Si), 30.1 (*Me*$_3$C), 30.4 (*Me*$_3$C), 32.3 (Me$_3$*C*Sn), 38.0 (Me$_3$*C*Sn). **^{29}Si{^{1}H} NMR** (59.63, $CDCl_3$): δ 5.2 ($^2J(^{29}Si–^{117/119}Sn)$ = 42 Hz), 1.8 (**8**). **^{119}Sn{^{1}H} NMR** (111.92, $CDCl_3$): δ –98 (51%, $^2J(^{119}Sn–^{117/119}Sn)$ = 351/367 Hz, $^2J(^{119}Sn–^{29}Si)$ = 44 Hz), 49 (39%, $^2J(^{119}Sn–^{117/119}Sn)$ = 351/367 Hz, $^2J(^{119}Sn–^{29}Si)$ = 41 Hz), –83 (5%, $(t\text{-}Bu_2SnO)_3$), 34 (5%, **8**). **Electrospray MS**: *m/z* (%), positive mode, 749.2 (100, $[(t\text{-}Bu_2SnO)_3 + H]^+$), 1059.2 (60, [**8** + *t*-Bu_2SnO + $8H_2O$ + Na]$^+$), 541.1 (32), negative mode, 587.1 (100, [**12** + OH]$^-$), 515.0 (50), 357.0 (48, $[Me_2(OH)SiCH_2(t\text{-}Bu_2)Sn(OH)_2]^-$).

Reaction of compound 8 with two molar equivalent (p-$MeOC_6H_4)_2$TeO

A mixture of (p-$MeOC_6H_4)_2$TeO (93 mg, 0.26 mmol) and **8** (84 mg, 0.13 mmol) in toluene (20 mL) was heated at reflux for 3 hours. The mixture was allowed to cool to room temperature and the solvent was evaporated in vacuo to give yellow viscous oil.

^{29}Si{^{1}H} NMR (59.63, $CDCl_3$): δ 6.9 ($^{2}J(^{29}Si–^{117/119}Sn)$ = 41 Hz), –10.4 ($^{2}J(^{29}Si–^{117/119}Sn)$ = 31 Hz), 1.8 (**8**), –11.4. **^{119}Sn{^{1}H} NMR** (111.92, $CDCl_3$): δ 35 (70%, $^{2}J(^{119}Sn–^{29}Si)$ = 41 Hz, $^{2}J(^{119}Sn–^{29}Si)$ = 32 Hz), 34 (11%, **8**), –239 (8%), –260 (8%), 43 (3%). **Electrospray MS**: *m/z* (%), positive mode, 451.0 (100, [(*p*-$MeOC_6H_4)_2TeO$ + $5H_2O$ + H]$^+$), 697.1 (26, [**13** + H]$^+$), 1019.2 (13, [**14** + H_2O + H]$^+$), negative mode, 733.1 (100, [**13** + H_2O + OH]$^-$), 431.1 (24, [**B** + $6H_2O$]$^-$), 407.0 (16), 393.0 (12, [**B** + $2H_2O$]$^-$), 357.0 (10, [**B**]$^-$); (**B** = $[Me_2Si(OH)CH_2(t\text{-}Bu_2)Sn(OH)_2]$).

Synthesis of *cyclo*-[Me_2SiCH_2{$Me_2N(CH_2)_3$}PhSnO*t*-Bu_2SnO], 16

A mixture of di-*tert*-butyltin oxide (60 mg, 0.240 mmol) and **7** (100 mg, 0.135 mmol) in $CHCl_3$ (25 mL) was heated at reflux for 5 hours. The mixture was allowed to cool to room temperature and the solvent was evaporated in vacuo giving white yellowish solid.

^{29}Si{^{1}H} NMR (59.63, $CDCl_3$): δ 6.5 ($^{2}J(^{29}Si–^{117/119}Sn)$ = 40 Hz), 4.5, 1.3, 1.3, 0.9, 3.3. **^{119}Sn{^{1}H} NMR** (111.92, $CDCl_3$): δ –23 (45%, $^{2}J(^{119}Sn–^{117/119}Sn)$ = 292 Hz), –89 (45%, $^{2}J(^{119}Sn–^{117/119}Sn)$ = 292 Hz), –55 (4%, **7**), –54 (3%, **7**), –66 (3%). **Electrospray MS**: *m/z* (%), positive mode, 620.1 (100, [**16** + H]$^+$), 372.0 (52, $[Me_2(OH)SiCH_2${$Me_2N(CH_2)_3$}

PhSn]$^+$), 991.3 (26), 741.2 (24, [**7** + H]$^+$), 540.1 (15, [(*t*-$Bu_2SnO)_2$ + H]$^+$), 1015.2 (7), 894.2 (6).

Synthesis of *cyclo*-[Me_2SiCH_2(*t*-Bu_2)SnOPh_2GeO] (17)

A mixture of Ph_2GeO (56 mg, 0.230 mmol) and **7** (85 mg, 0.115 mmol) in $CHCl_3$ (20 mL) was heated at reflux for 5 hours. The mixture was allowed to cool to room temperature and the solvent was evaporated in vacuo to give colorless oil.

^{29}Si{^{1}H} NMR (59.63, $CDCl_3$): δ 10.7 (90%, $^{2}J(^{29}Si–^{117/119}Sn)$ = 41 Hz), 4.6 (5%), 1.4 (5%). **^{119}Sn{^{1}H} NMR** (111.92, $CDCl_3$): δ –59 (96%, $^{2}J(^{119}Sn–^{29}Si)$ = 43 Hz, $^{2}J(^{119}Sn–^{73}Ge)$ = 60 Hz). **Electrospray MS**: *m/z* (%), positive mode, 614.1 (100, [**17** + H]$^+$), 536.0 (100, [**17** – Ph]$^+$), 894.2 (94, [**17** + Ph_2GeO + $2H_2O$ + H]$^+$, 370.1 (20).

3.5 References

1. Finch, C. A., *Brit. Polym. J.* **1985**, *17*, 321.
2. (a) Chojnowski, J., *J. Inorg. Organomet. Polym.* **1991**, *1*, 299; (b) Manners, I., *Angew. Chem. Int. Ed. Engl.* **1996**, *35*, 1602.
3. West, R., *J. Organomet. Chem.* **1986**, *300*, 327.
4. Allcock, H., *J. Inorg. Organomet. Polym.* **1992**, *2*, 197.
5. (a) Beckmann, J.; Jurkschat, K., *Coord. Chem. Rev.* **2001**, *215*, 267; (b) Fridrichova, A.; Mairychova, B.; Padelkova, Z.; Lycka, A.; Jurkschat, K.; Jambor, R.; Dostal, L., *Dalton Trans.* **2013**, 16403.
6. (a) Murugavel, R.; Voigt, A.; Walawalkar, M. G.; Roesky, H. W., *Chem. Rev.* **1996**, *96*, 2205; (b) P. Gates, D.; Manners, I., *J. Chem. Soc., Dalton Trans.* **1997**, 2525.
7. (a) Graalmann, O.; Klingebiel, U.; Clegg, W.; Haase, M.; Sheldrick, G. M., *Z. Anorg. Allg. Chem.* **1984**, *519*, 87; (b) Puff, H.; Boeckmann, M. P.; Kök, T. R.; Schuh, W., *J. Organomet. Chem.* **1984**, *268*, 197; (c) Graalmann, O.; Meyer, M.; Klingebiel, U., *Z. Anorg. Allg. Chem.* **1986**, *534*, 109; (d) Haoudi-Mazzah, A.; Mazzah, A.; Schmidt, H. G.; Noltemeyer, M.; Roesky, H. W., *Z. Naturforsch.* **1991**, *46b*, 587; (e) Mazzah, A.; Haoudi-Mazzah, A.; Noltemeyer, M.; Roesky, H. W., *Z. Anorg. Allg. Chem.* **1991**, *604*, 93; (f) Brisdon, B. J.; Mahon, M. F.; Molloy, K. C.; Schofield, P. J., *J. Organomet. Chem.* **1992**, *436*, 11; (g) Foucher, D. A.; Lough, A. J.; Manners, I., *Inorg. Chem.* **1992**, *31*, 3034; (h) Liu, F. Q.; Schmidt, H. G.; Noltemeyer, M.; Freire-Erdbrügger, C.; Sheldrick, G. M.; Roesky, H. W., *Z. Naturforsch.* **1992**, *47b*, 1085; (i) Liu, F. Q.; Roesky, H. W.; Schmidt, H. G.; Noltemeyer, M., *Organometallics* **1992**, *11*, 2965; (j) Gosink, H. J.; Roesky, H. W.; Noltemeyer, M.; Schmidt, H. G.; Freire-Erdbrügger, C.; Sheldrick, G. M., *Chem. Ber.* **1993**, *126*, 279; (k) Akkurt, M.; Kök, T. R.; Faleschini, P.; Randaccio, L.; Puff, H.; Schuh, W., *J. Organomet. Chem.* **1994**, *470*, 59; (l) Gosink, H. J.; Roesky, H. W.; Schmidt, H. G.; Noltemeyer, M.; Irmer, E.; Herbst-Irmer, R., *Organometallics* **1994**, *13*, 3420; (m) Montero, M. L.; Uson, I.; Roesky, H. W., *Angew. Chem.* **1994**, *106*, 2198; (n) Samuel, E.; Harrod, J. F.; McGlinchey, M. J.; Cabestaing, C.; Robert, F., *Inorg. Chem.* **1994**, *33*, 1292; (o) Liu, F. Q.; Uson, I.; Roesky, H. W., *J. Chem. Soc., Dalton Trans.* **1995**, 2453; (p) Haoudi-Mazzah, A.; Mazzah, A.; Gnado,

J.; Dhamelincourt, P., *J. Raman Spectrosc.* **1996**, *27*, 451; (q) Liu, F. Q.; Uson, I.; Roesky, H. W., *Z. Anorg. Allg. Chem.* **1996**, *622*, 819; (r) Beckmann, J.; Mahieu, B.; Nigge, W.; Schollmeyer, D.; Schürmann, M.; Jurkschat, K., *Organometallics* **1998**, *17*, 5697; (s) Hoebbel, D.; Nacken, M.; Schmidt, H.; Huch, V.; Veith, M., *J. Mater. Chem.* **1998**, *8*, 171; (t) Vaugeois, Y.; De Jaeger, R.; Levalois-Mitjaville, J.; Mazzah, A.; Worlem, M.; Grützmacher, H., *New J. Chem.* **1998**, *22*, 783; (u) Beckett, M. A.; Hibbs, D. E.; Hursthouse, M. B.; Malik, K. M. A.; Owen, P.; Varma, K. S., *J. Organomet. Chem.* **2000**, *595*, 241; (v) Gun'ko, Y. K.; Reilly, R.; Kessler, V. G., *New J. Chem.* **2001**, *25*, 528; (w) Li, Y.; Wang, J.; Wu, Y.; Zhu, H.; Samuel, P. P.; Roesky, H. W., *Dalton Trans.* **2013**, *42*, 13715; (x) Padělková, Z.; Švec, P.; Kampová, H.; Sýkora, J.; Semler, M.; Štěpnička, P.; Bakardjieva, S.; Willem, R.; Růžička, A., *Organometallics* **2013**, *32*, 2398; (y) Carbó, J. J.; González-del Moral, O.; Martín, A.; Mena, M.; Poblet, J.-M.; Santamaría, C., *Chem. Eur. J.* **2008**, *14*, 7930; (z) MMLevitsky; Zavin, B. G.; Bilyachenko, A. N., *Russ. Chem. Rev.* **2007**, *76*, 847 ; (aa) Postigo, L.; Vázquez, A. B.; Sánchez-Nieves, J.; Royo, P.; Herdtweck, E., *Organometallics* **2008**, *27*, 5588; (ab) Kung, M. C.; Riofski, M. V.; Missaghi, M. N.; Kung, H. H., *Chem. Commun.* **2014**, *50*, 3262; (ac) Nehete, U. N.; Chandrasekhar, V.; Jancik, V.; Roesky, H. W.; Herbst-Irmer, R., *Organometallics* **2004**, *23*, 5372.

8. Beckmann, J.; Jurkschat, K.; Schollmeyer, D., On the Reaction of (*t*-$Bu_2SnO)_3$ with Organochlorosilanes. Simple Formation of [(*t*-$Bu_2SnO)_2$(*t*-Bu_2SiO)]. In *Organosilicon Chemistry III*, Wiley **1997**; pp 403.
9. Beckmann, J.; Jurkschat, K.; Schollmeyer, D.; Schürmann, M., *J. Organomet. Chem.* **1997**, *543*, 229.
10. Beckmann, J.; Jurkschat, K.; Kaltenbrunner, U.; Pieper, N.; Schürmann, M., *Organometallics* **1999**, *18*, 1586.
11. Beckmann, J.; Jurkschat, K.; Pieper, N.; Schurmann, M., *Chem. Commun.* **1999**, 1095.
12. Pakes, P. W.; Rounds, T. C.; Strauss, H. L., *J. Phys. Chem.* **1981**, *85*, 2469.
13. Jurkschat, K.; Rosche, F.; Schurmann, M., *Phosphorus, Sulfur Silicon Relat. Elem.* **1996**, *115*, 161.
14. Morosin, B.; Harrah, L. A., *Acta Crystallogr. Sect. B* **1981**, *37*, 579.

15. Jurkschat, K., Tetraorganodistannoxanes: Simple Chemistry From a Personal Perspective. In *Tin Chemistry: Fundamentals, Frontiers, and Applications*, Davies, A. G.; Gielen, M.; Pannell, K. H.; Tiekink, E. R. T., Eds. Wiley: **2008**, and references cited therein.
16. Addison, A. W.; Rao, T. N.; Reedijk, J.; van Rijn, J.; Verschoor, G. C., *J. Chem. Soc., Dalton Trans.* **1984**, *0*, 1349.
17. (a) Dräger, M., *J. Organomet. Chem.* **1983**, *251*, 209; (b) Kolb, U.; Beuter, M.; Dräger, M., *Inorg. Chem.* **1994**, *33*, 4522; (c) Dräger, M., *Z. Anorg. Allg. Chem.* **1976**, *423*, 53; (d) Beuter, M.; Kolb, U.; Zickgraf, A.; Bräu, E.; Bletz, M.; Dräger, M., *Polyhedron* **1997**, *16*, 4005.
18. Beckmann, J.; Jurkschat, K., *Main Group Met. Chem.*, **1998**, 21, 113.
19. Cervantes-Lee, F.; K. Sharma, H.; Haiduc, I.; H. Pannell, K., *J. Chem. Soc., Dalton Trans.* **1998**, 1.
20. Beckmann, J.; Dakternieks, D.; Duthie, A.; Lewcenko, N. A.; Mitchell, C., *Angew. Chem.* **2004**, *116*, 6851.
21. Andrianov, K. A.; Golubenko, A., *J. Gen. Chem. USSR Engl. Transl.* **1975**, *45*.
22. Zickgraf, A.; Beuter, M.; Kolb, U.; Dräger, M.; Tozer, R.; Dakternieks, D.; Jurkschat, K., *Inorg. Chim. Acta* **1998**, *275–276*, 203.
23. Kandil, S. A.; Allred, A. L., *J. Chem. Soc. A* **1970**, 2987.
24. Puff, H.; Schuh, W.; Sievers, R.; Wald, W.; Zimmer, R., *J. Organomet. Chem.* **1984**, *260*, 271.
25. Beckmann, J.; Dakternieks, D.; Duthie, A.; Ribot, F.; Schürmann, M.; Lewcenko, N. A., *Organometallics* **2003**, *22*, 3257.
26. Roß, L.; Dräger, M., *Z. Naturforsch. B* **1984**, *39*, 868.

3.6 Appendix.

Crystallographic Data and Structure Refinements.

Intensity data for all crystals were collected on a XcaliburS CCD diffractometer (Oxford Diffraction) fitted with graphite-monochromated Mo Kα (λ = 0.71073 Å) radiation at 173 K.

The structure was solved with direct methods using SHELXS-97.[1] Refinements were carried out against F^2 by using SHELXL-97.[1] All non-hydrogen atoms were refined using anisotropic displacement parameters. The C−H hydrogen atoms were positioned with idealized geometry and refined using a riding model. For decimal rounding of numerical parameters and su values the rules of IUCr have been employed.[2] The figures were created using SHELXTL[3] and Diamond 3.2i.[4] The crystallographic data are given in tables C1 and C2.

References.

1. Sheldrick, G., *Acta Crystallographica Section A* **2008,** *64* (1), 112.
2. Clegg, W., *Acta Crystallographica Section E* **2003,** *59* (1), e2.
3. *Sheldrick, G. M. SHELXTL, release 5.1 Software Reference Manual; Brucker AXS, Inc.: Madison, Wisconsin, 1997.*
4. *Diamond - Crystal and Molecular Structure Visualization, Crystal Impact - Dr. H. Putz & Dr. K. Brandenburg GbR, Kreuzherrenstr. 102, 53227 Bonn, Germany http://www.crystalimpact.com/diamond*.

Table C1. Crystal data and structure refinements of the eight-membered *cyclo*-stannasiloxanes **6**–**8**.

	6	**7**	**8**
Empirical formula	$C_{30}H_{36}O_2Si_2Sn_2$	$C_{28}H_{50}N_2O_2Si_2Sn_2$	$C_{22}H_{52}O_2Si_2Sn_2$
Formula weight	722.15	740.26	642.20
Temperature / K	173(2)	173(2)	173(2)
Wavelength /°A	0.71073	0.71073	0.71073
Crystal system	Triclinic	Triclinic	Triclinic
space group	P -1	P -1	P -1
a /°A	9.1830(5)	8.5925(11)	8.8934(4)
b /°A	9.3227(4)	9.0370(7)	9.1366(4)
c /°A	10.3918(5)	11.0256(15)	10.8755(5)
α /°	63.553(5)	93.036(9)	77.908(4)
β /°	85.715(4)	97.894(11)	75.147(4)
γ /°	72.521(4)	102.579(9)	61.593(5)
Volume /°A^3	757.94(8)	824.63(17)	747.32(6)
Z	1	1	1
Dc /g.cm^{-3}	1.582	1.491	1.427
Absorption coefficient /mm^{-1}	1.751	1.613	1.765
F(000)	360	376	328
Crystal size /mm	0.24 x 0.22 x 0.16	0.42 x 0.25 x 0.05	0.50 x 0.50 x 0.33
Range for data collection /°	2.19 to 25.50	2.318 to 25.498	2.55 to 25.50
Reflections collected	6939	4842	8852
Independent reflections	2829	4842	2773
Refinement method	Full-matrix least-squares on F^2	Full-matrix least-squares on F^2	Full-matrix least-squares on F^2
Data / restraints / parameters	2829 / 0 / 165	4842 / 0 / 168	2773 / 0 / 129
Goodness-of-fit on F^2	1.036	1.111	1.352
Final R indices [$I>2\sigma(I)$]	R1 = 0.0173, wR2 = 0.0440	R1 = 0.0327, wR2 = 0.0869	R1 = 0.0163, wR2 = 0.0461
R indices (all data)	R1 = 0.0193, wR2 = 0.0444	R1 = 0.0382, wR2 = 0.0911	R1 = 0.0171, wR2 = 0.0463
Largest diff. peak and hole / e.A^{-3}	0.466 and -0.379	0.955 and -1.394	0.296 and -0.658

Table C2. Crystal data and structure refinements of the ladder-type organotinoxo clusters **10** and **11**.

	10	**11**
Empirical formula	C_{34} H_{64} O_6 Si_2 Sn_4	C_{50} H_{100} O_8 Si_2 Sn_6
Formula weight	1099.79	1597.62
Temperature / K	173(2)	173(2)
Wavelength /°A	0.71073	0.71073
Crystal system	Monoclinic	Monoclinic
space group	P 1 2/n 1	P 21/n
a /°A	14.2431(5)	9.9649(7)
b /°A	10.4123(3)	28.0445(11)
c /°A	15.5313(5)	12.2933(7)
α /°	90	90
β /°	106.366(3)	112.096(7)
γ /°	90	90
Volume /°A^3	2210.02(12)	3183.2(3)
Z	2	2
Dc /$g.cm^{-3}$	1.653	1.667
Absorption coefficient /mm^{-1}	2.325	2.399
F(000)	1088	1584
Crystal size /mm	0.50 x 0.05 x 0.04	0.38 x 0.10 x 0.07
Range for data collection /°	2.29 to 25.50	2.26 to 25.50
Reflections collected	22747	15653
Independent reflections	4134	5902
Refinement method	Full-matrix least-squares on F^2	Full-matrix least-squares on F^2
Data / restraints / parameters	4134 / 1 / 220	5902 / 1 / 312
Goodness-of-fit on F^2	0.893	0.833
Final R indices [$I>2\sigma(I)$]	R1 = 0.0197, wR2 = 0.0391	R1 = 0.0289, wR2 = 0.0506
R indices (all data)	R1 = 0.0307, wR2 = 0.0401	R1 = 0.0511, wR2 = 0.0523
Largest diff. peak and hole / e.A^{-3}	0.570 and -0.503	0.810 and -0.496

Table C3. Crystal data and structure refinements of the *cyclo*-tellurostannoxane [{(*p*-$MeOC_6H_4)_2TeOSn(t\text{-}Bu_2)CO_3\}_2$]·$2CHCl_3$, **15**.

Empirical formula	$C_{48}H_{66}Cl_6O_{12}Sn_2Te_2$
Formula weight	1540.29
Temperature / K	173(2)
Wavelength /°A	0.71073
Crystal system	Monoclinic
space group	P 21/c
a /°A	14.5191(6)
b /°A	12.2606(4)
c /°A	18.4010(9)
α /°	90
β /°	112.475(5)
γ /°	90
Volume /°A^3	3026.8(2)
Z	2
Dc /$g.cm^{-3}$	1.690
Absorption coefficient /mm^{-1}	2.087
F(000)	1512
Crystal size /mm	0.22 x 0.20 x 0.03
Range for data collection /°	2.25 to 28.00
Reflections collected	54371
Independent reflections	7301
Refinement method	Full-matrix least-squares on F^2
Data / restraints / parameters	7301 / 0 / 324
Goodness-of-fit on F^2	1.014
Final R indices [$I>2\sigma(I)$]	R1 = 0.0292, wR2 = 0.0563
R indices (all data)	R1 = 0.0453, wR2 = 0.0598
Largest diff. peak and hole / $e.A^{-3}$	0.904 and –0.759

Table C4. Selected bond lengths /Å and bond angles /° in the *cyclo*-tellurostannoxane [{(*p*-$MeOC_6H_4$)$_2$TeOSn(*t*-Bu_2)CO_3}$_2$]·2$CHCl_3$, **15**.

Sn(1)-O(1a)	2.0496(18)	Te(1)-O(1)	1.9224(19)
Sn(1)-O(22)	2.0986(19)	Te(1)-O(21)	2.4862(19)
Sn(1)-O(23)	2.312(2)	Te(1)-C(1)	2.109(3)
Sn(1)-C(21)	2.171(3)	Te(1)-C(11)	2.120(3)
Sn(1)-C(31)	2.159(3)	C(20)-O(21)	1.259(3)
O(22)-Te(1)	3.0678(23)	C(20)-O(22)	1.334(3)
O(22)-Te(1a)	3.2761(19)	C(20)-O(23)	1.279(3)
O(1a)-Sn(1)-O(23)	145.39(7)	O(1)-Te(1)-O(21)	170.20(7)
O(1a)-Sn(1)-O(22)	86.32(7)	O(1)-Te(1)-C(1)	93.02(10)
O(1a)-Sn(1)-C(21)	102.27(10)	O(1)-Te(1)-C(11)	91.08(10)
O(1a)-Sn(1)-C(31)	97.96(10)	O(21)-Te(1)-C(1)	78.89(9)
O(23)-Sn(1)-O(22)	59.56(7)	O(21)-Te(1)-C(11)	84.60(9)
O(23)-Sn(1)-C(21)	97.12(10)	C(1)-Te(1)-C(11)	97.66(11)
O(23)-Sn(1)-C(31)	92.57(9)	O(21)-C(20)-O(22)	120.630(226)
O(22)-Sn(1)-C(21)	113.61(11)	O(21)-C(20)-O(23)	124.774(264)
O(22)-Sn(1)-C(31)	115.85(10)	O(22)-C(20)-O(23)	114.595(260)
C(21)-Sn(1)-C(31)	127.28(12)	Te(1)-O(22)-Te(1a)	100.597(52)
Sn(1)-O(22)-C(20)	96.973(154)	Te(1a)-O(1a)-Sn(1)	127.99(10)
Sn(1)-O(23)-C(20)	88.867(155)	Te(1)-O(21)-C(20)	100.605(187)
Sn(1)-O(22)-Te(1)	171.665(93)	C(20)-O(22)-Te(1a)	172.444(163)
Sn(1)-O(22)-Te(1a)	79.988(63)	C(20)-O(22)-Te(1)	81.404(149)

4. $[Me_2(i\text{-}PrO)SiCH_2]_2SnBr_2$: Evidence for Intramolecular Si–O Bond Activation

4.1 Introduction

Organotin compounds have been used as catalysts for the curing of polysiloxanes for many years but the mechanism for the catalysis is not understood yet.[1] In fact, one task the catalyst has to fulfil is the activation of Si–O bonds by O→Sn coordination. Model compounds for which such activation is manifested by experimental data such as single crystal X-ray diffraction analyses are scarce. To the best of our knowledge the eight- and ten-membered rings (**A**)[2] and (**B**)[3], the trimetylsiloxy-substituted tinoxo clusters (**C**)[4] and (**D**)[5], and the tin(IV) complex (**E**)[6] , are the only such examples in which intramolecular O→Sn interactions were shown from oxygen atoms that are bound to silicon atoms.

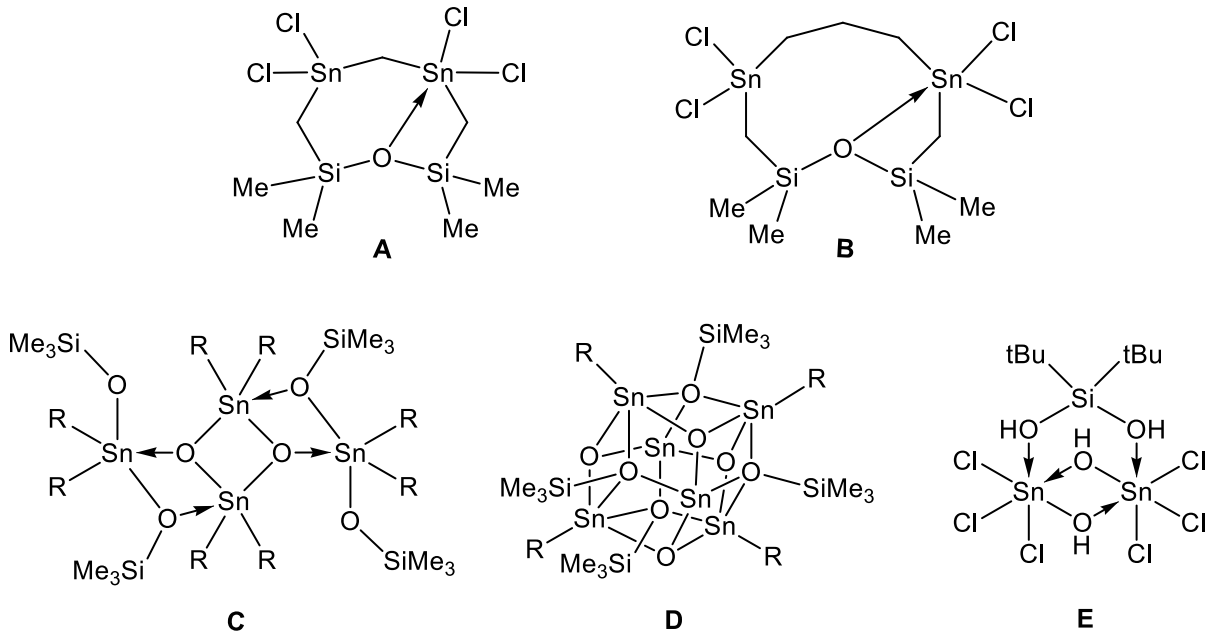

Chart 1.

One question to be answered is whether the interactions in **A** and **B** are attractive and induced by pure Lewis acid-base interaction or forced by the proximity of the corresponding atoms in the ring structure.

In this chapter we report the synthesis and molecular structure of the title compound $[Me_2(i\text{-}PrO)SiCH_2]_2SnBr_2$ which shows intramolecular O→Sn interactions involving an oxygen atom bound to silicon and carbon atoms that is not part of a ring. We also look, by variable temperature ^{119}Sn NMR spectroscopy, at the interaction between diorganotin dihalides, R_2SnX_2 (R = Me, $Me_2N(CH_2)_3$; X = Br, Cl) and trimethylethoxy silane, Me_3SiOEt, respectively hexamethylsiloxane, $Me_3SiOSiMe_3$. To the best of our knowledge, such simple investigations have not been reported yet. The experimental work is accompanied by DFT and MP2 calculations.

4.2 Results and Discussion

The reaction of $[Me_2(i\text{-}PrO)SiCH_2]_2SnPh_2$ (**1**) with elemental bromine gave the corresponding intramolecularly coordinated diorganotin dibromide $[Me_2(i\text{-}PrO)SiCH_2]_2SnBr_2$, **2**, as crystalline material in very good yield (eq 1).

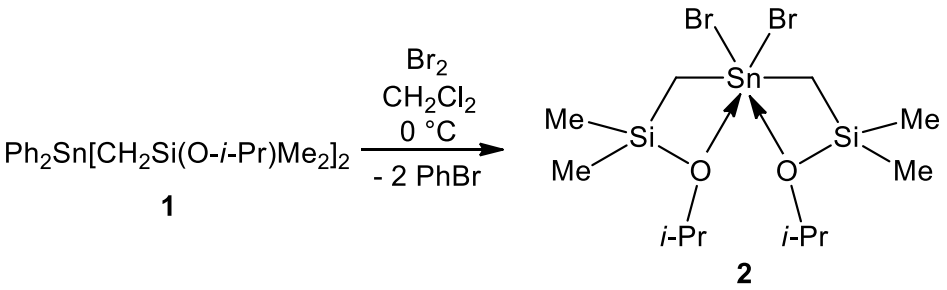

(1)

The solubility of compound **2** in common organic solvents such as dichloromethane, chloroform, acetonitrile, tetrahydrofuran, and toluene is very good.

Compound **2** crystallized in the monoclinic space group P2(1)/c with three independent molecules **2a**, **2b**, and **2c** that each appear four times in the unit cell. As result of the spatial arrangement each molecule is chiral. The centrosymmetric space group implies that the corresponding enantiomers are generated by mirroring to give the racemate. The molecular structure of **2a** is shown in Figure 1 and selected bond lengths and bond angles of **2a** are summarized in Table 1; those of **2b** and **2c** are given in the Appendix (Figure S4.1, Table D2).

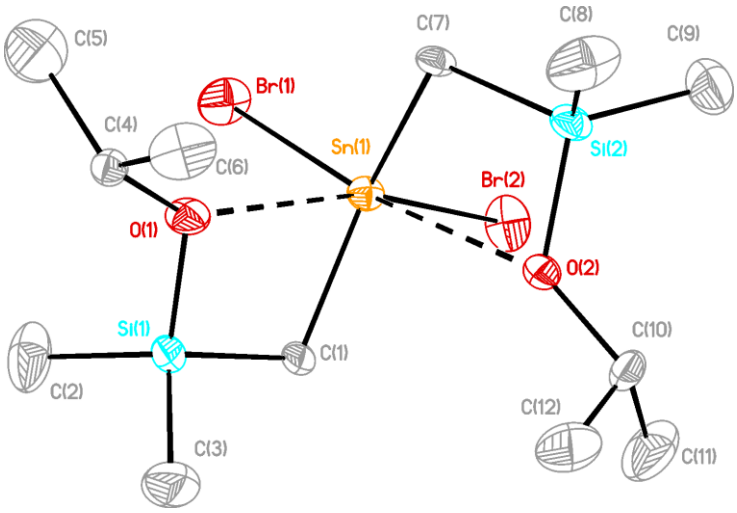

Figure 1. General view (SHELXTL) of a molecule of **2a** showing 30% probability displacement ellipsoids and the crystallographic numbering scheme. Hydrogen atoms are omitted for clarity.

The structures of **2a**, **2b**, and **2c** differ only slightly. Consequently, only that of **2a** is discussed in detail.

The Sn(1) atom can be seen as being [4+2]-coordinated with the Br(1), Br(2), C(1), and C(7) atoms forming a distorted tetrahedron with angles ranging between 132.4(2) (C(1)–Sn(1)–C(7)) and 100.25(3)° (Br(1)–Sn(1)–Br(2)) (mean angle 108.7°) that is doubly face-attacked by O(1) and O(2) at O–Sn distances of 2.946(4) and 2.912(4) Å (2.853(4) – 2.942(4)Å for **2b**, **2c**). These Sn–O distances are shorter than the sum of the van der Waals radii of oxygen and tin (3.70 Å).[7] They are also shorter than the intramolecular O–Sn distances observed for the eight- and ten-membered rings (**A**) (3.074(2) Å)[2] and (**B**) (3.312(2) Å),[3] respectively. The distances are in the same order of magnitude as the intramolecular O–Sn separations of 2.90(1)/2.92(1) Å found for bis(*o*-methoxyphenyl)tin dibromide, $(o\text{-}MeOC_6H_4)_2SnBr_2$.[8] The O(1) and O(2) atoms are trans to the Br(2) and Br(1) atoms, with Br(1)–Sn(1)–O(2) and Br(2)–Sn(1)–O(1) angles of 166.97(8) and 165.81(8)°, respectively. Interestingly, the Br(1)–Sn(1) (2.5240(8) Å) and Br(2)–Sn(1) (2.5164(8) Å) distances seem not to be affected by the O→Sn interactions. They are rather similar to the corresponding distances reported for diethyltin dibromide, Et_2SnBr_2, (2.505(4) Å)[9] and dicyclohexyltin dibromide, *cyclo*-Hex_2SnBr_2, (2.492(3), 2.516(2) Å)[10] that both contain tetrahedrally configurated tin

atoms. These findings support the interpretation of the O→Sn interaction in **2** being electrostatic rather than covalent.

The two four-membered rings that are formed as result of the intramolecular O→Sn interactions are nearly planar.

Table 1. Selected bond lengths (Å) and bond angles (deg) in **2a** and the optimized structures **2', 2''** and **2'''**.

	2a	**2' (B3LYP/def2-TZVP)**	**2'' (B97D/def2-TZVP)**	**2''' (MP2/def2-TZVP)**[a)]
Sn(1)–C(1)	2.103(6)	2.151	2.176	2.113
Sn(1) –C(7)	2.077(6)			
Sn(1)–O(1)	2.912(4)	3.317	3.175	2.833
Sn(1)–O(2)	2.946(4)			
Sn(1)–Br(1)	2.5240(8)	2.540	2.550	2.492
Sn(1)–Br(2)	2.5164(8)			
Si(1)–O(1)	1.639(4)	1.663	1.671	1.677
Si(2)–O(2)	1.640(4)			
Br(1)–Sn(1)–O(2)	166.97(8)	162.7	159.8	164.1
Br(2)–Sn(1)–O(1)	165.81(8)			
Br(1)–Sn(1)–O(1)	89.94(9)	87.6	92.9	90.1
Br(1)–Sn(1)–C(1)	105.02(18)	106.5, 108.4	105.4, 106.4	103.0, 106.0
Br(1)–Sn(1)–C(7)	105.74(16)			
Br(1)–Sn(1)–Br(2)	100.25(3)	102.8	105.5	105.2
O(2)–Sn(1)–O(1)	82.62(11)	85.9	72.6	75.0
O(2)–Sn(1)–C(1)	81.05(19)	81.3	76.6	76.2
O(2)–Sn(1)–C(7)	62.74(17)	56.7	59.4	65.4
O(2)–Sn(1)–Br(2)	89.05(8)	87.6	90.8	90.2
C(1)–Sn(1)–C(7)	132.4(2)	122.7	126.1	131.2
O(1)–Si(1)–C(1)	100.1(2)	103.9	103.2	101.2
O(2)–Si(2)–C(7)	101.5(2)			

[a)]For this calculation the *i*-propyl substituents were replaced by methyl ones and the symmetry was constraint to C_2 in order to reduce the calculation time.

A ^{119}Sn NMR spectrum of compound **2** in $CDCl_3$ solution showed a single resonance at δ 17 that is approximately 51 ppm low-frequency shifted with respect to the parent

tetracoordinated diorganotin dibromide $(Me_3SiCH_2)_2SnBr_2$ (δ 68.3, $CDCl_3$).[11] At –40°C the spectrum of **2** showed a resonance at δ 2. The ^{13}C NMR spectrum displayed a single resonance for the Si*C*H_2Sn carbon atom at δ 15.9 with $^1J(^{13}C–^{117/119}Sn)$ couplings of 312/326 Hz. These couplings are bigger than the $^1J(^{13}C–^{119}Sn)$ coupling of 296 Hz in $(Me_3SiCH_2)_2SnBr_2$. Finally, the $^2J(^1H–^{117/119}Sn)$ couplings of 107.6/112.3 Hz to the SiC*H*$_2$Sn protons in **2** are bigger than the corresponding $^2J(^1H–^{119}Sn)$ coupling of 89 Hz reported for $(Me_3SiCH_2)_2SnBr_2$. These results suggest the tin atom in compound **2** to exhibit a coordination number higher than four and that the strength of the O→Sn interaction increases slightly at low temperature.

An electrospray mass spectrum (ESI-MS, positive mode) of compound **2** showed a major mass cluster centered at m/z 885.1 that fits with the protonated hydrolysis product (**F**) (Chart 2, Figure 2).

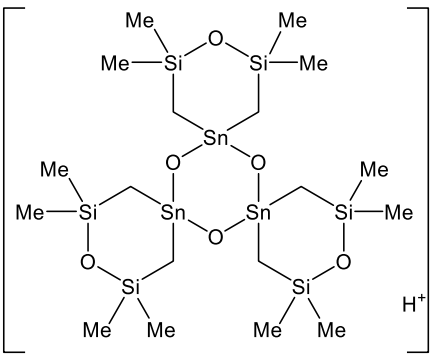

F *m/z* 885.1

Chart 2.

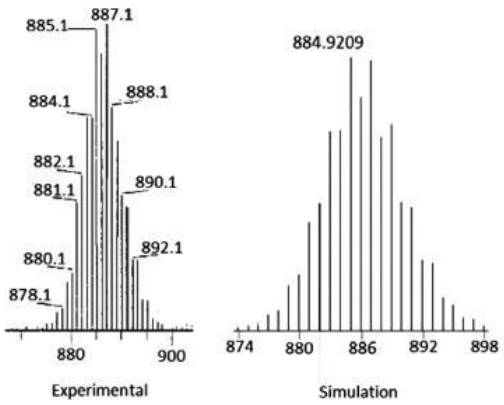

Figure 2. Experimental (from ESI MS) and simulated mass cluster for the hydrolysis product shown in Chart 2.

A ^{119}Sn NMR spectrum of compound **2** in $CDCl_3$ solution to which had been added one molar equivalent tetraphenylphosphonium bromide, Ph_4PBr, showed a major

resonance at *δ* –21 (integral 94) and a minor intense resonances at *δ* –48 (integral 6). Addition of a second molar equivalent Ph_4PBr caused low-frequency shifts of these signals to *δ* –38 (integral 98) and *δ* –65 (integral 2). At –40°C, a further low-frequency shift of the major signal to *δ* –69 was observed. The results are interpreted in terms of the equilibrium shown in eq 2 involving the tetraphenylphosphonium diorganotribromidostannate **3**.

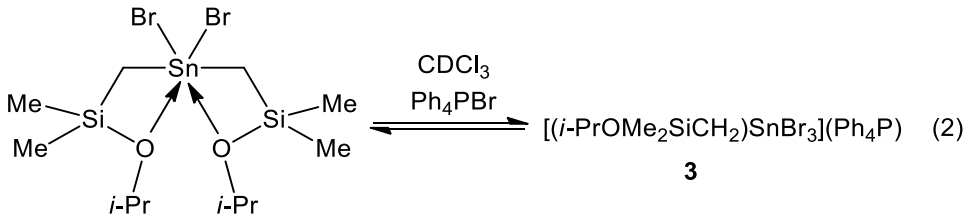

(2)

The equilibrium is fast on the ^{119}Sn NMR time scale at both room temperature and –40°C but the population of compound **3** increases at low temperature. An ESI-MS (negative mode) showed major mass clusters centered at m/z 620.8 (100%) and 576.9 (10–15%) that are assigned to the diorganotribromido and diorganodibromidohydroxido stannate complexes $[\{Me_2(i\text{-PrO})SiCH_2\}_2SnBr_3]^-$ and $[\{Me_2(i\text{-PrO})SiCH_2\}_2SnBr_2(OH)\cdot H_2O]^-$, respectively. Most remarkably, no mass clusters corresponding to species in which the SiO–*i*-Pr group is hydrolyzed were detected. Apparently, the coordination of the bromide ion at the tin atom prohibits Si–O bond activation. Attempts at isolating compound **3** failed.

Considering the results reported above we investigated the interaction of Si-bound oxygen atoms that are not part of a ring structure and that are not linked via a spacer with the Lewis-acidic tin moiety.

Thus, a ^{119}Sn NMR spectrum of a solution of dimethyltin dichloride, Me_2SnCl_2, in $CDCl_3$ to which had been added one molar equivalent trimethylethoxysilane, Me_3SiOEt, showed a single resonance at *δ* 132 that is 10 ppm low-frequency shifted with respect to Me_2SnCl_2 (*δ* 142).[12] Interestingly, the ^{29}Si NMR spectrum of the same solution displayed one resonance at *δ* 17.5 (integral approx 70) belonging to Me_3SiOEt and one resonance at *δ* 7.6 (integral approx 30) assigned to hexamethyldisiloxane, $Me_3SiOSiMe_3$. A rather similar result was observed for the ^{29}Si NMR spectrum recorded from a solution containing equimolar amounts of Me_2SnBr_2 and Me_3SiOEt. Apparently, activation of the Si–O bond in Me_3SiOEt took place. At –40°C, a further low-frequency shift of the ^{119}Sn resonance to *δ* 60 was observed.

Again, similar results were observed for a mixture consisting of equimolar amounts of Me_2SnBr_2 and Me_3SiOEt (T = 22°C: δ ^{119}Sn 66, T = –40°C: δ ^{119}Sn 59). In contrast, a ^{119}Sn NMR spectrum of a solution of dimethyltin dichloride, Me_2SnCl_2, in $CDCl_3$ to which had been added one molar equiv hexamethyldisiloxane, $Me_3SiOSiMe_3$, showed a single resonance at δ 142 both at room temperature and –40°C. Apparently, there is an equilibrium according to eq 3 that is completely on the left side for R = Me_3Si both at room and low temperature but that shifts to the right for R = Et at low temperature.

$$Me_2SnX_2 + Me_3SiOR \underset{}{\overset{CDCl_3}{\rightleftharpoons}} [Me_2SnX_2(Me_3SiOR)] \qquad (3)$$

X = Br, Cl
R = $SiMe_3$, Et

The results clearly indicate that the Si–O bond in a triorganoalkoxysilane such as Me_3SiOEt can be activated by a diorganotin dihalide such as Me_2SnX_2 (X = Br, Cl) but that hexaorganodisiloxane apparently cannot. In line with this statement is the observation that stirring a solution of dimethyltin dichloride, Me_2SnCl_2, and trimethylethoxysilane, Me_3SiOEt, in CH_2Cl_2 for 20 h at room temperature in the presence of air moisture affords, under formation of ethanol, full conversion of Me_3SiOEt to $Me_3SiOSiMe_3$.

From ESI MS we learned that addition of bromide anion to compound **2** caused enhanced stability against hydrolysis of the Si–O bond (see above). This implies that addition of bromide anion, as Ph_4PBr, to Me_2SnBr_2 should decrease the catalytic activity of the latter for Si–O hydrolysis. This is indeed the case as the ^{1}H, ^{13}C, and ^{29}Si NMR spectra in $CDCl_3$ of a mixture containing equimolar quantities of Me_2SnBr_2 and Me_3SiOEt and a droplet of water, and that had been stirred for four hours indicated approximately 60% to $Me_3SiOSiMe_3$ only.

Intramolecular N→Sn coordination in a functionalized diorganotin dichloride completely prohibits Si–O bond activation. Thus, the ^{1}H, ^{13}C, and ^{29}Si NMR spectra of a solution in $CDCl_3$ containing equimolar amounts of the intramolecularly coordinated diorganotin dichloride $[Me_2N(CH_2)_3]_2SnCl_2$,[13] Me_3SiOEt and a droplet of water that had been stirred for 4 h indicated no Si–O hydrolysis at all.

4.3 DFT calculations

In order to get more insight into the nature of the O→Sn interaction, DFT calculations using B3LYP and B97D density functional theory and the def2-TZVP basis set have been performed.[14] Remarkably, the gas phase optimization (**2'**in Table 1) gave a much longer O–Sn distance of 3.317 Å than the values found in the solid state. Even with the dispersion-corrected functional B97D (**2''** in Table 1), the O–Sn distances are predicted too long. On the other hand, the calculated Br–Sn bond distances of 2.540 and 2.550 Å fit well with the experimentally determined values. Moreover, the C–Sn and O–Si distances of 2.151 and 1.663 Å, respectively, are in good agreement with the molecular structure. The C–Sn–C angle is calculated to 122.7° and the Br–Sn–Br 102.8°. Here, it appears that B3LYP theory cannot handle the O→Sn interaction correctly. Hence, the C–Sn–C angle is predicted to be smaller than in the crystal structure. Using the B97D functional, the C–Sn–C angle widens to 126.1°, thus coming closer to the X-ray data, but the Br–Sn–Br angle deviates with 105.5° stronger from the experimental data. In the calculated structures, the configuration of the tin atom resembles more a regular tetrahedron than an octahedron.

NBO calculations revealed the absence of donor-acceptor interaction between the oxygen lone pairs and the tin atom. Wiberg bond indices of 0.021 between tin and oxygen atoms are not significant for any donor interaction as well. We relate the O→Sn contact to electrostatic interactions with regard to the NBO charges of +1.52 for tin (consistent with tin(IV))[15] and –0.88 for the oxygen atoms.

In order to perform MP2 calculations with a def2-TZVP basis set in a reasonable calculation time, in the model compound **2'''** the *i*-propyl substituents were replaced by methyl ones and the symmetry was constraint to C_2 (Table 1). The calculated model compound **2'''** fits well with the experimentally determined structure of **2** (Table 1). Especially, the O→Sn interaction is predicted correctly with a distance of 2.833 Å as compared to the Sn–O distances between 2.853(4) and 2.946(4) Å found in the solid state for compound **2**. The corresponding NBO calculations do not reveal a direct donor-acceptor interaction of the lone pairs of the oxygen atoms to the tin atom but interactions of these lone pairs with the antibonding orbitals of the surrounding substituents. For instance, the oxygen lone pairs bind with 7 kcal/mol into the σ*(Sn–Br) orbitals and with 2 kcal/mol into the σ*(Sn–C) orbitals. This finding can only be interpreted within the localised scheme of NBO calculations and has to be regarded

as further explanation for the hypercoordination at the tin atom. Taking into account the NBO charges as result of the MP2 calculation, the picture of the DFT calculations with dispersion functional B97D can be extended: using MP2 the tin atoms gains a positive charge of +1.83 whereas the oxygen atoms possess a NBO charge of –0.96. Consequently, the contribution of the electrostatic interaction between the tin and oxygen atoms is the most dominant part of this interaction.[16]

4.4 Conclusion

In conclusion, we have shown that Lewis-acidic diorganotin dihalides interact with triorganoalkoxysilanes and activate the Si–O bond. The interaction is electrostatic and this supports the interpretation of the Si–O bond to have considerable ionic character. The work is a modest contribution to the further understanding of the nature of the Si–O bond and its donor capacity, a topic that is still under some controversial debate,[17] and it might also contribute to catalyst design for polysiloxane formation. Furthermore, it was demonstrated that MP2 calculations handle O→Sn interactions more accurate than DFT calculations do.

4.5 Experimental Section

General Considerations

All solvents were dried and purified according to standard procedures and freshly distilled prior to use. If not otherwise stated, all reactions were carried out in an atmosphere of dry argon. $Me_2(i\text{-}PrO)SiCH_2Cl$ was synthesized according to literature method.[18] Bruker DPX-300 spectrometer was used to obtain ^{1}H, ^{13}C, ^{29}Si, ^{119}Sn, and ^{31}P NMR spectra. The ^{1}H, ^{13}C, ^{29}Si , ^{119}Sn, ^{31}P NMR chemical shifts δ are given in ppm and were referenced to Me_4Si (^{1}H, ^{13}C, ^{29}Si), Me_4Sn (^{119}Sn), and H_3PO_4 (^{31}P). Elemental analyses were performed on a LECO-CHNS-932 analyzer. The electrospray mass spectrum was recorded with a Thermoquest-Finnigan instrument using CH_3CN as the mobile phase.

DFT calculations

The calculations were performed with the program suite Gaussian09.[19] The geometry was calculated using the B3LYP or the B97D[14a] functional as implemented in Gaussian09. Furthermore, second-order Møller–Plesset perturbation theory (MP2) calculations have been performed using Gaussian09 as well. As basis set for geometry optimisations and NBO calculations, def2-TZVP has been used which includes an effective core potential on Sn.[14b] The stationary point has been characterised with frequency analysis and show the correct number of negative eigenvalues (zero for a local minimum). A NBO analysis was performed using NBO 3.0[20] as implemented in Gaussian09 Rev. B.01.[19]

Synthesis of $[Me_2(i\text{-}PrO)SiCH_2]_2SnPh_2$, 1

A solution of diphenyltin dichloride (20.6 g, 60 mmole) in tetrahydrofuran (100 mL) was added drop-wise to the Grignard reagent prepared from $Me_2(i\text{-}PrO)SiCH_2Cl$ (22.48 g, 135.0 mmole) and magnesium (3.94 g, 162.0 mmole) in tetrahydrofuran (150 mL). After the mixture had been stirred overnight at room temperature, the THF was removed in vacuo and the residue extracted three times under inert conditions

with hexane. The combined extracts were evaporated in vacuo to give 30.8 g of **1** (96%) as colorless liquid.

^{1}H NMR (300.13, $CDCl_3$): δ = 0.05 (s, 12H, *Me*$_2$Si), 0.42 (s, 4H, $^{2}J(^{1}H–^{117/119}Sn)$ = 74.3/77.2 Hz, SiC*H*$_2$Sn), 1.13 (d, 12H, $^{3}J(^{1}H–^{1}H)$ = 6.2 Hz, *Me*$_2$CH), 3.99 (m, 2H, $^{3}J(^{1}H–^{1}H)$ = 6.0 Hz, Me$_2$C*H*O), 7.35–7.63 (m, 10H, Ar H). **^{13}C{^{1}H} NMR** (75.48, $CDCl_3$): δ = –3.2 ($^{1}J(^{13}C–^{117/119}Sn)$ = 249/260 Hz, $^{1}J(^{13}C–^{29}Si)$ = 58 Hz, Si*C*H$_2$Sn), 1.2 ($^{1}J(^{13}C–^{29}Si)$ = 58.1 Hz, *Me*$_2$Si), 25.8 (*Me*$_2$CH), 64.7 (Me$_2$*C*HO), 127.9 ($^{3}J(^{13}C–^{117/119}Sn)$ = 49, C$_p$), 128.3 (C$_m$), 136.7 ($^{2}J(^{13}C–^{117/119}Sn)$ = 38, C$_o$), 141.5 ($^{1}J(^{13}C–^{117/119}Sn)$ = 468/490 Hz, C$_i$). **^{29}Si{^{1}H} NMR** (59.63, $CDCl_3$): δ = 15.1 (s, $^{2}J(^{29}Si–^{117/119}Sn)$ = 18 Hz, $^{1}J(^{29}Si–^{13}C)$ = 58 Hz). **^{119}Sn{^{1}H} NMR** (111.92, $CDCl_3$)**:** δ = –54 (93%, $^{2}J(^{119}Sn–^{29}Si)$ = 19 Hz, $^{1}J(^{119}Sn–^{13}CH_2)$ = 261 Hz, $^{1}J(^{119}Sn–^{13}C_i)$ = 489 Hz, $^{2}J(^{119}Sn–^{13}C_o)$ = 39 Hz, $^{3}J(^{119}Sn–^{13}C_m)$ = 49 Hz), –52 (7%, not assigned).

Synthesis of [Me$_2$(*i*-PrO)SiCH$_2$]$_2$SnBr$_2$, 2

Over a period of four hours, a solution of bromine (9.60 g, 60.0 mmol) in dichloromethane (50 mL) was added drop-wise at 0 °C to a solution of **1** (16.06 g, 30.0 mmol) in dichloromethane (50 mL). After stirring at 0 °C for two hours the mixture was allowed to reach room temperature and stirred overnight at ambient temperature. The solvent and phenyl bromide were removed in vacuo to give a solid residue. Recrystallization of this residue from hot hexane gave 14.2 g (87 %) of **2** as colorless single crystals of mp 69–70 °C suitable for X-ray diffraction analysis.

Anal. Calcd for $C_{12}H_{30}Br_2O_2Si_2Sn$ (541,05 g/mol): C, 26.64; H, 5.59. Found: C, 26.4; H, 5.55. **^{1}H NMR** (300.13, C_6D_6): δ = 0.13 (s, 12H, $^{4}J(^{1}H–^{117/119}Sn)$ = 5.8 Hz, *Me*$_2$Si), 1.03 (d, 12H, $^{3}J(^{1}H–^{1}H)$ = 6.2 Hz, *Me*$_2$CH), 1.13 (s, 4H, $^{2}J(^{1}H–^{117/119}Sn)$ = 107.6/112.3 Hz, SiC*H*$_2$Sn), 3.72 (m, 2H, $^{3}J(^{1}H–^{1}H)$ = 6.1 Hz, Me$_2$C*H*O). **^{13}C{^{1}H} NMR** (75.48, C_6D_6): δ = 1.4 ($^{1}J(^{13}C–^{29}Si)$ = 58 Hz, $^{3}J(^{13}C–^{117/119}Sn)$ = 17 Hz, Me$_2$Si), 15.9 ($^{1}J(^{13}C–^{117/119}Sn)$ = 312/326 Hz, Si*C*H$_2$Sn), 26.2 *Me*$_2$CH), 66.5 ((CH$_3$)$_2$*C*HO). **^{29}Si{^{1}H} NMR** (59.63, C_6D_6): δ = 15.0 ($^{2}J(^{29}Si–^{117/119}Sn)$ = 46 Hz, $^{1}J(^{29}Si–^{13}C)$ = 59 Hz). **^{119}Sn{^{1}H} NMR** (111.92, C_6D_6): δ = 18. **^{119}Sn{^{1}H} NMR** (111.92, $CDCl_3$): δ = 17 (room temperature), δ = 2 (T = –40 °C). **Electrospray MS**: m/z (%) 887.1 (100, [{[O(Me$_2$SiCH$_2$)$_2$Sn]O}$_3$ + H$^+$], 959.1 (10, [{[O(Me$_2$SiCH$_2$)$_2$Sn]O}$_3$ + 4H$_2$O + H$^+$], 590.9 (6, [{[O(Me$_2$SiCH$_2$)$_2$Sn]O}$_2$ + H$^+$].

Reaction of [Me$_2$(*i*-PrO)SiCH$_2$]$_2$SnBr$_2$, 2, with one molar equiv Ph$_4$PBr

A mixture of **2** (80 mg, 0.148 mmol), and tetraphenylphosphonium bromide (62 mg, 0.148 mmol) in $CDCl_3$ (1 mL) was stirred at room temperature for 5 minutes. Then an NMR sample was taken.

^{1}H NMR (300.13, $CDCl_3$): *δ* 0.16 (s, 12H, *Me*$_2$Si), 1.04 (d, 12H, $^3J(^1H–^1H)$ = 6.2 Hz, *Me*$_2$CH), 1.20 (s, 4H, $^2J(^1H–^{117/119}Sn)$ = 110.5/114.9 Hz, SiC*H*$_2$Sn), 3.91 (m, 2H, $^3J(^1H–^1H)$ = 6.0 Hz, (CH$_3$)$_2$C*H*O), 7.46–7.82 (m, 20 H, Ar H). **^{13}C{^{1}H} NMR** (75.47, $CDCl_3$): *δ* 0.75 ($^1J(^{13}C–^{29}Si)$ = 60 Hz, $^3J(^{13}C–^{117/119}Sn)$ = 16 Hz, *Me*$_2$Si), 17.8 ($^1J(^{13}C–^{117/119}Sn)$ = 344/360 Hz, $^1J(^{13}C–^{29}Si)$ = 57 Hz, Si*C*H$_2$Sn), 25.4 (*Me*$_2$CH), 65.4 (Me$_2$*C*HO), 116.9 ($^1J(^{13}C–^{31}P)$ = 89 Hz, C$_i$), 130.4 ($^3J(^{13}C–^{31}P)$ = 13 Hz, C$_m$), 133.9 ($^2J(^{13}C–^{31}P)$ = 10 Hz, C$_o$), 135.4 ($^4J(^{13}C–^{31}P)$ = 3 Hz, C$_p$). **^{29}Si{^{1}H} NMR** (59.63, $CDCl_3$): *δ* 15.3 ($^2J(^{29}Si–^{117/119}Sn)$ = 42 Hz). **^{119}Sn{^{1}H} NMR** (111.92, $CDCl_3$): *δ* –21 (94%), –48 (6%). **Electrospray MS**: m/z (%) Negative mode: 620.8 (100, [Me$_2$(*i*-PrO)SiCH$_2$]$_2$SnBr$_3^-$), 812.8 (25), 792.9 (25), 578.8 (10, [Me$_2$(*i*-PrO)SiCH$_2$]$_2$SnBr$_2$ + OH$^-$ + H$_2$O). Positive mode: 339.1 (100, Ph$_4$P$^+$).

Reaction of [Me$_2$(*i*-PrO)SiCH$_2$]$_2$SnBr$_2$, 2, with two molar equiv Ph$_4$PBr

A mixture of **2** (80 mg, 0.148 mmol), tetraphenylphosphonium bromide (124 mg, 0.296 mmol) in $CDCl_3$ (1 mL) was stirred at room temperature for 5 minutes. Then a NMR sample was taken.

^{1}H NMR (300.13, $CDCl_3$): *δ* 0.10 (s, 12H, *Me*$_2$Si), 0.96 (d, 12H, $^3J(^1H–^1H)$ = 5.8 Hz, *Me*$_2$CH), 1.16 (s, 4H, $^2J(^1H–^{117/119}Sn)$ = 110.5/114.9 Hz, SiC*H*$_2$Sn), 3.84 (m, 2H, $^3J(^1H–^1H)$ = 6.1 Hz, Me$_2$*C*HO), 7.39–7.75 (m, 20 H, Ar H). **^{13}C{^{1}H} NMR** (75.47, $CDCl_3$): *δ* 0.58 ($^1J(^{13}C–^{29}Si)$ = 59 Hz, $^3J(^{13}C–^{117/119}Sn)$ = 15 Hz, *Me*$_2$Si), 18.6 ($^1J(^{13}C–^{117/119}Sn)$ = 358/374 Hz, Si*C*H$_2$Sn), 25.2 (*Me*$_2$CH), 65.1 (Me$_2$*C*HO), 116.7 ($^1J(^{13}C–^{31}P)$ = 89 Hz, C$_i$), 130.3 ($^3J(^{13}C–^{31}P)$ = 13 Hz, C$_m$), 133.7 ($^2J(^{13}C–^{31}P)$ = 10 Hz, C$_o$), 135.2 ($^4J(^{13}C–^{31}P)$ = 3 Hz, C$_p$). **^{29}Si{^{1}H} NMR** (59.63, $CDCl_3$): *δ* 15.1 ($^2J(^{29}Si–^{117/119}Sn)$ = 37 Hz). **^{119}Sn{^{1}H} NMR** (111.92, $CDCl_3$): *δ* –38 (98.3%), –65 (1.7%). **Electrospray MS**: m/z (%) Negative mode: 620.8 (100, [Me$_2$(*i*-PrO)SiCH$_2$]$_2$SnBr$_3^-$), 578.8 (15, [Me$_2$(*i*-PrO)SiCH$_2$]$_2$SnBr$_2$ + OH$^-$ + H$_2$O). Positive mode: 339.1 (100, Ph$_4$P$^+$).

NMR Studies on the interaction of dimethyltin dihalides, Me_2SnX_2 (X = Br, Cl) with trimethylethoxy silane, Me_3SiOEt, and hexamethyldisiloxane, $Me_3SiOSiMe_3$, respectively

Dimethyltin dihalide (80 mg) and an equimolar amount of the corresponding silicon compound were dissolved in $CDCl_3$ (0.7 mL) and ^{119}Sn and ^{29}Si NMR spectra were recorded (Table 2).

Table 2.

		δ (^{119}Sn)		
R_2SnX_2	Me_3SiOR	22 °C	–40 °C	*δ* ^{29}Si (at 22 °C)
X = Cl	R = Me_3Si	142	142	7.6
X = Cl	R = Et	132	60	17.5 (70%), 7.6 (30%)
X = Br	R = Me_3Si	69	-	7.6
X = Br	R = Et	66	59	17.5 (70%), 7.6 (30%)

Reaction of Me_2SnCl_2 with Me_3SiOEt

A mixture of dimethyltin dichloride (150 mg, 0.68 mmol), trimethylethoxysilane (80mg, 0.68 mmol) and dichloromethane that was not dried (5mL) was stirred for 20 hours at room temperature. Then a NMR sample was taken.

$^{29}Si\{^1H\}$ NMR (59.63 MHz, C_6D_6): *δ* 7.5 ($(Me_3Si)_2O$).

Reaction of Me_2SnBr_2 with Me_3SiOEt

A mixture of dimethyltin dibromide (100 mg, 0.32 mmol), trimethylethoxysilane (38 mg, 0.32 mmol), one drop water and deuterated chloroform (1 mL) was stirred for 4 hours at room temperature. Then NMR sample was taken.

^1H NMR (300.13, $CDCl_3$): *δ* 0.05 (s, 9H, *Me*$_3$Si), 1.22 (t, 3H, *Me*CH_2OH), 1.37 (s, 6H, $^2J(^1H–\ ^{117/119}Sn)$ = 67.0 Hz, *Me*$_2SnBr_2$), 2.33 (s, *H*$_2O$), 3.69 (q, 2H, *MeCH*$_2OH$). **$^{13}C\{^1H\}$ NMR** (75.48, $CDCl_3$): *δ* 1.9 ($^1J(^{13}C–^{29}Si)$ = 60 Hz, *Me*$_3$Si), 8.30 ($^1J(^{13}C–\ ^{117/119}Sn)$ = 442/463 Hz, *Me*$_2SnBr_2$), 18.2 (*Me*CH_2OH), 58.4 (Me*C*H_2OH). **$^{29}Si\{^1H\}$ NMR** (59.63, $CDCl_3$): *δ* 7.6 ($(Me_3Si)_2O$).

Reaction of Me_2SnBr_2 with 2 Ph_4PBr and Me_3SiOEt

A mixture of dimethyltin dibromide (100 mg, 0.32 mmol), tetraphenylphosphonium bromide (272 mg, 0.65 mmol), trimethylethoxysilane (38 mg, 0.32 mmol), and one droplet of water in $CDCl_3$ (1.5 mL) was stirred for 4 hours at room temperature. Then an NMR sample was taken.

^{1}H NMR (300.13, $CDCl_3$): δ –0.22 (s, $(Me_3Si)_2O$), –0.19 (s, Me_3SiOEt), 0.87 (t, 3H, $MeCH_2O$), 1.35 (s, 6H, $^2J(^1H, ^{117/119}Sn)$ = 84.9 Hz, Me_2Sn), 2.68 (s (broad), H_2O), 3.35 (q, 2H, $MeCH_2O$), 7.34–7.70 (m, 40H, Ar H). **^{13}C{^{1}H} NMR** (75.48, $CDCl_3$): δ 0.7 (Me_3SiOEt), 1.2 $(Me_3Si)_2O$), 17.5 ($MeCH_2O$), 21.8 (Me_2Sn), 56.6 ($MeCH_2O$), 116.5 (d, $^1J(^{13}C–^{31}P)$ = 89 Hz, C_i), 130.0 (d, $^3J(^{13}C–^{31}P)$ = 13 Hz, C_m), 133.5 (d, $^2J(^{13}C–^{31}P)$ = 11 Hz, C_o), 135.0 (d, $^4J(^{13}C–^{31}P)$ = 3 Hz, C_p). **^{29}Si{^{1}H} NMR** (59.63, $CDCl_3$): δ 7.4 (60%, $(Me_3Si)_2O$), 15.0 (40%, Me_3SiOEt).

Reaction of $[Me_2N(CH_2)_3]_2SnCl_2$ with Me_3SiOEt

A mixture consisting of $[Me_2N(CH_2)_3]_2SnCl_2$ (150 mg, 0.41 mmol), trimethylethoxysilane (49 mg, 0.41 mmol), one drop of water and $CDCl_3$(1.5 mL) was stirred for 4 hours at room temperature. Then a NMR sample was recorded.

^{1}H NMR (300.13, $CDCl_3$): δ 0.08 (s, 9H, Me_3Si), 1.16 (t, 3H, $MeCH_2OSi$), 1.62 (t, CH_2Sn), 2.09 (m, $CH_2CH_2CH_2$), 2.65 (s, Me_2N), 2.72 (t, CH_2N), 3.62 (q, 2H, CH_3CH_2OSi). **^{13}C{^{1}H} NMR** (75.47, $CDCl_3$): δ –0.6 ($^1J(^{13}C–^{29}Si)$ = 59 Hz, Me_3Si), 18.4 ($MeCH_2OSi$), 21.1 ($CH_2CH_2CH_2$), 30.7 (CH_2Sn), 47.2 (Me_2Sn), 58.0 ($MeCH_2OSi$), 59.4 (CH_2N). **^{29}Si{^{1}H} NMR** (59.63, $CDCl_3$): δ 17.6 (Me_3SiOEt).

4.6 References

1. Cervantes, J.; Zárraga, R.; Salazar-Hernández, C., *Appl. Organomet. Chem.* **2012**, *26*, 157.
2. Schulte, M.; Schürmann, M.; Jurkschat, K., *Chem. Eur. J.* **2001**, *7*, 347.
3. Schulte, M.; Gabriele, G.; Schürmann, M.; Jurkschat, K.; Duthie, A.; Dakternieks, D., *Organometallics* **2003**, 22, 328.
4. Beckmann, J.; Jurkschat, K.; Kaltenbrunner, U.; Rabe, S.; Schürmann, M.; Dakternieks, D.; Duthie, A.; Müller, D., Organometallics *2000*, **19**, 4887.
5. Sita, L.; Xi, R.; Yap, G. P. A.; Liable-Sands, L. M.; Rheingold, A. L., *J. Am. Chem. Soc.* **1997**, *119*, 756.
6. Mazzah, A.; Haoudi-Mazzah, A.; Noltemeyer, M.; Roesky, H. W., *Z. anorg. Allg. Chem.* **1991**, *604*, 93.
7. Huheey, A. E.; Keiter, E. A.; Keiter, R. L., *Inorganic Chemistry: Principles of Structure and Reactivity*, 4th ed.; Harper Collins College: New York, 1993.
8. Ross, J.; Wardell, J.; Ferguson, G.; Low, J. N., Acta Crystallogr. **1994**, *50*, 1207.
9. Alcock, N. W.; Sawyer, J. F., *J. Chem. Soc., Dalton Trans.* **1977**, 1090.
10. Ganis, P.; Valle, G.; Furlani, D.; Tagliavini, G., *J. Organomet. Chem.* **1986**, *302*, 165.
11. Beckmann, J.; Henn, M.; Jurkschat, K.; Schürmann, M.; Dakternieks, D.; Duthie, A., *Organometallics* **2001**, *21*, 192.
12. Martínez, E. G.; González, A. S.; Casas, J. S.; Sordo, J.; Valle, G.; Russo, U., *J. Organomet. Chem.* **1993**, *453*, 47.
13. Pieper, N.; Klaus-Mrestani, C.; Schürmann, M.; Jurkschat, K.; Biesemans, M.; Verbruggen, I.; Martins, J. C.; Willem, R., *Organometallics* **1997**, *16*, 1043.
14. (a) Grimme, S., *J. Comput. Chem.* **2006**, *27*, 1787; (b) Weigend, F.; Ahlrichs, R., *Phys. Chem. Chem. Phys.* **2005**, *7*, 3297.
15. (a) Brendler, E.; Wächtler, E.; Heine, T.; Zhechkov, L.; Langer, T.; Pöttgen, R.; Hill, A. F.; Wagler, J., *Angew. Chem., Int. Ed.* **2011**, *50*, 4696; (b) Brendler, E.; Wächtler, E.; Heine, T.; Zhechkov, L.; Langer, T.; Pöttgen, R.; Hill, A. F.; Wagler, J., *Angew. Chem.* **2011**, *123*, 4793.
16. Hagemann, M.; Mix, A.; Berger, R. J. F.; Pape, T.; Mitzel, N. W., *Inorg. Chem.* **2008**, *47*, 10554.

17. (a) Weinhold, F.; West, R., *Organometallics* **2011**, *30*, 5815; (b) Grabowsky, S.; Hesse, M. F.; Paulmann, C.; Luger, P.; Beckmann, J., *Inorg. Chem.* **2009**, *48*, 4384.
18. Andrianov, K. A.; Golubenko, A., J. Gen. Chem. USSR Engl. Transl. 1975, 45.
19. Frisch, M. J.; Trucks, G. W.; Schlegel, H. B.; Scuseria, G. E.; Robb, M. A.; Cheeseman, J. R.; Scalmani, G.; Barone, V.; Mennucci, B.; Petersson, G. A.; Nakatsuji, H.; Caricato, M.; Hratchian, X. L., H. P.; Izmaylov, A. F.; Bloino, J.; Zheng, G.; Sonnenberg, J. L.; Hada, M.; Ehara, M.; Toyota, K.; Fukuda, R.; Hasegawa, J.; Ishida, M.; Nakajima, T.; Honda, Y.; Kitao, O.; Nakai, H.; Vreven, T.; Montgomery, J. A.; Peralta, J., J. E.; Ogliaro, F.; Bearpark, M.; Heyd, J. J.; Brothers, E.; Kudin, K. N.; Staroverov, V. N.; Keith, T.; Kobayashi, R.; Normand, J.; Raghavachari, K.; Rendell, A.; Burant, J. C.; Iyengar, S. S.; Tomasi, J.; Cossi, M.; Rega, N.; Millam, J. M.; Klene, M.; Knox, J. E.; Cross, J. B.; Bakken, V.; Adamo, C.; Jaramillo, J.; Gomperts, R.; Stratmann, R. E.; Yazyev, O.; Austin, A. J.; Cammi, R.; Pomelli, C.; Ochterski, J. W.; Martin, R. L.; Morokuma, K.; Zakrzewski, V. G.; Voth, G. A.; Salvador, P.; Dannenberg, J. J.; Dapprich, S.; Daniels, A. D.; Farkas, O.; Foresman, J. B.; Ortiz, J. V.; Cioslowski, J.; Fox, D. J. 2010.
20. Weinhold, F.; Landis., C. R., *Valency and Bonding;* Cambridge University Press: 2005.

4.7 Appendix.

Crystallographic Data and Structure Refinements.

Intensity data for the crystal were collected on Nonius Kappa CCD diffractometer fitted with graphite-monochromated Mo Kα (λ = 0.71073 Å) radiation at 173 K.

The structure was solved with direct methods using SHELXS-97.[1] Refinements were carried out against F^2 by using SHELXL-97.[1] All non-hydrogen atoms were refined using anisotropic displacement parameters. The C−H hydrogen atoms were positioned with idealized geometry and refined using a riding model. For decimal rounding of numerical parameters and su values the rules of IUCr have been employed.[2] The figures were created using SHELXTL.[3] The crystallographic data are given in table D1.

References.

1. Sheldrick, G., *Acta Crystallographica Section A* **2008,** *64* (1), 112.
2. Clegg, W., *Acta Crystallographica Section E* **2003,** *59* (1), e2.
3. *Sheldrick, G. M. SHELXTL, release 5.1 Software Reference Manual; Brucker AXS, Inc.: Madison, Wisconsin, 1997.*

Structural Data:

Table D1. Crystal data and structure refinements of the diorganotin dibromide $\{Me_2(i\text{-}PrO)SiCH_2\}_2SnBr_2$, **2**.

Empirical formula	$C_{12}\ H_{30}\ Br_2\ O_2\ Si_2\ Sn$
Formula weight	541.71
Temperature / K	173(2)
Wavelength /°A	0.71073
Crystal system	Monoclinic
space group	P2(1)/c
a /°A	13.6791(5)
b /°A	29.6551(10)
c /°A	16.4200(5)
α /°	90
β /°	90.540(3)
γ /°	90
Volume /°A^3	6660.6(4)
Z	12
Dc /$g.cm^{-3}$	1.618
Absorption coefficient /mm^{-1}	4.856
F(000)	3188
Crystal size /mm	0.24 x 0.21 x 0.12
Range for data collection /°	2.37 to 29.37
Reflections collected	61814
Independent reflections	16182
Refinement method	Full-matrix least-squares on F^2
Data / restraints / parameters	16182 / 132 / 658
Goodness-of-fit on F^2	0.683
Final R indices [$I>2\sigma(I)$]	R1 = 0.0472, wR2 = 0.1179
R indices (all data)	R1 = 0.1221, wR2 = 0.1371
Largest diff. peak and hole / $e.A^{-3}$	4.348 and -1.352

Molecular structure and selected bond lengths and bond angles of 2b and 2c from the molecular structure of $\{Me_2(i\text{-}PrO)SiCH_2\}_2SnBr_2$, 2.

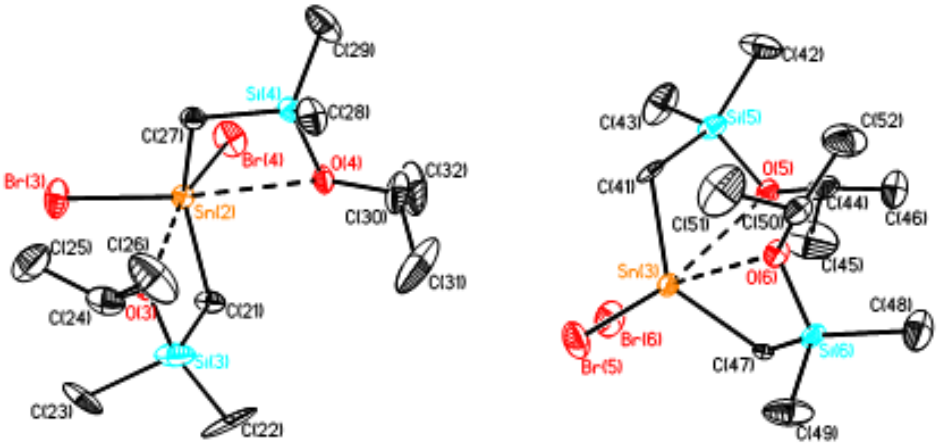

Figure S4.1. General view (SHELXTL) of the molecular structure of **2**b (left), and **2**c (right) showing 30% probability displacement ellipsoids and the crystallographic numbering scheme.

Table D2. Selected bond lengths /Å and bond angles /° in 2b and 2c.

2b		**2c**	
Sn(2)-C(21)	2.137(6)	Sn(3)-C(41)	2.123(6)
Sn(2)-C(27)	2.088(6)	Sn(3)-C(47)	2.074(6)
Sn(2)-O(3)	2.853(4)	Sn(3)-O(5)	2.942(4)
Sn(2)-O(4)	2.883(4)	Sn(3)-O(6)	2.877(4)
Sn(2)-Br(3)	2.5096(8)	Sn(3)-Br(5)	2.5099(9)
Sn(2)-Br(4)	2.4987(8)	Sn(3)-Br(6)	2.5204(9)
Si(3)-O(3)	1.653(4)	Si(5)-O(5)	1.618(5)
Si(4)-O(4)	1.640(4)	Si(6)-O(6)	1.631(5)
Br(3)-Sn(2)-O(4)	168.79(9)	Br(6)-Sn(3)-O(6)	165.41(9)
Br(4)-Sn(2)-O(3)	169.69(8)	Br(5)-Sn(3)-O(5)	164.85(9)
Br(3)-Sn(2)-O(3)	86.39(9)	Br(6)-Sn(3)-O(5)	89.06(9)

Br(3)-Sn(2)-C(21)	104.34(17)	Br(6)-Sn(3)-C(41)	104.63(18)
Br(3)-Sn(2)-C(27)	106.52(17)	Br(6)-Sn(3)-C(47)	104.33(18)
Br(3)-Sn(2)-Br(4)	98.80(3)	Br(6)-Sn(3)-Br(5)	100.65(3)
O(4)-Sn(2)-O(3)	87.30(13)	O(6)-Sn(3)-O(5)	82.31(13)
O(4)-Sn(2)-C(21)	80.91(18)	O(6)-Sn(3)-C(41)	81.5(2)
O(4)-Sn(2)-C(27)	63.65(18)	O(6)-Sn(3)-C(47)	63.5(2)
O(4)-Sn(2)-Br(4)	88.92(9)	O(6)-Sn(3)-Br(5)	90.32(9)
C(21)-Sn(2)-C(27)	133.3(3)	C(41)-Sn(3)-C(47)	134.9(3)
O(3)-Si(3)-C(21)	100.0(2)	O(5)-Si(5)-C(41)	99.8(2)
O(4)-Si(4)-C(27)	100.8(2)	O(6)-Si(6)-C(47)	100.2(2)

5. Summary

The main purpose of this work were the syntheses, structures and characterization of periphery-functionalized organotinoxo clusters and tin-containing heterocycles. These compounds are promising as catalysts for a diversity of organic reactions, and hold potential in material science.

In the first chapter, a series of novel organotin compounds containing the $Ph_2P(O)CH_2$ moiety was synthesized and characterized. The $Ph_2P(O)CH_2$-substituted organotin halides containing tin atoms with enhanced Lewis acidity show intermolecular P=O→Sn interactions. Reactions of the diorganotin dihalides $[Ph_2P(O)CH_2]RSnX_2$ (R = Ph, Me_3SiCH_2) with different stoichiometric amounts of di-*tert*-butyltin oxide afforded different types of diorganotinoxo clusters (Chart 1).

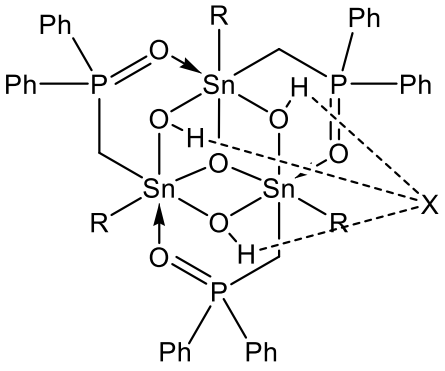

14, R = Ph, X = Br
15, R = Ph, X = I
16, R = Ph, X = Cl
17, R = Me_3SiCH_2, X = Br

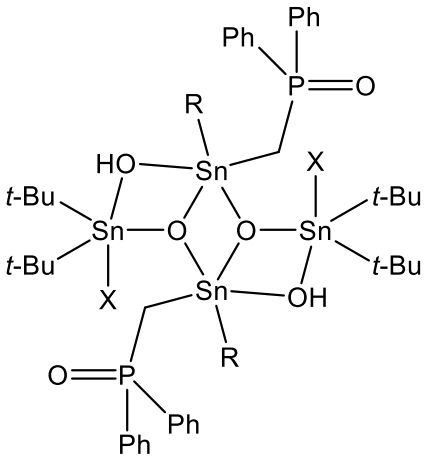

18, R = Ph, X = Cl
19, R = Me_3SiCH_2, X = Br
20, X = Me_3SiCH_2, Cl

Chart 1. $Ph_2P(O)CH_2$ functionalized O-capped clusters (left) and dimeric tetraorganodistannoxanes (right).

The reactions of $[Ph_2P(O)CH_2]RSnX_2$ with one molar equivalent *t*-Bu_2SnO afforded the O-capped clusters $[(Ph_2P(O)CH_2)R(\mu\text{-}OH)Sn]_3(\mu_3\text{-}O)(\mu_3\text{-}X)$ (**14**, R = Ph, X = Br;

16, R = Ph, X = Cl; **17**, R = Me_3SiCH_2, X = Br), being composed of cationic stannoxane core and a counter halide anion that is stabilized by three hydrogen bonds. Interestingly, by the reaction with sodium iodide, the O-capped cluster **14** suffers halide anion exchange providing the iodide containing analogous compound $[(Ph_2P(O)CH_2)Ph(\mu\text{-}OH)Sn]_3(\mu_3\text{-}O)(\mu_3\text{-}I)$, **15**, whereas no reaction with sodium fluoride was observed. The diorganotinoxo clusters **14**–**16** are isostructural. The reactions of the diorganotin dihalides $[Ph_2P(O)CH_2]RSnX_2$ with two molar equivalents *t*-Bu_2SnO afforded the ladder-like unsymmetrically substituted dimeric tetraorganodistannoxanes $[t\text{-}Bu_2(X)SnOSnR\{CH_2P(O)Ph_2\}(OH)]_2$ (**18**, R = Ph, X = Cl; **19**, R = Me_3SiCH_2, X = Br; **20**, R = Me_3SiCH_2, X = Cl). The complete hydrolysis of the diorganotin dibromide $[Ph_2P(O)CH_2](Me_3SiCH_2)SnBr_2$, **10**, in moist air afforded, after a long reaction time, under Sn–C cleavage the Sn_{12} monoorganotinoxo cluster $(Me_3SiCH_2Sn)_{12}O_{14}(OH)_6Br_2$, **10a**, consisting of the centrosymmetric macrocation $[(Me_3SiCH_2Sn)_{12}O_{14}(OH)_6]^{2+}$ and two bromide counter anions that are stabilized by hydrogen bonds. Recrystallization of the organotin trichloride $[Ph_2P(O)CH_2]SnCl_3$, **13**, from acetone in aerobic conditions gave some crystals of $[\{Ph_2P(O)CH_2SnCl_2(\mu\text{-}OH)\}_2\cdot 2C_3H_6O]$, **13a**, that is the first intermediate along the hydrolysis pathway of compound **13**. Compound **13a** is a polymer in the solid state as a result of hydrogen bridges.

Also reported in chapter 1 is the synthesis of the first tin-containing frustrated Lewis pair $[Ph_2PC_6H_4]t\text{-}Bu_2SnCl$, **29**. The compound shows no P→Sn interaction as proved by the absence couplings between these nuclei in the corresponding NMR spectra. This is a prerequisite for FLPs.

In the second chapter, a series of tin-substituted cyclic siloxanes and polyhedral oligomeric silsesquioxanes (POSS) was synthesized and characterized (Chart 2). The silicon atoms in these siloxanes are bound to one, two or three oxygen atoms. Halogenation and proto-destannylation of the mono-cyclic siloxane *cyclo*-$Ph_2Sn(CH_2Me_2Si)_2O$, **1**, the tri-cyclic siloxane $[\{Ph_2Sn(CH_2MeSi)_2O\}O]_2$, **12**, and of the tin-substituted POSS $(Ph_3SnCH_2SiO_{1.5})_8$, **20**, afforded the corresponding organotin halides *cyclo*-$PhISn(CH_2Me_2Si)_2O$, **2**, *cyclo*-$X_2Sn(CH_2Me_2Si)_2O$ (**3**, X = I; **4**, X = Br; **5**, X = Cl), $[\{X_2Sn(CH_2MeSi)_2O\}O]_2$ (**13**, X = I; **14**, X = Br; **15**, X = Cl), and $(Br_2PhSnCH_2SiO_{1.5})_8$, **21**, containing halogen substituents that are readily modifiable

by reactions with Grignard reagents. This was proved by the reaction of *cyclo*-PhISn($CH_2Me_2Si)_2O$, **2**, with the Grignard reagent $Me_2N(CH_2)_3MgCl$ affording the siloxane *cyclo*-{$Me_2N(CH_2)_3$}PhSn($CH_2Me_2Si)_2O$, **6**, which contains a periphery amine group.

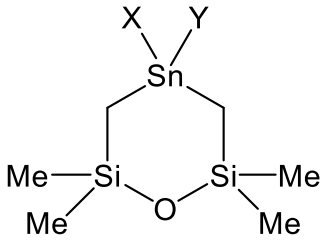

1; X = Y = Ph
2; X = I, Y = Ph
3; X = Y = I
4; X = Y = Br
5; X = Y = Cl
6; X = $Me_2N(CH_2)_3$, Y = Ph
7; X = $Me_2N(CH_2)_3$, Y = I

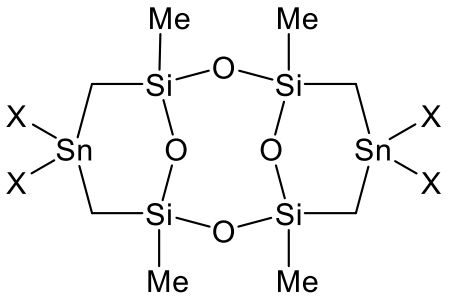

12; X = Ph
13; X = I
14; X = Br
15; X = Cl

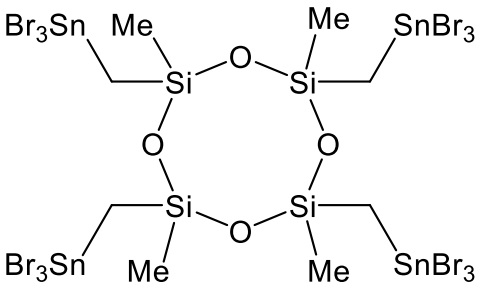

18

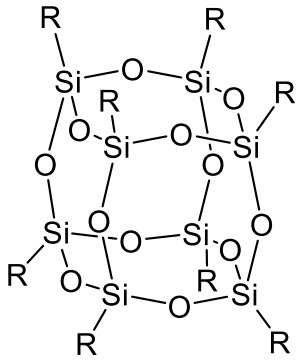

20, R = Ph_3SnCH_2
21, R = $PhBr_2SnCH_2$

Chart 2. Tin-substituted siloxanes and silsesquioxanes.

The reaction of the diorganotin halides *cyclo*-$X_2Sn(CH_2Me_2Si)_2O$ (**3**, X = I; **4**, X = Br; **5**, X = Cl), with *t*-Bu_2SnO afforded the corresponding symmetrically and/or the unsymmetrically substituted dimeric tetraorganodistannoxanes (Chart 3), and that is according to the halogen substituent bound to the tin atom.

The diorganotin diiodide **3** reacts with *t*-Bu_2SnO to give only the symmetrically substituted dimeric tetraorganodistannoxanes [$O(Me_2SiCH_2)_2(I)SnOSn($**X**$)(CH_2Me_2Si)_2O]_2$ (X = OH, I), **24**. In contrast, the diorganotin dichloride **5** reacts with

t-Bu_2SnO giving only the unsymmetrically substituted dimeric tetraorganodistannoxane $[O(Me_2SiCH_2)_2(Cl)SnOSn(Cl)t\text{-}Bu_2]_2$, **25**.

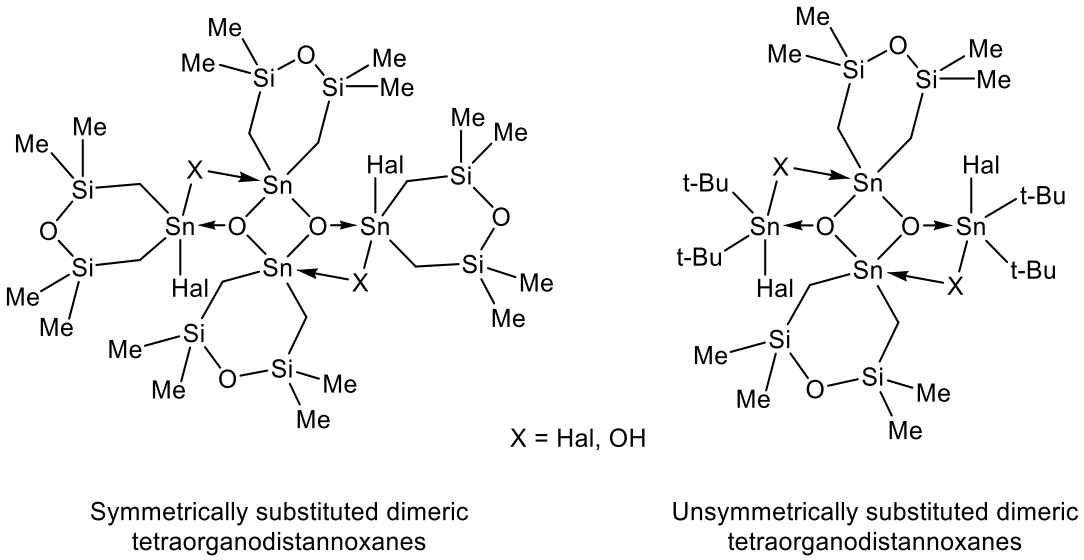

Chart 3. Symmetrically- and unsymmetrically-substituted dimeric tetraorganodistannoxanes.

The reaction of the diorganotin dibromide **4** with *t*-Bu_2SnO afforded the symmetrically- as well as the unsymmetrically substituted dimeric tetraorganodistannoxanes $[O(Me_2SiCH_2)_2(Br)SnOSn(\mathbf{X})(CH_2SiMe_2)_2O]_2$ (X = OH, Br), **26**, and $[O(Me_2SiCH_2)_2(\mathbf{X})SnOSn(Br)t\text{-}Bu_2]_2$ (X = OH, Br), **27**, respectively. Experiments to polymerize the six-membered siloxane *cyclo*-$Ph_2Sn(CH_2Me_2Si)_2O$, **1**, using different anionic initiators were not successful.

In the third chapter, novel eight membered stannasiloxanes *cyclo*-$(RR'SnOMe_2SiCH_2)_2$ (**6**, R = R' = Ph; **7**, R = Ph, R' = $Me_2N(CH_2)_3$; **8**, R = R' = *t*-Bu) were synthesized and completely characterized (Chart 4). Changing the organic substituents bound to the tin atom affects the chemical reactivity of the resulting eight-membered rings. Compound **6**, which has two phenyl substituents bound to the tin atom, reacts rapidly at room temperature with *t*-Bu_2SnO providing the six-membered stannasiloxane *cyclo*-$[Me_2SiCH_2(Ph_2)SnO(t\text{-}Bu_2)SnO]$, **9**. No reaction was observed as a solution of compound **6** was stirred with a variety of different diorganoelement oxides at different reaction conditions. On contact with air moisture, compound **9** surprisingly undergoes $Sn–C_{Ph}$ bond cleavage to give the ladder-like diorganotinoxo cluster $[PhSn(CH_2Me_2SiO)(\mu_3\text{-}O)Sn(\mu\text{-}OH)t\text{-}Bu_2]_2$, **10**. The latter

reacts with two molar equivalents *t*-Bu_2SnO affording the Sn_6 diorganotinoxo cluster [(*t*-Bu_2)(μ-OH)Sn(μ_3-O)Sn(Ph)(CH_2Me_2SiO)Sn(*t*-Bu_2)(μ_3-O)]$_2$, **11**.

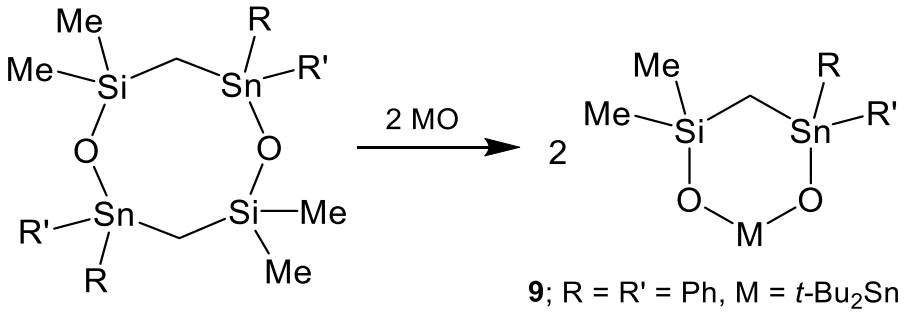

6; R = R' = Ph
7; R = $Me_2N(CH_2)_3$, R' = Ph
8; R = R' = *t*-Bu

9; R = R' = Ph, M = *t*-Bu_2Sn
12; R = R' = *t*-Bu, M = *t*-Bu_2Sn
13; R = R' = *t*-Bu, M = (*p*-MeO-$C_6H_4)_2Te$
16; R = Ph, R' = $Me_2N(CH_2)_3$, M = *t*-Bu_2Sn
17; R = Ph, R' = $Me_2N(CH_2)_3$, M = Ph_2Ge

Chart 4. Tin-containing *cyclo*-metallasiloxanes.

The eight-membered stannasiloxane **8**, containing two *t*-butyl substituents bound to the tin atom reacts at high temperatures with *t*-Bu_2SnO, respectively (*p*-$MeOC_6H_4)_2TeO$ providing the six-membered metallasiloxanes *cyclo*-[Me_2SiCH_2(*t*-Bu_2)SnO(*t*-Bu_2)SnO], **12**, and *cyclo*-[Me_2SiCH_2(*t*-Bu_2)SnO-(*p*-$MeOC_6H_4)_2TeO$], **13**, respectively. Furthermore, the reactions of the stannasiloxane *cyclo*-[{$Me_2N(CH_2)_3$}PhSnO$Me_2SiCH_2]_2$, **7**, with *t*-Bu_2SnO and Ph_2GeO provided the six-membered metallasiloxanes *cyclo*-[Me_2SiCH_2{$Me_2N(CH_2)_3$}-PhSnO(*t*-Bu_2)SnO], **16**, and *cyclo*-[Me_2SiCH_2{$Me_2N(CH_2)_3$}PhSnOPh_2GeO], **17**, respectively. Compound **17** is the first six-membered ring being composed of four different group 14 elements in the ring skeleton. The *cyclo*-metallasiloxanes *cyclo*-[CH_2(RR')SnO(Me_2)Si]$_2$ (**6**–**8**) and *cyclo*-[Me_2SiCH_2(RR')SnOMO] (**9**, **12**, **13**, **16**, and **17**) can be interpreted as model compounds for structurally modified silica surfaces. They also hold potential as single source precursors for new inorganic polymers and structurally modified polysiloxanes by the so-called Ring Opening Polymerization.

In the last chapter, it was shown that Lewis-acidic diorganotin dihalides interact with triorganoalkoxysilanes and activate the Si–O bond. The interaction is electrostatic and this supports the interpretation of the Si–O bond to have considerable ionic character.

6. Zusammenfassung

Das Hauptziel dieser Arbeit waren die Synthese, die Strukturaufklärung und die Charakterisierung periphär funktionalisierter Organozinncluster und zinnhaltiger Heterocyclen. Diese Verbindungen sind potentielle Katalysatoren für eine Vielzahl organischer Reaktionen und sind für die Materialwissenschaften interessant.

Im ersten Kapitel wird die Synthese und Charakterisierung einer Vielzahl von Organozinnverbindungen, welche den $Ph_2P(O)CH_2$-Substituenten enthalten, beschrieben. Die entsprechenden Organozinnhalogenide, welche Zinnatome mit gesteigerter Lewis-Acidität enthalten, zeigen P=O→Sn-Wechselwirkungen. Die Reaktionen der Diorganozinnhalogenide $[Ph_2P(O)CH_2]RSnX_2$ (R = Ph, Me_3SiCH_2) mit unterschiedlichen stöchiometrischen Mengen von Di-*tert*-butylzinnoxid ergeben verschiedene Arten von Diorganozinnoxoclustern (Abbildung 1).

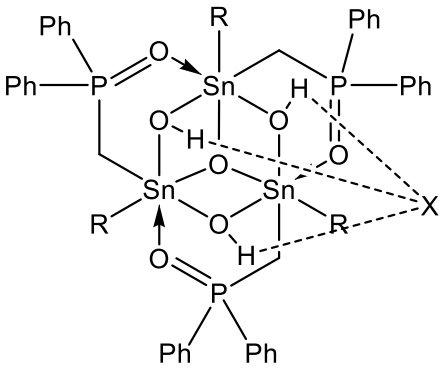

14, R = Ph, X = Br
15, R = Ph, X = I
16, R = Ph, X = Cl
17, R = Me_3SiCH_2, X = Br

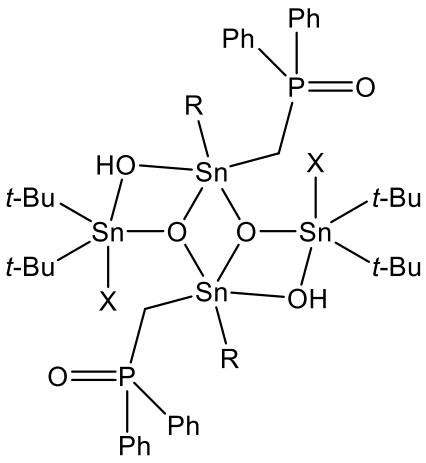

18, R = Ph, X = Cl
19, R = Me_3SiCH_2, X = Br
20, X = Me_3SiCH_2, Cl

Abbildung 1: $Ph_2P(O)CH_2$-funktionalisierte sauerstoffverbrückte Cluster (links) und dimere Tetraorganodistannoxane (rechts).

Die Reaktionen von $[Ph_2P(O)CH_2]RSnX_2$ mit einem Äquivalent *t*-Bu_2SnO lieferten die sauerstoffverbrückten Cluster $[(Ph_2P(O)CH_2)R(\mu\text{-}OH)Sn]_3(\mu_3\text{-}O)(\mu_3\text{-}X)$ (**14**, R = Ph, X = Br; **16**, R = Ph, X = Cl; **17**, R = Me_3SiCH_2, X = Br). Diese bestehen aus einem kationischen Stannoxankern und einem Halogenidanion, welches durch drei Wasserstoffbrückenbindungen stabilisiert wird. Beim sauerstoffverbrückten Cluster **14** wird durch die Reaktion mit Natriumiodid das Halogenidanion ausgetauscht, wodurch $[(Ph_2P(O)CH_2)Ph(\mu\text{-}OH)Sn]_3(\mu_3\text{-}O)(\mu_3\text{-}I)$,**15**, erhalten wird. Interessanterweise wird bei der analogen Reaktion von Verbindung **14** mit Natriumfluorid keine Produktbildung beobachtet. Die Diorganozinnoxocluster **14**–**16** besitzen die gleiche Struktur. Die Reaktion der Organozinndihalogenide $[Ph_2P(O)CH_2]RSnX_2$ mit zwei Äquivalenten *t*-Bu_2SnO lieferten die Leiter-artig aufgebauten unsymmetrisch substituierten dimeren Tetraorganodistannoxane $[t\text{-}Bu_2(X)SnOSnR\{CH_2P(O)Ph_2\}(OH)]_2$ (**18**, R = Ph, X = Cl; **19**, R = Me_3SiCH_2, X = Br; **20**, R = Me_3SiCH_2, X = Cl).

Die komplette Hydrolyse des Diorganozinndibromids $[Ph_2P(O)CH_2](Me_3SiCH_2)SnBr_2$, **10**, an der Luft ergab unter Sn–C-Bindungsspaltung den Sn_{12}–Monoorganozinnoxocluster $(Me_3SiCH_2Sn)_{12}O_{14}(OH)_6Br_2$,**10a**. Dieser besteht aus dem zentrosymmetrischen Makrokation $[(Me_3SiCH_2Sn)_{12}O_{14}(OH)_6]^{2+}$ und zwei Bromidgegenionen, welche durch Wasserstoffbrückenbindungen stabilisiert werden. Die Umkristallisation des Organozinntrichlorids $[Ph_2P(O)CH_2]SnCl_3$,**13**, aus Aceton an der Luft ergab einige Kristalle der Verbindung $[\{Ph_2P(O)CH_2SnCl_2(\mu\text{-}OH)\}_2\cdot 2C_3H_6O]$, **13a**). Diese Verbindung ist das erste Intermediat der Hydrolysereaktion des Organozinntrihalogenids **13**. Im Festkörper ist Verbindung **13a** aufgrund von Wasserstoffbrückenbindungen ein Polymer.

In Kapitel 1 wird ebenfalls die Synthese des ersten zinnenthaltenden frustrierten Lewis-Säure-Base-Paares $[Ph_2PC_6H_4]t\text{-}Bu_2SnCl$, **29**, beschrieben. Diese Verbindung zeigt keine P→Sn–Wechselwirkung, was durch die Abwesenheit der entsprechenden Kopplungen im ^{31}P– und ^{119}Sn–NMR-Spektrum belegt wird. Die fehlende Wechselwirkung ist eine Voraussetzung für frustrierte Lewis-Säure-Base-Paare.

Im zweiten Kapitel wird die Synthese und Charakterisierung einer Serie von cyclischen Zinn-substituierten Siloxanen und polyhedraler oligomerer Silsesquioxane (POSS) beschrieben (Abbildung 2). Die Siliciumatome dieser Siloxane sind an ein,

zwei oder drei Sauerstoffatome gebunden. Die Halogenierung und die Protodestannylation des monocylischen Siloxanes *cyclo*-$Ph_2Sn(CH_2Me_2Si)_2O$, **1**, des tricylischen Siloxanes $[\{Ph_2Sn(CH_2MeSi)_2O\}O]_2$, **12**, und des zinnsubstituierten POSSs $(Ph_3SnCH_2SiO_{1.5})_8$, **20**, lieferten die entsprechenden Organozinnhalogenide *cyclo*-$PhISn(CH_2Me_2Si)_2O$, **2**, *cyclo*-$X_2Sn(CH_2Me_2Si)_2O$ (**3**, X = I; **4**, X = Br; **5**, X = Cl), $[\{X_2Sn(CH_2MeSi)_2O\}O]_2$ (**13**, X = I; **14**, X = Br; **15**, X = Cl), und $(Br_2PhSnCH_2SiO_{1.5})_8$, **21**. Die in den Verbindungen enthaltenden Halogensubstituenten können für weitere Grignard-Reaktionen genutzt werden. Dies wurde durch die Reaktion von *cyclo*-$PhISn(CH_2Me_2Si)_2O$, **2**, mit dem Grignard-Reagenz $Me_2N(CH_2)_3MgCl$ bewiesen, wodurch das Siloxan *cyclo*-$\{Me_2N(CH_2)_3\}PhSn(CH_2Me_2Si)_2O$, **6**, erhalten wurde. Dieses enthält eine periphäre Amingruppe.

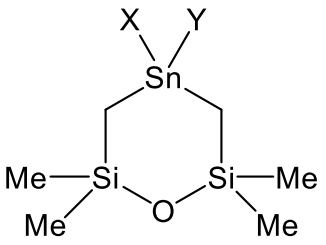

1; X = Y = Ph
2; X = I, Y = Ph
3; X = Y = I
4; X = Y = Br
5; X = Y = Cl
6; X = $Me_2N(CH_2)_3$, Y = Ph
7; X = $Me_2N(CH_2)_3$, Y = I

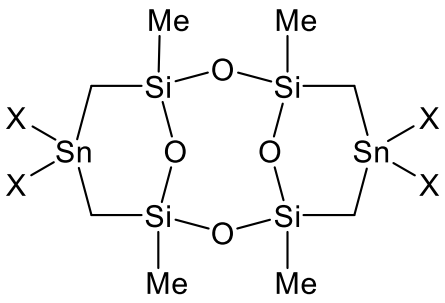

12; X = Ph
13; X = I
14; X = Br
15; X = Cl

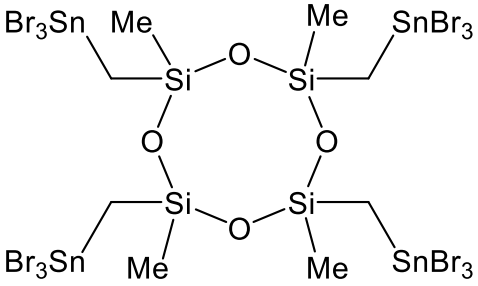

18

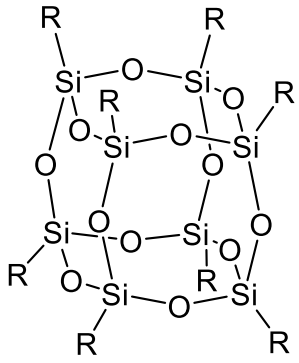

20, R = Ph_3SnCH_2
21, R = $PhBr_2SnCH_2$

Abbildung 2: Zinn-substituierte Siloxane und Silsesquioxane.

Die Reaktion des Diorganozinnhalogenids *cyclo*-$X_2Sn(CH_2Me_2Si)_2O$ (**3**, X = I; **4**, X = Br; **5**, X = Cl) mit *t*-Bu_2SnO lieferte die entsprechenden symmetrisch und/oder die unsymmetrisch substituierten dimeren Tetraorganodistannoxane (Abbildung 3). Diese Reaktivität beruht auf den Halogenatomen, welche an die Zinnatome gebunden sind.

Das Diorganozinndiiodid **3** reagiert mit *t*-Bu_2SnO ausschließlich zu den symmetrisch substituierten dimeren Tetraorganodistannoxanen $[O(Me_2SiCH_2)_2(I)SnOSn(X)(CH_2Me_2Si)_2O]_2$ (X = OH, I), **24**. Im Gegensatz dazu reagiert das Diorganozinndichlorid **5** mit *t*-Bu_2SnO nur zu dem unsymmetrisch substituierten dimeren Tetraorganodistannoxan $[O(Me_2SiCH_2)_2(Cl)SnOSn(Cl)t\text{-}Bu_2]_2$, **25**.

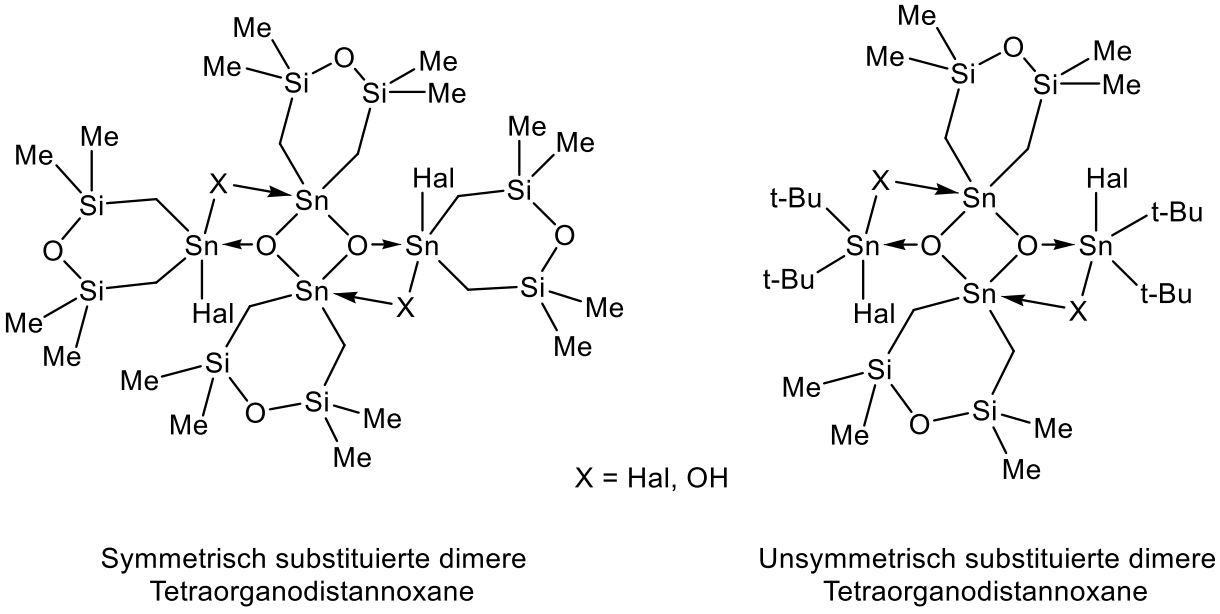

Abbildung 3: Symmetrisch und usymmetrisch substituierte dimere Tetraorganodistannoxane.

Die Reaktion des Diorganozinndibromids **4** mit *t*-Bu_2SnO lieferte sowohl die symmetrisch als auch die unsymmetrisch substituierten dimeren Tetraorganodistannoxane $[O(Me_2SiCH_2)_2(Br)SnOSn(\mathbf{X})(CH_2SiMe_2)_2O]_2$ (X = OH, Br), **26**, und $[O(Me_2SiCH_2)_2(\mathbf{X})SnOSn(Br)t\text{-}Bu_2]_2$ (X = OH, Br), **27**. Die Experimente zur Polymerisation des sechsgliedrigen *Cyclo* Siloxans, *cyclo*-$Ph_2Sn(CH_2Me_2Si)_2O$, **1**, waren nicht erfolgreich, wobei verschiedene anionische Starter getestet wurden.

Im dritten Kapitel wird über die Synthese und vollständige Charakterisierung der neuartigen achtgliedrigen ringförmigen Stannasiloxane *cyclo*-(RR'SnOMe$_2$SiCH$_2$)$_2$ (**6**, R = R' = Ph; **7**, R = Ph, R' = Me$_2$N(CH$_2$)$_3$; **8**, R = R' = *t*-Bu) berichtet (Abbildung 4). Durch die Variation der organischen substituenten am Zinnatom kann die Reaktivität der entsprechenden Achtringe beeinflusst werden. Verbindung **6**, in der zwei Phenylsubstituenten an das Zinnatom gebunden sind, reagiert bei Raumtemperatur schnell mit *t*-Bu$_2$SnO zu *cyclo*-[Me$_2$SiCH$_2$(Ph$_2$)SnO(*t*-Bu$_2$)SnO], **9**, welches einen sechsgliedrigen Ring enthält. Bei der Umsetzung einer Lösung von Verbindung **6** mit verschiedenen Diorganolementverbindungen wurde trotz unterschiedlicher Reaktionsbedingungen kein Umsatz beobachtet. Sobald Verbindung **9** mit Luft in Kontakt kommt, erfolgt eine Sn-C$_{Ph}$-Bindungsspaltung, wodurch der leiterartige Diorganozinnoxocluster [PhSn(CH$_2$Me$_2$SiO)(μ_3-O)Sn(μ-OH)*t*-Bu$_2$]$_2$, **10**, gebildet wird. Verbindung **10** reagiert mit zwei Äquivalenten *t*-Bu$_2$SnO zum Sn$_6$-Diorganozinncluster [(*t*-Bu$_2$)(μ-OH)Sn(μ_3-O)Sn(Ph)(CH$_2$Me$_2$SiO)Sn(*t*-Bu$_2$)(μ_3-O)]$_2$, **11**.

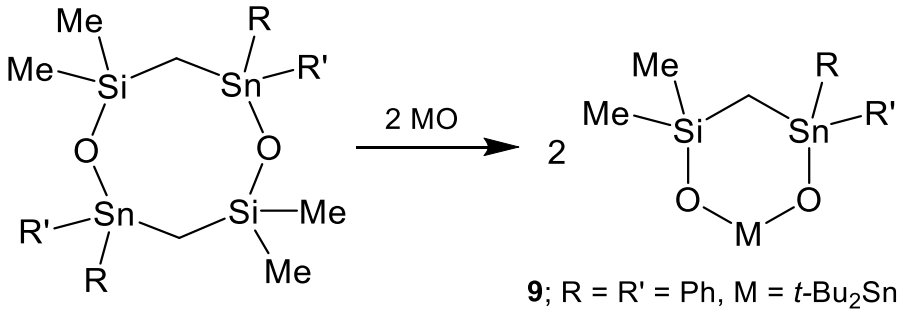

6; R = R' = Ph
7; R = Me$_2$N(CH$_2$)$_3$, R' = Ph
8; R = R' = *t*-Bu

9; R = R' = Ph, M = *t*-Bu$_2$Sn
12; R = R' = *t*-Bu, M = *t*-Bu$_2$Sn
13; R = R' = *t*-Bu, M = (*p*-MeO-C$_6$H$_4$)$_2$Te
16; R = Ph, R' = Me$_2$N(CH$_2$)$_3$, M = *t*-Bu$_2$Sn
17; R = Ph, R' = Me$_2$N(CH$_2$)$_3$, M = Ph$_2$Ge

Abbildung 4. *Cyclo*-Metallasiloxane.

Das ringförmige achtgliedrige Stannasiloxan, **8**, in dem zwei *tert*-Butylsubstituenten an das Zinnatom gebunden sind, reagiert bei hohen Temperaturen mit *t*-Bu$_2$SnO bzw. (*p*-MeOC$_6$H$_4$)$_2$TeO. Die Reaktion liefert die cyclischen sechsgliedrigen Verbindungen *cyclo*-[Me$_2$SiCH$_2$(*t*-Bu$_2$)SnO(*t*-Bu$_2$)SnO], **12**, und *cyclo*-[Me$_2$SiCH$_2$(*t*-Bu$_2$)SnO-(*p*-MeOC$_6$H$_4$)$_2$TeO], **13**. Desweiteren lieferten die Reaktionen des Stannasiloxanes *cyclo*-[{Me$_2$N(CH$_2$)$_3$}PhSnOMe$_2$SiCH$_2$]$_2$, **7**, mit *t*-Bu$_2$SnO und Ph$_2$GeO jeweils die ringförmigen sechsgliedrigen Metallasiloxane *cyclo*-

[Me_2SiCH_2{$Me_2N(CH_2)_3$}-PhSnO(*t*-Bu_2)SnO], **16**, and *cyclo*-[Me_2SiCH_2{$Me_2N(CH_2)_3$}PhSnOPh_2GeO], **17**. Die Verbindung **17** enthält den ersten sechsgliedrigen Ring, welcher vier verschieden Gruppe 14-Elemente in der Ringstruktur enthält. Die *cyclo*-Metallasiloxane *cyclo*-[CH_2(RR')SnO(Me_2)Si]$_2$ (**6**–**8**) und *cyclo*-[Me_2SiCH_2(RR')SnOMO] (**9**, **12**, **13**, **16**, und **17**) können als Modellverbindungen für modifizierte Kieselgeloberflächen betrachtet werden. Zusätzlich haben sie Potential für die Ringöffnungspolymerisation zur Darstellung neuer anorganischer Polymere und modifizierter Polysiloxane.

Im letzten Kapitel wurde gezeigt, dass die Lewis-sauren Diorganizinndihalogenide mit Triorganoalkoxysilanen wechselwirken und deren Si–O-Bindung aktivieren. Die Wechselwirkung ist elektrostatischer Natur und unterstützt die Interpretation der Si–O-Bindung als überwiegend ionische Bindung.

7. List of New Compounds

Chapter 1.

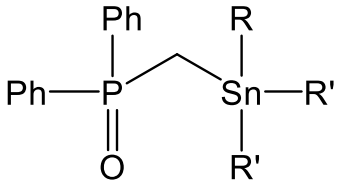

1, R = R' = Ph
2, R = Me_3SiCH_2, R' = Ph
3, R = R' = Cy

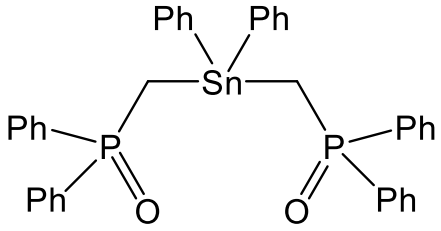

4

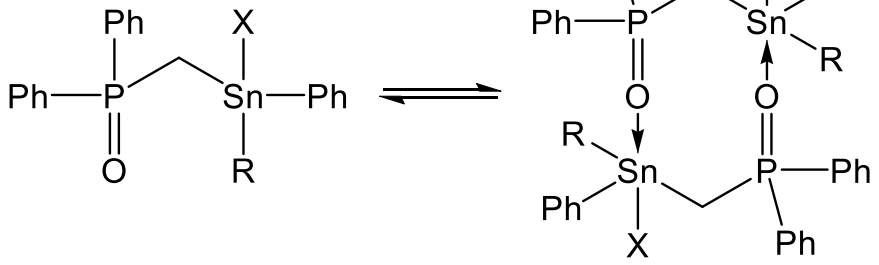

Monomer **Dimer**

5, R = Ph, X = I
6, R = Ph, X = Br
8, R = Me_3SiCH_2, X = I
9, R = Me_3SiCH_2, X = Br

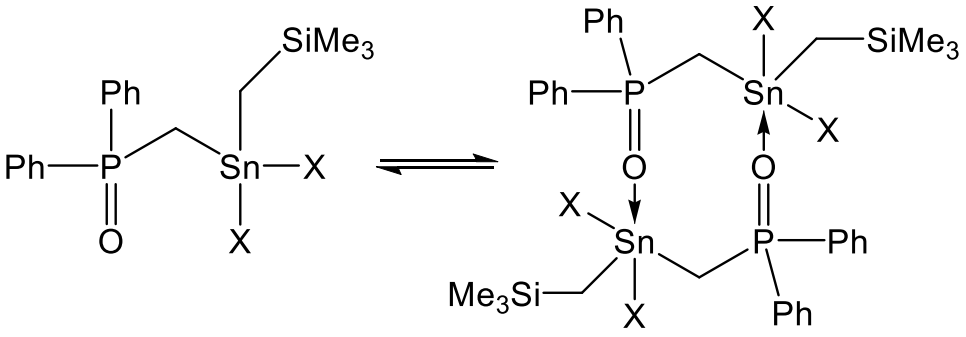

Monomer **Dimer**

10, X = Br
12, X = Cl

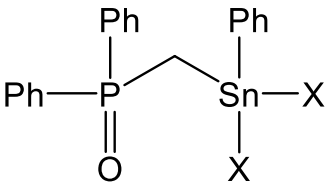

7, X = Br
11, X = Cl

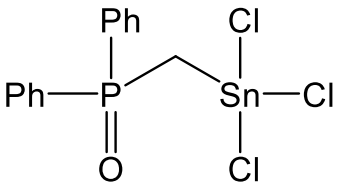

13

$(Me_3SiCH_2Sn)_{12}O_{14}(OH)_6Br_2$

10a

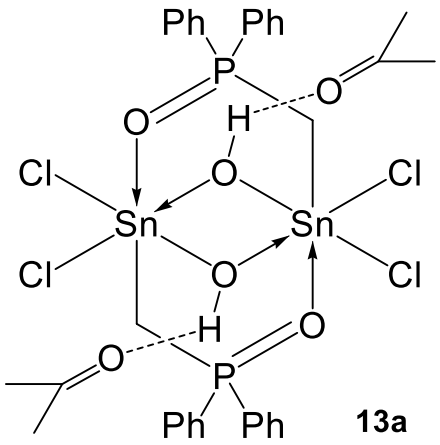

13a

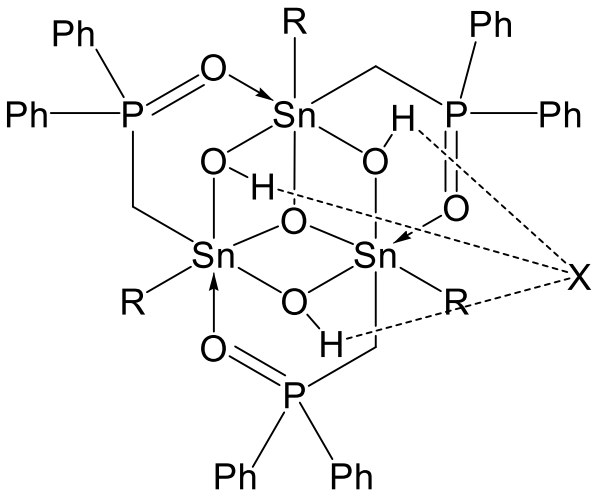

14, R = Ph, X = Br
15, R = Ph, X = I
16, R = Ph, X = Cl
17, R = Me_3SiCH_2, X = Br

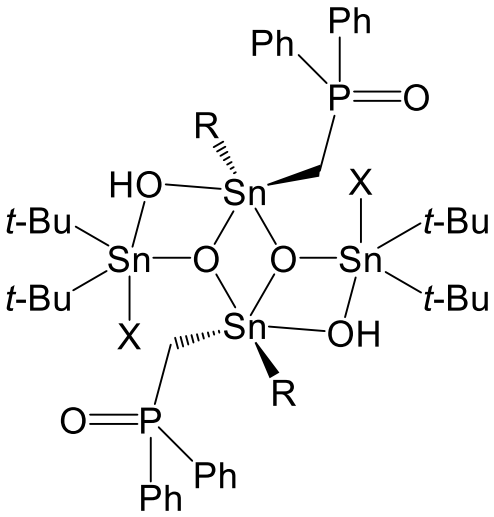

trans

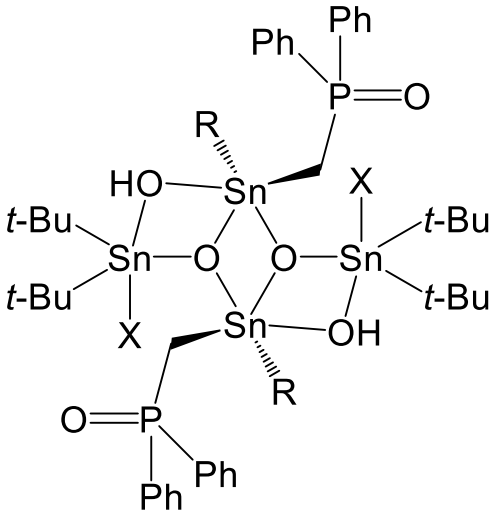

cis

18, R = Ph, X = Cl
19, R = Me_3SiCH_2, X = Br
20, X = Me_3SiCH_2, Cl

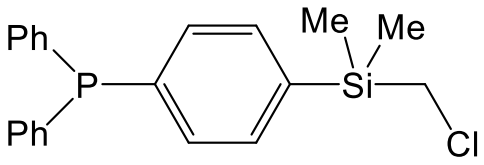

22

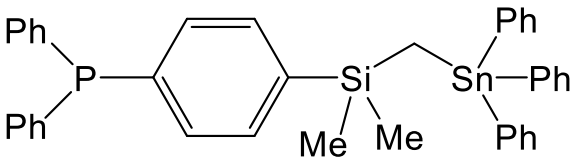

23

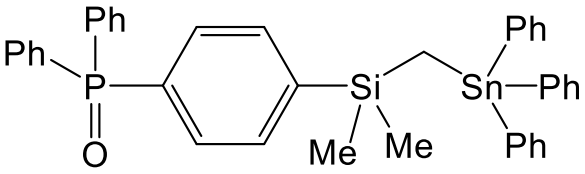

24

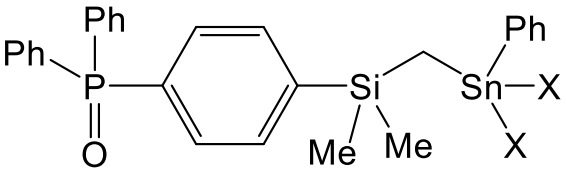

25, X = Br
26, X = Cl

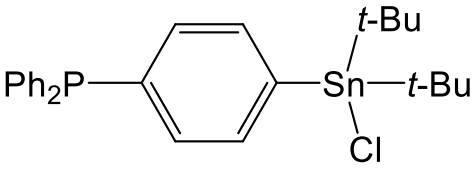

29

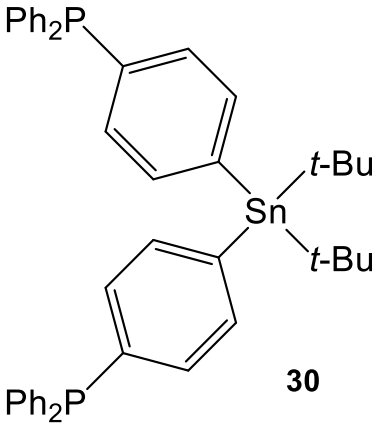

30

Chapter 2.

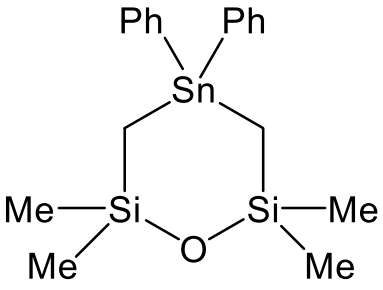

1

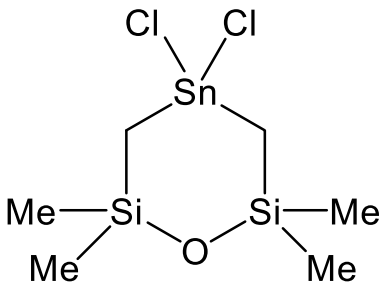

5

Compounds **1** and **5** were synthesized before by Mironov et al. however, no spectroscopic details or molecular structure were given. These compounds were synthesized in this work by different method and are completely characterization.

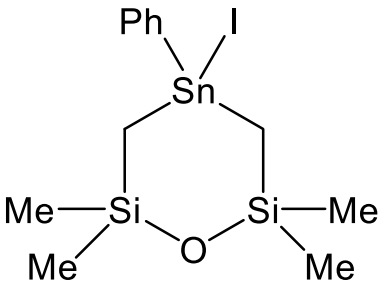

2

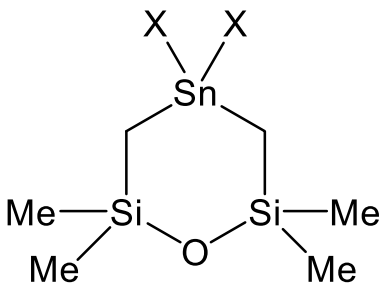

3, X = I
4, X = Br

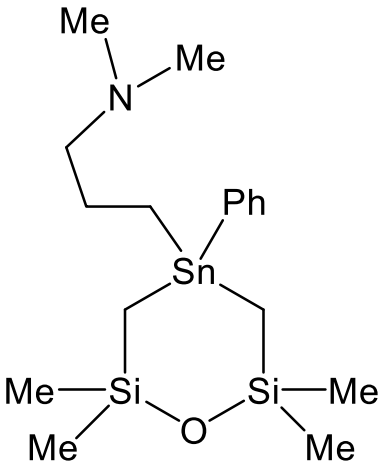

6

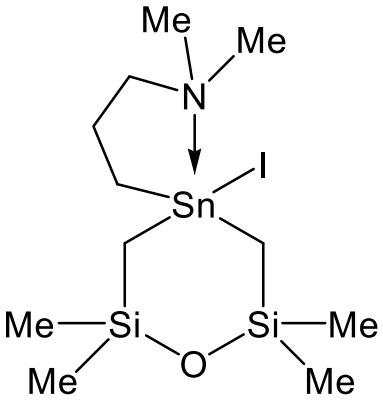

7

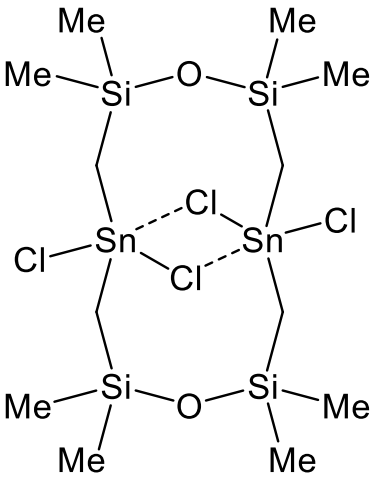

5a

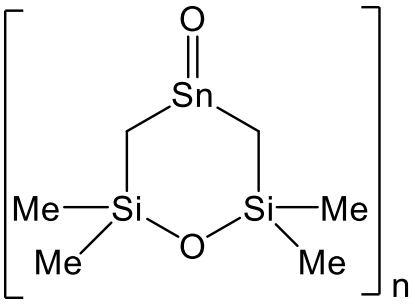

8

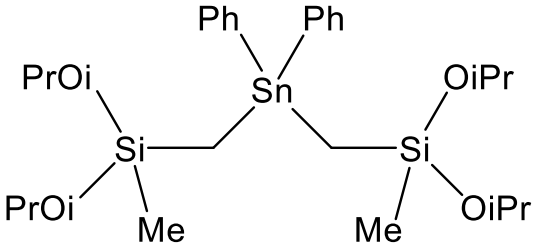

10

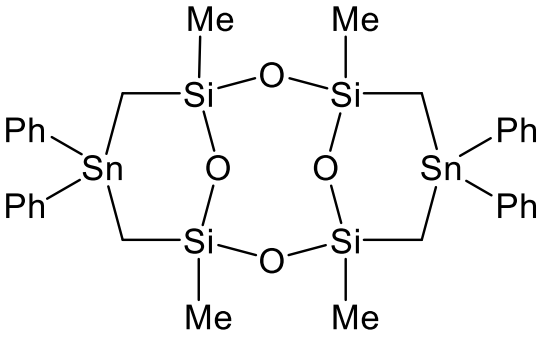

12

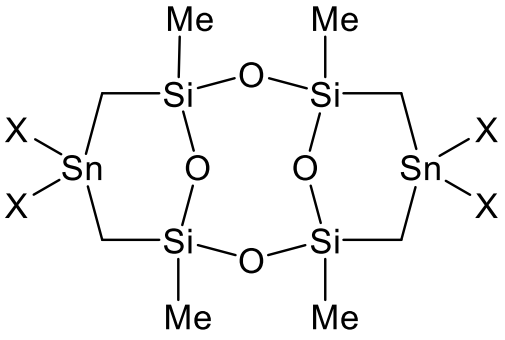

13, X = I
14, X = Br
15, X = Cl

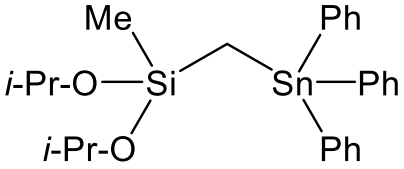

16

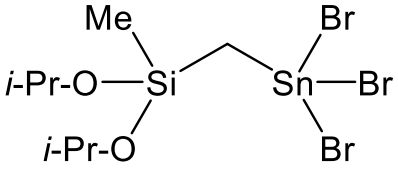

17

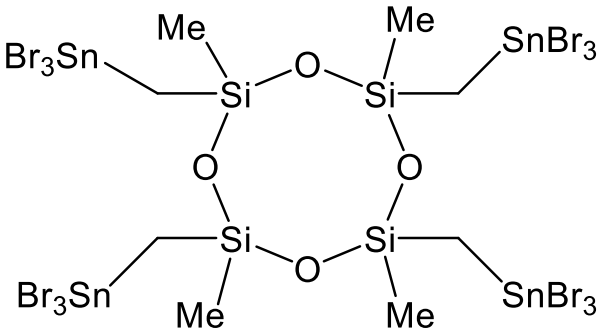

18

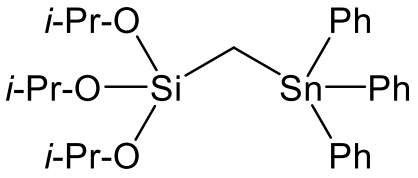

19

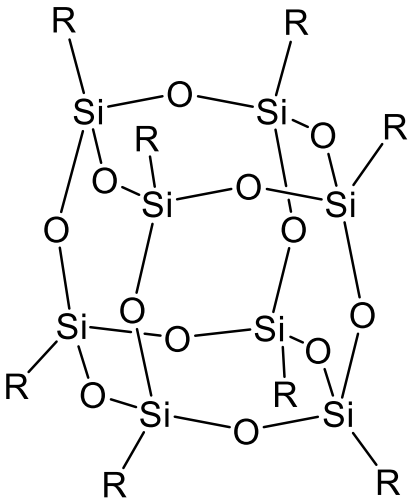

20, R = Ph_3SnCH_2

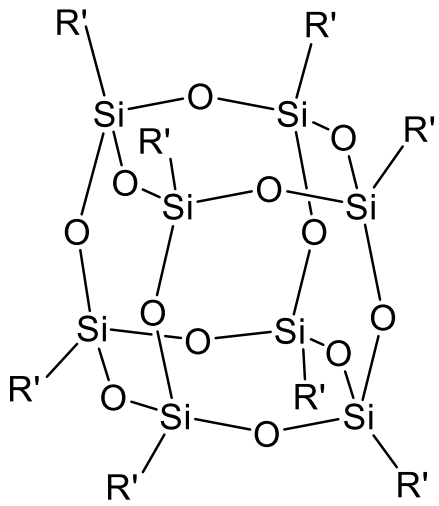

21, R' = $PhBr_2SnCH_2$

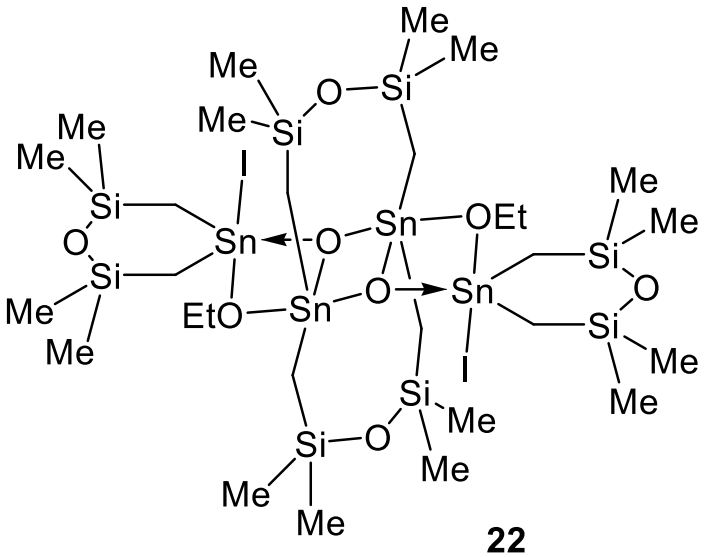

22

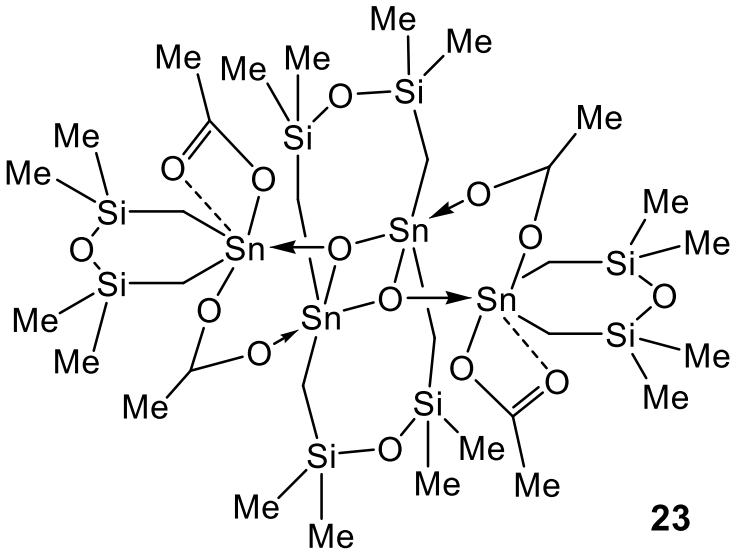

23

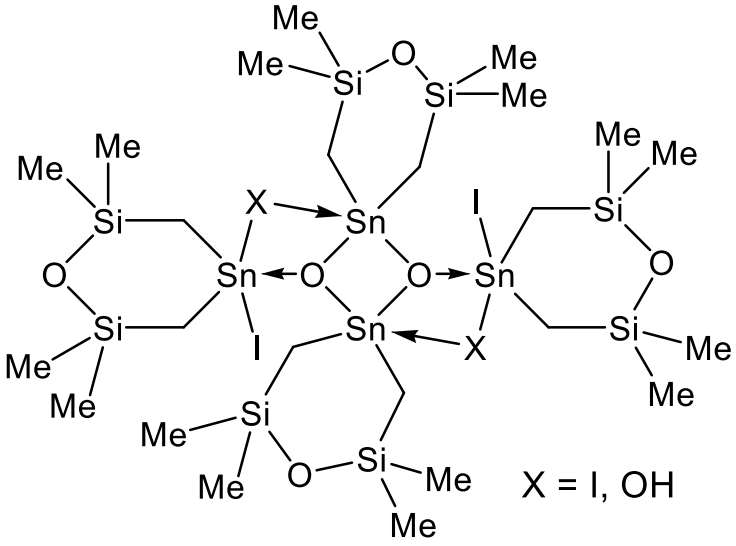

24

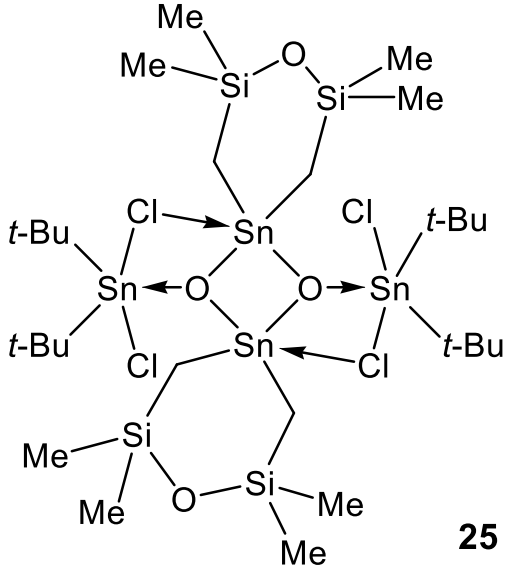

25

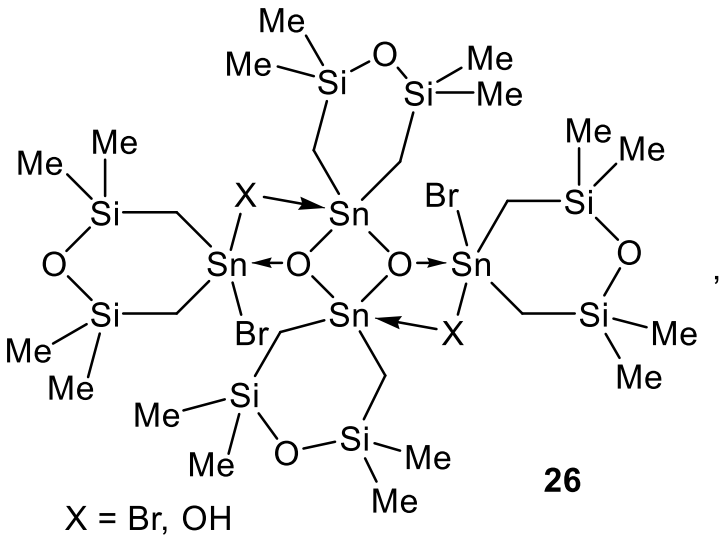

26

X = Br, OH

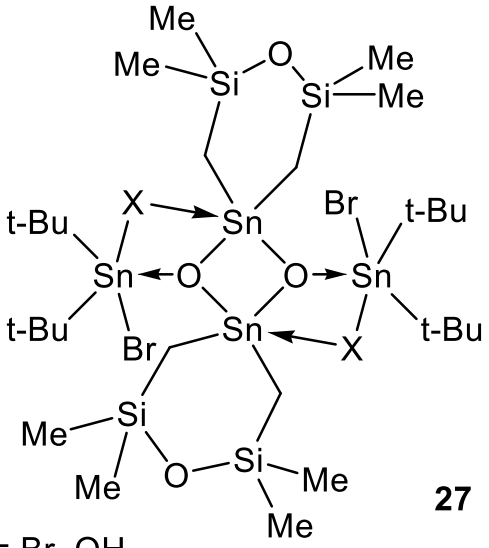

27

X = Br, OH

Chapter 3.

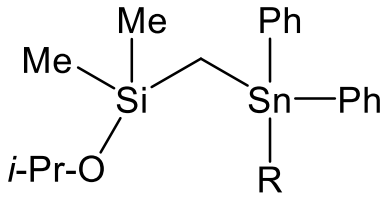

1, R = Ph
3, R = $Me_2N(CH_2)_3$

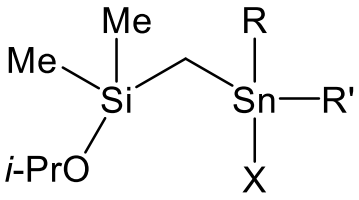

2, R = R' = Ph, X = I
4, R = Ph, R' = $Me_2N(CH_2)_3$, X = I
5, R = R' = *t*-Bu, X = Cl, OH

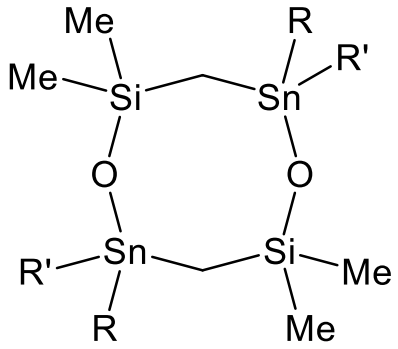

6, R = R' = Ph
7, R = $Me_2N(CH_2)_3$, R' = Ph
8, R = R' = *t*-Bu

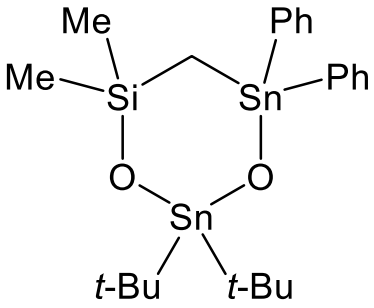

9

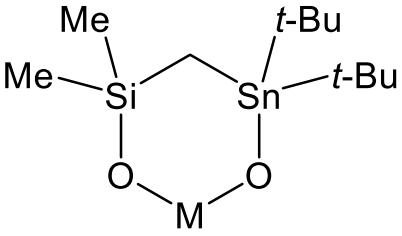

12, M = *t*-Bu_2Sn
13, M = (*p*-MeO-$C_6H_4)_2Te$

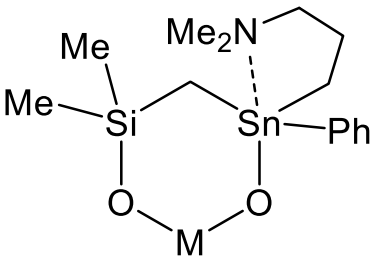

16, M = *t*-Bu_2Sn
17, M = Ph_2Ge

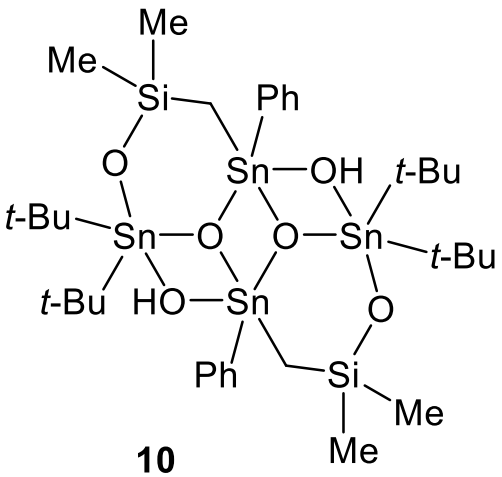
Me
Me
Si
Ph
O
Sn
OH
t-Bu
t-Bu
Sn
O
O
Sn
t-Bu
t-Bu
HO
Sn
O
Ph
Si
Me
Me

10

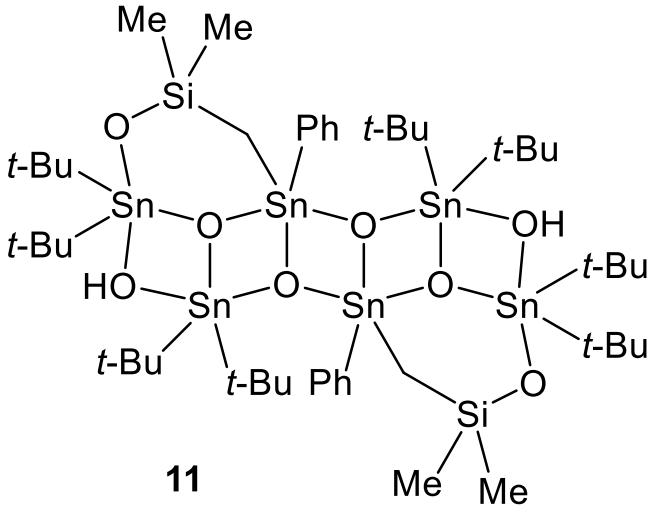
Me
Me
Si
O
Ph
t-Bu
t-Bu
t-Bu
Sn
O
Sn
O
Sn
OH
t-Bu
HO
Sn
O
Sn
O
Sn
t-Bu
t-Bu
t-Bu
Ph
O
Si
Me
Me

11

Chapter 4.

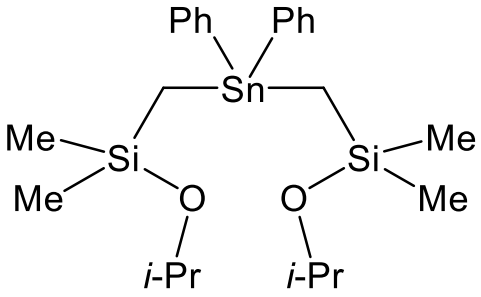

1

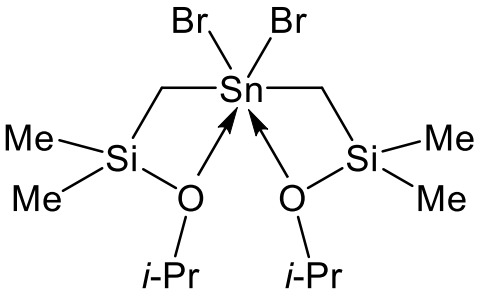

2

$[\{Me_2(i\text{-}PrO)SiCH_2\}SnBr_3](Ph_4P)$

3

8. CURRICULUM VITÆ

Personal Data

Name	Samer Baba Haj
Birthdate	06.07.1982
Birthplace	Damascus-Syria
Nationality	Syrian
Marital status	Married and have two Daughters
Confession	Muslim

Education

09.2012 – now	Research Assistant at TU Dortmund, Germany
08.2009 – now	PhD Student at TU Dortmund, Germany
10.2008 – 07.2009	Research Project in the Working Group Prof. Dr. Klaus Jurkschat, TU Dortmund.
10.2006 – 03.2008	Scientific Assistant at the Department of Chemistry, Damascus University, Syria
09.2004 – 09.2006 Syria	Diploma of Science in Chemistry, Damascus University,
09.2000 – 07.2004 Syria	Bachelor of Science in Chemistry, Damascus University,
09.1994 – 07.2000	Secondary School, Ibn-Khaldoon, Damascus, Syria
09.1988 – 06.1994	Primary School, Ibn-Hayan, Damascus, Syria

Publications

"$[Me_2(i\text{-}PrO)SiCH_2]_2SnBr_2$: Evidence for Intramolecular Si–O Bond Activation" Samer Baba Haj, Markus Schürmann, Ljuba Iovkova-Berends, Sonja Herres-Pawlis, Klaus Jurkschat, *Organometallics*, **2012**, *31*, 4716.

Dortmund, 27th. 05. 2015

Erklärung

Hiermit erkläre ich, dass ich die von mir vorgelegte Dissetration selbständig angefertigt und keine anderen als die in der Arbeit angegebenen Hilfen benutzt habe, und die Arbeit nicht zu einem anderen Zeitpunkt zum Zwecke der Promotion oder einer anderen Prüfung eingereicht wurde.

Dortmund, den 27 Mai 2015
Samer Baba Haj